Vol. 56 JANUARY, 1952 No. 1

THE JOURNAL OF PHYSICAL CHEMISTRY

(Registered in U. S. Patent Office)

Founded by Wilder D. Bancroft

CONTENTS

Symposium on Complex Ions and Polyelectrolytes

W. C. Waggener and R. W. Stoughton: Chemistry of Thorium in Aqueous Solutions. II. Chloride Complexing as A Function of Ionic Strength 1
Lawrence R. Thompson and W. K. Wilmarth: The Binuclear Peroxo Complex Compounds of Tri- and Tetrapositive Cobalt 5
Philip Wehner and J. C. Hindman: The Chloro Complexes of Ruthenium(IV) 10
Hans B. Jonassen, G. G. Hurst, R. B. LeBlanc and A. W. Meibohm: Inorganic Complex Compounds Containing Polydentate Groups. VI. Formation Constants of Complex Ions of Diethylenetriamine and Triethylenetetramine with Divalent Ions 16
Frederick R. Duke and Welby G. Courtney: Complexes in Oxidation–Reduction Reactions. The Copper(II)–Cyanide Reaction 19
Fred Basolo, John G. Bergmann and Ralph G. Pearson: Mechanism of Substitution Reactions in Complex Ions. I. Kinetics of the Aquation and Hydrolysis of Some C-Substituted Acetatopentamminecobalt(III) Ions 22
S. S. Jones and F. A. Long: Complex Ions from Iron and Ethylenediaminetetraacetate: General Properties and Radioactive Exchange 25
Robert A. Plane and Henry Taube: Observations of the Kinetics of the Exchange of Water between $Cr(H_2O)_6^{+++}$ and Solvent 33
R. K. Osterheld and L. F. Audrieth: Polymerization and Depolymerization Phenomena in Phosphate–Metaphosphate Systems at Higher Temperatures. Condensation Reactions Involving the Potassium Hydrogen Orthophosphates. 38
André Oth and Paul Doty: Macro-ions. II. Polymethacrylic Acid 43
Frederick T. Wall and Thomas J. Swoboda: Electrolytic Interaction of Nylon with Aqueous Solutions of Sodium Hydroxide 50
George E. Kimball, Melvin Cutler and Harold Samelson: A Theory of Polyelectrolytes 57
Edward H. deButts: The Distribution of Ions in Solutions of Weak Electrolytes 60
Herbert Morawetz and Walter L. Hughes, Jr.: The Interaction of Proteins with Synthetic Polyelectrolytes. I. Complexing of Bovine Serum Albumin 64
Fred Karush: The Interaction of Optically Isomeric Dyes with Bovine Serum Albumin 70
Irving M. Klotz, R. K. Burkhard and Jean M. Urquhart: The Binding of Organic Ions by Proteins. Comparison of Bovine and Human Serum Albumins 77
J. L. Oncley, E. Ellenbogen, D. Gitlin and F. R. N. Gurd: Protein–Protein Interactions 85
William J. Argersinger, Jr., and Arthur W. Davidson: Experimental Factors and Activity Coefficients in Ion Exchange Equilibria 92
Jack J. Grossman and Arthur W. Adamson: The Diffusion Process for Organolite Exchangers 97
J. T. Clarke, J. A. Marinsky, W. Juda, N. W. Rosenberg and S. Alexander: Electrochemical Properties of a Permionic Anion Membrane 100
K. S. Spiegler and C. D. Coryell: Electromigration in a Cation Exchange Resin. II. Detailed Analysis of Two-Component Systems 106
Jack Schubert: Ion Exchange Studies of Complex Ions as a Function of Temperature, Ionic Strength, and Presence of Formaldehyde 113
T. R. E. Kressman: Ion Exchange Separations Based upon Ionic Size 118
W. O. Milligan and Arthur L. Draper: Isobaric and Isothermal Studies in the System Soap–Water. II. 123
Robert D. Vold, Joseph Grandine, 2nd, and Hans Schott: Characteristic X-Ray Spectrometer Patterns of the Saturated Sodium Soaps 128
E. A. Hauser and D. S. le Beau: The Surface Structure and Properties of Colloidal Silica and Alumina 136
J. M. Honig and L. H. Reyerson: Adsorption of Nitrogen, Oxygen and Argon on Rutile at Low Temperatures; Applicability of the Concept of Surface Heterogeneity 140

Founded by Wilder D. Bancroft

THE JOURNAL OF PHYSICAL CHEMISTRY

(Registered in U. S. Patent Office)

Published monthly (except July, August and September) by the American Chemical Society at 20th and Northampton Sts., Easton, Pa.

Application pending for re-entry as second-class matter at the Post Office at Easton, Pennsylvania.

The *Journal of Physical Chemistry* is devoted to the publication of selected symposia in the broad field of physical chemistry and to other contributed papers.

Manuscripts originating in the British Isles, Europe and Africa should be sent to F. C. Tompkins, The Faraday Society, 6 Gray's Inn Square, London W. C. 1, England.

Manuscripts originating elsewhere should be sent to W. Albert Noyes, Jr., Department of Chemistry, University of Rochester, Rochester 3, N. Y.

Correspondence regarding accepted copy, proofs and reprints should be directed to Assistant Editor, Allen D. Bliss, Department of Chemistry, Simmons College, 300 The Fenway, Boston 15, Mass.

Business Office: American Chemical Society, 1155 Sixteenth St., N. W., Washington 6, D. C.

Advertising Office: American Chemical Society, 332 West 42nd St., New York 18, N. Y.

Articles must be submitted in duplicate, typed and double spaced. They should have at the beginning a brief Abstract, in no case exceeding 300 words. Original drawings should accompany the manuscript. Lettering at the sides of graphs (black on white or blue) may be pencilled in, and will be typeset. Figures and tables should be held to a minimum consistent with adequate presentation of information. Photographs will not be printed on glossy paper except by special arrangement. All footnotes and references to the literature should be numbered consecutively and placed on the manuscript at the proper places. Initials of authors referred to in citations should be given. Nomenclature should conform to that used in *Chemical Abstracts*, mathematical characters marked for italic, Greek letters carefully made or annotated, and subscripts and superscripts clearly shown. Articles should be written as briefly as possible consistent with clarity and should avoid historical background unnecessary for specialists.

Symposium papers should be sent in all cases to Secretaries of Divisions sponsoring the symposium, who will be responsible for their transmittal to the Editor. The Secretary of the Division by agreement with the Editor will specify a time after which symposium papers cannot be accepted. The Editor reserves the right to refuse to publish symposium articles, for valid scientific reasons. Each symposium paper may not exceed four printed pages (about sixteen double spaced typewritten pages) in length except by prior arrangement with the Editor.

Remittances and orders for subscriptions and for single copies, notices of changes of address and new professional connections, and claims for missing numbers should be sent to the American Chemical Society, 1155 Sixteenth St., N. W., Washington 6, D. C. Changes of address for the *Journal of Physical Chemistry* must be received on or before the 30th of the preceding month.

Claims for missing numbers will not be allowed (1) if received more than sixty days from date of issue (because of delivery hazards, no claims can be honored from subscribers in Central Europe, Asia, or Pacific Islands other than Hawaii), (2) if loss was due to failure of notice of change of address to be received before the date specified in the preceding paragraph, or (3) if the reason for the claim is "missing from files."

Annual Subscription: $8.00 to members of the American Chemical Society, $10.00 to non-members. Postage free to countries in the Pan American Union; Canada, $0.40; all other countries, $1.20. Single copies, $1.25; foreign postage, $0.15; Canadian postage, $0.05.

* * * (*Continued from first page of cover*) * * *

W. O. Milligan and L. W. Vernon: Crystal Structure of Heavy Metal Orthovanadates 145
Fred J. Edeskuty and Neal R. Amundson: Mathematics of Adsorption. IV. Effect of Intraparticle Diffusion in Agitated Static Systems 148
Victor P. Henri, Charles R. Maxwell, William C. White and Dorothy C. Peterson: The Chemical Effects of α-Particles upon Some Hydrocarbons in the Vapor State 153
R. J. Scott and H. E. Gunning: The Polymerization of Cyclopropane 156

THE JOURNAL OF PHYSICAL CHEMISTRY

Founded by Wilder D. Bancroft

VOL. LVI

1952

EASTON, PA.
MACK PRINTING COMPANY
1952

THE JOURNAL OF PHYSICAL CHEMISTRY

(Registered in U. S. Patent Office) (Copyright, 1952, by the American Chemical Society)

Founded by Wilder D. Bancroft

VOLUME 56 JANUARY 17, 1952 NUMBER 1

CHEMISTRY OF THORIUM IN AQUEOUS SOLUTIONS. II. CHLORIDE COMPLEXING AS A FUNCTION OF IONIC STRENGTH[1]

BY W. C. WAGGENER AND R. W. STOUGHTON

Chemistry Division, Oak Ridge National Laboratory, Oak Ridge, Tennessee

Received August 30, 1951

Chloride complexing of aqueous thorium has been studied as a function of ionic strength over the range 0.5–6.0 using the benzene–TTA solvent extraction method. Chloride data up to 4 *M* are explained in terms of successive complexing, and constants are estimated for formation of $ThCl^{+3}$, $ThCl_2^{+2}$, $ThCl_3^{+}$ and $ThCl_4$. Aqueous TTA–thorium species have been investigated by a new method, *viz.*, by measuring the partition of TTA, under suitable conditions, between a benzene phase and an aqueous phase, as a function of both thorium and chloride concentration. A single complex, monothenoyltrifluoroacetonethorium ion (*i.e.*, ThT^{+3}), has been found, and a tentative value for k_T ($Th^{+4} + HT_{aq} = ThT^{+3} + H^+$) at $\mu = 2.00$ is 6.6 ± 5%. There is no evidence for a double complex involving both TTA and chloride under our conditions.

Introduction

In the first paper of this series, Day and Stoughton[2] studied the interaction of aqueous thorium with a number of monobasic acids at a single ionic strength and acidity of 0.5. The present work was initiated to obtain additional chloride data required for thorium hydrolysis studies being conducted at different ionic strength,[3] as well as to exploit the advantages of the benzene–TTA extraction method employed.

This solvent extraction method involves measurement of the change in the distribution ratio of radioactive thorium (Th-234) between a benzene phase containing the chelating agent, thenoyltrifluoroacetone (TTA), and an aqueous phase containing varying concentration of anions—*viz.*, chloride—and perchlorate ion at constant ionic strength and acidity.

The following reactions involving aqueous thorium ion may occur

$$Th^{+4} + 4HT_B = ThT_{4B} + 4H^+ \qquad K_T \qquad (1)$$

$$Th^{+4} + H_2O = ThO^{++} + 2H^+ \qquad k_h \qquad (2a)$$

$$2Th^{+4} + H_2O = Th_2O^{+6} + 2H^+ \qquad k_h' \qquad (2b)$$

$$Th^{+4} + HT = ThT^{+3} + H^+ \qquad k_T \qquad (3)$$

$$Th^{+4} + nCl^- = ThCl_n^{+(4-n)} \qquad k_{nCl} \qquad (4)$$

where K_T, k_h, k_h', k_T and k_{nCl} stand for equilibrium constants with the substances in equations (1), (2a), (2b), (3) and (4), respectively, expressed in moles per liter, HT stands for TTA, T stands for the chelate radical, and the subscript B indicates benzene phase.

Under conditions where all aqueous thorium is in the form of Th^{+4}, equation (1) expresses the extraction of thorium into benzene–TTA, and the distribution ratio of thorium in the two phases is expressed by

$$R_o = \frac{[Th^{+4}]_A}{[ThT_4]_B} = \frac{1}{K_T} \times \frac{[H^+]_A^4}{[HT]_B^4} \qquad (5)$$

If the ThT^{+3} aqueous complex, equation (3) were taken into account, both the central part and the right-hand side of equation (5) would contain the factor $(1 + k_T[HT]/[H^+])$.

Thorium hydrolysis, which is best represented by equations (2a) and (2b), is negligible under conditions of acidity and thorium concentration employed.[3] If the relatively small amount of complexing represented by equation (3) be neglected then when chloride ion is present in the aqueous phase the ratio of the total thorium in the aqueous phase to that in the benzene phase is given by

$$R = \frac{[Th^{+4}] + [ThCl^{+3}] + [ThCl_2^{+2}] + \cdots + [ThCl_n^{+(4-n)}]}{[ThT_4]_B} \qquad (6)$$

(1) This document is based on work performed for the Atomic Energy Commission at the Oak Ridge National Laboratory.

(2) R. A. Day and R. W. Stoughton, *J. Am. Chem. Soc.*, **72**, 5662 (1950).

(3) K. A. Kraus and R. W. Holmberg, U. S. Atomic Energy Commission Declassified Report, AECD-2919 (1950).

from which may be derived the equation expressing the distribution ratio as a function of chloride ion concentration.

$$R = R_o(1 + k_{Cl}[Cl^-] + k_{2Cl}[Cl^-]^2 + \cdots + k_{nCl}[Cl^-]^n) \quad (7)$$

The constants k_{Cl}, k_{2Cl}, $\cdots$, k_{nCl} are the respective stability constants for possible chlorothorium species $ThCl^{+3}$, $ThCl_2^{+2}$, . . ., $ThCl_n^{+(4-n)}$, and are written as indicated in equation (4).

The stability constant for the monochlorothorium ion may be obtained at low chloride where the contribution of higher species is negligible, from the slope of the curve obtained by plotting R *versus* $[Cl^-]$, divided by R_o. The next higher species then may be estimated by plotting log $\{R/R_o - (1 + k_{Cl}[Cl^-])\}$ *versus* log $[Cl^-]$, inserting the value for k_{Cl} initially determined. The limiting slope at low chloride gives the chloride power dependence of the species, and its ordinate intercept at log $[Cl^-] = 0$ numerically equals the constant.

Stability constants for successive species may be estimated in turn by similar log–log plots. However, for the intermediate chlorothorium species which have small and only slightly different stabilities it is necessary to adjust the values of the constants by trial and error.

These constants could also be obtained by a least squares method. However, the method outlined here is easier to perform and, we believe, just as accurate.

The complexing of TTA by thorium in the aqueous phase according to equation (3) is significant, though relatively small (*i.e.*, under 10%). Zebroski[4] by the spectrophotometric method, measured k_T as a function of ionic strength in the range $\mu = 0.11$–2.11. Recently[5] he has reported that his former values are probably too high by a factor of nearly two.

During our present studies there arose a question of possible double complexes involving both TTA and chloride with thorium. If such complexing were appreciable our above interpretation in terms of k_{nCl} constants would be incorrect. By measuring the distribution of TTA, under suitable conditions, between a benzene phase and an aqueous phase as a function of thorium and of chloride, equation (3) has been verified as representing all Th^{+4}–TTA aqueous complexing of detectable magnitude, and a value for k_T was obtained in close agreement with Zebroski's later work.

For purposes of disproving double complexing, it was assumed that the following reactions involving TTA and thorium might be taking place in the aqueous phase

$$Th^{+4} + HT = ThT^{+3} + H^+ \qquad k_T \quad (3)$$

$$Th^{+4} + HT + Cl^- = ThClT^{+2} + H^+ \qquad k_{ClT} \quad (8)$$

Under conditions where the hydrolysis of thorium is negligible and its extraction into benzene also negligible, the partition of TTA between aqueous and benzene phases may then be written

$$D = \frac{[HT]_A + [ThT^{+3}]_A + [ThClT^{+2}]_A}{[HT]_B} \quad (9)$$

from which may be derived

$$D = D_o\left(1 + k_T\frac{[Th^{+4}]}{[H^+]} + k_{ClT}\frac{[Th^{+4}][Cl^-]}{[H^+]}\right) \quad (10)$$

where D_o stands for the aqueous-over-benzene TTA distribution in absence of thorium and chloride in the aqueous phase at a given ionic strength. The constant, k_T, may be evaluated in the absence of chloride from the slope of the line obtained by plotting D *versus* $[Th^{+4}]/[H^+]$. Then knowing k_T, the value of k_{ClT} could be obtained at constant $[Th^{+4}]/[H^+]$ from the slope of the curve obtained by plotting D *versus* $[Th^{+4}][Cl^-]/[H^+]$, should the third term in the brackets of equation (10) be of significant magnitude.

Experimental

Aqueous Chlorothorium Studies.—Reagent grade chemicals were used throughout. Sodium perchlorate used to maintain ionic strength was prepared in 8 M solution by neutralizing standardized $HClO_4$ with NaOH pellets. A visible amount of hydrated $Fe(OH)_3$, formed upon standing 2–3 days at a pH of 4 was filtered off after first boiling to eliminate carbonate, and diluting to volume. Analyses for sulfate and phosphate ions were reported as less than 0.001 M and and 0.0001 M, respectively.[6]

The TTA was obtained from M. Calvin of the University of California. It was repurified by vacuum distillation, and stored in darkness over P_2O_5. Crystals of the nearly colorless product melted at 42.8–43.2°.

The aqueous solutions for a given experiment at constant ionic strength and acidity were prepared as a group by pipetting measured volumes of components into 25-ml. volumetric flasks and diluting to the mark. The benzene–TTA stock solution as prepared contained TTA 2.5% in excess of the nominal molarity in order to accommodate a decrease in the total concentration of chelating agent due to aqueous phase solubility. Natural thorium, 10^{-6} or 10^{-5} M, and thorium tracer were introduced from 0.01 M $HClO_4$ solutions (previously equilibrated with benzene–TTA) by equilibrating overnight.

Equilibrations were performed in 15-ml. glass-stoppered centrifuge tubes which were rotated end-over-end at 45 r.p.m. in a thermostated water-bath with temperature controlled at 25 ± 0.1°. Duplicate 4-ml. volumes of 11 or 15 stock solutions of aqueous phase were equilibrated 1.5–3.5 hours with equal volumes of benzene–TTA containing Th-232 and tracer Th-234. Both phases were sampled as soon as practicable after centrifuging. Aliquots from the benzene phases were evaporated directly on 25-mm. glass plates for beta counting. Aliquots from the aqueous phases which contained salts were delivered to 2-ml. volumetric flasks, diluted, then equilibrated with 0.5 ml. of 0.5 M benzene–TTA. After centrifuging, the organic phases were transferred, *in toto*, to counting plates. The samples were counted with a G–M counter through a 20.7 mg./cm.^{2} aluminum absorber, whereby only the 2.32 mev. beta of UX_2 (1.1 minute Pa-234 daughter of Th-234) was counted, thereby making the count quite insensitive to small amounts of extraneous material. Material balances averaged 97–101% with a mean deviation of 1–2%.

Aqueous TTA–Thorium Studies.—A stock solution of 0.2 M $Th(ClO_4)_4$ in 0.057 M $HClO_4$ was prepared and its extraction into benzene–TTA was compared with that of carrier-free tracer Th-234 in 0.1 M $HClO_4$ in the following manner. Thorium nitrate was heated to dryness several times with $HClO_4$. The solid was taken up with enough 0.01 M $HClO_4$ to give a solution 0.234 M in thorium as determined by precipitating the oxalate and igniting to ThO_2. An aliquot of this solution was diluted tenfold with dilute $HClO_4$ and tracer added. The resulting solution which was approximately 0.38 M in acid and 0.0234 M in thorium was equilibrated with an equal volume of 0.25 M benzene–TTA. The aqueous-over-benzene distribution ratios determined from duplicate gravimetric analyses of each phase were 0.430 and 0.432. The corresponding ratio determined from

(4) E. L. Zebroski, University of California Radiation Laboratory classified thesis, BC-63, 1947.

(5) E. L. Zebroski and H. W. Alter, private communication.

(6) These analyses were performed through the courtesy of P. A. Thomason, Oak Ridge National Laboratory Analytical Division.

the average beta count of four plates prepared from each phase was 0.430.

In this experiment duplicate 4-ml. volumes of 11 aqueous stock solutions at $\mu = 2.0$, $[H^+] = 0.04\ M$, $[Cl^-] = 0$–$0.56\ M$ and $[Th] = 0$–$0.10\ M$ were equilibrated 6 hours with equal volume of $1.0 \times 10^{-4}\ M$ and $3.0 \times 10^{-4}\ M$ benzene–TTA. The concentrations of TTA in the benzene phases were measured spectrophotometrically at 320, 325 and 330 mμ after 5- and 25-fold dilutions, respectively. The concentrations of TTA extracted into the aqueous phases were determined by equilibrating 3-ml. aliquots, acidified to $0.5\ M$ in $HClO_4$ overnight with 3 ml. of fresh benzene. Then, the absorption of back extracted TTA was measured directly The acidity of each aqueous phase after equilibration was measured with a glass electrode-vibrating reed electrometer which was standardized against $0.050\ M$ $HClO_4$ in $1.95\ M$ $NaClO_4$.[7]

Results and Discussion

The results obtained for the interaction of aqueous thorium and chloride ions are presented graphically in Figs. 1–6. Table I gives a summary

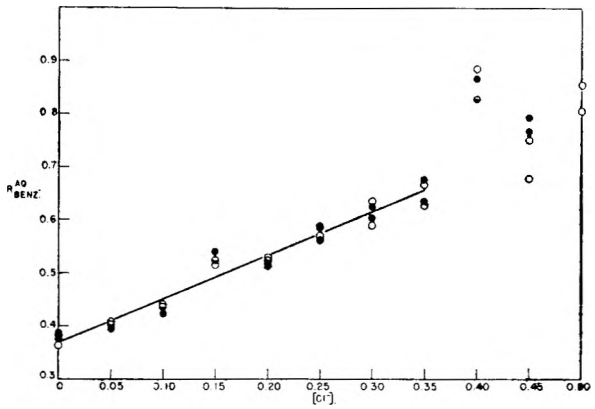

Fig. 1.—Distribution of thorium in the aqueous benzene system: equilibration 3.0 hr. at 25 ± 0.1°: ○, experimental points, first count of plates; ●, experimental points, second count of plates; ——, curve of equation $R^{aq.}_{benz.} = 0.368\{1 + 2.24[Cl^-]\}$. Aqueous phase ($\mu = 0.5$): $[Cl^-] = 0.00$–$0.50\ M$; $[ClO_4^-] = 0.50$–$0.00\ M$; $[Na^+] = 0.30$–$0.00\ M$; $[H^+] = 0.20\ M$. Benzene phase: $[HT] = 0.10\ M$; $[Th^{234}]$ = tracer level; $[Th^{232}] = 10^{-6}\ M$; (Th initially in benzene phase).

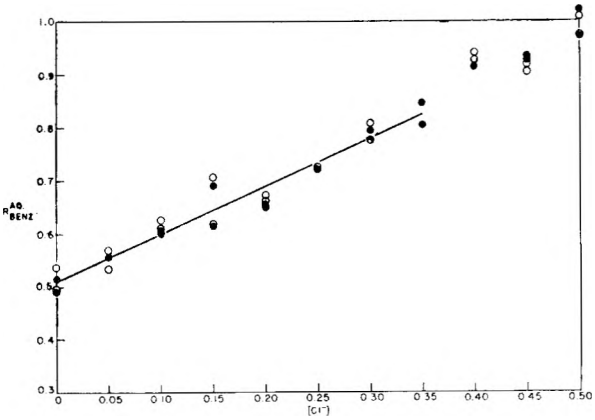

Fig. 2.—Distribution of thorium in the aqueous benzene system: equilibration 3.5 hr. at 25 ± 0.1°: ○, experimental points, first count of data; ●, experimental points, second count of data; ——, curve of the equation $R^{aq.}_{benz.} = 0.508\{1 + 1.78[Cl^-]\}$. Aqueous phase ($\mu = 0.7$): $[Cl^-] = 0.00$–$0.50\ M$; $[ClO_4^-] = 0.70$–$0.20\ M$; $[Na^+] = 0.50$–$0.00\ M$; $[H^+] = 0.20\ M$. Benzene phase: $[HT] = 0.10\ M$; $[Th^{234}]$ = tracer level; $[Th^{232}] = 10^{-6}\ M$; (Th initially in benzene phase).

(7) Measurements were the courtesy of R. W. Holmberg, Oak Ridge National Laboratory Chemistry Division.

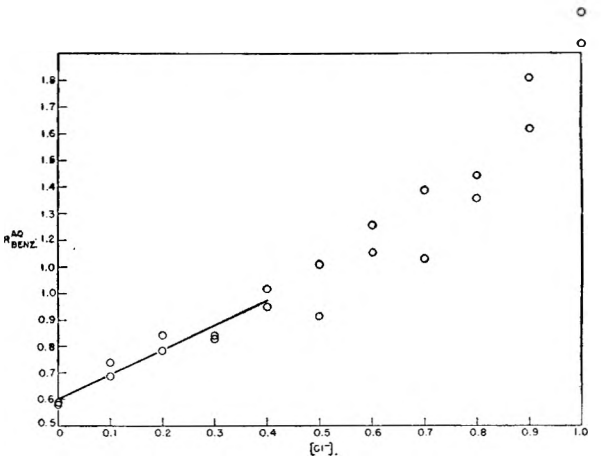

Fig. 3.—Distribution of thorium in the aqueous benzene system: equilibration 1.5 at 25 ± 0.1°; ○, experimental points; ——, curve of the equation $R^{aq.}_{benz.} = 0.601\{1 + 1.53[Cl^-]\}$. Aqueous phase ($\mu = 1.0$): $[Cl^-] = 0.00$–$1.00\ M$; $[ClO_4^-] = 1.00$–$0.00\ M$; $[Na^+] = 0.80$–$0.00\ M$; $[H^+] = 0.20\ M$. Benzene phase: $[HT] = 0.10$; $[Th^{234}]$ = tracer level; $[Th^{232}] = 10^{-5}\ M$; (Th initially in benzene phase).

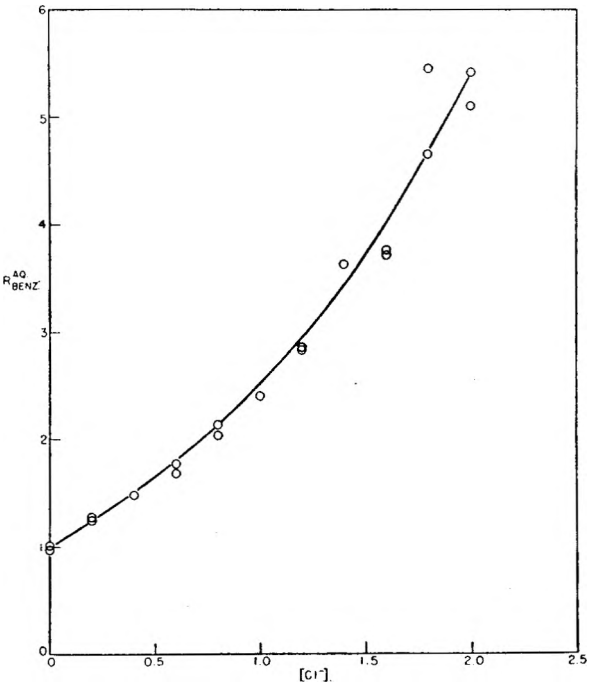

Fig. 4.—Distribution of thorium in the aqueous benzene system: equilibration 2.0 hr. at 25 ± 0.1°; ○, experimental points; ——, curve of the equation $R^{aq.}_{benz.} = 1.00\{1 + 1.21[Cl^-] + 0.10[Cl^-]^2 + 0.20[Cl^-]^3\}$. Aqueous phase ($\mu = 2.0$): $[Cl^-] = 0.00$–$2.00\ M$; $[ClO_4^-] = 2.00$–$0.00\ M$; $[Na^+] = 1.80\ M$; $[H^+] = 0.20\ M$. Benzene phase: $[HT] = 0.10\ M$; $[Th^{234}]$ = tracer level; $[Th^{232}] = 10^{-5}\ M$; (Th initially in benzene).

of constants. These equilibrium constants are concentration (not activity) constants and, as such, contain the activity coefficients of the various species involved as factors. These coefficients are assumed to remain essentially constant for a given experiment at constant ionic strength and changing chloride ratio. This assumption appears to be reasonable at all ionic strengths in the region of low chloride. Hence, our values for k_{Cl} should not be

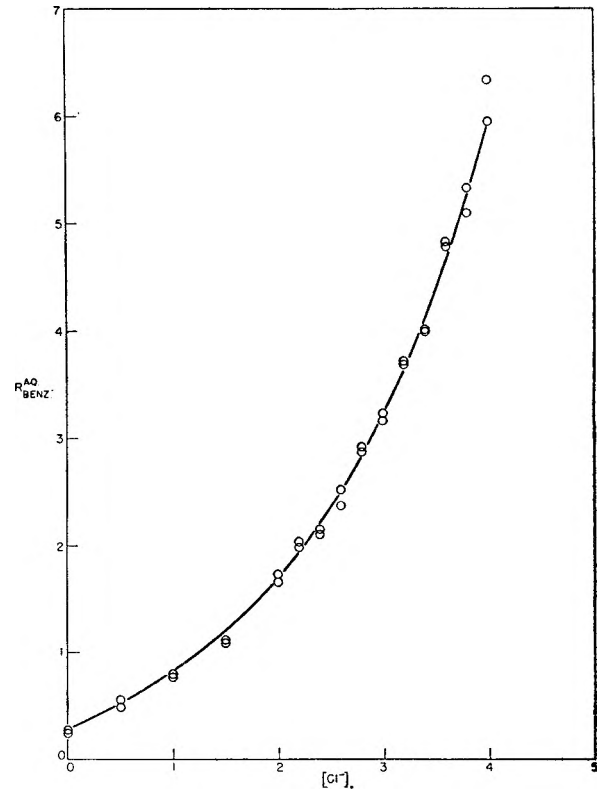

Fig. 5.—Distribution of thorium in the aqueous benzene system: equilibration 3.0 hr. at 25 ± 0.1°: ○, experimental points; ——, curve of equation $R_{benz.}^{aq.} = 0.280\{1 + 1.70[Cl^-] + 0.14[Cl^-]^2 + 0.10[Cl^-]^3 + 0.018[Cl^-]^4\}$. Aqueous phase ($\mu$ = 4.0): $[Cl^-]$ = 0.00–4.00 M; $[ClO_4^-]$ = 4.00–0.00 M; $[Na^+]$ = 3.68 M; $[H^+]$ = 0.32 M. Benzene phase: [HT] = 0.25 M; $[Th^{234}]$ = tracer level; $[Th^{232}] = 10^{-5}$ M; (Th initially in benzene phase).

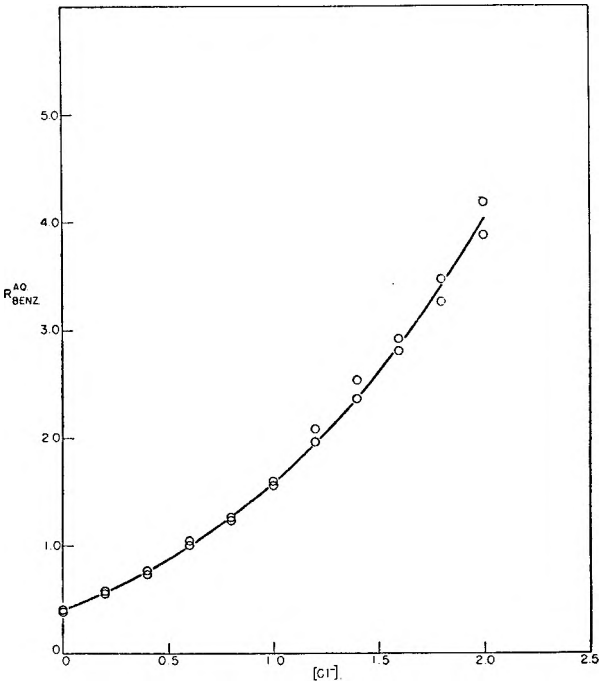

Fig. 6.—Distribution of thorium in the aqueous benzene system: equilibration 2.0 hr. at 25 ± 0.1°; ○, experimental points; ——, curve of equation $R_{benz.}^{aq.} = 0.396\{1 + 2.10[Cl^-] + 0.55[Cl^-]^2 + 0.35[Cl^-]^3\}$. Aqueous phase ($\mu$ = 6.0): $[Cl^-]$ = 0.00–2.00 M; $[ClO_4^-]$ = 6.00–4.00 M; $[Na^+]$ = 5.68 M; $[H^+]$ = 0.32 M. Benzene phase: [HT] = 0.25 M; $[Th^{234}]$ = tracer level; $[Th^{232}] = 10^{-5}$ M; (Th initially in benzene phase).

appreciably in error due to this assumption. The higher constants, k_{2Cl}, k_{3Cl} and k_{4Cl}, however, are expected to be more affected by change in medium, since they are important only at higher chloride.

TABLE I

EQUILIBRIUM CONSTANTS FOR CHLOROTHORIUM COMPLEXES AS A FUNCTION OF IONIC STRENGTH AT 25°

				Concentration constants of formation for chlorothorium species			
μ	$[H^+]$	[HT]	[Th]	k_{Cl}	k_{2Cl}[a]	k_{3Cl}[a]	k_{4Cl}[a]
0.5	0.20	0.10	10^{-5}	2.24			
0.5	.50	.25	10^{-6}	2.25			
0.7	.20	.10	10^{-5}	1.78			
1.0	.20	.10	10^{-6}	1.53			
2.0	.20	.10	10^{-5}	1.21	0.1 (0.083)	0.2 (2.0)	
4.0	.32	.25	10^{-5}	1.70	0.14 (0.082)	0.10 (0.71)	0.018 (0.18)
6.0	.32	.25	10^{-6}	2.10	0.55 (0.26)	0.35 (0.64)	

[a] Values in parentheses are constants of formation by addition of a single chloride ion to the preceding complex.

The concentration constant, k_{Cl} (for $Th^{+4} + Cl^- = ThCl^{+3}$) decreases from 2.24 at μ = 0.5 to a minimum of 1.21 at μ = 2.0, then increases to 2.10 at μ = 6.0. An approximate value for the corresponding activity constant k°_{Cl} (μ = zero), has been obtained assuming the Debye–Hückel equation holds up to an ionic strength of 2. A plot of log k_{Cl} *versus* $\mu^{1/2}/(1 + 2.465\ \mu^{1/2})$ gave a value of $k^\circ_{Cl} \approx 24$ on extrapolation to zero ionic strength. Kraus and Nelson[8] have found that a similar plot for the U(IV) hydrolysis agreed quite well with experiment in the region up to about μ = 2.0.

The value for k_{Cl} at μ = 0.5 obtained in the present studies is significantly higher than the value of 1.76 obtained by Day and Stoughton.[2] In this connection the distribution ratio, R_o, obtained by Day and Stoughton was 0.63 compared to the present value of 0.37. Ten per cent. of the discrepancy is due to our allowance for the solubility of TTA in the aqueous phase (see Experimental). Another difference was the purifying of the TTA for the present work. Values of R_o of up to unity have been obtained with old TTA samples whereas all values using the repurified material were of the order of 0.37. Day and Stoughton did not purify their TTA and may have had some water-soluble complexing agent impurity present. Such a possibility would explain their lower k_{Cl} and would mean that all their constants are too low.

Our results at ionic strength 4.0 are in substantial agreement with those of Zebroski, Alter and Heumann.[9] They have obtained the values 1.30, 0.125, 0.037 and 0.014 for k_{Cl}, k_{2Cl}, k_{3Cl} and k_{4Cl}, respectively.

It is noteworthy that our results for the formation of successively higher chlorothorium complexes do not follow even qualitatively the Bjerrum theory based upon statistical and electrostatic effects.[10] It was thought at first that the data up to 4.0 M chloride could be represented satisfactorily by the assumption of two chlorospecies, the mono- and the

(8) K. A. Kraus and F. Nelson, *J. Am. Chem. Soc.*, **72**, 3901 (1950).

(9) E. L. Zebroski, H. W. Alter and F. K. Heumann, private communication.

(10) N. Bjerrum, *Ergeb. exakt. Naturw.*, **5**, 125 (1926).

trichlorothorium ions. However, with additional data it has become apparent that while the mono- and trichloro ions are the predominant chlorothorium species at all concentrations up to 4 M chloride the di- and tetrachlorothorium species are present in measurable concentration. Table II illustrates the relative importance, percentagewise, of the thorium species in 1, 2 and 4 M chloride solution at an ionic strength of four.

TABLE II

RELATIVE PERCENTAGE OF AQUEOUS THORIUM SPECIES IN CHLORIDE SOLUTIONS AT AN IONIC STRENGTH OF 4.0 AND 25°

Species	Chloride concentration 1 M	2 M	4 M
Th^{+4}	33.8	16.5	4.8
$ThCl^{+3}$	57.5	56.2	32.3
$ThCl_2^{+2}$	4.7	9.3	10.6
$ThCl_3^{+}$	3.4	13.2	30.4
$ThCl_4$	0.6	4.8	21.9

Thenoyltrifluoroacetonothorium Ion.—The results of studies at an ionic strength of two are presented in Fig. 7. Data obtained in perchlorate solution by varying the concentration of thorium are indicated by the open circles. The dark circles represent additional points calculated from data at constant total thorium with varying chloride by correcting for the chlorothorium species present (see Fig. 4 and Table I). These two sets of data agree quite well and show no evidence for the existence of either complexes containing both chloride and TTA radical or complexes containing more than one TTA radical per thorium. The best straight line through these data gives a value of k_T between 6.4 and 6.8. In interpreting these data, the distribution ratio at zero thorium concentration (0.0114) was weighted higher than the other values, since it was an average of a larger number of experimental results.

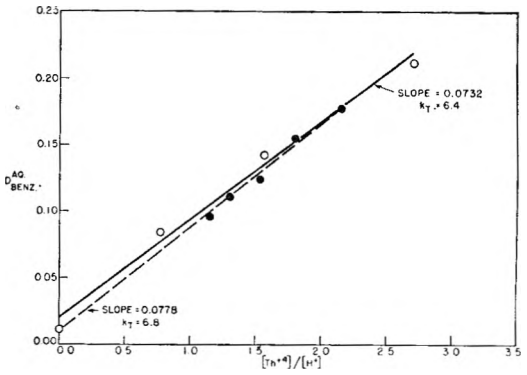

Fig. 7.—Distribution of thenoyltrifluoroacetone (HT) in the aqueous benzene system: ○, [Th] = 0.00–0.10 M; ●, $[Th^{+4}]$ + [Chloro-Th] = 0.10 M; [Cl] = 0.20–0.96 M; Aqueous phase (μ = 2.0): $[Th^{+4}]$ = 0.00–0.10 M; $[Na^+]$ = 0.00–1.96 M; $[H^+]$ = 0.04 M; $[ClO^-]$ = 0.04–2.00 M; $[Cl^-]$ = 0.00–0.96 M. Benzene phase (initially) [HT] = 1.0×10^{-4} and 3.0×10^{-4} M.

The effect of this complex is to make all the constants in equation (7) contain the factor $1/(1 + k_T[HT]/[H^+])$. Hence the true values for any of the constants are obtained by multiplying the values given in this paper by $(1 + k_T[HT]/[H^+])$. This factor is 1.08 at ionic strength 2.0 at equilibrium at $[H^+]$ = 0.32 M and $[HT]_B$ = 0.25 M. As a state of equilibrium with respect to the complex ThT^{+3} is not attained in much less than 25 hours due to the slowness of the TTA phase distribution, and since we shook the tubes for only 1.5 to 3.5 hours, the correction under the current experiments is much smaller, *i.e.*, nearer to unity. At other ionic strengths we believe the correction to be not much, if any, greater than at ionic strength 2.0. Hence we have not made the correction in the current work.

THE BINUCLEAR PEROXO COMPOUNDS OF TRI- AND TETRAPOSITIVE COBALT

BY LAWRENCE R. THOMPSON AND W. K. WILMARTH

Department of Chemistry, University of Southern California, Los Angeles, California

Received August 30, 1951

A repetition of the preparative work of A. Werner and others confirmed the existence of a series of green binuclear peroxo compounds containing a cobalt atom in the tetrapositive oxidation state. A second series of red compounds which Werner, using the concept of secondary valence forces, formulated as isomers proved to be the one electron reduction products of the green series and contained only tripositive cobalt. Analytically, the red compounds appeared to be isomeric because, while they are only weakly basic in solution, they normally precipitate as acid salts and thus differ from the green series by a single proton. The reported "isomeric conversions" are in reality all oxidation–reduction reactions and include the bromide-catalyzed disproportionation of the red series and reduction of the green series by hydroxide ion.

Introduction

The present research is the beginning of a systematic attempt to clarify the general chemical nature of a remarkable series of binuclear complex compounds containing cobalt in the tetrapositive valence state. This valence appears to be confined to polynuclear complexes in which the metal ions are linked through a peroxo bridge in the following fashion

$$[(A)_5\overset{3+}{Co}—O_2—\overset{4+}{Co}(A)_5]$$

The subscript five indicates that in addition to the peroxo bridge each cobalt atom is also bonded in the usual fashion to five other groups, some of which may be bridging groups between the cobalt atoms. A may be one or more of the conventional complexing groups; the charge on the complex ion will of course depend upon which groups are present.

It should be possible, in principle, to reduce each of these ions to the symmetrical unit

$$[(A)_5\overset{3+}{Co}—O_2—\overset{3+}{Co}(A)_5]$$

but it is only in the single case discussed below that the correct structure has been assigned to both the oxidized and reduced form of a particular binuclear skeleton. The fact that in this case the compounds cannot be inter-converted by oxidation or reduction without extensive decomposition has been partially responsible for the general acceptance of the view this is universally true. However, the principal sources of confusion depend upon several more involved and intriguing chemical properties which will become apparent in the historical survey below.

Compounds belonging to the general class of peroxo complex ions of cobalt have been known for a long time,[1] but no very systematic or logical consideration of the field occurred until the time of Alfred Werner.[2a,b] In the period 1898–1910 he prepared a number of complex compounds containing tetrapositive cobalt. Several of these, whose physical and chemical properties we have investigated in greater detail, are

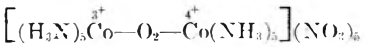

I

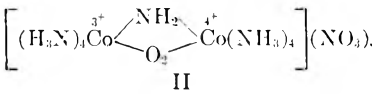

II

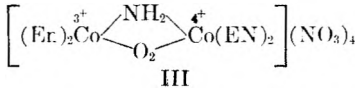

III

Compounds of the type II and III, which have a second bridging group, are usually less susceptible to bridge cleavage by a variety of reagents, and our studies have been largely concerned with these substances.

In addition to these compounds, Werner reported at least one case in which both cobalt atoms were in the conventional tripositive state.

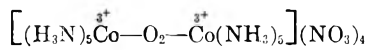

IV

Both compound I, which has the typical dark green color of the first group of compounds, and compound IV, which is red brown in color, were isolated from aerated ammoniacal cobaltous solutions. While the cations differ only in charge, Werner observed, as we have mentioned above, that attempts to reduce I to IV in solution resulted only in destruction of the peroxo bridge either by complete reduction or partial reduction to trivalent cobalt with simultaneous evolution of gaseous oxygen. Since it is known that solutions containing compound IV rather rapidly decompose with oxygen evolution, this result is not inconsistent with the existence of both I and IV in the solid state.

It is the unusual behavior of the bridged compound III, which is prepared from II by direct treatment with aqueous ethylenediamine, which is responsible for most of the erroneous conclusions drawn by Werner and all subsequent workers. If the red ethylenediamine solution is neutralized with concentrated nitric acid at room temperature the green nitrate III is precipitated, but if the nitric acid is slowly added at ice temperatures it is reported that a red compound analytically isomeric with III is obtained. Werner proposed the formula

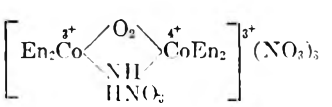

for the red nitrate. Aside from the possibility of dimorphic crystal forms, which is ruled out by the fact that the solutions are also green and red, respectively, an isomerism based upon these formulas is meaningless today. However, Werner's evidence for isomerism seemed rather compelling since he reported acidification reversibly converted the red nitrate to the green nitrate and subsequent addition of base reformed the red nitrate.

In addition, Werner found that the red nitrate could be converted to the green nitrate in preparative amounts merely adding bromide ion to the solution. To avoid confusion in the later discussion we may indicate at this point that the red nitrate is not really an isomeric compound, although it differs from the green nitrate by a single hydrogen atom, and, as we shall show later, it is correctly formulated as an acid salt containing only tripositive cobalt.

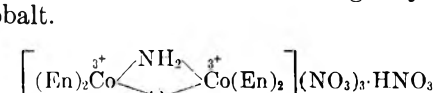

V

All of the above changes, in fact, are really oxidation–reduction reactions but of a rather unexpected sort.

The principal contribution of the later workers in this field has been to establish the paramagnetism, and hence presumably the tetrapositive valence, in compounds I, II and III and the diamagnetism of compound IV.[3,4,5]

The diamagnetism of V was established early in the present study, and it at once became apparent that if V contained tetrapositive cobalt, the fundamental unit would have to be at least a tetramer to contain an even number of electrons.

Subsequent study showed that the compounds were interconverted not only by acid and base but also by a variety of oxidizing and reducing agents. While it is obvious that the oxidation in the presence of acid is effected by the nitrate ion, the details of the reduction by hydroxide ion without oxygen evolution have not yet been clarified. Qualitative tests for hydrogen peroxide are negative, but direct addition of hydrogen peroxide indicates that it would be destroyed by some side reaction under these experimental conditions.

The apparent oxidation of the red nitrate by bromide ion appears to be a bromide-catalyzed disproportionation

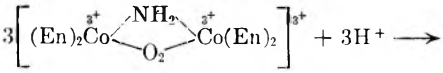

(1) E. Fremy, *Ann.*, **83**, 240 (1852).

(2) (a) A. Werner, *Ann.*, **375** 1 (1910); (b) A. Werner and A. Mylius, *Z. anorg. Chem.*, **16**, 246 (1898).

(3) K. Gleu and K. Rehm, *Z. anorg. allgem. Chem.*, **237**, 79 (1938).

(4) L. Malatesta, *Gazz. chim. ital.*, **72**, 287 (1942).

(5) J. P. Mathieu, *Bull. soc. chim.*, [5] **5**, 105 (1938).

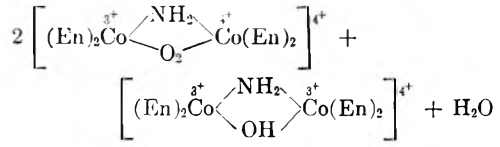

The appearance of the green nitrate in the predicted 66% yield was observed spectroscopically, thus establishing the stoichiometry, but the presence of the the second product containing the μ-hydroxo bridge has not been established with certainty and mononuclear compounds may also be present in the solution.

These experiments pretty well clarify the assignment of structure with the exception of a second red complex compound which Werner precipitated from solutions of either III or V after treatment with aqueous ammonia. Analysis indicated that the compound closely resembled III and V but contained only a tripositive cation, which was presumed to be formed by loss of a molecule of acid in the basic medium and represented as

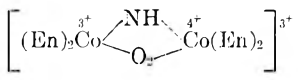

Since aqueous ammonia is known to reduce the green nitrate, and would favor the precipitation of a normal rather than an acid salt, we feel that this product differs from V only in the acid of crystallization. Imido bridges have been assigned to a number of binuclear cobalt compounds, but the neutral character of the amido bridge implies complete hydrolysis except in very strongly basic solution or in the solid state. We are planning to investigate a number of these cases in order to justify or completely discredit such structures.

Preparative Methods

(1) **Octaammine-μ-amido-μ-peroxodicobalt(III, IV) Tetranitrate (Compound II).**—Vortmann's fuscosulfate was prepared by Werner's[6] method, with some modification, resulting in improved yields. The neutralizing time was reduced to 3.5 hours and litmus was used to obtain the acid endpoint. The oxidized reaction mixture was allowed to stand two days before neutralization and two or three days just after neutralization. Yields were 19–23 g. from 100 g. of $Co(NO_3)_2 \cdot 6H_2O$.

The green constituent of the mixture was converted to the nitrate by Werner's method, again with several modifications. Two separate 20-g. portions of fuscosulfate were triturated for 10 minutes with 80-ml. portions of concentrated HNO_3, allowed to stand 24 hours and filtered. The entire 40-g. residue was stirred for 5–10 minutes in water at 60° to extract the peroxo compound. Another 100 ml. of water at 60° was poured through the filter and the combined filtrates treated with concentrated HNO_3 dropwise to precipitate the green peroxo nitrate.

(2) **Tetrakis-(ethylenediamine)-μ-amido-μ-peroxodicobalt-(III, IV) Tetranitrate (Compound III).**—Werner's[2,7] method of conversion by heating III in 10% ethylenediamine at 60° was used. Acidification of the reaction mixture at room temperature with concentrated HNO_3 gave the green peroxo nitrate in 75% yields.

(3) **Tetrakis-(ethylenediamine)-μ-amido-μ-peroxodicobalt-(III, III) Trinitrate ·1 Nitric Acid.**—Compound II was heated with 10% ethylenediamine at 60°, but the reaction mixture was acidified at −2.0 to −3.0° instead of at room temperature.[2,7] The red peroxo nitrate was obtained in yields of 65–70%.

To purify, 1.5 g. of crude red nitrate was dissolved in 25 ml. of water at room temperature, filtered and cooled in an ice–salt mixture. 30 drops of concentrated nitric acid was added, 5 drops at a time. The red crystals were washed with alcohol and ether; yield 80%.

(4) **Tetrakis-(ethylenediamine)-μ-amido-μ-peroxodicobalt-(III, III) Triiodide ·2 Hydrate.**—Twenty-seven ml. of a saturated, filtered solution of compound V was treated with 10 ml. of a saturated solution of KI. Ethyl alcohol was added until the dark brown-black precipitate turned red. After filtering and washing with alcohol, it was purified by dissolving in warm water and cooling in an ice-bath; yield of red-brown crystals, 40%.

One Electron Oxidation–Reduction Properties

The reaction

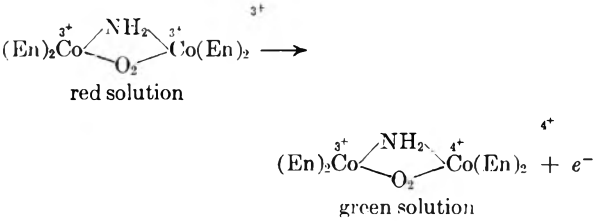

can be qualitatively studied by noting the readily observed reversible color changes indicated above. Oxidizing agents which effected the oxidation rapidly in acidic aqueous solution at 25° include MnO_4^-, HOCl, Br_2, BrO_3^-, NO_3^-. No immediate color change is observed with H_2O_2, Fe^{3+}, Ag^+, Hg^{2+} or $Cr_2O_7^{2-}$. Since both Br_2 and HNO_3 react rapidly, the standard electrode potential for the binuclear half cell must be more positive than −1.0 volt. It would appear that some oxidizing agents, such as $Cr_2O_7^{2-}$, are potentially capable of being reduced but the reduction is so slow that it was not observed during the relatively short period of the experiment.

It was possible, using standard $KMnO_4$, to titrate the reduced binuclear compound. 0.276 g. of the red nitrate dissolved in 10 ml. of water was titrated with 0.033 *N* $KMnO_4$ using the natural color of $KMnO_4$ as the indicator. One equivalent of the red nitrate was found to react with 1.15 equivalents of $KMnO_4$ solution. The 15% discrepancy may be due partially to the inherent difficulty of observing the end-point in the highly colored solutions, but either trace impurities or side reactions are also possible.

The reaction

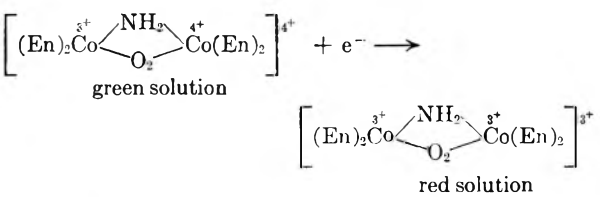

proceeds rapidly in the presence of NO_2^-, N_2H_4, $Fe(CN)_6^{4-}$, AsO_2^-, $S_2O_3^{2-}$ and OH^-, but slowly or not at all with Hg_2^{2+} or $NH_2OH \cdot HCl$. The oxidation of the hydroxide ion, apparently to the peroxide valence state, will be discussed below. Sn^{2+}, Fe^{2+}, I^- and SO_3^{2-} were rapidly oxidized but reduced the peroxo bridge as well as the tetrapositive cobalt atom.

Thiosulfate appeared to be the most suitable reagent for a quantitative titration, and a 0.1030 *N* solution of $Na_2S_2O_3$ was titrated with a solution of the green binuclear nitrate using an external KI starch indicator. One equivalent of the green nitrate oxidized 0.80 equivalent of thiosulfate. It should be noted that the discrepancy here is in the opposite direction to that observed in the first titration. It seems likely that some of the thiosulfate is being converted to sulfate rather than tetrathionate, although impurities or side reactions may also be at fault.

Acid and Base Oxidation–Reduction Conversions

The initial phases of the present research were concerned with establishing the experimental reproducibility of Werner's preparation and interconversion of the red and green nitrates. Since the oxidation–reduction nature of the reaction was not yet understood we felt that it was of prime importance not only to confirm the analytical evidence of the

(6) A. Werner, *Ber.*, **40**, 4609 (1907).

(7) A. Werner, *ibid.*, **47**, 1963 (1914).

"isomerism" but also to characterize the compounds using powder pattern and spectrophotometric methods.

Powder patterns were obtained using a Philips X-ray diffraction apparatus. A complete tabulation of the lines in terms of the conventional sin θ/λ values is unnecessary in the present paper; the strong lines are recorded below to identify the compounds. The red nitrate V has a very strong broad ring at sin $\theta/\lambda = 0.0613$ and three other strong rings appear at 0.0508, 0.1068 and 0.1142, respectively. The green nitrate III has its strongest ring at 0.0578 with strong rings also appearing at 0.0703, 0.1108, 0.1227 and 0.1440.

The red nitrate when converted to the green nitrate, and the green nitrate when converted to the red nitrate possessed patterns identical with the original red and green compounds; but, after standing for 18 days, the red nitrate made by conversion clearly showed the heavy characteristic ring of the green nitrate, indicating a slow conversion in the solid state. The mechanism of this process is still in doubt.

The first three rings of the octaamine nitrate II possessed values of 0.0658, 0.0731 and 0.0837 with other strong rings appearing farther out in the pattern.

The red-brown triiodide possessed characteristic rings of sin θ/λ equal to 0.1141, 0.1246 and 0.1348.

The conversion of the red to the green nitrate was achieved by adding concentrated nitric acid rapidly to a saturated solution containing 2 g. of the red nitrate; both solutions were at room temperature. On cooling in an ice-bath the green nitrate was isolated in 50–60% yields.

The green nitrate was converted to the red nitrate in the following fashion: 3 g. of green nitrate was dissolved in 75 ml. of water and 4 ml. of concentrated NH_3 (sp. gr. 0.927) were added dropwise. Keeping the temperature as far below 0° (−2° to −3°) as possible without freezing the solution, 5.5 ml. of concentrated HNO_3 was added, 3 drops at a time (to avoid warming up the solution). A residue of 0.6 g. was obtained which clearly was contaminated with the green nitrate. To the cooled mother liquor was added an additional 4.5 ml. of concentrated HNO_3 dropwise. 1.45 g. of red nitrate was obtained and purified as already described.

The spectra were obtained using a Beckman model DU photoelectric quartz spectrophotometer. Readings were taken from 800 mμ to as low as 220 mμ. When measurements were made in the near infrared, visible and near-ultraviolet regions, 1-cm. Corex absorption cells and a tungsten lamp were used. Below 350 mμ, 1-cm. silica cells and a hydrogen lamp were used.

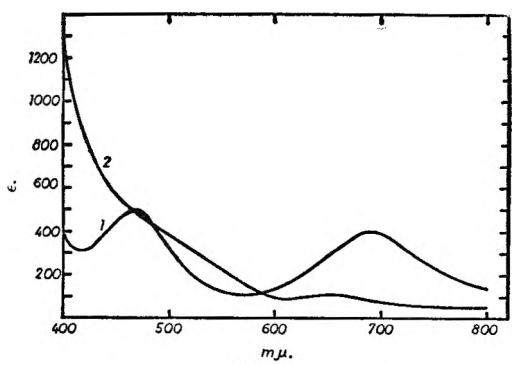

Fig. 1.

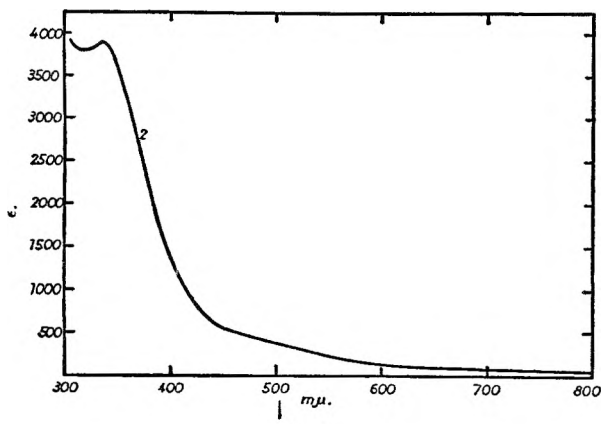

Fig. 2.

The spectra of the green nitrate III is plotted as curve I in Fig. 1. The extinction coefficient, plotted from 400–800 mμ has rather broad maxima at 470 and 690 mμ. The red nitrate V has only a large band in the ultraviolet with a foot extending into the visible with considerable absorption out to about 600 mμ. The small shoulder shown in Fig. 2 is probably real although the compounds used in these studies are probably not of the highest purity.

The spectra of a solution of green nitrate prepared by oxidation of a red nitrate solution with nitric acid had an absorption indistinguishable from curve I. A solution of the red nitrate prepared by adding aqueous sodium hydroxide to the green nitrate solution was almost identical with curve II, except the small shoulder was not quite so pronounced. While this conversion needs to be confirmed by more careful measurements, the agreement in spectra was so striking that it seems likely that minor impurities are responsible for the lack of complete quantitative agreement.

The oxidation of hydroxide ion in alkaline solution by the green nitrate proceeds without gas evolution, but qualitative tests for hydrogen peroxide after conversion were negative. Further studies showed that hydrogen peroxide does not react with either the red or green nitrate in acid solution and that it can be titrated quantitatively with permanganate. The oxygen evolution is readily observed throughout the titration and would certainly have been seen if it had been formed by oxidation of the hydroxide ion. If hydrogen peroxide was added to the green nitrate solution before the alkaline conversion it completely disappeared during conversion, apparently without appreciably affecting the permanganate titer of the resulting red solution. On the basis of this evidence one can conclude that hydrogen peroxide is a possible oxidation product, but its ultimate chemical fate has yet to be determined.

Discussion

While the principal questions regarding the existence and the gross structural features of these binuclear compounds have been resolved, we are only beginning to explore their more interesting details. Perhaps the most intriguing problem involves the detailed nature of the peroxo bridge, especially in those compounds containing tetrapositive cobalt. Several obvious alternatives can be suggested, and at present it is difficult to estimate their applicability. Gleu and Rehm[3] and others have postulated that the unpaired electron should be assigned to the oxygen bridge, and the considerable tendency for oxygen to exist in units containing an unpaired electron may lend some weight to this viewpoint. If one prefers the tetrapositive formulation, the symmetry of the structure would suggest two resonance forms in which either cobalt might be considered to be tetrapositive. Recently it has become increasingly apparent[8] that many polynuclear ions contain metal–metal bonds. In this sense, the resonance picture might be considered as equivalent to a three electron bond linking the metal atoms. Experimentally, it does seem that the peroxo bridge is a necessary structural feature, but its function may be either to contain the odd electron or to provide a geometrical unit in which the cobalt atoms are located at distances compatible with such a metal bond. We plan to systematically investigate the structural features of a number of polynuclear compounds in an effort to make some of the above discussion more meaningful in terms of experimental quantities.

(8) Phillip A. Vaughan, J. H. Sturdivant and Linus Pauling, *J. Am. Chem. Soc.*, **72**, 5477 (1950).

The present work suggests that, with the possible exception of compounds containing only the single peroxo bridge, it should be possible to study the energetics of formation of the symmetrical unit by one electron reduction. Preliminary measurements, using conventional methods, fix the potential at somewhat more positive than -1.0 volt for compound III. Extension of these studies to analogous compounds should clarify the effect of structural change upon the relative stabilities of the oxidized and reduced units. Polarographic studies have been initiated, but it is too early to evaluate the results.

The general tendency for the reduced unit to precipitate as an acid salt suggests that, in the solid state, the proton may reside upon the peroxo bridge. In solution it would appear that the compounds are only weakly basic in the reduced state and, as one might anticipate, completely neutral after oxidation. While the additional charge in the oxidized unit should increase the acidity of all protons in the complex ion, the amido bridge is, at most, still a very weak acid. We are rather interested in the question since the postulated μ-imido compounds can be reformulated, with the addition of only a single proton, as an amido binuclear unit containing one tri- and one dipositive atom. Resonance stabilization might permit the preparation of such a compound, although the increased number of electrons renders it less likely.

The unusual hydroxide reduction of the oxidized unit has been established largely on the basis of reversible color change and powder pattern and spectral characterization. One would anticipate a rather greater overvoltage than that observed for the hydroxide oxidation, and it seems likely that a follow process, which destroys added peroxide, facilitates the initial oxidation. Since the exploratory studies have involved compounds which may not be of the highest purity, careful analysis may reveal that the chemical change accompanying the reduction produces an entirely new binuclear series of peroxo compounds.

The bromide disproportionation has also been formulated largely on compound identification based on powder pattern and spectral evidence. The identification of valence states can be pretty well established in this way, but some minor changes in interpretation may be necessary when more complete analytical data become available.

The authors are indebted to the Office of Naval Research for supporting this work.

REMARKS

F. BASOLO: (1) You mention that the red ethylenediamine complex in aqueous solution undergoes a reversible change to a second red compound. This you suggest may be caused by

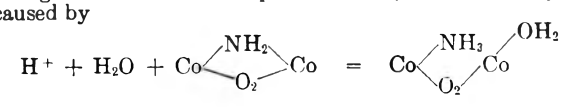

but point out that the acid dissociation constants for the two species are 10^{-2} and 10^{-7}, respectively. Do you not think this value of 10^{-7} is too small providing the assumed structure is correct? Merely on the basis of electrostatic forces, I should expect this $+4$ cation would be a stronger acid than say the $+3$ $Co(NH_3)_5H_2O^{+3}$ which has a value of 2.04×10^{-6}.

(2) The structure shown as number V may be further supported if it were possible to remove the additional molecule of nitric acid. Since this is rather commonly accomplished with Werner complexes of cobalt(III) merely by heating them at 110° for several hours, I am wondering if any such attempt was made to expel the nitric acid from compound V.

REPLY: (1) Experimentally one observes the quantitative disappearance of one mole of strong acid and the appearance of one mole of a titratable weak acid with a pK of approximately 7. It would seem to me that the only possible acid in the system of approximately this strength must be one formed from a cobalt-water bond. Our experience with several binuclear compounds has made us rather cautious in predicting their properties on the basis of similar mononuclear compounds. However, I believe a comparison of the relative acidities of hydrogen peroxide and ammonium ion might convince one that the peroxo group in this unit would have an acid weakening inductive effect as compared with the ammonia molecule. A further comparison of the acidity of hydronium ion and the aqueopentamine-cobaltic ion suggests that the over-all substitution of $(H_3N)_5Co\text{-}O_2\text{-}^{+1}$ for an ammonia in $(H_3N)_5Co(OH_2)^{3+}$ would almost certainly be acid weakening in spite of the increased positive charge.

(2) We have observed an apparently clean-cut thermal reaction on vacuum heating of compound V but the reaction may be more complex than the one you suggest.

L. F. AUDRIETH: Attention should be called to the fact that the nitrates of the μ-peroxo compounds are substances which approach "oxygen balance" from the explosives chemist point of view. Decammino μ-peroxodicobalt(III, IV) pentanitrate may be expected to be an extremely hazardous compound since it is an oxygen balanced substance. It can be assumed that its complete decomposition can be represented by the equation.

$$Co_2N_{15}H_{30}O_{17} \longrightarrow 2CoO + 7.5N_2 + 15H_2O$$

Care should be exercised in handling materials of this kind for they may be sensitive to friction and impact and most certainly to the application of heat.

We have had occasion to study the explosives characteristics of complex ammines containing coördinated or ionic oxygenated groups such as the nitrate, nitrite and perchlorate radicals (Tomlinson, Ottoson and Audrieth, *J. Am. Chem. Soc.*, **71**, 375 (1949)). Coördination compounds approaching oxygen balance represent a wide variety of explosive types; some possess appreciable sensitivity to friction and impact, and others, when properly initiated, have brisance values approaching conventional high explosives. Thus, for instance, tetrammine copper(II) nitrate is more sensitive to impact than is tetryl and has a brisance value about the same as that of lead azide. Hexammine chromium(III) nitrate is much more sensitive to impact than TNT and actually has a brisance value only slightly lower than that for TNT. The oxygen balance concept is an empirical concept but does have practical value since it makes possible the prediction of hazards which may be encountered in investigation of complex compounds.

REPLY: (1) Initially we were quite concerned about the possible explosive properties of these compounds, but all of the substances which we have prepared have been tested and none of them seem to be extremely sensitive to either shock or heat.

THE CHLORO COMPLEXES OF RUTHENIUM(IV)[1]

BY PHILIP WEHNER AND J. C. HINDMAN

Chemistry Division, Argonne National Laboratory, Chicago, Illinois

Received August 30, 1951

A study of the chloro complexes of Ru(IV) has been made in perchlorate media. The formation of these complexes is associated with the following color changes: reddish (Ru(IV)) → yellow → violet → yellow. The compositions of certain of the complexes identifiable with these colors have been studied by equilibrium and kinetic methods. Evidence indicates that the violet complex is the uncharged species $Ru(H_2O)_2(OH)_2Cl_2$ and is transformed by the addition of chloride ion to the yellow anionic complexes $[RuH_2O(OH)_2Cl_3]^-$ and $[Ru(OH)_2Cl_4]^-$. The violet complex grows from rapidly formed initial yellow complexes some of which appear to be polynuclear species.

Solutions of ruthenium(III) and -(IV) in perchloric acid are unstable with respect to the decomposition of perchlorate with consequent formation of chloride ion.[2] This behavior has emphasized the necessity of obtaining data concerning the ruthenium chloro complexes prior to undertaking any investigation of other ruthenium complex ion systems where it is desired to use perchlorate solutions as reference starting materials. The experiments summarized in this paper were intended primarily to furnish information as to the number and possible formulas of the chloro complexes formed by Ru(IV).

Experimental

The ruthenium(IV) perchlorate solutions used were 0.118 *M* or 0.305 *M* in Ru(IV) and 6.0 *M* in $HClO_4$. These stocks were presumably mixtures of at least two Ru(IV) species between which equilibrium is not rapidly established in perchloric acid alone.[2] The reaction mixtures were prepared by diluting aliquots of these stocks with the appropriate solution made from standardized solutions of HCl, NaCl, $NaClO_4$ and $HClO_4$. In all cases the ionic strength was kept constant at 6.2 *M* except where otherwise noted. Changes in the solutions were followed spectrophotometrically using a Cary Recording Spectrophotometer. The samples were contained in 2-cm. quartz cells, and the temperature of the cell compartment was thermostatically controlled.

As a guide to the assignment of charges for certain of the complexes transference experiments were run using a cell of the type described by McLane, Dixon and Hindman.[3] Examination of the 0.118 *M* stock by this technique (0.076 *M* Ru(IV) in 6 *M* $HClO_4$, 20 ma., 3 hours at 25°) showed only transference to the cathode indicating the species present are positively charged.

The Yellow(II) Complex.—Depending on the acid and chloride concentration, the addition of chloride to Ru(IV) perchlorate is followed by a series of color changes.

Ru(IV) (reddish) ⟶ violet ⟶ yellow $[Cl^-] < 0.1\ M$, $[H^+] < 0.4\ M$

Ru(IV) (reddish) ⟶ yellow ⟶ violet ⟶ yellow $[Cl^-] > 0.1\ M$, $[H^+] > 0.4\ M$

Each of the yellow transitions has been found to be associated with several complexes. The assignment of a formula to the first yellow species formed from the decay of the violet intermediate (designated Y(II)) has been used as a guide to the assignment of formulas to certain of the other complexes. The formula of this complex was deduced as follows: Series of samples in 6.0 molar $HClO_4$ having varying [Ru] to $[Cl^-]$ ratios were obtained by mixing x ml. of 0.305 *M* $[Cl^-]$ with $1 - x$ ml. of 0.305 *M* Ru(IV) perchlorate. The spectra of the samples were checked periodically for equilibrium and an analysis[4,5] of the data was made by plotting the observed optical density at a given wave length minus the calculated optical density for no reaction against x (Fig. 1). Since $D_{obsd.} - D_{calcd.}$ was a maximum at 0.75, n, the number of chloride ions in the complex, was

$$n = \frac{x}{1 - x} = \frac{0.75}{0.25} = 3.0$$

Corrections to this formula, due to the presence of the Y(III) complex, were found to be negligible.

On electrolysis of a 0.042 *M* Ru(IV) in 0.24 *M* HCl–5.4 *M* $HClO_4$ solution at 20 ma. for 6 hours at 25° this complex was transferred to the anode, an indication that it is negatively charged. Since, in addition, the Y(II) ⇄ Y(III) equilibrium has been found to be independent of hydrogen ion, the Y(II) complex must contain water. Based on a coördination number of 6,[6,7] the formula for the Y(II) complex containing the least number of chlorides is therefore $[RuH_2O(OH)_2Cl_3]^-$. The absorption spectrum of this complex, shown in Fig. 2, was obtained from a solution 0.0495 *M* in Cl^-, 1.00 *M* in H^+ and 6.2 *M* ionic strength. In this solution at equilibrium the predominant species is Y(II); correction for a small amount of Y(III) was made by the method of successive approximations. The molar extinction coefficient of the peak at λ 454 mμ was found to be 6,100.

The Yellow Complexes of Higher Chloride Content Y(III), Y(IV) and Y(V). Under a variety of conditions a yellow complex, designated Y(III), can be observed to grow at the expense of the Y(II) complex and eventually to exist in equilib-

(1) Presented at the Symposium on Complex Ions and Polyelectrolytes held under the auspices of the Division of Physical and Inorganic Chemistry and the Division of Colloid Chemistry at Ithaca, New York, June 18–21, 1951.

(2) P. Wehner and J. C. Hindman, *J. Am. Chem. Soc.*, **72**, 3911 (1950).

(3) C. K. McLane, J. S. Dixon and J. C. Hindman, Paper No. 4.3 "The Transuranium Elements," Plutonium Project Record of the National Nuclear Energy Series, McGraw-Hill Book Co., Inc., New York, N. Y., 1949.

(4) L. I. Katzin and E. Gebert, *J. Am. Chem. Soc.*, **72**, 5455 (1950).

(5) W. C. Vosburgh and G. R. Cooper, *ibid.*, **63**, 437 (1941).

(6) W. P. Groves and J. Sugden, W. P. Groves, Ph.D. Thesis, London, 1941, quoted by R. S. Nyholm, *Quart. Reviews*, **3**, 321 (1949).

(7) D. P. Mellor, *J. Proc. Roy. Soc. N. S. Wales*, **77**, 145 (1943).

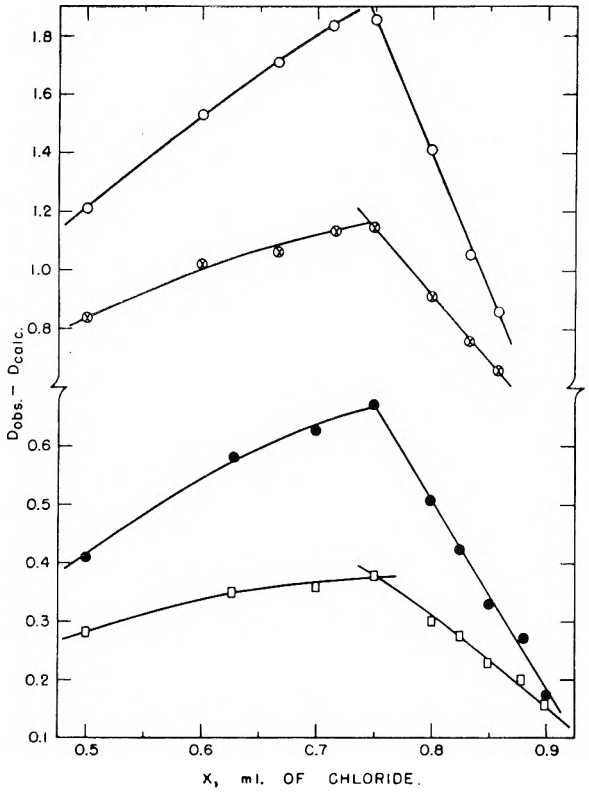

Fig. 1.—Plot of x *versus* $D_{obsd.} - D_{calcd.}$ for Y(II) complex. Series 1, after 49 days: ●, 454 mμ; □, 423 mμ. Series 2, after 55 days: ○, 354 mμ; ⊗, 428 mμ.

rium with it. The absorption spectrum of this new species is characterized by intense peaks at 385 and 254 mμ together with a minor peak at 476 mμ (Fig. 2). A noteworthy feature of the transformation is that as the 385 mμ peak grows in intensity it becomes asymmetric due to acquisition of a shoulder on the short wave length side. This behavior suggests that still another complex, designated Y(IV), with an absorption maximum in the region of 360 mμ, is being formed in relatively minor amounts. Support for this viewpoint is obtained in 10 *M* HCl, where partial resolution of the Y(III) and Y(IV) peaks occurs (Fig. 3).

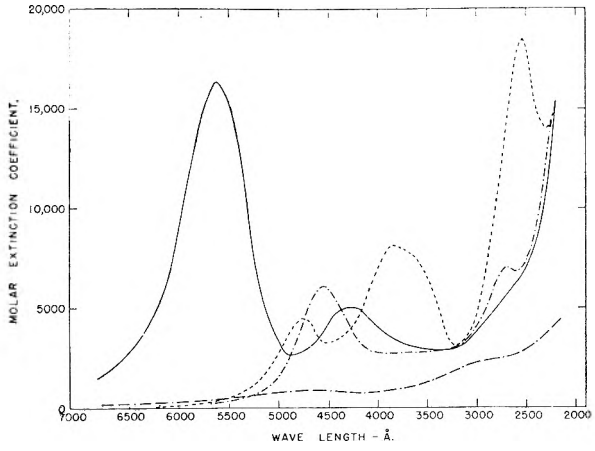

Fig. 2.—Absorption spectra of various Ru(IV) species: · — — —, Ru(IV) in 6 *M* $HClO_4$; ———, violet complex, $[Ru(H_2O)_2(OH)_2Cl_2]$; — · —, Y(II), $[RuH_2O(OH)_2Cl_3]^-$; – – – – – –, Y(III), $[Ru(OH)_2Cl_4]^=$.

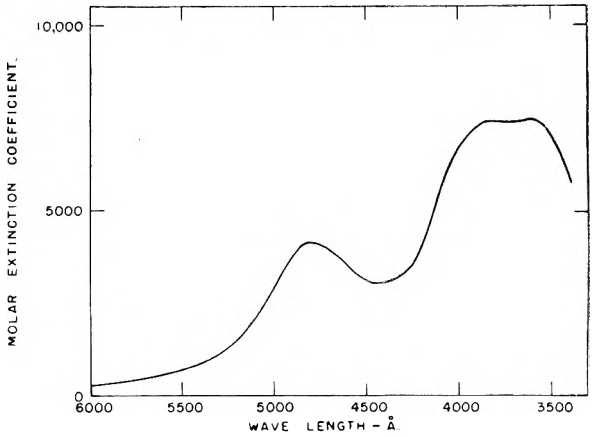

Fig. 3.—Ru(IV) in 10 *M* HCl after 70 days storage.

The spectrum of Y(III) (together with Y(IV)) shown in Fig. 2 was obtained from a solution 6.2 molar in Cl^-, 1 molar in H^+, and 1.95×10^{-4} molar in Ru(IV) after the spectral changes had reached apparent equilibrium (3 to 4 days, no further change in an additional 12 days). Corrections were made for the small amount of Y(II) present by a method of successive approximations using the Y(II) ⇄ Y(III) equilibrium constant obtained as described below. This spectrum gave the following values, for the molar extinction coefficients of the Y(III) peaks: 18,400 (254 mμ), 8,140 (385 mμ) and 4,500 (476 mμ).

In order to establish the formula of the Y(III) complex the effect of the chloride ion and hydrogen ion concentrations upon the Y(II) ⇄ Y(III) equilibrium was studied. Mixtures of approximately constant Ru(IV) concentration (1.18×10^{-4} *M*), constant hydrogen ion concentration (1.00 *M*) and varying chloride concentration were stored until their spectra had been at equilibrium for 6 to 12 days (total storage period ranged up to 21 days). The amounts of Y(II) and Y(III) in each solution were determined by a two-color analysis at the wave lengths 454 mμ and 385 mμ, using extinction coefficients of 2,750 (385 mμ) and 6,100 (454 mμ) for Y(II) and 8,140 (385 mμ) and 3,270 (454 mμ) for Y(III). A similar set of mixtures of constant chloride concentration and varying hydrogen ion concentration were analysed in the same manner. The results of the measurements are given in Tables I and II.

At the chloride concentrations involved in these experiments the asymmetry of the Y(III) peak at λ 385 was not as pronounced as is shown in Fig. 2; consequently it is believed that interference from Y(IV) was not serious. From Table I it is seen that the data can be satisfactorily interpreted on the basis that the equilibrium involves first order dependence on the chloride ion concentration. From Table II it is evident that the equilibrium is essentially independent of hydrogen ion concentration below $[H^+] = 1.00$ *M*; the departure from this independence at the high acidities is probably due to the increasing importance of an additional complex, Y(V), formation of which is acid dependent (see further discussion of Y(V) below).

The above results, together with the evidence concerning the formula of Y(II), indicate that the

TABLE I

EFFECT OF CHLORIDE ION ON THE Y(II) ⇄ Y(III) EQUILIBRIUM

$[H^+] = 1.00\ M$, $t = 25°$, $\mu = 6.2$

$[Cl^-]$ (m./l.)	D_{484}	D_{385}	$\frac{[Y(III)]}{[Y(II)]}$	$\frac{[Y(III)]}{[Y(II)][Cl^-]}$ (m./l.)$^{-1}$	$\frac{[Y(III)]}{[Y(II)][Cl^-]^2}$ (m./l.)$^{-2}$
0.100	1.320	0.880	0.223	2.23	22.3
.200	1.240	1.080	.484	2.42	12.1
.400	1.115	1.230	.876	2.19	5.48
.600	1.025	1.340	1.348	2.25	3.75

Mean, 2.28 ± 0.08

TABLE II

EFFECT OF HYDROGEN ION ON THE Y(II) ⇄ Y(III) EQUILIBRIUM

$[Cl^-] = 0.200\ M$, $t = 25°$, $\mu = 6.2$

$[H^+]$ (m./l.)	D_{484}	D_{386}	$\frac{[Y(III)]}{[Y(II)]}$
0.100	1.195	0.975	0.408
.398	1.210	0.975	.395
.864	1.260	1.000	.378
1.00	1.240	1.080	.484
6.20	1.083	1.295	1.07

Y(II) ⟷ Y(III) equilibrium can be represented by the equation

$$\underset{\text{Y(II)}}{[RuH_2O(OH)_2Cl_3]^-} + Cl^- \rightleftarrows \underset{\text{Y(III)}}{[Ru(OH)_2Cl_4]^-} + H_2O$$

Also, the results of Table II show that the value of the equilibrium constant found at $[H^+] = 1.00\ M$ (2.28 ± 0.08) is probably too high and that a better value would be $\bar{K}_{25°} = 1.9$.

Consistent with the above formula for Y(III) is the fact that when mixtures of Y(II) and Y(III)–Y(IV) are electrolyzed, the material transferred to the anode is enriched in Y(III)–Y(IV) relative to Y(II). This behavior indicates that the Y(III) and Y(IV) species are more negatively charged than Y(II).

In addition to the shoulder at 360 mμ due to Y(IV), which is most prominent at very high chloride concentrations, the Y(III) spectrum is altered at high acidities ($\geq 6\ M$) in a manner that suggests an additional complex, Y(V), is slowly formed in minor amounts. This species appears to have a broad maximum in the region 430–440 mμ but to have an absorption less intense than that of either Y(II) or Y(III). While it is likely that Y(IV) and Y(V) correspond to $[RuCl_5OH]^=$ and $[RuCl_6]^=$, this has not yet been established, for solutions have not yet been obtained in which these complexes are the predominant species.

The Violet Complex.—This complex is observed, as a transitory intermediate, under almost all conditions at which Ru(IV) and Cl^- react at finite rates. Under conditions that produce appreciable concentrations of the violet complex the relationship of the violet complex as the precursor of Y(II) is clearly evident. From a run ($[H^+] = 0.87\ M$, $[Cl^-] = 0.2\ M$, $[Ru] = 1.18 \times 10^{-4}\ M$) in which at one time about 77% of the Ru(IV) existed as the violet complex, the qualitative spectrum of this complex was obtained. The actual extinction coefficients (see Fig. 2) were obtained by studying the decay of the violet complex to Y(II) under conditions ($[H^+] = 6.0\ M$, $[Cl^-] = 0.25\ M$; $[H^+] = 1.00$, $[Cl^-] = 0.5\ M$) where nearly pure Y(II) was obtained (corrections were applied for small amounts of Y(III)). Using the known extinction coefficients of Y(II) and the qualitative violet spectrum, the amounts of Ru(IV) present as the violet species at various stages of the transition were calculated by a method of successive approximations. The average of seven such determinations gave 16.4 ± 0.7 × 10^3 as the value of E_m at λ 562 mμ and 5.0 ± 0.2 × 10^3 at 427 mμ.

Because of the transitory nature of the violet complex the bulk of the effort to elucidate its formula has been concerned with the kinetics of its formation and decay. The effect of hydrogen ion and chloride ion concentration upon the growth and decay of the species is illustrated in Figs. 4 and 5 summarized in Tables III and IV. From the curves shown in these figures it has been possible to establish the orders in chloride and hydrogen ion concentrations of the rate of conversion of the violet species to Y(II).

If the rate of decay of the violet complex to Y(II) obeys the relation

$$\left(\frac{dV}{dt}\right)_2 = \bar{k}_2\,[V]$$

then the total amount of the complex decaying to Y(II) will be given by

$$V_T = \int \bar{k}_2 [V]\,dt$$

where the integration is to be carried out from zero time until the violet species has completely vanished. However, if all of the Ru(IV) has passed through the violet species, V_T must equal the initial Ru(IV) concentration, so that

$$[Ru(IV)]_0 = \bar{k}_2 \int [V]\,dt$$

$$\bar{k}_2 = \frac{[Ru(IV)]_0}{\int [V]\,dt}$$

$$\bar{k}_2 = \int \frac{E_V}{\frac{D_V}{l[Ru(IV)]_0}}\,dt$$

where D_V is the optical density of the violet species at λ 562 mμ, l is the cell length, and E_V the molar extinction coefficient of the violet species at λ 562 mμ. Since the denominator of the last expression is merely the area under the curves illustrated in Figs. 4 and 5, $\bar{k}_2$ may be readily obtained by graphical integration.

In addition to the assumption that all of the Ru(IV) passes through the violet species, two other assumptions are inherent in the above treatment. One is that the rate is first order in the concentration of violet species, which seems reasonable, and the other is that the rate of the back reaction, Y(II) → Violet, is small in comparison to the forward rate. Experience indicates that the latter assumption is acceptable except at very low chloride concentrations. That the assumption that all of the Ru(IV) passes through the violet species probably becomes invalid at very high acidities is suggested by the data of Fig. 4, which shows that as the hydrogen ion concentration increases the observed maximum amount of the violet complex rises and then falls.

Table III shows the $\bar{k}_2$ values obtained by the above integration method for the series of runs at

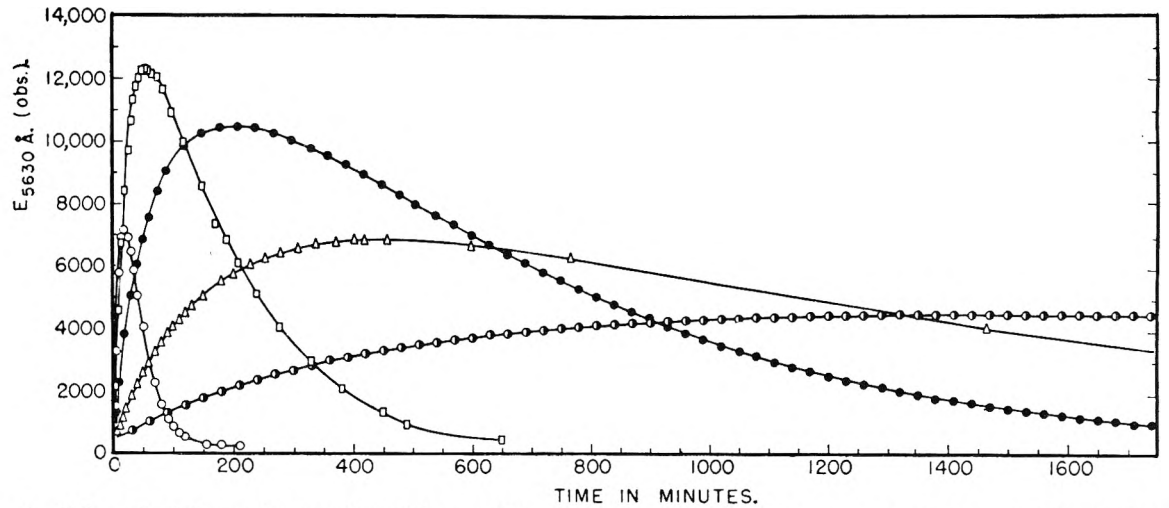

Fig. 4.—Effect of acidity on the growth and decay of the violet complex; $t = 25°$, $\mu = 6.2$, $[Cl^-]^- = 0.200\ M$, [Ru] = $1.18 \times 10^{-4}\ M$; $[H^+]$: ○, 6.2 M; □, 0.999 M; ●, 0.4035 M; △, 0.206 M; ◑, 0.1052 M.

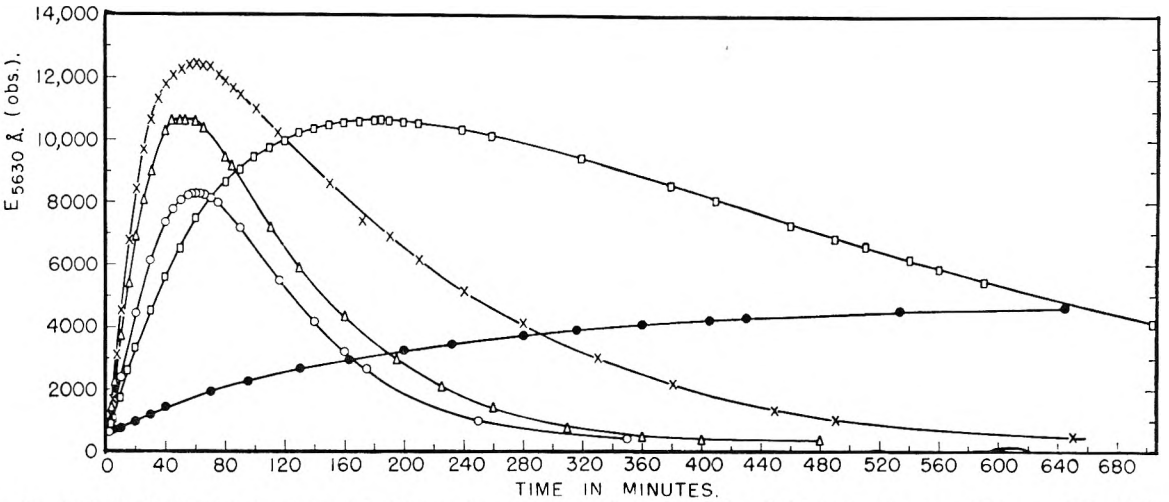

Fig. 5.—Effect of chloride ion concentration on the growth and decay of the violet complex; $t = 25°$, $\mu = 6.2$, $[H^+] = 1.00\ M$, [Ru] = $1.17 \times 10^{-4}\ M$; ○, $[Cl^-]$: 0.0600 M; △, 0.397 M; ×, 0.199 M; □, 0.0995 M; ●, 0.0495 M.

constant hydrogen ion concentration and varying chloride ion concentration (data of Fig. 5).

TABLE III

EFFECT OF CHLORIDE ION CONCENTRATION ON THE RATE CONSTANT FOR VIOLET → Y(II)

$t = 25°$, $\mu = 6.2$

$[Cl^-]$ (m./l.)	$[H^+]$ (m./l.)	$\bar{k}_2$ (min.$^{-1}$)	$\frac{\bar{k}_2}{[H^+][Cl^-]}$	$\frac{\bar{k}_2}{[H^+][Cl^-]^2}$
0.600	1.002	0.0154	0.026	0.043
.3973	0.9953	.0115	.029	.073
.199	0.999	.00608	.031	.15
.0995	1.001	.00249	.026	.25
.0495	0.998	.000662	.013	.27

It is evident that, except for the run at very low chloride concentration, a reasonably satisfactory rate constant can be obtained if $\bar{k}_2$ is considered to contain a term involving the first power of the chloride concentration. It is believed that the departure of the run at $[Cl^-] = 0.0495\ M$ from this regularity is probably due to the increasing importance of the Y(II) → Violet rate at the low chloride concentrations.

Table IV lists the $\bar{k}_2$ values obtained in the same manner for the series of runs at constant chloride concentration and varying hydrogen ion concentration (data of Fig. 4).

TABLE IV

EFFECT OF HYDROGEN ION CONCENTRATION ON THE RATE CONSTANT FOR VIOLET → Y(II)

$t = 25°$, $\mu = 6.2$

$[H^+]$ (m./l.)	$[Cl^-]$ (m./l.)	$\bar{k}_2$ (min.$^{-1}$)	$\frac{\bar{k}_2}{[Cl^-][H^+]}$	$\frac{\bar{k}_2}{[Cl^-][H^+]^2}$
6.20	0.200	0.0426	0.034	0.0055
0.999	.199	.00608	.031	.031
.4035	.199	.001923	.024	.059
.206	.200	.000912	.022	.11
.1052	.199	.000497	.024	.23

It is evident that $\bar{k}_2$ must also include a term involving the first power of the hydrogen ion concentration. The deviations from constancy at $[H^+] \geq 1\ M$ are probably due, in part, to failure of all the Ru(IV) to pass through the violet species.

The complete rate equation for the transition Violet → Y(II) may thus be written as

$$-\left(\frac{dV}{dt}\right)_2 = k_2[H^+][Cl^-][V]$$

where k_2 is of the magnitude 0.023 min.$^{-1}$ (m./l.)$^{-2}$ at 25°. Coupled with transference data on the violet complex this equation leads to a plausible formula for the violet complex.

Mixtures of 0.06 M Ru(IV) in 0.24 M [Cl^-] and 6 M [H^+] containing appreciable concentrations of the violet species were chilled to 0° and electrolyzed 6 hours at 20 ma. The violet complex was not transferred in either direction, an indication that this is an uncharged species. The only simple formulas that represent neutral species and also satisfy the above kinetic relation for decay to Y(II) are $Ru(OH)_2Cl_2$ and $Ru(OH)_3Cl$. If the violet were $Ru(OH)_3Cl$, the acquisition of the first additional chloride ion would have to be rate determining inasmuch as no species intermediate between the violet complex and Y(II) are observed spectrophotometrically. This step would be followed by the fast addition of the second chloride ion to yield the Y(II). But this fast step would be either essentially the same as the initial slow step, *i.e.*, the addition of chloride ion to a neutral species, or, even worse, the addition of chloride ion to a negatively charged species. It does not seem likely that such a rate relationship between these steps would actually exist.

On the other hand, if the violet complex were $Ru(OH)_2Cl_2$, the rate data would comply with the simple interpretation that the violet species is transformed to yellow (II) by the acid-catalyzed addition of chloride ion

$$\underset{\text{Violet}}{Ru(H_2O)_2(OH)_2Cl_2} + Cl^- \xrightarrow{(H^+)} \underset{\text{Y(II)}}{[RuH_2O(OH)_2Cl_3]^-} + H_2O$$

This interpretation seems much more likely than that based on the formula $Ru(OH)_3Cl$ and therefore it is believed that the violet complex is the dihydroxo dichloro species shown in the above equation. Though the acid catalysis of the chloride addition seems somewhat surprising, it may actually be a rather general phenomenon in the case of these hydroxy ruthenium species. Thus qualitative studies indicate that the Y(II) → Y(III) transformation is accelerated by hydrogen ion even though the equilibrium between these species is independent of acidity.

The Initial Yellow Complexes, Y(IA), Y(IB) and Y(IC).—Several features of the data shown in Figs. 4 and 5 indicate that the formation of the violet complex proceeds via a rather complicated set of reactions. Thus, the time at which the violet species reaches its maximum growth becomes independent of chloride ion concentration when this concentration exceeds 0.2 M. In addition, the curves of Figs. 4 and 5 show brief initial induction periods in which the rate of growth of the violet complex increases markedly (for example, see Fig. 6 which shows the initial portions of the curves of Fig. 5). Such behavior suggests that the violet complex is formed from a species which itself has a finite rate of formation, and that one of these steps involves a reaction with hydrogen ion and becomes rate determining at high chloride concentrations.

In addition, studies of the effect of the initial Ru(IV) concentration on the rate of growth of the violet species show that the steps leading to the violet complex are not strictly first order in ruthenium under all conditions. In Fig. 7 are shown the apparent extinction coefficients of the violet complex, D_V/l[Ru], as a function of time for a series of runs at constant chloride and hydrogen ion concentrations but varying initial ruthenium concentrations. If the growth and decay of the violet species were first order in ruthenium concentration, the curves of

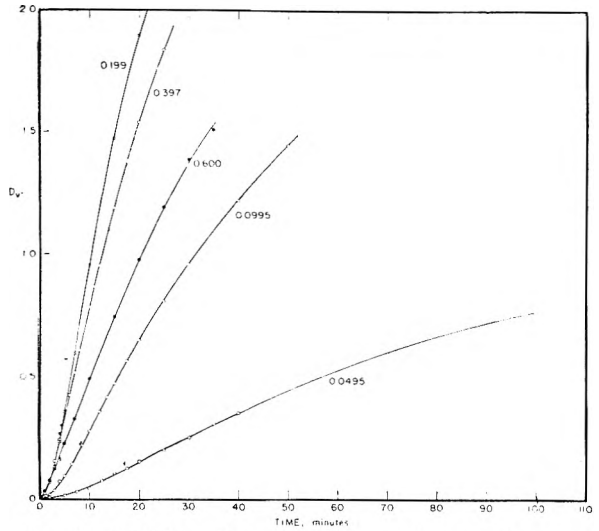

Fig. 6.—Initial portions of violet complex growth curves of Fig. 5. Chloride concentrations as indicated; arrows mark ends of induction periods. Actual ordinates of [Cl^-] = 0.0495 M curve are one-half the indicated values.

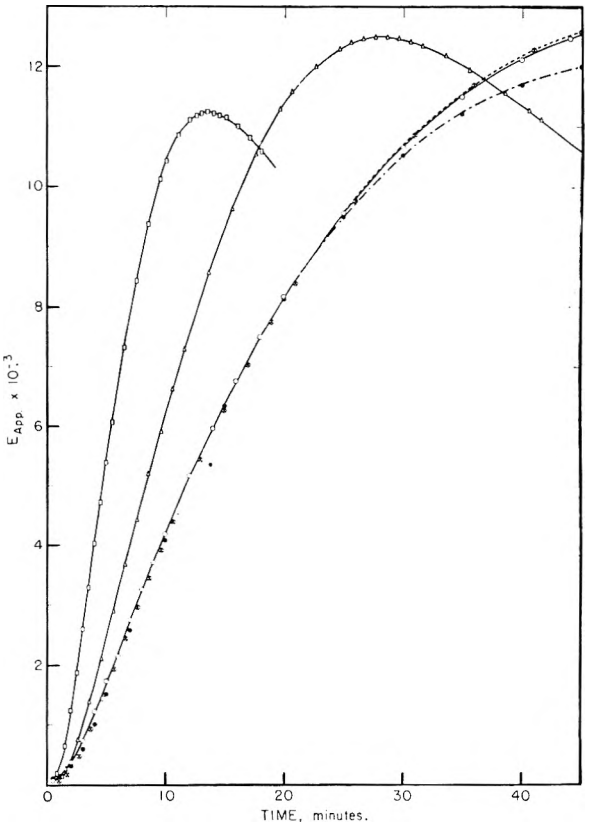

Fig. 7.—Effect of initial ruthenium concentration on the rate of growth of the violet complex; [H^+] = 1.00 M, [Cl^-] = 0.2 M, μ = 6.2, t = 25°, and [Ru]$_0 \times 10^4$ in m./l.: ○, 1.79; ●, 1.17; ⊗, 0.897; △, 0.343; □, 0.171.

Fig. 7 should coincide. It is observed that this is the case at Ru(IV) concentrations above 9×10^{-5} M, but that at concentrations below this value the relative rate of formation of the violet species increases and the duration of the induction period decreases. Such behavior suggests that the reverse rates of the steps leading to the violet complex are not negligible and that polymeric species are probably involved in these steps.

Though these observations indicate that other complexes are formed prior to the violet species, it has not been possible to obtain from the kinetic data on the growth of the violet complex unequivocal information concerning these earlier steps and species. However, it seems reasonable to suppose that the earlier species indicated by the kinetic data are identical with the initial yellow complexes that are observed prior to the violet complex under a variety of conditions.

Examination of the spectra immediately after the addition of Ru(IV) to chloride solutions reveals the following effects. At low chloride and/or hydrogen ion concentrations (*e.g.*, $[Cl^-] < 0.05$ M, $[H^+] = 1$ M, $[Ru] = 1.29 \times 10^{-4}$ M; $[Cl^-] = 1$ M, $[H^+] < 0.1$ M) a general increase in the level of the Ru(IV) absorption occurs without any evidence for definite absorption bands. Under such conditions either no further reaction is evident after long storage or the formation of the violet and/or later complexes is extremely slow. At higher chloride and hydrogen ion concentrations at least three definite absorption bands are formed with maxima at 369, 443 and 420 mμ (the appearance of these bands under extreme conditions are shown in Fig. 8). These maxima appear to be associated with three yellow complexes, designated Y(IA), Y(IB) and Y(IC), respectively.

Though these complexes are formed very rapidly (within a few minutes) at the higher chloride and acid concentrations, they do not appear to have reached equilibrium before the growth of the later species, such as the violet complex, begins to mask their spectra. This fact, together with the incomplete resolution of their absorption maxima and the general intensification of the Ru(IV) background absorption, makes the quantitative study of these initial yellow complexes very difficult. Consequently their formulas have not been obtained and their relationship to the violet complex has not been clearly established. Certain qualitative information concerning these species has, however, been obtained.

The fractions of Y(IA) and Y(IB) initially formed at 6.2 M chloride ion concentration and hydrogen ion concentrations of 0.06 and 1.00 M appear to the same, although on standing the Y(IA) species grows at the expense of the other complex, more so at the lower acid concentration. The amount of both complexes increases with increasing chloride concentration at constant acidity. It is further observed that at constant chloride concentration of 0.2 M, the concentrations of Y(IB) and Y(IC) increase with increasing acidity and that in 6.0 to 10.6 M acid Y(IC) becomes the predominant complex. Thus, the Y(IA) complex appears to be the most hydrolyzed species and the Y(IC) the least.

On the basis of these observations concerning the growth of the violet complex a conjecture as to the

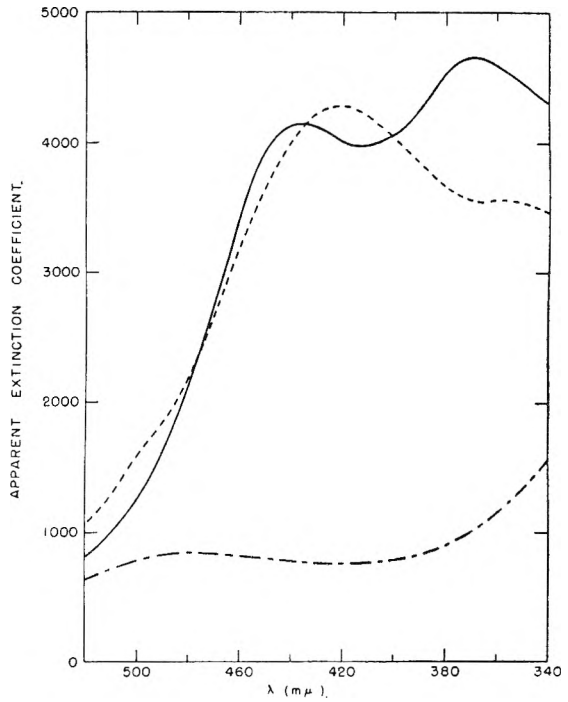

Fig. 8.—Absorption spectra of Ru(IV) in solutions of composition: ———, $[H^+] = 1.0$ M, $[Cl^-] = 6.2$ M; – – – – – –, $[H^+] = 10.6$ M, $[Cl^-] = 0.2$ M; – – – –, $[HClO]_4 = 6$ M. Spectra taken approximately 30 seconds after mixing.

nature of the Y(I) complexes and the steps leading to the violet complex may be made as follows. Apparently the initial steps at acid concentrations below 6 M are the rapid additions of chloride ion to the Ru(IV) perchlorate forming the complexes Y(IA) and Y(IB) in the ratio of the species of Ru(IV) initially present in the stock. Inasmuch as the violet complex is a dihydroxo species and appears to be formed *via* a step involving hydrogen ion (which becomes rate determining at chloride concentrations above 0.2 M), the Y(IA) and Y(IB) complexes are presumably more highly hydrolyzed than is the violet. In view of the indications that these complexes are polymers they may thus correspond to types such as

$(HO)_3ClRu—OH—Ru(OH)_2Cl$ Y(IA)
$(HO)_2ClRu—OH—Ru(OH)_2Cl^+$ Y(IB)

though the actual degree of polymerization is not known.

Formation of these initial complexes appears to be followed by the adjustment of their concentrations to the hydrogen ion concentration of the solution (such adjustment with respect to hydrogen ion concentration is known to be slow in the absence of chloride ion[2]), and then by the slow hydrogen ion dependent step, which it seems plausible to assume would involve breakdown of the polymer chain to the less hydrolyzed Y(IC)

$$(HO)_2ClRu—OH—Ru(OH)_2Cl^+ + H^+ \longrightarrow \underset{\text{Y(IC)}}{2\ Ru(OH)_2Cl^+} + H_2O$$

Further addition of chloride ion would then yield the violet species

$$Ru(OH)_2Cl^+ + Cl^- \longrightarrow \underset{\text{(Violet)}}{Ru(OH)_2Cl_2}$$

INORGANIC COMPLEX COMPOUNDS CONTAINING POLYDENTATE GROUPS. VI. FORMATION CONSTANTS OF COMPLEX IONS OF DIETHYLENETRIAMINE AND TRIETHYLENETETRAMINE WITH DIVALENT IONS[1]

BY HANS B. JONASSEN, G. G. HURST,[2a] R. B. LEBLANC,[2b] AND A. W. MEIBOHM[2c]

Richardson Chemical Laboratories, Tulane University, New Orleans, Louisiana

Received August 30, 1951

The formation for the ions Mn(II), Fe(II), Co(II) and Zn(II) have been measured with diethylenetriamine and triethylenetetramine at 30° and 40°. Formation constants and other thermodynamic properties have been calculated for these complexes. The order of stability of these complexes is related to the second ionization potential of the metal.

The authors[3,4] previously measured the formation curves and determined the formation constants of the complexes of diethylenetriamine (abbr. dien) and triethylenetetramine (abbr. trien) with nickel(II) and the copper(II) ions. This paper reports the determination of the formation curves and formation constants of the complexes of these two polyamines with the manganese(II), the iron(II) the cobalt(II) and the zinc(II) ions at 30 and 40° and some of the thermodynamic values calculated from these data.

The method used for the measurements is the *p*H method developed by J. Bjerrum.[5] The specific equations for the complexes of dien and trien were developed previously.[3,4]

From the stepwise acid–base dissociation constants of dien H_3^{+3} and trien H_4^{+4} and the *p*H's of solutions containing known concentrations of the metal ion, a mineral acid, and dien or trien the concentrations of the free amine and of the complexed amine can be calculated. From these the values of $\bar{n}$, the mean number of amine molecules coördinated to each metal ion, and *p*(dien) or *p*(trien), the negative logarithm of the free dien or trien concentration, can be computed. These quantities substituted into the following equations, yield the values of the formation constants of the complex ion $Me(dien)^{+2}$ and $Me(dien)_2^{+2}$.

$$\log k_1 = p(\text{dien}) + \log \frac{\bar{n}}{1-\bar{n}} - \log\left[1 + \frac{(2-\bar{n})[\text{dien}]k_2}{1-\bar{n}}\right]$$

$$\log k_2 = p(\text{dien}) + \log \frac{\bar{n}-1}{2-\bar{n}} + \log\left[1 + \frac{\bar{n}}{(n-1)[\text{dien}]k_1}\right]$$

Similar equations[5] have been derived for the complex ions $Me(trien)^{+2}$ and $Me_2(trien)_3^{+4}$

$$\log k_1 = p(\text{trien}) + \log \frac{\bar{n}}{1-\bar{n}}$$

$$\log k_{3:2} = p(\text{trien}) + \log \frac{\bar{n}-1}{1.5-\bar{n}}$$

The log k values can also be obtained from the formation curves at $\bar{n} = 0.5$ and $\bar{n} = 1.5$ for the dien complexes and $\bar{n} = 0.5$ and $\bar{n} = 1.25$ for the trien complexes.

The partial aminium complexes which Schwarzenbach obtained by modification of Bjerrum's method could not be identified under the conditions of this investigation.[6]

Spectrophotometric investigations of the metal-amine solutions under the various conditions given in Schwarzenbach's work showed that only the density values of the absorption characteristics change with change in conditions. It seems unlikely that the amine and aminium complexes have the same absorption characteristics.

Experimental

Stock solutions of all the metal ions except the iron(II) ion were prepared by dissolving a mole of the C.P. nitrate salt in a liter of solution. These solutions were standardized by electrodeposition and/or precipitation as the pyrophosphate. Boiled distilled water was used for these solutions. A rapid stream of nitrogen was passed through the cobalt(II) and the manganese(II) solutions for ten hours to ensure the absence of appreciable quantities of dissolved oxygen.

A stock solution of iron(II) ion was prepared by dissolving 5.6 g. of C.P. iron powder in about 60 ml. of 6 *N* HCl. The solution was filtered and diluted to a liter with boiled distilled water. Dissolved oxygen and any trace of iron(II) were removed by bubbling hydrogen through the solution for twelve hours in the presence of few drops of colloidal palladium and indigo tetrasulfonate as catalysts. The iron was determined gravimetrically as the oxide, the chloride as AgCl, and the excess HCl by potentiometric titration in an atmosphere of nitrogen.

A 2 *M* KNO_3 stock solution and a 4 *M* KCl stock solution were prepared by weighing the dry salts and dissolving in the required amount of solution. A 1 *M* HNO_3 solution was prepared from boiled C.P. HNO_3 and standardized with Reagent Grade Na_2CO_3.

Technical grade dien or trien from Carbide and Carbon Chemicals Corporation was purified as previously described.[7] It was dissolved in a liter of solution, and titrated potentiometrically with the standard 1 molar acid.

The solutions (except for that of the iron(II) ion) used for the measurements were prepared in 100-ml. volumetric flasks. They contained 0.1 *M* of metal ion, 0.1 *M* of HNO_3, 1.00 *M* of KNO_3 and KCl, and varying concentrations of the amines. The 1 molar stock solution of the amines also was 1 molar in KCl.

The solutions for the iron(II) ion measurements were

(1) Presented at the Symposium on Complex Ions and Polyelectrolytes, Ithaca, New York, June 18–21, 1951. Abstracted from the Ph.D. dissertations of R. B. LeBlanc and A. W. Meibohm, February, 1950.

(2) Present addresses: (a) Department of Chemistry, Mississippi Southern College, Hattiesburg, Miss. (b) Department of Chemistry, Texas Agricultural and Mechanical College, College Station, Texas. (c) Department of Chemistry, Valparaiso University, Valparaiso, Indiana.

(3) H. B. Jonassen, R. B. LeBlanc and R. M. Rogan, *J. Am. Chem. Soc.*, **72**, 4968 (1950).

(4) H. B. Jonassen and A. W. Meibohm, THIS JOURNAL, **55**, 726 (1951).

(5) J. Bjerrum, "Metal Ammine Formation in Aqueous Solution," P. Hasse and Son, Copenhagen, 1941.

(6) G. Schwarzenbach, *Helv. Chim. Acta*, **33**, 974 (1950).

(7) H. B. Jonassen, R. B. LeBlanc, A. W. Meibohm and R. M. Rogan, *J. Am. Chem. Soc.*, **72**, 2430 (1950).

0.01 *M* in iron(II) ion, 0.01 *M* in HCl, 1.27 *M* in KCl, and of varying concentrations in amine. In order to minimize oxidation HCl and KCl were substituted for HNO_3 and KNO_3, and the concentrations of the iron(II) ion and the acid were decreased to 0.01 *M*. The concentration of the KCl was increased to 1.27 *M* to make the salt concentration the same as that used for the measurements for the acid–base constants of the amines and the formation constants of the other metal complexes.

The solutions of the cobalt(II) ion, the iron(II) ion and the manganese(II) ion were prepared up to the point of addition of the stock solution of the metal ion. Nitrogen was bubbled through the solutions in the volumetric flasks for 45 minutes to remove dissolved oxygen, whereupon the metal ion solution was added. This precaution was taken since these three ions are easily oxidized in basic solution by dissolved oxygen.

The *p*H's of all the solutions were measured at 30 ± 0.2° and 40 ± 0.2°. A Beckman model G *p*H meter, standardized with Beckman buffer solutions (*p*H's of 4, 7 and 10) was used. An atmosphere of nitrogen was maintained over the solutions of the manganese(II), the iron(II) and the cobalt(II) ions during the measurements.

Results

Table I contains the data and calculations on the manganese(II) ion and dien at 30°. The two formation constants of the manganese(II) ion and dien complexes at 30° calculated from points on the formation curve are shown in Table II.

TABLE I

*p*H MEASUREMENTS OF MANGANESE(II) SOLUTIONS CONTAINING DIETHYLENETRIAMINE AT 30°

$C_{Mn(II)} = 0.0949M$. $C_{KNO_3} + C_{KCl} = 1.00M$; C_a = total concentration of hydrogen ions bound to dien; C_{dien} = total concentration of dien in solution; C'_{dien} total concentration of dien not bound in a complex ion; $\bar{n}_{dien}$ = average number of hydrogen ions attached to one uncomplexed dien molecule.

C_{dien}	*p*H	$\log \frac{\bar{n}_{dien}}{dien}$	$\bar{n}_{dien}$	C_a	C'_{dien}	$\bar{n}$	*p*(dien)
0.0450	5.25	3.15	2.25	0.0999	0.0443	0.008	10.15
.0551	7.52	4.44	1.98	.1001	.0507	.046	5.44
.0655	7.84	3.80	1.96	.1001	.0510	.153	4.80
.0850	8.10	3.29	1.93	.1001	.0519	.349	4.29
.0900	9.15	3.19	1.92	.1000	.0523	.400	4.19
.1047	8.26	2.97	1.90	.1000	.0523	.549	3.97
.1179	8.35	2.80	1.88	.0999	.0531	.683	3.80
.1302	8.42	2.66	1.86	.1002	.0539	.804	3.66
.1451	8.52	2.47	1.83	.0999	.0547	.953	3.47
.1600	8.62	2.28	1.79	.0995	.0557	1.099	3.28
.1901	8.73	2.07	1.73	.0996	.0574	1.293	3.07
.1999	8.88	1.80	1.65	.0998	.0606	1.468	2.80
.2198	0.01	1.55	1.56	.0998	.0642	1.640	2.55
.2402	0.20	1.24	1.40	.1002	.0718	1.777	2.24
.2598	9.40	0.91	1.20	.0996	.0835	1.859	1.91
.2850	9.62	0.58	0.96	.0996	.1035	1.913	1.58

Figure 1 shows the formation curves at 30° for dien and the iron(II), the cobalt(II), the zinc(II), manganese(II), copper(II) and nickel(II) ions, respectively.

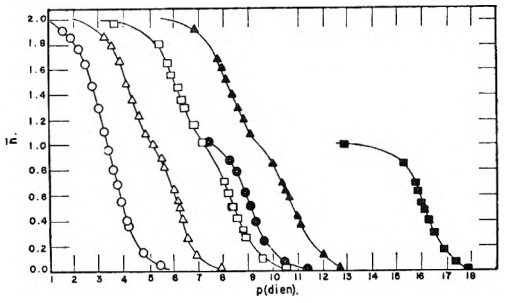

Fig. 1.—Formation curves of diethylenetriamine and the following ions at 30°: Mn, —○—; Co —□—; Cu, —■—; Fe, —Δ—; Ni, —▲—; Zn, —●—.

TABLE II

FORMATION CONSTANTS OF MANGANESE(II) AND DIETHYLENETRIAMINE AT 30°

$$\Delta = -\log\left(1 + \frac{(2-\bar{n})[\text{dien}]k_2}{(1-\bar{n})}\right)$$

$\bar{n}$	*p*(dien)	$\log \frac{\bar{n}}{1-\bar{n}}$	Δ	log k_1
0.153	4.80	−0.74	−0.01	4.05
.349	4.29	− .27	− .04	3.98
.400	4.19	− .18	− .05	3.96
.549	3.97	+ .09	− .09	3.98
.683	3.80	+ .33	− .16	3.97
.804	3.66	+ .61	− .28	3.99
			Average	3.99

$$\Delta = \log\left(1 + \frac{\bar{n}}{(\bar{n}-1)[\text{dien}]k_1}\right)$$

$\bar{n}$	*p*(dien)	$\log \frac{\bar{n}-1}{2-\bar{n}}$	Δ	log k_2
1.099	3.28	−0.96	+0.50	2.82
1.293	3.07	− .38	+ .19	2.88
1.468	2.80	− .06	+ .08	2.82
1.640	2.55	+ .25	+ .04	2.84
1.777	2.24	+ .54	+ .02	2.80
			Average	2.83

Table III shows the values of the formation constants at 30° and 40°, the free energies of binding, and the heats of binding of the complexes of dien with the four ions. The data for nickel(II) ion and the copper(II) ion which were previously reported[3] are included for comparison.

TABLE III

THERMODYNAMIC VALUES FOR COMPLEX IONS OF DIETHYLENETRIAMINE AND DIVALENT METAL IONS

All values in kcal./mole; ΔH values = $\Delta H_{305}°$

Cation	*T*, °C.	log k_1	log k_2	$-\Delta F_1$	$-\Delta F_2$	$-\Delta H_1$	$-\Delta H_2$
Mn(II)	30	3.99	2.83	5.5	3.9	4	5
Mn(II)	40	3.89	2.72	5.6	3.9		
Fe(II)	30	6.23	4.13	8.6	5.7	9	8
Fe(II)	40	6.03	3.95	8.6	5.7		
Co(II)	30	8.47	6.07	11.8	8.4	9	10
Co(II)	40	8.26	5.83	11.8	8.4		
Ni(II)	30	10.81	8.14	15.0	11.2	12	13
Ni(II)	40	10.54	7.83	15.1	11.2		
Cu(II)	30	16.11		22.3		20	
Cu(II)	40	15.64		22.4			
Zn(II)	30	9.14		12.7		8	
Zn(II)	40	8.95		12.8			

Figure 2 shows the formation curves of the complexes of triethylenetetramine and divalent metal ions.

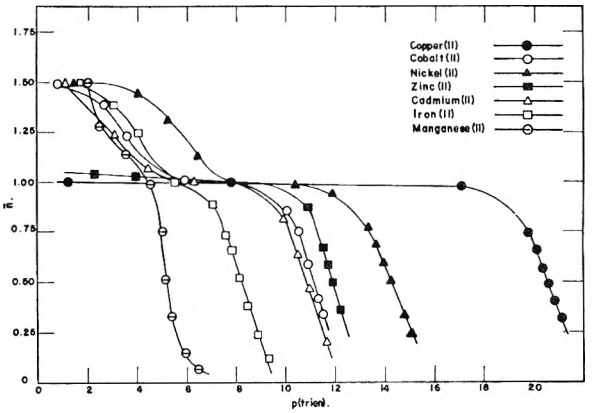

Fig. 2.—Formation curves: complex ions of all cations at 30°.

Table IV gives the thermodynamic values obtained for the complex ions of triethylenetetramine with the above divalent metal ions as well as cadmium(II) ions at temperatures of 30 and 40°.

TABLE IV

THERMODYNAMIC VALUES OF COMPLEX IONS OF TRIETHYLENETETRAMINE AND DIVALENT METAL IONS

All values in kcal./mole, ΔH values = $\Delta H_{308}°$

Cation	T, °C.	log k_1	log $\beta_{2:2}$	$-\Delta F_1$	$-\Delta F_{2:2}$	$-\Delta H_1$	$-H_{2:2}$
Mn(II)	30	5.43	2.84	7.5	3.9	4	4
Mn(II)	40	5.31	2.72	7.6	3.9		
Fe(II)	30	8.31	3.92	11.5	5.4	9	9
Fe(II)	40	8.08	3.70	11.6	5.3		
Co(II)	30	11.21	3.38	15.5	4.7	9	4
Co(II)	40	11.03	3.27	15.8	4.7		
Ni(II)	30	14.34	5.63	19.8	7.8	13	9
Ni(II)	40	14.01	5.41	20.1	7.8		
Cu(II)	30	20.62		28.6		22	
Cu(II)	40	20.08		28.8			
Zn(II)	30	11.94		16.5		4	
Zn(II)	40	11.81		16.9			
Cd(II)	30	10.92	3.19	15.1	4.4	4	4
Cd(II)	40	10.79	3.07	15.5	4.4		

Discussion

Formation of Complexes.—As shown in Table III the manganese(II), the iron(II), the cobalt(II) and the nickel(II) ions exhibit a coördination number of six complexing with two dien molecules.

The copper(II) ion and the zinc(II) ion exhibit a coördination number less than six, but still coördinate two dien molecules. As was explained previously[3] the equations for the calculations of formation constants are applicable to these ions for an $\bar{n}$ value greater than one only if all the amino nitrogens are coördinated to the metal ion. This is not the case in the copper and zinc ions and only the first formation constant for these complexes, therefore, can be obtained from these data.

Figure 2 shows that in each case the formation of a complex ion of triethylenetetramine with one metal ion occurs. In the presence of excess amine expansion of the coördination sphere occurs for all but the copper(II) and zinc(II) ions.

Comparison of the data of cadmium(II) and zinc(II) shows that the 1:1 complex ion is more stable for zinc(II) than for cadmium(II) and that the coördination sphere of zinc(II) is not expanded to a coördination of six whereas that of the cadmium(II) ion is. It is to be expected that the larger cadmium(II) would act in this manner.

The equations of the method of this paper require that all nitrogen atoms of triethylenetetramine be coördinated to the central metal ion. The coördination number of six thus requires a formula $[M_2A_3]^{+4}$.

It is possible to postulate other formulas for these complexes such as MA_2 where two of the nitrogen atoms of one of the amines would not be coördinated. However, spectrophotometric studies[8] and polarographic studies of several of these complexes indicate that the complex ion with the highest amine to metal ion ratio is the 3/2:1 complex.

The steep increase in the formation curves of the cadmium(II) and manganese(II) complex ions with trien shown in Fig. 2 is no doubt due to the fact that at these high concentrations of amine polymeric hydroxy complexes may exist which will change the pH and thereby the $\bar{n}$ and p(amine) value. Such polymers would not allow coördination of all nitrogen atoms in the amines and Bjerrum's method would not be valid.

A previous polarographic investigation of the complex ion formed between cadmium(II) and triethylenetetramine[9] gave log k values of 13.9 for the 1:1 complex ion. However, the log k values for this complex compound obtained in this investigation is 10.9, and the value for the 3:2 complex ion was estimated to be 3.1.

The difference in these values of the 1:1 complex ion can be expected since a large excess of the amine (100:1) and greater is present in polarographic investigation whereas the excess of amine in the solution from which these data were obtained was never larger than 2:1. At such small excess the above authors found that the electrode process was irreversible indicating the possible presence of other complex ions. The complex $(Cd_2\ trien_3)^{+4}$ found in this investigation is in accord with such conclusions.

Order of Stability of Ions.—The order of stability of the complex ions of the same metal ion is that expected from the nature of the amine. The stability of the ions formed by $\beta\beta'\beta''$-triaminetriethylamine (tren), an isomer of triethylenetetramine indicated that steric effects are important.[6] It is sterically impossible for this amine to enter a planar configuration as required by the copper(II) ion and the decrease in stability, relative to the tri-

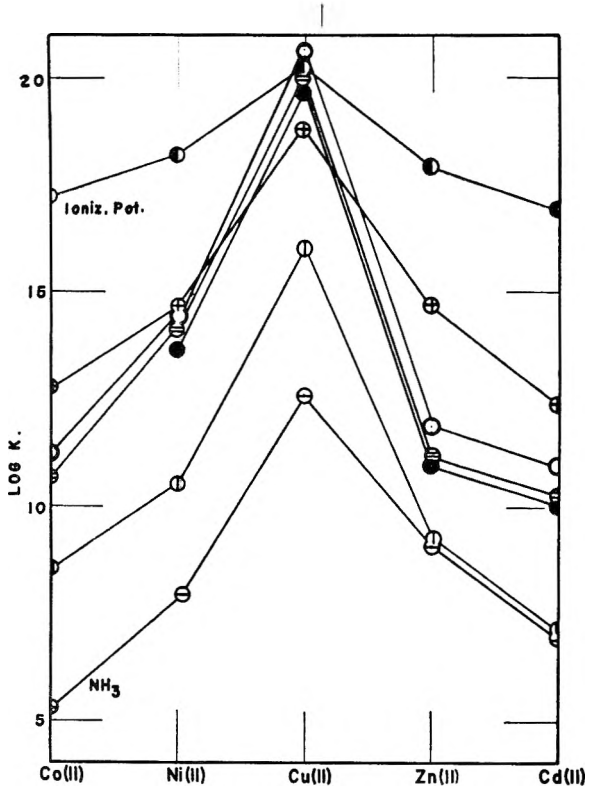

Fig. 3.—Relative stability of complex ions, coördination number of four: ethylenediamine, —⊖—; propylenediamine, —●—; diethylenetriamine, —①—; triethylenetetramine, —○—; β,β',β''-triaminotriethylamine, —⊕—.

(8) H. B. Jonassen and B. E. Douglas, *J. Am. Chem. Soc.*, **71**, 4094 (1949).

(9) B. E. Douglas, H. A. Laitinen and J. C. Bailar, Jr., *ibid.*, **72**, 2484 (1950).

ethylenetetramine complex ion, is indicative of the strain present in the ion.

The determination of the formation constants at two temperatures permits calculation of the free energy of the ions and approximate heats of formation of the complex ions. These are given in Table IV.

A comparison of the data of the first and second step equilibria in the complex ions containing triethylenetetramine and diethylenetriamine shows that the increase in stability in the second step equilibrium is very much smaller for the trien complexes than for the dien complex ions. This is to be expected since the second step of the trien complexes involves formation of dinuclear complex ions.

No evidences of the hydrogen complexes reported by Schwarzenbach were obtained in this investigation.

Irving and Williams[10] have recently reviewed the stability of complex ions of bivalent metals. For the ions, Cu(II), Ni(II), Co(II), Zn(II) and Cd(II) the stability decreases in that order irrespective of the nature of the coördinating group.

(10) H. Irving and J. P Williams, *Nature*, **162**, 746 (1948).

Calvin and Melchior[11] obtained the same order of stability. Attempts by these authors to relate the order of stability to some property of the metal atom or ion showed that the correlation was best obtained between the second ionization potential of the gaseous atoms and the relative stability of the complex.

Figure 3 shows the logarithms of the stability constants of complex ions with various amines with a coördination number of four which have been studied quantitatively along with the second ionization potentials as given by Latimer.[12] Since only a very few data are available for Fe(II) and Mn(II) complexes with this coördination number these values are not included but the decrease in the second ionization potential observed for these ions is also found in the log k data of their complexes. Similar results are indicated by the meager data available for complexes with a coördination number of six.

(11) M. Calvin and N. C. Melchior, *J. Am. Chem. Soc.*, **70**, 3270 (1948).

(12) W. M. Latimer, "The Oxidation States of the Elements and Their Potentials in Aqueous Solutions," Prentice-Hall, Inc., New York, N. Y., 1938, pp. 14–15.

COMPLEXES IN OXIDATION-REDUCTION REACTIONS. THE COPPER(II)-CYANIDE REACTION

BY FREDERICK R. DUKE AND WELBY G. COURTNEY

Contribution No. 122 from the Institute for Atomic Research and Department of Chemistry, Iowa State College, Ames, Iowa

Received August 30, 1951

Many homogeneous oxidation-reduction reactions have been shown to involve coördination complexes as intermediates. In the present work, copper(II) is shown to coördinate four cyanide ions, this complex ion then yielding $Cu(CN)_3^=$ and CN radical; high concentrations of ammonia are present in the reaction mixture in order to compete with the cyanide ions for the coördination positions on the copper(II) ion, thereby bringing the rate of the reaction into a measurable range. A possible reason for the necessity of four cyanide ions in the reacting complex is discussed.

Out of the studies on the mechanism of electron transfer have come some promising possible generalizations. One of these might be stated as follows: coördination complexes are involved mechanistically as intermediates in homogeneous ionic oxidation-reduction reactions. This hypothesis appears to be particularly applicable to reactions involving cationic oxidants and anionic or "Lewis-base" reductants. For example, systems in which such complexes have been observed as intermediates are Fe(III)–I^-,[1] Mn(III)–$C_2O_4^=$,[2,3] Ce(IV)–glycol,[4] Ce(IV)–Cl^-,[5] Fe(III)–$SO_3^=$,[6] Ce(IV)–$C_2O_4^=$,[7] and a number of others.

A point of further interest in connection with these coördination intermediates is any relationship which might exist between the number of oxidizable anions in the complex and the rate of "electron transfer." For instance, the complex FeI_2^+ yields ferrous ion very much more rapidly than does the complex FeI^{+2}; $Mn(C_2O_4)^+$ yields manganous very much more rapidly than does $Mn(C_2O_4)_2^-$.

The present work examines the Cu(II)–CN^- reaction from the points of view outlined above.

(1) A. V. Hershey and W. C. Bray, *J. Am. Chem. Soc.*, **58**, 1760 (1936).

(2) F. R. Duke, *ibid.*, **69**, 2885 (1947).

(3) H. Taube, *ibid.*, **70**, 1216 (1948).

(4) F. R. Duke and A. A. Forist *ibid.*, **71**, 2790 (1949).

(5) F. R. Duke and J. Anderegg unpublished data.

(6) F. R. Duke and A. Bottoms, unpublished data.

(7) S. D. Ross and C. G. Swain, *J. Am. Chem. Soc.*, **69**, 1325 (1947).

Experimental

Reagent grade chemicals were used. Acidified cupric chloride stock solution was standardized through thiosulfate against $K_2Cr_2O_7$ with a small quantity of Na_2CO_3 added, and potassium cyanide was standardized against $AgNO_3$ with the iodide end-point. The ammonia was cooled, diluted, standardized against HCl, and thereafter kept in an ice-box, as were all solutions containing ammonia. Kinetic runs were made at 0° ± 0.1°, maintained by a bath of melting ice in a dewar flask.

Separate erlenmeyer flasks containing 50 ml. of the desired cupric ammonia solution and a cyanide solution of appropriate concentration were cooled to equilibrium in the ice-bath. Five ml. of the cyanide solution were then added to the rapidly shaken copper solution by means of a pipet calibrated to give 5.00 ± 0.02 ml. Five-ml. portions of the reacting solution were removed by a calibrated pipet at known times and quenched in 2 ml. of a solution containing 0.2 M zinc nitrate in approximately 10 M ammonia. The optical density at 600 mμ of the quenched solution was observed and compared against an empirical curve constructed from the optical densities of known cupric copper concentrations under identical conditions except for the colorless cuprous cyanide complexes. The concentration of total cupric copper in the reacting solution was thus determined. Concen-

trations of other ions subsequently cited likewise refer to the reacting solution.

The ionic strength of the reacting solution was maintained at 1.0 with sodium nitrate. The ammonia concentrations remained sufficiently standard over 18 hours, and the cyanide solutions for even longer. Optical measurements were performed on a Coleman Universal Spectrophotometer, Model 14.

A separate study was made to determine the cause of the distinct violet color resulting from the addition of cyanide to ammoniated cupric copper. The optical density at 614 mμ of the copper–ammonia–cyanide mixture was measured as a function of time, since it is unstable. Extrapolation over 20 seconds to zero time gave D_0, the extinction at zero time. The above wave length was chosen from fast test runs as the approximate maximum in the absorption spectrum of the violet species. These optical measurements were made with a Cary Recording Spectrophotometer, Model 12, Serial 15.

Results and Discussion

It was noticed that a shift from blue to blue-violet occurred when CN^- was added to ammoniacal cupric solutions. The violet color absorbed most strongly light of wave length 615 mμ. The effect of varying CN^- at constant Cu^{++} on the extinction was determined at this wave length and found to be linear in CN^-. Since $K = Cu(CN)_x^{2-x}/(Cu^{++})(CN)^x$ and $Cu(CN)_x^{2-x} = KE$, where E is the extinction, $K(Cu^{++})(CN^-)^x = KE$, or at constant Cu^{++}, $(CN^-)^x = K'E$. The straight line variation of E with (CN^-) indicates that $x = 1$ and that the inconsequential amounts of copper and cyanide are stored as $CuCN^+$ at high ammonia concentrations. Thus we were able to conclude that the Cu^{++} could be represented by total copper concentration and that CN^- initially was equal to total cyanide concentration.

The stoichiometry of the reaction was found to be $8CN^- + 2Cu^{++} \rightarrow 2Cu(CN)_3^= + (CN)_2$. Cyanogen was found to hydrolyze slowly compared with the rate of the oxidation reaction.

Plots were prepared of Cu^{++} *vs.* time. Some typical curves are shown in Fig. 1. From these

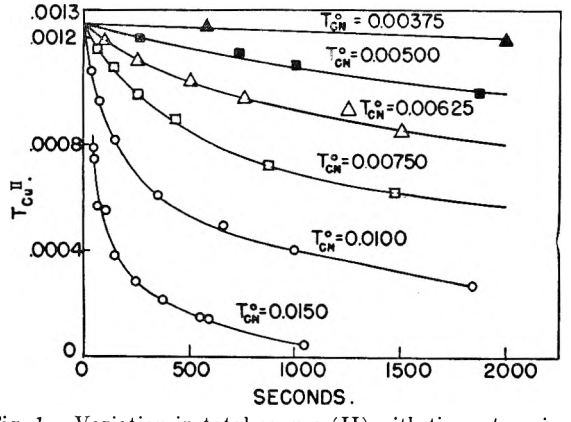

Fig. 1.—Variation in total copper (II) with time at various cyanide concentrations.

plots, $-d\,Cu/dt$ was determined by the plane surface mirror technique, both at zero time and other times. The zero time rates are uncomplicated by the presence of cuprous copper and were therefore analyzed first. Plots were made of log $(-R_0)$ *versus* log α for constant original copper(II), $T^\circ_{Cu^{II}}$, where R_0 is the initial reaction rate and the zero

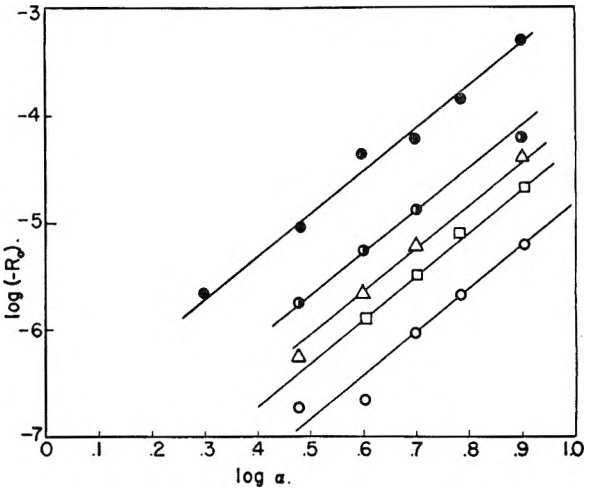

Fig. 2.—Plot for the determination of kinetic order in copper (II) and cyanide.

time ratio of CN^- to Cu^{++} is α (Fig. 2). These plots were found to have a slope of 4 for a variety of values of α, and intercepts appropriate to the equation: $-R_o = kT^{\circ 5}_{Cu^{II}}\alpha^4$. This result indicates a rate expression

$$-R_o = -(dT_{Cu^{II}}/dt)_o = k''(Cu^{++})_o(CN^-)^4_o \quad (1)$$

Next, the effect of variation in (NH_3) was considered. Utilizing the cupric–ammonia stability constants K'_n where $K'_n = [Cu(NH_3)^{II}_n]/[Cu(NH_3)^{II}_n][NH_3]$, and the relation $T_{Cu^{II}} = [Cu(NH)^{II}_4] + [Cu(NH_3)^{II}_5]$, since the concentrations of less-ammoniated species can be calculated to be insignificant and that of the cyanide complex is assumed to be insignificant, it can easily be shown that

$$(Cu^{II}) = \frac{T_{Cu^{II}}}{k'_1k'_2k'_3k'_4a^4_{NH_3} + k'_1k'_2k'_3k'_4k'_5a^5_{NH_3}} \quad (2)$$

where a_{NH_3} is the activity of the ammonia. Also, since $(CN^-) = T_{CN^-} = T^\circ_{CN^-} - 4T_{Cu^{II}} + 4T^\circ_{Cu^{II}}$ from stoichiometry, the integrable rate equation is

$$-R = \frac{kK_{II}(T_{Cu^{II}})(T^\circ_{CN^-} - 4T^\circ_{Cu^{II}} + 4T_{Cu^{II}})^4}{k'_1\cdots k'_4a^4_{NH_3} - k'_1\cdots k'_5a^5_{NH_3}} \quad (3)$$

$$-R = kK'(T_{Cu^{II}})(T^\circ_{CN^-} - 4T^\circ_{Cu^{II}} - 4T_{Cu^{II}})^4 \quad (4)$$

Equation (4) reduces to (1) at zero time. Integration of (4) gives

$$\ln\frac{1}{x} + 12x - 24x^2 + 64x^3 - \left(\ln\frac{1}{x_0} + 12x_0 - 24x_0^2 + 64x_0^3\right) = kK'(T^\circ_{CN^-} - 4T^\circ_{Cu^{II}})^4 \times t \quad (5)$$

where $x = T_{Cu^{II}}/T^\circ_{CN^-} - 4T^\circ_{Cu^{II}} + 4T_{Cu^{II}})$ and x_0 refers to zero time. Equation (6), $X - X_0 = K''t$, corresponding to (5) is valid for all conditions other than $T^\circ_{CN^-} - 4T^\circ_{Cu^{II}} = 0$, when (4) must be reintegrated.

The slow reaction may involve $Cu(CN)_4(NH_3)^=$ rather than $Cu(CN)_4^=$ as the disproportionating species, and in this case (2) is replaced by

$$(Cu(NH_3)^{II}) = \frac{T_{Cu^{II}}}{k'_2k'_3k'_4a^3_{NH_3} + k'_2k'_3k'_4k'_5a^4_{NH_3}} \quad (7)$$

K' now becomes

$$\frac{K_{VI}}{k_2'k_3'k_4'a_{NH_3}^3 + k_2' \cdots k_6'a_{NH_3}^4} \quad (8)$$

A similar treatment could be given for an intermediate complex of $Cu(CN)_4(NH_3)_2^=$.

The validity of the mechanism which has been postulated may be experimentally verified by the use of (6), for the product kK' should be independent of copper(II) and cyanide concentrations. The role of ammonia in the intermediate complex is carried in K', per equation (4) or (8). For the excessive ammonia concentrations, K' is a true constant. Plots were prepared where the left side of equation (6) was calculated and graphed *vs.* t. Figure 3 exemplifies these plots. The lines which resulted were straight and had the slopes, K'', indicated in column 4 in Table I.

TABLE I

PSEUDO AND TRUE CONSTANTS FOR $\mu = 1$, $T = 0°$

T_{NH_3}	T^0_{CuII}	$T^0_{CN^-}$	K''	kK_{II} for $Cu(CN)_4^=$	kK_{IV} for $Cu(CN)_4(NH_3)^=$
12.5	0.00125	0.0150	5.3×10^5	2.8×10^{26}	3.3×10^{30}
	.00125	.0100	4.8×10^5	2.7	3.2
	.00150	.0120	4.9×10^5	2.7	3.2
	.00150	.00900	7.0×10^5	3.6	4.2
	.00200	.00800	.....	3.0	3.6
	.00250	.0100	.....	2.9	3.4
	.00300	.00900	5.3×10^5	2.8	3.3
	.00600	.0120	4.8×10^5	2.5	3.0
	.00600	.00900	6.3×10^5	3.3	3.9
	.00600	.00600	5.1×10^5	2.7	3.2
11.2	.00300	.00900	9.9×10^5	2.8×10^{26}	4.0×10^{30}
	.00300	.00600	9.2×10^5	2.8	4.0
10.5	.00200	.00600	1.2×10^6	2.9×10^{26}	4.1×10^{26}

The last two columns of Table I indicate the results of an attempt to determine the role of ammonia in the reaction by calculating the denominator of K' in the two mechanisms mentioned previously. If we now substitute the formal concentrations of ammonia, T_{NH_3}, for activities, the denominator of K' in (4) becomes $2.4 \times 10^{15}\ T^4_{NH_3} + 1.5 \times 10^{15}\ T^5_{NH_3}$ or in (8), $3.6 \times 10^{10}\ T^5_{NH_3} + 2.3 \times 10^{10}\ T^4_{NH_3}$. The values of kK_{II} and kK_{IV} in Table I are calculated under these conditions and should therefore be considered as independent of variations in copper(II), cyanide or ammonia. These values definitely disallow any categorical statements regarding the function of ammonia in the reaction, except that ammonia greatly lowers the rate in closest agreement with the assumption that $Cu(CN)_4^=$ is the intermediate species. The high inverse dependence of the rate on ammonia concentration precluded the possibility of obtaining data over wide ammonia variations.

In searching for a reason why four CN^- ions must be in the complex for the reaction to proceed, we tentatively arrived at the conclusion that cuprous cyanide complexes having less than three cyanides must have very high free energy, too high to represent to any measurable extent the kinetic product of the reaction. Another way of saying essentially the same thing is that the activated complex must have substantially the properties of the product, and the high energy products represent activated complexes of considerably higher free energy than that involving four cyanide ions.

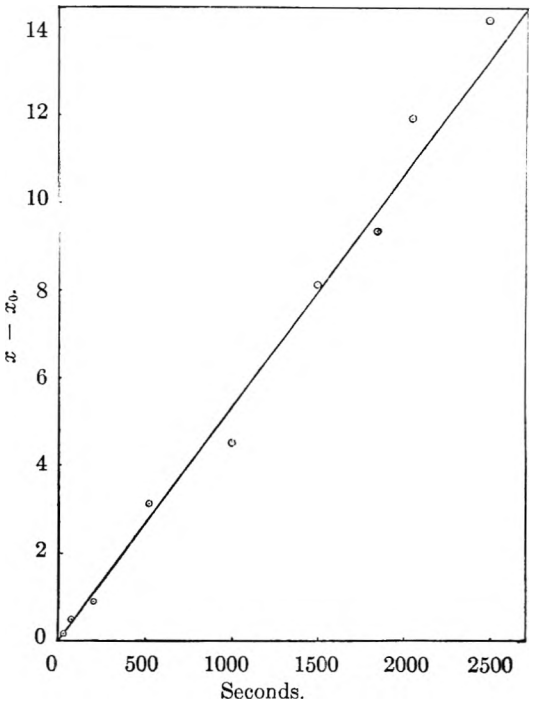

Fig. 3.—Plot testing equation (6).

This work was performed in the Ames Laboratory of the Atomic Energy Commission.

REMARKS

ROBERT E. CONNICK: The authors have stressed an interpretation of the data in terms of an activated complex structurally very similar to known or plausible complex ions. It should be pointed out that such a picture is not unique and the activated complex may consist of an arrangement of atoms quite unlike the stable complex ion. The kinetic data will be fitted equally well as long as the stoichiometric composition of the activated complex is the same.

Thus one could interpret a first order rate law for the decomposition of the ceric–glycol complex in two steps: first, the dissociation of the complex into ceric ion and glycol; and, second, the collision of these two species to form the activated complex. The geometrical arrangement in space of the ceric ion and glycol might be completely unlike that of the stable complex.

Such an interpretation, when applied to the copper cyanide reaction gives a plausible rationalization of the observed fourth order dependence on cyanide ion concentration. Thus the activated complex may consist of the copper with three cyanide groups arranged around it in positions similar to those found in the product, $Cu(CN)_3^{--}$. The fourth cyanide ion would be the one oxidized and could have a position completely unrelated to any stable complex ion. For example, it may be turned 180° from its normal coordination configuration.

It is of course impossible to deduce from kinetic data the structural arrangement of the atoms within the activated complex.

REPLY: My attitude on this question is consistent with the principle of accepting the simpler of two possible alternatives which cannot be distinguished.

Further, the existence of an interatomic orbital involving the oxidant and reductant could provide a convenient path for the electrons. Perhaps compelling evidence will show up in the future in favor of one or the other of these possible views.

I agree with Dr. Connick that both points of view should be presented for the sake of scientific completeness.

MECHANISM OF SUBSTITUTION REACTIONS IN COMPLEX IONS. I. KINETICS OF THE AQUATION AND HYDROLYSIS OF SOME C-SUBSTITUTED ACETATOPENTAMMINECOBALT(III) IONS[1]

BY FRED BASOLO, JOHN G. BERGMANN AND RALPH G. PEARSON

Department of Chemistry, Northwestern University, Evanston, Illinois

Received August 30, 1951

The rates of aquation and hydrolysis of several C-substituted acetatopentamminecobalt(III) ions have been measured. These have been found to be dependent upon the base strength of the coördinated ligand but independent of its size. This has been interpreted to mean either that the incoming group approaches the complex largely from a position opposite to that of the group being displaced or that the substitution occurs by means of an ionization mechanism. In addition it was found that there is a hundredfold spread in the rates of hydrolysis as compared to only tenfold for the rates of aquation in the same series of ions containing ligands of different base strengths. This has been interpreted as being due to a change in the residual positive charge on the central cobalt atom having a greater effect on the approach of a negatively charged hydroxide ion than on that of a neutral water molecule.

I. Introduction

The mechanism of substitution reactions in complex ions has been of interest to coördination chemist ever since the acceptance of Werner's coordination theory of valence. Some of the approaches to an elucidation of these mechanisms have included studies in stereochemistry[2-5] chemical kinetics[6,7,8] and isotope exchange.[9,10] Bailar has written an excellent review on the stereochemistry of complex compounds[11] in which he summarizes some of the views on this subject of reaction mechanism. Werner has interpreted his observations as being indicative of no correlation between the positions occupied by the incoming and outgoing groups during a substitution reaction. It would be of interest to know, however, if the incoming group approaches the complex from the same side or from a position opposite to that of the outgoing group. In an attempt to contribute to the solution of this problem, an investigation has been made of the reaction rates of various C-substituted acetatopentamminecobalt(III) ions. The rates of aquation and hydrolysis have been determined for two series of such complex ions, one containing acetato groups of different base strength while the other contains acetato groups of analogous base strength but of different steric requirements.

II. Experimental

A. Preparation of Compounds.—The starting material used for the synthesis of the necessary compounds was carbonatopentamminecobalt(III) nitrate made according to the procedure of Werner and Goslings.[12] In general all of the acetato complexes were prepared by the reaction of the carbonato complex with an excess of the desired acid. The techniques employed to isolate these salts from solution varied slightly depending upon their solubility characteristics. In every case the compound was analyzed for ammonia using the method described by Horan and Eppig.[13]

The general method of synthesis may be illustrated by a description of the procedure for the preparation of acetatopentamminecobalt(III) nitrate. Five grams (0.018 mol) of carbonatopentamminecobalt(III) nitrate is suspended in 15 ml. of water and 12 g. (0.2 mol) of glacial acetic acid is added. The reaction mixture is concentrated on a steam-bath for 90 min. during which time a red crystalline salt separates. After cooling to room temperature, 50 ml. of water is added and the product is collected on a filter. The mother liquor is removed from the filter flask and then the salt is washed with 50 ml. of cold water followed by alcohol and ether and dried at 50°; yield 3 g. *Anal.* Calcd. for $[Co(NH_3)_5C_2H_3O_2](NO_3)_2$: NH_3, 26.0. Found: NH_3, 26.2. An additional 2 g. (over-all yield 83%) of the salt may be obtained by adding 15 g. of ammonium nitrate to the mother liquor. The precipitated salt is collected, washed and dried as described above.

Essentially the same procedure was used for the preparation of all these compounds except that in every case other than that of the acetato complex the salts were sufficiently soluble so they did not separate during the digestion of the reaction mixture. In all instances, except for the isobutyrate and pivalate, the nitrate compounds were separated from the solution by the addition of an excess of ammonium nitrate to the reaction mixture. In case of the isobutyrato and pivalato derivatives, these were isolated by the addition of the concentrates to absolute alcohol. All of the complexes were isolated as the nitrate salts. Good evidence that the complex ions contain the acetato groups and not nitrate comes from the fact that under these same conditions the aquation of $[Co(NH_3)_5NO_3]^{+2}$ is much more rapid—$k(70°)$ $(min.^{-1}) = 2 \times 10^{-1}$.

B. Procedure for Determining the Rates of Aquation.—The aquation reaction for all of these complex ions may be illustrated by the equation $[Co(NH_3)_5X]^{+2} + H_2O \rightarrow [Co(NH_3)_5H_2O]^{+3} + X^-$. The aquo complex, $[Co(NH_3)_5H_2O]^{+3}$, resulting from this aquation is an acid of ionization constant $2.04 + 10^{-6}$.[14] The rates of aquation were followed by titrating the amounts of this acid produced using a standard solution of sodium hydroxide. It was found that thymol blue served as a suitable indicator, providing the concentration of the complex did not exceed 0.01 *M*. The aquations were all run at 70 ± 0.05°, with solutions approximately 0.004 *M* in complex containing two equivalents of perchloric acid. From time to time samples (25 ml.) were withdrawn and discharged into some cracked ice to quench the reaction. The solution was then titrated with 0.0755 *N* NaOH from a microburet graduated directly to 0.01 ml. Rate constants were obtained by plotting the usual first order expression against the time.

C. Procedure for Determining the Rates of Hydrolysis.—The hydrolysis reaction for all of these complex ions may

(1) This investigation was supported by a grant from the United States Atomic Energy Commission under Contract AT(11-1)-89-Project No. 2.

(2) A. Werner, *Ber.*, **44**, 873 (1911); *Ann.*, **386**, 1 (1912).

(3) A. Werner, *Ber.*, **45**, 1228 (1912).

(4) J. C. Bailar, Jr., and W. Auten, *J. Am. Chem. Soc.*, **56**, 774 (1934).

(5) J. C. Bailar, Jr., J. H. Haslam and Eldon M. Jones, *ibid.*, **58**, 2226 (1936).

(6) A. B. Lamb and J. W. Marden, *ibid.*, **33**, 1873 (1911).

(7) J. N. Brönsted, *Z. physik. Chem.*, **122**, 383 (1926).

(8) F. J. Garrick, *Trans. Faraday Soc.*, **34**, 1088 (1938); *Nature*, **139**, 507 (1937).

(9) G. W. Ettle and C. H. Johnson, *J. Chem. Soc.*, 1490 (1939).

(10) A. W. Adamson, J. P. Welker and M. Volpe, *J. Am. Chem. Soc.*, **72**, 4030 (1950).

(11) J. C. Bailar, Jr., *Chem. Revs.*, **19**, 67 (1936).

(12) A. Werner and N. Goslings, *Ber.*, **36**, 2380 (1903).

(13) H. A. Horan and H. J. Eppig, *J. Am. Chem. Soc.*, **71**, 581 (1949).

(14) J. N. Brönsted and K. Volqvartz, *ibid.*, **134**, 97 (1928).

be designated by the equation $[Co(NH_3)_5X]^{+2} + OH^- \rightarrow [Co(NH_3)_5OH]^{+2} + X^-$. The procedure used to follow the rate of hydrolysis is similar to that described for the aquation reaction. However, in this case the unreacted hydroxide ion is determined by titration with standard hydrochloric acid using thymol blue as an indicator. The hydrolyses were carried out at 25 ± 0.05° with solutions approximately 0.004 *M* in complex plus an equivalent amount of sodium hydroxide. The usual second order function was plotted against time to get the rate constants.

III. Results and Discussion

A. Acetato Groups with Different Base Strengths.—Among the simplest substituted acetic acids having appreciably different dissociation constants are the haloacetic acids. The base strength of the anions of these acids will vary inversely as the dissociation constant of the corresponding acids. Accordingly, the reaction rates of the trifluo-, trichloro-, dichloro- and monochloroacetatopentamminecobalt(III) nitrates have been investigated. Some representative data collected on the aquation reactions are plotted in Fig. 1 and for the hydrolysis reactions in Fig. 2. In all cases duplicate runs were made with better than ±10% precision in the value for the rate constant.

The rate constants for these reactions along with those for the glycolato and acetato derivatives are summarized in Table I.

TABLE I

ACETATO GROUPS WITH DIFFERENT NUCLEOPHILIC CHARACTER

$Co(NH_3)_5X(NO_3)_2$ X⁻	Diss. const. H X	Aquation, 70° k (min.⁻¹)	Hydrolysis 25° k (liters mole⁻¹ min.⁻¹)
CF_3COO	5×10^{-1}	3.3×10^{-3}	4.4
CCl_3COO^-	2×10^{-1}	3.2×10^{-3}	4.3
$CHCl_2COO^-$	5×10^{-2}	9.6×10^{-4}	1.6
CH_2ClCOO^-	1.4×10^{-3}	3.5×10^{-4}	2.5×10^{-1}
CH_2OHCOO^-	1.5×10^{-4}		7.0×10^{-2}
CH_3COO^-	1.8×10^{-5}	4.9×10^{-4}	4.2×10^{-2}

It can be seen that considerable correlation is found between rates of reaction and the acidity of the particular coördinated acetato group. That the correlation is not perfect is clearly illustrated in Fig. 5. It is felt that some of the discrepancies may result from the experimental difficulties encountered in making accurate measurements of these rate constants. Unfortunately all of these complex ions in solution have a tendency to liberate ammonia as typified for the aquation reaction by the equation

$$[Co(NH_3)_5X]^{+2} + (n+1)H_2O \longrightarrow [Co(NH_3)_{5-n}(H_2O)_{n+1}]^{+3} + X^- + nNH_3$$

and for the hydrolysis reaction by

$$[Co(NH_3)_5X]^{+2} + (n+1)OH^- \longrightarrow [Co(NH_3)_{5-n}(OH)_{n+1}]^{+3-n} + X + nNH_3$$

Lamb and Marden[6] experienced this same difficulty and made a study of this decomposition of acidopentamminecobalt(III) ions showing that the evolution of ammonia appears to be autocatalyzed. Actually what appears to happen is that the first ammonia molecule comes off from the complex ion with difficulty, but then the next four ammonias are displaced rather readily. That ammonia is liberated during these reactions was confirmed by sweeping the ammonia out of the reaction mixture with a stream of air and into a solution containing Nessler reagent.

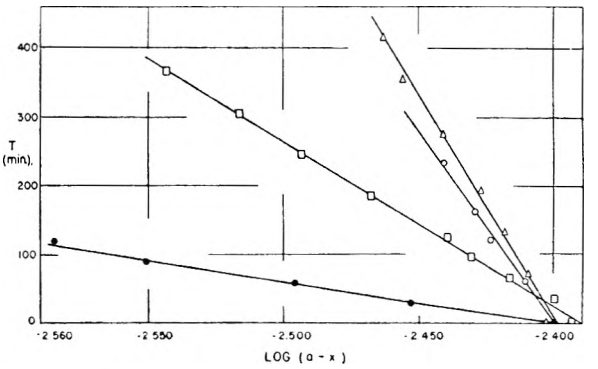

Fig. 1.—Aquation of $[Co(NH_3)_5 X]^{+2}$ at 70°: X^- = ●, CCl_3COO^-; Δ, CH_2ClCOO^-; □, CH_2ClCOO^-; ○, CH_3COO^-.

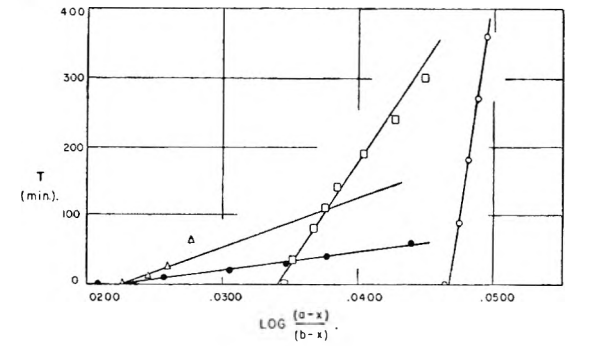

Fig. 2.—Hydrolysis of $[Co(NH_3)_5 X]^{+2}$ at 25°: X^- = ●, CCl_3COO^-; □, CH_2ClCOO^-; Δ, $CHCl_2COO^-$; ○, CH_3COO^-.

This was done with the aquation reactions after the excess acid had been neutralized with sodium carbonate. Qualitative tests of this type resulted in only very faint or no coloration of the Nessler solution after the mixture had been allowed to stand at the conditions of our experiment for less than four hours. However, after standing for a period longer than five hours there resulted a marked coloration of the Nessler solution indicating that appreciable quantities of ammonia had been evolved.

As soon as an appreciable amount of ammonia is released, data collected by the titration method become meaningless. For this reason most of the rates reported in Table I and II are for the initial stages of the reaction, from 5 to 10% completion. However, the stronger acids are displaced rapidly enough compared to ammonia so that their complexes may be followed considerably further (up to 60% for trifluoracetato). The assumed kinetics, first order for aquation and second order for hyrolysis, were based chiefly on the results obtained from these more rapid reactions. Also the possible effect of hydrogen ion on the rate of the aquation reaction was checked for the trifluoracetato and for the acetato complexes. The rates were found to be the same in 0.004 and 0.008 *M* acid so that catalysis by hydrogen ions is not important. Likewise the hydroxide ion concentration has been varied in the hydrolysis of the trichloroacetato and isobutyrato complexes. In all cases there was found a first order rate dependence upon the concentration of hydroxide ion.

It is of interest to note that the hydrolysis curve of Fig. 5 is more nearly linear than would be an an-

alogous curve for the aquation reactions. Also the spread in the rates of hydrolysis (100-fold) is greater than the spread in the rates of aquation (10-fold). This is reasonable if it is assumed that the effect of changing the nature of the acid ligand works in two ways. First, the stronger acid ligand forms a weaker bond with the central cobalt ion and is more easily removed than a weaker acid ligand. This would be true if the process of removing a substituted acetate ion from a positive cobalt ion is similar to the process of removing it from a positive hydrogen ion. Second, the stronger acid group leaves a greater effective positive charge on the central cobalt ion. This would greatly facilitate the approach of a negatively charged hydroxide ion, but would have only a small effect on the approach of a neutral water molecule.

B. Acetato Groups with Comparable Base Strength but Different Steric Requirements.—A second series of "substituted" acetic acids were chosen in which the dissociation constants are not too different. However, in this series the hydrogen atoms attached to the methyl group in acetic acid are progressively replaced by methyl groups—*i.e.*, CH_3CH_2COOH, $(CH_3)_2CHCOOH$, and $(CH_3)_3CCOOH$. The data collected for the rates of aquation and hydrolysis of the acidopentamine-cobalt(III) ions containing these "substituted" acetato groups are plotted in Figs. 3 and 4. The rate constants for these reactions are summarized in Table II.

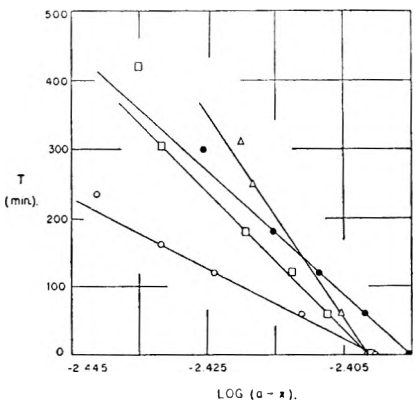

Fig. 3.—Aquation of $[Co(NH_3)_5X]^{+2}$ at 70°: X^- = ○, CH_3COO^-; △, $(CH_3)_2CHCOO^-$; □, $CH_3CH_2COO^-$; ●, $(CH_3)_3CCOO^-$.

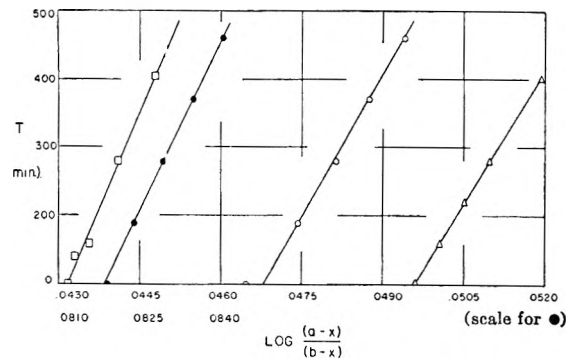

Fig. 4.—Hydrolysis of $[Co(NH_3)_5X]^{+2}$ at 25°: X^- = ○, CH_3COO^-; □, $CH_3CH_2COO^-$; △, $(CH_3)_2CHCOO^-$; ●, $(CH_3)_3CCOO^-$.

TABLE II

"ACETATO" GROUPS WITH DIFFERENT STERIC REQUIREMENTS

$Co(NH_3)_5X(NO_3)_2$ X⁻	Diss. const. H X × 10⁻⁵	Aquation 70° k (min.⁻¹) × 10⁻⁴	Hydrolysis 25° k (liters mole⁻¹ min.⁻¹) × 10⁻²
CH_3COO^-	1.8	4.9	4.2
$CH_3CH_2COO^-$	1.4	1.9	2.7
$(CH_3)_2CHCOO^-$	1.5	1.6	3.4
$(CH_3)_3CCOO^-$	1.0	2.6	1.8

These results indicate that the rates of aquation and of hydrolysis for these complexes are at least comparable. These reactions could not be followed to more than 10% completion because of interference due to the evolution of ammonia as previously described. It is therefore felt that some of the variations observed may well be attributed to the experimental difficulties.

IV. Conclusions

A consideration of molecular models[15] clearly shows that an approach to the central metal atom by the incoming group from the same side as that of the group being displaced becomes increasingly more difficult as the size of the group attached to the carboxyl gets larger. In all of the compounds investigated, an approach from a position opposite to that of the group being displaced is equally available. Since the rate data indicate that comparable rates of aquation and hydrolysis are observed if the groups have similar base strengths regardless of the steric hindrance at the front of the ion, it seems reasonable to conclude that in these examples either the incoming group approaches the complex largely from the back side (side opposite to the outgoing group) or the substitution occurs by means of an ionization mechanism. Additional support is given to this supposition by the fact that even in the series of compounds where the basic property of the coördinated groups do change, the relative rates of reaction are those to be expected without taking into account the frontal steric changes accompanying these changes in nucleophilic properties as shown in Fig. 5.

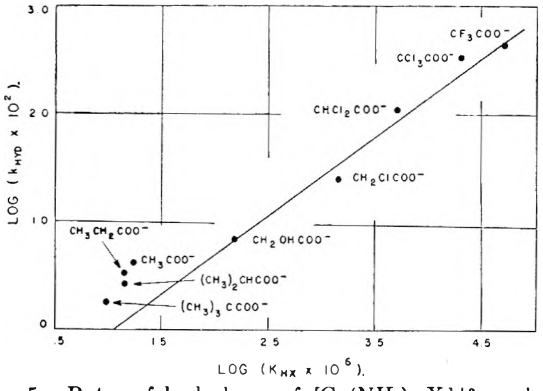

Fig. 5.—Rates of hydrolyses of $[Co(NH_3)_5X]^{+2}$ *vs.* base strengths of X^-.

(15) The central cobalt(III) atomic model was constructed using the hexacovalent radius of Co(III) given by Pauling[16] and the linear scale dimensions of 1 cm. in the model equal to 1 Å. in the atom adopted for the Fisher-Hirschfelder-Taylor atom models.

(16) L. Pauling, "The Nature of the Chemical Bond," Cornell University Press, Ithaca, N. Y., 1945, p. 182.

REMARKS

VICTOR K. LAMER: What is the slope of the line in the plot in Fig. 5 of the log of the specific rate of hydrolysis against the log of the base strength of the group being replaced?

RESPONSE: The line has a slope of approximately 0.8.

F. R. DUKE: On what basis is the S_N2 mechanism for the reactions postulated?

RESPONSE: Both kinetic and stereochemical data on numerous substitution reactions involving cobalt(III) complexes suggest the reaction path is primarily that commonly referred to as S_N2. Although this appears plausible since it has been shown by various investigators that these reactions are second order and likewise they are not accompanied by racemization, it has not been unequivocally established.

HENRY TAUBE: How do you know that the C–O bond is not broken rather than the Co–O bond when the groups are replaced? Tracer experiments conducted by J. P. Hunt and A. C. Rutenberg at the University of Chicago show that in the replacement by water of carbonate in $Co(NH_3)_5CO_3^+$ the C–O bond is severed rather than the Co–O bond.

RESPONSE: To begin with I do not feel the two systems are analogous as the evolution of carbon dioxide may well enhance the breaking of the carbon–oxygen bond. I am also of the opinion that our results would support cleavage of the cobalt–oxygen bond. If the bond broke between carbon and oxygen one may expect that the rates of reaction would decrease with increasing steric hindrance as is the case with the hydrolysis of esters. Since we found that the rates of reactions were not dependent on steric hindrance, it would appear that the approach is from the opposite side of the cobalt which remains unchanged. This in turn suggests that the cleavage occurs between cobalt and oxygen.

COMPLEX IONS FROM IRON AND ETHYLENEDIAMINETETRAACETATE: GENERAL PROPERTIES AND RADIOACTIVE EXCHANGE

BY S. S. JONES[1] AND F. A. LONG

Department of Chemistry, Cornell University, Ithaca, N. Y.

Received August 30, 1951

The complex ion formed from ferrous ion and ethylenediamine tetraacetate ion, $FeY^=$, has a dissociation constant of about 10^{-14}. It is easily and rapidly oxidized to the ferric complex. The acid H_2FeY is quite strong as is HFeY. The ferric complex is much more stable; the dissociation constant, determined by a radioactive indicator method is about 10^{-24}. However $FeY^=$ undergoes photosensitized reduction in the presence of sunlight. The radioactive exchange between the iron of $FeY^=$ and Fe^{++} is instantaneous at *p*H values of from 2 to 5. The analogous ferric exchange at 25° is much slower. In the *p*H range from 1 to 2.5 the rate of exchange depends on *p*H in a complex manner and analysis of the exchange data shows that at least three separate kinetic terms enter.

Introduction

Ethylenediaminetetraacetate ion, which is customarily abbreviated as $Y^{==}$, forms stable complexes with a variety of di- and trivalent metal ions. The ratio of metal to ethylenediaminetetraacetate is invariably one and since the latter ion contains six potential coördinating groups, there is the interesting possibility that the $Y^{==}$ ion alone is so arranged around the metal ion as to give an octahedral structure. Early studies on the complex ions were made principally by Pfeiffer[2–4] and Brintzinger[5–7] and co-workers. Schwarzenbach and coworkers[8–14] have studied several of the complexes with emphasis on the analytical applications. Of particular interest are the *pK* values of the acid H_4Y; according to Schwarzenbach and Ackerman[10] in 0.1 molar potassium chloride at 20°, these are: $pK_1 = 2.00$; $pK_2 = 2.67$; $pK_3 = 6.16$; $pK_4 = 10.26$.

Very little has been reported on the complex of ferrous ion and ethylenediaminetetraacetate. Schwarzenbach and Biedermann[12] mention somewhat incidentally that ferrous ion is one of several divalent metal ions which can be determined quantitatively with this complexing agent, which implies that the complex is moderately stable. The ferric complex has been studied somewhat more extensively. Brintzinger prepared the compounds HFeY and $NH_4FeY \cdot H_2O$ and discussed qualitatively the properties of solutions of the complex ion. He concluded that the complex is relatively unstable. Klemm[15] reports that the compound HFeY has a magnetic susceptibility similar to that of ferric salts and concludes that the bonding in FeY^- is ionic. Schwarzenbach, *et al.*,[12] studied the titration curves of mixtures of ferric ion and Na_2H_2Y and concluded that in basic solution the complex becomes $FeYOH^=$.

One way to obtain information on the stability of complex ions is to study the rate of exchange of the metal ion in the complex with the free metal ion using radioactive indicators. Preliminary studies on the radioactive exchange of several complex ions of $Y^{==}$ with the hydrated metal ions have been reported earlier[16] and it was shown that the ferric, cobaltic and nickelous complexes exhibited slow exchange whereas the ferrous and cobaltous complexes underwent rapid exchange. When, as is the case with the ferric complex, the exchange is slow

(1) Knolls Atomic Power Laboratory, General Electric Company, Schenectady, N. Y.

(2) P. Pfeiffer and W. Offermann, *Ber.*, **75B**, 1 (1942).

(3) P. Pfeiffer and H. Simons, *ibid.*, **76B**, 847 (1943).

(4) P. Pfeiffer, *ibid.*, **77A**, 59 (1944).

(5) H. Brintzinger and G. Hesse, *Z. anorg. allgem. Chem.*, **249**, 113 (1942).

(6) H. Brintzinger, H. Thiele and U. Müller, *ibid.*, **251**, 285 (1943).

(7) H. Brintzinger and S. Munkelt, *ibid.*, **256**, 65 (1948).

(8) G. Schwarzenbach, *Helv. Chim. Acta*, **29**, 1338 (1946).

(9) G. Schwarzenbach, W. Biedermann and F. Bangerter, *ibid.*, **29**, 811 (1946).

(10) G. Schwarzenbach and H. Ackermann, *ibid.*, **30**, 1798 (1947).

(11) G. Schwarzenbach and H. Ackermann, *ibid.*, **31**, 1029 (1948).

(12) G. Schwarzenbach and W. Biedermann, *ibid.*, **31**, 459 (1948).

(13) G. Schwarzenbach and W. Biedermann, *Chimia*, **2**, 56 (1948).

(14) G. Schwarzenbach, *Helv. Chim. Acta*, **32**, 839 (1949).

(15) W. Klemm, *Z. anorg. allgem. Chem.*, **252**, 225 (1944).

(16) F. A. Long, S. S. Jones and M. Burke, Brookhaven Conference Report No. BNL-C-8 (1948).

but measurable it is of additional interest to determine the rate law.

The following sections give the results of a more detailed study of the ferrous and ferric complexes. These studies show that the ferric complex is actually highly stable whereas the ferrous complex is relatively unstable with respect both to dissociation and to oxidation. The radioactive exchange of ferric iron in the complex with free ferric ions is shown to be *p*H dependent and to follow a complex rate law.

Materials and Procedures

Ethylenediaminetetraacetic acid was obtained in a specially purified grade from the Bersworth Chemical Company of Framingham, Massachusetts. It was dried in a vacuum oven at 60° for 12 to 24 hours before use. Titration curves indicated a purity of 100 ± 1% for the dried acid.

Radioactive iron, a mixture of Fe^{55} and Fe^{59}, was obtained as a ferric chloride solution from the Atomic Energy Commission, Oak Ridge, Tennessee. The iron was freed from radioactive impurities, principally Co^{60}, by extraction of the ferric chloride solution with diethyl or diisopropyl ether. Radioferric sulfate was prepared by repeated evaporation of ferric chloride solution to near-dryness with sulfuric acid. Active ferrous sulfate solutions were prepared by reduction of radioferric sulfate with hydroxylamine sulfate. Radioferric perchlorate solutions were made by repeated precipitation of the hydroxide which was finally dissolved in an accurately known quantity of perchloric acid. Other chemicals were of reagent grade.

Two solid compounds of the ferric complex, $NH_4FeY \cdot H_2O$ and HFeY, were prepared using procedures similar to that of Brintzinger, *et al.*[6] Due to the manner of preparation the ammonium salt contained small amounts of impurities. However, the acid, HFeY, was quite pure.

ANALYSIS OF THE DRIED ACID

	C, %	H, %	N, %	Fe, %
Observed	34.97	4.24	7.97	16.07
Observed	34.79	3.69	8.13	16.08
Observed	...	..	..	16.10
Calcd. for HFeY	34.80	3.80	8.12	16.18

Comparison with the theoretical analysis for the formula HFeY clearly shows that there is no water in the coördination sphere of the acid. This fact was further confirmed by titration of the acid with standard base.

Absorption spectra were determined with a model DU Beckman quartz spectrophotometer. Measurements of *p*H were made with a laboratory model Beckman *p*H meter. Except where noted otherwise, all exchange runs were carried out at 25.00 ± 0.1°. Precipitation was carried out in fritted glass funnels and solutions of the separated exchange species were diluted in volumetric containers for counting.

The iron in a few of the solutions was electroplated on copper disks using a procedure similar to that described by Hahn.[17] However, in most cases the solutions were counted directly. To accomplish this, a dipping counter of the sort described by Solomon and Estes[18] was surrounded by a glass jacket in such a way that solutions could be poured in at the top, counted, and removed through a stopcock at the bottom. Solutions of the complex did not cause counting difficulties but it was necessary to count ferric ion in strongly acid solutions to prevent the adsorption of ferric ion or its hydrolysis products on the glass surface. As long as water solutions of roughly the same salt content were counted, no correction for differences in radiation absorption was needed. Background and coincidence corrections were made on all counts.

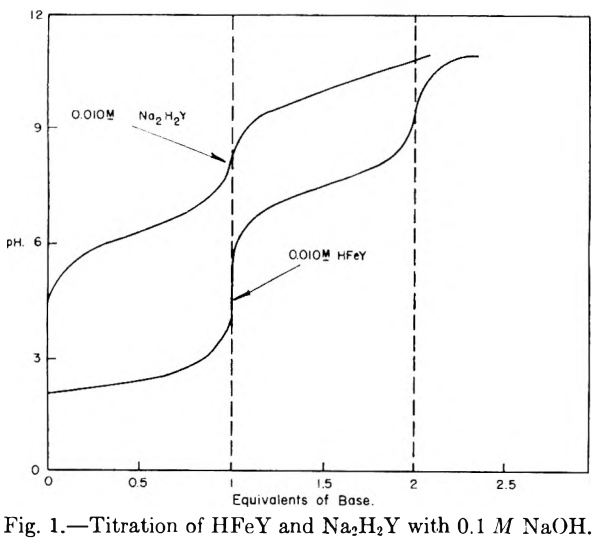

Fig. 1.—Titration of HFeY and Na_2H_2Y with 0.1 *M* NaOH.

Properties of the Ferric Complex.—A solution of FeY^- is stable to acidified permanganate at room temperature. Sulfide solutions cause a color change followed by partial precipitation. Thiocyanate ion causes a definite color change with moderately acid solutions of the complex, but the normal red color of the ferric thiocyanate complex is produced only when the solutions are highly acid. The FeY^- complex does not react with orthophenanthroline. It is not decomposed by phthalate, benzoate or phosphate ions (at *p*H 5) or by an ammonia–ammonium ion buffer. It is however decomposed by alkali hydroxides giving ferric hydroxide; cupferron also precipitates the iron.

Titration Curves.—The titration of the acid HFeY is compared in Fig. 1 with the last half of the curve for the acid H_4Y. The latter is clearly a weak acid and breaks are evident for neutralization of the second and third protons. In contrast HFeY, down to *p*H 7, behaves like a completely strong monobasic acid. However, at still higher *p*H values a second inflection occurs and, as noted by Schwarzenbach,[12] this is accompanied by a color change which is without doubt due to formation of the complex, $FeYOH^=$.

Spectrum.—Figure 2 gives the absorption spectrum of the ferric complex at high and low *p*H and also the spectrum of the ferrous complex. For all solutions the complex was 0.0125 molar and the absorption path length was 1.00 cm. The absorp-

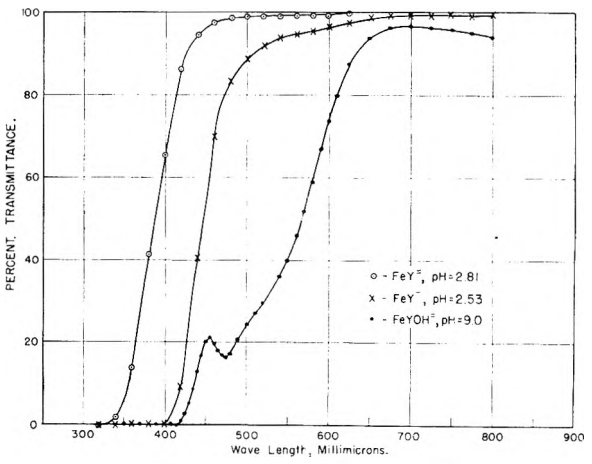

Fig. 2.—Absorption spectra: solutions are 0.0125 *M*; path length is 1.00 cm.

(17) P. F. Hahn, *Ind. Eng. Chem., Anal. Ed.*, **17**, 45 (1945).

(18) A. K. Solomon and H. D. Estes, *Rev. Sci. Instruments*, **19**, 47 (1948).

tion of the ferric complex at *p*H 2.5 is such as to give a yellow color to the solution. At *p*H 9 the absorption band has moved considerably into the longer wave lengths so that the complex $FeYOH^{=}$ has deeper orange color. In contrast to these the ferrous complex appears to be essentially colorless. An incidental point is that solutions of the ferric complex obey Beer's law.

The continuous variation method of Job[19] as modified by Vosburgh[20] has been used to determine whether FeY^{-} is the only complex formed in acid solution. The procedure is to mix two solutions of equal molarities, one of ferric ion and one of complexing agent in differing ratios and then measure the optical densities of the mixtures at selected wave lengths. One plots Z, the difference between observed optical density and that calculated assuming no reaction, against a composition function, X. Z will be a maximum or minimum for a composition where the reactants are combined just in reacting proportions. In the present case solutions were prepared by mixing 0.0025 molar phthalate buffered solutions of Na_2H_2Y and ferrous sulfate and then oxidizing to obtain the ferric complex. All solutions were at *p*H 2.75 ± 0.1 and optical densities were measured at wave lengths 360, 380 and 400 millimicrons. Figure 3 gives the results. The ordinates are $Z = D - L[e_1M(1 - X) + e_2MX]$ and X, where X is volume fraction of Na_2H_2Y solution in the mixture, e_1 and e_2 are molar extinction coefficients for ferrous and Na_2H_2Y solutions, respectively; M is the molarity of solutions used, L is optical path length and D is observed optical density. For all three wave lengths the Z *versus* X plots are essentially intersecting straight lines with a maximum at $X = 0.5$. This result indicates that the only complex formed under these conditions is FeY^{-}, *i.e.*, a 1:1 ratio of ferric and complexing agent.

Photosensitivity.—Solutions of FeY^{-} are stable indefinitely when stored in the dark or even in red glass containers. However in sunlight the complex undergoes a light induced reduction rather similar to that observed with solutions of ferrioxalate and ferricitrate ions. Studies have been made of this photosensitized reduction using 0.01 molar solutions of the ferric complex at high and low acidity and with and without contact with air. At either high or low acidity a solution of FeY^{-} in a Pyrex glass container is converted to the colorless ferrous complex after standing in sunlight for a few hours. The reaction may be represented approximately as

$$FeY^{-} + h\nu = FeY^{=} + \text{Decomp. Pdts. of } H_4Y$$

If the resulting solution is now kept in the dark and exposed to air the ferric complex is reformed by the reaction

$$FeY^{=} + 1/2\ H_2O + 1/4\ O_2 = FeY^{-} + OH^{-}$$

Since this reaction produces hydroxide ions, if less than one equivalent of acid was initially present some of the hydroxy complex, $FeYOH^{=}$, is formed and the oxidized solution will have an orange color.

(19) P. Job, *Ann. Chim.* (10) **9**, 113 (1928).

(20) W. C. Vosburgh and G. R. Cooper, *J. Am. Chem. Soc.*, **63**, 437 (1941).

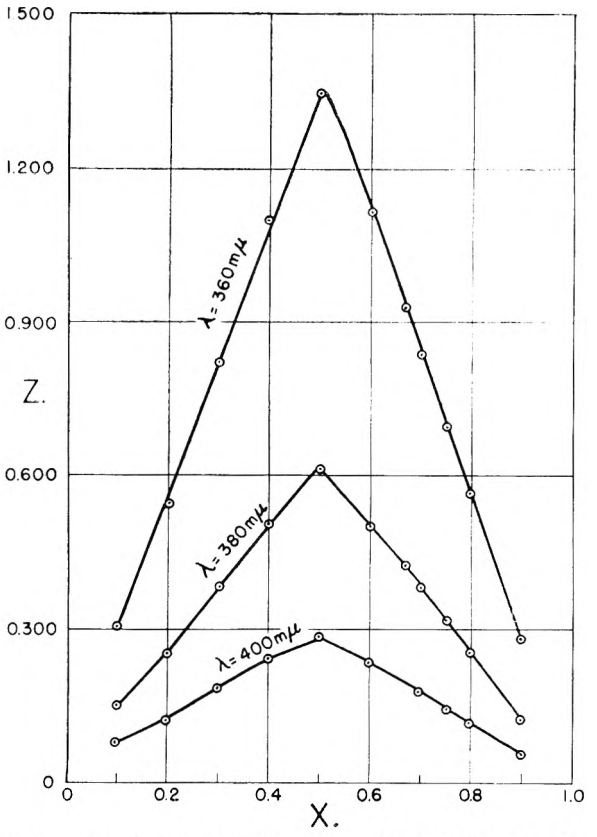

Fig. 3.—Continuous variation study with Fe^{+++} and H_2Y^{-}.

On repeated photoreduction and subsequent oxidation enough hydroxide is formed to decompose the complex and precipitate ferric hydroxide. However, if the solutions are kept from contact with air the first formed $FeY^{=}$ will persist indefinitely. Because of this photosensitivity of FeY^{-} solutions the majority of experiments with it were performed in red glass containers.

Properties of the Ferrous Complex.—No solid salts of this complex have been prepared and even aqueous solutions of it are rather difficult to work with, partly because the dissociation constant of the complex is comparatively high but more importantly because the complex is very easily oxidized. Thus even weak oxidizing agents rapidly oxidize the complex to FeY^{-}; dissolved oxygen also rapidly affects the oxidation when the *p*H is only moderately high. As an example, solutions of 0.004, 0.010 and 0.012 molar $FeY^{=}$, all at a *p*H of 2.5, were prepared using distilled water and a minimum of agitation; even so, in 8 minutes oxidation took place to the extent of 65%, 40% and 35%, respectively. For ordinary solutions the rate controlling step is clearly diffusion of air since with shaking all solutions are completely oxidized in a few minutes. The qualitative experiments listed below were done with minimum exposure to air and, as discussed later, for more quantitative experiments air was rigorously excluded.

The ferrous complex is not precipitated by ammonia at *p*H 9; however alkali hydroxides do decompose it giving a mixture of ferrous and ferric hydroxides. The iron in the complex is not removed by ferricyanide ion but is by alkali or ammonium

sulfide and by orthophenanthroline. A solution of 0.025 molar $FeY^{=}$ initially at a *p*H of 2.3 will in a few hours show a definite precipitate of the solid acid H_4Y. These results indicate a moderate stability of the ferrous complex if not subjected to oxidizing conditions.

Titration Curves.—Figure 4 gives titration curves for solutions of H_2FeY under varying conditions. One would expect this acid to be fairly strong and thus the predicted titration curve is one with a single inflection at a *p*H of 7 when two equivalents of base have been added. In Fig. 4 it can be seen that when a fairly concentrated solution is titrated with stirring by nitrogen the curve is close to that predicted. However for titrations done in the presence of air there is a notable trend toward an earlier inflection point. This is to be expected if any oxidation of the complex occurs since the oxidation reaction in acid is

$$H_2FeY + 1/4\ O_2 = HFeY + 1/2\ H_2O$$

All the titration curves of Fig. 4 were made up from stoichiometric amounts of solid ferrous sulfate and Na_2H_2Y solution. For the curve to the left the solution had free access to air and was motor stirred. The curve shows that oxidation to HFeY was complete. The intermediate curve represents a more vigorous attempt to exclude air but oxidation to the extent of about 50% still occurred. Even in the third and most favorable case about 16% oxidation occurred. The conclusion from these experiments is that the acid H_2FeY doubtless is a strong dibasic acid but for the acid to show its true properties air must be entirely excluded.

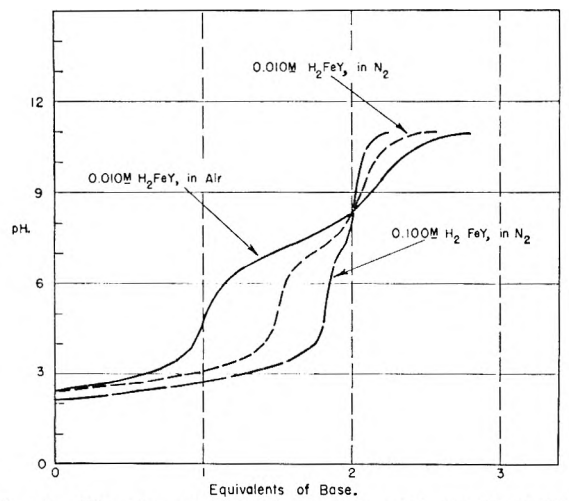

Fig. 4.—Titration of H_2FeY solutions with 0.1 *M* NaOH.

One can use the change in *p*H accompanying the oxidation of the ferrous complex to compare its rate of oxidation with that of ferrous ion. Specifically a solution was prepared containing 0.10 molar ferrous ion, 0.10 molar $FeY^{=}$ and 0.05 molar H^+ and then the increase with time of the *p*H of the solution was followed. The solution was exposed to air and stirred at each *p*H measurement. The significant point is that the *p*H rose to the value of the first inflection point (about *p*H 6) before a detectable amount of ferric hydroxide was formed. This means that approximately 50% of the ferrous complex was oxidized before a measurable amount of oxidation of the ferrous ion occurred. Additional qualitative experiments lead to the same conclusion, that the ferrous complex, at all *p*H values, is oxidized by oxygen at a considerably greater rate than is ferrous ion itself. Because of this sensitivity to oxidation, it is highly unlikely that the analytical determination of ferrous ion using this complex, as suggested by Schwarzenbach and Biedermann, can actually be done.

Spectrum of $FeY^{=}$.—Figure 2 shows the absorption spectrum for this complex in the visible region. Because of the ease of oxidation of these solutions extreme care was used in their preparation. The calculated amount of analyzed ferrous sulfate was weighed directly into an absorption cell. Then the cell was filled completely with a mixture of 0.0100 molar Na_3HY and 0.0025 molar Na_2H_2Y and the cell top sealed in place with wax before any significant amount of the solid salt had dissolved. After the solid had dissolved and the solution mixed the spectrum was measured. No visible color showed in the solution until the cell was opened at the end of the experiment. A duplicate run gave the same spectrum and the same final *p*H of the solution (2.81). Although traces of the ferric complex may still have been present, these results show that the ferrous complex is almost, perhaps entirely, colorless.

Dissociation Constants.—Approximate values for the equilibrium constants have been obtained for both the ferrous and ferric complexes using rather different procedures in the two cases. The ferrous complex is of lower stability so that in solutions of intermediate acid concentration there is extensive dissociation with concomitant formation of weak acids from the $Y^{=}$ ion. Consequently a determination of the actual hydrogen ion concentration in a mixture of the complex and a known amount of acid, combined with a knowledge of the acidity constants for ethylenediaminetetraacetic acid permits a calculation of the dissociation constant for the complex. Thus using Schwarzenbach's values for the ionization constants of the acid the following equations may be written, where the subscript zero refers to total concentrations before dissociation.

$$(H^+)_0 - (H^+) = (Y^{=}) [4 \times 10^{21.09}(H^+)^4 + 3 \times 10^{19.09}(H^+)^3 + 2 \times 10^{16.42}(H^+)^2 + 10^{10.25}[H^+] + (HSO_4^-)$$

$$(Y^{=}) = \frac{(H^+)_0 - (H^+) - (HSO_4^-)}{10^{21.69}(H^+)^4 + 10^{19.56}(H^-)^3 + 10^{16.72}(H^+)^2 + 10^{10.26}(H^+)}$$

$$(Fe^{++}) = \sum_{x=0}^{4} H_xY^{x-4}$$

$$= (Y^{=})[10^{21.09}(H^+)^4 + 10^{19.09}(H^+)^3 + 10^{16.42}(H^+)^2 + 10^{10.26}(H^+) + 1]$$

$$(FeY^{=}) = (FeY^{=})_0 - (Fe^{++})$$

Duplicate determinations of the dissociation constants were made, with extreme care to avoid oxidation of the complex. Since the results were identical (measured *p*H values of 2.80 and 2.81) calculations for only one of them are given in Table I. The activity coefficient of hydrogen ion was estimated from the results for solutions of hydrochloric

acid in barium chloride[21] and the concentration of bisulfate ion was calculated using Klotz and Eckert's[22] value of the apparent ionization constant of this ion at the given ionic strength. The accuracy of these determinations is low; the reason is that the hydrogen ion concentration at equilibrium is so low that relatively small errors in its determination make a large change in the dissociation constant. However, on the basis of these two results one can say that the concentration dissociation constant for FeY^- ion is approximately 10^{-14}.

TABLE I

DISSOCIATION CONSTANT OF FeY^-, 25°

$(Na_2FeY)_0$, M	0.0125
$(Na_2SO_4)_0$, M	.0050
$(H_2SO_4)_0$, M	.0075
pH	2.81
f_{H^+}	.80
$(H^+) = a_{H^+}/f_{H^+}$, M	.00194
(HSO_4^-), M	.00096
(Y^{---}), M	$10^{-13.64}$
(Fe^{++}), M	.0047
(FeY^-), M	.0078
K_D	$10^{-13.9}$

A similar procedure cannot be used for the much more stable ferric complex; its dissociation constant has been evaluated using the radioactive indicator method of Cook and Long.[23] In fact, the detailed procedure is much the same as that used by these authors for the nickel complex of ethylenediaminetetraacetate ion. A solution containing 0.025 molar of the ferric complex, 0.60 molar hydrogen ion and enough sodium perchlorate to give an ionic strength of 2.02 was held at 25° to permit equilibrium dissociation of the complex. Then equal volumes of this solution and one of 0.025 molar radioactive ferric perchlorate were mixed. An extrapolation of data on the per cent. exchange for this mixture as a function of time shows an "instantaneous exchange" at zero time of 15% (see curve A of Fig. 5). This instantaneous exchange results from the mixing of the radioactive ferric ion with the non-radioactive ferric ion from the equilibrium dissociation of the complex; its value is related to the fractional dissociation of the complex by

$$f = \frac{d(a + b)}{a + db}$$

where f is the fractional exchange, d is the fractional dissociation of the complex in the original equilibrated solution and a and b are total concentrations of added ferric ion and complex ion in the solution after mixing. In the present case $a = b$ and d calculates to be 0.081. Thus in the original complex solution the ferric ion concentration is 0.081 × 0.025 or 0.00203 molar. In this highly acid solution it can be shown that the predominating equation for the dissociation is

$$FeY^- + 4H^+ = Fe^{+++} + H_4Y$$

i.e., essentially all of the Y^{---} ion is removed as the

(21) H. S. Harned and C. G. Geary, *J. Am. Chem. Soc.*, **59**, 2032 (1937).

(22) I. M. Klotz and C. F. Eckert, *ibid.*, **64**, 1878 (1942).

(23) C. M. Cook, Jr., and F. A. Long, to be published.

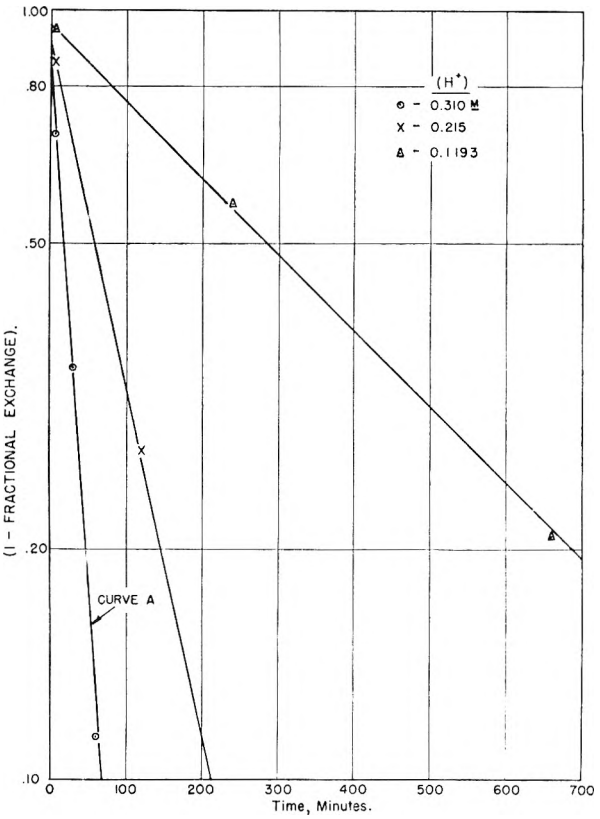

Fig. 5.—Fractional exchange *versus* time in strongly acid solutions. Concentrations of FeY^- and of Fe^{+++} are 0.0125 M.

undissociated acid. This simplifies calculation of the dissociation constant and one can write

$$\frac{(Fe^{+++})^2}{[(FeY^-)_0 - (Fe^{+++})][(H^+)_0 - 4(Fe^{+++})]^4} = \frac{K_D}{K_A}$$

where K_D is the concentration dissociation constant, K_A is the over-all dissociation constant for the acid H_4Y, $10^{-21.09}$ from Schwarzenbach's data, and the zero subscripts refer to total concentrations in the original solution before dissociation. Using the above value for the ferric ion concentration we calculate $K_D = 10^{-23.9}$, which confirms the conclusion that the ferric complex is highly stable. A similar calculation for a second solution for which the immediate exchange was 10% gave $K_D = 10^{-23.7}$. This value of $K_D = 10^{-24}$ can only be considered approximate since the ionic strength of the equilibrated solution is much higher than the value of 0.1 used by Schwarzenbach in his determination of the acidity constants.

FeY^-–Fe^{++} Exchange.—Three experiments were made on this exchange; the data are given in Table II. In all cases the concentrations of complex and ferrous ion were equal. The experiments at low pH were done with only moderate precautions to minimize contact with the air. However, the run at pH 4.7 was done in an all-glass apparatus designed so that all solutions could be flushed with purified nitrogen and thereafter kept from exposure to air; without this precaution oxidation of the complex would have been very rapid and extensive. Separations were made by removing the ferrous ion with an ammonia–ammonium

ion buffer. Counts were usually made on both fractions and the completeness of separation was confirmed by analysis of the fractions for iron.

The data of Table II show that at *p*H values of 4.7 and lower this exchange is essentially instantaneous. This is the expected result in view of the comparatively large dissociation constant listed earlier for this complex.

TABLE II

DATA ON FeY^-–Fe^{++} EXCHANGE 25 ± 2°

($FeSO_4$)	(Na_2FeY)	*p*H	Ionic str.	$t_{1/2}$ for Exchange, min.
0.0125	0.0125	1.50	0.14	<1
.0150	.0150	2.49	.15	<1
.0125	.0125	4.74	.22	<1

FeY^-–Fe^{+++} Exchange.—From the high stability of the ferric complex it might be expected that this exchange would be slow and this is found to be true. Preliminary experiments using solutions of radioactive ferric sulfate and of the sodium or ammonium salt of the complex showed that at 25° the half-time for exchange is several hours at acid concentrations of around 0.01 molar and, further, that the rate of exchange is strongly dependent on acidity. It was therefore decided to investigate the kinetics of this exchange in detail. To avoid uncertainties about other complex ions, all studies were made in perchlorate solutions; in addition the majority of studies were made at a high and constant ionic strength of 1.10.

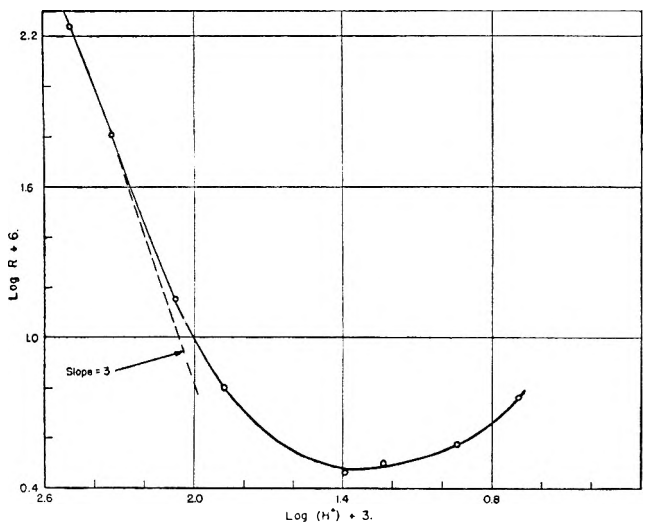

Fig. 6.—log *R* *versus* log (H^+): concentrations of Fe^{+++} and FeY^- are 0.0125 *M* and ionic strength is 1.10.

For most exchange experiments the solution of complex ion was made up using the solid acid, HFeY, sodium perchlorate, and perchloric acid. The radioactivity was usually in the ferric perchlorate solution. Most separations were made by precipitating the ferric ion as ferric hydroxide using an ammonia–ammonium ion buffer as the precipitating agent. However as a check, separations were made by precipitation of the ferric ion with benzoate ion, phthalate ion, phosphate ion and also by ether extraction of ferric thiocyanate. In no case was there noted any dependence of the exchange rate on the method of precipitation. However, with the separation of the ferric ion as the hydroxide, iron analysis of the separated fractions showed that usually from 2 to 5% of the complex was also decomposed; consequently radioactivity counts were generally made on the complex fraction.

Exchange rate was determined in the usual manner by plotting log (1 − fraction exchange) *versus* time to get the half-time. From this the rate, *R*, is calculated from the relation

$$R = \frac{ab}{a+b}\left(\frac{0.693}{t_{1/2}}\right)$$

where *a* and *b* are concentrations of complex ion and of added ferric ion in the exchange mixture and the half-time is in minutes. Typical plots of per cent. exchange *versus* time are given in Fig. 5. It is seen that the plots are all linear indicating no complications in the exchange process. For all but the most acid solutions the plots extrapolate to zero exchange at zero time. For the very acid runs the points extrapolate to give an immediate exchange at zero time, *e.g.*, Curve A in Fig. 5. This is of course due to the equilibrium dissociation of the complex discussed previously. For all these cases the amount of immediate exchange is relatively small, hence the rates were calculated using the apparent concentrations of complex ion and ferric ion, *i.e.*, ignoring the changes due to dissociation. Calculations showed that this approximation made in the worst case only a 1% error in the rate. It is however important to use the true half-time, the time when (1 − fraction exchange) is half its extrapolated value at zero time.

A log–log plot of *R* at constant reactant concentrations against hydrogen ion concentration is shown in Fig. 6. The complex character of this plot clearly indicates that at least two kinetic terms enter in the rate law. In actual fact the rate law involves at least three separate terms; hydrogen concentration enters in one to the third power, in another to the zero power and in a third to the inverse first power. Although for each of these terms there is a *p*H range in which it is dominant, the contributions invariably overlap some; this makes the determinations of the separate rate constants and orders rather complex.

Table III gives values for the exchange rate in solutions of low *p*H Runs 1, 2, 3 and 5 can be used to determine the order of the rate at high acid with respect to hydrogen ion, assuming that one kinetic term is dominant. Since all concentrations but hydrogen ion are constant one can write

$$\text{Rate} = k(H^+)^z$$

and thus the slope of a plot of log *R* against log(H^+) should give the value of *z*. Actually the points for these runs are the four points on the left of Fig. 6 and it can clearly be seen that these give at high acidity a slope of 3. Thus in highly acid solutions the rate is third order in hydrogen ion concentration. At somewhat lower acidities the slope is lower as would be expected if a term involving hydrogen ion to a lower power is beginning to enter.

Runs 6 to 10 serve to determine the order of this

TABLE III

FeY^-–Fe^{+++} EXCHANGE AT HIGH ACIDITY, 25°

No.	$(Fe^{+++})_0$	$(FeY^-)_0$	(H^+)	Ionic Strength	$t_{1/2}$, min.	10^5R
1	0.0125	0.0125	0.310	1.10	25	17.3
2	.0125	.0125	.215	1.10	68	6.37
3	.0125	.0125	.119	1.10	308	1.41
4	.0125	.0125	.119	0.194	420	1.03
5	.0125	.0125	.0751	1.10	676	0.64
6	.0250	.0250	.191	0.482	105	8.25
7	.0125	.0125	.191	.482	120	3.61
8	.00625	.00625	.191	.482	135	1.60
9	.0125	.0250	.191	.482	72	8.02
10	.0250	.0125	.191	.482	116	4.98

first term with respect to the principal reactants. Writing the general rate as

$$R_1 = k_1(Fe^{+++})^x(FeY^-)^y(H^+)^z$$

where R_1 refers to the contribution to the rate from the first kinetic term, one can write for these runs at constant acidity

$$R_1 = k''(Fe^{+++})^x(FeY^-)^y$$

The tabulated data all indicate that the rate is first order in the complex ion and zero order in ferric ion but with a significant contribution at lower acidities from another kinetic term which is first order in each. Thus the half-times for runs 6 to 8 are roughly constant, indicating a first order reaction but do decrease with increasing concentration as would be expected if a second order term also enters to a smaller extent. The results for runs 9 and 10 show particularly clearly that the reaction is essentially first order in complex ion and zero in ferric ion. The rate for run 9 is almost identical with that of 6 indicating the rate is independent of changes in ferric ion. Run 10 has half the complex and double the ferric concentration of 9 and the rate is about half that of 9.

The conclusion from these runs is that at high acidity the rate may be written

$$R = k_1(FeY^-)(H^+)^3 + k_2(FeY^-)^a(Fe^{+++})^b(H^+)^c$$

with preliminary indications that a and b are one and c is zero. These latter orders are in fact confirmed by the lower acidity runs of Table III. Thus one can write this equation as

$$\frac{R}{(FeY^-)} = k_1(H^+)^3 + k_2(Fe^{+++})$$

and a plot of $R/(FeY^-)$ *versus* $(H^+)^3$ will give values for both k_1 and k_2. Such a plot has been made for solutions containing constant ferric ion concentration, and the points fall rather well in a straight line. The slope of the plot gives $k_1 = 0.47$ liter^3 mole^{-3} min.$^{-1}$ and the intercept gives a tentative value of $k_2 = 0.02$ liter mole^{-1} min.$^{-1}$.

The runs at still lower acidity given in Table IV permit a more accurate determination of the second kinetic term and also a study of the third. As shown by runs 11 to 14 the rate of the exchange does not continue to decrease with increasing pH but actually increases. This suggests a term in which hydrogen ion enters to an inverse power. Since it is known from the work of Rabinowitch and Stockmayer[24] that at these lower acidities the first hydrolysis of ferric ion is significant, an obvious possibility is that the third term involves reaction of the species $FeOH^{++}$ and therefore that the hydrogen ion concentration enters to the inverse first power. Thus a plausible rate equation at low acidity where the contribution from the first kinetic term is negligible, is

$$R_{23} = k_2(Fe^{+++})(FeY^-) + k_3\frac{(Fe^{+++})(FeY^-)}{(H^+)}$$

If this is correct then a plot of $R/(Fe^{+++})(FeY^-)$ against $1/(H^+)$ should give a straight line of slope k_3 and intercept k_2. Furthermore, if as implied by the above rate equation ferric ion and complex ion enter to the first power in both kinetic terms, points for runs with different concentrations of the principal reactants should all fall on the same curve. It should however be noted that due to hydrolysis of ferric ion, the hydrogen will be slightly higher than that added and the ferric ion will be lower. A plot of this sort is shown in Fig. 7. The values of R_{23} used are simply the values of the observed rate minus the calculated contribution for the first kinetic term. The values for ferric and hydrogen ion concentration have been calculated using for the hydrolysis constant of ferric ion a value of 6.35×10^{-4}; this is the value calculated for an ionic strength of 1.1 from the data of Stockmayer and Rabinowitch. The straight line through the points deliberately emphasizes the data at higher acidity since there is a possibility of further hydrolysis at the lowest acidities. From the line of Fig. 7 $k_2 = 1.5 \times 10^{-2}$ liter mole^{-1} min.$^{-1}$ and $k_3 = 9 \times 10^{-5}$ min.$^{-1}$.

TABLE IV

FeY^-–Fe^{+++} EXCHANGE AT LOWER ACIDITY, 25°

No.	$(Fe^{+++})_0$	$(FeY^-)_0$	$(H^+)_0$	Ionic strength	$t_{1/2}$, min.	$R \times 10^5$
11	0.0125	0.0125	0.0241	1.10	1480	0.292
12	.0125	.0125	.0165	1.10	1370	.316
13[a]	.0125	.0125	.0085	1.10	900	.481
14	.0125	.0125	.0035	1.10	740	.585
15	.0250	.0250	.0329	1.10	790	1.10
16	.00625	.00625	.00823	1.10	2320	0.093
17	.0125	.0250	.0165	1.10	960	.60
18	.0250	.0125	.0165	1.10	1016	.57
19	.0125	.0125	.0035	0.0915	354	1.22
20	.0125	.0125	.0241	0.0991	790	0.55

[a] This run disagrees considerably with the others and is not used in later calculations.

All the data in Table IV are consistent with the fact that the order of both the second and third

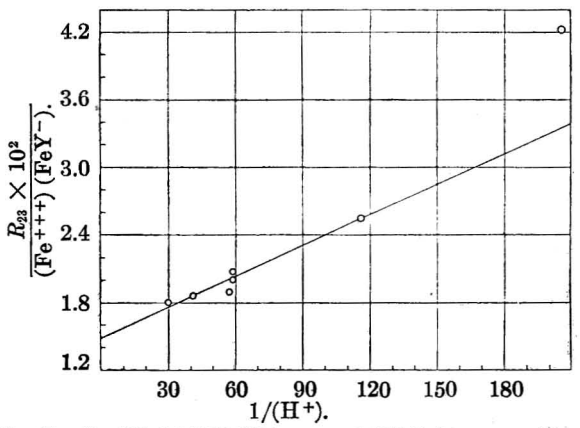

Fig. 7.—$R_{23}/(Fe^{+++})(FeY^-)$ *versus* $1/(H^+)$ for runs at low acidity.

(24) E. Rabinowitch and W. H. Stockmayer, *J. Am. Chem. Soc.*, **64**, 335 (1942).

terms is first in both complex ion and ferric ion. For example the data of runs 15 and 16 fall nicely on the line of Fig. 7. Of particular interest is a comparison of runs 17 and 18 with 12; at the same acidity doubling either ferric or complex ion concentration doubles the rate.

The over-all rate equation at ionic strength 1.1 appears to be

$$R = 0.47(FeY^-)(H^+)^3 + 0.015(FeY^-)(Fe^{+++}) + 9 \times 10^{-6}\frac{(FeY^-)(Fe^{+++})}{(H^+)}$$

Since we are assuming that the third term involves the first hydrolysis of ferric ion, we can use the previously quoted value for the hydrolysis constant and rewrite this as

$$R = 0.47(FeY^-)(H^+)^3 + 0.015(FeY^-)(Fe^{+++}) + 0.14(FeY^-)(FeOH^{++})$$

Table V gives for the various acidities the contributions of each of the terms of the rate equation to the total rate and also gives a comparison of the observed and calculated rates. The only region where there is a consistent deviation of the calculated from the observed is in the region around 0.1 molar hydrogen ion; here the calculated rate is consistently low. The most likely explanation for this deviation is that a term involving ferric ion, complex ion and hydrogen ion, each to the first power, makes some contribution in this *p*H region. However, our data are not accurate enough to justify detailed consideration of a fourth kinetic term.

As a matter of fact a three-term rate law of the type

$$R = k_1(FeY^-)(H^+)^3 + k_2(FeY^-)(Fe^{+++})(H^+) + \frac{k_3(FeY^-)(Fe^{+++})}{(H^+)}$$

will, with the proper choice of rate constants, fit the observed data only slightly less well than the equation given earlier. Because of this we conclude that there is a real uncertainty about the order with respect to hydrogen ion of the second term.

For solutions of low ionic strength the predicted primary kinetic salt effects are: no salt effect for the first term; large negative salt effects for both the second and third terms. Although none of the rates was measured in solutions of sufficiently low ionic strength to expect the limiting laws to hold, the observed salt effects are still of some interest. In the high acidity region where the first term is dominant, a small positive salt effect is observed, *e.g.*, runs 3 and 4. In the low acidity regions where the second and third kinetic terms are dominant, *e.g.*, runs 19 and 20, there is a negative salt effect but as would be expected its magnitude is much smaller than the limiting law prediction.

TABLE V

COMPARISON OF OBSERVED AND CALCULATED RATES

Run	(H^+)	10^5R_1	10^5R_2	10^5R_3	10^5R_{123}	$10^5R_{obsd.}$
1	0.310	17.6	0.23	...	17.8	17.3
2	.215	5.84	.23	0.05	6.07	6.37
3	.119	0.99	.23	.01	1.23	1.41
5	.0751	.26	.23	.02	0.51	0.64
11	.0244	.009	.229	.056	.294	.292
12	.0170	.003	.225	.079	.307	.316
14	.0049	....	.208	.255	.463	.585
15	.0331	.04	.93	.17	1.14	1.10
16	.00863	....	.055	.038	0.093	0.093
17	.0170	.006	.450	.159	.615	.60
18	.0174	.003	.452	.155	.61	.57

From the rate law one may write down plausible mechanisms for the exchange process. In the highly acid solutions the rate-determining step is clearly an acid induced dissociation, for example

$$FeY^- + 2H^+ = H_2FeY^+ \quad \text{Equil.}$$
$$H_2FeY^+ + H^+ = Fe^{+++} + H_3Y^- \quad \text{Rate Det.}$$

For the second and third terms the obvious mechanisms are simple bimolecular processes

$$FeY^- + \overset{*}{F}e^{+++} = \overset{*}{F}eY^- + Fe^{+++} \quad \text{Slow}$$

and

$$FeY^- + \overset{*}{F}eOH^{++} = \overset{*}{F}eY^- + FeOH^{++} \quad \text{Slow}$$

It is of some interest that the rate constant for the second of these bimolecular reactions is about tenfold larger in spite of the lower net charge on the hydroxoferric ion.

REMARKS

F. A. LONG (Communicated): After our paper was submitted to this symposium, an article by G. Schwarzenbach and J. Heller (*Helv. Chim. Acta*, **34**, 576 (1951)) became available which gives the results of a detailed e.m.f. study of equilibrium constants for the ferrous and ferric complexes of ethylenediaminetetraacetate. For the ferrous complex these authors give $pK_D = 14.2$ and for the ferric complex $pK_D = 25.1$, both in good agreement with our less precise results.

Schwarzenbach and Heller also report studies on the titration of the acids of these two complexes. They conclude that the acid HFeY is strong and that the acid H_2FeY is strong in the first proton but somewhat weak in the second.

ARTHUR E. MARTELL: At what ionic strength was the dissociation constant of FeY^- determined to be 10^{-24}?

RESPONSE: The ionic strength was about unity, but it may possibly have been somewhat higher than that.

A. E. MARTELL: A study of the effect of added electrolyte on the stability of CaY^{-2} has just been completed at Clark University. The results indicate a decrease in log K (stability constant) from about 10.5 to 8.5 as the ionic strength is increased from zero to unity. This seems to be in line with the difference between your dissociation constant of 10^{-24} at ionic strength of unity, and 10^{-25} in 0.1 M potassium chloride reported by Schwarzenbach.

A. E. MARTELL (further comments personally communicated after the talk): (1) Dr. Jones mentioned sodium and lithium ions as examples of metals which have negligible interaction with the ethylenediaminetetraacetate^{-4} ion. On the other hand Schwarzenbach has reported stability constants of the order of magnitude of 10^1 and 10^3 for these two ions, respectively. While it may be argued that these interactions are negligible, considerable interaction apparently takes place with another complexing agent, the anion of aminobarbituric acid, –N,N-dracetic acid. In this case I believe that the stability constant reported by Schwarzenbach for the lithium ion is about 10^5.

(2) Sometimes it is desirable to further purify ethylenediaminetetraacetic acid (EDTA) for experimental purposes. This may be accomplished by recrystallization from hot water. However, because of the low solubility of the acid, even in boiling water, the method is a tedious one if appreciable amounts are desired. I have found a convenient method to be (1) long stirring of the acid in a large volume of hot water (to remove soluble sodium salts) followed by (2) extraction of the filtered and washed acid with water in a soxhlet. In cases where sodium ions are not objectionable, recrystallization of the disodium salt from hot water is, of course, the most convenient method of purification.

HENRY TAUBE: It seems possible that the various terms in the rate law have similar interpretations. In every case

it can be assumed that the slow step is removal of the chelating group from ferric ion. This removal is facilitated by ions which associate with Y^{---}. Parallel processes take place with various types of cations—H^+, Fe^{+++}, $FeOH^{++}$—functioning. A test of the role which the metal ions play would be to study the rate of exchange in the presence of an ion such as Al^{+++} which is not involved in the net exchange process.

OBSERVATIONS OF THE KINETICS OF THE EXCHANGE OF WATER BETWEEN $Cr(H_2O)_6^{+++}$ AND SOLVENT

BY ROBERT A. PLANE[1] AND HENRY TAUBE

The George Herbert Jones Laboratory, University of Chicago, Chicago, Illinois

Received August 30, 1951

The rate of the exchange $Cr(H_2O)_6^{+++}$–H_2O has been found to be first order in $Cr(H_2O)_6^{+++}$, and to increase with the concentration of anion. For solutions at varying high salt concentration, the rate varies directly with concentration of anion. The anions decrease in effectiveness for promoting the exchange in the order NO_3^-, ClO_4^-, Cl^-, Br^-. With Cl^- as the only anion present, the rate of exchange greatly exceeds the rate of formation of the ion $Cr(H_2O)_5Cl^{++}$. The activation energy for the exchange in the perchlorate system is 24 ± 2 kcal./mole and the *pz* factor *ca.* 6×10^{13} l. mole^{-1} min.$^{-1}$. The rate of exchange is markedly increased by Cr^{++}, slightly by $Cr_2O_7^=$, and is induced by the reaction of Cr^{+++} with Ce^{+4}. The effect of Cr^{++} is greatly enhanced by Cl^-.

Some observations on the rate of exchange of water between hydrated cations and solvent have already been published.[2,3,4] The ions investigated were Al^{+++}, Cr^{+++}, Fe^{+++}, Co^{+++}, Co^{++}, Ga^{+++} and Th(IV). Of these, only Cr^{+++} showed a measurably slow rate of exchange of the bound water with the solvent. A few results were obtained[4] on the kinetics of exchange in the chromic ion–water system, but the investigation was by no means complete.

In the present work, a study in some detail of the kinetics of water exchange for the hydrated chromic ion was undertaken. The results of the work already referred to proved that chromic ion in the presence of acid and perchlorate ion exists as the species $Cr(H_2O)_6^{+++}$. It seemed of interest to learn whether the exchange of water with the solvent resembles that of other complex ion substitution reactions in its kinetic properties such as rate law and activation energy. The hope that the results of the investigation would have a direct bearing on the problem of the mechanism of substitution in hexacoördinated complex ions provided an additional stimulus for undertaking the work.

Besides the aspects of general interest referred to, the system $Cr(H_2O)_6^{+++}$–H_2O presents some of specific interest. The system can serve as a tool in the study of the rate of electron transfer between $Cr(H_2O)_6^{+++}$ and chromium in other oxidation states. If the rate of exchange of water between Cr^{++} aq. (for example) and solvent is rapid, Cr^{++} aq. must increase the rate of exchange between $Cr(H_2O)_6^{+++}$ and H_2O at least to the extent fixed by the rate of electron transfer between Cr^{++} aq. and $Cr(H_2O)_6^{+++}$. The catalytic effect exerted in the $Cr(H_2O)_6^{+++}$–H_2O exchange will therefore set an upper limit on the rate of electron transfer. The investigations of this type can be extended also to unstable oxidation states of chromium, by studying the $Cr(H_2O)_6^{+++}$–H_2O exchange induced by oxidizing agents acting on Cr^{+++} aq. or of reducing agents acting on $CrO_4^=$.

(1) A.E.C. Predoctoral Fellow, 1950–1951.

(2) J. P. Hunt and H. Taube, *J. Chem. Phys.*, **18**, 757 (1950).

(3) H. L. Friedman, H. Taube and J. P. Hunt, *ibid.*, **18**, 759 (1950).

(4) J. P. Hunt and H. Taube, *ibid.*, **19**, 602 (1951).

Where applicable, the method seems a particularly good one for studying the rate of electron transfer, since it does not require that the oxidation states undergoing electron exchange be separated. The sampling procedure involves only removal of a small fraction of the solvent by distillation and, assuming reasonable kinetic behavior, negligible effects will be introduced by it.

Experimental

Definitions.—Most of the symbols used in the paper are defined in Table I.

TABLE I

MEANING OF SYMBOLS

M	concentration in moles per liter
Q	the mole ratio H_2O/CO_2 used in isotopic equilibration of the two species.
R	the normalized ratio mass 46/mass 44 obtained from the mass spectrometer measurements
K	the equilibrium constant for the reaction: $CO_2^{16} + H_2O^{18} = CO^{16}O^{18} + H_2O^{16}$
N_c°	the mole fraction of $CO^{16}O^{18}$ in normal CO_2
N_s^t	the mole fraction H_2O^{18} in the solvent water of a reacting solution. The right-hand superscript designates the time
$t_{1/2}$	the half-time for water exchange in any experiment expressed in hours.
r	the rate of the reaction carrying the isotopic exchange
k_2	defined by $r = k_2$ $(Cr(H_2O)_6^{+++})$(Anion). In most cases, the anion is ClO_4^-. Units of k_2: l. mole^{-1} min.$^{-1}$

General Procedure.—The methods used in the research were essentially those described elsewhere.[4] Water enriched O^{18} was added to the chromic salt and other substances dissolved in water of ordinary isotopic composition. Periodically, the solvent was removed for isotopic analysis by distillation. The concentration of O^{18} in the water was determined by allowing the water to equilibrate with CO_2, and analyzing the CO_2 by a mass spectrometer. The change with time of isotopic composition in the solvent samples is a measure of the rate of exchange of water between chromic ion and the solvent.

The sampling procedure differed slightly from the vacuum distillation used by Hunt and Taube.[4] Inert gas at a pressure of 12 mm. was maintained in the apparatus during distillation. The time of distillation was thereby prolonged to about 3 minutes, and the process was made more controllable. In each distillation *ca.* 0.2 of the water was removed. To ensure complete equilibration of CO_2 and H_2O, the substances were left in contact for about 20 exchange half-lives, 6 days. In earlier experiments, CO_2 was separated

from H_2O after only 3 days in contact. The earlier data are noticeably less precise.

The only oxyanions which have been added to the solutions are ClO_4^-, $CrO_4^=$ and NO_3^-. Their exchange characteristics are sufficiently well known so that allowance for these effects can be made. Perchlorate ion has been shown[4] to exchange immeasurably little with water during the time of the experiments under the prevailing conditions. Chromate ion exchanges rapidly with the solvent in acid solution.[5] The exchange of NO_3^- with water was followed for a solution 3.0 M in $LiNO_3$ and 0.5 M in HNO_3. Even after 45 days, the isotopic composition of the water had not changed outside the limits of the precision of the measurements, ± 0.1% in the value of N_s. Complete exchange of the nitrate would have resulted in a 20% change in the value of N_s.

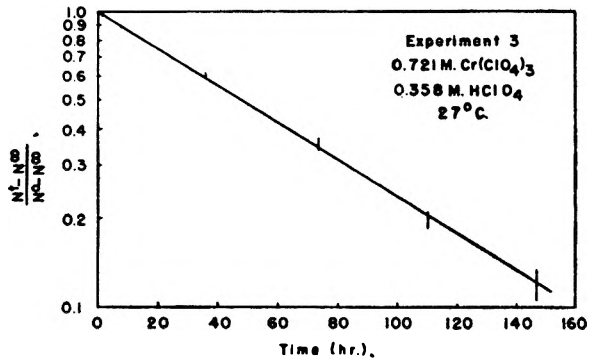

Fig. 1.—Kinetics of the exchange: $Cr(H_2O)_6^{+++}$–H_2O.

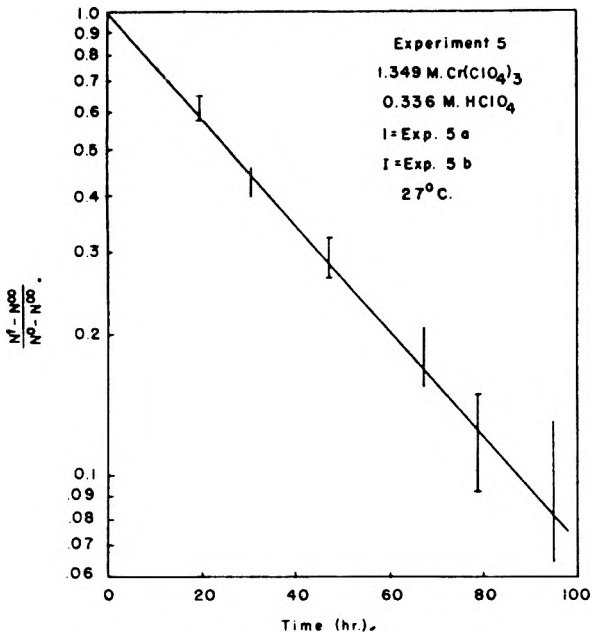

Fig. 2.—Kinetics of the exchange: $Cr(H_2O)_6^{+++}$–H_2O.

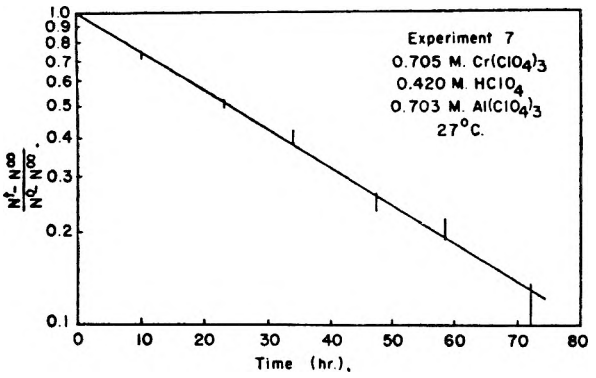

Fig. 3.—Kinetics of the exchange: $Cr(H_2O)_6^{+++}$–H_2O.

Materials.—Chromic perchlorate was purified by repeated recrystallization from water of a commercial C.P. sample. Different preparations have been used, without noticing a difference in the observations. $NaClO_4$ was prepared by crystallization from a solution made by combining A.R. NaOH and A.R. $HClO_4$. Aluminum perchlorate was prepared by crystallization from the solution obtained on fuming aluminum nitrate in 30% $HClO_4$. Cerous perchlorate was prepared in a similar manner. $Ce(ClO_4)_4$ aq. in $HClO_4$ aq. was prepared by the double decomposition of $Ce(HSO_4)_4$ aq. in $HClO_4$ aq. with Ba^{++} ($Ba(OH)_2$). The procedure of Lingane and Peesok[6] was followed in preparing $Cr(ClO_4)_2$ aq. The solutions contain zinc ion at a molar concentration one-half that of the chromous ion. Kept from air, they were stable for many hours, and were found to give no test for Cl^-. The sodium bromide, sodium dichromate, chromic nitrate and perchloric acid were A.R. grade, used without further purification.

Treatment of the Data.—The value of N_s was calculated from the measured values of R, Q and N_c° and the known value[7] of K using the equation

$$N_c = \frac{R}{K + R} + \frac{R}{Q(1 + R)} - \frac{N_c^\circ}{Q}$$

N_s thus obtained is directly proportional to the mole fraction of O^{18} in the solvent water, and for the purposes of the rate data, it is unnecessary to correct for the fractionation on distillation.

For all experiments but one[8] a straight line was obtained in the plot of log $(N_s^t - N_s^\circ)$ against t (*cf.* Figs. 1, 2 and 3 for representative data). The rate of the chemical reaction producing the exchange in each experiment is related to the slope k by the equation[9]

$$r = k \frac{(Cr(H_2O)_6^{+++})(H_2O)}{6(Cr(H_2O)_6^{+++}) + (H_2O)}$$

The r calculated in this manner refers to the rate of exchange of all six water molecules.

Since (H_2O) is large compared to $6(Cr(H_2O)_6^{+++})$, the term on the right-hand side reduces practically to $k(Cr(H_2O)_6^{+++})$. Hence, the constancy of k(or of $t_{1/2}$) will be a test of a rate law for the exchange having the rate proportional to the first power of chromic ion concentration. The rate law: $r = k_2(Cr(H_2O)_6^{+++})(\text{anion})$ has also been tested, and the values of k_2 calculated applying it have been recorded for most of the experiments. The data on catalysis were treated by setting r as established from the slope as the sum of two terms, of which one represents the normal rate in the absence of catalyst, and the other, the contribution by the catalytic path.

Since the water bound by chromic ion even in the most concentrated solutions used is only a small fraction of the water in the system, very high precision in the sampling, equilibration and isotopic analysis stages is required in order to obtain even reasonably accurate values of the specific rates. The accuracy of the values decreases as the chromic salt concentration decreases. To keep the accuracy

(5) G. R. Mills, *J. Am. Chem. Soc.*, **62**, 2833 (1940).

(6) J. J. Lingane and R. L. Peesok, *Anal. Chem.*, **20**, 425 (1948).

(7) At 25°, K = 2.078; H. C. Urey, *J. Chem. Soc.*, 562 (1947).

(8) In this experiment chloride ion was the only anion present. The experiment is described in a later section of this paper.

(9) R. B. Duffield and M. Calvin, *J. Am. Chem. Soc.*, **68**, 557 (1946).

within the range $\pm 10\%$, it was necessary to work with solutions of chromic salt 0.5 *M* or higher in concentration. Accurate data at lower salt concentrations could be obtained if a suitable precipitating agent were found for $Cr(H_2O)_6^{+++}$. The properties of the agent would need to be such that H_2O coördinated to Cr^{+++} could easily be removed from the product salt. A search was made for such a reagent but without success, and the present work therefore does not cover the interesting range of dilute chromic solutions.

Results

Table II contains a summary of the results of experiments performed to establish the rate law for the reaction.

TABLE II

VARIATION OF RATE WITH CONCENTRATION OF $Cr(H_2O)_6^{+++}$ AND ClO_4^- (TEMP. 27.0°)

No.	Concentrations: Cr^{+++}	ClO_4^-	H^+	Other salt	$t_{1/2}$, hr.	$k_2 \times 10^6$, min.
1	0.450	1.760	0.444	None	80 ± 15	78 ± 15
2[a]	.721	2.515	.358	None	48 ± 5	87 ± 9
3	.939	3.208	.391	None	39 ± 3	82 ± 6
4a	1.118	3.723	.373	None	32 ± 2	84 ± 5
4b	1.118	3.723	.373	None	34 ± 2	79 ± 5
5a[b]	1.349	4.362	.336	None	27 ± 2	81 ± 6
5b[b]	1.349	4.362	.336	None	26 ± 2	84 ± 6
6	0.827	5.195	.353	2.363 $NaClO_4$	27 ± 2	73 ± 5
7[c]	.705	4.659	.420	0.703 $Al(ClO_4)_3$	25 ± 2	90 ± 7

[a] *Cf.* Fig. 1. [b] *Cf.* Fig. 2. [c] *Cf.* Fig. 3.

The earlier work[4] indicated that the rate of reaction is higher than first order in salt concentration. This behavior has been borne out by the present experiments which cover a much wider range of salt concentration. $t_{1/2}$ is far from constant, and decreases as the salt concentration increases. The values of k_2 are satisfactorily constant however. Experiments 6 and 7 compared with 5a and 5b are important in showing that the second order variation in salt concentration is produced by the product $(Cr(H_2O)_6^{+++})(ClO_4^-)$ rather than the product $(Cr(H_2O)_5^{+++})$.[2]

The effects of anions other than ClO_4^- have been studied, and the data relating to them are presented in Table III.

TABLE III

THE DEPENDENCE OF RATE OF EXCHANGE ON THE IDENTITY OF ADDED ANION (TEMP. 27.0°)

No.	Composition: (Cr^{+++})	(H^+)	Anion	$t_{1/2}$, hr.	$k_2 \times 10^6$, min.
16[a]	1.134	0.847	4.25 *M* Cl^-	35 ± 2	67 ± 4
24	0.812	.303	2.74 *M* NO_3^-	28 ± 2	137 ± 10
8	1.352	.349	4.41 *M* NO_3^-	16.5 ± 0.5	133 ± 4
9[b]	0.841	.359	2.882 *M* ClO_4^-, 2.313 *M* Br^-	29 ± 2	66 ± 10

[a] Solution made up using freshly prepared blue $Cr(H_2O)_6Cl_3$. [b] Bromide was added as NaBr. The specific rate was calculated subtracting the contribution by the perchlorate path as given by the specific rate in Table II from the total rate, and attributing the residual rate to Br.

In addition to the experiments reported, one was done for comparison with Exp. 16, but using chromic chloride at *ca.* 0.6 *M*. In this experiment, the rate of exchange was observed to be very rapid initially, but it diminished gradually during the course of the experiment, $t_{1/2}$ based on the final stages being considerably in excess of 35 hr. No explanation for this behavior has been found. The sample of $Cr(H_2O)_6Cl_3$ had stood for several days before the second experiment was done. However the solution prepared from it was blue, and all the chloride was precipitated at once on the addition of Ag^+. Transformation of the blue form to green chromic chloride cannot be the explanation of the behavior. It is possible that an unknown catalyst which was destroyed during the reaction was responsible for the unusual behavior noted in the experiment.

The effect on the rate in the presence of ClO_4^- of changing the concentration of acid was studied by Hunt and Taube.[4] Their data are summarized in Table IV. Included is the result of an experiment performed in the course of the present work.

TABLE IV

EXPERIMENTAL RESULTS SHOWING THE REACTION RATE AS A FUNCTION OF ACID CONCENTRATION (TEMP. 25.0°)

No.	Concentrations: $Cr(ClO_4)_3$	$HClO_4$	$k_2 \times 10^6$ (min.) 25°
I[a]	1.093	0.000 (*p*H 2)	84 ± 5
II[a]	1.100	.0956	73 ± 5
IV[a]	0.810	.090	80 ± 5
V[a,b]	.810	.090	70 ± 5
4[b]	1.118	.373	63 ± 4
III[a]	1.084	1.12	65 ± 4

[a] Results obtained by Hunt and Taube.[4] [b] Corrected to 25° using measured temperature coefficient.

When the data are expressed in terms of the k_2 rate law, a slight increase in rate as the concentration of acid increases is observed. The variation, while outside of experimental error, is too slight to suggest formulation of a rate law, and may be due to a salt effect. It may be noted from Table IV that the specific rate obtained in the present work is in reasonable agreement with the earlier work.

The data obtained in a study of the variation of rate with temperature are shown in Table V. The activation energy calculated from the data for the lower temperature interval is 23 ± 2 kcal. and for the higher is 26 ± 2. Using the average value for the activation energy, *pz* for the reaction is calculated as 6×10^{13} l. mole^{-1} min.$^{-1}$.

TABLE V

RESULTS OF EXPERIMENTS AT DIFFERENT TEMPERATURES

No.	Temp., °C.	Concentrations: $Cr(ClO_4)_3$	$HClO_4$	$t_{1/2}$, hours	$k_2 \times 10^6$, min.
10	20.15	1.113	0.370	80 ± 4	34 ± 2
4	27.00	1.118	.372	33 ± 2	81 ± 6
11	35.01	1.106	.368	10.5 ± 0.5	250 ± 14

Exposure of samples to the light of a 100-watt incandescent bulb at a distance of 3 in., and increasing the surface (Pyrex) to volume ratio by a factor of 4 did not result in a noticeable change in rate of exchange. The effect of these variations in conditions was tested on samples in the series for experiment 3, Table II.

Table VI presents a summary of experiments performed to test catalysis of the $Cr(H_2O)_6^{+++}$–H_2O exchange by oxidizing agents, including $Cr_2O_7^=$.

A definite catalysis of the exchange by $Cr_2O_7^=$ can be noted from the results in Table VI. Ceric ion exerts an even more marked catalytic effect. Under the conditions of the experiments, Ce^{IV} is

TABLE VI

EFFECT OF OXIDIZING AGENTS ON THE RATE OF THE EXCHANGE $Cr(H_2O)_6^{+++}$–H_2O

Temp. 27°; ClO_4^- present

No.	Composition (Cr⁺⁺⁺)	(H⁺)	Other	$t_{1/2}$, hr.	Residual rate[a] × 10⁴ mole l.⁻¹ min.⁻¹
12	0.990	0.514	0.184 *M* $Na_2Cr_2O_7$	26	1.1 ± 0.4
13[b]	0.784	.71	$(Ce^{IV})_0 = (Ce^{III})_0$ = 0.0493 *M*	17	2.6 + .4
18[c]	1.032	.80	$(Ce^{IV})_0 = (Ce^{III})_0$ 0.024 *M*	18	2.4 ± .4
19	0.744	.69	0.18 *M* $Ce^{(III)}$, 0.0164 *M* $Na_2Cr_2O_7$	29.5	0.5 ± .4

[a] In the absence of catalyst, r in each case would be about 2.5×10^{-4} mole $l.^{-1}$ $min.^{-1}$ the exact value depending on the concentration of $Cr(ClO_4)_3$. [b] Exchange 19 ± 2% complete in first 7 min. [c] Exchange 9 ± 2% complete in first 16 min.

reduced rapidly, the major part being consumed a few minutes after mixing. During the first interval of time, considerable exchange is observed (19% in experiment 13), and following this there is a continued constant catalysis throughout the duration of the experiment, which is independent of the initial amounts of Ce^{IV} used (*cf.* experiments 13 and 18). Experiment 19 proves that the continued catalysis is not due to interaction of the products Ce^{III} and $Cr_2O_7^=$. In evaluating experiments 13 and 18, it should be noted that the net oxidation of $Cr(H_2O)_6^{+++}$ to form the exchangeable species $Cr_2O_7^=$ accounts for only a small fraction of the initial induction.

Attempts to induce the $Cr(H_2O)_6^{+++}$–H_2O exchange by the action of reducing agents on $Cr_2O_7^=$ were without success. The solutions used were *ca.* 0.80 *M* $Cr(ClO_4)_3$, 0.73 *M* $HClO_4$ and 0.14 *M* $Na_2Cr_2O_7$. The reducing agent, in one case Fe^{++}, in the other AsO_2^-, each used in amount so as to make the initial concentration 0.052 *M*, was added slowly over a 3-minute interval. Calculation of isotope balance showed that within experimental error, ±2% of total exchange, exchange in $Cr(H_2O)_6^{+++}$–H_2O was not induced.

Chromous ion exerts a marked catalytic effect on the exchange $Cr(H_2O)_6^{+++}$–H_2O. The results of three experiments on this aspect of the work are presented in Table VII.

TABLE VII

CATALYSIS OF THE EXCHANGE $Cr(H_2O)_6^{+++}$–H_2O BY Cr^{++}

Temp. 27°; ClO_4^- present

No.	Composition[a] (Cr⁺⁺⁺)	(Cr⁺⁺)[b]	(H⁺)	(NaCl)	$t_{1/2}$, hr.	k_2'[c]
20	0.99	0.099–0.039	0.30	.....	6.5 ± 1.5	0.023 ± 0.011
25	1.05	.173– .151	.33	.....	2.1 ± 0.2	.028 ± .004
23	1.03	.081– .074	.33	0.011 *M*	0.9 ± 0.1	.143 ± .02

[a] Each solution contains Zn^{++} at a concentration one-half that of the initial chromous concentration. [b] (Cr^{++}) was determined at zero time and at the time of final sampling. Both values are recorded. [c] Calculated on the assumption that the catalytic term is $k_2'(Cr^{++})(Cr^{+++})$.

Owing to the marked decrease in Cr^{++} in experiment 20, the result is rather inaccurate and the rate law for the catalysis is not proven. The effect of Cl^- in enhancing catalysis by Cr^{++} is very striking.

Two other experiments were performed on catalysis by chromous ion. The results however cannot be compared directly with those presented in Table VII since the final concentration of chromous ion was not determined, and later work showed that there was considerable loss of chromous ion during the handling procedure to which the solutions were subjected. In one of the experiments, the initial composition corresponded approximately to that recorded for experiment 20; the half-time for the $Cr(H_2O)_6^{+++}$–H_2O exchange was however very much shorter, only 0.3 ± 0.1 hr. The chromous solution used in this experiment had stood for *ca.* 12 hours before being used, and had developed a green color. Tests showed chloride ion to be absent. From the procedure followed in preparing the solutions, (differing from that used for the other experiments) it seems possible that F^- or a reduction product of NO_3^- was present and produced the anomalous effects.

An experiment was performed to measure the rate of exchange between Cr^{++} aq. and water. For a solution 0.394 *M* in $Cr(ClO_4)_2$, 0.197 *M* $Zn(ClO_4)_2$ and 0.403 *M* in $HClO_4$, the exchange was observed to be complete in two minutes. The experiment incidentally shows that exchange of Zn^{++} aq. and solvent is also very rapid.

Discussion

The observations recorded in Table II show that the half-time for the exchange of $Cr(H_2O)_6^{+++}$ with water depends markedly on the concentration of salt, and that the half-time is fixed by the concentration of the anion ClO_4^-. It has been found that with both ClO_4^- and NO_3^- as anions, the rate varies as the product $(Cr(H_2O)_6^{+++})(anion)$. Although the concentration of the anion has a marked effect on the rate, changing the nature of the anion in the series NO_3^-, ClO_4^-, Cl^-, Br^- affects the rate by only a factor of about two.

In attempting to arrive at an understanding of the role which the anions play, it is difficult to separate salt effects (which imply a general ion atmosphere effect exerted by the anions) from chemical effects (which imply a well-defined participation by the anion in the activated complex) since the experiments were performed in solutions at high varying salt concentration. An argument which favors a chemical interpretation is that the magnitude of the effect exerted by the anions seems large for a salt effect on rate-determining reactions of the type

$$Cr(H_2O)_6^{+++} \longrightarrow Cr(H_2O)_5^{+++}$$

or

$$Cr(H_2O)_6^{+++} + H_2O \longrightarrow$$

By either mechanism, the activated complex differs only in extent of hydration from the reactants and the variation of activity coefficient with concentration would be expected in each case to be similar for both states. The fact that empirically the rate can be expressed as the product $k_2(Cr(H_2O)_6^{+++})(anion)$ for both the ClO_4^- and NO_3^- is also an argument in favor of a chemical interpretation, but is only of limited value. On the view that the activated complex contains $Cr(H_2O)_6^{+++}$ and an anion, it is very remarkable that the rate is independent of ionic strength over the range of high values covered.

Of the chemical effects which an anion may exert, the mode by which it operates forming a complex

ion $Cr(H_2O)_5X^{++}$ which then aquatizes can be rejected at least for the system containing Cl^-. Under the conditions of the experiments, the half-time for the formation of the chloro complex in equilibrium amount is in excess of 150 hours. It is so long in fact that the solutions were not appreciably green even after the water exchange reaction was essentially complete. A possible mode of action for the negative ion is that water in its hydration sphere is replaced by a water molecule oriented about the chromic ion in the first sphere and the additional interaction resulting therefrom reduces the energy required to remove water from the cation. This type of mechanism is similar to that demonstrated by Swain[10] for substitutions on carbon. Another possibility is that the energy levels for chromic ion are sufficiently affected by the charge of the anions to lower the activation energy for replacement of water.

In respect to *pz* factor and activation energy, there is nothing peculiar about the exchange $Cr(H_2O)_6^{+++}$–H_2O. Many substitution reactions in hexacoördinated complex ions have frequency and energy factors about the same in magnitude as was observed for the exchange reaction.

The catalysis of the exchange $Cr(H_2O)_6^{+++}$–H_2O by $Cr_2O_7^=$ is too great to be explained by the exchange of Cr(III) and Cr(VI).[11] The effect of chromate ion may simply be that of an anion which because of the higher charge is particularly effective in promoting exchange by the k_2 path. On this basis k_2 for $Cr_2O_7^=$ would be 9 times as great as for ClO_4^-. Another possibility is that $Cr_2O_7^=$ in contact with Cr^{+++} generates Cr(IV) and Cr(V).[12] Since these ions have vacant inner *d* orbitals, the exchange of associated water with solvent is expected to be rapid.[4] If electron exchange with Cr(III) is rapid, they can be expected to act as catalysts for the $Cr(H_2O)_6^{+++}$–H_2O exchange. It seems likely that these intermediates explain at least in part the experiments with ceric ion. There is some difficulty however in fitting both the initial induction and the continued catalysis to the model. To explain the continued catalysis as due to Cr(IV) or Cr(V), it must be assumed that ceric ion persists, although at low concentration, for long periods of time. If both the rate of formation of Cr(IV), for example, and if destruction are of the same order in ceric ion, the steady state concentration of Cr(IV) will be independent of the concentration of oxidizing agent and a constant steady state concentration of Cr(IV) will be maintained. The experiments with reducing agents added to $Cr_2O_7^=$ are inconclusive. The rate of oxidation of Fe^{++} and AsO_2^- by Cr(IV) and Cr(V) may be so rapid that the intermediates are kept at concentrations too low to be effective in the catalysis of the $Cr(H_2O)_6^{+++}$–H_2O exchange.

The experiments with chromous ion added demonstrate the usefulness of this indirect method of studying rate of electron transfer between different oxidation states of the same element. It can be applied conveniently however only in systems such as the present one, in which one ion exchanges associated groups much less rapidly than the other. Since Cr^{++} has been shown to exchange rapidly with solvent, an upper limit for the rate of electron transfer between Cr^{++} and Cr^{+++} under the conditions of our experiment of 0.028 l. mole^{-1} min.$^{-1}$ can be set. It seems very likely that electron transfer is the only path for the $Cr(H_2O)_6^{+++}$–H_2O exchange opened up by Cr^{++}, and that the value mentioned above measures the specific rate of the Cr^{++}–Cr^{+++} electron exchange. Catalysis of the exchange by Cl^- is not unexpected in view of the behavior of the other systems of this type.[13,14] The observations made on the catalysis by Cr^{++} of the exchange between $Cr(H_2O)_6^{+++}$ and water make reasonable an electron transfer mechanism for the catalysis by Cr^{++} of the dissolution of $CrCl_3$ in water.[15] The reaction is ordinarily slow, but can become very rapid when Cr^{++} or certain reducing agents are added. Conversion of Cr^{+++} in a matrix of Cl^- to Cr^{++} by electron transfer makes possible the rapid release of Cl^-. Since there is not net consumption of Cr^{++}, the process can continue.

Acknowledgment.—This work was supported by the Office of Naval Research under contract N6-ori-02026. The funds for the purchase of the mass spectrometer used in the research were supplied by the Atomic Energy Commission under Contract At(11-1)-92.

REMARKS

F. A. LONG: The fact that the $t_{1/2}$ values are so nearly the same for the three different anions, perchlorate, nitrate and bromide, makes it seem quite possible that the differences are simply due to salt effects on the reaction of the $Cr(H_2O)_6^{+++}$ complex with water.

RESPONSE: If the anion is excluded from the activated complex, the reaction in question becomes an ion-dipole reaction. Don't you think a factor of three is rather large for a secondary salt effect?

RESPONSE (F. A. Long): There are examples of ion-dipole reactions which show even larger salt effects.

RESPONSE (R. A. Plane): Perhaps we are saying the same thing in different words. We must conclude that at least in the chloride case, the exchange does not proceed by formation of a complex ion. Since it is an outer sphere effect, it is equivalent to what you call an activity effect.

ROBERT E. CONNICK: Would you care to make some remarks about the role of the anion in the exchange if the intermediate $Cr(H_2O)_5X^{++}$ is excluded.

RESPONSE (R. A. Plane): Several mechanisms can be postulated. The anion can be "hydrated" by one of the H_2O molecules coordinated to Cr^{+++}, and thus assist in the removal of the water molecule. Or, a complex of the type $Cr(H_2O)_6$ anion^{++} may be formed which rapidly exchanges water.

RESPONSE (R. E. Connick): In the first case, should not the effectiveness of the anion in catalysis be related to base strength, and permit calculation of the relative effectiveness of anions?

RESPONSE (R. A. Plane): The relation is not simple because the difference in the energy of hydration of the anion by solvent water and water attached to Cr^{+++} is in question.

FRED BASOLO: In all your work you discuss water ex-

(10) C. C. Swain, *Record of Chemical Progress*, **12**, 21 (1951). Review.

(11) H. E. Menker and C. S. Garner, *J. Am. Chem. Soc.*, **71**, 371 (1949).

(12) F. H. Westheimer, *Chem. Revs.*, **45**, 429 (1949).

(13) D. J. Meier and C. S. Garner, *J. Am. Chem. Soc.*, **73**, 1894 (1951)—catalysis of Eu(II)-Eu(III) by Cl^-.

(14) W. F. Libby, private communication—catalysis of Ce(III)-Ce(IV) by F^-.

(15) R. Abegg and Fr. Auerbach, "Handbuch der Anorganischen Chemie," Bd. 4, Abt. 1, S. Hirzel, Leipzig, 1921, pp. 75–76.

change for hydrated metal ions. Have you investigated the analogous situation with more stable complex ions of the type $[Co(NH_3)_5H_2O]^{+++}$ or $[Co(NH_3)_4(H_2O)_2]^{+++}$?

RESPONSE: Work has been started by Rutenberg and Taube on the exchange of $Co(NH_3)_5H_2O^{+++}$ with water. The exchange in this system proceeds at about the same rate as for $Cr(H_2O)_6^{+++}$. Some observations which have been made indicate that the rate is independent of the anion concentration when $SO_4^=$ is the anion.

POLYMERIZATION AND DEPOLYMERIZATION PHENOMENA IN PHOSPHATE–METAPHOSPHATE SYSTEMS AT HIGHER TEMPERATURES.[1] CONDENSATION REACTIONS INVOLVING THE POTASSIUM HYDROGEN ORTHOPHOSPHATES

BY R. K. OSTERHELD[2,3] AND L. F. AUDRIETH

Noyes Laboratory of Chemistry, University of Illinois, Urbana, Illinois

Received August 30, 1951

Methods of differential thermal analysis, X-ray diffraction, chemical analysis together with dehydration studies have been employed to investigate the condensation reactions which take place when the potassium hydrogen orthophosphates and mixtures thereof are heated to higher temperatures. Potassium dihydrogen orthophosphate is converted directly into the insoluble potassium metaphosphate, dehydration beginning at a temperature above 200°. Heating curves for the anhydrous dipotassium hydrogen orthophosphate indicate that conversion proceeds in two steps, the first beginning at about 282° involving loss of one-half of the constitutional water to yield an intermediate whose composition can be represented by the formula $2K_2HPO_4 \cdot K_4P_2O_7$, and the second, around 400° corresponding to complete dehydration to the pyrophosphate, $K_4P_2O_7$.

The preferred first reaction for any mixture containing both the mono- and dihydrogen orthophosphates leads to tripotassium monohydrogen pyrophosphate in accordance with the equation: $KH_2PO_4 + K_2HPO_4 \rightarrow K_3HP_2O_7 + H_2O$ (A). Using equimolar ratios of the reactants this process goes to completion at 245°. The effect of further heating of such mixtures depends upon the initial mole ratios of the reactants. Excess of the dipotassium hydrogen orthophosphate results in formation of potassium triphosphate: $K_3HP_2O_7 + K_2HPO_4 \rightarrow K_5P_3O_{10} + H_2O$ (B). If no excess of the monohydrogen orthophosphate is present condensation of two moles of the tripotassium hydrogen pyrophosphate takes place to give the intermediate tetraphosphate whose disproportionation is believed to account for the formation of metaphosphate and triphosphate as reaction products: $2K_3HP_2O_7 \rightarrow [K_6P_4O_{13} + H_2O] \rightarrow KPO_3 + K_5P_3O_{10} + H_2O$ (C). Reactions (B) and (C) take place readily at 325°. Any excess of potassium dihydrogen orthophosphate over that required for the reaction represented by equation (A) will be converted into metaphosphate.

Introduction

The aggregation reactions effected by the heating of various hydrogen orthophosphates have been the subject of considerable study. Most of this work, however, has been concerned only with the ultimate reaction products and has been limited largely to a study of the behavior of the sodium hydrogen orthophosphates. Much of the work in this field has been purely empirical. To produce a given sodium polyphosphate any mixture of sodium hydrogen phosphates having the proper sodium to phosphorus ratio is heated to an appropriate temperature. Whereas such an approach is effective from a technological point of view, it serves to obscure some of the more interesting scientific aspects of these reactions, which, in themselves, may become of technological importance.

The phosphates resemble the molybdates, chromates and vanadates with respect to the formation of isopoly (condensed) acids, but differ from the latter in one important aspect. Whereas the aggregation (dehydration polymerization) of molybdates, chromates and vanadates may be accomplished readily in aqueous solution by the addition of acid, it is necessary to employ high temperature, essentially ansolvous acidic media to bring about the conversion of orthophosphates into poly- and metaphosphates. Such reactions therefore represent polymerization processes occurring in high temperature acid systems. For preparative purposes, the hydrogen ion is generally the acid employed, that is, adjustment of acidity is accomplished by using the appropriate hydrogen phosphate, or mixture of hydrogen phosphates, as the starting material.[4] It is noteworthy, however, that other high temperature acids, both protonic (ammonium and hydrogen sulfate ion) and nonprotonic (sulfur trioxide and dichromate ion), will cause these aggregation reactions to take place. It is also possible to bring about the reverse process at higher temperature, that is, depolymerization of polyphosphates by the use of appropriate bases, just as the polyanions of Cr(VI), Mo(VI) and V(V) are degraded to the simple ortho-ions in aqueous solution by raising the *p*H. Fusion of sodium polymetaphosphate melts with oxides, hydroxides, carbonates, sulfides and fluorides effects such depolymerization.[4,5] It is only recently[4,6] that the fundamental nature of these high temperature polymerization–depolymerization reactions as acid–base phenomena has been emphasized.

There is presented in the experimental portion of

(1) Presented at the Symposium on Complex Ions and Polyelectrolytes, Ithaca, N. Y., June 18–21, 1951. Abstracted from a thesis submitted by R. K. Osterheld to the Graduate College of the University of Illinois in partial fulfillment of the requirements for the Degree of Doctor of Philosophy, 1950.

(2) Victor Chemical Works Research Fellow in Chemistry 1948–1950.

(3) Baker Laboratory of Chemistry, Cornell University, Ithaca, New York.

(4) O. F. Hill and L. F. Audrieth, THIS JOURNAL, **54**, 699 (1950).

(5) O. F. Hill, Thesis, University of Illinois, 1948.

(6) L. F. Audrieth and G. T. Moeller, *J. Chem. Education*, **20**, 219 (1943).

this paper the results of a study of the aggregation reactions which the potassium hydrogen orthophosphates, and mixtures thereof, undergo at higher temperatures. It had already been recognized that the thermal behavior of the potassium mono- and dihydrogen orthophosphates is different from that of the corresponding sodium salts. The method of differential thermal analysis was used to determine the course of the condensation reactions. The identity of the intermediate and final products was verified by chemical methods and by X-ray diffraction analysis. The specific objectives were (a) to define more clearly the mechanism of the reaction leading to the formation of potassium triphosphate and (b) attempt the preparation of potassium tetraphosphate by a high temperature aggregation reaction. The latter objective was not realized, even though it had been shown that discrete polyanions become more stable toward thermal treatment as the size of the cation is increased.[7,8]

Experimental Procedures

Differential thermal analyses were carried out in a small electric furnace heated at a controlled rate of eight to ten degrees per minute. Weights of sample were standardized at ten grams. Sample temperatures were recorded continuously by means of a Wheelco recorder. The differential in temperature between the sample and a similar amount of ignited aluminum oxide was recorded simultaneously on a Brown recorder. The temperature sensing units for both these purposes were bare junction Pt–90Pt 10Rh thermocouples. The thermocouple and recorder combination used to determine sample temperature was calibrated periodically against benzoic acid (m. 122.5°), potassium dichromate (m. 397.5°), potassium sulfate (tr. 583.0°), and sodium chloride (m. 800.4°). The temperatures recorded are considered accurate to ± 5°.

The analytical procedure recommended by Jones[9] was used for determination of orthophosphate. The Bell method was employed for the quantitative determination of pyro- and triphosphate.[10] Since potassium metaphosphate is insoluble in water, it was collected on an ashless filter paper, then ignited for an hour at 575°, followed by an hour at 800°.

Thermal Behavior of the Individual Reactants. Potassium Dihydrogen Orthophosphate.—Thermal analysis of potassium dihydrogen orthophosphate showed that the rate of dehydration becomes appreciable at 208°. At about 258° a strong endothermic process takes place, during which water is lost rapidly and the material froths. The resulting dehydration product, potassium metaphosphate, melts at 805°. Although it is possible to prepare disodium dihydrogen pyrophosphate by partial thermal dehydration of sodium dihydrogen orthophosphate, there is disagreement in the literature about the formation of appreciable amounts of dipotassium dihydrogen pyrophosphate as an intermediate in the conversion of potassium dihydrogen orthophosphate to potassium metaphosphate. The dehydration process was therefore studied at 245°, since the behavior at this temperature is of particular importance to a later stage of the present investigation. Data for the reaction are presented graphically in Fig. 1. It will be noted that at 245° water is lost steadily by potassium dihydrogen orthophosphate until essentially complete conversion to potassium metaphosphate has occurred. The analytical data for samples taken at stages during the process show that no appreciable amounts of any intermediate are present at any time, and that potassium metaphosphate appears early in the dehydration. Thermal analysis of a sample of dipotassium dihydrogen pyrophosphate prepared in another way further showed that its decomposition commences below 200°, becoming rapid at 230°.

(7) H. Flood and T. Förland, *Acta Chem. Scand.*, **1**, 781 (1947).
(8) H. Flood and A. Muan, *ibid.*, **4**, 364 (1950).
(9) L. T. Jones, *Ind. Eng. Chem., Anal. Ed.*, **14**, 536 (1942).
(10) R. N. Bell, *Anal. Chem.*, **19**, 97 (1947).

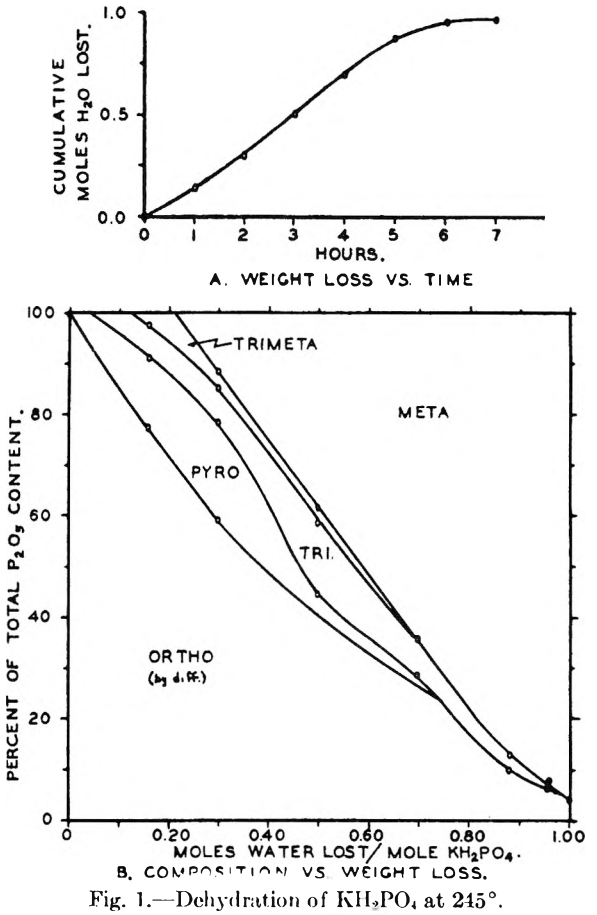

Fig. 1.—Dehydration of KH_2PO_4 at 245°.

Potassium Monohydrogen Orthophosphate.—Anhydrous potassium monohydrogen orthophosphate was prepared by dehydration, at 200°, of reagent grade $K_2HPO_4 \cdot 3H_2O$. The heating curve for the anhydrous material showed that the conversion into potassium pyrophosphate proceeds in two steps: one starting at 282° and a second around 400°. Samples heated at 325° lose one-half of their constitutional water. The second half can be removed by heating to 400°. Analyses of the "half-dehydrated" and completely dehydrated samples showed them to contain 51.3 and 96.7%, respectively, of the phosphorus content as pyrophosphate. With the exception of several minor lines, all the lines in the X-ray diffraction pattern of the intermediate material could be ascribed to K_2HPO_4, the starting material, or to $K_4P_2O_7$, the ultimate product. Further studies are planned to elucidate the nature of the intermediate material and the reason for the two stages in the aggregation process.

Thermal Behavior of Potassium Dihydrogen–Monohydrogen Orthophosphate Mixtures.—Samples representing 2:1, 2:2, 3/2:2 and 1:2 mole ratios of the dihydrogen to monohydrogen orthophosphate were prepared by thoroughly mixing and grinding together the proper amounts of the anhydrous materials. Differential thermal analysis data for these mixtures are presented in Fig. 2 in the form of approximate redrawings of the curves obtained. Data for the individual reactants are similarly presented for comparison.

From an examination of these data, it seems likely that the initial reaction is the same for each of the various mixtures. A reaction starts in each mixture around 180–200° and increases in rate up to 230–250°. Comparison with the heating curves for the pure reactants makes it clear that this reaction is not due to either component acting as an individual. Pure potassium dihydrogen orthophosphate undergoes a rapid endothermal process in the vicinity of 260°, as do mixtures rich in this component. The relative magnitude of this arrest becomes smaller as the KH_2PO_4 content is decreased, indicating that this particular break in the first three curves represents the same process. Pure dipotassium monohydrogen phosphate undergoes no change below about 280°. In the curves for the mixtures shown in Fig. 2 the two

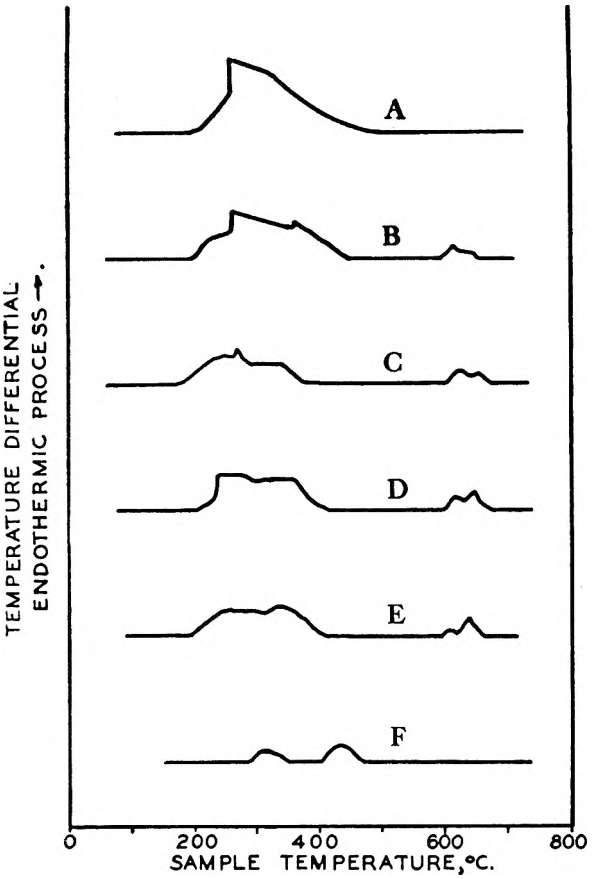

Fig. 2.—Thermal analyses for KH_2PO_4–K_2HPO_4 mixtures; over-all reaction: A, $KH_2PO_4 \rightarrow KPO_3$; B, $2KH_2PO_4 + K_2HPO_4 \rightarrow 3/2KPO_3 + 1/2K_5P_3O_{10}$; C, $2KH_2PO_4 + 2K_2HPO_4 \rightarrow KPO_3 + K_5P_3O_{10}$; D, $3/2KH_2PO_4 + 2K_2HPO_4 \rightarrow 1/2KPO_3 + K_5P_3O_{10}$; E, $KH_2PO_4 + 2K_2HPO_4 \rightarrow K_5P_3O_{10}$; F, $2K_2HPO_4 \rightarrow K_4P_2O_7$.

upper breaks at 618° and 650° represent, respectively, the eutectic for the $K_5P_3O_{10}$–KPO_3 system and the incongruent melting point of $K_5P_3O_{10}$. The relative magnitudes of these breaks change properly in accord with the composition.

A temperature of 245° was chosen as one which would be likely to bring the initial reaction to completion in a reasonable time period without inducing further reaction. Samples containing 2:1, 2:2 and 1:2 mole ratios of potassium dihydrogen to monohydrogen orthophosphate were prepared by two methods: (a) those termed "ground mixtures" were mixed and ground together as thoroughly as possible and (b) those called "intimate mixtures" were prepared by evaporating a solution of the reactants as quickly as possible to bring about rapid, intimate cocrystallization of the components. These mixtures were heated to constant weight at 245°. Table I presents data for the weight losses (calculated as moles of water) experienced by these mixtures in reaching constant weight, and reports the analyses of the products obtained. The data for the three mole ratio mixtures will be considered separately.

Reaction in Equimolar KH_2PO_4–K_2HPO_4 Mixtures.—When equimolar mixtures of potassium dihydrogen and monohydrogen orthophosphate were heated to constant weight at 245°, the weight losses were found to correspond to the evolution of 2.04, 2.05, 2.02 and 2.06 moles of water per two moles of each reactant. The possible reactions which would lead to this result are

$$2KH_2PO_4 + 2K_2HPO_4 \longrightarrow 2K_3HP_2O_7 + 2H_2O \quad (1)$$

$$2KH_2PO_4 + 2K_2HPO_4 \longrightarrow 2KPO_3 + 2H_2O + (2K_2HPO_4) \quad (2)$$

$$2KH_2PO_4 + 2K_2HPO_4 \longrightarrow K_2H_2P_2O_7 + K_4P_2O_7 + 2H_2O \quad (3)$$

$$2KH_2PO_4 + 2K_2HPO_4 \longrightarrow K_5P_3O_{10} + 2H_2O + (KH_2PO_4) \quad (4)$$

$$2KH_2PO_4 + 2K_2HPO_4 \longrightarrow KPO_3 + K_4P_2O_7 + 2H_2O + (KH_2PO_4) \quad (5)$$

Although each of these equations accounts for the observed weight loss, the last three are believed to be unlikely since they presuppose that KH_2PO_4 or $K_2H_2P_2O_7$ are stable at 245°. Equations (3) and (5), which involve the direct dehydration: $2K_2HPO_4 \rightarrow K_4P_2O_7 + H_2O$, as an independent reaction, are also unlikely since this reaction does not take place to an appreciable extent below 280°.

Table I presents a comparison of analytical data for constant weight products at 245° from "ground" and "intimate" mixtures with the compositions predicted for each of the five possible reactions listed above. Equations (1) and (3) agree most closely with the experimental data for equimolar mixtures. Perfect agreement with theory cannot be expected for reactions of this kind. While sintering takes place during early stages of the reaction, no appreciable liquid phase is present to ensure

TABLE I

REACTION OF VARIOUS MONO- AND DIHYDROGEN PHOSPHATE MIXTURES AT 245°[a]

A. Weight loss, as moles of water, in achieving constant weight at 245°

Type of sample	Mole ratios, KH_2PO_4:K_2HPO_4 2:1	2:2	1:2
Ground	1.96	2.05	1.28
Intimate	1.98	2.04	1.21
Theoretical 1	2.00	2.00	1.00
for 2	2.00	2.00	1.00
equation 3	1.50	2.00	1.50
4	1.00	2.00	2.00
5	2.50	2.00	2.00

B. Analyses of products obtained by heating to constant weight at 245°

Type of sample	% P as	Mole ratios, KH_2PO_4:K_2HPO_4 2:1	2:2	1:2
Ground	PO_3^-	8.0	10.8	5.0
	$P_3O_{10}^{-5}$	0.0	2.8	9.0
	$P_2O_7^{-4}$	87.9	64.2	52.0
Intimate	PO_3^-	5.8	0.0	0.9
	$P_3O_{10}^{-5}$	0.0	0.0	1.7
	$P_2O_7^{-4}$	89.8	79.4	62.0
Theoretical for	PO_3^-	33.3	0.0	0.0
equation 1	$P_3O_{10}^{-5}$	0.0	0.0	0.0
	$P_2O_7^{-4}$	66.7	100.0	66.7
equation 2	PO_3^-	66.7	50.0	33.3
	$P_3O_{10}^{-5}$	0.0	0.0	0.0
	$P_2O_7^{-4}$	0.0	0.0	0.0
equation 3	PO_3^-	0.0	0.0	0.0
	$P_3O_{10}^{-5}$	0.0	0.0	0.0
	$P_2O_7^{-4}$	100.0	100.0	100.0
equation 4	PO_3^-	0.0	0.0	0.0
	$P_3O_{10}^{-5}$	50.0	75.0	100.0
	$P_2O_7^{-4}$	0.0	0.0	0.0
equation 5	PO_3^-	66.7	25.0	33.3
	$P_3O_{10}^{-5}$	0.0	0.0	0.0
	$P_2O_7^{-4}$	33.3	75.0	66.7

[a] The differences from 100% correspond to orthophosphate.

thorough mixing of the reactants. The slow dehydration of the dihydrogen phosphate, KH_2PO_4, is a competing reaction at 245°. It is evident, however, that the use of the intimate mixture tends to eliminate this side reaction.

Of the possibilities that correspond most closely with the analytical data, equation (1) has been chosen as representing the major reaction at 245° for several reasons: (a) the X-ray pattern indicates that none of the usual potassium phosphates is a major constituent of the product, (b) $K_2H_2P_2O_7$ is normally not stable at 245°, and (c) the conversion of K_2HPO_4 to $K_4P_2O_7$ will normally not take place below 280° at an appreciable rate.

Reaction in 1:2 Molar Ratio KH_2PO_4–K_2HPO_4 Mixtures.—The experimental data for mixtures containing a 1:2 mole ratio of potassium dihydrogen to monohydrogen orthophosphate are presented in Table I, together with the results predicted by the following possible reactions (equations based on the same premises as those in the preceding section but modified to take into account the different mole ratio of reactants)

$$KH_2PO_4 + 2K_2HPO_4 \longrightarrow K_3HP_2O_7 + H_2O + (K_2HPO_4) \quad (1)$$

$$KH_2PO_4 + 2K_2HPO_4 \longrightarrow KPO_3 + H_2O + (2K_2HPO_4) \quad (2)$$

$$KH_2PO_4 + 2K_2HPO_4 \longrightarrow {}^1/_2K_2H_2P_2O_7 + K_4P_2O_7 + 1\ {}^1/_2H_2O \quad (3)$$

$$KH_2PO_4 + 2K_2HPO_4 \longrightarrow K_5P_3O_{10} + 2H_2O \quad (4)$$

$$KH_2PO_4 + 2K_2HPO_4 \longrightarrow KPO_3 + K_4P_2O_7 + 2H_2O \quad (5)$$

It is apparent from these equations and from the data reported in Table I that the actual weight losses experienced at 245° by the 1:2 mixtures do not agree closely with any of the possibilities presented. The data agree best with the requirements for the first three equations. In a later section evidence will be presented for a second reaction commencing near 250° which may be responsible for high observed weight losses for this mixture.

The analytical data show, once again, that the use of intimate mixtures tends to eliminate a side reaction which is appreciable in the ground mixtures. The analytical data for the product obtained from the intimate mixture are in good agreement with the requirements of equation (1) and no other.

Reaction in 2:1 Molar Ratio KH_2PO_4–K_2HPO_4 Mixtures.—The possible reactions in 2:1 mole ratio mixtures, that correspond to those considered in the previous sections, may be represented by the equations

$$2KH_2PO_4 + K_2HPO_4 \longrightarrow K_3HP_2O_7 + KPO_3 + 2H_2O \quad (1)$$

$$2KH_2PO_4 + K_2HPO_4 \longrightarrow 2KPO_3 + 2H_2O + (K_2HPO_4) \quad (2)$$

$$2KH_2PO_4 + K_2HPO_4 \longrightarrow K_2H_2P_2O_7 + {}^1/_2K_4P_2O_7 + 1\ {}^1/_2H_2O \quad (3)$$

$$2KH_2PO_4 + K_2HPO_4 \longrightarrow {}^1/_2K_5P_3O_{10} + H_2O + (1\ {}^1/_2KH_2PO_4) \quad (4)$$

$$2KH_2PO_4 + K_2HPO_4 \longrightarrow 2KPO_3 + {}^1/_2K_4P_2O_7 + 2\ {}^1/_2H_2O \quad (5)$$

From the data presented in Table I it can be seen that the observed weight losses for the reaction at 245° in mixtures of this composition agree well with the first two equations. However, the analytical data, presented in the same table, are in complete disagreement with the composition expected on the basis of equation (2). The data are in fair agreement with a process represented by equation (1). It is possible in this case that a $K_2H_2P_2O_7$ intermediate in the KH_2PO_4 dehydration to KPO_3 is stabilized by the $K_3HP_2O_7$ formed according to equation (1). Heating the intimate sample for which data are reported in Table I to 270° brought its composition into better agreement with equation (1) (analyses, % P as: PO_3^- 32.1, $P_3O_{10}^{-5}$ 0.0, $P_2O_7^{-4}$ 56.1).

Conclusions Concerning the Interaction of KH_2PO_4 and K_2HPO_4 at 245°.—A consideration of both the weight loss and analytical data (chemical and X-ray) for the reaction taking place at 245° between several different mole ratios of potassium dihydrogen and monohydrogen orthophosphates shows that the preferred reaction may be represented by the equation: $KH_2PO_4 + K_2HPO_4 \rightarrow K_3HP_2O_7 + H_2O$. Absolute agreement with theory is a practical impossibility since allowance must be made for the inherent nature of solid-phase reactions, which may not go to completion, and for the fact that side reactions are likely to take place.

The Effect of Higher Temperatures

Products obtained by heating to constant weight at 245° starting mixtures consisting of 2:2 and 1:2 mole ratios of potassium dihydrogen to monohydrogen orthophosphate are of special interest. The first of these products consists largely of the previously unreported tripotassium monohydrogen pyrophosphate; the second yields potassium triphosphate upon heating to a sufficiently high temperature.

The differential analysis curves reproduced schematically in Fig. 3 depict the effect of further heating on samples already heated to constant weight at 245°. Figure 3 shows that a sample of 1:2 mole ratio (curve B) which has reached constant weight at 245° needs to be heated only to a slightly higher temperature before another process begins to take place. In fact, it is likely that this second process takes place to an appreciable extent even at 245°. This would explain the higher than theoretical weight losses observed for samples of this composition when heated to constant weight at 245° and also accounts for the presence of triphosphate in such a product (see Table I). The mixture consisting initially of $KH_2PO_4 + 2K_2HPO_4$, undergoes the following reaction at 245°

$$KH_2PO_4 + 2K_2HPO_4 \longrightarrow K_3HP_2O_7 + K_2HPO_4 + H_2O$$

It reacts further at a somewhat higher temperature according to the equation

$$K_3HP_2O_7 + K_2HPO_4 \longrightarrow K_5P_3O_{10} + H_2O$$

Differential curve 3-B indicates that this reaction can be completed at 325°. The "tailing off" of the the curve above 400° may be due to the decomposition of unreacted K_2HPO_4. As before, the two upper arrests correspond to the eutectic in the $K_5P_3O_{10}$–KPO_3 system and the incongruent melting point of $K_5P_3O_{10}$, respectively. The strength of

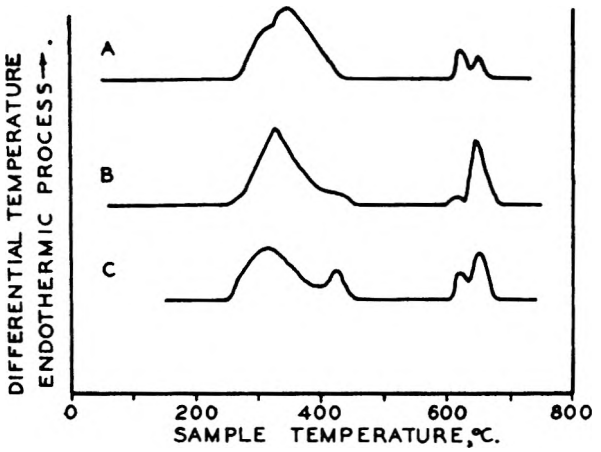

Fig. 3.—Thermal analyses for samples previously heated at 245°: Sample A: $2KH_2PO_4 + 2K_2HPO_4$ } First heated to
B: $KH_2PO_4 + 2K_2HPO_4$ } constant weight at 245°
C: $K_3HP_2O_7 + K_2HPO_4$, synthetic mixture, see text.

Reaction A: $2K_3HP_2O_7 \rightarrow K_5P_3O_{10} + KPO_3$
B: $K_3HP_2O_7 + K_2HPO_4 \rightarrow K_5P_3O_{10}$
C: $K_3HP_2O_7 + K_2HPO_4 \rightarrow K_5P_3O_{10}$

the latter arrest indicates the final product is essentially pure $K_5P_3O_{10}$.

A synthetic mixture of equimolar quantities of $K_3HP_2O_7$ and K_2HPO_4 was prepared by mixing K_2HPO_4 with the product obtained by heating an equimolar mixture of KH_2PO_4:K_2HPO_4 to constant weight at 245°. The differential thermal analysis for this mixture is presented as Fig. 3-C. The resemblance to Fig. 3-B is clear, although the reaction is not as clean-cut. This is to be expected since the synthetic mixture constitutes a less intimate composition than that used in 3-B. This is also the reason for the increased strength of the break at 420°, corresponding to the second half of the dehydration of K_2HPO_4, and for the fact that the two upper breaks indicate that less $K_5P_3O_{10}$ was produced.

An intimate mixture of the mole ratio KH_2PO_4–$2K_2HPO_4$ which had first been heated to constant weight at 245° was heated subsequently at 325° to constant weight. A separate sample of the original KH_2PO_4–$2K_2HPO_4$ mixture was heated to constant weight at 325° directly. Analyses for these products are presented in Table II. It is clear that the reaction to produce potassium triphosphate may be completed at 325°.

Figure 3-A shows the effect of further heating upon the product obtained at 245° from an equimolecular KH_2PO_4–K_2HPO_4 mixture. The major reaction in this case takes place at a higher temperature than that which characterizes the $K_3HP_2O_7$–K_2HPO_4 reaction. It is postulated that two moles of tripotassium monohydrogen pyrophosphate condense with the elimination of water to form an unstable tetraphosphate intermediate, which immediately disproportionates to triphosphate and metaphosphate

$$2K_3HP_2O_7 \longrightarrow (K_6P_4O_{13}) + H_2O$$
$$(K_6P_4O_{13}) \longrightarrow K_5P_3O_{10} + KPO_3$$

The small "bump" on the initial side of the major break in curve 3-A may be due to the $K_3HP_2O_7$–K_2HPO_4 reaction discussed previously. The tripotassium monohydrogen pyrophosphate prepared by thermal dehydration at 245° is never pure; some unreacted orthophosphate is also present.

TABLE II

ANALYTICAL DATA FOR SAMPLES HEATED TO CONSTANT WEIGHT AT 325°

Thermal treatment	% P as	Mole ratios, KH_2PO_4:K_2HPO_4 2:2	1:2
Heated to constant	PO_3^-	24.0	4.1
weight at 325° in	$P_3O_{10}^{-5}$	75.6	91.5
steps	$P_2O_7^{-4}$	0.0	0.0
Heated to constant	PO_3^-		4.3
weight at 325° di-	$P_3O_{10}^{-5}$		95.0
rectly	$P_2O_7^{-4}$		0.0
Theoretical	PO_3^-	25.0	0.0
	$P_3O_{10}^{-5}$	75.0	100.0
	$P_2O_7^{-4}$	0.0	0.0

A sample of a ground mixture consisting of equimolar quantities of KH_2PO_4 and K_2HPO_4 which had previously been heated to constant weight at 245° (to effect conversion to $K_3HP_2O_7$) was subsequently heated at 325° until constant weight was achieved. Analyses for this material are given in Table II. They agree well with the expected composition and are in accord with the postulated reaction given above.

Conclusions

The preferred first reaction in any mixture containing the compounds KH_2PO_4 and K_2HPO_4 is the formation of tripotassium monohydrogen pyrophosphate

$$(A)\quad KH_2PO_4 + K_2HPO_4 \longrightarrow K_3HP_2O_7 + H_2O$$

This reaction can be carried essentially to completion at 245°.

The effect of further heating depends upon the initial mole ratios of the reactants. If K_2HPO_4 is present in excess, heating at a higher temperature will result in the formation of potassium triphosphate in accordance with the equation

$$(B)\quad K_3HP_2O_7 + K_2HPO_4 \longrightarrow K_5P_3O_{10} + H_2O$$

If no excess monohydrogen orthophosphate is present, a temperature slightly higher than that necessary for the reaction just given causes condensation of two moles of the $K_3HP_2O_7$ to give tetraphosphate as a postulated intermediate. The latter disproportionates to triphosphate and metaphosphate.

$$(C)\quad 2K_3HP_2O_7 \longrightarrow (K_6P_4O_{13}) + H_2O$$
$$(K_6P_4O_{13}) \longrightarrow K_5P_3O_{10} + KPO_3$$

Both reactions (B) and (C) will take place at 325°. Excess KH_2PO_4 over that required for reaction (A) will be converted into potassium metaphosphate slowly at 245°, but more rapidly at a slightly higher temperature.

Acknowledgment.—The authors are grateful for the advice and encouragement offered to them by Dr. Howard Adler, Dr. W. H. Woodstock and Dr. R. N. Bell of the Victor Chemical Works Research Laboratories, Chicago Heights, Illinois.

MACRO-IONS. II. POLYMETHACRYLIC ACID

BY ANDRÉ OTH[1] AND PAUL DOTY

Gibbs Laboratory, Department of Chemistry, Harvard University, Cambridge 38, Massachusetts

Received August 30, 1951

Two fractions of polymethacrylic acid having molecular weights of 43,000 and 90,000 were investigated as a function of the degree of neutralization and concentration by the following methods: light scattering, viscosity, potentiometric titration and conductance. Except in the non-ionized case, the concentration dependence of the scattering is similar to that already anticipated theoretically and considered to be characteristic of polyelectrolytes. The dissymmetry likewise exhibits a characteristic concentration dependence and its extrapolation to zero concentration permits the evaluation of the size of the polyion under these conditions. It is found that the expansion of the higher molecular weight fraction over the unperturbed size is about fivefold in the root-mean-square end-to-end separation. If the intrinsic viscosity data are determined from extrapolation of Fuoss's equation and the size estimated by means of the Flory–Fox equation, values consistent with the dissymmetry results are obtained. The concentration dependence of the *p*H at a given degree of neutralization appears to be different from that previously assumed and as a consequence a somewhat different expression for the apparent *p*H at infinite dilution is obtained, *i.e.*, $[pH]_0^\alpha = 7.70 - 2.45 \log (1 - \alpha)/\alpha$. The limiting conductance is interpreted to show that the net charge on the polyion deviates from the titration value beyond about 40% neutralization.

The present state of knowledge concerning the behavior of polymeric electrolytes in solution derives principally from investigations of viscosity,[2–8] electrometric titration,[9–11] conductance[12–15] and diffusion.[16] However, the interpretation of much of the data so obtained rests upon theories[17–20] that are as yet unproven. Moreover, thermodynamic investigations, such as those of osmotic pressure, sedimentation, equilibrium and light scattering, have not been adequately brought to bear on the basic problems of the intermolecular and intramolecular interactions in polymeric electrolytes. In an attempt to improve this situation we have carried out a coördinated study of polymethacrylic acid fractions by means of light scattering techniques combined with measurements of viscosity, electrometric titration and conductance as a function of polymer concentration and extent of neutralization.

The results presented here are restricted to solutions of the polyacid and its sodium salt: that is, solutions with added electrolyte are not included in this present study. It may seem that this limitation narrows the investigation to a particularly simple case. Actually the reverse is true. In attempting to characterize macromolecules and their interactions it is essential to perform measurements over a dilute concentration range in which contacts between the solute molecules are essentially limited to binary contacts and then to extrapolate (generally in a linear fashion) the data to zero concentration. In the case of uncharged polymer molecules, the molecular size remains approximately constant in the dilute concentration range and the absolute value of the concentration in this range (usually about 0.1 to 1.0 g./100 cc.) is large enough to produce an adequate response in most procedures employed. It is these two conditions that do not appear to apply in aqueous solutions of partially or completely dissociated polymeric electrolytes. In these cases the size of the molecule appears to increase greatly upon dilution and the concentration range required for reliable extrapolation may be shifted to much lower values. Some experiments in which the effective size of the polyion and its gegenion atmosphere appear to be stabilized by adjustment of the gegenion concentration will be presented later.

I. Experimental Procedures

A. Preparation and Fractionation of Polymethacrylic Acid.—The polymethacrylic acid was prepared in a manner similar to that used by Arnold and Overbeek.[9] A 10% aqueous solution of the freshly distilled monomer was polymerized at 25° using the hydrogen peroxide–ferrous sulfate initiator system. The amount of initiator used was chosen in order to produce a polymer having a weight average molecular weight of about 100,000. The polymerization was stopped after it was 60% complete. The polymer was precipitated by butanone and then redissolved in water and dialyzed. A crude fractionation was carried out by the addition of 5 *N* hydrochloric acid to a 2% aqueous solution of the polymer. By this process two fractions, A and B, were obtained and these were refractionated into three fractions each, A_1, A_2, A_3 and B_1, B_2, B_3. These fractions were dialyzed and then electrodialyzed in order to remove all small ions. Only fractions A_2 and B_1 were used in this study.

B. Viscosity Measurements and Estimation of Molecular Weights.—The viscometer employed throughout this study had the following characteristics: capillary radius, 0.227 mm.; volume of bulb, 2.91 cc.; length of capillary, 7.7 cm.; efflux time for water, 210 sec.; gradient for water, 1010 $sec.^{-1}$; Hagenbach correction, 1.0%. All measurements were made at 25°.

(1) Department of Chemistry, University of Liege, Liege, Belgium.

(2) H. B. Bungenberg de Jong, and Ong Sia Gwan, *Kolloid chem. Beihefte*, **31**, 89 (1930). For other references to early work, see "Colloid Science," (Edited by J. R. Kruyt) Vol. II, Elsevier, New York, N. Y., 1949, pp. 213–223.

(3) R. M. Fuoss and V. P. Strauss, *Ann. N. Y. Acad. Sci.*, **51**, 836 (1949).

(4) R. M. Fuoss and V. P. Strauss, *J. Polymer Sci.*, **3**, 602, 603 (1948).

(5) M. Heidelberger and F. E. Kendall, *J. Biol. Chem.*, **95**, 127 (1932).

(6) A. Katchalsky and H. Eisenberg, *J. Polymer Sci.*, **6**, 145 (1951).

(7) H. Markovitz and G. E. Kimball, *J. Chem. Soc.*, **5**, 115 (1950).

(8) H. Staudinger, "Die hochmolecularen organischen Verbindungen," Verlag Julius Springer, Berlin, 1932.

(9) R. Arnold and J. Th. G. Overbeek, *Rec. trav. chim.*, **69**, 192 (1950).

(10) R. K. Cannan, A. H. Palmer and A. C. Kibrick, *J. Biol. Chem.*, **142**, 803 (1942). For other references see Chapter 20, "Protein, Amino Acids and Peptides," Cohn and Edsall, Reinhold Publishing Corp., New York, N. Y., 1943.

(11) A. Katchalsky and J. Gillis, *Rec. trav. chim.*, **68**, 879 (1949).

(12) R. M. Fuoss and V. P. Strauss, *J. Poly. Sci*, **3**, 246 (1948).

(13) J. R. Huizenga, P. F. Grieger and F. T. Wall, *J. Am. Chem. Soc.*, **72**, 2636 (1950).

(14) F. T. Wall and E. H. deButts, *J. Chem. Phys.*, **17**, 1330 (1949).

(15) F. T. Wall, G. S. Stent and J. J. Ondrejcin, THIS JOURNAL, **54**, 979 (1950).

(16) J. R. Huizenga, P. F. Grieger and F. T. Wall, *J. Am. Chem. Soc.*, **72**, 4228 (1950).

(17) J. J. Hermans and J. Th. G. Overbeek, *Rec. trav. chim.*, **67**, 761 (1948); *Bull. soc. chim. Belg.*, **57**, 154 (1948).

(18) A. Katchalsky, O. Kunzle and W. Kuhn, *J. Polymer Sci.*, **5**, 283 (1950).

(19) A. Katchalsky and P. Spitnik, *ibid.*, **2**, 432 (1947).

(20) (a) W. Kuhn, O. Kunzle and A. Katchalsky, *Helv. Chim. Acta*, **31**, 1994 (1948); (b) O. Kunzle, *Rec. trav. chim.*, in press.

Inasmuch as Arnold and Overbeek[9] had used viscosity data of 2 N sodium nitrate solutions of completely neutralized methacrylic acid for the estimation of molecular weights, using the intrinsic viscosity–molecular weight relation for polymethyl methacrylate in benzene, similar measurements were made with our fractions in order to compare the molecular weight of our fractions with theirs. Using the relation mentioned[21]

$$M = 2.42 \times 10^5 [\eta]^{1.32} \qquad (1)$$

the results obtained were: for fraction A_1, $[\eta] = 0.450$, $M = 84{,}000$; for fraction B_2, $[\eta] = 0.265$, $M = 42{,}000$. On the basis of the molecular weight determinations discussed in the next paragraph, it appears that these results are essentially correct indicating that the state of coiling of the polyion at high ionic strength is comparable to that of its methyl ester in benzene solution. This conclusion is similar to that reached by Katchalsky and Eisenberg[6] when 2 N sodium hydroxide was used as the solvent.

C. Light Scattering Measurements and the Determination of Molecular Weight.—The light scattering photometer employed in these studies has been described by Brice, Halwer and Speiser.[22] For further details of its calibration and the procedures used, reference should be made to Doty and Steiner.[23] The solutions were cleaned by centrifuging for at least four hours at 20,000 g. The solvent used for the molecular weight determinations was hydrochloric acid solution having a pH of 1.55. In this solvent the ionization of the polymethacrylic acid was negligible ($\alpha \cong 0.001$). The limiting dissymmetry (45°/135°) was unity for fraction B_1 and 1.025 for fraction A_2. In the latter case the limiting c/R_{90} ratio has been corrected by 1.5%. The light scattering data are summarized in Table I.

TABLE I

LIGHT SCATTERING DATA FOR TWO POLYMETHACRYLIC ACID FRACTIONS IN HYDROCHLORIC ACID SOLUTION

Fraction A_2			Fraction B_1		
c, g./cc.	$R_{90} \times 10^5$	$Kc/R_{90} \times 10^5$	c, g./cc.	$R_{90} \times 10^5$	$Kc/R_{90} \times 10^5$
0.01005	29.1	1.421	0.01000	15.75	2.63
.00471	15.2	1.275	.00500	8.45	2.46
.00286	9.82	1.204	.00250	4.31	2.40
.00166	5.90	1.171	.00125	2.21	2.35
.00091	3.30	1.145			
0		1.125	0		2.32
$s = 1.025$	$P(90) = 0.985$		$z = 1.00$	$P(90) = 1.00$	
$M = 1/(1.125 \times 10^{-5} \times 0.985) = 90{,}300$			$M = 1/(2.32 \times 10^{-5}) = 43{,}100$		
$B = 0.15 \times 10^{-4}$ cc. moles/g.^{2}			$B = 0.16 \times 10^{-4}$ cc. moles/g.^{2}		

$\lambda = 4370$ Å., $dn/dc = 0.1594$, $K = 2\pi^2 n_0^2 (dn/dc)^2 / N_0 \lambda^4 = 4.15 \times 10^{-7}$

Some of the data for fraction A_2 are plotted in Fig. 1 in accordance with the basic equation

$$K(c/R_{90})P(90) = 1/M + 2Bc \qquad (2)$$

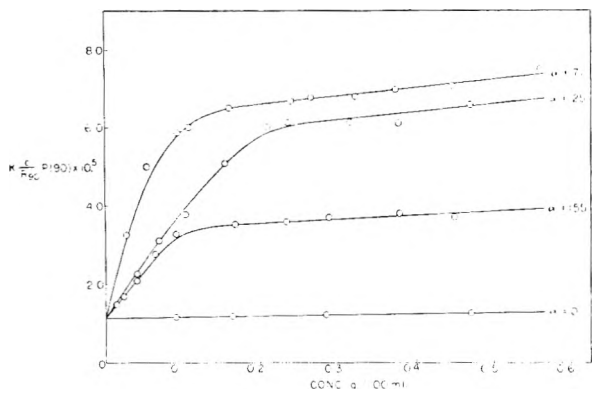

Fig. 1.—Plot of $(Kc/R_{90})P(90)$ against c for polymethacrylic acid, fraction A_2, at different degrees of ionization. Data taken from Table II.

(21) J. H. Baxendale, S. Bywater and M. G. Evans, *J. Polymer Sci.*, **1**, 237 (1946).

(22) B. A. Brice, M. Halwer and R. Speiser, *J. Opt. Soc.*, **40**, 768 (1950).

(23) P. Doty and R. F. Steiner, *J. Chem. Phys.*, **18**, 1211 (1950).

D. Potentiometric Titration and Conductance Measurements.—A Beckman pH meter, model G, was used for the determination of pH at 25°. For these measurements the solutions were prepared with the usual precautions in order to avoid carbon dioxide absorption. The dilutions and pH measurements were made under streaming nitrogen with a Beckman pH Meter, model G, at 25°. Without the use of nitrogen, the drift of the pH was evident at ionizations greater than $\alpha = 0.5$. Conductivity measurements were made with a relatively simple conductance bridge, Model RC, of the Industrial Instrument Co. A soda lime trap was used to close the conductivity cell. These measurements were likewise made at 25°.

II. Light Scattering

A. Absolute Intensity Data.—In the investigation which has preceded this one,[24] the behavior of solutions of a protein salt (bovine serum albumin carrying fifty charges) was studied. In this case the polyion is small and rigid; consequently, the variations in the dissymmetry which were observed were due entirely to the effects of external interference. It was found that the value of Kc/R_{90} rose sharply from the intercept at zero concentration, gradually fell off and after reaching a concentration of about 0.4 g./100 cc. was nearly independent of concentration. This behavior was shown to be consistent with concept of the protein ion and its gegenion atmosphere behaving as either a hard or, better, a soft sphere whose size was comparable with that of the gegenion atmosphere and which therefore varied in size approximately inversely as the cube root of the concentration of gegenions and hence of protein. The data could be represented by expressions derived for three closely related models. For the case of non-repelling hard spheres

$$Kc/R_\theta = \frac{1}{MP(\theta)} [1 + 2(B'/M)c\Phi(hD)] \qquad (3)$$

where $B' = (2/3)\pi D^3 N_0$, N_0 being Avogadro's number and D the hard sphere diameter. The quantity $\Phi(hD)$ is the common scattering function $(3/x^3)(\sin x - x \cos x)$ where $x = hD$ and $h = (4\pi/\lambda')\sin(\theta/2)$. If the potential between particles is of the form $\ln[1 - \exp(-r/r_0)^2]$, which is a good approximation to the potential between charged particles, one can derive the expression

$$Kc/R_\theta = \frac{1}{MP(\theta)} [1 + \pi^{3/2}(N_0/M)cr_0^3 \exp(-h^2 r_0^2/4)] \qquad (4)$$

At higher concentrations these equations become somewhat inadequate since only the second virial coefficient has been used in their derivation. In the absence of gegenions that do not belong to the protein salt the hard sphere diameter, D, or the distance of average approach of centers, r_0, is assumed to be inversely proportional to the cube root of the concentration. Therefore, the coefficients of the last term in both equation (3) and (4) are concentration independent and the concentration dependence of $Kc/R\theta$ is due solely to the variation of the function $\Phi(hD)$ or the exponential as a consequence of the dependence of D and r_0 on concentration. This functional relation is satisfactory for representing the observed data for serum albumin. A similar concentration dependence of Kc/R is to be expected for polymethacrylic acid when sufficiently ionized except insofar as it may be modified by the variation in size of the polyion with concentration and by much larger charges which the polyion may bear.

The reduced intensity at 90°, R_{90}, and the dissymmetry, z (45°/135°), have been measured as a function of concentration at several different extents of ionization and are presented in Table II and graphed in Fig. 1 for fraction A_1. In obtaining these data the solution at a concentration of about 0.5 g./100 cc. is brought to the desired state of ionization by the addition of dilute NaOH solution. The solution and solvent are then made optically clean by centrifuging at 20,000 g. for at least five hours at about 5°. The solvent in this case is doubly distilled water. In principle the pH of the water should be that of the solution but in this particular system those pH values are so close to that of distilled water that adjustment is not necessary. The scattering measurements were made in two ways. (1) For concentrations below 0.1 g./100 cc. the semi-octagonal cell is filled with 50 cc. of optically clean water ($z < 1.1$)

(24) P. Doty and R. F. Steiner, *ibid.*, in press.

and the concentrated solution is gradually added and mixed by means of a magnetically rotated, glass-enclosed iron nail. (2) At higher concentrations the cell is filled with 50 cc. of the concentrated solution and dilutions are made stepwise with optically clean water. For the concentration range in which the minimum occurs, measurements were made in both ways. It was demonstrated that centrifugation had not significantly altered the concentration of the solution.

It will be recalled that R_0 is the quantity of thermodynamic significance. In work with polymers this is usually derived from measurements of R_{90} by dividing the latter by $P(90)$ which in turn is evaluated from the limiting dissymmetry, $[z]$. However, in view of the unusual concentration dependence of z it is believed that R_0 is better approximated by using $P(90)$ derived from the dissymmetry observed at each concentration. The difference between these two procedures generally amounts to only a few per cent. The data plotted in Fig. 1 for $\alpha = 0$ are taken from Table I.

It is noted that the concentration dependence of Kc/R_{90} is of the nature anticipated and that the initial slope as well as the remainder of the data increase with α. The data for different values of α are consistent with a common intercept but the precision is not sufficient to prove this for the higher degrees of ionization. The precision attained in this work was not accomplished without considerable effort since the excess scattering over that of water was only 10 to 100%.

The data in Fig. 1 can be rather well represented by equations (3) and (4) by choosing a value of D or r_0 to fit the data at high concentration and then providing for an appropriate increase in D or r_0 with decreasing concentration. In the former study of serum albumin[24] equation (3) was found to fit the observed data within a small difference resulting from the use of a hard sphere potential rather than an electrostatic potential when the following points were considered: (1) the contribution of the counter-ions present due to the acid required to maintain the relatively low pH, (2) the macro-ion possessed a finite size which was independent of concentration, (3) the hard sphere diameter was the sum of the mean diameter of the protein molecule and a counter-ion atmosphere whose effective thickness varied as the inverse cube root of the concentration of counter-ions. When considering the present data the first point need not be considered. The second and third points must be considered together since the size of the macro-ion is in this case variable. If the finite size of the macro-ion is neglected, it was found that the concentration dependence must be much less pronounced, say about inverse sixth root of concentration, in order to obtain moderate agreement. A more reasonable alternative, especially in view of the discussion of the viscosity behavior below, is to permit the effective diameter, D, to increase toward a limiting size upon dilution. This is in contrast to the limit of infinite size used for the serum albumin. Within the precision of Fig. 1 a variety of forms of the concentration dependence of D can be employed. Among these is the particular form $D^3 = A/(1 + B\sqrt{c})$ which is analogous to the reduced specific viscosity. Although these data do not justify an attempt to elicit a precise form of the concentration dependence of D, the following might be said in summary. The initial slopes are not infinite but do increase with charge. Therefore, the value of D appears to reach a limiting value upon dilution which is a monotonic function of the charge. The value of Kc/R_{90} at which the curves essentially level off at higher concentration is a measure of the extent to which the solution is filled with spheres of diameter D.

The curves for $\alpha = 0.25$, 0.45 and 0.71 differ little from each other and, moreover, are very similar in shape and absolute value with the corresponding data for serum albumin which carried only fifty charges. The insensitivity to the value of α beyond 0.25 is probably due to a compensation between the further increase in charge and a corresponding increase in gegenion concentration which might in part be due to association of gegenions with the polyion at larger degrees of ionization. The similarity with serum albumin, despite the much greater charge on the polyion must be a reflection of the net interaction in each case being about the same. This is understandable inasmuch as the charges on serum albumin reside within a relatively small volume giving rise to interactions that approach those of point charges; the charges on the polyions are so widely distributed that much less effective repulsions exist between flexible molecules.

TABLE II

LIGHT SCATTERING DATA FOR FRACTION A_2 AS A FUNCTION OF DEGREE OF IONIZATION

α	c. (g./cc.) $\times 10^2$	$R_{90} \times 10^5$	$[z]$	$K(c/R_{90})P(90) \times 10^5$
0.155	0.0151	0.357	1.25	1.46
	.0258	.566	1.19	1.645
	.0412	.726	1.15	2.08
	.0666	.900	1.12	2.77
	.0925	1.06	1.12	3.27
	.168	1.77	1.14	3.51
	.233	2.36	1.18	3.57
	.269	2.80	1.19	3.72
	.379	3.54	1.20	3.82
	.450	4.28	1.21	3.72
0.25	0.0232	0.454	1.45	1.574
	.0418	.600	1.39	2.22
	.0695	.775	1.26	3.08
	.1045	.971	1.24	3.73
	.154	1.04	1.25	5.075
	.209	1.16	1.30	6.01
	.235	1.27	1.33	6.10
	.314	1.67	1.35	6.11
	.377	2.02	1.35	6.09
	.471	2.23	1.42	6.61
0.45	0.0208	0.250	1.65	2.30
	.0374	.355	1.60	2.99
	.0623	.479	1.565	3.74
	.080	.580	1.52	4.07
	.125	.766	1.40	5.14
	.187	.927	1.45	6.20
	.249	1.15	1.52	6.40
	.299	1.34	1.55	6.47
	.374	1.66	1.57	6.50
0.71	0.0268	0.222	1.70	3.25
	.0536	.301	1.63	4.97
	.092	.455	1.56	5.86
	.1085	.749	1.49	6.47
	.1955	.840	1.51	6.91
	.266	1.10	1.63	6.75
	.322	1.25	1.74	6.76
	.374	1.43	1.72	6.96
	.448	1.70	1.72	7.06
	.560	1.99	1.75	7.38
	.700	2.44	1.75	7.50

B. **Dissymmetry Data.**—Equations (3) and (4) lead to the following expressions for dissymmetry

$$z = [z]\frac{1 + 2(B'/M)c\Phi(h_2D)}{1 + 2(B'/M)c\Phi(h_1D)} \qquad (5)$$

and

$$z = [z]\frac{1 + \pi^{3/2}(N_0/M)cr_0^3\exp(-h_2^2r_0^2/4)}{1 + \pi^{3/2}(N_0/M)cr_0^3\exp(-h_1^2r_0^2/4)} \qquad (6)$$

where h_1 and h_2 are evaluated at $\theta = 45$ and 135, respectively. If D and r_0 are independent of concentration, as in uncharged macromolecules, both of these expressions show that with increasing concentration the dissymmetry, z, falls rapidly at first and then more slowly from the limiting value, $[z]$, at zero concentration. The absolute magnitude of the charge increases with D and r_0. On the other hand, if D and r_0 are assumed to be inversely proportional to the cube root of the concentration in the case of protein salts, z will drop from its limiting value to quite low values at extremely low concentrations and then rise (convex upward) more slowly approaching the original value of $[z]$ asymptotically.

An examination of the dissymmetry data in Table II (Fig. 2) shows that the level of the dissymmetry increases with the degree of neutralization and that the concentration

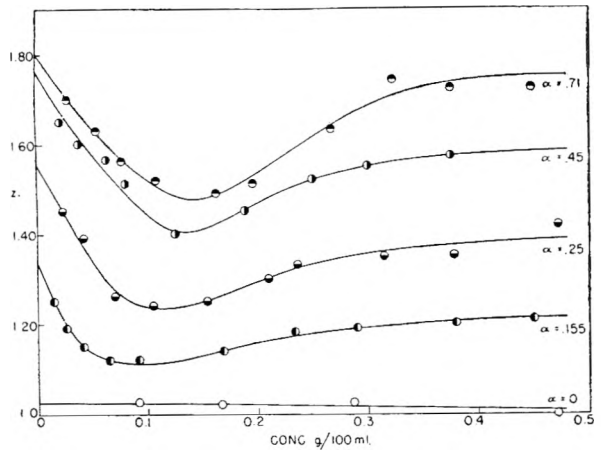

Fig. 2.—Plot of dissymmetry against c for polymethacrylic acid, fraction A_2, at different degrees of ionization. Data taken from Table II.

dependence is intermediate between the two cases described in the foregoing paragraph. Below concentrations of 0.1 g./100 cc. z increases with decreasing c in a regular manner which appears to permit reasonably precise extrapolation. Essentially the same intercepts as those shown are obtained if $1/(z-1)$ is plotted against concentration as is often the practice with neutral polymers. From the limiting values of z assignments of the mean radius can be interpreted in terms of either random coils or rods. Consideration of the actual magnitudes observed indicates that the results should be interpreted in terms of random coils. For example, if $[z]$ at $\alpha = 0.71$ were due to rod-shaped particles, they would be only half the contour length of the polymer molecule. This conceptual difficulty does not occur if one accepts the random coil model. In this case the data require that the coil be expanded until its root-mean-square separation of its ends, R, is about one-third the contour length of the molecule. At this degree of expansion the Gaussian approximation begins to fail but the error which results in this particular case should not exceed a few per cent. The measurement of the angular intensity distribution would provide a more direct resolution of this point but the low level of scattering in this system has discouraged such work for the present. We conclude, then, that upon charging the molecules of fraction A_2 their size as measured by R increases from about 170 to 1180 Å. at zero concentration as given in Table III. The contour length of the chain is 2660 Å. The size of the uncharged polymer is deduced from viscosity measurements discussed in the next section. The value of z in this case is too small for use in the precise determination of R; it places an upper limit of 210 Å. on R.

The concentration dependence of z displayed in Fig. 2 cannot be easily accounted for quantitatively. This is not surprising inasmuch as both the interaction between the polyions as well as their size may vary considerably in the concentration range studied. The fundamental limitation to interpretation probably lies in neglecting virial coefficients higher than the second (equation 6). Moreover the fitting of the concentration dependence of z puts much more rigorous demands on the theory than the fitting of the concentration dependence of Kc/R_{90}. In particular it is not possible to explain the return of z to high values, comparable to $[z]$, at high concentrations without requiring the size of the polyion to be essentially independent of concentration. This requirement appears to be unacceptable for several reasons. First, in non-electrolyte polymer solutions, there is a direct proportionality between the size R and the slope B. Alternatively we would expect R to be directly related to the effective diameter D. In either view the data in Fig. 1 would indicate that the size of the polyion decreases significantly with concentration. Second, the viscosity data discussed below lead to the same conclusion. Therefore, it would appear that the difficulty lies in the inadequacy of the theory for the concentration dependence of z at high concentration.

To test this conclusion we have examined the dissymmetry at $\alpha = 0.71$ upon diluting isoionically from concentrations of 0.266 and 0.700 g./100 cc. These two concentrations bracket the range in which high dissymmetries are exhibited. The measurements, which will be published later, showed a sharp drop upon dilution and a mild rise again after passing through minima. The intrinsic dissymmetries were found to be 1.32 and 1.25, respectively, corresponding to R = 650 and 750 Å. Since isoionic dilution of the serum albumin solutions under similar circumstances[24] showed that the effective diameter D was held constant by such a procedure, we may take this as an indication that R is at least as small as 650 Å. at c = 0.7 g./100 cc. and increases to 1180 at infinite dilution. This supports the interpretation of the R_{90} measurements and the viscosity data.

TABLE III

MEASUREMENTS AND ESTIMATES OF R FOR TWO FRACTIONS OF POLYMETHACRYLIC ACID AS A FUNCTION OF THE DEGREE OF IONIZATION

Fraction	α	$[\eta]$	pK	R'	R_z	R_η	R_t	R_{kkk}
A_2	0.001	0.115			(210)	171	142	142
	.155	3.70	6.64	334	710	540	895	1700
	.25	18.5	7.01	446	940	925	1185	2100
	.45	45.5	7.57	640	1110	1250	1710	2400
	.68	55.5	8.18	786		1340	2100	2560
	.71				1180			
	.75						2530	
B_1	0.001	0.063				109	100	100
	.08	0.465	6.16	114		212	280	430
	.20	2.27	6.83	188		360	480	875
	.35	10.5	7.3	264		600	685	1080
	.50		7.70	326			850	1180
	.75	13.9	8.39	394		658	1015	1250
	1.00	13.4				650		1250

III. Viscosity Measurements

It has been shown[3,4] that the specific viscosity–concentration data of polymeric electrolytes can be well represented by the expression

$$\frac{\eta_{sp}}{c} = \frac{A}{1 + B\sqrt{c}} \tag{7}$$

By plotting the data according to this equation in reciprocal form, a straight line is obtained which apparently allows the intrinsic viscosity to be determined by extrapolation. Recently the following relation relating intrinsic viscosity, $[\eta]$, to R has been proposed[25] and shown to be valid in a number of cases.

$$R^3 = \frac{M[\eta]}{2.1 \times 10^{21}} \tag{8}$$

By combining these two relations a new method for determining the value of R for polymeric electrolytes results. Such a procedure is, however, open to some criticism. First, the use of equation (8) in preference to others such as those due to Kuhn and Kirkwood and Riesman may not find universal agreement. We believe that at present the Flory–Fox equation has received the widest experimental verification. Second, can one expect an equation derived for randomly coiled chains to hold when the molecules are extended so that R may be as much as 45% of the contour length? In reply one can only state that up to this degree of extension, the polymer chain of this length is still essentially Gaussian and that on a time scale comparable to the gradient employed in the viscosity measurements the molecule will probably be spherically symmetrical. Therefore, despite the extreme state of extension, equation (8) may still be applicable. However, since this is the first experience with applying this equation to such extended molecules, the results should be interpreted with caution.

The viscosity measurements for the two fractions of polymethacrylic acid as a function of c and α are shown in Table IV. Some of the data for fraction A_2 are plotted in accordance with equations (7) in Fig. 3 where the linear behavior is evident. The values of A, which we consider equal to $[\eta]$, and B are also given in Table IV. It is interesting to note that although B as a function of α passes through a flat maximum, it appears to be independent of molecular weight.

The values of R calculated from equation (8) are listed in Table III, under the heading R_η. Although the differences

(25) P. J. Flory and T. G. Fox, *J. Polymer Sci.*, **5**, 745 (1950).

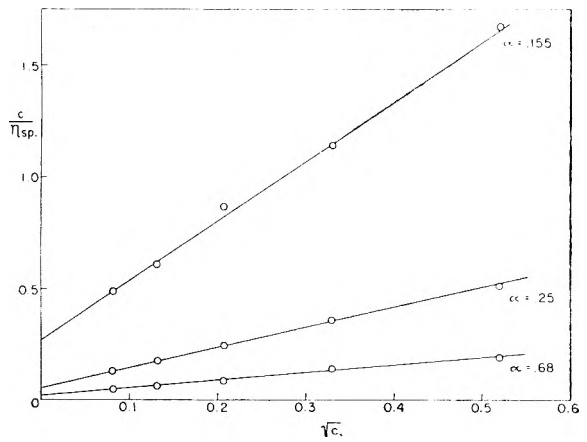

Fig. 3.—Plot of the reciprocal reduced specific viscosity against the square root of concentration for polymethacrylic acid, fraction A_2, at several degrees of ionization.

between these values and those of R_z are for the most part beyond that of probable experimental error, assuming that the methods of extrapolation are valid, the comparison reveals no major discrepancies. Thus this interpretation of the viscosity results is consistent with the light scattering results.

TABLE IV

SPECIFIC VISCOSITY DATA FOR TWO POLYMETHACRYLIC ACID FRACTIONS AS A FUNCTION OF DEGREE OF IONIZATION AND CONCENTRATION

	Fraction A_2			
c, (g./100 cc.)	α = 0.155	α = 0.25	α = 0.45	α = 0.68
0.272	0.600	1.98	4.20	5.27
.107	0.877	2.804	6.50	7.84
.0432	1.145	4.10	9.52	11.70
.0174	1.640	5.715	13.16	16.6
.00697	2.046	7.77	18.2	21.4
A	(3.70)	(18.5)	(45.5)	(55.5)
B	(9.85)	(16.8)	(18.4)	(18.2)

	Fraction B_1				
c, (g./100 cc.)	α = 0.08	α = 0.20	α = 0.35	α = 0.75	α = 1.0
0.2166	0.121	0.403	1.222	1.71	1.705
.1083	.158	0.552	1.66	2.20	2.19
.0541	.193	1.702	2.18	2.90	2.92
.0271	.228	0.909	2.89	3.80	4.04
.0135	.281	....	3.68	4.95	4.81
A	(.465)	(2.27)	(10.5)	(13.9)	(13.4)
B	(6.0)	(9.75)	(16.1)	(16.1)	(15.2)

It is interesting to note that the value of a occurring in the equation

$$[\eta] = KM^a \qquad (9)$$

increases from 0.82 to 1.87 upon ionization (α = 0.001 to α = 0.7). Since these values are based on only two fractions, the accuracy cannot be high, but they are consistent with a transition from a small coil to a highly extended configuration in agreement with similar measurements of Katchalsky and Eisenberg.[6]

IV. Potentiometric Titrations

A. Theory.—In two recent theoretical studies relations between the difference in the apparent pK (which depends on the degree of ionization) and the intrinsic pK of the monomeric acid, *i.e.*, pK_0, and the ratio of the size of the polyion at degree of ionization α and uncharged, R_α/R_0 have been proposed. The equation derived by Hermans and Overbeek[4] is

$$[\mathrm{pH}]_0^\alpha + \log(1-\alpha)/\alpha - pK_0 = C\frac{\alpha Ze^2}{DkTR'} \qquad (10)$$

$[\mathrm{pH}]_0^\alpha$ refers to pH at zero concentration and degree of ionization α

C = a constant having a value between 0.52 and 0.56
Z = degree of polymerization
e = electronic charge
D = dielectric constant

$$R' = [(\bar{5}/36)R_0^2(1 + R_\alpha^2/R_0^2)]^{1/2} \qquad (10a)$$

By a somewhat different procedure which ignores the effects of gegenions, Katchalsky and Gillis[11] conclude that

$$pK - pK_0 = 2.4 \times 10^{-5}\lambda/(2\lambda' sb^2)^{1/3} \qquad (11)$$

where

$\lambda = 1 + \ln(3R_\alpha^2/2R_0^2)$
$\lambda' = \ln(3R_\alpha^2/2R_0^2) - 1$
s = no. of monomer units per statistical element of uncharged, randomly coiled, polymer; taken as 3 in this work as a result of viscosity measurements; a value of 4 is sometimes used by other workers
b = length of monomer in chain direction, 2.52 Å.

In addition the value of n, defined by the relation

$$\mathrm{pH} = pK - n\log(1-\alpha)/\alpha \qquad (12)$$

is found to be related to the expansion factor in the following way

$$n - 1 = 0.821 \times 10^{-5}\lambda/(2\lambda' sb^2)^{1/3} \qquad (13)$$

B. Evaluation of pK at Zero Concentration.—In order to test these relations the pH has been measured as a function of polymer concentration at several values of α. The results for fraction B_1 are given in Table V. Since the pH is

TABLE V

TITRATION DATA FOR POLYMETHACRYLIC ACID (FRACTION B_1). THE OBSERVED pH AS A FUNCTION OF DEGREE OF NEUTRALIZATION

c, (g./100 cc.)	α = 0.08	α = 0.20	α = 0.35	α = 0.50	α = 0.75
0.2166	4.47	5.54	6.04	6.73	7.78
.1083	4.61	5.70	6.24	6.94	8.03
.05415	4.77	5.88	6.40	7.08	8.26
.02707	4.83	6.02	6.56	7.21	8.46
.01353	4.98	...	6.72	7.38	8.56
$D = [p\mathrm{H}]^\alpha$	5.16	6.35	7.02	7.68	8.92
E	2.16	2.56	3.13	3.10	3.53

concentration dependent the need for extrapolating to zero concentration in order to evaluate pK is evident. It has been stated[19] that the concentration dependence could be represented by adding a term in $c^{1/2}$ onto equation (12).

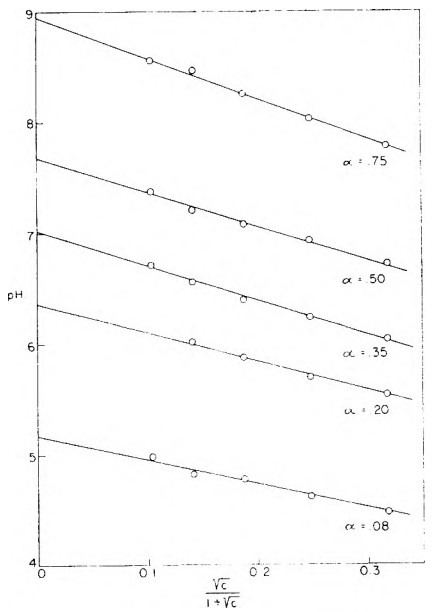

Fig. 4.—Plot of pH as a function of $\sqrt{c}/(1+\sqrt{c})$ for polymethacrylic acid, fraction B_1, at several degrees of ionization.

However, this proved inadequate for the present data. In analogy with the Debye-Hückel expressions for the activity coefficients for electrolytes, the term $D\sqrt{c}/(1 + E\sqrt{c})$ was added to expression (12). It was found that when E was given the value of unity and c expressed in g./100 cc. the data could be fitted as shown in Fig. 4. The earlier data of Katchalsky and Spitnik[19] are also well fitted by this type of plot. Likewise titration data of β-lactoglobulin[5] in the acid range are represented by this type of plot with $E = 0.5$. On the basis of very limited data, therefore, it appears that this is an improvement in representing the concentration dependence of the activity coefficients of macroions. The values of $[pH]_0^\alpha$ obtained by the extrapolations shown in Fig. 4 are plotted against $\log(1 - \alpha)/\alpha$ in Fig. 5. The straight line representation found here leads to the expression of the titration data in the form

$$[pH]_0^\alpha = 7.70 - 2.45 \log(1 - \alpha)/\alpha \qquad (14)$$

The values of the constants found by Katchalsky and Spitnik[19] were 7.02 and 2.0, respectively. The principal reason for this difference lies in the different methods of extrapolation to zero concentration. Since our data covered a larger range of concentration and extended to more dilute solutions, we believe it correct to use our values in the following calculations. It should be added that the data of Arnold and Overbeek[9] which were obtained at only one polymer concentration are considerably higher than ours at the lower values of α.

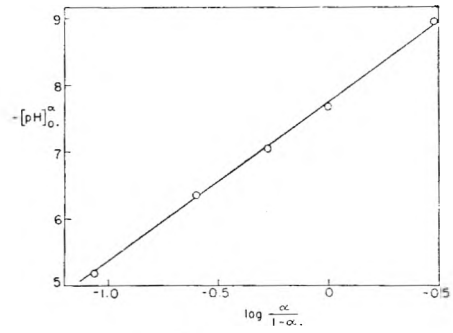

Fig. 5.—Plot of $-[pH]_0^\alpha$ against $\log \alpha/(1 - \alpha)$ for polymethacrylic acid, fraction B_1.

C. Estimation of Molecular Size and Slope of Titration Curve.—The values of pK found by extrapolation are listed in Table III together with the values of R' derived from equation (10a). Using the values of R_0 corresponding to the size estimated from viscosity measurements of the hydrochloric acid solution ($\alpha = 0.001$), the values of R have been calculated and are listed under R_t. These values are somewhat larger than those obtained from dissymmetry and viscosity at lower values of α. At larger α values R_t is considerably higher than the other estimates. This increasing divergence with α may be expected inasmuch as the theory on which equation (9) is based assumed only moderate expansion of the coiled molecule.

Turning now to an examination of the other theoretical relation, equation (10), one finds that no comparison can be made. This is because the expression on the right side does not yield values in the range observed. Thus when $R_\alpha/R_0 = 8$, the right side of equation (9) has a value of 5.0 whereas the observed value, that is, the left side of equation (9), is about 2.0.

In view of this experience with equation (10) one cannot expect a very satisfactory prediction of the value of the slope constant, n, from equation (12). Choosing a value of $R_\alpha/R_0 = 8$, this being approximately the case for both fractions near $\alpha = 0.5$, we find from equation (12) a value of $n = 1.83$ which is to be compared with an observed value of 2.45.

D. Activity Coefficients of Polymeric Ions.—The form of the activity coefficient described in Section B above invites some speculation. Putting the activity coefficient in the Debye-Hückel form, equation (12) may be written as

$$pH = pK - n \log(1 - \alpha)/\alpha - nZ^{*2}A\sqrt{m}/(1 + a\beta m) \qquad (15)$$

A and β are the usual constants having values of 0.505 and 0.329. The ionic diameter is represented by a and the effective charge by Z^*. As before m is equal to the molality of gegenions. At $\alpha = 0.5$ it is found that $Z^* = 3.25$ and $a = 12.7$ Å. Thus one might imagine that the proton behaves as though in solution with gegenions of these characteristics or that a part of the polymer chain defined in this manner were the effective unit in determining the activity of hydrogen ions. In order for the observed concentration dependence to be preserved as a function of α it is necessary that both Z^* and a vary inversely as $\sqrt{\alpha}$. Thus upon going to higher degrees of ionization the charge and size of the chain segment acting on each proton decreases and upon going to states of smaller ionization Z^* and a increase until at states of low α the entire polyion acts as the gegenion to the proton. However, it is most unlikely that the potential of the hydrogen ions with respect to the polyions is in all cases sufficiently small compared to kT for the Debye-Hückel theory to be valid. Therefore, these conclusions are merely a description of the situation in familiar though not strictly applicable terms.

V. Conductance Measurements

In formulating a satisfactory concept of polyelectrolyte solutions, it is necessary to know to what extent the gegenions are associated with polyions. In particular one wonders if the absence of even moderate changes in light scattering and viscosity in the range of $\alpha = 0.5$ to 1.0, in comparison with the radical changes found in the 0 to 0.4 range of α may not be due to the association of gegenions at higher values of α. To obtain some information on the variation of the effective charge of the polyion with degree of ionization conductance experiments were undertaken. Meanwhile, however, these questions have been answered in a very elegant manner by means of transference and diffusion experiments.[13,16,19]

The specific conductance of fraction B_1 was measured as a function of concentration at five different degrees of ionization. The reduced specific conductance is recorded in Table VI. The concentration dependence at constant α was found to follow a relation of the form

$$\kappa/c = (\kappa/c)_0 - A\sqrt{c} + Bc \qquad (16)$$

In order to evaluate the effective charge of the polyion as a function of the degree of neutralization, we compute the

TABLE VI

REDUCED SPECIFIC CONDUCTANCE OF POLYMETHACRYLIC ACID (FRACTION B_1) AS A FUNCTION OF THE DEGREE OF IONIZATION AND CONCENTRATION

c, (g./100 cc.)	$\kappa/c \times 10^3$ $\alpha = 1.0$	$\alpha = 0.75$	$\alpha = 0.50$	$\alpha = 0.35$	$\alpha = 0.20$
0.2166	4.23	3.43	3.06	2.43	1.47
.1083	4.44	3.70	3.27	2.75	1.775
.0541	4.73	3.99	3.54	2.95	1.93
.0271	5.24	4.14	3.84	3.18	.....
.0216	....	....	....	....	2.20
.01353	5.69	4.66	4.12	3.32	.....
$(\kappa/c)_0$	(6.70)	(5.57)	(4.75)	(3.78)	(2.55)
$A\ 10^2$	1.08	0.905	0.636	0.418	0.240
$B\ 10^2$	1.18	0.96	0.575	0.276	0.0122

limiting molar conductivity, $\Lambda_0 = 1000\ (\kappa/c)$ where c is expressed in moles of monomeric units (mol. wt. 86) per liter. Then if λ_0^- is the limiting molar conductance of the polyion, Z' is the effective charge of the polyion and λ_0^+ is the equivalent conductance of the counterion (Na = 51.0), we have

$$\Lambda_0 = Z'\lambda_0^+ + \lambda_0^- \qquad (16a)$$

Now the mobility of the polyion is given by the expression

$$\mu = (\Lambda_0 - Z'\lambda_0^+)/Z'F \qquad (17)$$

where F represents the number of faradays. The mobility, μ, can also be expressed as

$$\mu = (HeZ')/f \qquad (18)$$

where H represents the applied electric field and f the frictional constant of the migrating particle. If it is assumed that the value of f is proportional to $[\eta]$, *i.e.*, $f = k[\eta]$, we have by combining the two preceding equations and com-

bining all the constants into a single one, D, equal to $He f/k$, the equation

$$DZ'^2/[\eta] + Z'\lambda_0^- - \Lambda_0 = 0 \qquad (19)$$

Thus if D is known, we can evaluate Z' from $[\eta]$ and Λ_0 for the corresponding degree of neutralization.

Since D is not independently known, we can to a first approximation evaluate it by assuming that for low values of ($\alpha < 0.30$) the effective number of charges Z' is equal to the titration charge αZ: then we can solve the quadratic equation for Z', rejecting the root which leads to a value of Z' larger than the corresponding αZ. The results are shown in Fig. 6 where it is seen that up to nearly $\alpha = 0.5$, the effective charge is essentially equal to the titration charge but that it increases much more slowly thereafter with increasing neutralization. At $\alpha = 1.0$, $Z' = 0.6\,Z$. The curve shown in Fig. 6 is in nearly quantitative agreement with that obtained from transference and diffusion measurements.[13,15,16] This cation binding is most clearly shown by the lack of proportionality between $(\kappa/c)_0$ and α in Table VI.

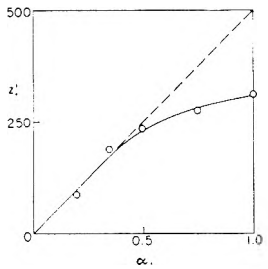

Fig. 6.—The net charge per polyion as a function of the degree of neutralization α for polymethacrylic acid, fraction B_1.

VI. Discussion

The foregoing data and their interpretation provide a consistent picture of the limiting size and interaction of polymeric electrolytes at low concentration as a function of the degree of neutralization. With increasing ionization the polymer molecule expands, rapidly at first, and then more slowly reaching a maximum size (for the sample studied about seven times its original root-mean-square end-to-end distance) at about 60 to 80% neutralization. The expansion as a function of α is shown in Fig. 7 for fraction A_2. As in the case of ordinary electrolytes, there is a rather academic ambiguity concerning the real concentration at which this description holds. Over the concentration range covered by our measurements most of the gegenions could be considered as belonging to the ionic atmosphere of the polyions or as being associated with them. In extrapolating to zero concentration, it is implied that this situation persists. Yet at infinite dilution most of the gegenions would in time leave the polyion. Thus at truly infinite dilution after equilibrium has been attained, the polyion is involved with only a few ions resulting from the ion product of water and the picture we have drawn probably does not apply. However in a practical sense, at some less degree of dilution but still at concentrations less than that experimentally accessible, the polyion we have described probably exists and its characterization is important since the behavior of real solutions of finite concentration can be so conveniently referred: it is the goal to which polyions at finite concentration tend upon dilution.

It is interesting to note the discrepancy between our results and the theory of Kuhn, Kunzle and Katchalsky[20] which attempts to relate the expansion of the polyion to its degree of ionization and hence to various physical properties. The predictions of their theory are shown in Fig. 7 as taken from Table III. These values are much larger than indicated by our data and for large α correspond to nearly complete extension. This disagreement is essentially a reflection of their assumption that the effect of gegenions was negligible at high dilution. It is unlikely that there is any way to determine the characteristics of polyions completely separate from gegenions. Their claim that such conditions exist in dilute solutions is not supported by these investigations or their own if properly assessed. In the interpretation of their viscosity data on polymethacrylic acid (Fig. 7, reference 20) their extrapolation to zero concentration falls short of that which would have resulted from equation (7) by a factor of 1.8. On the other hand, the molecular weight assumed for this polymer was less by 6.5 than later measurements[6] showed it to be. The ratio of these two factors, *i.e.*, 6.8/1.8, is approximately the extent to which (R_α^2/R_0^2) deduced from their theory differs from that derived from the data in Table III.

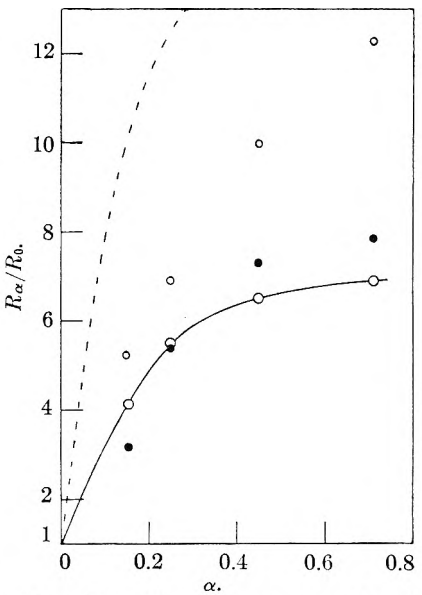

Fig. 7.—The ratio of the root-mean-extension of the polymethacrylic acid, fraction A_2, R_α/R_0 as a function of the degree of neutralization as determined from dissymmetry and viscosity measurements. The results calculated from titration data are also shown. The dashed line is calculated from the theory of Kuhn, Kunzle and Katchalsky.[22] R_0 has been computed from $[\eta] = 0.115$. Since this is abnormally low, presumably due to hydrogen bonding,[16] use of $[\eta] = 0.450$ (Part I) as a closer approximation to the size of the unperturbed coil may be preferred. Doing this increases R_0 by a factor of 1.58 and correspondingly alters the scale of this figure by the same amount. ○, dissymmetry; ●, viscosity; ⊙, titration.

Only qualitative statements can be made about the concentration dependence of the size of the polyion. The Kc/R_{90} data show that D decreases with concentration and we deduce that the size of the polyion must likewise decrease. The dissymmetry measurements when isoionic dilutions are made lead to the same conclusion. In the particular case of fraction A_2 at $\alpha = 0.71$ it would appear from both types of measurements that R decreases about 2- to 4-fold upon increasing the concentration from zero to 0.5%.

The well-known variation of η_{sp}/c with c leads to the same qualitative conclusion. To obtain more precise information from viscosity measurements two contributions to the value of η_{sp}/c must be eliminated so that that portion due only to polyion size can be evaluated. The first contribution is the electroviscous effect, that is, the augmentation of η_{sp}/c by the counterion atmosphere. The fact that size determinations based on extrapolation to infinite dilution where the effect of the gegenions should be maximal are consistent with those from light scattering indicate that the electroviscous effect is unimportant. Measurements of this effect in the serum albumin system, to be published later, show likewise that the effect, although important at low viscosities as in protein solutions, is negligible in polyelectrolytes of high molecular weight. We conclude that the observed values of η_{sp}/c for solutions of polysalts is due to the size of the polyions and their interactions; the effect of the gegenions *directly* is negligible. Therefore, only the effect of interactions must be taken into account. On the basis of preliminary experiments it appears that this may be done at least to a good approximation, by making isoionic dilutions from various points on the η_{sp}/c *versus* c curve for the polysalt. Further investigation along these lines by both viscometric and light scattering measurements will probably clarify the problem of the concentration dependence of the polyion size.

It may be useful to remark at this point that the success of Fuoss's approximate equation

$$\frac{\eta_{sp}}{c} = \frac{A}{1 + B\sqrt{c}} \qquad (7)$$

to represent the viscosity of many polyelectrolyte solutions is consistent with the views outlined here. This is readily seen by comparing this with the corresponding equation for ordinary electrolytes

$$\frac{\eta_{sp}}{c} = \frac{A\sqrt{c}}{1 + B\sqrt{c}} \qquad (20)$$

In the later case η_{sp}/c increases without limit upon dilution. This is consistent with the assumption that the size of the counterion cloud, which is in this case solely responsible for the increased viscosity over that of the solvent, varies inversely with the square or cube root of the concentration and thus reaches infinite size at zero concentration. With polyelectrolytes on the other hand, η_{sp}/c approaches a finite limit of A with decreasing concentration. This is consistent with the size of the polymer ion being the controlling factor, the value of A reflecting the limiting size to which the polyion expands.

Finally mention should be made of three other reports of light scattering observations on polymeric electrolytes[26,27,28] which have appeared recently. In all of these the diminution of R_{90} with increasing charge was observed and in one case[28] the dissymmetry showed the characteristic minimum similar to that in Fig. 2. However, the essentially qualitative nature of these observations and their restriction to relatively high concentration prevents further comparison.

Acknowledgment.—The authors wish to thank the Research Corporation for financial support which made this work possible.

(26) W. M. Cashin, *J. Colloid Sci.*, **6**, 271 (1951).
(27) R. M. Fuoss and D. Edelson, *J. Polymer Sci.*, **6**, 767 (1951).
(28) F. T. Wall, J. W. Drenan, M. R. Hatfield and C. L. Painter, *J. Chem. Phys.*, **19**, 585 (1951).

ELECTROLYTIC INTERACTION OF NYLON WITH AQUEOUS SOLUTIONS OF SODIUM HYDROXIDE

BY FREDERICK T. WALL AND THOMAS J. SWOBODA[1]

Noyes Chemical Laboratory, University of Illinois, Urbana, Illinois

Received August 30, 1951

Theoretical equations have been derived to describe the interaction of fibrous nylon suspended in aqueous acids or bases. To test the theory, experiments have also been carried out using undrawn nylon fibers with aqueous sodium hydroxide. Good agreement is observed between theory and experiment, and the results have been used to calculate equilibrium constants for the ion absorption and neutralization processes. The numbers of carboxyl and amino groups within the nylon are also calculated and the results are found to be in good agreement with titrations carried out in solution.

Introduction

When an insoluble substance containing ionizable groups is placed in an aqueous solution of an electrolyte, ion absorption or ion exchange generally occurs. In particular, if the substance is a polymer like nylon, whose molecules contain carboxyl and amino end groups, one can expect marked interactions with acids and bases. Indeed it is presumed that acid dyes attach themselves to nylon through salt formation with the amino end-groups.[2] Since nylon provides a relatively simple model of a solid acid–base system, we have carried out quantitative studies of its interactions with aqueous alkali. The experimental results have also been compared with a simple theory based on mass action considerations.

Gilbert and Rideal[3] have already treated theoretically the interactions of wool with electrolytes and have compared their conclusions with the experimental results of Steinhardt[4–6] and others.[7] Since wool is presumed to have equal numbers of acid and base groups, the theoretical equations assume quite

(1) Chemical Department, E. I. du Pont de Nemours and Company, Wilmington 98, Delaware.
(2) McGrew and Schneider, *J. Am. Chem. Soc.*, **72**, 2547 (1950).
(3) Gilbert and Rideal, *Proc. Roy. Soc. (London)*, **182A**, 335 (1944).
(4) Steinhardt and Harris, *Bur. Stand. J. Res.*, **24**, 335 (1940).
(5) Steinhardt, *ibid.*, **28**, 191 (1942).
(6) Steinhardt, Fugitt and Harris, *ibid.*, **30**, 123 (1943).
(7) Speakman and Stott, *Trans. Faraday Soc.*, **31**, 1425 (1935).

simple forms. Nylon, on the other hand, can have almost any ratio of acid to base end-groups; hence, it provides a more drastic test of the theoretical considerations involved.

Suppose that a certain nylon fiber, which is to be immersed in a solution of an appropriate electrolyte, contains all total A_0 carboxyl groups and B_0 amino groups. Let us further suppose, for the sake of our present discussion, that A_0 is greater than B_0. Then since the proton affinity of an amino group is greater than that of the carboxylate ion, we can expect that the fiber will initially contain approximately B_0 positive ($-NH_3^+$) and B_0 negative ($-COO^-$) groups as well as $A_0 - B_0$ un-ionized carboxyls (–COOH). If the fiber is now placed in a solution of sodium hydroxide, for example, we can expect the following over-all reactions to occur

$$—COOH + Na^+ + OH^- \longrightarrow —COO^-Na^+ + H_2O$$

and

$$—NH_3^+ + —COO^- + Na^+ + OH^- \longrightarrow —COO^-Na^+ + —NH_2 + H_2O$$

By the symbol $-COO^-Na^+$ we shall mean a sodium ion attached to the fiber, presumably in the neighborhood of a negatively charged carboxyl group.

The reactions written above imply that both fiber and solution remain electrically neutral; of course this will not be exactly the case, but it will be very nearly true for fibers that are large compared to colloidal sized particles. It is evident that if appreciably different amounts of positive and negative ions were taken up by the fiber, a prohibitively large fiber potential would be set up; hence it will be assumed that equivalent amounts of positive and negative ions react. In any event, the interaction of the fiber with alkali will take place in two distinct stages, the first involving un-ionized carboxyls and the second involving pairs of ionized groups. Therefore, we can predict (as is verified experimentally) that the base titration of solid nylon (with $A_0 > B_0$) will be accompanied by a break occurring approximately after the completion of the first reaction and before the start of the second.

Theory

Although our experiments were carried out only with sodium hydroxide acting on nylon with excess acid end-groups, it would seem appropriate to deal theoretically with six different possibilities. These involve titration with either acids or bases of nylons with $A_0 > B_0$, $A_0 = B_0$, and $A_0 < B_0$. The theory is a generalization of that developed by Gilbert and Rideal[3] who made use of Fowler's[8] statistical methods and also took cognizance of the possible existence of an electrical potential on the fiber.

Certain assumptions concerning the nature of the fiber and of the absorption processes will be made in the development of the titration equations; these assumptions can be summarized as follows. The acidic and basic polymer end-groups, which are presumed to be randomly distributed throughout the fiber, are the specific sites occupied by absorbed ions. All carboxyl sites are assumed to be identical with respect to their interactions with ions, irrespective of whether or not neighboring sites are occupied; similarly, all amino sites are identical. Each site can interact with only one ion, which then makes this site unavailable for further absorption.

When nylon fibers are suspended in an aqueous solution of either a monovalent acid or monovalent base, two or more of the following reactions can take place

$$—COO^- + H^+ \rightleftharpoons —COOH \quad (1)$$

$$—COO^- + B^+ \rightleftharpoons —COO^-B^+ \quad (2)$$

$$—NH_2 + H^+ \rightleftharpoons —NH_3^+ \quad (3)$$

$$—NH_3^+ + A^- \rightleftharpoons —NH_3^+A^- \quad (4)$$

$$H^+ + OH^- \rightleftharpoons H_2O \quad (5)$$

In these equations, –COOH and $-NH_2$ represent the carboxyl and amino end-groups, respectively, within the nylon fiber, and B^+ and A^- represent the cation of a base and the anion of an acid. The significance of the remaining symbols obviously follows.

As suggested earlier, let us define A_0 and B_0 as the total concentrations of carboxyl and amino end-groups in the fiber, to be expressed as moles per gram of fiber. We can therefore assert that

$$A_0 = [—COO^-] + [—COOH] + [—COO^-B^+] \quad (6)$$

and

$$B_0 = [—NH_2] + [—NH_3^+] + [—NH_3^+A^-] \quad (7)$$

where the bracketed terms represent the concentrations of the enclosed end-group species, likewise expressed in moles per gram of fiber. Certain fractions, θ_1, θ_2, θ_3 and θ_4 are further defined by the equations

$$[—COOH] = \theta_1 A_0 \quad (8)$$

$$[—COO^-B^+] = \theta_2 A_0 \quad (9)$$

$$[—NH_3^+] = \theta_3 B_0 \quad (10)$$

$$[—NH_3^+A^-] = \theta_4 B_0 \quad (11)$$

$$[—COO^-] = (1 - \theta_1 - \theta_2)A_0 \quad (12)$$

$$[—NH_2] = (1 - \theta_3 - \theta_4)B_0 \quad (13)$$

Equations expressing the free energy changes accompanying reactions (1) through (5) can now be written in terms of the quantities just defined.

$$\Delta\mu_1 = \Delta\mu_1^\circ + RT \ln \frac{\theta_1}{1 - \theta_1 - \theta_2} - RT \ln [H^+] + F\psi \quad (14)$$

$$\Delta\mu_2 = \Delta\mu_2^\circ + RT \ln \frac{\theta_2}{1 - \theta_1 - \theta_2} - RT \ln [B^+] + F\psi \quad (15)$$

$$\Delta\mu_3 = \Delta\mu_3^\circ + RT \ln \frac{\theta_3}{1 - \theta_3 - \theta_4} - RT \ln [H^+] + F\psi \quad (16)$$

$$\Delta\mu_4 = \Delta\mu_4^\circ + RT \ln \frac{\theta_4}{\theta_2} - RT \ln [A^-] - F\psi \quad (17)$$

$$\Delta\mu_5 = \Delta\mu_5^\circ - RT \ln [OH^-] - RT \ln [H^+] \quad (18)$$

$\Delta\mu_i$ represents the free energy change per unit of reaction concerned, while $\Delta\mu_i^\circ$ is the corresponding standard value. The last term in each of equations (14) through (17) is the contribution to the free energy of reaction which can be attributed to the charge on the fiber.[3] The quantity ψ is the electrostatic potential of the fiber, and F is the value of the faraday.

It will be necessary to subdivide the subsequent development into the several aforementioned cases. These cases will include separate treatments of the absorption of acids and of bases subject to a further

(8) Fowler and Guggenheim, "Statistical Mechanics," Cambridge University Press, 1939, p. 426.

breakdown according to the relative numbers of acidic and basic end-groups within the fibers.

A. Titration with Acid.—It is obvious in this instance, where no base is involved, that $\theta_2 = 0$. Now let us consider in order three possibilities, namely, $A_0 < B_0$, $A_0 = B_0$, and $A_0 > B_0$.

Case 1. $A_0 < B_0$.—Before reacting with a solution, practically all of the carboxyl groups in a fiber with $A_0 < B_0$ will be ionized to carboxyl ions and an equivalent number of amino groups ionized to ammonium ions. Thus when acid is added to the solution, the protons find two possible absorption sites available, namely, the carboxyl ions and the un-ionized amine groups. Obviously the amino groups of the nylon are the sites preferred by the protons, so it will be assumed that the amino groups become completely saturated with protons before absorption of protons by the carboxyl ions begins. The absorption of acid by these fibers is thus divided into two regions corresponding to $0 < \theta_4 < \frac{B_0 - A_0}{B_0} = \theta_4^*$ and $\theta_4^* < \theta_4 < 1$. These regions must be treated individually.

Subcase (a). $0 < \theta_4 < \frac{B_0 - A_0}{B_0} = \theta_4^*$.—As protons are absorbed by the amino groups, an equivalent number of acid anions must also be absorbed. These anions form salt linkages with the alkyl ammonium ions, thus contributing to the following over-all reaction which is a combination of reactions (3) and (4)

$$-NH_2 + H^+ + A^- \rightleftharpoons -NH_3^+A^- \qquad (19)$$

After sufficient time, the fibers will come to equilibrium with the solution in which they are suspended. At equilibrium

$$\Delta\mu_3 + \Delta\mu_4 = 0 \qquad (20)$$

Hence

$$\Delta\mu_3^\circ + \Delta\mu_4^\circ + RT \ln \frac{\theta_4}{1 - \theta_3 - \theta_4} - RT \ln[H^+][A^-] = 0 \qquad (21)$$

It will be noticed that the two electrostatic potential terms present in the parent equations (16) and (17) do not appear in equation (21). This cancellation occurs, of course, because the two terms are of equal magnitude and opposite sign.

Since the solution contains only acid, and since protons and anions are absorbed in equivalent amounts, it follows that

$$[H^+] = [A^-] \qquad (22)$$

It is obvious, under these particular circumstances, that

$$\theta_1 = 0 \qquad (23)$$

and

$$\theta_3 = \frac{A_0}{B_0} \qquad (24)$$

Equation (21) can then be rewritten with $[A^-]$ and θ_3 eliminated and the natural logarithm converted to a common logarithm

$$\log \frac{\theta_4}{1 - \frac{A_0}{B_0} - \theta_4} = 2 \log [H^+] - \frac{2.303}{RT}(\Delta\mu_2^\circ + \Delta\mu_4^\circ) \qquad (25)$$

Further simplification leads to

$$\log \frac{\theta_4}{\theta_4^* - \theta_4} = -2pH + \alpha_1 \qquad (26)$$

where

$$\alpha_1 = -\frac{2.303}{RT}(\Delta\mu_3^\circ + \Delta\mu_4^\circ) \qquad (27)$$

The quantity α_1 is a constant at any given temperature. Thus the desired titration equation, which relates the pH of the acid solution to a function of the amount of acid absorbed, has been obtained for the condition that $0 < \theta_4 < \theta_4^*$.

Subcase (b). $\frac{B_0 - A_0}{B_0} = \theta_4^* < \theta_4 < 1$.—For this absorption region, the acid concentration of the suspending solution has been increased to a point where all of the amino sites are covered with protons. Further absorption of protons takes place at the carboxyl ion sites of the fiber giving rise to the over-all

$$-COO^- + -NH_3^+ + H^+ + A^- \rightleftharpoons -COOH + -NH_3^+A^- \qquad (28)$$

Proceeding in the same manner as before, we have at equilibrium

$$\Delta\mu_1^\circ + \Delta\mu_4^\circ + RT \ln \frac{\theta_1\theta_4}{\theta_3(1 - \theta_1)} - RT \ln[H^+][A^-] = 0 \qquad (29)$$

Here again the electrostatic potential terms have cancelled. Besides equation (22), the following additional equalities hold

$$\theta_3 = (1 - \theta_4) = (1 - \theta_1)\frac{A_0}{B_0} \qquad (30)$$

Making use of these relationships, equation (29) can be reduced to the desired expression in terms of pH and θ_4.

$$\log \frac{(\theta_4 - \theta_4^*)\theta_4}{(1 - \theta_4)^2} = -2pH + \alpha_2 \qquad (31)$$

$$\alpha_2 = \frac{-2.303}{RT}(\Delta\mu_1^\circ + \Delta\mu_4^\circ) \qquad (32)$$

Case 2. $A_0 = B_0$.—The similarity of this case to the upper absorption region, $\theta_4^* < \theta_4 < 1$, of Case 1 is obvious. Thus equations (28) and (29) also apply here. However, since $A_0 = B_0$, equation (30) is modified to

$$\theta_3 = (1 - \theta_4) = (1 - \theta_1) \qquad (33)$$

and the final titration equation becomes

$$\log \frac{\theta_4}{1 - \theta_4} = -pH + \frac{\alpha_2}{2} \qquad (34)$$

This is precisely the titration equation developed by Gilbert and Rideal.[3] It should be noted that in this instance, one equation is sufficient to describe the absorption of acid from zero to total saturation.

Case 3. $A_0 > B_0$.—In this case, all amino and an equivalent number of carboxyl groups are initially ionized with the excess carboxyl groups un-ionized and taking no part in the reaction. Therefore, the absorption is described by a single titration equation which shares some of the simplicity of Case 2. The over-all reaction is given by equation (28) and the corresponding free energy expression by equation (29). Equations (30) also hold, although the relative magnitudes of A_0 and B_0 are, of course, reversed. Thus the final equation obtained is

$$\log \frac{(\theta_4 - \theta_4^*)\theta_4}{(1 - \theta_4)^2} = -2pH + \alpha_2 \qquad (35)$$

where θ_4^* is still defined as $(B_0 - A_0)/B_0$ but is now a negative quantity. Remington and Gladding[9] offered a similar equation in their recent work on nylon fibers.

B. Titration with Base.—When a simple base, such as sodium hydroxide, is added to the solution in which nylon fibers are suspended, the driving force for the absorption process is supplied by the tendency of the hydroxyl ions to strip protons from the end-groups of the fiber and to react with them to form water. Now it is evident that the protons should first be removed from the carboxyl sites, after which they are taken away from the ammonium groups. Any tendency of the fiber to take on a prohibitedly high negative charge by means of proton removal is counteracted by the absorption of an equivalent number of sodium ions which become associated with the negatively charged carboxyl end-groups. Thus the net effect is the stoichiometric absorption of NaOH by the fiber followed by the elimination of water. Since no acid is now involved, it is obvious that $\theta_4 = 0$. Here too it is necessary to consider the three possibilities, $A_0 < B_0$, $A_0 = B_0$ and $A_0 > B_0$. Let us now consider the derivation of titration equations for the various fibers.

Case 1. $A_0 < B_0$.—In the normal fiber (with $A_0 < B_0$) the transfer of protons from the carboxyl groups to an equivalent number of amino groups is complete. Since the excess amino groups remain un-ionized, they will not take part in the subsequent absorption of base. Therefore, the absorption process involves the removal of protons from the

(9) Remington and Gladding, *J. Am. Chem. Soc.*, **72**, 2553 (1950).

ammonium groups and the absorption of the cations of the base by the carboxyl groups

$$-COO^- + -NH_3^+ + B^+ + OH^- \rightleftharpoons -COO^-B^+ + -NH_2 + H_2O \quad (36)$$

Noting that $\theta_1 = \theta_4 = 0$, we have at equilibrium

$$\Delta\mu_2^\circ - \Delta\mu_3^\circ + \Delta\mu_5^\circ + RT \ln \frac{\theta_2(1-\theta_3)}{(1-\theta_2)\theta_3} - RT \ln[B^+][OH^-] = 0 \quad (37)$$

Here again the two electrostatic potential terms of the parent equations do not appear because of their equal magnitudes and opposite signs.

Since only base is added to the solution and the absorption of cations by the fibers is accompanied by the formation of water, it follows that

$$[B^+] = [OH^-] \quad (38)$$

This equation, in combination with equation (18), can be used to eliminate both $[B^+]$ and $[OH^-]$ from equation (37). There is then obtained, after simplification and a change to common logarithms

$$\log \frac{\theta_2(1-\theta_3)}{(1-\theta_2)\theta_3} = -2\log[H^+] - \frac{2.303}{RT}(\Delta\mu_2^\circ - \Delta\mu_3^\circ - \Delta\mu_5^\circ) \quad (39)$$

The following relationship exists between θ_2 and θ_3

$$\theta_3 = (1-\theta_2)\frac{A_0}{B_0} \quad (40)$$

so equation (39) becomes

$$\log \frac{(\theta_2 - \theta_2^*)\theta_2}{(1-\theta_2)^2} = 2p\mathrm{H} + \alpha_3 \quad (41)$$

where

$$\theta_2^* = \frac{A_0 - B_0}{A_0} \quad (42)$$

and

$$\alpha_3 = \frac{-2.303}{RT}(\Delta\mu_2^\circ - \Delta\mu_3^\circ - \Delta\mu_5^\circ) \quad (43)$$

θ_2^* is a negative quantity similar to θ_4^* of case 3 for acid titration.

Case 2. $A_0 = B_0$.—This example is similar to the previous one, differing only insofar as no un-ionized amino groups are present. Since these groups do not participate in the absorption, their absence results in simplification of the titration equation. Thus, because $A_0 = B_0$, θ_2^* becomes equal to zero and the titration equation becomes

$$\log \frac{\theta_2}{1-\theta_2} = p\mathrm{H} + \frac{\alpha_3}{2} \quad (44)$$

Case 3. $A_0 > B_0$.—Here all the amino groups and an equivalent number of carboxyl groups are ionized, but there still remains an excess of un-ionized carboxyl groups. Thus, for this fiber there are two distinct absorption stages, one involving the $0 < \theta_2 < \frac{A_0 - B_0}{A_0} = \theta_2^*$, and the second occurring in the range $\theta_2^* < \theta_2 < 1$, where θ_2^* is now positive. Each of these regions must be considered separately.

Subcase (a). $0 < \theta_2 < \frac{A_0 - B_0}{A_0} = \theta_2^*$.—The over-all reaction for this subcase is

$$-COOH + B^+ + OH^- \rightleftharpoons -COO^-B^+ + H_2O \quad (45)$$

At equilibrium

$$-\Delta\mu_1^\circ + \Delta\mu_2^\circ + \Delta\mu_5^\circ + RT \ln \frac{\theta_2}{\theta_1} - RT \ln [B^+][OH^-] = 0 \quad (46)$$

Here again the electrostatic potential terms of the parent equations cancel out. We also note that $\theta_3 = 1$ and

$$(1 - \theta_1 - \theta_2) = \frac{B_0}{A_0} \quad (47)$$

With the additional help of equations (18) and (38), there is obtained upon simplification

$$\log \frac{\theta_2}{\theta_2^* - \theta_2} = 2p\mathrm{H} + \alpha_4 \quad (48)$$

where

$$\alpha_4 = -\frac{2.303}{RT}(-\Delta\mu_1^\circ + \Delta\mu_2^\circ - \Delta\mu_5^\circ) \quad (49)$$

Subcase (b). $\frac{A_0 - B_0}{A_0} = \theta_2^* < \theta_2 < 1$.—This subcase bears a close resemblance to Case 1. At the start of absorption in both instances, the fiber contains an equivalent number of carboxyl and alkyl ammonium groups for participation in the subsequent absorption. Thus, the over-all reaction for both cases is given by equation (36) and the free energy by equation (37). Here again, $\theta_1 = 0$ and equations (38) and (40) apply, except that the relative magnitudes of A_0 and B_0 are reversed. Proceeding as we did in Case 1, we obtain the titration equation

$$\log \frac{(\theta_2 - \theta_2^*)\theta_2}{(1-\theta_2)^2} = 2p\mathrm{H} + \alpha_3 \quad (50)$$

Experimental

In the theoretical section of this study, equations have been derived which should describe the absorption of either a monovalent acid or a monovalent base by nylon fibers. Two of the cases considered have already been subject to experimental investigation; one involved the absorption of acid by nylon fibers for which $A_0 > B_0$,[9] and the second was concerned with the absorption of acid by fibers with $A_0 = B_0$, except that wool instead of nylon actually was used.[10,11] The foregoing analysis of the effect of various end group ratios on the absorption pattern for nylon fibers has indicated that in certain instances the absorption should differ significantly from that observed in previous studies.

The absorption of acid by fibers with $A_0 < B_0$ or the absorption of base by fibers with $A_0 > B_0$, should manifest two distinct regions. The experimental portion of the present study has been devoted to an investigation of the absorption of base by nylon fibers for which $A_0 > B_0$. The two stages of absorption involved in this case provide the opportunity for a more rigorous test of the theoretical development.

The nylon used in this work consisted of undrawn fibers of the so-called 66 variety (polyhexamethylene adipamide) which contained about 82×10^{-6} mole of carboxyl end-groups and 42×10^{-6} mole of amino end-groups per gram of polymer as determined by the titration method of Waltz and Taylor.[12] These fibers were allowed to come to equilibrium with solutions of sodium hydroxide, the concentrations of which were so chosen that the absorption varied from approximately zero to total saturation of the fibers.

When the concentration of the equilibrium sodium hydroxide solution was between 0.01 and 0.2 molar, which corresponded to the upper portion of the absorption region, the following procedure was used. Three to five grams of nylon fibers and 50 to 75 ml. of sodium hydroxide solution were placed in a 100-ml. Pyrex weighing bottle equipped with a tightly fitting cover which was greased and held firmly in place with rubber bands. The vessel was placed in a 25° constant temperature bath for at least 100 hours to permit the attainment of equilibrium. At the end of this period samples of the equilibrium solution were withdrawn for chemical analysis. Knowing accurately the weight of nylon, the volume of solution, as well as the initial and equilibrium concentrations of the solution, the amount of sodium hydroxide absorbed by the fiber could be calculated.

Carbonate-free sodium hydroxide solutions were used throughout this work. In all phases of the work, the solutions were protected from air by an atmosphere of nitrogen. Dry nylon fibers absorb water from the air so rapidly that it was found necessary to determine the moisture content by weighing samples of the fibers before and after heating in a 75° oven for six hours. Chemical analyses of both the initial and equilibrium sodium hydroxide solutions were obtained by titrating samples of these solutions with standard potassium acid phthalate. When the volume of solution available for analysis was small and the concentration low, microtechniques were employed.

In the lower portion of the absorption region for the nylon fibers, the concentrations of the equilibrium solutions and

(10) Gilbert, *Proc. Roy. Soc. (London)*, **183A**, 167 (1944).

(11) Lemin and Vickerstaff, *J. Soc. Dyers and Colourists*, **63**, 405 (1947).

(12) Waltz and Taylor, *Anal. Chem.*, **19**, 448 (1947).

the amounts of sodium hydroxide absorbed were so small that the chemical method described above was inadequate. Accordingly, radioactive tracer techniques were substituted whenever the concentration of the equilibrium solution lay between 0.0001 and 0.01 molar.

Since the concentrations of most of the initial sodium hydroxide solutions were below the range for chemical analysis, more concentrated solutions were first prepared and chemically analyzed. These solutions were then diluted by known factors to the desired low concentrations. A small amount of radioactive sodium (Na^{22}) was introduced into these solutions before transferring the required volume over the nylon fibers in the reaction vessel. After the required period for attainment of equilibrium, the large bulk of equilibrium solution was poured off the fibers. A count of the radioactivity of a measured volume of this equilibrium solution and also of a sample of the initial solution was made. Under the conditions of the experiment, the concentrations of the initial and equilibrium solutions were proportional to their radioactive counts, thus permitting calculation of the concentrations of the equilibrium solutions. From these concentrations it was possible to calculate the amount of sodium hydroxide absorbed by the fibers and the *p*H of the equilibrium solution.

For almost half of the reactions carried out, an additional direct determination of the amount of sodium hydroxide absorbed by the fibers was made. At the end of the reaction, after the bulk of the equilibrium solution had been poured off, the fibers were mechanically squeezed as dry as possible. The weight of residual solution still on the fibers was obtained by weighing the soaked fibers and subtracting the weight of the dry fibers. The fibers and residual solution were then dissolved in 88% phenol. The resulting viscous solution was diluted to a convenient volume with a 1:10 mixture of 95% sulfuric acid and ethanol. The radioactive count of this solution was then measured. Again taking advantage of the proportionality existing between radioactive count and amount of sodium hydroxide, it was possible to calculate the moles of sodium hydroxide absorbed by the fibers after correcting for the radioactive count of the residual solution clinging to the fibers.

Relative radioactive counts of the various solutions were obtained by placing 25-ml. samples of these solutions into glass cells which fitted snugly around a Geiger–Mueller tube. The Geiger–Mueller tubes used were self-quenching with a wall thickness of 30 mg./cm.^{2} They were sensitive to beta and gamma emissions with energies above 0.35 mev. These tubes were used in conjunction with a Model 163 Scalar of the Nuclear Instrument and Chemical Corporation. The sodium isotope (Na^{22}) used in this work was available as its chloride salt in aqueous solution. The concentration of salt in this solution was less than 10^{-7} mole per liter and only a few tenths of a milliliter was added to each 300 to 500 ml. of initial sodium hydroxide solution. Therefore no correction had to be made to compensate for the addition of this material to the solutions. The amount of Na^{22} added to the sodium hydroxide solutions gave these solutions activities equivalent to 1000 to 2000 counts per minute. Radioactive counts ranging from 100 to 700 per minute were obtained for the solutions of dissolved nylon. Background corrections of 40 to 50 counts per minute were applied. Coincidence correction curves for each Geiger tube used were obtained by means of the dilution method. Such corrections were applied to the radioactive counts whenever necessary, but they were never much greater than 1%. Duplicate counts were made involving times sufficiently long to insure a statistical error of less than 2%. Since Na^{22} has a half-life of 3.0 years, no decay corrections were necessary.

Results and Conclusions

Experiments involving interaction of the nylon fibers with sodium hydroxide solutions were carried out for twenty-four different concentrations. In each instance, the amount of sodium hydroxide absorbed and the concentrations of the equilibrium solution were determined. The results of these measurements are given in Table I. The values given in the second column were obtained from measurements made on the solutions, whereas those in the third column were obtained from a direct measurement of the amount of sodium in the fibers. The concentrations of the equilibrium sodium hydroxide solutions, expressed in moles per liter, are tabulated in the fourth column. The measurements for experiments numbered 1 through 6 were made by conventional chemical means, whereas radioactive tracer techniques were used for the remainder of the reactions. The last column in the table contains values for the *p*H of the equilibrium solution as calculated from the concentration data of column four.

TABLE I

SUMMARY OF RESULTS

Reaction number	$[-COO^-Na^+] \times 10^6$ Indirect	Direct	$[OH^-] \times 10^3$	*p*H
1	79.4		194.6	13.29
2	77.6		135.3	13.10
3	76.0		78.27	12.89
4	68.7		42.17	12.63
5	63.0		26.90	12.43
6	58.0		17.25	12.24
7	44.4		8.73	11.94
8		40.1	7.08	11.85
9	39.2		5.83	11.77
10		35.4	5.07	11.70
11	31.7		2.98	11.47
12	29.2	30.3	2.54	11.41
13	23.4		1.43	11.16
14	17.7	18.2	1.16	11.06
15	11.2		0.83	10.92
16	12.8	11.8	.79	10.90
17	5.37	5.61	.53	10.72
18	2.06		.40	10.60
19	0.74	0.53	.35	10.54
20	.23		.25	10.40
21	.57	0.26	.24	10.38
22	.14	.13	.14	10.15
23	.05		.09	9.97
24	.02	.008	.08	9.87

The nylon fibers employed in this study contained a larger number of carboxyl than amino end-groups. The theoretical discussion presented earlier indicates that the absorption of sodium hydroxide by such fibers should take place in two steps subject to equations (48) and (50). This absorption pattern is qualitatively reflected in the titration curve of Fig. 1, in which the moles of sodium hydroxide absorbed are plotted against the *p*H of the equilibrium solution. As would be expected, the solid line curve of this graph contains two steps. The first step corresponds to the removal of protons from the un-ionized carboxyl groups, the second to their removal from the ammonium groups. The point of inflection between the two steps occurs at $[-COO^-Na^+] = A_0 - B_0$, which is the number of excess un-ionized carboxyl groups in the fiber. This point, it should be recalled, also corresponds to θ_2^* of equations (48) and (50). The broken line curves drawn on the graph in the neighborhood of $A_0 - B_0$ represent the hypothetical completion of the first absorption process and the beginning of the second.

The titration equations (48) and (50) enable us to make a quantitative interpretation of the absorp-

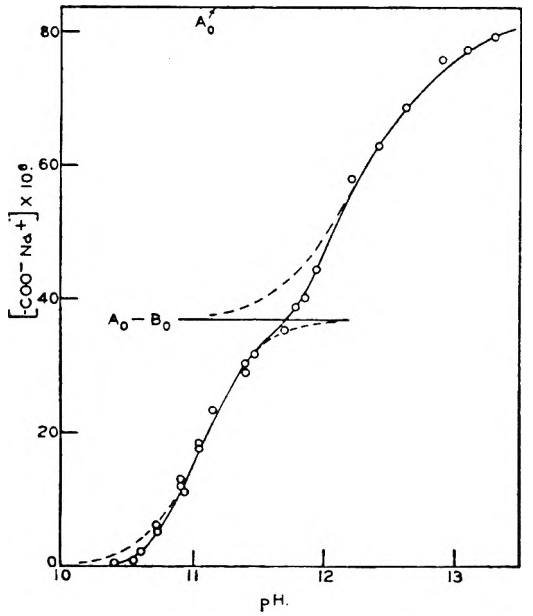

Fig. 1.—Amount of absorbed sodium ions plotted against pH of solution.

tion data for the fibers studied in this work. These equations can be written

$$\frac{\theta_2[H^+]^2}{(\theta_2^* - \theta_2)} = e^{\alpha 4} \quad (51)$$

and

$$\frac{(\theta_2 - \theta_2^*)\theta_2[H^+]^2}{(1 - \theta_2)^2} = e^{\alpha 3} \quad (52)$$

Taking advantage of the fact that $\theta_2^* = A_0 - B_0/A_0$ and $K_w = [H^+][OH^-]$ and letting $k_1 = e^{\alpha 4}/K_w^2$ and $k_2 = e^{\alpha 3}/K_w^2$, we obtain

$$\frac{[-COO^-Na^+]}{\{(A_0 - B_0) - [-COO^-Na^+]\}[OH^-]^2} = k_1 \quad (53)$$

and

$$\frac{[-COO^-Na^+]\{[-COO^-Na^+] - (A_0 - B_0)\}}{\{A_0 - [-COO^-Na^+]\}^2[OH^-]^2} = k_2 \quad (54)$$

In these expressions, k_1 and k_2 are the "equilibrium constants" for the reactions which occur during the first and second stages of the absorption. Equations (53) and (54) can be rewritten in the forms

$$\sigma = \frac{[-COO^-Na^+]}{[OH^-]^2} = -k_1[-COO^-Na^+] + k_1(A_0 - B_0) \quad (55)$$

and

$$\tau = \sqrt{\frac{[-COO^-Na^+]\{[-COO^-Na^+] - (A_0 - B_0)\}}{[OH^-]^2}} = -\sqrt{k_2}[-COO^-Na^+] + \sqrt{k_2}A_0 \quad (56)$$

Thus, if σ is plotted against $[-COO^-Na^+]$ for the first stage of the absorption, a straight line should be obtained with a slope equal to $-k_1$ and an abscissa intercept equal to $(A_0 - B_0)$. Similarly for the second stage, a plot of τ against $[-COO^-Na^+]$ should give a straight line with a slope equal to the negative square root of k_2 and an abscissa intercept equal to A_0. Values of σ for $[-COO^-Na^+] < (A_0 - B_0)$ and those of τ for $[-COO^-Na^+] > (A_0 - B_0)$ are given in Table II. It should be noted that the σ plot must be made before τ can be computed.

TABLE II

VALUES FOR σ AND τ

$[-COO^-Na^+] \times 10^6$ Indirect	Direct	σ Indirect	Direct	$\tau \times 10^3$
79.4				0.298
77.6				.449
76.0				.696
68.7				1.109
63.0				1.403
58.0				2.028
44.4				2.090
	40.1			1.600
39.2				1.629
	35.4		1.38	
31.7		3.57		
29.2	30.3	4.53	4.70	
23.4		11.44		
17.7	18.2	13.15	13.52	
11.2		16.25		
12.8	11.8	20.51	18.91	
5.37	5.61	19.11	19.97	
2.06		12.88		
0.74	0.53	6.04	4.33	

In Figs. 2 and 3, values of σ and τ are plotted against $[-COO^-Na^+]$. While the points are somewhat scattered, the data plotted in these two graphs do determine two straight lines. Thus the existence of two constants k_1 and k_2, as required by the theoretical analysis and defined in equations (53) and (54), is confirmed by the experimental data. The slopes of the two lines give for the equilibrium

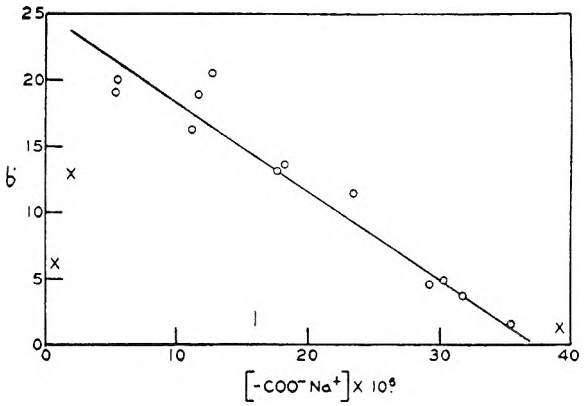

Fig. 2.—Plot of σ *vs.* amount of absorbed sodium ions for first stage of titration.

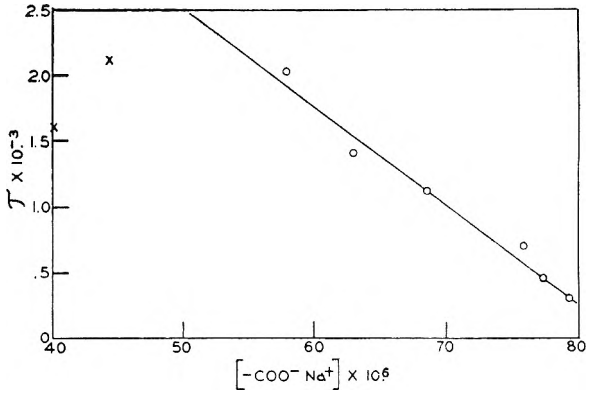

Fig. 3.—Plot of τ *vs.* amount of absorbed sodium ions for second stage of titration.

constants of the two absorption stages the values $k_1 = 6.8 \times 10^5$, and $k_2 = 5.5 \times 10^3$. The relative magnitudes of the equilibrium constants reflect the fact that more free energy is required to remove a proton from the ammonium groups of the fiber than from the less basic carboxyl groups. From the abscissa intercepts of the two lines, there are obtained the values $A_0 = 84 \times 10^{-6}$ and $B_0 = 47 \times 10^{-6}$ for the mole of carboxyl and amino end-groups, respectively, per gram of fiber. These numbers compare reasonably well with the values $A_0 = 82 \times 10^{-6}$ and $B_0 = 42 \times 10^{-6}$ obtained outside this Laboratory by an entirely independent method.[12]

Before passing on to other considerations, a more critical examination of Figs. 2 and 3 and the data represented there is in order. In both figures, certain points occurring in the region of $[-COO^-Na^+] = A_0 - B_0$ are represented by crosses. These points correspond to the transition from the first to the second stages of the alkali absorption and are seen in Fig. 1 as the points approximately midway between the dashed "theoretical" curves.

In Fig. 2, the values of σ corresponding to $[-COO^-Na^+] < 3 \times 10^{-6}$ are also represented on the graph by crosses; they likewise do not conform to equation (55) However, the experimental circumstances indicate that this divergence can be attributed to inaccuracy of the work done in the low

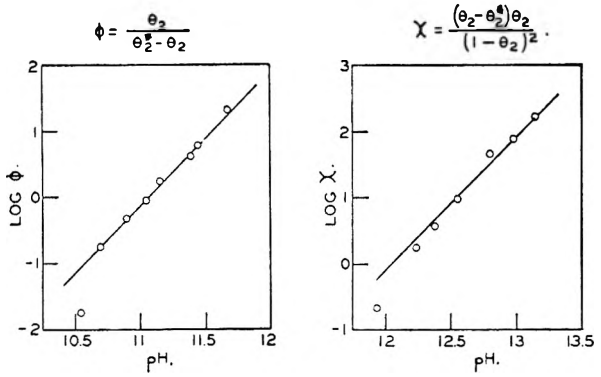

Fig. 4.—Plots of log ϕ and log χ *vs.* *p*H. Straight lines have correct theoretical slope equal to 2.

*p*H region rather than to a real deviation from theory. The fact that the solutions were substantially unbuffered is undoubtedly responsible for the difficulty. All reasonable precautions were taken to guard against extraneous depression of the *p*H, but these precautions obviously were insufficient to cope with the problem. Attempts were made during the course of the experimental work to check by direct measurement the *p*H values of these solutions which were calculated from the radioactive count data. These direct measurements were made with a glass electrode used in conjunction with a calomel reference cell and a laboratory model *p*H meter. In the upper portion of this first absorption stage, where $[-COO^-Na^+] > 3 \times 10^{-6}$, the calculated and directly measured *p*H values were in good agreement; but in the low *p*H region in question, the observed values were considerably below those obtained by calculation. It is probable that neither the observed nor the calculated values are of much quantitative significance, so we can conclude that the data for experiments 18 through 24 have only qualitative meaning. Since these reactions were concerned only with the small initial absorption, it is felt that the dubious character of the data does not detract from the significance of the results obtained for the remainder of the absorption process.

Another method for illustrating the agreement between the theoretical analysis of the absorption process and the experimental data involves the direct application of equations (48) and (50). For simplicity of notation, let us define

$$\phi = \frac{\theta_2}{(\theta_2^* - \theta_2)} \text{ and } \chi = \frac{(\theta_2 - \theta_2^*)\theta_2}{(1 - \theta_2)^2}$$

Using the aforementioned values of A_0 and B_0 to determine θ^*, values of log ϕ and log χ, respectively, have been calculated and plotted against *p*H in Fig. 4. According to equations (48) and (50), the points in each of these graphs should be on straight lines with slope equal to two. The straight lines drawn in Fig. 4 are lines which have the correct theoretical slope; in this respect the graphs demonstrate agreement of experiment with theory.

A THEORY OF POLYELECTROLYTES

BY GEORGE E. KIMBALL, MELVIN CUTLER AND HAROLD SAMELSON

Department of Chemistry, Columbia University, New York 27, New York

Received August 30, 1951

Several theories have been developed to account for properties of polymeric materials containing ionizing groups, when they are dissolved in solvents such as water. Certain Debye-Hückel approximations are inaccurate, but the Donnan potential method is applicable in many cases. We have developed a satisfactory model and theory, which depends on the validity of the Poisson–Boltzmann equation, and the legitimacy of replacing the chain force by a central force.

Introduction

The term polyelectrolyte will be used in this paper to denote any high polymeric material which contains ionic groups attached to the polymer chains. The chain may be linear, or crosslinked. The ions may correspond to the ions of strong electrolytes, for example quaternary ammonium groups (chain)-NR_3^+, or to the ions of weak electrolytes, such as carboxyl ions, (chain)-COO^-.

The properties of such molecules of interest here are those observed in ionizing solvents such as water. The solvent must always contain the counterions of the polyelectrolyte formed by its original dissociation, and frequently contains added salt, which has a marked effect on the properties of the polyelectrolyte.

A number of theories have been developed to account for the properties of these substances, notably by Kuhn, Katchalsky and Künzle[1-3] and by Hermans and Overbeek.[4] These theories have generally followed the lines of the Debye–Hückel theory of strong electrolytes, a procedure which is open to question because of the high electrical potentials which are produced in polyelectrolytes. In this paper it will be shown that the Debye–Hückel approximations are extremely inaccurate, but that the method used by Donnan[5] for estimating potentials across semipermeable membranes may be applied in many cases.

The Electrostatic Problem

Let us first consider the example of a single, rigid, spherical polyelectrolyte molecule immersed in a large volume of uni-univalent salt solution. The polyelectrolyte molecule can be considered as a fixed concentration of immovable ions decreasing from a high value at the center to zero at large distances. If r is the distance from the center, we may represent this as a function $c_0(r)$. If the ions of the polyelectrolyte are singly charged, this distribution of ions creates a distribution of electrical charge density

$$q_0(r) = ec_0(r) \tag{1}$$

If the molarity of the ambient salt solution is M, the concentration of "movable" positive ions will be a function $c_1(r)$ and that of negative ions a function $c_2(r)$, both functions approaching M as r increases.

We now introduce the usual assumptions that $c_1(r)$ and $c_2(r)$ are governed by the Boltzmann equation

$$c_1(r) = M \exp\left(-\frac{e\psi(r)}{kT}\right) \tag{2a}$$

$$c_2(r) = M \exp\left(\frac{e\psi(r)}{kT}\right) \tag{2b}$$

where $\psi(r)$ is the electrostatic potential determined by the Poisson equation

$$\nabla^2\psi = -\frac{4\pi}{D} q(r) \tag{3}$$

Here $q(r)$ is the net charge density

$$q(r) = e\,(c_0(r) + c_1(r) - c_2(r)) \tag{4}$$

Combining these equations gives

$$\nabla^2\psi = -\frac{4\pi e}{D} c_0(r) + \frac{8\pi Me}{D} \sinh\frac{e\psi}{kT} \tag{5}$$

If we define

$$u = \frac{e\psi}{kT} \tag{6a}$$

$$\kappa^2 = \frac{8\pi Me^2}{DkT} \tag{6b}$$

$$x = \kappa r \tag{6c}$$

$$f(x) = \frac{c_0(r)}{2M} \tag{6d}$$

Then equation (5) reduces to

$$\frac{1}{x^2}\frac{\mathrm{d}}{\mathrm{d}x}\left(x^2\frac{\mathrm{d}u}{\mathrm{d}x}\right) = \sinh u - f(x) \tag{7}$$

We seek the solutions of this differential equation which satisfy the boundary conditions that u is finite for $x = 0$ and approaches zero sufficiently rapidly as x approaches infinity.

Equations of the type of (7) have been attacked by two different methods of approximation. One method, originally applied by Debye and Hückel,[6] approximates by the assumption that u is small enough so that $\sinh u \approx u$. If we denote the solution obtained by this approximation by v, then v satisfies the differential equation

$$\frac{1}{x^2}\frac{\mathrm{d}}{\mathrm{d}x}\left(x^2\frac{\mathrm{d}v}{\mathrm{d}x}\right) = v - f(x) \tag{8}$$

By using Green's functions, this can be solved to give the solution

$$v = \frac{1}{x}\int_0^\infty K(x,y)\, y\, f(y)\, \mathrm{d}y \tag{9}$$

where

$$\begin{aligned} K(x,y) &= \sinh y\, e^{-x} \qquad (y < x) \\ &= \sinh x\, e^{-y} \qquad (y > x) \end{aligned} \tag{10}$$

(1) A. Katchalsky, O. Künzle and W. Kuhn, *J. Polymer Sci.*, **5**, 283 (1950).

(2) W. Kuhn, O. Künzle and A. Katchalsky, *Helv. Chim. Acta*, **31**, 1994 (1948).

(3) O. Künzle, *Rec. trav. chim.*, **68**, 699 (1949).

(4) J. J. Hermans and J. T. G. Overbeek, *ibid.*, **67**, 761 (1948).

(5) F. G. Donnan, *Z. Elektrochem.*, **17**, 572 (1911).

(6) D. A. MacInnes, "Principles of Electrochemistry," Reinhold Publishing Corp., New York, N. Y., 1939, p. 138.

The other method of approximation is essentially that used by Donnan[5] in studying membrane equilibria, and consists of neglecting the derivative term in equation (8). We therefore define as the reduced Donnan potential the function

$$w(x) = \sinh^{-1} f(x) \tag{11}$$

We shall show that of these two approximations to u, w is the better under the conditions found in polyelectrolytes. The demonstration depends on the following four theorems, which are proved rigorously in the appendix.

Theorem 1: The functions $u(x)$, $v(x)$ and $w(x)$ are nowhere negative.

Theorem 2: The function $v(x)$ is greater than $u(x)$ for all values of x.

Theorem 3: There are values of x for which $u(x)$ is greater than $w(x)$, and also values of x for which $w(x)$ is greater than $u(x)$, and hence there is at least one value of x for which $u(x)$ equals $w(x)$.

Theorem 4: If df/dx is negative for all values of x, then $u(0)$ is less than $w(0)$.

To illustrate the use of these theorems consider the case of an imaginary polyelectrolyte in which $c_0(r)$ is a constant inside a sphere and vanishes outside. Then $f(x)$ is a constant, f_0, for $x < a$ and zero for $x > a$. Equations (9) and (11) then give

$$v = f_0 \left(1 - \frac{a+1}{x} e^{-a} \sinh x\right) \qquad (x < a)$$
$$= f_0 (a \cosh a - \sinh a)\, e^{-x}/x \qquad (x > a) \tag{12}$$
$$w = \sinh^{-1} f_0 \qquad (x < a) \tag{13}$$
$$= 0 \qquad (x > a)$$

For typical polyelectrolyte dimensions, a is of the order of 5 to 10. Near the center of the polyelectrolyte, v is approximately equal to f_0, while w is $\sinh^{-1} f_0$. For $f_0 = 10$, which again is typical, we would have $v \approx 10$ and $w \approx 3$. Since both v and w are larger than u by Theorems 2 and 4, w must be nearer to u than v is.

That this situation is general can be seen from equation (9). The kernel $K(x, y)$ has a sharp peak on the line $x = y$, and becomes small when x differs from y by about unity. If the charge distribution is spread out so that $f(x)$ varies only slightly in a range of unity in x ($1/\kappa$ in r) the integral in (9) can be approximated by replacing $f(y)$ by a Taylor series

$$f(y) = f(x) + (y - x)f'(x) + \frac{1}{2}(y - x)^2 f''(x) + \cdots$$

Substituting this series into (9) gives

$$v = f(x) + 2f'(x)\left(1 - \frac{e^{-x}}{x}\right) + \cdots \tag{14}$$

which shows that if $f(x)$ is slowly varying, v is approximately equal to $f(x)$. But w is $\sinh^{-1} f$. If f is small these approximations are the same, but in regions where f is large w is much smaller than v. Since both are larger than u, w must be the better approximation.

In cases where $f(x)$ is slowly varying, it is now clear that the Donnan potential w is the proper approximation to use. If this approximation is used in equation (2) we find

$$c_1(r) = \frac{1}{2}\{c_0 + \sqrt{c_0^2 + 4M^2}\} \tag{15a}$$

$$c_2(r) = \frac{1}{2}\{-c_0 + \sqrt{c_0^2 + 4M^2}\} \tag{15b}$$

The Distribution of the Bound Ions

Up to now we have considered the ions of the polyelectrolyte as fixed in position. Actually these ions can move, but are restricted in their motion by the forces of the polymer chain. These forces counteract the tendency of the ions to diffuse and the repulsions between their charges, and keep the polyelectrolyte molecule together. To represent these forces in a tractable way, we shall use the device of replacing the chain force by a force of attraction to a fixed center. It is well known that the links of an uncharged polymer chain are normally distributed, *i.e.*, if it were not for the electrostatic forces, the concentration of ions would be of the form

$$c_0(r) = A\, e^{-r^2/2\sigma^2} \tag{16}$$

where A and σ are constants. If we replace the chain forces by a central force $F(r)$ whose potential is $V(r)$, the Boltzmann law requires

$$c_0(r) = Ae^{-V(r)/kT} \tag{17}$$

Comparing (16) and (17) shows we must put

$$V(r) = \frac{kTr^2}{2\sigma^2} \tag{18}$$

and

$$F(r) = -\frac{kTr}{\sigma^2} \tag{19}$$

In other words the force must be directly proportional to the distance from the center, and directly proportional to the absolute temperature.

If we now include the effect of the electrostatic repulsions, equation (16) must be modified to

$$c_0(r) = Ae^{-r^2/2\sigma^2} e^{-e\psi/kT} \tag{20}$$

This, together with the Donnan approximation to the potential

$$\sinh \frac{e\psi}{kT} = \frac{c_0}{2M} \tag{21}$$

gives a pair of simultaneous equations for ψ and c_0. The solution of these equations is

$$\psi = \frac{kT}{e} \ln \sqrt{1 + \frac{A}{M} e^{-r^2/2\sigma^2}} \tag{22}$$

$$c_0 = \frac{Ae^{-r^2/2\sigma^2}}{\sqrt{1 + \frac{A}{M} e^{-r^2/2\sigma^2}}} \tag{23}$$

To determine the parameters in these equations, we note first that σ characterizes the chain restoring force. It can be estimated from the size of similar, but uncharged, polymer molecules, being in fact given by

$$\sigma^2 = \frac{1}{3} R^2 \tag{24}$$

where R is the root-mean-square distance of a link of such a polymer from the center.

The constant A must be determined to give the correct total number of ions, z, on the polyelectrolyte. The relationship is

$$z = \int_0^\infty \frac{4\pi r^2 A e^{-r^2/2\sigma^2}}{\sqrt{1 + \frac{A}{M} e^{-r^2/2\sigma^2}}}\, dr \tag{25}$$

If in this equation we put $A = bM$, and $r = y\sigma\sqrt{2}$

$$z = 8\pi\sqrt{2}\sigma^3 Mb\int_0^\infty y^2 e^{-y^2}(1 + be^{-y^2})^{-1/2}\,dy \quad (26)$$

$$= 8\pi\sqrt{2}\sigma^3 Mb\,I(b) \quad (27)$$

where

$$I(b) = \int_0^\infty y^2 e^{-y^2}(1 + be^{-y^2})^{-1/2}\,dy \quad (28)$$

Values of the functions $I(b)$ and $bI(b)$ are given in Table I.

TABLE I

b	$I(b)$	$bI(b)$
0	0.432	0.0
1	.387	0.387
3	.327	.930
10	.242	2.419
30	.1672	5.02
100	.1040	10.40
300	.0644	19.32
1000	.0371	37.1
3000	.0220	65.9
10000	.01220	122.0
30000	.00710	213.1

For larger values of b, $I(b) \approx (\pi/2b)^{1/2}$.

To grasp the behavior of the polyelectrolyte as the salt concentration is varied, consider the value of r at which $r^2c_0(r)$ is a maximum, *i.e.*, the "most probable" value of r. This is located at the root of the equation

$$\left(1 - \frac{r^2}{\sigma^2}\right) + be^{-r^2/2\sigma^2}\left(1 - \frac{r^2}{2\sigma^2}\right) = 0 \quad (29)$$

which varies from $r = \sigma$ for small values of b to $r = \sigma\sqrt{2}$ for large value of b. Since equation (27) shows that b is small for large values of M and large for small values of M it follows that in high salt concentrations the polymer has the same "most probable" radius as the corresponding uncharged polymer, and extends as the salt concentration is reduced, but by not more than a factor $\sqrt{2}$ in radius.

This is a much smaller extension than has been obtained by previous theories. This is because of the fact that previous theories have introduced much higher electric fields. In the present theory the electric field has been shown to be small, and the main effect causing the extension of the chain is the diffusion tendency of the counter ions, which in dilute salt solutions essentially doubles the diffusion tendency of the ions of the polyelectrolyte.

Discussion

The applications of this model of polyelectrolytes to viscosity measurements and titration curves will be discussed in later papers. It may be pointed out here that the extension of the model to viscosity measurements involves additional assumptions concerning the permeability of the polyelectrolyte to the flow of solvent, and that the titration curves involve questions of chemical equilibrium under unusual conditions. However, neither of these problems can be discussed except in the light of a model of the action of the salt solution on the polyelectrolyte molecule.

The correctness of the model we have presented here depends only on the validity of the Poisson–Boltzmann equation, and the legitimacy of replacing the chain forces by a central force. The limits of the validity of the Poisson–Boltzmann equation have been discussed at great length, and there are serious objections to its use at high potentials. Nevertheless it is still the only tractable approximation available, and is used here for lack of a better approximation.

The main objection to the use of the central field approximation is the assumption that σ has the same value in a polyelectrolyte as for an uncharged polymer. This in effect neglects any stiffening of the chain by the repulsions of the ions. As the counter-ions affect these repulsions, this stiffening may be considerable, and would have the effect of making σ larger in dilute salt solutions, thus increasing the degrees of stretching. As a result, this model may be expected to become a poor approximation in very dilute salt solutions. Nevertheless these objections do not hold in moderate salt concentrations and there the model should be a reasonably good approximation.

Appendix

Proofs of Theorems

Theorem 1.—Suppose that there is an interval x_1, x_2 over which v is negative. The lower bound, x_1, is either 0, or a point at which $u = 0$, and the upper bound, x_2, is either ∞ or a point at which $u = 0$. Consider the integral

$$I_1 = \int_{x_1}^{x_2} u\,\frac{d}{dx}\left(x^2\,\frac{du}{dx}\right)dx$$

Using equation (7) this can be put in the form

$$I_1 = \int_{x_1}^{x_2} x^2 u\,(\sinh u - f)\,dx$$

which must be positive. Also by integrating by parts, it can be written

$$I_1 = x^2 u\,\frac{du}{dx}\Big|_{x_1}^{x_2} - \int_{x_1}^{x_2} x^2\left(\frac{du}{dx}\right)^2 dx$$

The integrated part vanishes at both limits, and the remaining integral term is obviously negative. This is a contradiction, so there can be no interval in which u is negative. The proof for v is similar, and the theorem for w is obvious.

Theorem 2.—Suppose there is an interval x_1, x_2 over which $v < u$. The lower bound x_1 is either 0, or a point at which $u = v$ and $v' < u'$. The upper bound x_2 is either ∞, or a point at which $u = v$ and $v' > u'$. Now consider

$$I_2 = \int_{x_1}^{x_2}\left[v\,\frac{d}{dx}\left(x^2\,\frac{du}{dx}\right) - u\,\frac{d}{dx}\left(x^2\,\frac{dv}{dx}\right)\right]dx$$

By equations (7) and (8) this may be written

$$I_2 = \int_{x_1}^{x_2}[v(\sinh u - u) + f(u - v)]x^2\,dx$$

which is clearly positive. On the other hand, the integration can be carried out directly, giving

$$I_2 = \left[x^2\left(v\,\frac{du}{dx}\,u - \frac{dv}{dx}\right)\right]_{x_1}^{x_2}$$

which is negative or zero. This is a contradiction. Hence r must everywhere be greater than a.

Theorem 3.—The integral

$$I_3 = \int_0^\infty \frac{d}{dx}\left(x^2\,\frac{du}{dx}\right)dx$$

$$= \left[x^2\,\frac{du}{dx}\right]_0^\infty = 0$$

But by equation (7)

$$I_3 = \int_0^\infty x^2 (\sinh u - f)\, dx$$
$$= \int_0^\infty x^2 (\sinh u - \sinh w)\, dx$$

Since the integral vanishes, sinh u must be greater than sinh w in some regions and less in others, and the theorem follows.

Theorem 4.—Suppose $u(0) > w(0)$, so that $\sinh u(0) > f(0)$. Let x_1 be the upper bound of the interval in which $\sinh u(x) > f(x)$. By Theorem 3 this interval is finite, and at x_1, $\sinh u(x) = f(x)$ and $\frac{d}{dx}(\sinh u - f) < 0$. Consider

$$I_4 = \int_0^{x_1} \frac{d}{dx}\left(x^2 \frac{du}{dx}\right) dx$$
$$= \left[x^2 \frac{du}{dx}\right]_0^{x_1}$$

The value at the lower limit is 0, hence

$$I_4 = x_1^2 \left(\frac{du}{dx}\right)_{x_1}$$

But by equation (7)

$$I_4 = \int_0^{x_1} x^2 (\sinh u - f)\, dx$$

which is positive. Hence

$$\left(\frac{du}{dx}\right)_{x_1} > 0$$

On the other hand, at x_1

$$\frac{d}{dx}(\sinh u - f) = \frac{d}{dx}(\sinh u - \sinh w) < 0$$

which requires

$$\left(\frac{dw}{dx}\right)_{x_1} > \left(\frac{du}{dx}\right)_{x_1}$$

and hence

$$\left(\frac{dw}{dx}\right)_{x_1} > 0$$

But this also requires $\left(\frac{df}{dx}\right)_{x_1} > 0$ while it was postulated that $\left(\frac{df}{dx}\right) < 0$ for all values of x. Hence the supposition leads to a contradiction and the theorem is proved.

DISTRIBUTION OF IONS IN SOLUTIONS OF WEAK ELECTROLYTES

BY EDWARD H. DEBUTTS[1]

Mallinckrodt Chemical Laboratory, Harvard University, Cambridge, Mass.

Received August 30, 1951

Using the successive ionization constants of a weak electrolyte, it is possible to calculate the concentrations of all ions present in a solution of that electrolyte at any specified average degree of ionization, but when the number of dissociation steps becomes large, the determination of such a distribution curve by this method becomes an almost impossible task. The manner in which the concentration of any particular ion of a weak electrolyte, relative to its concentration at some arbitrary point, varies with average degree of ionization may be found by direct analysis of potentiometric titration data. With an s-basic acid, it is shown that the concentration or number of ions of charge i at a degree of ionization, α, can be determined by $\ln \frac{(n_{s-i})\alpha}{(n_{s-i})_{max.}} = \int_{\alpha = i/s}^{\alpha} (i - s\alpha) d(-\ln a_{H^+})$. Here the subscripts indicate the range over which the integration is run. This equation has been tested by application to the titration curve of 1,2,3-propanetricarboxylic acid. A comparison of the resulting distribution curve to that obtained by the classical method is made. It is seen that the two methods are equivalent. By numerical integration of the titration curve of a polymeric acid, one can obtain similar curves. It is also feasible to use this tool to test theoretical titration curves which are in the literature. These are of the form $pH + \log \frac{1-\alpha}{\alpha} = pK_0 + 0.434\, \Delta F/kT$. ΔF can be written as the product of the degree of ionization and a function of the dimensions of the polymer and the ionic strength. Thus $\Delta F = \alpha F(R,w)$. Using these results, it is shown that the distribution curve can be calculated by the equation $\frac{(n_{s-i})\alpha}{(n_{s-i})_{max.}} = \left\{\left(\frac{\alpha}{i/s}\right)^{i/s}\left(\frac{1-\alpha}{1-i/s}\right)^{1-i/s} \exp - [f(R, w)/2kT][\alpha - i/s]^2\right\}^s$. Curves are shown which illustrate the sensitivity of the method and some predicted plots are compared with experiment.

If one has at his disposal the various equilibrium constants which characterize the dissociation of a weak electrolyte, then it is possible to calculate the concentrations of all ions present at any particular average degree of ionization of that electrolyte. When the number of dissociation steps is small, this is not a difficult task. However, if the number of equilibria involved is large, then these calculations become extremely laborious. In addition, the uncertainty involved in the estimation of the various mass law constants increases. When one considers the case of the polymeric electrolytes, it is for all practical purposes impossible to calculate the distribution curves of the ions present by the method outlined above.

It has been found to be possible to evaluate the manner in which the relative concentration of an ion of any specified charge varies with average degree of ionization by direct analysis of potentiometric titration data. In effect, the method to be discussed by-passes the calculation of the individual dissociation constants. We shall derive from mass-law considerations the basic equations involved. After doing this, we shall show by an example that relative distribution curves obtained by our method are the same as those obtained classically. Finally there will be suggested a method by which some of the theoretical titration curves in the literature can be checked against actual titration data.

Without loss of generality, the development of the necessary equations can be accomplished by working with a hypothetical polybasic acid. Following the notation suggested by Wall and deButts,[2] let us assume that we are dealing with a solution of N molecules and ions of an s-basic acid. In this solution suppose that there are n_{s-i} ions of charge i and

(1) Hercules Experiment Station, Wilmington, Delaware.

(2) F. T. Wall and E. H. deButts, *J. Chem. Phys.*, **17**, 1330 (1949).

that the average degree of ionization is α. Clearly

$$\sum_{i=0}^{s} n_{s-i} = N \qquad (1)$$

and

$$\alpha = \frac{\sum_{i=0}^{s} i\, n_{s-i}}{s \sum_{i=0}^{s} n_{s-i}} \qquad (2)$$

To develop the end-result in as simple a manner as possible, let us divide the numerator and denominator of (2) by n_s, the number of uncharged molecules in our solution and then examine the quotients n_{s-i}/n_s. By simple algebraic manipulation of the various expressions for the equilibrium constants, it can be seen that

$$n_{s-i}/n_s = \left(\prod_{J=1}^{i} K_J \right) f_s/f_{s-i}(a_{H^+})^i \qquad (3)$$

Here K_J is the Jth ionization constant, the f's represent the activity coefficients of the ions and a_{H^+} is the activity of the hydrogen ion in the solution.

Upon substitution of equations (3) into (2), we obtain

$$\alpha = \frac{\sum_i (i f_s/f_{s-i}(a_{H^+})^i \prod_{J=1}^{i} K_J}{\sum_i f_s/f_{s-i}(a_{H^+})^i \prod_{J=1}^{i} K_J} \qquad (4)$$

or

$$\alpha = \frac{1}{s} \frac{\partial \ln \left[f_s/f_{s-i}(a_{H^+})^i \prod_{J=1}^{i} K_J \right]}{\partial(-\ln a_{H^+})} \qquad (5)$$

Both equations (4) and (5) have been derived previously.[3]

By substituting the result of (3) in (5) and requiring that the concentration of acid be held constant we obtain

$$\alpha = -\frac{1}{s} \frac{\partial \ln n_s}{\partial(-\ln a_{H^+})} \qquad (6)$$

This result was reported in a previous publication[2] but the derivation there was based on a model. Here no model has been assumed, and the equation should be valid for any weak electrolyte which dissociates to give an ion of the parent material and an ion which is common to all equilibria. It will not apply to compounds whose ions can assume mixed charges.

Equation (6), while interesting, is not terribly useful. If, however, we take the logarithm of (3) and differentiate, we obtain

$$\frac{\partial \ln n_{s-i}}{\partial(-\ln a_{H^+})} = i + \frac{\partial \ln n_s}{\partial(-\ln a_{H^+})} \qquad (7)$$

And when we make the substitution indicated by (6) we see that

$$\frac{\partial \ln n_{s-i}}{\partial(-\ln a_{H^+})} = i - \alpha s \qquad (8)$$

The most obvious implication of this result is that when the average degree of ionization is numerically equal to the charge on a given ion divided by the basicity of the acid, the concentration of that ion passes through a maximum. In addition we see that if we have an analytical expression for α in terms of $(-\ln a_{H^+})$ we can calculate the distribution curve directly. Failing this, we can obtain the same information by numerical integration of the potentiometric titration curve.

To demonstrate this latter course, and to show that the method outlined here is equivalent to that previously reported, we replotted data obtained by Morton[4] on 1,2,3-propanetricarboxylic acid and calculated a relative distribution curve for the doubly charged ion by integration around the point $\alpha = {}^2/_3$. In Fig. 1 this curve is compared to that reported by Morton. The circles represent points obtained from the dissociation constants and the curve shows the variation of the ratio of the concentration of the doubly charged ion at various average degrees of ionization $[(n_1)_\alpha]$ to its concentration at the point where it is maximum $[(n_1)_{max.}]$. It is seen that the two methods are equivalent.

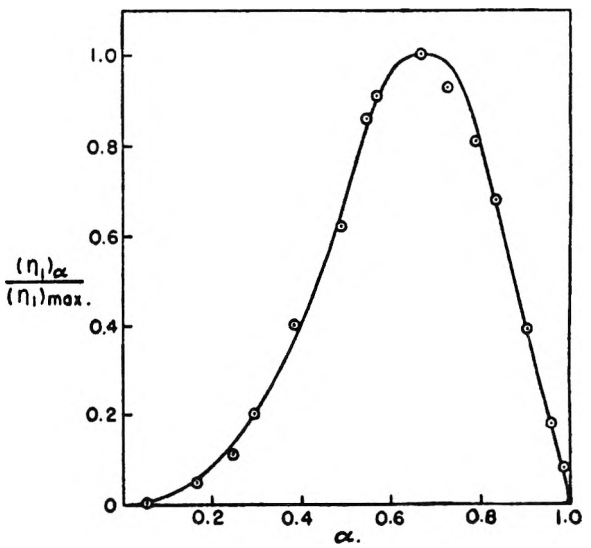

Fig. 1.—Relative distribution curve for the doubly charged ion of 1,2,3-propanetricarboxylic acid: ⊙, calculated from ionization constants; ——, calculated directly from titration curve.

If we turn now from acids of very low basicity to those of very high basicity, we find that there are reported theoretical expressions which relate the degree of ionization to the activity of the hydrogen ion.[5-7] All of these have the form

$$p\mathrm{H} + \log \frac{1-\alpha}{\alpha} = pK_0 + 0.4343 \frac{\Delta F_\alpha}{kT} \qquad (9)$$

Here pH is taken to be equal to $(-\log a_{H^+})$, K_0 is the inherent ionization constant, and $\Delta F_\alpha/kT$ is the electrical free energy of ionization. We note further that the free energy can be factored according to

$$\Delta F_\alpha = \alpha f(R,w) \qquad (10)$$

Here R is a measure of the dimensions of the ions

(3) J. Wyman, Jr., *Adv. in Protein Chem.*, **4**, 407 (1948).

(4) C. Morton, *Trans. Faraday Soc.*, **24**, 14 (1928).

(5) E. J. Cohn and J. T. Edsall, "Proteins, Amino Acids and Peptides," Reinhold Publishing Company, New York, N. Y., 1943, p. 476.

(6) J. J. Hermans and J. Th. G. Overbeek, *Rec. trav. chim.*, **67**, 761 (1948).

(7) A. Katchalsky and J. Gillis, *ibid.*, **68**, 879 (1949).

and w is the ionic strength. Equation (9) can thus be written (using natural logarithms)

$$-\ln a_{H^+} + \ln \frac{1-\alpha}{\alpha} = -\ln K_0 + \alpha f(R,w)/kT \quad (11)$$

If we differentiate this expression with respect to $(-\ln a_{H^+})$, holding R, w, and T constant, substitute the result in (8), and integrate between the limits of $\alpha = i/s$ (where n_{s-i} is maximum) and α, there is obtained after simplification

$$\frac{(n_{s-i})_\alpha}{(n_{s-i})_{max.}} = \left(\frac{\alpha}{i/s}\right)^{i/s}\left(\frac{1-\alpha}{1-i/s}\right)^{1-i/s} \exp\left[-\frac{f(R,w)}{2kT}(\alpha - i/s)^2\right]^s \quad (12)$$

When one is dealing with acids of high basicity, the ratio of concentrations is of significant value over a very small range of α (*cf.* Fig. 2 or 3), so that

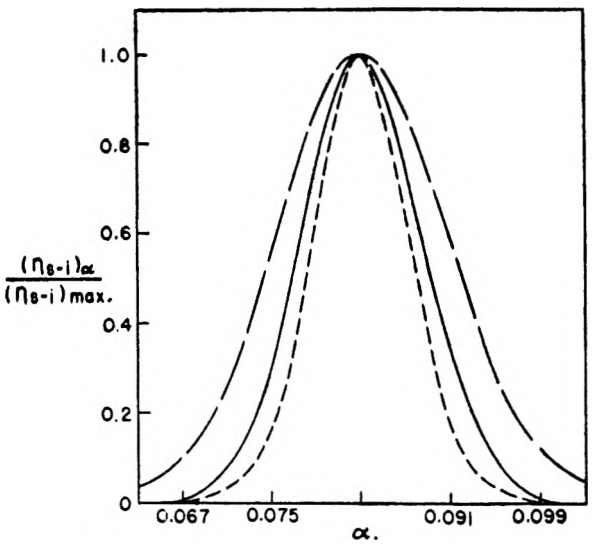

Fig. 2.—Effect of basicity on relative distribution curve; $i/s = 0.083$, $f(R,w)/2kT = 11$: – – –, $s = 512$; ——, $s = 1024$; – – –, $s = 1615$.

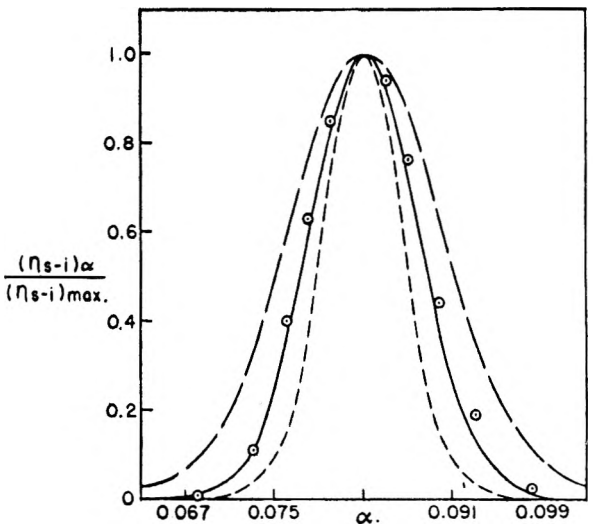

Fig. 3.—Effect of $f(R,w)/2kT$ on relative distribution curve. Comparison of theoretical curves with experiment: – – –, $f(R,w)/2kT = 0$ (no electrical interaction); ⊙, $f(R,w)/2kT \cong 4.5$ (experiment); ——, $f(R,w)/2kT = 7.0$ (Cohn and Edsall); – – –, $f(R,w)/2kT = 17.7$ (Katchalsky and Gillis).

one can expand the exponential and obtain as an excellent approximation

$$\frac{(n_{s-i})_\alpha}{(n_{s-i})_{max.}} = \left(\frac{\alpha}{i/s}\right)^{i/s}\left(\frac{1-\alpha}{1-i/s}\right)^{1-i/s}\left[1 - \frac{f(R,w)}{2kT}(\alpha - i/s^2\right]^s \quad (13)$$

It is this form which we have used in our calculations.

Since the relative distribution curves can be obtained either directly from experiment or from theory, it is natural to use these curves to test the theoretical expressions in the literature. The question of sensitivity of the method arises. It will be useful if (a), it is not too sensitive to basicity (*i.e.*, molecular weight), (b) it is reasonably sensitive to the function $f(R, w)$ and (c) the data required for numerical integration can be obtained with sufficient accuracy.

If one examines Figs. 2 and 3, it is seen that the first two requirements are met satisfactorily. To obtain the family of curves in Fig. 2, we varied the basicity, s, while holding the free energy function constant. It is seen that when we change the number of ionizable groups by a factor of two, distinguishable plots are obtained. If the basicities were changed by only 10%, then on the scale we use the curves would not be perceptibly different from those shown. We can, of course, measure the basicity of polymeric acids to about 1 or 2% so that errors in the distribution curve due to errors in measurement of basicity will not be noted. If now we hold the basicity constant, and vary $f(R, w)$, the curves in Fig. 3 are obtained. The reason for choosing the values of $f(R, w)/kT$ will be evident later. The point we wish to make now is that small errors in the exponential will not drastically alter the distribution plots, but large errors will. This means that calculation of distribution curves from theory, using dimensional and molecular weight data from experiment, will show reasonably large deviations from the experimental distribution curve only if the validity of the theory is to be seriously questioned.

The situation with regard to the data required for the numerical integration is not so satisfactory. When the data in the literature are examined and an attempt is made to prepare a distribution curve based on these data, it is evident that they are not sufficiently accurate. To obtain the points which are shown in Fig. 3, it was necessary to assume one more significant figure in α and in pH than was justified. Thus the plot shown is not extremely meaningful. This difficulty can very probably be overcome by use of a differential titration apparatus.

In addition to showing the manner in which variation in the electrical free energy function alters the plot of relative concentrations *versus* degree of ionization, Fig. 3 also illustrates an experimental curve and the predictions of three different theories. Before discussing the actual plots, it would probably be wise to describe the manner in which they were derived. The numerical integration of the titration curve is more conveniently performed if equation (8) is cast into the form

$$\frac{1}{s}\ln\frac{(n_{s-i})_\alpha}{(n_{s-i})_{max.}} = \int_{\alpha=i/s}^{\alpha}(i/s-\alpha)(\mathrm{d}-\ln a_{H^+}) \quad (8a)$$

The value of the integral is then obtained from a plot of $(i/s - \alpha)$ against $(-\ln a_{H^+})$ by measurement of the appropriate areas around the point where $(i/s - \alpha)$ has the value zero. The values of $(n_{s-i})_\alpha/(n_{s-i})_{max.}$ result.

In the case shown, we used data reported by Arnold and Overbeek[8] for the neutralization of polymethacrylic acid in 10^{-4} M potassium chloride solution. The degree of polymerization based on viscosity measurements is 1615. The value of i/s is 0.083. When these are substituted in equation (13), we have

$$\frac{(n_{s-i})_\alpha}{(n_{s-i})_{max.}} = \left\{1.33115\,\alpha\left(\frac{1-\alpha}{\alpha}\right)^{0.917}\left[1-\frac{f(R,w)}{2kT}(\alpha-i/s)^2\right]\right\}^{1615} \quad (13a)$$

The three theoretical distribution curves were calculated from this formula.

Unfortunately the work of Hermans and Overbeek[6] cannot be tested without independent measurements of the coil dimensions. We can, however, examine cases where $f(R, w)/2kT$ is zero, and where this function takes the form described by Katchalsky and Gillis[7] and in Cohn and Edsall.[5]

Katchalsky and Gillis relate the mean "end-to-end" distance, h_α, to the degree of ionization by

$$h_\alpha^3 = \frac{s^2\alpha^2e^2h_0^2}{3DkT}\left(\ln\frac{3h_\alpha^2}{2h_0^2}-1\right) \quad (14)$$

Since h_0^2 can be determined from theory, we are able by (14) to calculate the manner in which h_α changes as α increases. The value of h_α at some particular α (in this case 0.083) can then be substituted in their free energy expression

$$\frac{f(R,w)}{2kT} = \frac{se^2}{DkTh_\alpha}\times\left[1+\ln\frac{3h_\alpha^2}{2h_0^2}\right] \quad (15)$$

On the basis of equation (14), the value of h_α is found to be 33.0×10^{-6} cm. In turn the value of (15) is 17.7. This theory of course neglects the effect of counter ions on the conformation of the polymeric species.

In the case of the titration curve reported in the monograph edited by Cohn and Edsall,[5] we have

$$\frac{f(R,w)}{2kT} = \frac{se^2}{2DkT}\left[\frac{1}{R_0(1+KR_0)}\right] \quad (16)$$

Here K is the familiar Debye reciprocal radius and R_0 was taken to be that dimension shown by Debye to be related to the mean square end to end distance of non-charged polymers by

$$R_0^2 = \frac{5}{18}h_0^2 \quad (17)$$

In our example K is 0.74×10^6 cm.$^{-1}$ and h_0 is calculated to be 5.23×10^{-6} cm. It follows that $f(R, w)/2kT = 7.0$. It should be mentioned that this theory assumes that the dimensions of the polymer coil do not change as α increases.

The manner in which the relative concentrations vary with average degree of ionization using these values of $f(R, w)/2kT$ is compared to experiment in Fig. 3. The broadest curve is that which results when one assumes that ionization proceeds on a statistical basis, *i.e.*, $f(R, w)/kT = 0$. It is quite evident that the assumption of no electrical interaction is invalid. It is likewise clear that the effect of counter ions is felt at rather low concentrations for the Katchalsky and Gillis theory gives us too high a value for the free energy term. Surprisingly enough the equation of Cohn and Edsall results in a plot which is quite close to experiment. This means that expansion of the coil is suppressed rather drastically by the sodium, hydrogen, and potassium ions present in the solution. Indeed a fit to experiment can be obtained from their expression if we use 1.28 as the value of h_α/h_0. This is to be contrasted with the value 6.3 predicted by (14). In closing we must reemphasize the fact that the experimental points are considerably in error. Because of this we can conclude only that the ionic strength of the solution with which we are working is too high for the work of Katchalsky and Gillis to be valid.

(8) R. Arnold and J. Th. G. Overbeek, *Rec. trav. chim.*, **69**, 192 (1950).

THE INTERACTION OF PROTEINS WITH SYNTHETIC POLYELECTROLYTES. I. COMPLEXING OF BOVINE SERUM ALBUMIN.

BY HERBERT MORAWETZ[1] AND WALTER L. HUGHES, JR.

University Laboratory of Physical Chemistry Related to Medicine and Public Health, Harvard University, Boston, Mass.

Received August 30, 1951

The precipitation of bovine serum albumin by four synthetic polyelectrolytes was studied as a function of *p*H, ionic strength, polymer/protein ratio and the degree of polymerization of the resin. Bovine serum albumin recovered from its complex with polymethacrylic acid had the same optical activity, solution viscosity and crystallizability as the original material and seemed, therefore, to be in its native state. Anion binding, characteristic of serum albumin, was considered to cause the shift of the precipitation curves to lower *p*H in the presence of chloride or thiocyanate and to account for the high stability of albumin complexes with a copolymer of styrene and maleic anhydride. It was shown that oxyhemoglobin can be separated from serum albumin in the interisoelectric range by precipitation with polymethacrylic acid.

I. Introduction

It has long been recognized that the coprecipitation of proteins at *p*H values lying between their isoelectric points presents problems in any scheme of protein fractionation.[2] Green suggested[3] that the separations could be enhanced by approaching the precipitation zone from the direction where all the proteins bear charges of the same sign. More recently a fractionation scheme has been described[4] which takes advantage of protein–protein interaction for the separation of groups of proteins. The value of the method depends on the presence of specifically interacting proteins in the original mixture.

This principle can be extended to the isolation of individual proteins from binary mixtures by the addition of a new charged component. On looking about for such charged components one is immediately attracted to the synthetic polyelectrolytes[5,6] since they are readily available and may be tailored to fit the problem. Furthermore, in many cases they are known to form highly insoluble precipitates with specific counter-ions, thus suggesting a method for their eventual removal from the protein system.

The synthetic materials can be made very cheaply and in great variety by copolymerization of a large number of readily available monomers or by chemical modification of polymers and copolymers. Since they can be made with a much greater density of ionizable groups than that characteristic of proteins, it may be expected that they will displace proteins from their salt-like complexes, permitting a more quantitative separation of normally interacting proteins. Before attempting protein separations a study of the interaction of polyelectrolytes with pure individual proteins seemed indicated, and bovine serum albumin was chosen as the first to be investigated, since its high solubility in water would put particularly stringent requirements on an efficient precipitating reagent.

(1) Public Health Service Research Fellow of the National Heart Institute.

(2) E. J. Cohn, *J. Gen. Physiol.*, **4**, 697 (1922).

(3) A. A. Green, *J. Am. Chem. Soc.*, **60**, 1108 (1938).

(4) E. J. Cohn, *et al.*, *ibid.*, **72**, 465 (1950).

(5) Naturally occurring polyelectrolytes such as protamines[7,8] nucleic acids[9] and gum arabic,[10] have frequently been shown to precipitate proteins under suitable conditions.

(6) Synthetic polyelectrolytes have also been used lately for the precipitation of bacterial suspensions.[11]

(7) F. Haurowitz, *Kolloid-Z.*, **74**, 208 (1936).

(8) A. Kleczkowski, *Biochem. J.*, **40**, 677 (1946).

(9) K. B. Björnesjö, and T. Teorell, *Arkiv Kem. Mineral Geol.*, **A19**, No. 34 (1945).

(10) H. G. Bungenberg de Jong, "Colloid Science," Vol. II, Elsevier Press, Inc., New York, N. Y., 1949, Chapter 10.

(11) E. Katchalski, in preparation.

II. Experimental

The bovine serum albumin (BSA) was a crystallized sample obtained from Armour and Company. A stock solution of 1% was made up and the albumin concentration determined by ultraviolet absorption measurement using the optical density data of Cohn, Hughes and Weare.[12] The solution was kept frozen at −17° in small ampules and melted only immediately before use.

The oxyhemoglobin was prepared by Miss Virginia Gossard according to the method described by Drabkin.[13] Its concentration was calculated from the optical density at 350 mμ using the data reported by Sidwell, Munch, Barron and Hogness.[14]

Polymethacrylic acid (MA) was prepared from glacial methacrylic acid which was distilled at reduced pressure under nitrogen and kept frozen at −17°. The monomer was mixed with five parts by weight of benzene, benzoyl peroxide catalyst added (1.5% of the weight of the monomer) and the polymerization was carried out by heating for two days at 60°. The resin suspension was washed with acetone and ether and vacuum-dried at 70°. The yield was 98%, the intrinsic viscosity in methanol 1.05. Some of the polymer was fractionated by precipitating twice from aqueous solution at *p*H 6.8 and a calcium acetate concentration of 0.05 *M*. The precipitate was dissolved in 5% sodium hydroxide, dialyzed three days against *M*/100 hydrochloric acid, the solution frozen and vacuum evaporated.

Polymethacrylic acid samples of a range of different molecular weights were prepared at 60° from solutions of 10 ml. of glacial methacrylic acid (Rohm and Haas) in 40 ml. of methyl ethyl ketone with different amounts (29 mg., 83 mg., 165 mg., and 328 mg.) of azo-bis-isobutyronitrile catalyst. After 24 hours the polymerization was essentially complete. The precipitated resin was washed with ether, dissolved in water, dialyzed for two days and dried from the frozen state. Intrinsic viscosities in methanol were 1.58, 1.11, 0.79 and 0.57.

Methacrylic acid–vinylpyridine copolymer was prepared from 2-vinylpyridine (Reilly Tar & Chem. Co.) distilled at reduced pressure under nitrogen immediately before use. A monomer mixture containing 1.5 mole per cent. vinylpyridine was polymerized in methyl ethyl ketone solution at 60° to a conversion of 12%. The copolymer had an absorption coefficient $E^{1\%}_{1\ cm.}$ 27.0 at 265 mμ in solution of *p*H 4.0.

Polyvinylamine hydrobromide (PVA) prepared by the method of Reynolds and Kenyon[15] was supplied by the Eastman Kodak Co. It analyzed 60.27% bromine and 11.34% nitrogen. The intrinsic viscosity in 0.15 *N* sodium chloride (based on the concentration of polyvinylamine) was 1.12.

Maleic anhydride–styrene copolymer (MAS) containing

(12) E. J. Cohn, W. L. Hughes, Jr., and J. H. Weare, *J. Am. Chem. Soc.*, **69**, 911 (1947).

(13) D. L. Drabkin, *J. Biol. Chem.*, **164**, 703 (1946).

(14) A. E. Sidwell, Jr., R. H. Munch, E. S. G. Barron and T. R. Hogness, *ibid.*, **123**, 335 (1938).

(15) D. D. Reynolds and W. O. Kenyon, *J. Am. Chem. Soc.*, **69**, 911 (1947).

50 mole per cent. of each monomer was obtained from Carbide and Carbon Chemicals Co. (Resin SYHM). The intrinsic viscosity in methyl ethy lketone was 0.31. This resin is soluble in water only after hydrolysis of the anhydride groups (achieved rapidly by treatment with dilute alkali and more slowly by stirring in water at 80°).

Methacrylic acid–diethylaminoethyl methacrylate copolymer (DEMMA) was prepared as described in a previous communication.[16] It contained 54.6 mole per cent. methacrylic acid, had an isoelectric point of 8.0 and an intrinsic viscosity in pyridine of 1.5.

Ground glass stoppered tubes were used for mixing the albumin and polyelectrolyte solutions, using a total volume of 10 ml. for each experiment. When it was desired to vary *p*H at low ionic strength, stock solutions of the polyelectrolytes were made up to different degrees of neutralization and mixed in varying proportions so as to avoid exposing the protein to local concentrations of acid or alkali. Acetate buffers were used when it was desired to keep the *p*H at a given value while investigating the effect of another variable. After introducing all reagents precooled to 0°, the stoppered tube was inverted several times and left standing at 0°, for at least three hours although equilibrium was apparently attained much more rapidly. The precipitate was separated in a refrigerated centrifuge and the supernatant was used for analysis and *p*H determination on a glass electrode at 25°.

Analyses were carried out by determinations of the optical density with a Beckman spectrophotometer using 1-cm. quartz cells to hold the appropriately diluted samples. Since many of the supernatants from protein precipitations were slightly hazy, buffers had to be added to produce clear solutions before the absorption measurements. In such cases the blanks contained the same buffer concentration. Supernatants from precipitation with anionic polymers were diluted with an equal amount of $M/10$ disodium phosphate unless they contained alkaline earths cations, in which case a mixture of five parts $M/4$ trisodium citrate and one part $M/4$ citric acid was used. Supernatants from polyvinylamine precipitations were diluted with acetate buffer of *p*H 4.00 and ionic strength 0.8. Polymers MAS and PVA had characteristic UV absorption maxima and the concentrations of albumin and polymer could be obtained from optical density measurements at two wave lengths (see Fig. 1). The results obtained from analyzing the supernatants from a series of experiments involving precipitation with MAS were checked by dissolving the precipitate in disodium phosphate solution and analyzing in a similar manner. The amounts of protein and polymer found in the two phases added up to the quantities known to be present within an average error of 6%. Copolymer DEMMA had an absorption coefficient $E^{1\%}_{1\ cm.}$ 0.55 at 280 mμ due probably to light scattering from the very high molecular weight material. The resin had no characteristic absorption maximum and no attempt was made to interpret optical densities in terms of protein concentration. Polymethacrylic acid had $E^{1\%}_{1\ cm.}$ 0.385 at 280 mμ and its contribution to the optical densities of supernatants from albumin precipitation was neglected.

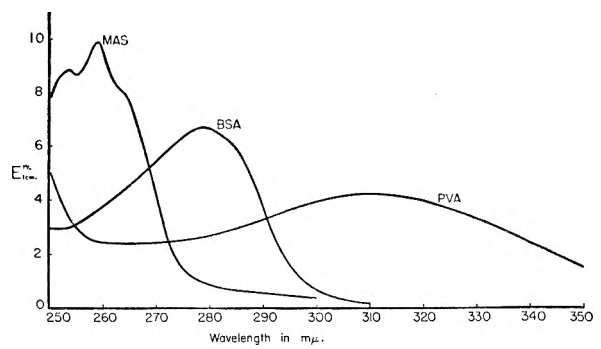

Fig. 1.—Ultraviolet absorption spectra of bovine serum albumin at *p*H 4, maleic anhydride–styrene copolymer and polyvinylamine.

(16) T. Alfrey, Jr., R. M. Fuoss, H. Pinner and H. Morawetz, in preparation.

Viscosity measurements were carried out in an Ostwald type viscosimeter at 25°.

Optical activity was determined using a 20-cm. polarimeter tube and allowing 15 minutes after mixing the reagents before taking a reading. Two samples were prepared by mixing partially neutralized resin solutions with a concentrated solution of BSA, so that no precipitation occurred. One sample was made by precipitating BSA by polymethacrylic acid at *p*H 4.0 and redissolving the precipitate by addition of disodium phosphate. The protein concentration was calculated from the optical density at 280 mμ, after allowing for the absorption of the resins.

III. Results

A. Polymethacrylic Acid.—The effect of the resin/protein ratio on the precipitation of BSA by MA in buffered solution at various *p*H values is shown in Fig. 2. Resin addition beyond an optimum amount increases albumin solubility. Holding the resin/protein ratio constant and studying

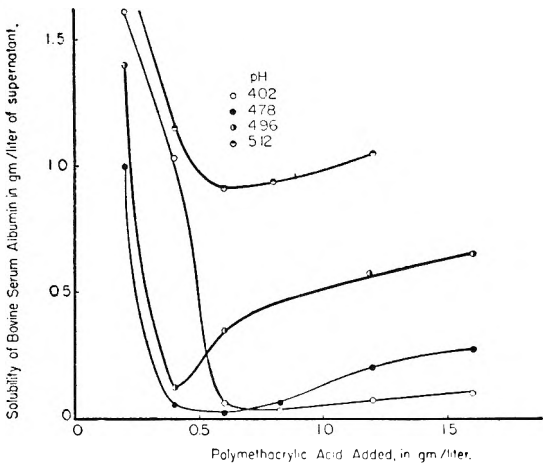

Fig. 2.—Precipitation of bovine serum albumin by polymethacrylic acid: effect of resin/protein ratio at constant *p*H; $\Gamma/2$ = 0.04 (acetate buffer); BSA concn. = 1.82 g./liter.

the albumin precipitation as a function of *p*H at different concentrations of acetate buffer and in the presence of thiocyanate, the data plotted in Fig. 3 were obtained. Acetate

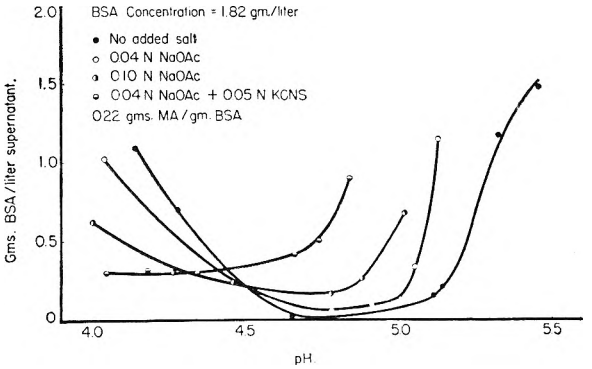

Fig. 3.—Precipitation of bovine serum albumin by polymethacrylic acid: effect of acetate and thiocyanate.

has little effect on the complex formation but thiocyanate produces a considerable shift of the precipitation curve to lower *p*H values. Figure 4 shows that both the molecular weight of the polymer and the precipitation temperature are only of secondary importance.

Results obtained in a study of the interaction between alkaline earth cations and a copolymer of methacrylic acid with a small amount of vinylpyridine were used in selecting the optimum conditions for polymethacrylic acid precipitation. The pyridine residues facilitated the determination of the polymer by optical density measurement at 265 mμ and were not expected to produce an important change in the

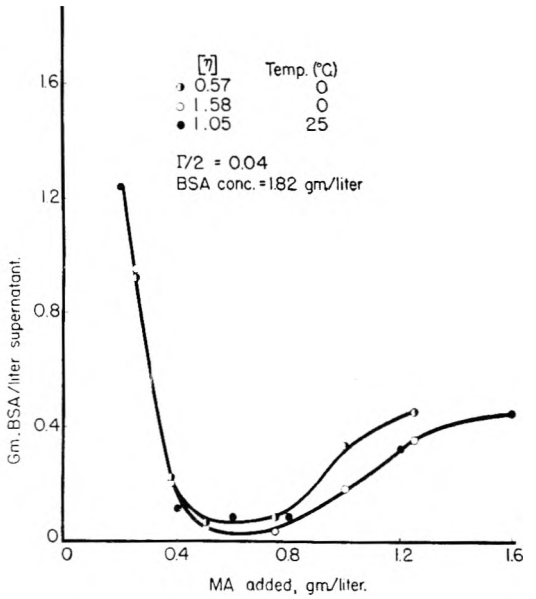

Fig. 4.—Precipitation of bovine serum albumin by polymethacrylic acid: effect of temperature and molecular weight ($\sim [\eta]$) of resin.

properties of the polyelectrolyte above *p*H 5. It was found that the efficiency of the precipitation increased in the order $Mg^{++} < Ca^{++} < Ba^{++}$, the polymer salt being most insoluble in the *p*H range 6.0 to 6.5. As little as 0.01% MA is flocculated from 1% BSA solution by 0.04 *M* barium chloride, and no protein is carried down with the polymer.

Three criteria were used for the absence of protein denaturation: optical activity, solution viscosity and crystallizability. Table I lists results of optical activity measurements. Since some of the readings were as low as 2°, the differences between the optical activities found for the various samples are within the probable experimental error. They are also in satisfactory agreement with the value of 78° ± 2° found by Cohn, Hughes and Weare.[12]

TABLE I

EFFECT OF POLYELECTROLYTES ON THE OPTICAL ACTIVITY OF BOVINE SERUM ALBUMIN

BSA concn., g./l.	G. resin/g. BSA	Resin	*p*H	Specific optical activity
29.0	0.00	.....	5.33	−75°
28.5	.47	MA, 45% neutralized	6.00	−78
13.8	.49	MAS, 53% neutralized	6.46	−75
14.2	.45	MA, added at *p*H 4 ppt. redissolved by Na_2HPO_4	5.28	−76

The BSA used had an intrinsic viscosity of 0.43 and could be crystallized at −5° from a 20% solution containing 0.1 *M* acetic acid, 0.5 *M* sodium acetate and 40% by volume of ethanol. It was found that small amounts of polymethacrylic acid raise substantially the intrinsic viscosity and inhibit completely the crystallizability of the protein. These two criteria were used, therefore, to prove the separation of the pure albumin from its complex with the polymer, as well as the preservation of the protein in the native state.

The BSA was precipitated at *p*H 4.71 by 0.4 g. of fractionated polymethacrylic acid per gram protein. The precipitate was redissolved at *p*H 5.38 and the resin precipitated by making the solution 0.05 molar in barium chloride. After centrifugation, the supernatant was filtered through fritted glass, dialyzed for two days and dried from the frozen state. The recovered protein had an intrinsic viscosity of 0.44 and crystallized under similar conditions as the starting material with comparable yields.

That proteins can be separated in the interisoelectric range by use of polyelectrolytes, as postulated, has been demonstrated by the separation of oxyhemoglobin and BSA. At 1.9% BSA, 2.5% oxyhemoglobin, ionic strength 0.08 and *p*H 5.75 the optimum MA/oxyhemoglobin ratio was found to be 0.15. Under these conditions 91% of the oxyhemoglobin was precipitated while all of the albumin remained in solution.

B. Maleic Anhydride–Styrene Copolymer.—Copolymer MAS had a characteristic ultraviolet absorption spectrum and it was, therefore, possible to follow the concentration of both components in equilibrium with resin–albumin precipitates. The effect of varying the amount of MAS added to a BSA solution is shown in Table II. These data cannot

TABLE II

EFFECT OF THE RESIN/PROTEIN RATIO ON THE PRECIPITATION OF A 0.31% BOVINE SERUM ALBUMIN SOLUTION BY MALEIC ANHYDRIDE–STYRENE COPOLYMER

Initial g. MAS/g. BSA	*p*H	Supernatant BSA g./l	Supernatant MAS, g./l.	Precipitate, g. MAS/g. BSA
0.09	5.39	2.71	0.13	0.11
.17	5.70	2.20	.34	.13
.26	5.25	1.07	.36	.16
.43	4.62	0.49	.80	.16
.57	4.42	.10	1.11	.23
.86	4.27	.06	1.75	.26

be readily interpreted since the degree of ionization of both resin and protein vary simultaneously with their relative amounts in solution. When the resin/protein ratio was kept constant and the degree of resin neutralization was varied, the results represented in Fig. 5 were obtained. Conversely, the variation of the resin/protein ratio in buffered solutions at *p*H 4.77 and 5.16 gave the data shown in Fig. 6. Any MAS added beyond a given amount remained in solution and the addition of excess resin increased the albumin solubility from its minimum to a new characteristic level. The insolubility of the resin–protein complex in sodium chloride solution is apparent from the data of Table III.

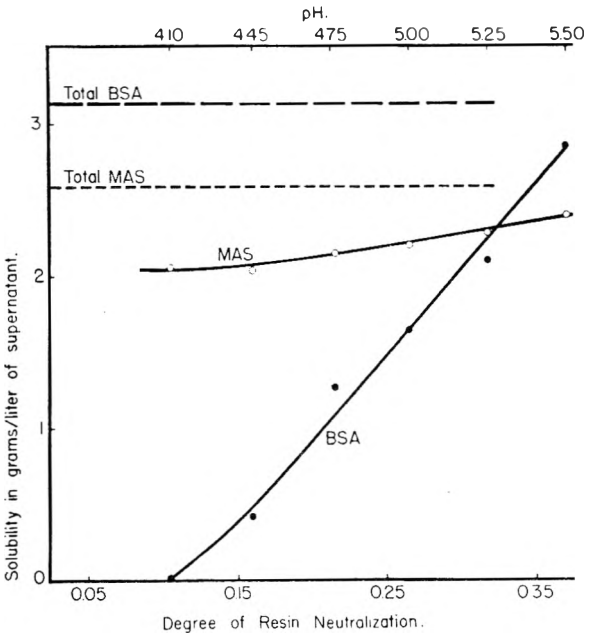

Fig. 5.—Precipitation of bovine serum albumin by maleic anhydride–styrene copolymer: effect of the degree of resin neutralization.

Although the albumin precipitate with MAS dissolved on raising the *p*H of the solution, the complex proved to be very stable and all attempts at its dissociation failed. The presence of the resin increased the protein solubility above its isoelectric point at low ionic strength and high ethanol concentration. In fact, a solution containing 3 g./l. BSA, 1.3 g./l. of half-neutralized MAS and 30% by volume of ethanol, could not be precipitated by addition of 95% ethanol or anhydrous acetone. Calcium acetate solution added

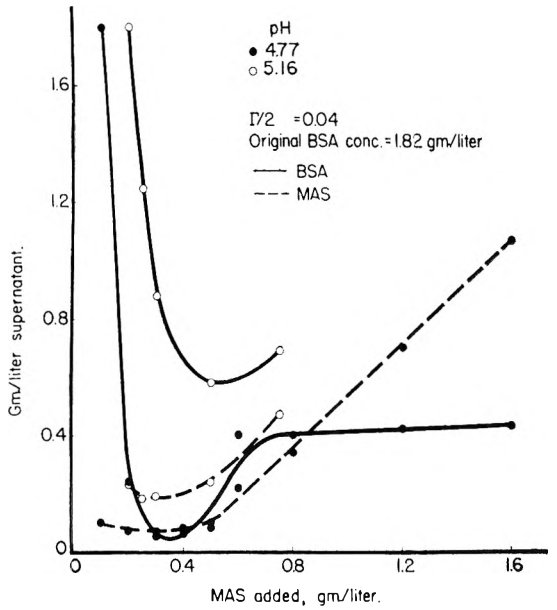

Fig. 6.—Precipitation of bovine serum albumin by maleic anhydride–styrene copolymer: effect of resin/protein ratio at constant *p*H.

in the *p*H range 6.2 to 6.4 precipitated all the protein with the resin. The precipitation became progressively less complete at higher *p*H values, but the resin/protein ratio was essentially the same in the precipitate and the supernatant. Optical activity measurements (Table I) indicate that no protein denaturation is involved in this complex formation.

TABLE III

EFFECT OF IONIC STRENGTH ON THE PRECIPITATION OF BOVINE SERUM ALBUMIN BY MALEIC ANHYDRIDE–STYRENE COPOLYMER

3.1 g./l. BSA, 2 g./l. MAS, degree of resin neutralization 0.106

Normality of sodium chloride	Supernatant BSA, g./l.	Supernatant MAS, g./l.
0.000	0.19	1.29
.017	.38	0.68
.033	.37	.54
.050	.20	.47
.067	.21	.38
.083	.19	.33

C. **Polyvinylamine.**—The precipitation of BSA by PVA leads to the formation of a precipitate which has the appearance of a highly viscous second liquid phase in contrast to

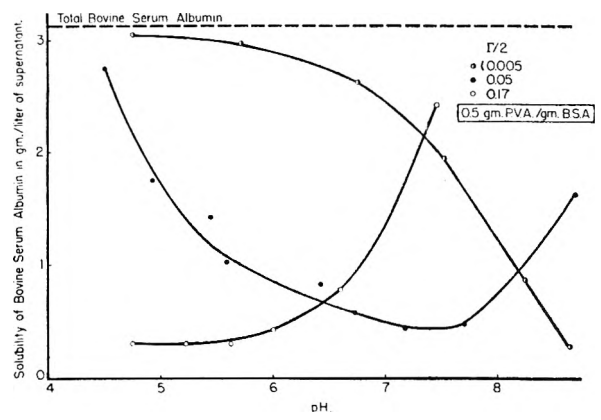

Fig. 7.—Precipitation of bovine serum albumin by polyvinylamine as a function of *p*H: effect of sodium chloride.

TABLE IV

PRECIPITATION OF SERUM ALBUMIN WITH POLYVINYLAMINE

3.1 g./l. BSA, 1.6 g./l. PVA

Mole sodium hydroxide/equivalent polyvinylamine hydrobromide	Normality of sodium chloride	*p*H	Supernatant BSA, g./l.	Supernatant PVA, g./l.
0.145	0.00	3.95	3.05	1.60
.333	.00	4.76	3.05	1.61
.521	.00	5.70	2.97	1.53
.630	.00	6.78	2.62	1.58
.738	.00	7.53	1.94	1.33
.846	.00	8.25	0.86	0.98
.955	.00	8.67	.22	.46
.145	.05	4.51	2.76	1.48
.239	.05	4.93	1.75	1.28
.333	.05	5.42	1.37	1.18
.427	.05	5.82	1.03	1.10
.521	.05	6.42	0.82	0.98
.630	.05	6.73	.58	.85
.738	.05	7.18	.44	.72
.846	.05	7.70	.47	.63
.955	.05	8.70	1.63	.91
.145	.17	4.74	0.31	0.80
.239	.17	5.22	.31	.76
.333	.17	5.63	.31	.70
.427	.17	6.00	.42	.72
.630	.17	6.60	.79	.72
.738	.17	7.44	2.44	1.41
Effect of 32 Volume % Ethanol				
0.521	0.00		0.55	1.00
.738	.00		.09	0.86
.955	.00		.04	.30

the flocculent precipitates observed with the anionic polymers. Addition of chloride results in a surprisingly large shift of the precipitation curve toward lower *p*H values and an even greater effect is produced by thiocyanate (see Table IV and Figs. 7 and 8). Ethanol reduces the solubility of the BSA complex with PVA.

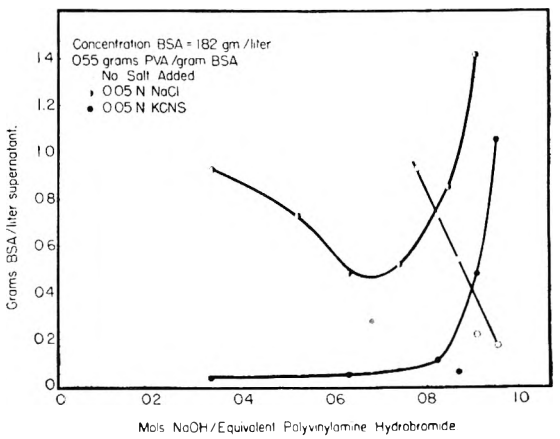

Fig. 8.—Precipitation of bovine serum albumin by polyvinylamine as a function of the degree of neutralization.

All the albumin could be precipitated by alcohol in the presence of PVA, but some of the resin was carried down with it. At 1.8 g./l. BSA, 1 g./l. PVA, 40% ethanol by volume, *p*H 4.77, ionic strength 0.04 and −5°, the precipitate contained all the BSA with 30% of the PVA. Conversely, the precipitation of polyvinylamine by sulfate in the *p*H range 5–6 did not precipitate any of the protein. It was found, however, that at high protein/resin ratios the polyvinylamine sulfate tended to remain in colloidal suspension and could not be satisfactorily separated.

D. Diethylaminoethyl Methacrylate–Methacrylic Acid Copolymer.—When 1% solutions of the amphoteric polyelectrolyte DEMMA and of BSA were mixed a precipitate was formed, the amount depending on the ratio of the solutions taken. The precipitation was always very incomplete as can be seen from the optical densities of the supernatants plotted in Fig. 9. The precipitate formed only at extremely low ionic strength and dissolved in 0.005 *N* sodium chloride.

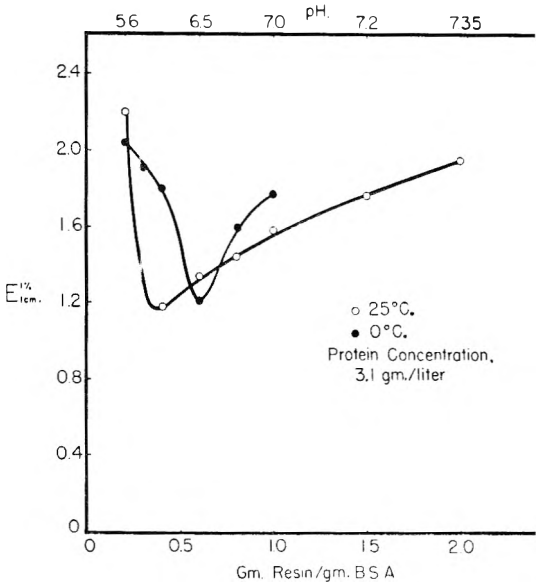

Fig. 9.—Interaction of bovine serum albumin with a methacrylic acid–diethylaminoethyl methacrylate copolymer. Extinction at 280 mμ is plotted *vs.* resin/protein ratio.

IV. Discussion

The solubility studies here reported include so many complicating factors that no more than a qualitative interpretation of the results is justified. In principle, the complexing of proteins with polyelectrolytes may be regarded as an extension of the use of polyvalent ions for protein precipitation[4]. Previous studies have indicated that protein precipitation by such naturally occurring polyelectrolytes as gum arabic[10] and protamines[8] can take place only at low ionic strength. Among the synthetic polyelectrolytes used in the present investigation only the ampholyte DEMMA formed such easily dissociable complexes with bovine serum albumin, while the albumin precipitates with the cationic and anionic polymers were surprisingly stable at relatively high salt concentrations. This stability of the complex may be related to the flexibility of the polymer chain, permitting a close approach of its ionic charges to the opposite charges of the protein.

It was generally found that a critical ratio of resin to protein was required for maximum precipitation (Figs. 2 and 6). The solubilization of the precipitate on addition of either component implies the formation of soluble complexes, as observed in antigen–antibody reactions. Maximum precipitation would be expected to coincide with the formation of isoelectric complexes and Bungenberg de Jong[10] has shown that this is the case for the gelatin–gum arabic system. Computing the charge of polymethacrylic acid from titration data obtained in the absence of albumin, maximum protein precipitation is found to correspond to about 20 anionic polyelectrolyte charges per BSA molecule, at *p*H 4.02, 4.78 and 4.96 while a higher ratio of anionic charges is required at *p*H 5.12. This is more than the albumin charge at any but the lowest of these *p*H values,[17] but the proximity of the oppositely charged colloid reduces the electrical free energy of ionization and undoubtedly increases the charges of both components to values which are difficult to estimate.

The effect of the resin/protein ratio on complex formation at constant *p*H could be studied particularly well with copolymer MAS, since both components could be determined spectrophotometrically in the supernatant (Figs. 5 and 6). The data indicate that with increasing amounts of MAS added to a given amount of albumin, the resin/protein ratio in the precipitate increases to a maximum and any further resin remains entirely in solution. The constant albumin solubility in the presence of large amounts of resin may be interpreted as characterizing the solubility of the resin–albumin complex of this limiting composition. The results resemble somewhat those obtained by Björnesjö and Teorell[9] in their extensive study of the precipitation of ovalbumin by thymonucleic acid.

The precipitation equilibria were almost independent of the molecular weight of polymethacrylic acid (Fig. 4), as would be expected, since it is known that for any but very low molecular weight polyelectrolytes the electrical field due to the ionized chain molecules is almost independent of their degree of polymerization.[18]

While the precipitation of BSA with the anionic polymers was reversed rather sharply in the neighborhood of the isoelectric point of the protein, polyvinylamine added at low salt concentration became an effective precipitant only above *p*H 7 (Fig. 7). The low tendency of serum albumin to complex with basic colloids has been ascribed by Haurowitz[7] to a steric configuration in which most of the anionic groups are located in the interior of the molecule.

The precipitation of BSA with polyvinylamine was shifted to much lower *p*H values when chloride or thiocyanate were added to the solution (Figs. 7 and 8). The effect to be expected from such salt addition could be ascribed in general to a combination of the following factors: (a) Reduced electrostatic interaction of the oppositely charged colloids due to increased counter-ion density. (b) Increase in the negative charge of the albumin due to anion binding. (c) Increase in the polyelectrolyte charge due to a reduction of the electrical free energy of ionization.

The experimental data indicate that factors (b) and (c) outweigh the effect of increased counter-ion density. The observation that thiocyanate is more effective than chloride is in accord with the relative affinity of serum albumin for these two anions. Scatchard, Scheinberg and Armstrong found[19] that isoelectric human serum albumin

(17) C. Tanford, *J. Am. Chem. Soc.*, **72**, 441 (1950).

(18) A. Katchalski and P. Spitnik, *J. Polymer Sci.*, **2**, 432 (1947).

(19) G. Scatchard, I. H. Scheinberg and S. H. Armstrong, Jr., *J. Am. Chem. Soc.*, **72**, 535, 540 (1950).

bound six chloride ions and sixteen thiocyanate ions when the free anion concentration was 0.05 *N*. On the other hand, no specific anion binding is observed with soluble synthetic polyelectrolytes.[16]

Thiocyanate shifts also the BSA–polymethacrylic acid precipitation curve to lower *p*H values, (Fig. 3) but the effect is much less pronounced than in PVA precipitation. This may be due to a competition of the polymeric acid for the cationic centers at which thiocyanate ions can be bound to albumin.

The anion binding characterizing serum albumin is no doubt responsible for the striking stability of the BSA complex with copolymer MAS containing a phenyl group for every two carboxyls. The precipitation range extends in this case well beyond the isoelectric point of the protein and the complex seems to be stable even in solution at higher *p*H, as indicated by the failure of all attempts to separate the components. It is significant, that copolymer MAS can be separated from γ-globulin,[20] which does not exhibit anion binding. This interpretation is supported by Ballou, Boyer, Luck and Lum reporting the relative affinity of serum albumin for acetate and phenylacetate.[21] Similar conclusions were reached by Klotz in comparing the albumin binding of succinate and the anions of various aromatic acids.[22]

The present studies of the interaction of serum albumin with synthetic polyelectrolytes were undertaken to evaluate their utility as reagents for protein fractionation. The removal of added reagents and the recovery of the protein in its native state are prerequisites of any fractionation process. Polymethacrylic acid and polyvinylamine could be precipitated quantitatively from albumin solutions by barium and sulfate ions, respectively, provided the polyelectrolyte was freed of its low molecular weight fraction. Bovine serum albumin recovered from its precipitate with polymethacrylic acid was found to be unchanged with respect to intrinsic viscosity, specific optical rotation and crystallizability. Similar tests for denaturation could not be carried out with albumin recovered from its polyvinylamine complex, because of the lack of available PVA. However, the albumin recovered in these experiments also appeared grossly unaltered. The optical activity of serum albumin has frequently been shown to increase sharply on denaturation[23–25] and it is therefore significant that even the albumin complex with maleic anhydride–styrene copolymer retained the specific optical activity characteristic of albumin in the native state, although the forces binding the protein to the polyelectrolyte were too strong to allow separation of the components. Preliminary studies with M. J. Hunter in this Laboratory have also shown that liver esterase retained its activity following coprecipitation with serum albumin and polymethacrylic acid.

In confirmation of these results may be mentioned prior studies on the interaction of enzymes with nucleic acids and protamines. Thus Warburg and Christian used nucleic acid to precipitate enolase and recovered it without loss of activity.[26] Krebs showed that the inactivation of phosphorylase by salmine or polylysine is reversed by precipitating the basic colloid with insulin.[27] Large organic anions can also be used under proper conditions as protein precipitants without resulting denaturation.[28]

The application of polyelectrolytes for protein fractionation was illustrated by the separation of albumin and oxyhemoglobin in their interisoelectric range, using polymethacrylic acid reagent. In the usual procedure the interaction of the proteins is avoided by carrying out the separation at a *p*H below the isoelectric point of albumin, although oxyhemoglobin is rather unstable in this region. The avoidance of extreme *p*H values may be of advantage in other separations of relatively labile proteins. For blood proteins, whose isoelectric points are usually acid to the *p*H of optimal stability, the use of basic resins would appear preferable.

The phenomenon of anion binding by serum albumin indicates that polyelectrolytes may even prove useful in albumin separations from other proteins of the same isoelectric point. This might be effected either by making the albumin more negative by addition of a strongly bound anion, or by use of such polyelectrolytes as copolymer MAS containing groups known to enhance anion binding.

(20) E. Alameri, private communication.

(21) G. A. Ballou, P. D. Boyer, J. M. Luck and F. G. Lum, *J. Clinical Investigation*, **23**, 454 (1944).

(22) I. M. Klotz, *J. Am. Chem. Soc.*, **68**, 2299 (1946).

(23) H. W. Aten, C. J. Dippel, K. J. Keuning and J. Van Doren, *J. Colloid Sci.*, **3**, 65 (1948).

(24) W. Pauli and W. Koelbl, *Koll. Bei.*, **41**, 417 (1935).

(25) R. B. Simpson, Doctoral thesis, Princeton, 1949.

(26) O. Warburg and W. Christian, *Biochem. Z.*, **310**, 384 (1942).

(27) E. G. Krebs, private communication.

(28) T. Astrup and A. Birch-Anderson, *Nature (London)*, **160**, 637 (1947).

THE INTERACTION OF OPTICALLY ISOMERIC DYES WITH BOVINE SERUM ALBUMIN

BY FRED KARUSH

The Children's Hospital of Philadelphia and The Department of Pediatrics, The University of Pennsylvania School of Medicine, Philadelphia, Penna.

Received August 30, 1951

The binding by bovine albumin of the optically isomeric forms of an anionic azo dye was investigated with a view to clarifying the extent and limitations of the configurational adaptability of the combining regions of the protein. The range of moles of dye bound per mole of protein (r) was 1 to 17. In addition to the equilibrium dialysis measurements of the binding, observations were made of the absorption spectra of the bound dyes and of the inhibitory effect of colorless structurally related anions. It was found that the same albumin sites bind the *d* and *l* forms of the dye although some selectivity is evident. This discrimination is manifested both in the divergence of the binding curves for small values of r and in the different spectral shifts of the bound dyes at $r = 0.5$. It is concluded that the dye is bound by an attractive three-point interaction probably over the whole range of r studied and that the combining regions of the protein possess a high degree of configurational adaptability. The sigmoid shape of the binding curve for the *d* dye has been interpreted as arising from a structural alteration of the protein. It is suggested that the initial binding of the dye causes the rupture of secondary intramolecular bonds leading to a partial and reversible opening-up and thereby making additional combining regions available. It appears that the *l* dye also effects such a transformation but the absence of the sigmoid shape here is attributed to the large initial slope of the binding curve. Arguments are presented to support the view that at least a portion of the entropy increase which is almost invariably observed in protein–anion combination arises from this structural alteration of the protein.

In a recent discussion[1] of the binding properties of serum albumins we suggested that these proteins possess a number of combining regions characterized by a high degree of configurational adaptability. This adaptability was associated with the ability of these regions to assume a large number of equilibrium configurations of approximately equal energy. The formation of a complex between an organic anion and the protein was ascribed to the stabilization through combination of that configuration which permitted maximum interaction of the protein groups with the appropriate groups of the anion. This kind of picture seems to be necessary to account for the large association constants observed and to explain the wide variations in structure which can be accommodated by the same protein sites.

A study of the binding of optically isomeric anionic dyes was undertaken in an effort to clarify this phenomenon and evaluate its significance under the least ambiguous conditions experimentally possible. The dye selected for this study was phenyl-(*p*-(*p*-dimethylaminobenzeneazo)-benzoylamino)-acetic acid.

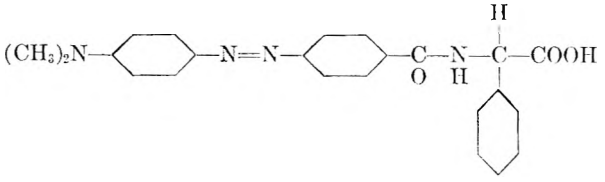

Its use was suggested by the experiments of Landsteiner and van der Scheer,[2] in which the dextro and levo forms of phenyl-(*p*-aminobenzoylamino)-acetic acid were diazotized and separately coupled to proteins. These hapten–proteins were used as immunizing antigens to produce antibodies directed against the stereoisomeric haptenic groups. By the appropriate precipitin tests it was demonstrated that the configurational difference between the isomers was reflected in the different specificities of the homologous antisera. This clearly established that the combination of the haptenic group with the homologous antibody was a three-point interaction involving the three substituents on the asymmetric carbon atom. Such a three-point interaction is a necessary condition for the purposes of our investigation. That this condition would be satisfied with the dye above in its interaction with albumin was rendered probable by the immunochemical study of Landsteiner and van der Scheer as well as by more general considerations based on the chemical nature of the groups present in the dye.

Experimental

The preparation of the optically active dyes, as well as the inactive dye, was carried out essentially by the procedure described by Ingersoll and Adams[3] with minor variations. The starting material was *dl*-phenylaminoacetic acid obtained from Eastman Kodak Company. The resolution of this racemic mixture into the levo and dextro forms was effected by fractional crystallization of the salts formed by these compounds with *d*- and *l*-camphorsulfonate, respectively, according to the method developed by Ingersoll.[4] The levo form of the amino acid was obtained first by addition of *d*-camphorsulfonic acid, recrystallization of the precipitated salt and hydrolysis with aqueous ammonia. To obtain the pure *d*-amino acid the isomeric mixture remaining in the first supernatant was treated with ammonia to recover the partially resolved amino acid. This was dissolved in water and inactive camphorsulfonic acid added to yield by fractional crystallization the *d*-amino acid *l*-sulfonate. Recrystallization and treatment with ammonium hydroxide resulted in the desired product.

The phenylaminoacetic acid was condensed with *p*-nitrobenzoyl chloride to form phenyl-(*p*-nitrobenzoylamino)-acetic acid. This was converted to phenyl-(*p*-aminobenzoylamino)-acetic acid by reduction with ferrous sulfate and ammonia and recrystallized from water. The melting points of the dextro and levo forms of this compound agreed with those given by the above authors. Ten-ml. solutions in 1 *N* HCl were prepared with 0.5000 g. of the *l*-isomer and 0.3794 of the *d*-isomer. These solutions gave observed rotations with a sodium light source of $-9.27°$ for the former and $+7.00°$ for the latter compound. These values agree to within 1% with the results reported by Ingersoll and Adams.[3] The *p*-amino compounds were diazotized and coupled to dimethylaniline in acetate buffer. The resulting dyes were recrystallized three times from 60% aqueous alcohol. The active dyes readily formed needle-shaped crystals whereas the racemic dye appeared amorphous. The melting points of

(1) F. Karush, *J. Am. Chem. Soc.*, **72**, 2705 (1950).

(2) K. Landsteiner and J. van der Scheer, *J. Exptl. Med.*, **48**, 315 (1928).

(3) A. W. Ingersoll and R. Adams, *J. Am. Chem. Soc.*, **44**, 2930 (1922).

(4) A. W. Ingersoll, *ibid.*, **47**, 1168 (1925).

the dyes derived from the active intermediates were both 189–190° in agreement with Ingersoll and Adams. The melting point of the inactive dye, not reported by these authors, was approximately 218°. Also these authors were unable to measure the optical rotations of the dyes. We shall designate the dye derived from *d*-phenyl-(*p*-aminobenzoylamino)-acetic acid as the *d*-I_p dye and that derived from the corresponding levo form as the *l*-I_p dye. The designation I_p dye will be used for the purpose of chemical identification without regard to stereoisomerism.

The measurement of the absorption spectra of the *d*-I_p dye and *l*-I_p dye as well as the *dl*-I_p dye showed that the shapes of the absorption curves were identical both in the visible and ultraviolet regions, from 220 to 600 mμ. However, the *d*- and *l*-I_p dyes gave an apparent molar extinction coefficient which was 1.7% lower than that for the *dl*-I_p dye. We attribute this difference to the presence of tightly bound water in the crystals of the active dyes. Apparently the drying conditions employed, six hours at 100° over P_2O_5 *in vacuo*, were inadequate to remove this water. Prolonged exposure of the dye to higher temperatures was deleterious. Confirmation of our interpretation was furnished by elementary analysis of the *dl*-I_p dye and the *l*-I_p dye. The former gave a value of 68.6% for carbon in agreement with the value of 68.6% calculated for $C_{23}H_{22}O_3N_4$ whereas the latter contained 67.6% carbon, 1.5% less than above.

For reasons which will become apparent below the binding of the structurally related dye *p*-(*p*-dimethylaminobenzeneazo)-benzoylaminoacetic acid was measured. This dye, designated H_p, was prepared by the diazotization of *p*-aminohippuric acid and the coupling of the diazonium salt to dimethylaniline in acetate buffer. It was recrystallized three times from methylcellosolve and melted at 227°.

The protein used in this study was crystallized bovine serum albumin supplied by Armour and Company. Stock solutions of the protein in water at a concentration of 1.50×10^{-4} *M* were made up periodically and stored in the frozen state. Correction was made for the moisture and ash content of the protein and a molecular weight of 69,000 was used.

The protein binding of the dyes was determined by the method of equilibrium dialysis as previously described.[1] Initial volumes of 10 ml. inside and outside the dialysis bag were used. The inside solution usually contained 3.00×10^{-5} *M* albumin in 0.0500 *M* phosphate buffer, *p*H 7.0 and the outside solution contained the dye in the same buffer. Duplicate measurements were always made and their agreement was usually within 1%. Equilibration was effected by overnight rocking in a constant temperature bath maintained at 25.0 ± 0.1°. Since the dye was adsorbed to the dialysis bag an appropriate correction for this effect was made. Over the range of free dye concentration encountered in this work, from 3×10^{-6} to 4×10^{-4} *M*, the average amount of adsorbed *l*-I_p dye was 8.4% of the total free dye without any consistent difference in the amounts adsorbed at low and high concentrations. For the *d*-I_p dye the adsorption is somewhat lower, 7.1%, and for the *dl*-I_p dye a value of 7.7% was used.

The absorption spectra of the dyes were determined with the model DU Beckman spectrophotometer. As noted above, the shapes of the absorption curves were identical. In Fig. 3 is shown part of the absorption curve of the dye in 0.05 *M* phosphate buffer, *p*H 7.0. The absorption maximum in the visible spectrum occurs at 470 mμ with a value of the molar extinction coefficient, ε, of 2.90×10^4. A minimum appears at 342 mμ with $\epsilon = 0.295 \times 10^4$ and another maximum at 278 mμ with $\epsilon = 1.19 \times 10^4$. The dye concentrations in the outside solutions of the dialysis tubes were determined by measurement of the optical density of appropriate dilutions of these solutions. Adherence to Beer's law was established for the range of concentrations encountered in the analytical procedure using a 1-cm. absorption cell. Measurement of the absorption at high concentrations, up to 74×10^{-5} *M*, with a reduced light path revealed no change in the shape of the absorption curve. From this constancy we infer that the dye is monomolecularly dispersed in the range of free dye concentration employed in this study.

Results and Discussion

The Binding Curves and Their Significance.—The experimental results for the albumin binding of the *d*-I_p dye, *l*-I_p dye and *dl*-I_p dye are represented in Fig. 1 in the form of a plot of r/c *vs.* r, where r is the average number of dye ions bound per protein molecule at free dye concentration c. Through the experimental points have been drawn the best smooth curves and these have been linearly extrapolated to the vertical axis. The intercepts have the values 40.4×10^4, 29.1×10^4 and 19.3×10^4 for the *l*-I_p dye, *dl*-I_p dye and *d*-I_p dye, respectively. The reasons for presenting the results in the form of an r/c *vs.* r plot will be clear from the following discussion.

On the assumption that there are n binding sites per protein molecule with intrinsic association constants K_i and, furthermore, that there is no interaction among the bound ions, the law of mass action leads to the following relation between r and c

$$r = \sum_i \frac{K_i c}{1 + K_i c} \quad (i = 1, 2, \ldots n) \qquad (1)$$

Scatchard[5] has pointed out that for the case of equal K_i's, equation (1) can be rearranged to give

$$r/c = nK - rK \qquad (2)$$

and that a plot of r/c against r will serve as a test of the validity of the above assumptions. Deviations from linearity can arise from interaction of the bound ions and from unequal association constants.

It is apparent from Fig. 1 that the dye binding does not adhere to the simple assumptions of equation (2). The binding curve of the *l*-I_p dye is characterized by a decreasing negative slope with increase in r. Its shape is very similar to that found for the binding of another anionic azo dye.[1] In the latter case the binding curve was quantitatively interpreted in terms of the existence of two groups of sites characterized by two considerably different association constants.

In contrast to the *l*-I_p dye, the binding of the *d*-I_p dye exhibits a strikingly different behavior. This contrast is of particular interest both because of its relation to the configurational difference of the optical isomers and because it appears to represent the first case of a sigmoid-shaped binding curve. From this shape it can be inferred that the binding of the first few *d*-I_p dye ions either results in the availability of additional combining regions or otherwise facilitates the binding of additional *d*-I_p dye ions.

An increase in available sites as a consequence of the combination of dye ions with the protein could be readily accounted for if such combination involved the opening-up or partial unfolding of the protein molecule. It has previously been suggested by Klotz[6] that the value of n may indeed vary with the number of bound ions. This suggestion was based on the wide variation in the values of n reported for several anions and on the absence of even a single case of a soluble albumin complex in which a plot of r *vs.* log c exhibits a limiting value of r.

Aside from the shape of the *d*-I_p dye curve, there are other less direct indications of a structural change of the protein associated with anion binding. Studies with inorganic anions, alkyl sulfates and an-

(5) G. Scatchard, *Ann. N. Y. Acad. Sci.*, **51**, 660 (1949).

(6) I. M. Klotz, *Cold Spr. Harb. Symposium Quant. Biol.*, **14**, 97 (1950).

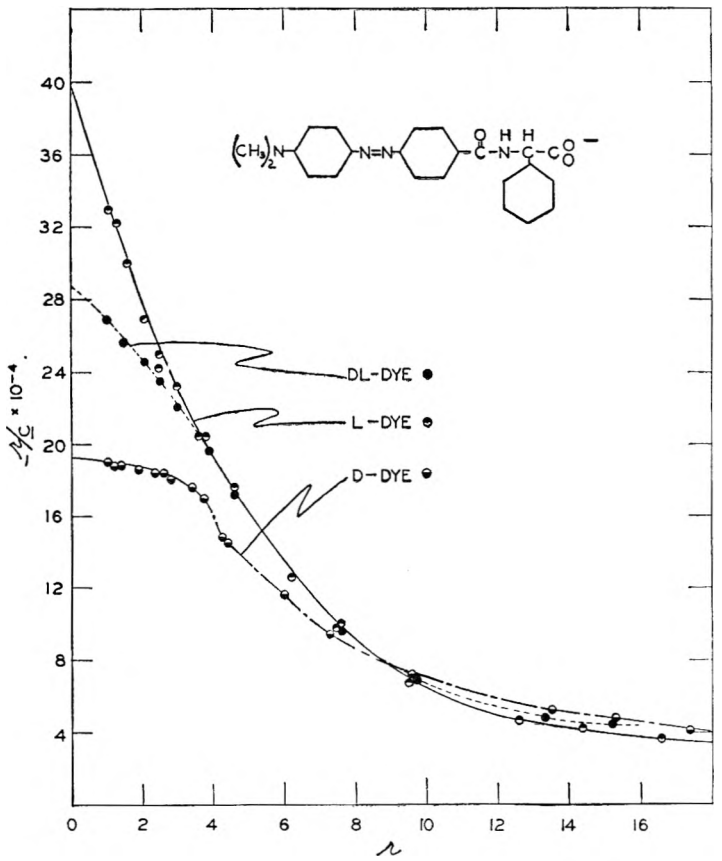

Fig. 1.—Binding curves of the isomeric I_p dyes: 3×10^{-5} M albumin in 0.05 M phosphate buffer, pH 7.0 at 25°.

ionic azo dyes have demonstrated that the association of these ions with albumin is characterized by a positive value of the entropy (ΔS^0) and that this is the dominant term in determining the value of ΔF^0.[6] The entropy change has been interpreted as due to the release of ion-bound water attendant upon the charge neutralization which occurs when the anion is bound to the cationic group. Quantitatively, however, this interpretation does not account for the observed wide variation of ΔS^0, from 8.7 e.u. for chloride ion to 24.0 e.u. for dodecyl sulfate. In particular, it is difficult to see why ΔS^0 for octyl sulfate (16.7 e.u.) should be about 7 e.u. less than that for dodecyl sulfate on the basis of charge neutralization. It appears likely to us, rather, that part of the entropy increase in anion binding is due to the reversible conversion of the protein to a less condensed state involving the rupture of intramolecular bonds. This picture is consistent with the structural interpretation of the d-I_p dye binding curve suggested above.

Another related argument in favor of this view is to be found in the efficacy of dodecyl sulfate as a denaturing agent. At a concentration as low as 0.01 M this detergent can cause extensive unfolding of horse serum albumin, as revealed by the increase in asymmetry of the protein.[7] At the same time about 110 molecules of detergent are bound per molecule of albumin. In much more dilute solutions the detergent is strongly bound to bovine albumin without denaturation, and a value of $n = 14$ has been deduced from the binding curve.[8] Dodecyl sulfate is the most strongly bound anion yet studied thermodynamically and exhibits the largest entropy change observed.[6] It is thus reasonable to infer that its strong binding in dilute solutions is causally related to its denaturing action at higher concentration. The picture involved here is that with increasing concentration of detergent there is an increasing availability of sites, and amount of detergent bound, associated with a continuous, or perhaps stepwise, unfolding of the molecule. If such a structural transformation does indeed occur when the number of anions bound is small, then we must conclude from the available evidence that, under these conditions, the structural changes are reversible and do not greatly alter the gross geometry of the protein. The latter is suggested by the ability of horse albumin to bind about 55 detergent molecules without measurable change of molecular shape.[7]

We have already noted the fact that the l-I_p dye curve does not exhibit a sigmoid shape and is very similar to the binding curve of an anionic azo dye previously described.[1] This does not however exclude the possibility that the same phenomenon found with the d-I_p dye may be involved in the binding of these other dyes. In fact, as is discussed below, the position of dl-I_p dye curve relative to the other curves furnishes cogent evidence for the view that the binding of the l-I_p dye is associated with similar structural changes in the protein. It is not unlikely that the failure to observe the sigmoid shape with these dyes is due to the large negative initial slope which would tend to obscure the effect under discussion.

The fact that optically isomeric dyes are bound differently by bovine albumin raises a number of interesting questions with important structural implications. The first problem to be considered is whether or not the same sites are involved in the binding of the d- and l-I_p dyes. A partial answer to this question is found in the comparison of the observed binding curve for the dl-I_p dye with a theoretical binding curve calculated from the d- and l-curves. This calculation is made on the assumption that there are no common binding sites for the d- and l-I_p dyes and that in their binding the isomeric dyes are also otherwise independent of each other. In Fig. 2 the broken line, representing the theoretical curve, falls above the observed curve and is considerably higher in the region of large values of r. It is in this region, of course, where the effect of competition of the isomers for common sites would be most evident. We may conclude, therefore, that the same combining regions of the albumin are involved in the binding of both isomers. That there is some selectivity in the reac-

(7) H. Neurath and F. W. Putnam, *J. Biol. Chem.*, **160**, 397 (1945).

(8) F. Karush and M. Sonenberg, *J. Am. Chem. Soc.*, **71**, 1369 (1949).

tion of these sites with the isomeric dyes, however, is evident from the divergence of the *d*- and *l*-curves for small *r*. This divergence indicates that there are a small number of sites, perhaps only one or two, which bind the *l*-isomer preferentially.

For values of *r* larger than 9 we note that the *d*- and *l*-curves are rather close and, furthermore, that the *dl*-curve falls between them. This means that those sites associated with large values of *r* bind both isomers and, in fact, almost equally well. We have suggested for the *d*-I_p dye that these additional sites become available as a consequence of structural alterations of the protein associated with the initial binding of the dye anions. It follows therefore, that the *l*-I_p dye must also similarly effect a structural change in the protein resulting in the appearance of additional combining regions.

The discrimination exercised by bovine albumin in its binding of the isomeric dyes reveals that the combination of dye and protein, for small values of *r*, involves a three-point interaction between them. This means that aside from the carboxyl group, which is undoubtedly linked to a cationic group, both the phenyl group attached to the α-carbon and the substituent group containing the azo linkage are involved in the interaction with the protein. These interactions contribute to the stabilization of the complex, that is, decrease the free energy of the reaction. For the azo substituent this effect is indicated by the relatively strong binding of both the *d*-I_p dye and *l*-I_p dye, a condition which is characteristic of anionic azo dyes. It is more directly demonstrated by the fact that, as can be estimated from Table II and Fig. 1, the *l*-I_p dye is bound about 100 times as strongly as phenylacetate. The important contribution of the α-phenyl group is unequivocally evident from the binding of the H_p dye, which differs from the I_p dye only by the absence of this group. The binding of the H_p dye was measured under the same conditions as that used for the I_p dyes. Its weaker tendency to complex is indicated by an extrapolated value of 3×10^4 for r/c as $r \rightarrow 0$. This value is less than one-sixth that for the *d*-I_p dye and one-thirteenth that for the *l*-I_p dye.

The divergence of the *d* and *l* binding curves at low *r* implies that the sites responsible for this differentiation possess a configurational asymmetry which is common to all or most of the albumin molecules. Thus, if in a large collection of such molecules the participating protein groups were randomly arranged with respect to the cationic centers, then the observed interaction between the dye and the protein should not be different for the isomeric forms. That there is a common pattern of asymmetry among the several sites on the same molecule is also suggested by the binding curves, particularly by the fact that the *dl*-curve consistently falls between the curves for the isomeric dyes. However the available information is inadequate to permit a definitive statement on this matter.

With respect to those combining regions which are involved in the binding at large values of *r*, the evidence suggests that here too there is an attractive three-point interaction between the dye and protein. This conclusion can be surmised from the fact that the isomers are not bound equally and that the r/c values even up to $r = 15$ are larger than the limiting value of 3×10^4 found for the H_p dye. The observation, as discussed below, that the spectral shift for the bound isomeric dyes at $r = 15$ are very close to those for $r = 5$ is also consistent with this view.

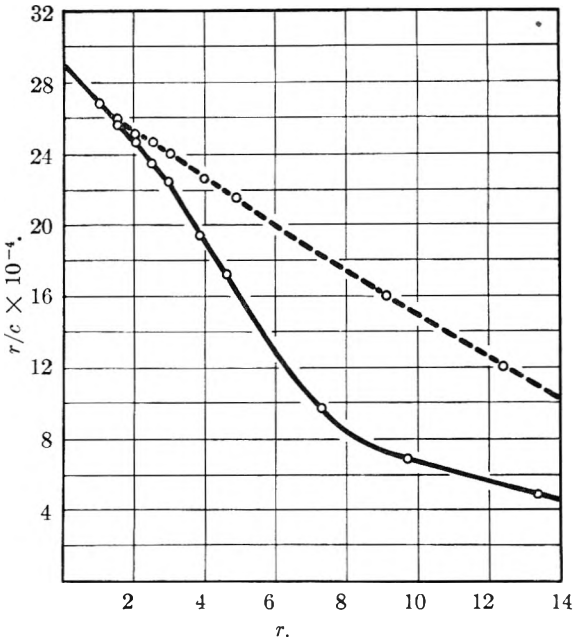

Fig. 2.—Comparison of the observed and calculated (upper curve) binding curves for the *dl*-I_p dye.

The differences observed in the binding of the isomers are a reflection of the limitations in the configurational adaptability of the combining regions. On the other hand the ability of these sites to form strong complexes with both isomers attests to the extreme structural accommodation of which they are capable. From the configurational point of view the geometrical relation between the optical isomers represents a difference which is much greater, for example, than that associated with position isomerism. In contrast to the sharp selectivity which enzymes and antibodies exhibit in their reactions with optical isomers, the adaptability of albumin assumes distinctive proportions.

In this connection we may point out an ambiguity in the conception of configurational adaptability which does not lend itself readily to experimental clarification. This arises from our inability to specify which groups of the protein are involved in formation of a complex. Thus a particular combining region may bind the optical isomers equally well but we are unable to decide from this fact whether the same individual protein groups, *e.g.*, a phenolic group of a tyrosine residue, are linked to the constituent groups of both dye isomers or whether only the same kinds of protein groups participate, different amino acid residues being involved for the two isomers.

The Absorption Spectra of the Bound Dyes.—The combination of both the *d*-I_p dye and *l*-I_p dye with bovine albumin results in a change in the absorption spectra of the dyes. This spectral

shift has served to provide additional evidence for the selective behavior of the protein. The absorption spectra of the dyes at several values of r were determined under the same conditions used in the binding experiments, *i.e.*, in 0.0500 M phosphate buffer, pH 7.0 with 3.00×10^{-5} M albumin. The temperature was maintained at 25° with a thermostated cell compartment. The total dye concentrations were approximately 2×10^{-5}, 20×10^{-5} and 74×10^{-5} M and optical density readings were made with path lengths of 10, 1 and 0.2 mm., respectively. The actual dye concentrations were

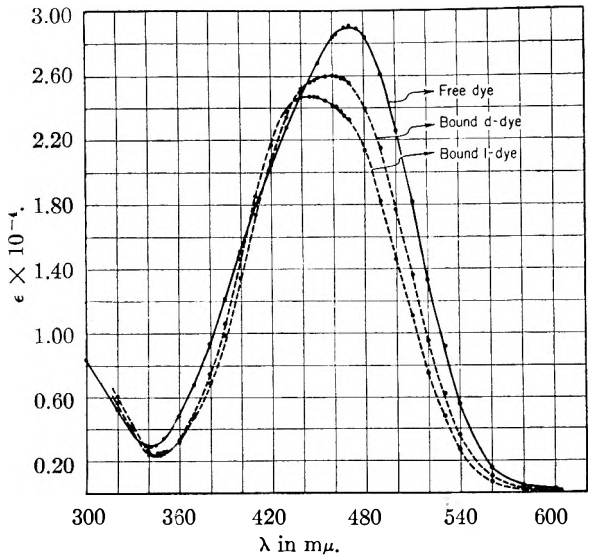

Fig. 3.—Absorption spectra for free and bound I_p dye at $r = 0.5$.

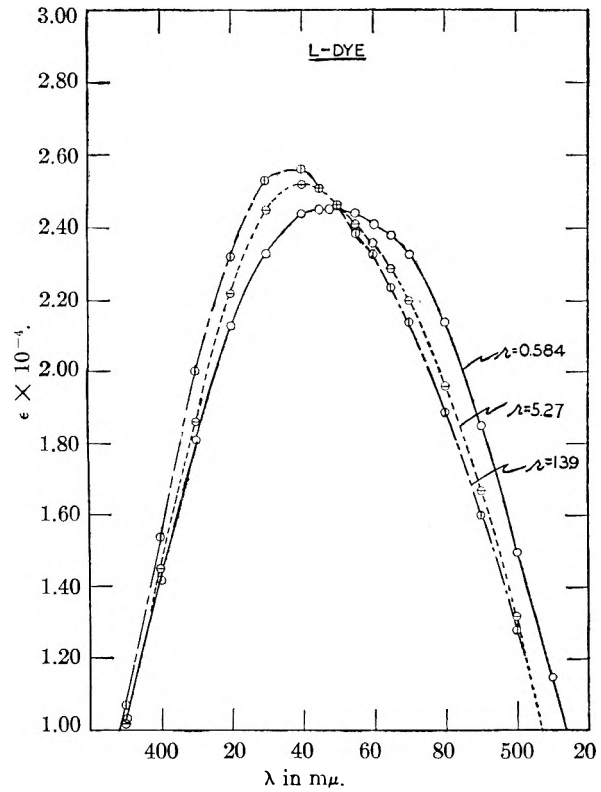

Fig. 4.—Absorption spectra of bound l-I_p dye at various values of r.

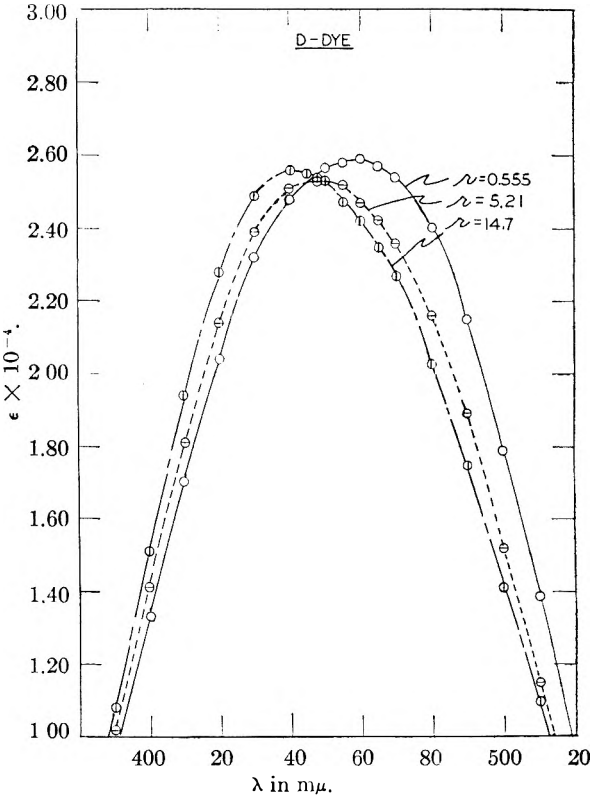

Fig. 5.—Absorption spectra of bound d-I_p dye at various values of r.

accurately determined and the distribution between the free and bound forms calculated from the binding curves. With this information the absorption spectra of the dyes were computed. These are shown in Figs. 3, 4 and 5. In Table I are presented the values of r at which the spectra were measured together with the corresponding molar extinction coefficients at the wave length of maximum absorption. These spectra represent, of course, an average of the contributions made by the dye ions bound at different sites.

TABLE I

ABSORPTION RESULTS FOR BOUND I_p-DYES AT VARIOUS VALUES OF r IN 0.0500 M PHOSPHATE BUFFER AND 3×10^{-5} M ALBUMIN; T = 25°

Isomer	Total dye concn. in m./l. × 10⁵	% of dye free	r	$\lambda_{max.}$ in mμ	ε at $\lambda_{max.}$ × 10⁴
l	1.922	8.9	0.584	448	2.45
d	1.964	15.2	0.555	460	2.58
l	19.22	17.7	5.27	440	2.52
d	19.64	20.4	5.21	448	2.53
l	73.8	43.5	13.9	440	2.56
d	74.2	40.7	14.7	440	2.56
Free dye	....	..	....	470	2.90

An examination of the absorption spectra reveals that for all values of r there is a substantial spectral shift. For $r = 0.5$, however, the bound d- and l-isomers exhibit a considerable difference in the extent to which the protein affects their absorption properties. This observation provides independent evidence that the sites involved in the binding at small r interact differently with the d and l forms of the dye. It agrees well with the binding results

TABLE II

EFFECT OF STRUCTURALLY RELATED ANIONS (0.001 *M*) ON BINDING OF *l*-1_p DYE BY BOVINE SERUM ALBUMIN, 0.05 *M* PHOSPHATE, *p*H 7.0, 25°. PROTEIN CONCN. = 3.00×10^{-5} *M*, INITIAL DYE CONCN. (OUTSIDE) = 9.50×10^{-5} *M*

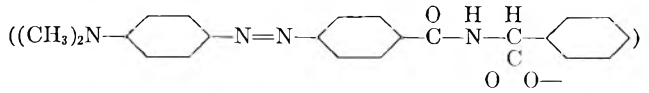

Anion	Structural formula	Free concn. $c \times 10^5$ *M*	r_I	r_I/r^a
None		0.996	2.45	
Acetate		1.016	2.43	0.97
p-Aminohippurate	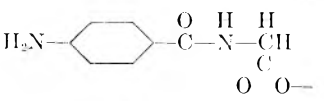	1.076	2.39	.916
Hippurate	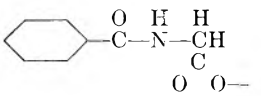	1.282	2.24	.762
l-Phenyl-(*p*-aminobenzoylamino)-acetate	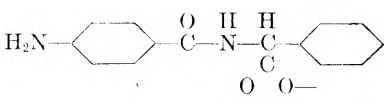	1.35	2.19	.720
Phenylacetate	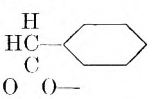	1.47	2.11	.655
dl-Phenyl-(*p*-nitrobenzoylamino)-acetate	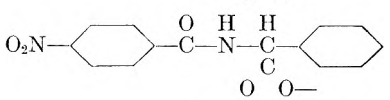	1.63	1.99	.577
dl-Phenyl-(benzoylamino)-acetate	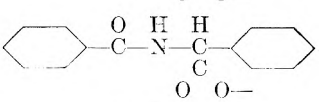	1.65	1.97	.567
d-Phenyl-(benzoylamino)-acetate[b]	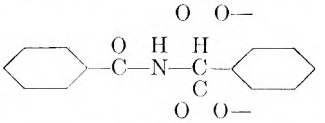	1.626	1.92	.560
l-Phenyl-(benzoylamino)-acetate[b]	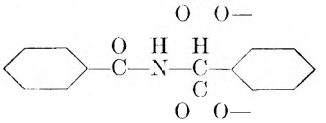	1.630	1.92	.557

[a] r_I is the average number of dye anions bound per protein molecule at free dye concn. (c) in presence of competitor; r is the corresponding quantity in absence of competitor at same (c). [b] Initial dye concn. was 9.29×10^{-5} *M*.

although a binding difference is not a necessary concomitant of a spectral difference.

The spectra for larger values of r show significant relations both with respect to the spectra for the same dye and with respect to the spectra for the isomers at the same r. For each isomer it is evident that the spectra for the two higher r values are distinctly altered relative to that observed for r = 0.5. This alteration is not in the direction toward the spectrum of the free dye, however. It appears, therefore, on the basis of the optical results that the interaction between dye and protein does not grow less intimate with increasing r. Furthermore the closeness of the spectra for r = 5 and r = 14 or 15 for each dye is quite striking in view of the different portions of the binding curves to which they refer. The indication here is that the bound dye molecules at the two r's are combined in much the same way. Indeed they may even possess more or less equal binding constants in spite of the fact that the curvature of the binding curves would suggest the contrary conclusion. The similarity of the spectra can, in fact, be further increased by taking into account that contribution to the curves for r = 5 which is due to the site or sites which give rise to the spectra observed with r = 0.5. This correction was made with the assumption that one site out of the five occupied produced these spectra. These corrected spectra are shown in Fig. 6.

A comparison of the spectra for the bound isomers reveals that at r = 5 and higher the differences observed with r = 0.5 are considerably reduced. In other words the protein sites exert about the same influence on the absorption properties of the bound dye regardless of its configuration. This behavior is consistent with the binding curves, since these demonstrate that the *d*- and *l*-isomers are bound almost equally well, and fits in with the view that these sites possess a high degree of adaptability. There is, however, some difference between the *d* and *l* binding curves at large r and it is perhaps more than a coincidence that there is a small but consistent difference between the spectra of the bound isomeric dyes as r changes from 5 to 15. This

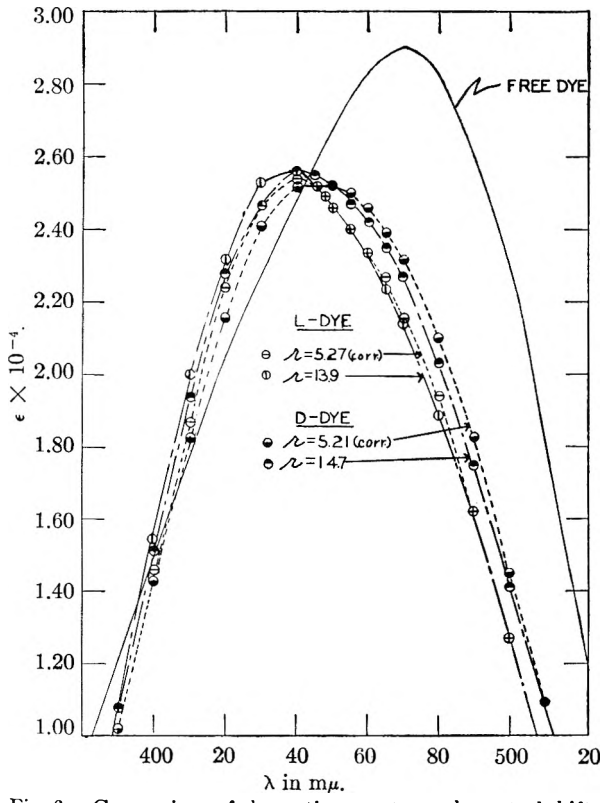

Fig. 6.—Comparison of absorption spectra and spectral shifts for the active I_p dyes at indicated values of r.

is apparent in Fig. 6 for wave lengths larger than 450 mμ. These binding and spectral differences suggest the possibility that the sites involved may have a common pattern of asymmetry which enables them to exercise a small but consistent selectivity with respect to the *d*- and *l*-isomers.

Inhibitory Effects of Structurally Related Anions.—In an effort to secure additional information about the adaptability of the combining regions a study was made of the inhibitory effect of colorless anions structurally similar to the dye on the binding of the latter. Among these inhibitors were included optical isomers whose configurational relation to the isomeric I_p-dyes was known by virtue of their synthesis from the same active intermediates used for the dye preparations. The inhibitor was always used in an initial concentration in the protein solution of 2.00×10^{-3} *M* to yield in the equilibrated system a concentration of 1.00×10^{-3} *M* uncorrected for the small amount bound to the protein.

The first experiments of this kind involved the use of the *d* and *l* forms of phenyl-(*p*-aminobenzoylamino)-acetate with both the *d*- and *l*-I_p dyes. The results here showed practically no difference in the behavior of the isomeric inhibitors. As with the I_p dyes the valid interpretation of these results is contingent upon the demonstration that there is or is not a three-point interaction of the inhibitor with the protein. For this purpose the inhibitory effect of the group of anions shown in Table II was evaluated. This was done with a view to ascertaining the contributions to complex formation made by the various groups attached to the α-carbon. It is evident that the α-phenyl and the benzoylamino groups enhance the binding of the inhibitor. From this we infer that phenyl-(benzoylamino)-acetate is bound, to at least some of the protein sites, through an attractive three-point interaction involving the carboxyl group in addition to the two aromatic groups. On the other hand, this conclusion cannot be stated unequivocally for the *p*-amino derivative described above although a similar three-point interaction is not excluded for this compound.

Since the suitability of phenyl-(benzoylamino)-acetate for our purpose was established the inhibitory effect of its *d* and *l* forms on the binding of the isomeric I_p dyes was determined. The results are presented in Fig. 7 in the form of a plot of r_I/r *vs.* c where r_I and r represent the number of dye anions bound per protein molecule with and without inhibitor, respectively, at the same free dye concentration c. This kind of plot readily reveals the extent to which the inhibitor has rendered the protein sites unavailable to the dye at various concentrations of the latter. This plot is also useful in that the limiting value of r_I/r can be used to estimate an average association constant for the inhibitor, as is easily shown with the use of equation (2). For the inhibitor under consideration this constant is of the order of 1×10^3. The range of r_I encompassed by the results of Fig. 7 is 0.8 to 3.

These inhibition experiments clearly demonstrate that both isomers are effective with respect to both dyes though not equally so in the case of the *l*-I_p dye. These observations substantiate the conclusion reached on the basis of the dye binding curves that the same sites can bind both forms of optically active anions. Thus the configurational adaptability of these sites again manifests itself.

Nevertheless a distinctive difference between the *d* and *l* dyes in the competitive effect of the isomeric inhibitors is apparent. With respect to the *l*-I_p dye

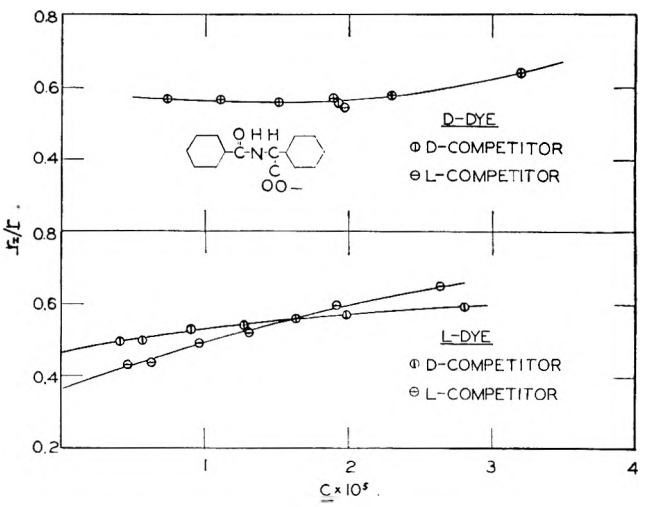

Fig. 7.—The inhibitory effect of the *d* and *l* forms of a structurally related colorless anion, phenyl-(benzoylamino)-acetate, on the dye binding. r_I and r are observed values at the indicated concentration of free dye (c) with and without inhibitor, respectively. Inhibitor concentration = 1.00×10^{-3} *M*.

the *l* competitor is more effective at low *c* than the *d* anion, up to r_I equal to about 2, but the reverse obtains at higher *c*. This behavior can be correlated with the dye binding curves since in these the *l* dye is also bound more strongly at small *r* than the *d* dye but this relation is reversed for larger *r*. This implies a selectivity by the sites binding at small *r* in favor of the *l* structure whereas those sites which become available as a consequence of dye bound to the other sites exhibit a preference for the *d* structure. With respect to the *d*-I_p dye the equal effectiveness of the competitive anions over the entire range studied is not readily accounted for in a manner which is consistent with our interpretation of the *l* dye results. Though the identity of the curves at small *c* can be explained, the difficulty is that a divergence of the inhibition curves analogous to that for the *l* dye would also be expected for the *d* dye. However an extension of these experiments involving a wider range of *c* (and r_I) is required before the significance of our current findings can be assessed. We may also note that the *d* dye inhibition curves exhibit a minimum, a feature which is undoubtedly related to the sigmoid shape of the binding curve of the *d*-I_p dye. A more detailed interpretation of this observation awaits further studies.

THE BINDING OF ORGANIC IONS BY PROTEINS. COMPARISON OF BOVINE AND HUMAN SERUM ALBUMINS[1]

BY IRVING M. KLOTZ, R. K. BURKHARD[2,3] AND JEAN M. URQUHART

Department of Chemistry, Northwestern University, Evanston, Illinois

Received August 30, 1951

Quantitative binding studies have been carried out to compare the interactions of human and bovine albumin, respectively, with each of four azobenzene anions. At *p*H 6.8 crystallized human albumin binds methyl orange with an affinity about the same as that of bovine albumin. At *p*H 9, however, the former protein is markedly superior to the latter. Variations in the affinity of human albumin for anions have been observed with samples obtained by different methods of preparation. All the albumins examined showed increased binding as the *p*H was increased from 6.8 to 9.2. Buffer effects cannot be responsible for this increase. Since electrostatic factors should produce the opposite effect, it is concluded that access to new or auxiliary binding sites becomes possible at the higher *p*H. Spectra of anion–albumin complexes clearly reveal a reversible change in the configuration of human albumin molecules as the *p*H is raised. New types of binding site become available. A comparison of these spectra with those of the anions in simple solvents gives some indication of the side chains involved in these interactions.

Introduction

Among the many proteins which have been examined for their ability to bind anions, serum albumin is exceptional in its possession of a very strong affinity for these small ions. The general impression obtainable in a comparison of binding data from various sources is that bovine albumin and human albumin possess closely comparable affinities toward anions. Thus the extent of binding of sulfonamides by human serum[4] differs only slightly from that observed with crystallized bovine albumin.[5] Similarly the intrinsic constant for complex formation with chloride ion is 44 for human albumin[6] compared to 27 for bovine albumin.[7]

In the present paper the affinities of albumin from bovine and human sources are compared under essentially identical conditions. In addition the optical properties of anion–protein complexes under comparable conditions are described. Although binding abilities of different albumins have been found to be similar in magnitude at some *p*H's, substantial differences appear for certain anions at other *p*H's. Furthermore, absorption spectra of the complexes indicate marked differences in the *nature* of the interaction of organic ions with albumins of different origin. These variations in behavior make available a method of obtaining some insight into the configurational differences between these proteins.

Experimental

Absorption Spectra.—The absorption of light by the organic anions examined was measured with the Beckman spectrophotometer, model DU, at approximately 25°. One-centimeter cells were used and extinction coefficients, ϵ, were calculated from the equation

$$\epsilon = \frac{1}{cd} \log_{10} (I_0/I)$$

where I_0 is the intensity of the light emerging from the solvent, I the intensity of the light emerging from the solution, c the molar concentration of the solute and d the thickness of the absorption cell in centimeters.

Dialysis Experiments.—The extent of binding of each of the compounds studied was measured by the differential dialysis technique described previously.[8] Experiments were carried out with mechanical shaking for an eighteen-hour period in an ice-bath at 0.0 ± 0.1°. The protein concentration was between 0.1 and 0.2%.

Reagents.—Of the azo compounds used, two were obtained commercially and two synthesized. The methyl orange was a reagent grade sample obtained from Merck and Co., Inc. Methyl red was a commercial sample but was purified by extraction with toluene, followed by recrystallization first from toluene and then from a pyridine–water mixture until a constant melting point was reached. The observed melting point of a sample dried at 110° was 178–

(1) This investigation was supported by grants from the Office of Naval Research (Project No. NR121-054) and the Rockefeller Foundation. Presented at the Twenty-fifth National Colloid Symposium, under the auspices of the Divisions of Colloid and of Physical and Inorganic Chemistry of the American Chemical Society at Ithaca, New York, June 18–20, 1951.

(2) Junior Fellow of the National Institutes of Health, 1948–1950.

(3) Department of Chemistry, Kansas State College, Manhattan, Kansas.

(4) B. D. Davis, *J. Clin. Invest.*, **22**, 753 (1943).

(5) I. M. Klotz and F. M. Walker, *J. Am. Chem. Soc.*, **70**, 943 (1948).

(6) G. Scatchard, I. H. Scheinberg and S. H. Armstrong, Jr., *ibid.*, **72**, 535 (1950).

(7) I. M. Klotz and J. M. Urquhart, THIS JOURNAL, **53**, 100 (1949).

(8) I. M. Klotz, F. M. Walker and R. B. Pivan, *J. Am. Chem. Soc.*, **68**, 1486 (1946).

179° (uncorrected); the value reported in the literature[9] is 181–182°.

4′-Dimethylaminoazobenzene-3-carboxylic acid and 4′-dimethylaminoazobenzene-4-carboxylic acid ("meta methyl red" and "para methyl red," respectively) were prepared according to the procedure used in the synthesis of methyl red,[9] except that *m*- and *p*-aminobenzoic acids, respectively, were used as starting reagents in the coupling with dimethylaniline. The crude products were extracted and recrystallized in the same manner as was methyl red. The samples were dried at 110°. Pertinent analytical data are listed below.

	Melting point, °C. Obsd.	Liter.[a]	Nitrogen, % Found	Calcd. for $C_{15}H_{15}O_2N_3$
Meta methyl red	199–200	210	15.88	15.61
Para methyl red	271–273	...	15.85	15.61

[a] A. Thiele and O. Peter, *Z. anorg. u. allgem. Chem.*, **173**, 169(1928).

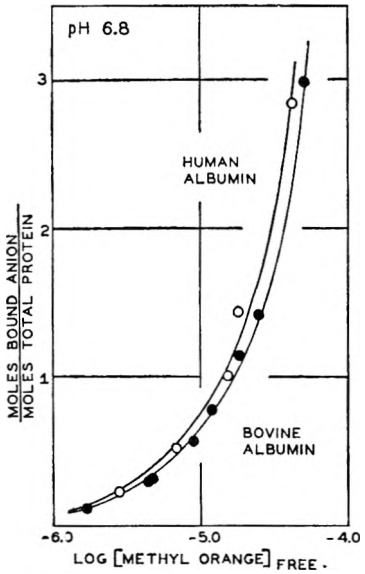

Fig. 1.—Relative affinities for methyl orange (I) of human albumin (lot 179-5x), ○, and of bovine albumin, ●, at *p*H 6.8. Experiments carried out at 0° in phosphate buffer.

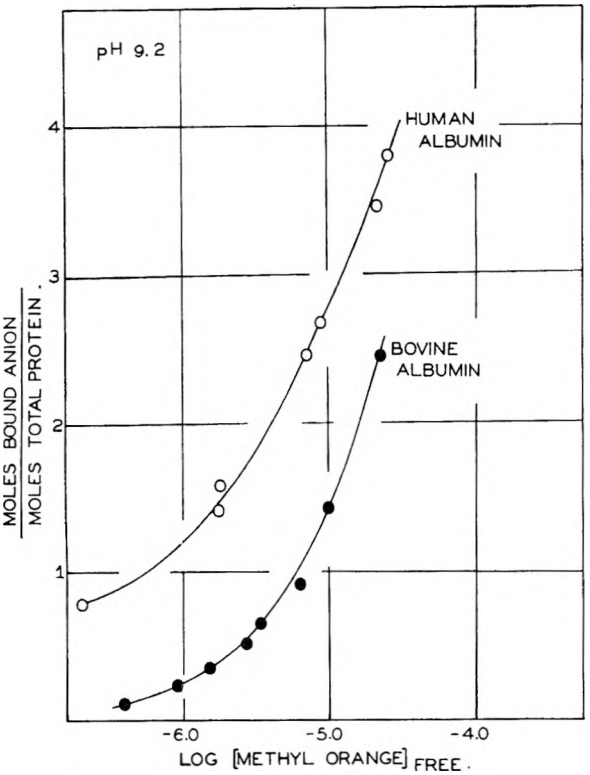

Fig. 2.—Relative affinities for methyl orange (I) of human albumin (lot 179-5x), ○, and of bovine albumin, ●, at *p*H 9.2. Experiments carried out at 0° in borate buffer.

(9) "Organic Syntheses," Coll. Vol. I, John Wiley and Sons, Inc. New York, N. Y., 1941, pp. 374–377.

As a further check on the purity of the dyes prepared in this manner, meta methyl red was subjected to chromatographic analysis.[10] The column contained 60–200 mesh alumina that had been washed first with hydrochloric acid and then with water and finally activated. The dye was placed on the column and then eluted with each of three solvents: dilute hydrochloric acid, dilute potassium hydroxide and basic potassium sulfanilate. In each case only a single component was eluted.

Crystallized bovine serum albumin was purchased from Armour and Co. The β-lactoglobulin came from Dr. T. L. McMeekin of the Eastern Regional Research Laboratory. Three samples of human albumin were studied. The crystallized preparations labelled lot 179-5x and Decanol 10, respectively, were gifts of Professors E. J. Cohn and W. L. Hughes, Jr., of the Harvard Medical School.[11] The former sample was crystallized with the aid of chloroform, the latter with the aid of decanol. A third sample of human albumin was obtained from Drs. P. H. Bell and R. O. Roblin, Jr., of the American Cyanamid Co. It had been prepared from contaminated plasma by standard blood-bank procedures and according to Dr. Bell had a purity of 97–99% as estimated by electrophoretic methods. We are deeply indebted to each of these sources for their coöperation and generosity.

Buffers were prepared from reagent grade phosphate and tetraborate salts. The phosphate buffers were 0.10 *M*, the borate 0.050 *M*. The organic solvents, ethyl alcohol, *n*-amyl alcohol, N-*n*-butylacetamide and N,N-di-*n*-butylacetamide, were commercial samples of high purity.

Results and Discussion

Comparison of Binding Energies.—The relative affinities of human and bovine albumin for a specific organic ion vary markedly with *p*H. Figures 1 and 2, for example, illustrate some of the data obtained with methyl orange (I) at *p*H's 6.8 and 9.2. The degree of binding is represented in graphs of

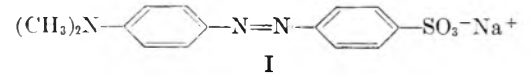

I

the average number of bound ions per mole of protein, *r*, *versus* the logarithm of the concentration of free anion, (A). A comparison of these two graphs shows that both proteins bind methyl orange with almost equal affinities at *p*H 6.8, but that human albumin is markedly superior to bovine at *p*H 9.2. From curves[12,13] published previously in connection with other problems, it is apparent that the relative standing of the two proteins at *p*H 7.6 parallels that at *p*H 9.2.

A comparison of binding affinities can also be expressed in terms of the energy differences involved. Free energies of binding can be evaluated from these data by methods described in detail previously.[7,8] If the binding sites all have the same intrinsic constant, *k*, then

$$\lim_{(A)\to 0}\left[\frac{r}{(A)}\right] = nk \qquad (1)$$

(10) We are indebted to Dr. David Zaukelies for carrying out these experiments.

(11) E. J. Cohn, W. L. Hughes, Jr., and J. H. Weare, *J. Am. Chem. Soc.*, **69**, 1753 (1947).

(12) I. M. Klotz, H. Triwush and F. M. Walker, *ibid.*, **70**, 2935 (1948).

(13) I. M. Klotz and J. M. Urquhart, *ibid.*, **71**, 1597 (1949).

where n is the total number of available sites for the anion on one protein molecule. As this equation implies, one may plot $r/(A)$ *versus* (A) and obtain nk from the extrapolated intercept at (A) = 0.

For a single set of binding sites, furthermore

$$nk = k_1 \qquad (2)$$

where k_1 represents the equilibrium constant for the first anion complexed with the protein. Thus k_1 may also be calculated from an extrapolation of the experimental binding data and hence ΔF_1° may be computed from the general thermodynamic relation

$$\Delta F_1^\circ = -RT \ln k_1 \qquad (3)$$

Values of ΔF_1° for complexes of methyl orange with each albumin at *p*H 6.8 and at *p*H 9.2 are listed in Table I. Again it is apparent that the energy of binding of methyl orange by human serum albumin is very close to that for bovine albumin at *p*H 6.8 but substantially greater at *p*H 9.2.

TABLE I

COMPARISON OF BINDING AFFINITIES AT 0° FOR BOVINE AND HUMAN SERUM ALBUMIN

		Bovine Serum Albumin		Human Serum Albumin	
Anion	*p*H	$\left[\frac{r}{(A)}\right]_{A=0} \times 10^{-5}$	ΔF_1°, cal. mole^{-1}	$\left[\frac{r}{(A)}\right]_{A=0} \times 10^{-5}$	ΔF_1°, cal. mole^{-1}
Methyl orange	6.83	0.72	−6080	0.82	−6140
	9.18	3.2	−6900	14	−7660
Methyl red	6.83	1.20	−6350	1.57	−6500
	9.18	2.4	−6730	3.3	−6900
Meta methyl red	6.83	3.9	−6980	4.2	−7040
	9.18	3.9	−6980	5.5	−7190
Para methyl red	6.83	0.82	−6150	1.6	−6510
	9.18	2.6	−6790	4.6	−7100

Very similar results have been obtained with a related series of azo compounds, methyl red (II) and its meta and para isomers, (III) and (IV), respectively.

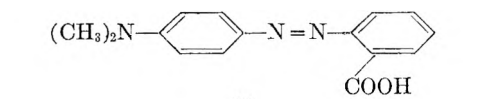

II

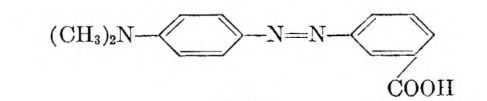

III

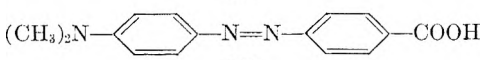

IV

As the data in Figs. 3–8 and in Table I indicate, human albumin in all cases forms stronger complexes with these anions than does bovine albumin. With the ortho and meta compounds, however, the differences between the two species of protein are small.

Effect of *p*H.—It seems pertinent to point out that for each compound the extent of binding increases as the *p*H is raised from 6.8 to 9.2, no matter which of the two proteins is used. Such behavior is indeed surprising, for one would expect a decrease in affinity of the protein for anions as the negative charge on the protein is increased. That this electrostatic factor is operative has been demonstrated in the acid region in experiments with methyl orange[13] as well as with chloride ion.[6]

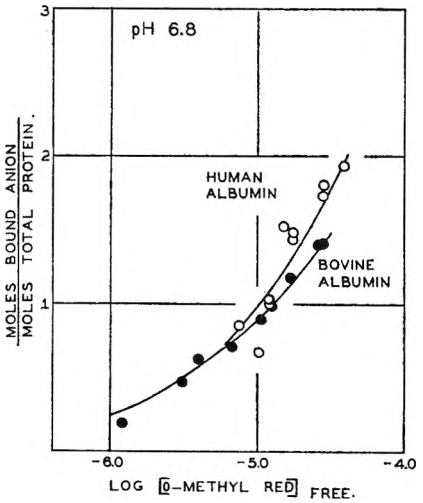

Fig. 3.—Relative affinities for methyl red (II) of human albumin (lot 179-5x), ○, and of bovine albumin, ●, at *p*H 6.8; temperature, 0°; phosphate buffer.

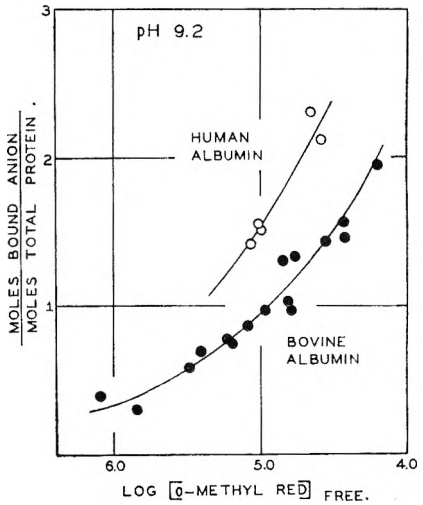

Fig. 4.—Relative affinities for methyl red (II) of human albumin (lot 179-5x), ○, and of bovine albumin, ●, at *p*H 9.2; temperature, 0°; borate buffer.

At first glance one might attribute the unexpected behavior of albumin in the region of *p*H 6.8 to 9.2 to the influence of the buffer. Marked variations in binding because of the differences in buffer present have been observed in previous experiments.[7] In the present situation, however, a few rapid calculations indicate that buffer effects are not the cause of the differences in binding.

If the buffer is competing with the dye anion,[7,12] then the limiting value of $r/(A)$ as (A) approaches zero is given not by equation (1) but by the expression

$$\lim_{(A)\longrightarrow 0}\left[\frac{r}{(A)}\right] = \frac{nk}{1+k_B(B)} \qquad (4)$$

where k_B represents the binding constant for the buffer and (B) its concentration. For phosphate

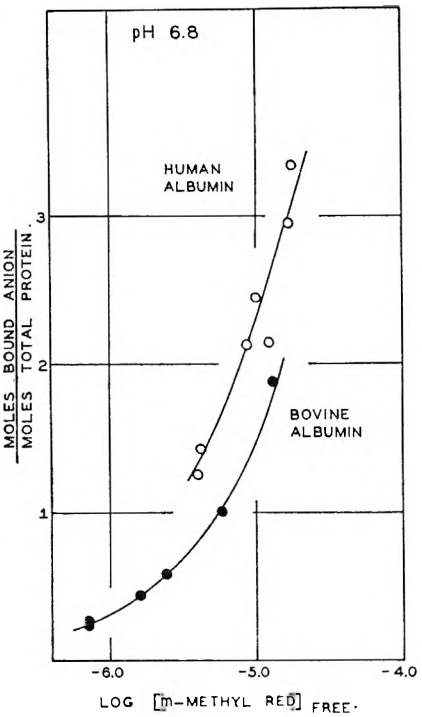

Fig. 5.—Relative affinities for meta methyl red (III) of human albumin (lot 179-5x), ○, and of bovine albumin, ●, at *p*H 6.8; temperature, 0°; phosphate buffer.

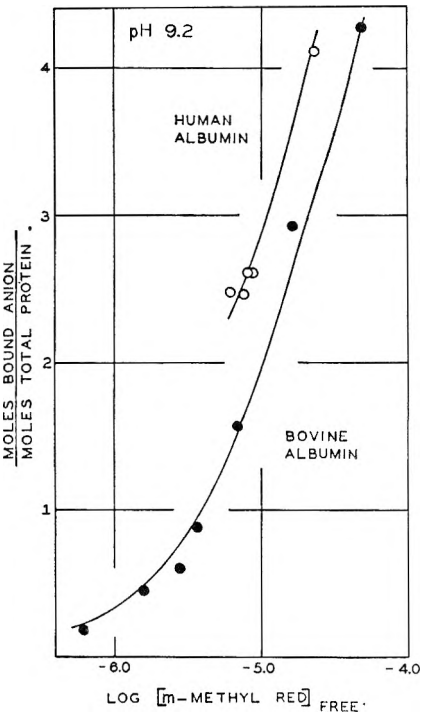

Fig. 6.—Relative affinities for meta methyl red (III) of human albumin (lot 179-5x), ○, and of bovine albumin, ●, at *p*H 9.2; temperature, 0°; borate buffer.

buffers k_B has been shown[14] to be[7] approximately

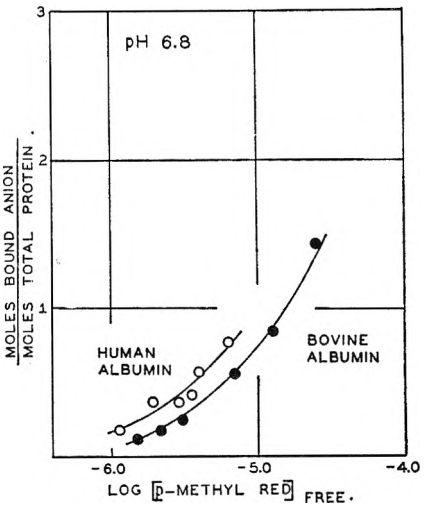

Fig. 7.—Relative affinities for para methyl red (IV) of human albumin (lot 179-5x), ○, and of bovine albumin, ●, at *p*H 6.8; temperature, 0°; phosphate buffer.

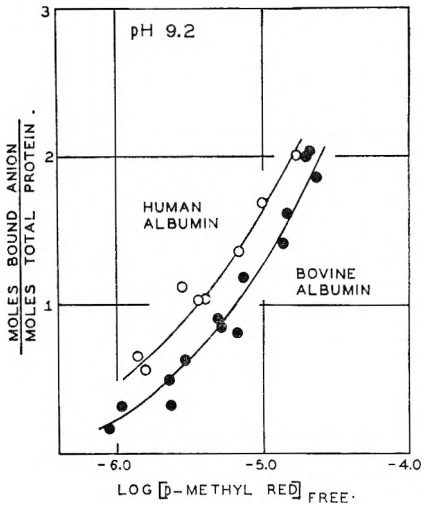

Fig. 8.—Relative affinities for para methyl red (IV) of human albumin (lot 179-5x), ○, and of bovine albumin, ●, at *p*H 9.2; temperature, 0°; borate buffer.

15. In a solution of approximately 0.1 *M* concentration, the effect of the buffer would be to reduce the extrapolated value of $r/(A)$ by a factor of about 2.5. One might expect, therefore, a difference in binding energy between the experiments at *p*H 6.8 and at *p*H 9.2 of RT ln (2.5) or 500 calories due to the difference in buffer effects. The electrostatic effect, however, would tend to counteract this buffer influence. For each additional negative charge placed on the protein the energy of binding should decrease by about 40 calories/mole.[8] Reference to Tanford's[15] titration curve indicates that albumin at *p*H 9.2 carries about 20 more negative charges than at *p*H 6.8. The electrostatic effect, therefore, should amount to approximately 800 calories, a value more than sufficient to counterbalance the buffer influence.

Thus from electrostatic considerations, even when suitably corrected for buffer effects, one would expect a decrease in extent of binding of anions by al-

(14) In this calculation, the assumption was made that glycine ions exert no competitive effect in binding by albumin. This assumption seems to be warranted, for on the basis of it a k of 27 was calculated for the binding constant of chloride ion with bovine serum albumin, whereas direct measurements by Scatchard, Scheinberg and Armstrong[6] led to a value of 44 for the binding constant of chloride with human albumin. In view of the slightly greater affinity of the latter protein for anions, a k of 44 is essentially in agreement with that of 27 for the former protein.

(15) C. Tanford, *J. Am. Chem. Soc.*, **72**, 441 (1950).

bumin as the *p*H is increased. An increase is actually observed. Evidently, then, some additional factor must be operative. An uncovering of new sites on the protein molecule as the *p*H is raised in the neighborhood of 7–9 could account for the increased binding. On first thought such an interpretation does not seem very attractive since increases in *p*H in this region tend to decrease the number of cationic loci on the protein. As will be shown shortly, however, the optical properties of certain albumin–anion complexes point clearly to a modification in the nature of the binding sites as the *p*H is raised from 7 to 9.

Comparison of Binding Ability of Human Albumins.—Since three samples of human albumin were available at various times during the course of this study, it seemed desirable to compare their binding abilities. Figure 9 summarizes the results obtained with the two crystallized samples at *p*H 6.8. The sample (Decanol 10) crystallized with the aid of decanol shows a slightly, but significantly, lower affinity for methyl red. The drop may be due to the presence of small amounts of residual decanol in the protein, but no attempt was made to remove this alcohol and examine the residual protein.

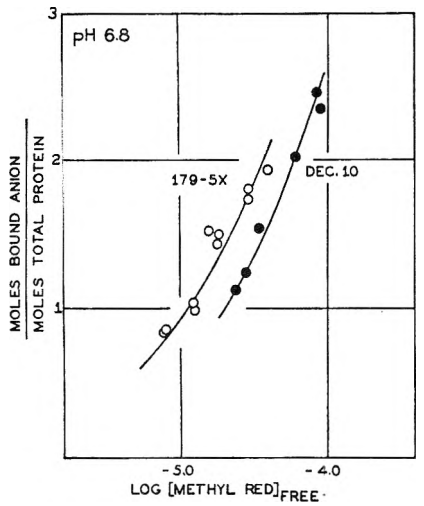

Fig. 9.—Comparison of affinities for methyl red (II) of crystallized human albumins at *p*H 6.8; lot 179-5x, ○; lot Decanol 10, ●; temperature, 0°; phosphate buffer.

A comparison was also made of the binding ability of the Cyanamid sample with the crystallized material 179–5x, and the results, with methyl orange, are illustrated in Fig. 10. Once again the latter sample showed the greater affinity. The Cyanamid material in the solid state had a slight brownish tinge probably due to combined bilirubin in the protein, and it is possible that the bilirubin combines with sites which otherwise would be available to the reference anion, methyl orange. Martin[16] has demonstrated that interactions of albumin with bilirubin are strong.

Among the three samples of human albumin examined, that crystallized with the aid of chloroform, 179-5x, shows the greatest affinity for anions, at least for the azo-dye type used in these studies. It should be pointed out, therefore, that if either of

(16) N. H. Martin, *J. Am. Chem. Soc.*, **71**, 1230 (1949).

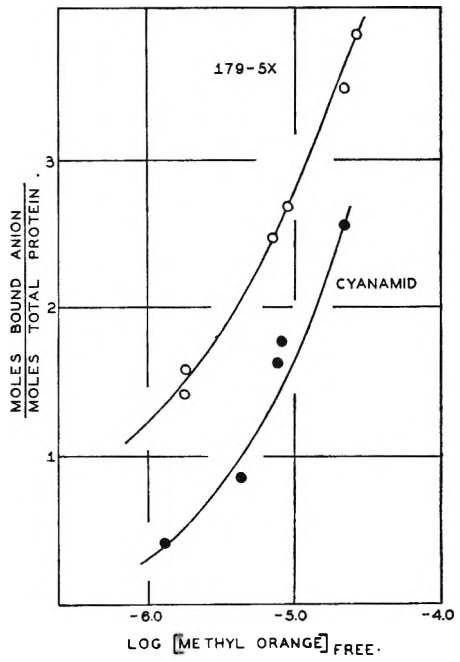

Fig. 10.—Comparison of affinities for methyl orange (I) of samples of human albumin at *p*H 9.2; lot 179-5x, ○; Cyanamid, ●; temperature, 0°; borate buffer.

the other two human albumins had been used in the studies summarized in Table I, the distinction from bovine albumin would have been definitely smaller. Thus it is obviously desirable to specify the details of the method of crystallization of the protein as well as its species origin.

In the light of these differences among samples of human albumin purified in different ways it is striking to recall in passing that the relatively drastic treatment with O-methylisourea to prepare guanidinated albumin[17] does not affect binding ability.[13]

Spectra of Complexes with Proteins.—The effect of *p*H on the optical characteristics of methyl orange complexes with albumin is illustrated by the graphs in Fig. 11. The presence of bovine albumin lowers the absorption maximum and shifts its peak by roughly the same amount at each of the four *p*H's 5.7, 6.9, 7.6 and 9.2. On the other hand, with human albumin the spectrum of the anion-protein complex at *p*H 5.7 differs markedly from that at *p*H 9.2. The absorption at *p*H 5.7 is similar to that of methyl orange in any one of several organic solvents, as will be shown shortly. On the other hand, the spectrum at *p*H 9 is reminiscent of that of the acid form of this indicator. Thus there seems to be a pronounced difference in the *nature* of the protein–anion interaction at the two *p*H's, in addition to the small differences in the extent of binding cited earlier.

The three available preparations of native human albumin have been examined in this connection. All behaved comparably in their over-all effects, though they showed differences in the degree of exaltation of the spectrum of methyl orange, or in the *p*H at which the transition in their optical effects

(17) W. L. Hughes, Jr., H. A. Saroff and A. L. Carney, *ibid.*, **71**, 2476 (1949).

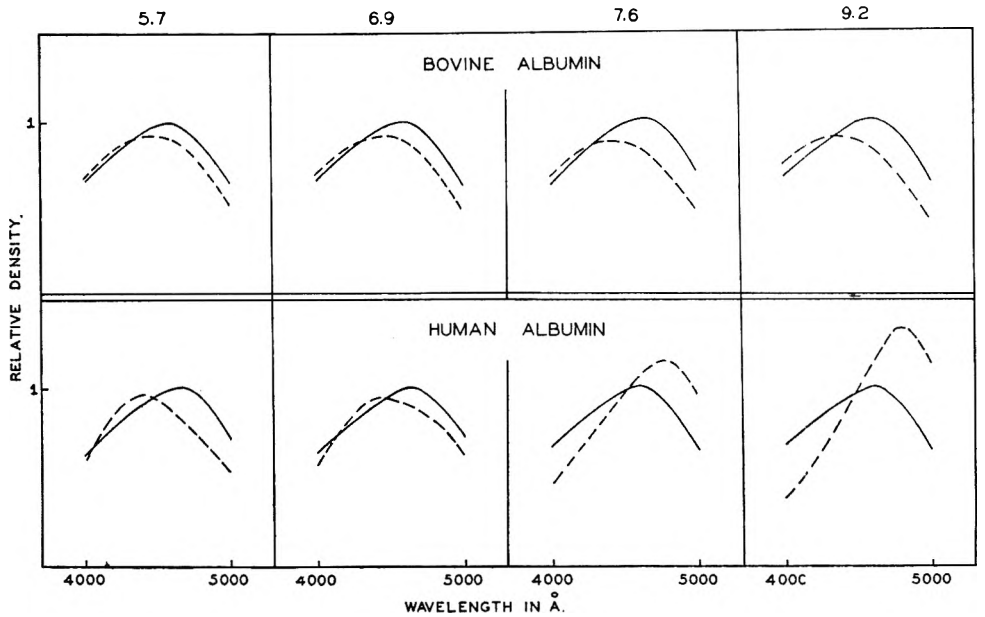

Fig. 11.—Comparison of effects of bovine albumin and of human albumin (lot 179-5x) on spectra of methyl orange at each of a series of *p*H's (listed at top of figure). In each case the optical density of methyl orange in buffer alone was assigned a relative value of 1 at the maximum to facilitate comparison of protein effects.

occurred. Thus the Cyanamid sample produced a larger effect at *p*H 7.6 than did the crystallized albumin lot 179-5x (Fig. 12). Between the two crystallized albumins, the outstanding difference in behavior occurred at *p*H 6.9 (Fig. 13), where the sample 179-5x produced a shift in the spectrum of methyl orange toward lower wave lengths, whereas the decanol sample caused an exaltation in absorption and a shift toward higher wave lengths. At this same *p*H, 6.9, the Cyanamid albumin hardly affected the spectrum of methyl orange.

As is apparent from Fig. 11, lot 179-5x at *p*H 7.6 produces the same type of optical shift with methyl orange as does lot Decanol 10 at *p*H 6.9. Similarly, the effect of the Cyanamid sample increases with increasing *p*H. The essential difference between these albumins lies, then, in the *p*H at which the transition in type of spectrum occurs. The albumin crystallized with the aid of decanol produces the anomalous spectrum at a *p*H lower than that required by the other two types of protein. In all cases, however, some modification occurs in the protein which makes new sites available for interaction with organic anions.

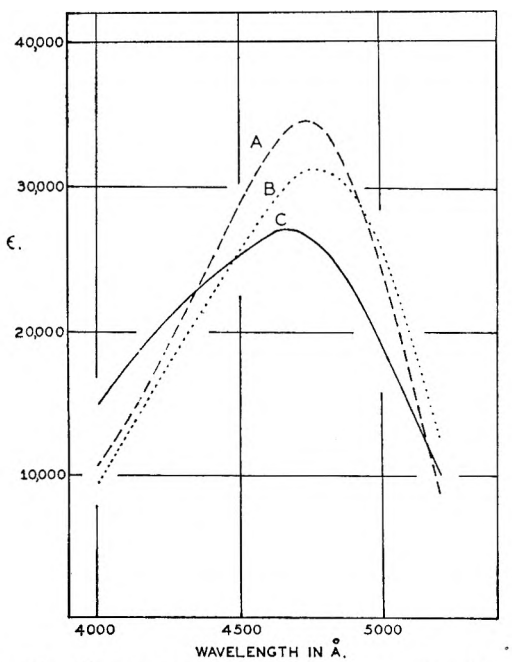

Fig. 12.—Comparison of effects of two samples of human albumin on spectrum of methyl orange in phosphate buffer at *p*H 7.6; Cyanamid, A; lot 179-5x, B; methyl orange alone, C; each protein at 0.2% concentration.

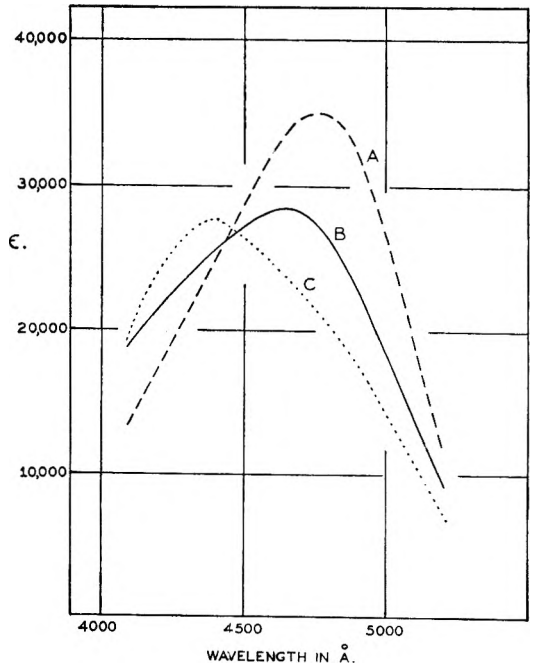

Fig. 13.—Comparison of effects of crystallized human albumins on spectrum of methyl orange in phosphate buffer at *p*H 6.9; lot 179-5x (0.2%), C; lot Decanol 10 (0.15%), A; methyl orange alone, B.

The reversibility of the spectroscopic effect has been demonstrated with both types of crystallized human albumin. In each case the procedure used was the following. A sample of the albumin was dissolved in a phosphate buffer at a *p*H of 7.7 and divided into two portions. The effect on the spectrum of methyl orange was measured with one portion. To the second portion a known quantity of standard HCl was added to bring the *p*H to 6.9. Again the effect on the optical absorption of methyl orange was measured and the results obtained were compared with those observed with a sample of albumin dissolved originally in a phosphate buffer at *p*H 6.9. No significant difference was observed in the spectra of the two albumin samples at *p*H 6.9. Some typical readings have been assembled in Table II. The reproducibility is not quite as good as can usually be obtained, but normally no correction has to be made for the dilution effect of the added acid. There is no doubt that the effect of *p*H can be reversed, and, furthermore, that each protein returns to the state it characteristically exhibits at *p*H 6.9. That is, despite the large difference in behavior of each type of crystallized human albumin at *p*H 6.9, an increase in *p*H and subsequent return to *p*H 6.9 does not bring both proteins to a common pattern. Each protein undergoes a change in configuration during the alteration in *p*H, yet is capable of returning to its characteristic structure if the acidity is also returned to its original value.

TABLE II

DEMONSTRATION OF REVERSIBILITY OF OPTICAL INTERACTION OF HUMAN SERUM ALBUMIN WITH METHYL ORANGE

	Molecular extinction coefficient			
	Lot 179-5x		Lot Decanol 10	
Wave length, mμ	Sample kept at *p*H 6.88	Sample originally at *p*H 7.68, adjusted to *p*H 6.88	Sample kept at *p*H 6.88	Sample originally at *p*H 7.70, adjusted to *p*H 6.88
410	19,200	19,000	13,300	13,500
420	....	....	16,950	....
430	26,400	26,000	20,700	20,800
440	27,700	27,200	24,500	....
450	26,300	26,400	28,200	27,800
460	24,600	24,800	32,000	31,200
470	....	....	34,400	33,200
480	20,300	20,600	34,800	33,200
490	....	....	32,400	30,800
500	14,200	14,500	27,300	....

In the experiments described so far, suitable buffers were used to maintain the desired *p*H. Since some concern might be raised by the presence of buffer ions, a spectrum was also obtained for methyl orange in the presence of human albumin (Cyanamid) at *p*H 9.1, with the *p*H being adjusted merely by the addition of dilute sodium hydroxide. The absorption curve obtained did not differ significantly from that shown in Fig. 11 for human albumin at *p*H 9 in borate buffer. Thus it is apparent that the anomalous spectrum produced by human albumin at *p*H's above about 7 is not dependent on the presence of specific buffer ions.

Among the other proteins which have been examined for their affinity toward methyl orange anions, only β-lactoglobulin shows an appreciable degree of binding.[13] The spectrum of the complex with this protein has also been examined at several *p*H's and the results are illustrated in Fig. 14. Evidently, β-lactoglobulin behaves in a manner analogous to bovine rather than to human albumin.

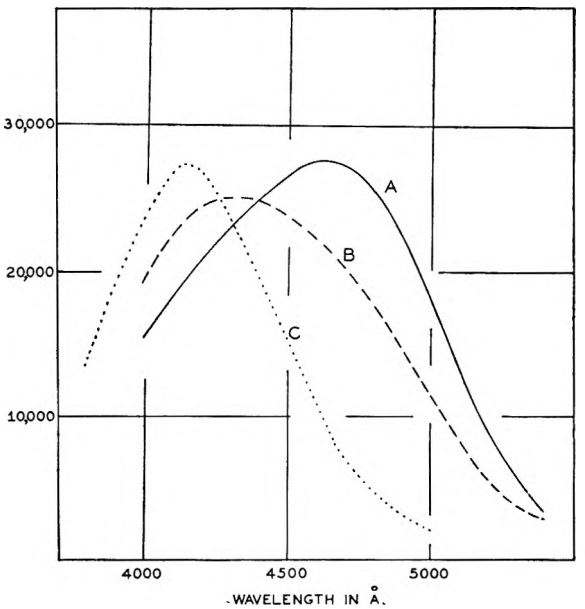

Fig. 14.—Effect of β-lactoglobulin on spectrum of methyl orange: methyl orange alone, A; with protein (*ca.* 0.1%) at *p*H 6.8, B; with protein (0.8%) at *p*H 9.2, C.

Significance of the Spectra.—The large differences in the spectra of methyl orange complexes with bovine and human albumin, respectively, suggest the existence of major differences in the molecular environment of the small anion when it is combined with the protein. A clue to the nature of these differences can be obtained from an examination of the spectra of methyl orange in a variety of simpler solvents.

Methyl orange, normally in the form of a sodium salt, is not readily soluble in organic solvents particularly of the aliphatic type. Sufficient solute has been dissolved, nevertheless, to obtain spectra in each of two alcohols and two amides. The absorption curves in ethyl alcohol, *n*-amyl alcohol, N-*n*-butylacetamide and N,N-di-*n*-butylacetamide, respectively, are illustrated in Fig. 15. It is of interest to note that each of these curves has a peak in the neighborhood of 420 mμ, *i.e.*, at shorter wave lengths than aqueous solutions of methyl orange. The spectra in these organic solvents thus are similar to those of aqueous methyl orange complexes with bovine albumin at all *p*H's, or with human albumin at *p*H's below about 7.

The alcohols and amides used have no special structural feature in common. All, of course, have aliphatic chains of some length, but that of ethyl alcohol is quite short. If we keep in mind that the methyl orange was used in the form of its sodium salt, it seems most likely that the common feature among the four organic solvents is that they are incapable of ionizing the methyl orange salt to an appreciable extent. Thus the solute molecules probably occur as ion pairs, $Na^+ \ldots {}^-O_3SR$ in these

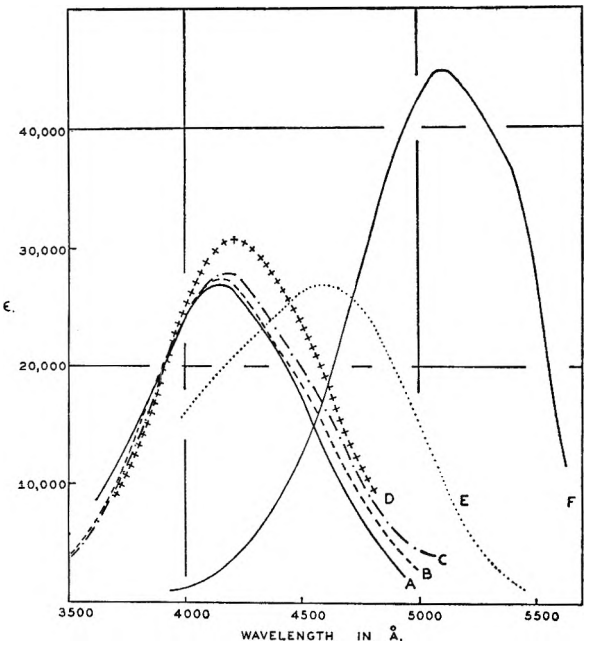

Fig. 15.—Absorption spectra of methyl orange in various solvents: N,N-di-*n*-butylacetamide, A; *n*-amyl alcohol, B; ethyl alcohol, C; N-*n*-butylacetamide, D; water, *p*H 7.7, E; 0.01 *M* HCl in water, *p*H 1.98, F.

solvents. Evidently then a spectrum with a peak in the neighborhood of 420 mμ is a reflection of the short-range electrostatic interaction between a cation, such as Na^+, and the azosulfonate ion, RSO_3^-, for in aqueous solution the freely ionized RSO_3^- shows a maximum slightly above 460 mμ.

On the basis of optical properties, therefore, one should interpret the spectral shifts of methyl orange complexes with bovine albumin as strongly electrostatic in origin, for the shift is in the same direction as is obtained in the non-aqueous solvents described. Thus the spectra agree with chemical evidence[13] in ascribing binding largely to interactions, represented by $P\text{–}NH_3^+ \ldots {}^-O_3SR$, between cationic loci of the protein molecule and the small anion.

On the other hand, the anomalous spectra produced by human albumin at the higher *p*H's mentioned are distinctly different from those obtained in the non-aqueous solvents. The peaks with human albumin are shifted toward higher wave lengths, as compared with non-complexed methyl orange. In this respect they remind one of the spectrum of methyl orange in an acidified aqueous solution (Fig. 15).

In acid solutions, the methyl orange anion picks up a hydrogen ion either at the dimethylamino or azo nitrogen.[18] It is tempting, therefore, to attribute the spectrum of methyl orange in a human albumin complex to contributory bonding with a hydrogen donor group from the protein, leading to a linkage which may be represented as $P\text{—}OH\cdots N\langle^{R_3}_{R_2}{}^{R_1}$. The nitrogen atom of the anion again could be either one of the two in the azo linkage or that of the dimethylamino group. The hydroxyl group from the protein could originate in side chains of serine, threonine or tyrosine residues. Of these three residues, the phenolic hydroxyl of tyrosine is likely to act most as a hydrogen donor since resonance with the benzene ring would favor a structure of the form 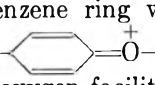 , in which the positively-charged oxygen facilitates hydrogen bonding.

This picture of the specific interaction of methyl orange with human albumin raises a number of immediate questions. On the basis of the information presented it is not possible to decide whether electrostatic bonding between the SO_3^- substituent of the azo molecule and a cationic locus on the protein also contributes to the stability of the complex. The presence of electrostatic bonding could be detected if the source of the anomalous spectral effect could be removed. In this connection experiments with iodinated albumin suggest themselves, for if the tyrosine residues are converted to diiodotyrosine groups, the acidity of the phenolic hydroxyl is increased so greatly that few such groups could act as hydrogen donors at *p*H 9. Furthermore, it would be desirable to establish clearly which of the nitrogens on the methyl orange molecule is involved in the interaction which leads to the acid-type spectrum with human albumin. Such an identification might be made from a study of interactions with related small anions in which substituents have been introduced which could block the approach either to the azo nitrogens or to the dimethylamino nitrogen. Finally, the major problem still remains of explaining the differences between human and bovine albumin in configurational terms.

Studies with suitably modified albumins and with related azobenzene anions, designed to answer these questions, have been carried out and will be described in a subsequent paper.

Conclusions

The experiments which have been described here lead to three important conclusions. It is apparent, first, that human albumin, irrespective of method of preparation, undergoes a marked change in configuration in the *p*H region near 7. This transformation is a reversible one, at least insofar as the optical criteria used here are concerned. Its origin, however, is not clear. It seems possible that the increase in charge on the protein with increasing *p*H may increase the electrostatic repulsion between regions within the molecule so that an alteration in folding is brought about. On the other hand, it is also conceivable that the change in shape is due to the breaking of specific inter-chain bonds involving histidine or α-amino side chains whose *pK*'s fall in this critical region near 7. Whatever the cause of the change in intramolecular bonding, it is clear that as a result new side chains are made available for interactions with specific anions.

It is also evident from the data presented that increases in binding ability of both human and bovine albumin as the *p*H is increased cannot be ascribed to buffer effects. Since the increases are contrary to what one should expect from electro-

(18) I. M. Kolthoff, "Acid-Base Indicators," The Macmillan Co., New York, N. Y., 1937, p. 228.

static considerations, it seems likely again that the reason lies in the availability of additional or auxiliary sites which augment the ability of the protein molecule to remove specific anions from the aqueous phase.

Finally, one may conclude that although bovine and human albumin exhibit binding abilities of the same order of magnitude, significant differences nevertheless do appear in the extent of interaction with specific anions. These differences may be greater at one *p*H than at another. They must be a reflection of differences in configuration around the cationic loci on the protein molecule. That such differences in configuration affect interactions with anions of different structure has been emphasized by Karush[19] in his analysis of binding constants in competitive interactions with albumin. Examination of the spectra of specific anion-protein complexes allows one to obtain a more revealing clue as to the molecular character of these configurational differences.

(19) F. Karush, *J. Am. Chem. Soc.*, **72**, 2714 (1950).

PROTEIN-PROTEIN INTERACTIONS

BY J. L. ONCLEY, E. ELLENBOGEN, DAVID GITLIN AND F. R. N. GURD

The University Laboratory of Physical Chemistry Related to Medicine and Public Health, Harvard University, the Department of Pediatrics, Harvard Medical School, and the Children's Medical Center, Boston, Massachusetts

Received August 30, 1951

The interaction between human β-liproprotein and γ-globulin has been studied by measuring the solubilities of the separate components and of their mixtures. The β-lipoprotein has a minimum solubility at *p*H 5.4, while γ-globulin has a solubility minimum at about *p*H 7.3. Their mixtures are much less soluble between these *p*H values, with a broad minimum near *p*H 6.7. The solubility is highly dependent upon ionic strength. This interaction has little specificity, and is weak, easily reversed by high ionic strength or change of *p*H. The interaction between insulin "monomers" has been studied by measuring the sedimentation constant as a function of the concentration of insulin, and of the *p*H and ionic strength of the medium. A reaction between 3 molecules of insulin of molecular weight 12,000 (I) to give a "trimer" of molecular weight 36,000 (I_3) is postulated. This interaction appears to have a high degree of specificity, but is relatively weak, again easily reversed by changes of *p*H and ionic strength. The interaction between human serum albumin and its homologous equine antibody is similar to other antibody–antigen reactions already described. It has been studied by redissolving specific precipitates in a known excess of serum albumin, and making quantitative measurements of the total protein, and free albumin (from ultracentrifuge studies). The interaction is found to be highly specific, and difficult or impossible to reverse by changes of *p*H or ionic strength.

There are no interactions more interesting and important than those between proteins. The extent of reaction, as judged by the extent and specificity of the forces involved, varies over wide limits. We would like to discuss several of these protein–protein interactions which have been studied in our laboratory recently.

Interaction of β-Lipoprotein and γ-Globulin (with F. R. N. Gurd[1])

It has long been recognized that proteins or other polyelectrolytes will form interaction complexes when the two reactants bear net charges of opposite sign. As early as 1894, Kossel[2] pointed out that just as the nucleic acids precipitated proteins from acid solution, so the strongly basic protamines precipitated proteins from alkaline solution. This striking property of protamines to form precipitates with proteins was the basis for Kossel's well-known theory that the protamines were the fundamental units of proteins to which other materials could be added in a variety of ways. Following Kossel, the precipitation of proteins by protamines and histones received considerable attention.[3–11]

Nearly all the investigations of this kind have involved the interaction of either the highly basic protamines or the strongly acidic nucleic acids with proteins which were isoelectric at less extreme *p*H values. It was pointed out in 1938 by Green,[12] however, that similar interactions between proteins of opposite net charge were to be expected during fractionation of serum proteins. Attention was drawn to the fact that solubility curves obtained under conditions of such complex formation would show a broad region of low solubility with a minimum lying somewhere between the minima of the pure components. Since the shape of such a solubility curve need not be abnormal, it would be easy to draw the erroneous conclusion that a definite single protein component had been precipitated. Even if specific analysis were made for one component in such a mixture and its minimum solubility determined, the apparent isoelectric point so obtained would still be in error.

In the present investigation, the involvement of β-lipoprotein in some such interaction with other plasma protein components was first suggested by the discrepancy between the apparent solubility minimum near *p*H 6.0 found for the β-lipoprotein

(1) F. R. N. Gurd, Ph.D. Dissertation, Harvard University, 1949.

(2) A. Kossel, *Deutsche Med. Wochenschr.*, 147 (1894); *Z. physiol. Chem.*, **22**, 156 (1896).

(3) L. Bauman, *Am. J. Med. Sci.*, **198**, 475 (1939).

(4) F. Bischoff, *Am. J. Physiol.*, **117**, 182 (1936).

(5) F. P. Gay and T. B. Robertson, *J. Exp. Med.*, **16**, 479 (1912).

(6) H. C. Hagedorn, B. N. Jensen, N. B. Krarup and I. Wodstrup, *Acta Med. Scand., Suppl.*, **78**, 678 (1936).

(7) M. A. Lissitzin and N. S. Alexandrowskaja, *Z. physiol. Chem.*, **221**, 156 (1933).

(8) T. B. Robertson, *J. Biol. Chem.*, **13**, 499 (1912).

(9) C. L. A. Schmidt, *ibid.*, **25**, 63 (1916).

(10) D. A. Scott and A. M. Fisher, *J. Pharm. Exp. Therap.*, **58**, 78, 93 (1936).

(11) B. Ugglas, *Biochem. Z.*, **61**, 469 (1914).

(12) A. A. Green, *J. Am. Chem. Soc.*, **60**, 1108 (1938).

in crude plasma fractions[13] and the minimum about *p*H 5.4 found for the purified β-lipoprotein.[15] The hypothesis that interaction of the β-lipoprotein with the plasma proteins of highest isoelectric point, the γ-globulins,[14] was responsible for this apparent shift of isolectric point led to the study of their interactions.

Human serum β-lipoprotein was prepared as previously described.[15]

Human serum γ-globulin consisted of Fraction II-1,2 (Lot L-413) prepared by method 9.[14]

Solubility determinations were carried out in the manner previously described.[15] The separate determination of β-lipoprotein and γ-globulin in mixtures was made in either of the following two ways. In the first method determinations were made for N and total cholesterol, from which the quantities of the two proteins were calculated on the assumption that the β-lipoprotein contained 31% cholesterol and 4.2% N[15] and the γ-globulins no cholesterol and 16% N.[14] In the second method the optical density of the mixture after diluting with *p*H 8.0 phosphate buffer of ionic strength 0.1 was determined in the Beckman quartz spectrophotometer at 320 mμ as well as at 279 mμ. The E (1%, 1 cm.) for the γ-globulin was found to be 0.091 and 14.5, respectively, while corresponding values for the β-lipoprotein varied with the age of the preparation and required daily measurements on the stock solution of known concentration.[16] Values for E (1%, 1 cm.) of the β-lipoprotein varied from 7.6 to 14.5 at 279 mμ and 1.7 to 3.6 at 320 mμ. The separate concentrations of β-lipoprotein and γ-globulin were calculated by solving the two simultaneous equations obtained from the measurements at these two wave lengths. Agreement between the two methods of calculation was always within 5% and usually within 2%.

Other determinations were made as described previously.[15]

The effect of the presence of γ-globulins on the solubility of β-lipoprotein as a function of *p*H and of ionic strength (Γ/2) is shown in Fig. 1. Over the entire range of conditions employed the γ-globulins were completely soluble in the absence of β-lipoprotein. The dotted curves showing the solubility of the β-lipoprotein in the presence of the γ-globulins are in sharp contrast with the behavior of the purified β-lipoprotein[15] as given by the solid lines. The data show both a striking decrease in the solubility of the β-lipoprotein in the mixtures over the *p*H range between the isoelectric regions of the β-lipoprotein and γ-globulin, and a marked effect of ionic strength on the interaction.

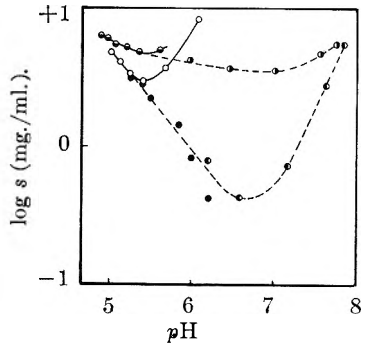

Fig. 1.—Interaction of β-lipoprotein with γ-globulin. Solubility of β-lipoprotein as a function of *p*H in aqueous solutions at 0°. γ-Globulin absent: ○, 0.01 ionic strength acetate buffer; ◒, 0.02 ionic strength acetate buffer. γ-Globulin present: ●, 0.01 ionic strength acetate buffer; ◐, 0.01 ionic strength phosphate buffer; ◑, 0.02 ionic strength phosphate buffer.

In Table I are shown the mole ratios of γ-globulin to β-lipoprotein in the precipitates formed at varying *p*H values and at ionic strengths of 0.01 and 0.02. For the calculation of the mole ratios, molecular weights of 1,300,000 and 156,000 were taken for the β-lipoprotein and γ-globulin.[17] The ratios showed a steady trend towards larger values as the *p*H or the concentration of γ-globulin is increased. From these results it appears that the complexes of β-lipoprotein with γ-globulin form a continuous series of solid solutions, with very likely a number of different species of complex present in any particular precipitate.

TABLE I

COMPOSITION OF PRECIPITATES FORMED BY INTERACTIONS OF γ-GLOBULIN (MOL. WT. 156,000) AND β-LIPOPROTEIN (MOL. WT. 1,300,000) IN AQUEOUS PHOSPHATE BUFFERS AT 0°

		Protein in system, μm./l.		Protein in ppt., μm./l.		Molecular ratio, γ/β	
*p*H	Γ/2	γ-Glob.	β-lipoprot.	γ-Glob.	β-lipoprot.	In system	In ppt.
6.20	0.01	52.0	4.4	9.0	3.8	11.8	2.4
6.62	0.01	52.0	4.4	13.5	4.1	11.8	3.3
7.17	0.01	52.0	4.4	15.8	3.8	11.8	4.1
7.62	0.01	52.0	4.4	9.1	2.2	11.8	4.1
5.98	0.02	59.0	4.5	1.6	1.3	13.1	1.2
6.46	0.02	59.0	4.5	3.7	1.7	13.1	2.2
7.00	0.02	59.0	4.5	4.5	1.8	13.1	2.6
7.53	0.02	59.0	4.5	2.9	0.8	13.1	3.4
6.79	0.01	5.7	4.5	tr.	tr.	1.3	...
6.80	0.01	11.4	4.5	4.3	1.8	2.6	2.3
6.84	0.01	23.0	4.5	7.6	3.4	5.2	2.2
6.84	0.01	41.0	4.5	14.1	4.2	9.2	3.4
6.84	0.01	58.0	4.5	17.1	4.3	13.0	4.0

These results may be interpreted qualitatively in terms of the interaction of positively charged γ-globulins with negatively charged β-lipoprotein, leading to the formation of salt-like complexes. As would be expected, the effect disappeared at *p*H values where both proteins bore on the average the same sign of net charge. The strong influence of neutral salts on the precipitation of the complexes is undoubtedly due to the combination of an effect on the equilibrium in solution between simple molecules and complexes, where the shielding action of the ions would be expected to promote dissociation, and the fundamentally similar effect of increased solubility of the complexes. In systems of this sort the relative magnitude of the two effects may be expected to involve the dipole moments of the separate species and of the interaction complexes.

Since the solubility of proteins is generally least when they bear a low net charge, presumably the most insoluble of the interaction complexes would be those in which the net negative charge of the β-lipoprotein would be most nearly neutralized by the γ-globulin molecules bearing net positive charges. Accordingly it should be expected that the higher the *p*H the higher the ratio of γ-globulins to β-lipoprotein in the precipitated complexes, an expectation borne out strikingly by the results in Table I. The higher ratios of γ-globulins to β-lipoprotein in the precipitated complexes with increasing ratios in the total system shows the interaction to involve more than simple electrostatic interactions, however. The great inhomogeneity of the γ-globulins, especially with respect to isoelectric point,[18] makes impossible a quantitative treatment of the results. At any given *p*H the γ-globulins exhibit a great variety of charged forms, and, at least over the *p*H range of about 6 to 8, γ-globulin molecules bearing both net positive charges and net negative charges would be present, and may be expected to enter into interactions with each other as well as with the β-lipoprotein.

Experiments of Cohn and Mittelman[19] on the interaction of γ-globulins with serum albumin in alcohol-water mixtures showed that strong protein–protein interactions other than that between γ-globulins and β-lipoprotein could take place

(13) This conclusion was based on solubility curves made with Fractions II+III and III-0[14] in which the quantities of cholesterol dissolved at various *p*H values were measured. We are indebted to Drs. D. A. Richert and P. M. Gross, Jr., for many of these measurements.

(14) J. L. Oncley, M. Melin, D. A. Richert, J. W. Cameron and P. M. Gross, Jr., *J. Am. Chem. Soc.*, **71**, 541 (1949).

(15) J. L. Oncley, F. R. N. Gurd and M. Melin, *ibid.*, **72**, 458 (1950).

(16) The progressive changes in the absorption spectrum of β-lipoprotein have been correlated with autoxidation of the fatty acids present. Any direct effect of age on the solubility properties of the β-lipoprotein has not been detected.

(17) J. L. Oncley, G. Scatchard and A. Brown, THIS JOURNAL, **51**, 184 (1947).

(18) R. A. Alberty, *J. Am. Chem. Soc.*, **70**, 1675 (1948).

(19) E. J. Cohn and D. Mittelman, Abstracts of Papers, 112th Meeting, American Chemical Society, 29C, 1947.

among the proteins of human plasma. Preliminary experiments have shown that γ-globulins interact with the components of a variety of plasma protein fractions to form insoluble complexes. However, the quantitative importance of γ-globulins and β-lipoprotein, comprising as they do about 11% and 5%, respectively, of the total plasma proteins, necessarily makes the interaction of β-lipoprotein with γ-globulins of special interest in plasma fractionation. The demonstration of the strong tendency of β-lipoprotein to interact with γ-globulins throws some light on the results of earlier studies on the separation of plasma protein components. Some at least of the plasma euglobulins studied by earlier workers[20,21,22] very probably involved complex formation with lipoproteins. Indeed, the previous failures to isolate human serum β-lipoprotein were very likely due to its strong tendency to form complexes with other proteins. It is particularly interesting that the interaction complexes described here have the properties which led Sørensen to declare[23] that proteins were "reversible dissociable component systems."

Interaction of Insulin Monomers (with E. Ellenbogen[24])

There is now a great deal of evidence that the molecular weight of insulin should be 12,000. Probably the first published indication that this molecular weight should be taken for insulin was the X-ray study of Crowfoot.[25] She reported the cell molecular weight to be 39,700, which became 37,600 when corrected for 5.4% of moisture. Later revision of the probable moisture content to 10.1%[26] gives 36,000 for this value. In addition, Crowfoot found that this insulin molecule possesses a trigonal symmetry which indicated that the atoms are present in triple point arrays, suggesting that the elementary cell contains 3 or $3n$ molecules. This should give 12,000 or $12{,}000/n$ for the X-ray molecular weight. She further states that "...it is scarcely possible that a giant molecule should possess true trigonal symmetry...it is more probable that three molecules should associate in solution and that this is the unit of which Svedbergh has determined the molecular weight...[25]."

The existence of the small molecular weight molecule, which we will call the insulin monomer to avoid confusion, is also suggested by relaxation times obtained in dielectric dispersion studies of insulin dissolved in mixtures of propylene glycol and water.[27] The low dielectric constant of these solvents would be expected to favor the formation of monomer, as will be discussed later, although the full significance of this experiment was not recognized until much later. Recent ultracentrifuge experiments in these solvents has shown that the sedimentation constants of these solutions are very low, and of the order of magnitude demanded by the monomer. Because of the high viscosity of this solvent, it was not possible to make precise measurements of such a low sedimentation constant, however.

Minimum molecular weights have been calculated from the amino acid composition of insulin.[26,28] These studies have given an average minimum molecular weight of 12,000.

Except for a few acid solutions studies by Sjögren and Svedberg,[29] the first study of acid solutions in the ultracentrifuge which clearly indicated a low molecular weight for insulin were those of Moody.[30] In a doctoral dissertation, he reports that solutions of insulin at *p*H 3.0 in 1.6% glycerol give a sedimentation constant of about 1.75 *S*, and a diffusion constant of 15×10^{-7}. Using $\bar{v} = 0.75$, he obtained a molecular weight of about 11,000. We have carried out studies in acid solutions from September, 1946, to the present,[24] and Fredericq and Neurath have recently published[31] results of their study. These studies are all in quite good agreement with a molecular weight in acid solutions of 12,000, except for a few experiments of Fredericq and Neurath in $H_2PO_4^-$ which led them to suggest a minimum molecular weight of 6,000. There are a number of difficulties which arise if one accepts this low value, however, and it does not seem consistent with our studies. Light scattering studies of Doty[32] have never yielded values lower than about 12,000, and sedimentation velocity studies in our laboratory have given no indications of a minimum weight less than 12,000. We have therefore taken 12,000 as the most likely value for the insulin monomer.

Ultracentrifuge studies in neutral solutions have consistently yielded higher molecular weight values, although these have varied from 35,000 to 46,000. It is difficult to determine from these data whether the insulin "polymer" in this *p*H range consists of three or four insulin monomers. The more recent workers favor 48,000 for the molecular weight, but this figure was arrived at largely because of the low diffusion constant used, and leads to a rather large value for f/f_0. From viscosity measurements in acid solutions, and at *p*H 7.2 and an ionic strength of 0.1, we observed an Einstein viscosity coefficient smaller than 3.5, and hence should expect f/f_0 to be not much over 1.1. We have found that the partial specific volume used by most workers (0.749) is too large and favor a value of about 0.71 or 0.72. Also our diffusion constant measurements lead us to favor the lower molecular weight (36,000). At this time, however, we must consider this to be only a tentative value.

Gutfreund has published osmotic pressure measurements and studies in the velocity ultracentrifuge[33,34] which he interprets as showing an equilibrium between an insulin monomer of 12,000 molecular weight and "...the apparent formation of molecules consisting of three units in the crystal, while in solution the molecule can consist of up to four units."

(20) H. Chick, *Biochem. J.*, **7**, 318 (1913).
(21) W. B. Hardy, *J. Physiol.*, **33**, 251 (1905).
(22) H. C. Haslam, *Biochem. J.*, **7**, 492 (1913).
(23) S. P. L. Sørensen, *Compt. rend. trav. lab. Carlsberg*, **18**, No. 5 (1930).
(24) E. Ellenbogen, Ph.D. Dissertation, Harvard University, 1949.
(25) D. Crowfoot, *Proc. Roy. Soc. (London)*, **A164**, 580 (1938).
(26) A. C. Chibnall, *J. Int. Soc. Leather Trades Chemists*, **30**, 1 (1946).
(27) E. J. Cohn, J. D. Ferry, J. J. Livingood and M. H. Blanchard, *Science*, **90**, 183 (1939).
(28) C. Fromageot, *Cold Spring Harbor Symp. Quant. Biol.*, **14**, 49 (1950).
(29) B. Sjögren and T. Svedberg, *J. Am. Chem. Soc.*, **53**, 2657 (1931).
(30) L. S. Moody, Ph.D., Dissertation, Univ. of Wisconsin, 1944.
(31) E. Fredericq and H. Neurath, *J. Am. Chem. Soc.*, **72**, 2606 (1950).
(32) P. Doty, M. Gellert and B. Rabinovitch, *J. Am. Chem. Soc.*, in press.
(33) H. Gutfreund, *Biochem. J.*, **42**, 156, 544 (1948).
(34) H. Gutfreund and A. G. Ogston, *ibid.*, **40**, 432 (1946).

Pedersen[35] also has recent data not in good agreement with the simple picture of an equilibrium between monomer and trimer insulin units of molecular weight 12,000 and 36,000. He obtains a molecular weight of 42,000 at neutral *p*H values, and near 24,000 in solutions at *p*H 2.55 (which he considers could better be about 21,000). There are thus major problems in any simple interpretation of the behavior of insulin solutions.

Crystalline beef zinc insulin (Lot No. 280,177) was kindly furnished us by the Eli Lilly Company, Indianapolis, Indiana. It was found to contain 15.5% N and 0.93% Zn. Zinc free insulin was prepared for some experiments by dialysis in collodion bags against 0.03 *N* HCl solutions.

Sedimentation experiments were carried out in an air-driven type ultracentrifuge[36,37] equipped with a Philpot schlieren optical system.[38] They were carried out at a speed of 54,000 r.p.m., corresponding to centrifugal fields of approximately 200,000 to 240,000 g. The sedimentation diagrams normally were sufficiently symmetrical to compute the weight-average sedimentation constant by observing the rate of sedimentation of the median of the diagram, rather than the more accurate formula using $s_w = (3s_m - s_t)/2$, where s_w is the weight-average sedimentation constant, s_m the sedimentation constant calculated from the median, and s_t the sedimentation constant calculated from the mode.[39] The sedimentation constants were calculated by plotting log distance against corrected times, and was reduced to the value expected for sedimentation in a medium with the viscosity and density of water at 20°. In most cases we also calculated apparent diffusion constants from the shape of the sedimentation diagram. The weight-average value was obtained from the second moment, m_2, and area, A, of the diagram, using the equation $D_w = m_2/(2tA)$.

Net charge was determined from measurements with the glass electrode of MacInnes and Belcher,[40] using activity coefficients for hydrochloric acid determined under comparable conditions, as described by Tanford.[41] All measurements were made using 10 mg./ml. of insulin.

We have carried out a number of ultracentrifuge experiments with the insulin system in order to study the equilibrium with the monomer unit which appears to be stable only in acid solution. Two types of experiments were performed. In one type we have varied the insulin concentration (from about 3 to 60 mg /ml. whenever possible) and held the *p*H and ionic strength constant in each series of experiments (Fig. 2). In the second type we have varied the *p*H (and hence the net charge of the insulin), holding the ionic strength constant for each series of measurements, and maintaining a constant insulin concentration of 10 mg./ml. (Fig. 3). In acid solutions, the sedimentation constant is observed to be a function of the *p*H, the ionic strength, the insulin concentration, and the dielectric constant. Below *p*H 2 there is little effect of the hydrogen ion concentration, but a marked one for changes in the ionic strength. The effects at *p*H values higher than 2, but below the lower limit of the range of insolubility can best be explained in terms of the net charge on the molecules at each *p*H. This has been done in Fig. 4, where the same data presented in Fig. 3 is plotted against net charge (on the basis of the 12,000 molecular weight monomer).

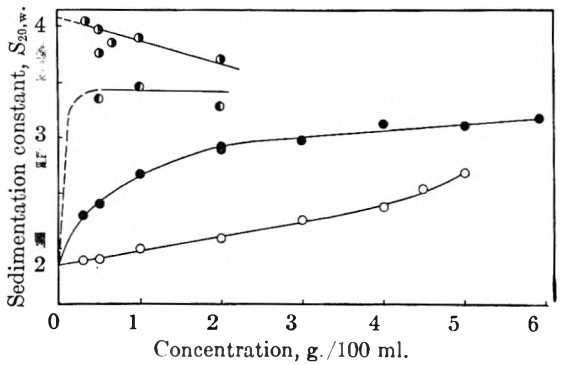

Fig. 2.—Sedimentation constant of insulin as a function of insulin concentration: ○, *p*H 2.0, 0.1 *M* sodium chloride; ●, *p*H 3.0, 0.1 *M* sodium chloride; ◐, *p*H 7.2, 0.1 ionic strength sodium phosphate buffer; ◑, *p*H 7.3, 0.1 ionic strength sodium phosphate buffer + 0.58 *M* sodium chloride.

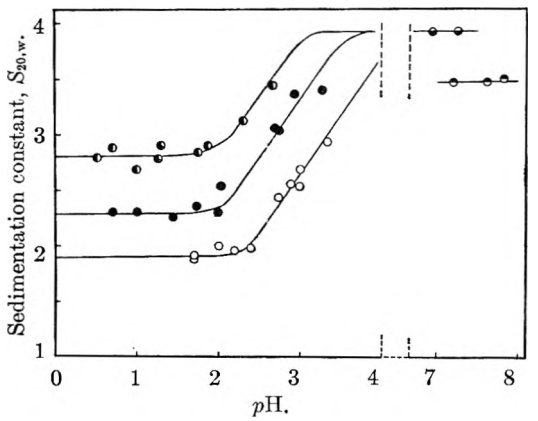

Fig. 3.—Sedimentation constant of insulin (10 mg./ml.) as a function of *p*H and ionic strength. Studies from *p*H 0 to 4 made in sodium chloride–hydrochloric acid mixtures, ionic strength of sodium chloride: ○, 0.1 *M*; ●, 0.2 *M*; ◐, 0.3 *M*. Studies from *p*H 7 to 8 made in sodium phosphate buffers of 0.1 ionic strength; ◓, no added sodium chloride; ◒, 0.4–0.6 *M* sodium chloride added.

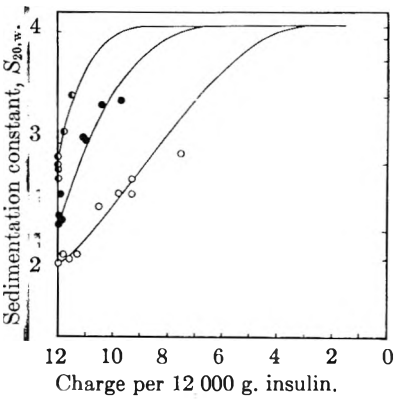

Fig. 4.—Sedimentation constant of insulin (10 mg./ml.) as a function of net charge and ionic strength: ○, 0.1 *M* sodium chloride; ●, 0.2 *M* sodium chloride; ◐, 0.3 *M* sodium chloride.

We have attempted to describe these observations in terms of an association equilibrium which is given in terms of an electrostatic repulsive force and an almost constant attractive force, due to short range forces of some kind. A decrease in the electrostatic repulsion, dependent upon ionic strength, dielectric constant and net charge, will always favor polymerization of monomer units. These reductions of the electrostatic interactions may be produced by lowering the net charge, increasing the ionic strength, or increasing the dielectric constant. The sedimentation constants

(35) K. O. Pedersen, *Cold Spring Harbor, Symp. Quant. Biol.*, **14**, 140 (1950).

(36) J. H. Bauer and E. G. Pickels, *J. Exp. Med.*, **65**, 565 (1937).

(37) E. G. Pickels, *Rev. Sci. Inst.*, **9**, 358 (1938); **13**, 426 (1942).

(38) J. St. L. Philpot, *Nature*, **141**, 283 (1938).

(39) I. Jullander, *Arkiv. Kemi, Mineral. Geol.*, **21A**, No. 8, p. 30 (1945).

(40) D. A. MacInnes and D. Belcher, *Ind. Eng. Chem., Anal. Ed.*, **5**, 199 (1933).

(41) C. Tanford, *J. Am. Chem. Soc.*, **72**, 441 (1950).

in the acid region at high ionic strengths, and in neutral solutions where the net charge is small, illustrate this behavior. Since the net charge changes little or not at all below *p*H 2, we see that hydrogen ion concentrations higher than this value will cause only an ionic strength effect. Insulin is a most interesting molecule to study in this way, since there is no evidence that these very acid conditions cause any appreciable denaturation of the insulin.

The effect of varying the insulin concentration can be seen by an application of the mass law. Neglecting any dimers, or polymers of more than three monomers units, we may write the chemical reaction

$$3\mathrm{I} \rightleftharpoons \mathrm{I}_3 \qquad (1)$$

and the mass law equilibrium as

$$K_{13} = (\mathrm{I}_3)/(\mathrm{I})^3 \qquad (2)$$

Here (I_3) represents the molecular concentration of insulin trimer, (I) that for the insulin monomer, and K_{13} is the association constant for the reaction. If we let α be the weight fraction of insulin in the associated (trimer) form, and c be the total concentration of insulin in g./100 ml., then $(\mathrm{I}_3) = 10\,c\alpha/36{,}000$, and $(\mathrm{I}) = 10c(1-\alpha)/12{,}000$, where we assume the molecular weights 12,000 and 36,000 for the monomer and trimer forms. We then can write equation (2) as

$$K_{13} = 4.8 \times 10^5\, \alpha/c^2\,(1-\alpha)^3 = 4.8 \times 10^5\, K'_{13} \qquad (2a)$$

where K'_{13} is defined as $\alpha/c^2(1-\alpha)^3$. It is difficult to express α as an analytic function of K_{13} and c, but we can easily compute α as a function of c for a number of assumed values of K'_{13} (as hence K_{13}). Such functions are shown in Fig. 5.

If we could directly measure the sedimentation constant, s, as a function of concentration, c, our problem could be ended here, since

$$s = s_1(1-\alpha) + s_3\alpha = s_1 + \alpha(s_3 - s_1) \qquad (3)$$

and α could be computed from the observed values of s when we assumed proper values for s_1 and s_3. However, in the ultracentrifuge we must deal with the sedimentation velocity of a boundary through which the concentration is varying from zero to the concentration of the solution used to fill the cell (corrected suitably for the dilution factor due to the sector-shape of the cell). Since there are indications from measurements of light scattering in this system that equilibria between monomer and trimer molecules is very rapidly obtained,[42] we thus have a different α value at each point in the boundary region, corresponding to the concentration at that point. We can compute the weight average sedimentation constant at concentration c as

$$s_c = \int_0^c s_i dc_i \Big/ \int_0^c dc_i = (1/c) \int_0^c s_i dc_i \qquad (4)$$

Substituting s_i from equation 3, we obtain

$$s_c = s_1 + (s_3 - s_1)/c \int_0^c \alpha_i dc_i \qquad (4a)$$

Equation (1) gives us α_i as a function of c (and K_{13}), so that s_c is a function of the concentration

(42) P. Doty and J. T. Edsall, *Adv. Prot. Chem.*, **6**, 91, 93 (1951).

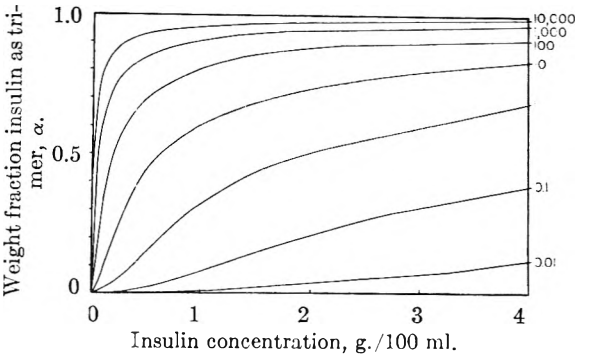

Fig. 5.—Weight fraction of insulin in trimer form (α) as a function of insulin concentration, from equation (2a). Values on right indicate values of the constant K'_{13}. The constant $K_{13} = 4.8 \times 10^5 K'_{13}$.

c, and the parameters K_{13}, s_1 and s_3. Or we may find values of K_{13} from observed s_c values at a given value of c (assuming s_1 and s_3). The scale at the right of Fig. 4 gives this relationship at an insulin concentration, c, of 10 mg./ml., using $s_1 = 1.85$ and $s_3 = 4.06$.

Now we have obtained an estimate of the equilibrium constant under different conditions of net charge and ionic strength, and hence can compute the free energy for reaction (1) under these varying conditions. Estimates of the repulsive forces involved in this reaction may be obtained by calculation of the work done when placing a number of charges upon the surface of a sphere of volume equal to that of the insulin molecule. The electrostatic part of the chemical potential of an insulin ion of charge z_i and radius b is[43]

$$\mu_i^e = (Ne^2z^2/2D)[1/b_i - \kappa/(1+\kappa a_i)] \qquad (5)$$

where N is Avogadro's number, e the electronic charge, D the dielectric constant, κ the familar Debye-Hückel parameter (equal to $0.329 \times 10^8 \sqrt{\Gamma/2}$ at 25° in water), and a_i is the sum of the radii of the insulin ion (positively charged) and the chloride ion (when the ionic strength of the solution is due to NaCl and HCl). We have taken b_1 and a_1 (for the monomer) to be 15.6 Å. and 18.1 Å., respectively, and b_3 and a_3 (for the trimer) to be 22.5 Å. and 25.0 Å. The electrical free energy for reaction (1) is then

$$\Delta\mu_{13}^e = \mu_3^e - 3\mu_1^e \qquad (6)$$

and is a function of the charge per 12,000 g. of insulin, and of $\Gamma/2$ (and hence of the ionic strength). At the maximum charge of +12, $\Delta\mu_{13}^e$ varies from about 17,000 cal. at 0.1 ionic strength to 12,500 cal. at 0.3 ionic strength. As the charge is reduced, $\Delta\mu_{13}^e$ decreases rapidly, and the attractive term in the total free energy becomes predominant.

The magnitude of the attractive force has been estimated by calculating the free energy for the reaction from the K_{13} values of Fig. 4, using the equation

$$\Delta\mu_{13} = \Delta\mu_{13}^e + \Delta\mu_{13}^a = -2.303\,RT \log K_{13} \qquad (7)$$

Values of from −21,000 to −18,000 cal. are thus obtained for $\Delta\mu_{13}^a$, and the predicted sedimentation

(43) G. Scatchard, in Cohn and Edsall, "Proteins, Amino Acids and Peptides," Reinhold Publ. Corp., New York, N. Y., p. 57, 1943.

constants as a function of net charge (per monomer unit) as shown in Fig. 6. The agreement between these computed curves and the observed ones in Fig. 4 leaves much to be desired, but the qualitative agreement obtained is probably all that should be expected in view of the rather crude nature of both experiment and theory at the present time. Binding of ions other than hydrogen, as suggested for SCN^- by Fredericq and Neurath[31] would have a great deal of influence on these calculations.

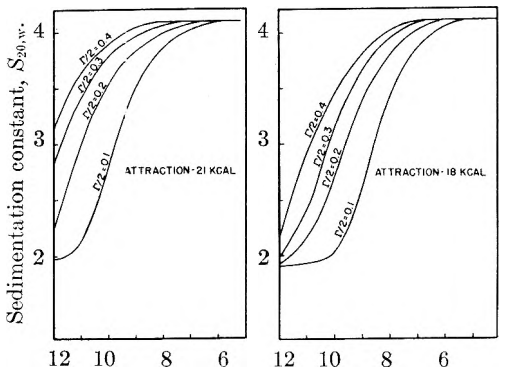

Fig. 6.—Calculated variation of the sedimentation constant for insulin solutions.

We must also attempt to estimate the importance of other equilibria on the calculations we have just described. If we consider that the shape of the insulin monomer and trimer are those recently proposed by Low from studies of the unit cell dimensions of crystals of both zinc insulin and insulin sulfate,[44] then there will be three common surfaces produced by reaction (1) to make the trimer, and we can take an attractive energy of about −6000 or −7000 cal. per common face. This does not seem to be at all unreasonable in magnitude, and might be accounted for by a close fitting of lipophilic groups on the insulin. If this attractive force has such a simple origin, however, there would not seem to be any *a priori* reasons for believing that polymers of the insulin monomer other than the trimer might not exist. Simple calculations based on this picture indicate that the reactions yielding the trimer (with three common faces) are more important than those involving the dimer with only one common face[44a]). As the net charge becomes smaller, and especially at high ionic strengths, the higher polymers appear to become more stable. This might explain why some experiments in the neutral range yield values for the molecular weight of insulin which appear to be larger than 36,000. In the last few months, Mr. Henry Dix, working with us on this problem, has found some insulin preparations which appear to have molecular weight values above 36,000 even at *p*H 3 when the insulin concentration is high. The stability of such high polymers might also explain the maximum observed in the solubility curve for insulin in glycine, which occurs at the unexpectedly low value of 0.5 *M* glycine.[27] The high dielectric constants of these solvents might favor the formation of high polymers of very low solubility, which overcome the usual "salting-in" behavior of glycine.

Another difficult problem whose solution has eluded us to date, is that concerned with the boundary spreading observed during these ultracentrifuge studies. We have obtained rather normal values of apparent diffusion constant at *p*H 1–2 (at 0.1 ionic strength), and at *p*H 7. Where the equilibrium of reaction (1) shows considerable amounts of both components, larger values are obtained, as would be expected. However, the observed values are as large as 30×10^{-7} cm.^{2}/sec., whereas we have not been able to calculate any theoretical values greater than about 15×10^{-7} when we assume a rapid equilibrium. If the reaction is quite slow, and especially if some dimer and higher polymers were present, the high values observed would be demanded by theory. As mentioned before, however, light scattering studies would seem to exclude the possibility of a slow reaction. We have also studied solutions where there was much boundary spreading, both immediately after mixing, and after 48 hours standing at room temperature, and could find no differences in the sedimentation diagrams obtained.

Although there are, then, many uncertain points concerning the behavior of insulin solutions under these conditions, it would seem that the molecular weight of insulin would best be considered as 12,000 and that it does react to give higher molecular weight polymers. In sufficiently dilute solutions, we would expect that insulin would dissociate even when the polymer molecules were rather stable, however, and it appears very probable from these studies that under the conditions specified for biological activity tests for insulin, it is the monomer which is the biologically active unit.

It is interesting to note that recent studies of Schwert[45] indicate that polymerization reactions of this same character are of importance in both α- and γ-chymotrypsin. Although he did not study the effects of ionic strength and dielectric constant, these systems form reversible equilibria (probably between monomer and dimer forms) which are dissociated by decrease in *p*H and/or decrease in protein concentration.

Interaction of Human Serum Albumin with Its Homologous Equine Antibody (with D. Gitlin)

There have been many studies of the interaction of protein antigens, such as human serum albumin, with their homologous antibodies. As the amount of antigen, G, added to the antibody, A, is increased, increasing amounts of precipitate formed by combination of antigen and antibody are obtained,

(44) B. W. Low, *Cold Spring Harbor Symp. Quant. Biol.*, **14**, 77 (1950).

(44a) NOTE ADDED IN PROOF.—Considerable evidence is now available[32,33] to indicate that the dimer equilibrium may be of much importance and that the tetramer equilibrium also must be considered. More recent studies by Dr. B. W. Low (in press) indicate that the orientation and shape of the monomer unit in the orthorhombic cell is different from that proposed earlier. The present model based on the close packing of cylindrical rods is 44 Å. long. Lateral close packing of the molecules leads to the formation of the dimer, trimer, tetramer, etc. The trimer formed in this way does not correspond to the orientation of the trimer unit in rhombohedral zinc-insulin crystals.

(45) G. W. Schwert, *J. Biol. Chem.*, **179**, 655 (1949).

until it rises to a maximum. Additional amounts of antigen cause a decrease in the amount of precipitate formed, and finally the precipitate vanishes in the so-called inhibition zone. In general, it has been found that the reactions of equine antibodies[46–52] differ from those of rabbit and most other animals in that a marked inhibition zone occurs not only with excess antigen, but also with excess antibody.

Chemical theories to explain this interaction have been proposed by many investigators, but only upon the application of quantitative analytical methods to antigen–antibody systems of known molecular size has the stoichiometry become apparent.[53] Such studies of the specific precipitates formed by the reactions of antigen and antibody indicate that the molecular ratio of antigen to antibody varies continuously, but usually starts and ends at specific ratios. In the diphtheria toxin–antitoxin system, for example, these extreme values closely approximate the formulas A_4G and AG.[51]

In the inhibition zones it is more difficult to obtain evidence as to the chemical composition of the complexes formed. One of the most direct methods is to mix accurately known amounts of antibody and antigen, and then by ultracentrifugal analysis of the solution determine the amount of free antigen or antibody present in the solution. The sedimentation constant and amount of the complexes formed can also be determined if they are not too heterogeneous. This method was first applied by Heidelberger and Pedersen in the ovalbumin anti-ovalbumin (rabbit) system.[54] A more comprehensive study was that of Pappenheimer, Lundgren and Williams on the diphtheria toxin antitoxin (equine) system.[50] The later workers were thus able to show that the empirical composition of the complex in the region of antigen excess varied from AG to AG_2 as more antigen was added, closely approximating AG_2 for large antigen excess. Similar studies in the region of antibody excess indicated the empirical formula A_8G. Complexes with the molecular weight predicted by these simple formulas were also observed, but much of the total mass of the complex was also observed to sediment more rapidly, as would be expected if a further aggregation occurred.

It has recently been shown that the reaction between human serum albumin and its homologous equine antibody results in the toxin–antitoxin type of precipitation curve.[46] Studies of this reaction by application of light-scattering methods have made possible investigations of the kinetics of aggregation in this system.[55] We wish here to report on a study of the molecular composition of the complexes formed by this system in the region of antigen excess.

The equine antiserum used throughout was that described as "Bleeding #3" in the earlier reports.[46,55] Studies of this antiserum indicated that practically all of the antibody present was of the "complete" or "precipitating" form.

Crystallized human serum albumin employed as antigen was preparation "Decanol 10"[56] obtained from Dr. W. L. Hughes, Jr., of this Laboratory.

Solutions of purified antigen–antibody complexes were obtained by adding to a given amount of equine antiserum an amount of human serum albumin calculated to bring the reaction to the equivalence zone. The mixture was incubated at 37° for 1 hour and then placed at 1° for 24 hours. After making up to definite volume, the solution thus formed was dialyzed against saline-buffer of total ionic strength 0.15 (0.10 sodium chloride + 0.05 phosphate buffer at pH 7.5) for 24 hours. The solutions were run in the ultracentrifuge as described in the previous section. That component having the sedimentation constant of albumin was considered as free antigen.

Because of the method used for the preparation of purified complexes, the antibody excess zone was not studied and observations in the ultracentrifuge were limited to the zone of antigen excess.

TABLE II

INTERACTION OF HUMAN SERUM ALBUMIN (MOL. WT. 69,000) AND ITS HOMOLOGOUS EQUINE ANTIBODY (MOL. WT. 184,000)[a]

Region of antibody excess. No antibody was observed in any of these ultracentrifuge experiments or by ring tests.

	Total protein present in system, mg./ml..		Ratio of albumin to antibody in system		Albumin found, mg./ml.		Ratio of albumin to antibody in complex	
	Albumin G	Antibody A	Weight ratio	Molecular ratio	Unbound	Bound in complex	Weight ratio	Molecular ratio
I	6.0	12.2	0.49	1.31	0.7	5.3	0.44	1.18
II[b]	7.1	8.3[b]	0.86	2.30	2.6	4.5	0.54	1.44
III	10.0	10.6	0.94	2.50	3.5	6.5	0.61	1.63
IV	6.1	4.5	1.35	3.60	2.8	3.3	0.73	1.95
V	11.3	5.6	2.02	5.40	7.1	4.2	0.75	2.00

[a] Assumed molecular weight from that of equine diphtheria antitoxin (ref. 56). [b] Solution II was formed by equilibrating half of the solution V with additional specific precipitate.

The composition of the solutions, and the ultracentrifugal estimates of the amount of excess antigen are reported in Table II. It will be noted that as the amount of antigen in the reaction system was increased relative to the amount of antibody, the amount of antigen bound per unit weight of antibody increased until it reached a limiting ratio of about 0.75. The molecular weight of human serum albumin is 69,000,[56] and if one assumes 184,000 for the average molecular weight of the equine antibodies as was obtained for the equine antitoxin,[57] this corresponds to a limiting molecular composition of 2.0 moles of human serum albumin per mole of equine antibody.

As was observed by Pappenheimer, Lundgren and Williams, the protein concentration of the solutions studied, as obtained from the total area under the sedimentation diagram in the ultracentrifuge, was usually less than that calculated to be present suggesting the presence of larger complexes sedimenting very rapidly. Of great interest is the fact that several distinct antigen-antibody complexes existed in these solutions. At least three components exclusive of that component designated as albumin could be observed. As the amount of antigen in the system was increased, the complexes of greater molecular weight decreased in concentration until a relatively homogeneous antigen-antibody complex existed, consistent with a molecular composition of 2 moles of human serum albumin to one mole of antibody.

(46) D. Gitlin, C. S. Davidson and F. H. Wetterlow, *J. Immunol.*, **63**, 415 (1949).

(47) S. B. Hooker and W. C. Boyd, *Ann. N. Y. Acad. Sci.*, **43**, 107 (1942).

(48) G. A. Hottle and A. M. Pappenheimer, Jr., *J. Exp. Med.*, **74**, 545 (1941).

(49) A. M. Pappenheimer, Jr., *ibid.*, **71**, 263 (1940).

(50) A. M. Pappenheimer, Jr., H. P. Lundgren, and J. W. Williams, *ibid.*, **71**, 247 (1940).

(51) A. M. Pappenheimer, Jr., and E. S. Robinson, *J. Immunol.*, **32**, 291 (1937).

(52) H. P. Treffers, M. Heidelberger and J. Freund, *J. Exp. Med.*, **86**, 83 (1947).

(53) M. Heidelberger, *J. Am. Chem. Soc.*, **60**, 242 (1938).

(54) M. Heidelberger and K. O. Pedersen, *J. Exp. Med.*, **65**, 393 (1937).

(55) D. Gitlin and H. Edelhoch, *J. Immunol.*, **66**, 67 (1951).

(56) E. J. Cohn, W. L. Hughes, Jr., and J. H. Weare, *J. Am. Chem. Soc.*, **69**, 1753 (1947).

(57) M. L. Petermann and A. M. Pappenheimer, Jr., THIS JOURNAL, **45**, 1 (1941).

It should be noted that the solution II was formed by equilibrating part of the solution V with additional specific precipitate, increasing the relative amount of antibody in the system as compared to the latter solution. This clearly demonstrates the reversibility of the aggregation reaction.

It is thus seen that in the antigen excess region of the reaction between equine antibody and human serum albumin, the solution formed contains several complexes of definite antigen–antibody composition. The relative proportions in which these complexes appear depend upon the relative amounts of antigen and antibody in the system. The fact that the relative proportions of these complexes can be altered from a relatively single complex as seen in experiment V to that in experiment II by increasing the relative amount of antibody in the system would further indicate the dependence of the composition of the antigen-antibody complexes upon the amounts of antigen and antibody in the system. It would thus appear that these complexes exist in equilibrium with each other and the amount of free antigen in the system.

It does not appear likely that these complexes are polymers of a simple complex, all possessing a single antigen-antibody ratio. In such a system, the smallest complex would shift (probably increase) in molecular weight as the antigen-antibody ratio in the monomer system increases, and the molecular weights of the complexes would be multiples of each other. This does not appear to be the case.

We have just described three protein–protein interactions which have recently been studied in our laboratories. A fourth reaction of this type is that of the mercury salt of mercaptalbumin, AlbSHgOH, with mercaptalbumin, AlbSH. The properties of this interaction have been described in some detail by Hughes[58] and by Edsall.[42] More recently, we have studied the corresponding reaction where a bifunctional organic mercurial

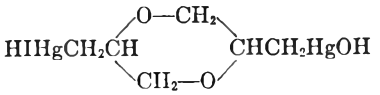

replaces the mercury ion.[59]

Although these interactions involve very different systems, and have been studied by different methods, the similarities in the kinds of forces which we call upon to explain the results obtained are most striking. The principal forces in the β-lipoprotein, γ-globulin system, electrostatic in character, are also responsible for the dissociation of the insulin polymers. There is much more specificity in the insulin reaction, however, introduced by the short-range attractive forces which are so important to antigen–antibody and enzyme-substrate interactions. The attractive forces involved in the mercaptalbumin system, while apparently simple in origin, are highly specific. Further studies of such interactions, especially these simpler ones, will do much to increase our knowledge of all protein-protein interactions.

REMARKS

GERSON KEGELES: It is suggested that the equilibrium between the various protein species may possibly be influenced by the ultracentrifuge itself when it is used to study this equilibrium. For if the partial specific volumes of the reactants differ from those of the products, then under the high pressures attained in the ultracentrifuge, that direction of the reaction should be favored, according to Le Chatelier's principle, which results in a decrease of volume. It is therefore suggested that the existence of such an effect might be studied by examining the equilibrium as a function of the speed of the ultracentrifuge.

(58) W. L. Hughes, Jr., *Cold Spring Harbor Symp. Quant. Biol.*, **14**, 79 (1950).

(59) R. Straessle, *J. Am. Chem. Soc.*, **73**, 504 (1951)

EXPERIMENTAL FACTORS AND ACTIVITY COEFFICIENTS IN ION EXCHANGE EQUILIBRIA

BY WILLIAM J. ARGERSINGER, JR., AND ARTHUR W. DAVIDSON

Department of Chemistry, University of Kansas, Lawrence, Kansas

Received August 30, 1951

In aqueous ion exchange experiments on exchangers such as Dowex 50, the total process has been found to include, in addition to equivalent exchange of ions, both water absorption and electrolyte adsorption by the solid exchanger. Although the quantity of water absorbed and the extent of electrolyte adsorption may be determined and corrected for, yet analysis of each of the equilibrium phases for both components provides the best data for the calculation of exchange equilibrium constants. The equilibrium system consists of a non-ideal liquid electrolyte solution and a non-ideal solid resin solution. Mean activity coefficients for the mixed electrolytes, when available, may be combined with exchange data for the calculation, through the Gibbs–Duhem equation, of both the equilibrium constant for the exchange process and the activity coefficients of the resin components as functions of composition. These activity coefficients, at a fixed resin composition, should be independent of the ionic strength of the equilibrium aqueous phase. The constancy of resin activity coefficients has been verified for the Na–H exchange system at three ionic strengths. The mean value of the equilibrium constant for this system is 1.69. Similar calculations have been made for the Ag–H system at 1 *M* ionic strength. Here the resin activity coefficients are greater than unity, and the value of the equilibrium constant has been found to be 13.7.

Even though the mechanism, kinetics and equilibrium of many cation exchange systems have been studied,[1–3] and reports of applications of cation exchange in both industry[3] and research[3–5] are exceedingly numerous, yet few investigations of exchange reactions have been carried out under rigorously simple and reproducible conditions with the primary aim of determining the true thermodynamic equilibrium constant for the process. A program of such investigations of exchange systems involving some of the more important uni- and bivalent cations was initiated in this Laboratory some time ago. In the course of the study a large amount of exchange data for fairly concentrated solutions has been obtained,[6] the total process occurring in exchange has been to some degree clarified, and a start has been made toward the determination of activity coefficients

(1) A. W. Davidson, W. J. Argersinger, Jr., R. W. Stoenner and W. K. Lowen, Technical Report to the Office of Naval Research, NR 057158, Feb., 1949.

(2) H. P. Gregor, *J. Am. Chem. Soc.*, **73**, 642 (1951).

(3) F. C. Nachod, "Ion Exchange," Academic Press Inc., New York, N. Y., 1949.

(4) R. E. Connick and S. W. Mayer, *J. Am. Chem. Soc.*, **73**, 1176 (1951).

(5) R. J. Myers, "Advances in Colloid Science," Vol. I, Interscience Publishers Inc., New York, N. Y., 1942.

(6) W. K. Lowen, R. W. Stoenner, W. J. Argersinger, Jr., A. W. Davidson and D. N. Hume, *J. Am. Chem. Soc.*, **73**, 2666 (1951).

in the exchanger phase, and from these the true equilibrium constant for the exchange process.[7,8]

The initial research involved exchange of simple univalent cations on the phenolsulfonic acid–formaldehyde resin known as Dowex 30.[9] It was soon established, however, that this exchanger is not entirely stable, especially toward oxidizing agents such as silver ion in acid solution. Consequently, all subsequent work has been done on Dowex 50,[10] a sulfonated polystyrene polymer, which is stable even in concentrated acid or salt solutions and is not oxidized by silver ion or similar oxidants in these solutions. From considerations of practical utility, the measurements were made for the most part in solutions of unit ionic strength.

In the first series of investigations, initial and equilibrium concentrations of both cations were determined, in accord with rather common practice, in the solution phase only; the equilibrium composition of the entire system was calculated from these data, together with the known initial number of equivalents of solid exchanger. It was observed, however, that in general the concentration increase of a cation in solution exceeded the concentration decrease of the other exchanging cation. The discrepancy was not due to decomposition of the resin, as had been the case with Dowex 30 as exchanger, but was later found to arise principally from absorption of water, or of solution, by the partially dried resin. In the simpler exchange systems the sole assumption of water absorption accounted for the change in ionic strength of the solution during exchange, and permitted the calculation of exchange equilibrium quotients, to be designated as K_m.

In exchange reactions involving silver and thallous ions, however, the variation in ionic strength could not be so readily explained. The discrepancy between the concentration changes for the two ions was generally smaller than in exchanges involving hydrogen and alkali metal ions, and decreased, changing sign, with increased proportion of silver or of thallous ion in the solution. Adsorption of the silver or thallous ion on the resin was thus indicated. In these exchanges, then, a constant amount of water absorption was assumed, and the experimental concentration data were used to calculate the amount of adsorbed silver or thallous ion, the equilibrium composition of the solid exchanger, and the equilibrium quotient for the process.

The equilibrium quotient, the proper quotient of ionic molalities in the solution and resin component mole fractions in the solid phase, was found not to be constant, but to vary regularly with equilibrium resin composition. The variation may be attributed to two sources: the non-ideal nature of the liquid electrolyte solution, and the non-ideal nature of the solid exchanger solution. The former is easily corrected for, at least in principle, by the use of ordinary mean activity coefficients for the electrolytes in the solution. However, there are but few cases in which such coefficients are known for mixed electrolyte solutions, especially at ionic strengths as high as unity. Hence, by extension of the Lewis ionic strength principle, the appropriate ratio of mean activity coefficients of the exchanging electrolytes was assumed constant at constant ionic strength, and equal to the proper ratio of the coefficients of the separate electrolytes each in its own pure solution. This assumption naturally does not improve the results so far as constancy with respect to composition change is concerned, but the actual values, K_a, obtained for the equilibrium quotient by the application of this correction may be regarded as having greater validity than the uncorrected K_m values. For solutions containing alkali metal ions and hydrogen ions, mean activity coefficients are known as functions of composition at constant total ionic strength, and these may be used to calculate improved values of the equilibrium quotients. The values so obtained are somewhat more nearly constant, but still exhibit a trend as the equilibrium composition of the system varies, which must be due to the variation from constancy of the proper ratio of activity coefficients of the components of the solid exchanger solution. In the first investigations, attempts were made to use empirical Margules expansions[11] for the resin activity coefficients, but with little success.

The range of values of the equilibrium quotients K_m and K_a, and their values for equimolar final resin compositions, are given in Table I for each of a number of exchange reactions with Dowex 50 in solutions of approximately constant unit ionic strength at 25°. In each case, the quotient applies to the reaction in which the first ion of the pair replaces the second in the resin.

TABLE I

EQUILIBRIUM QUOTIENTS IN EXCHANGE REACTIONS

Exchange reaction	K_m	K_a	K_m at $N = 0.5$	K_a at $N = 0.5$
Sodium–hydrogen	0.9– 1.6	1.4– 2.4	1.33	2.25
Ammonium–hydrogen	1.1– 2.2	2.2– 4.4	1.56	3.15
Silver–hydrogen	4.0– 6.2	13 –20	5.4	18
Thallous–hydrogen	4.7– 6.0	21 –27	5.3	24
Thallous–ammonium	2.7– 3.9	5.1– 7.4	3.3	5.3
Nickel–hydrogen	1.0– 6.0	4.0–24	3.0	12
Calcium–hydrogen	5.5–17	24 –72	9.5	42
Calcium–nickel	1.7– 3.5	1.8– 3.6	2.4	2.5

In each case the experimental data give K_m as a function of equilibrium resin composition. Some apparent hysteresis was observed in the last three systems, presumably primarily because of the uncertainties involved in the calculation of the resin composition solely from solution concentration measurements. The effect of the nature of the anion was found quite negligible.

At the completion of this first series of investigations it was decided, in view of the uncertainty in calculation of resin composition, that a detailed study of simple systems should be undertaken in order to determine experimentally the several distinct factors involved in the usual exchange process. Of particular interest were the previously postulated water absorption and electrolyte adsorption effects which, with the solution composi-

(7) W. J. Argersinger, Jr., A. W. Davidson and O. D. Bonner, *Trans. Kans. Acad. Sci.*, **53**, 404 (1950).

(8) A. W. Davidson, W. J. Argersinger, Jr., W. K. Lowen, R. W. Stoenner and O. D. Bonner, Final Report to the Office of Naval Research, NR 057158, Feb., 1950.

(9) W. C. Bauman, *Ind. Eng. Chem.*, **38**, 46 (1946).

(10) W. C. Bauman and J. Eichorn, *J. Am. Chem. Soc.*, **69**, 2830 (1947).

(11) J. Kielland, *J. Soc. Chem. Ind.*, **54**, 232T (1935).

tion, establish the equilibrium composition of the resin phase.

For the study of water absorption, the ammonium–hydrogen exchange on Dowex 50 at 25° in solutions of constant unit ionic strength was chosen. In all exchange experiments the initial pure resin had been dried, for convenience, to an arbitrary degree, and the previous results had indicated the occurrence of water absorption by such partially dried resins. Direct measurements of water uptake, by both the ammonium and the hydrogen forms of the resin, were made by complete dehydration of water-saturated samples. Each pure resin was found to have a characteristic reproducible total capacity for water. The capacity is independent of particle size, within limits, and independent also of the previous history of the resin with respect to either exchange or drying. The capacity of the mixed resins is a linear function of the composition on a mole fraction basis. Indirect calculations of water absorption from the change in total ionic strength of solution during exchange are generally in good agreement with these direct measurements.

In the exchange reactions involving silver or thallous ions, it had been necessary to postulate electrolyte adsorption as well as water absorption in order to explain the observed changes in ionic strength during exchange. This effect was more carefully studied not only in the silver–hydrogen exchange, but also in the ammonium–hydrogen exchange; for it was now found to be more general than had been supposed (although much more pronounced in the silver system than in the ammonium system). The equilibrium resin in an exchange experiment was filtered off with suction, superficially dried by gentle pressing between filter papers, and then washed with pure water. The electrolyte removed from the resin by washing in this manner is termed "adsorbed electrolyte"; this arbitrary designation, although certainly not entirely correct, is nevertheless convenient from the experimental viewpoint. Such "adsorbed electrolyte" may indeed consist in part merely of adhering solution, but in most cases the results indicate in addition the presence of more firmly bound material. Since similar washing of the pure forms of the resin indicated no appreciable exchange under these conditions, the experimentally determined composition of the washed resin was taken as its equilibrium composition in the exchange reaction. In every case the final analysis of the washed resin corresponded to a total exchange capacity in agreement, within the small experimental error, with that of the initial resin.

The washings from the resin were analyzed for both cations involved in the exchange. The total amount of electrolyte adsorbed, and the ratio of the amounts of the two cations, both vary with the composition of the resin and that of the solution. Typical experimental results are shown in Table II for the silver–hydrogen exchange system. It should be noted that these data refer to adsorption by a mixed resin from a mixed solution; the concentration of silver ion in the solution increases from zero to 1 *M* as the mole fraction of silver resin increases from zero to unity.

TABLE II

ELECTROLYTE ADSORPTION IN SILVER–HYDROGEN SYSTEM AT UNIT IONIC STRENGTH

Mole fraction of Ag resin at equilibrium	Equivalent of Ag^+ adsorbed per equiv. of resin	Equivalent of H^+ adsorbed per equiv. of resin	Total equivalent adsorbed per equiv. of resin
0	....	0.0098	0.0098
0.177	0.0006	.0116	.0122
.477	.0014	.0147	.0161
.701	.0042	.0219	.0261
.815	.0098	.0275	.0373
.935	.0276	.0289	.0565
.981	.0577	.0223	.0800
1.000	.0909	....	.0909

Similar results were obtained for the ammonium–hydrogen system, but here the magnitude of adsorption, of the order of 0.030 equivalent of total electrolyte per equivalent of resin, is much more nearly constant. In view of the differences in nature between the two resin pairs, this difference was not unexpected.

The problem of the direct determination of the magnitude of this postulated adsorption is complicated by the fact that in such experiments exchange must generally occur also. It is planned, however, to study the uptake of electrolyte from mixed solutions by resin mixtures carefully made up in each case to the appropriate equilibrium composition. In this way it is hoped that exchange will be avoided, or at least drastically reduced, and that adsorption on such equilibrium resins may be directly determined. However, the measurement of adsorption of a single electrolyte by a particular resin of constant composition, over a range of concentration of the electrolyte in solution, seems to be unattainable, particularly if the ionic strength is to be maintained constant.

A third factor which must be considered in determining the equilibrium resin composition from measured changes in solution concentrations, is the change in solution volume resulting from the exchange of electrolytes of different apparent molal volumes. In the silver–hydrogen exchange in nitrate solutions, since the densities of 1 *M* solutions of silver nitrate and nitric acid are nearly identical, this effect is negligible. In the ammonium–hydrogen exchange in chloride solutions, however, the apparent molal volumes of the two electrolytes in 1 *M* solution differ by about 2%; so that in an exchange experiment in which considerable exchange occurs, there is observed an appreciable volume change, approximately proportional to the extent of exchange.

The results of these studies have thus shown that the total equilibrium composition of an exchange system is determined not only by the extent of simple ion exchange, but also by absorption of water by the exchanger, by adsorption of electrolyte by the exchanger, and by the variation in apparent molal volume of the solute during exchange. These three factors, which in general are neither negligible nor compensating, invalidate any attempt to calculate resin compositions directly from measurements of changes of solution concentrations alone. As a typical illustration, in one run in the ammonium–hydrogen investigation the equilibrium mole frac-

tion of ammonium resin as calculated from the observed change in ammonium ion concentration in solution was 0.756, while the value calculated from the observed change in hydrogen ion concentration was 0.865. On the other hand, the value computed from measured concentration changes and electrolyte adsorption, with corrections for volume changes due to water absorption and to the difference in apparent molal volumes of the solutes, was 0.850, and the experimentally obtained value, from direct analysis of the resin, was 0.849. While it is thus possible to calculate the equilibrium resin composition fairly closely, it is scarcely more difficult, and probably more accurate, always to determine the composition experimentally. This has been done in all our subsequent work.

As has been mentioned, the equilibrium quotients determined from experimental exchange data vary with the composition of the exchange system, because of the non-ideal nature of both liquid and solid solutions. If the activity coefficients of the electrolytes in the aqueous solution are available as functions of composition, however, it is possible to calculate from the exchange data the true equilibrium constant and the activity coefficients of the resin components.[7,12]

For a simple univalent ion exchange we may define the equilibrium quotient K_m, the apparent equilibrium constant K_a, and the true equilibrium constant K as

$$A^+ + B\,Res \rightleftharpoons B^+ + A\,Res$$

$$K_m = \frac{m_{B^+}N_A}{m_{A^+}N_B};\quad K_a = K_m\left(\frac{\gamma_{BX}}{\gamma_{AX}}\right)^2;\quad K = K_a\frac{f_A}{f_B}$$

In these expressions m represents molality in the aqueous solution, N mole fraction in the solid exchanger phase, γ mean electrolyte activity coefficient (X is the anion in the solution), and f activity coefficient of resin component on a mole fraction basis, with pure resin as the standard state. The differential form of the logarithmic relation between K and K_a may be combined with the Gibbs–Duhem equation at constant temperature and pressure for the solid solution phase

$$d\ln f_A - d\ln f_B = -d\ln K_a$$
$$N_A\,d\ln f_A + N_B\,d\ln f_B = 0$$

These two differential expressions may readily be solved as simultaneous equations for $d\ln f_A$ and $d\ln f_B$. Integration with the boundary conditions $f_A \to 1$ as $N_A \to 1$ and $f_B \to 1$ as $N_B \to 1$ gives the results

$$\ln f_A = -N_B\ln K_a + \int_{N_A}^{1}\ln K_a\,dN_A$$

$$\ln f_B = N_A\ln K_a - \int_{0}^{N_A}\ln K_a\,dN_A$$

Finally, substitution of these values in the initial logarithmic equation for the true equilibrium constant yields

$$\ln K = \int_0^1 \ln K_a\,dN_A$$

Since K_a is known as a function of resin composition, *i.e.*, of N_A, the values of $\ln f_A$, $\ln f_B$ and $\ln K$ may readily be obtained by graphical integration.

(12) E. Högfeldt, E. Ekedahl and L. G. Sillén, *Acta Chem. Scand.*, **4**, 556, 828, 829 (1950).

So long as the exchanger may be considered a solid solution of the two forms of the resin, not only the equilibrium constant for the exchange process, but also the activity coefficients of the resin components should be independent of the ionic strength of the aqueous medium. The constancy of activity coefficients has been tested with data for three sets of exchange experiments in the sodium–hydrogen system with Dowex 50 at 25°, at constant ionic strengths, respectively, of 1.0 *M*, 0.3 *M* and 0.1 *M*. The equilibrium composition of each phase was determined directly by analysis for both components; thus explicit consideration of the complicating factors previously discussed was unnecessary. The experimentally determined values of the equilibrium quotient K_m were converted to values of the apparent equilibrium constant K_a by the use of activity coefficient data for sodium chloride–hydrochloric acid solutions from the literature.[13] The values of K, and of f_{Na} and f_H, the activity coefficients of the resin components, are given in Table III.

TABLE III

EQUILIBRIUM CONSTANTS AND RESIN ACTIVITY COEFFICIENTS IN SODIUM–HYDROGEN EXCHANGE ON DOWEX 50 AT 25°

Ionic strength = Mole fraction of Na resin	1.0 *M* f_{Na}	1.0 *M* f_H	0.3 *M* f_{Na}	0.3 *M* f_H	0.1 *M* f_{Na}	0.1 *M* f_H
0.0	0.865[a]	1.000	0.879[a]	1.000	0.881[a]	1.000
.1	.867	0.999	.879	1.000	.881	1.000
.2	.870	.999	.879	1.000	.881	1.000
.3	.876	.996	.883	0.997	.881	1.000
.4	.884	.992	.887	.995	.883	0.999
.5	.894	.983	.899	.984	.894	.992
.6	.909	.963	.917	.960	.912	.965
.7	.933	.916	.940	.917	.936	.920
.8	.964	.836	.966	.847	.961	.848
.9	.986	.720	.989	.735	.983	.745
1.0	1.000	.532[a]	1.000	.583[a]	1.000	.505[a]

$$K = \frac{a_{H^+}a_{NaRes}}{a_{Na^+}a_{HRes}} = 1.73,\ 1.0\ M;\ 1.68,\ 0.3\ M;\ 1.66,\ 0.1\ M$$

[a] Extrapolated values.

As is indicated by Table III, the agreement among the values of the equilibrium constant for the three sets of experiments is reasonably good. Except at the very ends of the composition range, where some extrapolation is required, the agreement among the values of the activity coefficient at any given composition is also satisfactory. The over-all correspondence seems to justify the treatment of the exchanger phase as a non-ideal solid solution, in which the variation of $\log f_{Na}$ and $\log f_H$ with composition cannot be described by simple one-term Margules expressions.

It should be remarked that exchanges involving ions of higher valence may be treated in an exactly analogous manner, if the equivalent fraction in the resin phase, instead of the mole fraction, is used as independent variable for the integration.[7,12]

The extension of the method to exchanges other than the sodium–hydrogen system requires a knowledge of solution activity coefficients. Of particular interest was the silver–hydrogen exchange; here, however, the requisite activity coefficient data

(13) H. S. Harned and B. B. Owen, "The Physical Chemistry of Electrolytic Solutions," Reinhold Publishing Corp., New York, 1950.

were not available in the literature. Since the evaluation of K_a from the exchange data involves only the *ratios* of coefficients, rather than the individual values, a single set of measurements of the electromotive forces of appropriate cells will suffice to give the needed information.

The use of the usual hydrogen gas electrode is prevented by ordinary chemical reaction between silver ion in acid solution and gaseous hydrogen; for this reason, as well as for experimental convenience, the glass electrode was chosen as a substitute. Cells were set up of the general type

Ag, AgCl | HCl (m_0) | glass | HNO_3 (m_1), $AgNO_3$ (m_2) | Ag

$$E = E^\circ - \frac{RT}{F} \ln \frac{a_{HNO_3}}{a_{AgNO_3}} = E^\circ - \frac{RT}{F} \ln \frac{m_1}{m_2} - \frac{2RT}{F} \ln \frac{\gamma_{HNO_3}}{\gamma_{AgNO_3}}$$

where a represents activity, m molality and γ mean activity coefficient. In principle, experimental measurements of the electromotive forces of such cells as a function of total ionic strength of the mixed solution should permit the evaluation of the constant E° by means of obvious extrapolation techniques.[13] In practice, however, such evaluation is interfered with by the so-called "acid error" of the glass electrode; the quantity E° varies slowly with acid strength of the solution.[14] Hence, the glass electrodes were calibrated in hydrochloric acid solutions, and the E° values so obtained were assumed to be valid for nitric acid solutions of the same acid strength. Although this assumption could not be tested by direct experiment, the error is believed to be slight.

The ratio of the mean activity coefficients of nitric acid and silver nitrate was then determined as a function of solution composition from the experimental electromotive force data for solutions of constant total ionic strengths of 1.0, 0.5, 0.2 and 0.1 M. In each study the mole fraction of silver nitrate in the mixed solute was varied from 5 to 95%. In the more concentrated solutions, the activity coefficient ratio is far from constant, changing by 4–6% over the range 5 to 95% silver nitrate. In the dilute solutions, however, the ratio is nearly constant, changing over the range mentioned by about 1% only. In all cases the rate of variation of the ratio is very much less over the intermediate composition range than at the ends of the scale; in other words, the ionic strength principle holds well under these conditions even at relatively high ionic strengths.

Data for the silver–hydrogen exchange on Dowex 50 at 25° were obtained for solutions of approximately constant total ionic strength of unity. The equilibrium resin composition was determined from direct analysis of the washed resin by exhaustive exchange; the effluent solutions, as well as the equilibrium solution samples, were analyzed by standard methods for hydrogen ion and silver ion. The exchange data were combined with the independently obtained solution activity coefficient data to calculate values of K_a, the apparent equilibrium constant, from which in turn the activity coefficients of the resin components and the true equilibrium constant were derived by graphical integration. The results are summarized in Table IV.

(14) M. Dole, "The Glass Electrode," John Wiley and Sons, Inc., New York, N. Y., 1941.

TABLE IV

SILVER–HYDROGEN EXCHANGE ON DOWEX 50 AT 25°

Ionic strength 1 M; $K = \frac{a_{H^+} a_{AgRes}}{a_{Ag^+} a_{H\ Res}} = 13.7$ at 25°

Mole fraction of Ag resin	f_{Ag}	f_H
0.0	1.42[a]	1.00
.1	1.35	1.00
.2	1.29	1.01
.3	1.24	1.02
.4	1.19	1.05
.5	1.16	1.07
.6	1.12	1.12
.7	1.08	1.18
.8	1.05	1.29
.9	1.02	1.53
1.0	1.00	3.05[a]

[a] Extrapolated values.

In contrast with the behavior of the sodium–hydrogen system, the activity coefficients of the resin components in the silver–hydrogen system are found to be greater than unity.[12] This difference may be due to the greater dissimilarity between the silver and hydrogen resins, as compared with the sodium and hydrogen resins.

Similar experiments to determine activity coefficient ratios and exchange data for the computation of exchange equilibrium constants are planned for other systems to which the present methods are applicable. These include, for example, exchange reactions involving mercurous, cadmium, zinc and thallous ions. In certain systems, the necessity for separate exchange solution analyses and activity coefficient ratio determinations may be obviated by the use of electromotive force measurements on the exchange solution itself, to give directly the appropriate ratio of solution activities. Some work of this nature has been reported by Marshall and Gupta.[15]

In addition to the obvious direct applications of equilibrium constant data of the sort here discussed to ordinary ion separations, at least two other applications may be mentioned. Since each actual ion exchange process may be regarded as an ordinary chemical reaction, it is possible to calculate the equilibrium constant for a given exchange from those for two other independent processes which may be combined to give the exchange under consideration. Such "triangular" relationships have been tested for the ammonium–thallous–hydrogen and calcium–nickel–hydrogen systems, with fairly good results. Finally, if the resin activity coefficients are independent of solution ionic strength, and depend only on the composition of the solid phase, then it should be possible, once these coefficients have been determined for a given exchanger, to apply them in the determination of mean activity coefficients in mixed electrolyte solutions at any ionic strength of interest. However, since the liquid solution contains three components, the Gibbs–Duhem equation for this solution contains a third term involving the activity of water; hence such a calculation would require additional information such as vapor pressure or freezing point data.

(15) C. E. Marshall and R. S. Gupta, *J. Soc. Chem. Ind.*, **52**, 433 (1933).

THE DIFFUSION PROCESS FOR ORGANOLITE EXCHANGERS

BY JACK J. GROSSMAN AND ARTHUR W. ADAMSON

Department of Chemistry, University of Southern California, Los Angeles 7, California

Received August 30, 1951

The film diffusion mechanism of Adamson and Grossman[1] has been demonstrated to be reliable. It is found that diffusion is the sole rate controlling process for the sulfonated polystyrene resins. Conditions which favor film diffusion are (1) a small film permeability D°/R°, (2) a large particle permeability D/R, (3) a small diffusion efficiency f, *i.e.*, dilute outer solutions, completely dissociated resins, low internal void space, and a large exchange capacity. It was found that film diffusion for the Na–Cs exchange begins a detectable transition to intermediate diffusion at 0.001 molar outer solution concentrations and above. Dissociation of the acid resin made particle diffusion rate controlling for the H–Cs exchange in concentrations greater than 8×10^{-4} molar although intermediate diffusion characteristics are still observable.

It was shown mathematically, in a previous note,[1] that it should be possible to demonstrate which mechanism, film diffusion or mass action, is rate controlling for exchanger systems. During the present investigation it became evident that, for organolites, although mass action could be ruled out, neither particle nor film diffusion alone is rate controlling. This coupled process has been referred to as the *Intermediate* mechanism by Kressman and Kitchener.[2] The present development provides a unified method for distinguishing not only the different rate processes, chemical and diffusional exchange, but also the relative proportion of film and particle diffusion.

Previous studies[3-6] have not satisfied the optimum requisites of the film diffusion theory in that only for complete exchange does the functional difference between the mass action and film diffusion expressions become sufficiently different to allow experimental detection. Thus, Juda and Carron[5] found that bimolecular kinetics described their rate data for the Na^+–H^+ exchange in dilute solution; they did not, however, venture any conclusions as to the actual nature of the rate-determining step. Other workers[2,3,4,7,8] have assumed that the rate constant dependence upon flow velocity and stirring rate, outer solution concentration, particle size and low activation energies were sufficient criteria for postulating the diffusional mechanism. It seems probable now that these are indeed sufficient.

Theory

It was shown[1] that the permeation rate of species A in the exchange reaction

$$A^+ + BR = B^+ + AR \qquad (1)$$

through a bounding liquid film of thickness R° into a spherical organolite particle with surface area Σ, with the restriction of resin electroneutrality, is

$$P_A = -P_B = \frac{D_A^\circ D_B^\circ}{R^\circ}\left(\frac{KC_AQ_B - C_BQ_A}{D_AQ_A + KD_BQ_B}\right) \qquad (2)$$

D_A° and D_B° are the solution diffusion constants of the two species A and B, C_A, C_B, Q_A and Q_B are the outer solution concentrations and the mole fractions on the resin sites of the two exchanging species and K is the concentration equilibrium constant. The quantities $\bar{C}_A$ and $\bar{C}_B$ are the interstitial (perhaps virtual) concentrations presumed to be in instantaneous equilibrium with the exchanger, hence governed by

$$K = \frac{\bar{C}_BQ_A}{\bar{C}_AQ_B} \qquad (3)$$

For film diffusion alone, the rate expression (2) may be integrated, and if the outer solution concentration for the species B, in the resin phase originally, be kept equal to zero while that for species A kept constant and equal to C_A°, one finally obtains

$$-\frac{1}{t}\ln(1 - Q_A) = \left(1 - \frac{KD_B^\circ}{D_A^\circ}\right)\frac{Q_A}{t} + k$$

where

$$k = \frac{\Sigma D_A^\circ KC_B^\circ}{ER^\circ} \qquad (4)$$

Thus film diffusion can be distinguished simply from chemical exchange since the latter is given by

$$-\frac{1}{t}\ln(1 - Q_A) = k$$

and the slope of the plot of $(1/t)\log(1 - Q_A)$ *vs.* Q_A/t will be zero.

Even keeping the restriction that $C_B = 0$, $C_A = C_A^\circ$ a constant, in examining the equations for coupled film and particle diffusion, one finds that equation 2 introduces a non-linear boundary condition. However, the addition of the further restrictions that $D_A^\circ = D_B^\circ$, similarly for the resin diffusion constants $D_A = D_B$, and $K = 1$ reduces the problem to that of particle heat transfer with radiation.[9] While very specialized, the solution, nevertheless, provides some insight into the general problem.

Defining the new variable $u = r(Q_A^\infty - Q_A)$, r measuring the distance from the center of the particle of radius R, Fick's second law of diffusion, written in spherical polar coördinates, is

$$D\frac{\partial^2 u_A}{\partial r^2} = \frac{\partial u_A}{\partial t} \qquad (5)$$

and the boundary conditions are

$$\frac{\partial u_A}{\partial r} + \left(\theta - \frac{1}{R}\right)u_A = 0 \qquad \text{at } r = R \qquad (6)$$

$$u_A^\circ = rQ_A^\circ(r) \qquad \text{at } t = 0 \qquad (7)$$

$$u_A = 0 \qquad \text{at } r = 0 \qquad (8)$$

(1) A. W. Adamson and J. J. Grossman, *J. Chem. Phys.*, **17**, 1002 (1949).

(2) T. R. E. Kressman and J. A. Kitchener, *Discussions of the Faraday Society*, **7**, 90 (1949).

(3) G. E. Boyd, A. W. Adamson and L. S. Myers, Jr., *J. Am. Chem. Soc.*, **69**, 2836 (1947).

(4) G. E. Boyd, A. W. Adamson and L. S. Myers, Jr., *ibid.*, **72**, 4807 (1950).

(5) W. Juda and M. Carron, *ibid.*, **70**, 3295 (1948).

(6) F. C. Nachod and W. Wood, *ibid.*, **66**, 1300 (1944).

(7) D. K. Hale and D. Reichenberg, *Discussions of the Faraday Society*, **7**, 79 (1949).

(8) R. Kunin and R. J. Myers, THIS JOURNAL, **51**, 1111 (1947).

(9) L. R. Ingersoll, O. J. Zobel and A. C. Ingersoll, "Heat Conduction," 1st Edition, McGraw-Hill Book Company, Inc., New York N. Y., 1943, pp. 169–174.

where

$$\theta = \frac{D^\circ f}{DR^\circ}; \quad f = \frac{VC_A}{\alpha E Q_A} \tag{9}$$

V is the solvent vol./g. resin and α is the degree of ionization. The general solution for the average concentration $<Q_A>$, in the resin at time t may be written as

$$\frac{Q_A^\infty - <Q_A>}{Q_A^\infty - Q_A^\circ} = \frac{6\theta^2}{R^2} \sum_{a=1}^{\infty} \frac{A_a \sin^2 m_a R}{m_a^4} e^{-Dm_a^2 t} \tag{10}$$

where the coefficients A_a are given by

$$A_a = \frac{m_a^2 R^2 + (\theta R - 1)^2}{m_a^2 R^2 + (\theta R - 1)\theta R} \tag{11}$$

The eigenvalues m_a are discussed below.

Equation 10 permits an examination of the intermediate case since the diffusional exchange character is regulated by the ratio

$$\frac{RD^\circ f}{DR^\circ} \equiv \frac{RD^\circ VC_A^\circ}{DR^\circ E\alpha} \tag{12}$$

such that as it approaches zero, equations 10 and 11 reduce to the film diffusion equations derived previously by Boyd, Adamson and Myers[3]

$$\frac{Q_A^\infty - <Q_A>}{Q_A^\infty - Q_A^\circ} = e^{-\frac{3D^\circ f}{RR^\circ}t} \tag{13}$$

and as the ratio approaches infinity, the particle diffusion equation

$$\frac{Q_A^\infty - <Q_A>}{Q_A^\infty - Q_A^\circ} = \frac{6}{\pi^2} \sum_{n=1}^{\infty} \frac{1}{n^2} e^{-\frac{n^2\pi^2 Dt}{R^2}} \tag{14}$$

is recovered.[3]

Apparatus and Materials

Radioactive tracer techniques were used as an analytical tool for determining the resin concentrations continuously throughout the exchange run. Figure 1 shows, in block diagram form, the flow system and counting arrangement. The specially designed shallow bed lucite cell is shown in detail in Fig. 2.

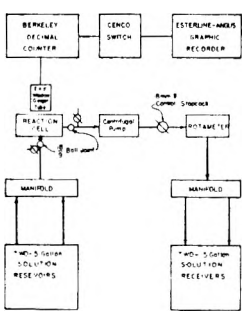

Fig. 1.—Flow diagram and counting circuit.

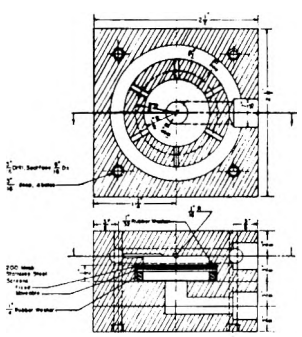

Fig. 2.—Lucite reaction cell.

The sulfonated polystyrene resin, Dowex 50, was furnished by the Dow Chemical Company, Midland, Michigan, and prepared as described by Marinsky.[10] After conversion to the hydrogen resin form and graded, air dried, with US standard series sieves, it was titrated with CsOH to which the radioactive isotope, Cs^{134} (0.7 and 1.8 mev. gammas, half-life 1.7 yr.) had been added. The radiocesium was shipped from the Oak Ridge Laboratories, Oak Ridge, Tennessee, as Cs_2CO_3. Solution concentrations were determined either by dilution or, in the case of HCl, by conductiometric titration. All chemicals were of C.P. grade.

(10) J. A. Marinsky, Office of Naval Research, Technical Report No. 34 ONR Contract N5 ori-07806, NR-026-001.

A 25-mg. radiocesium resin sample was introduced between the cell screens, the cell assembled, and connected into the flow system. The initial activity was determined as well as the background beforehand and at the completion of the run. The geiger tube was connected to a standard amplifier with a scale of 1000, and the scaled pulses were automatically recorded by means of an Esterline Angus Graphic Recording milliameter, operated with a chart speed of 12 in./min. Solution was circulated through the system by a centrifugal pump, the flow velocity regulated with a Pyrex, 8 mm. $ stopcock, and measured with a rotameter, range 0.4 to 3.7 l./min. Circulating large volumes of solution over a semi-micro resin sample guaranteed constant solution concentrations.

Experimental Results

The initial time was fixed by extrapolating the activity *vs.* arbitrary chart time back to the initial activity. Corrections were made for background and coincidence, the latter was 1.5% per 1000 cts./min. By plotting $(1/t) \log (A^\circ/A)$ *vs.* Q/T, where A is the activity at time t and A° the initial activity, the slope is found graphically and then used to compute the rate constant for each point. The expected deviation of 3% due to a 1000 count sampling is reflected in the 4% average deviation of individual rate constants from the mean. However, the large number of individual rate constant determinations reduce the probable error of the average value to 0.8%. If this degree of precision is desired, one should apply a least squares analysis to the slope determination.

TABLE I

FILM DIFFUSION RATE DATA AT 21°

Run[a] No.	Flow velocity, cm./sec.	Solution concn. × 10^3 M	Slope m	$k \times 10^3$ / 2.303	k / 2.303 × C_A°
3 H–CsR	24.8	1.816	0.475	0.269	0.148
5 H–CsR	48.4	1.816	.471	.364	.201
1 H–CsR	48.4	0.808	.401	.360	.446
2 H–CsR	18.4	0.923	.414	.160	.173
6 Na–CsR	48.4	1.799	.263	.708	.394
7 Na–CsR	48.4	0.976	.266	.329	.337

[a] Resin Dowex 50 (60–70 mesh).

The remaining data are represented graphically in Figs. 3 to 7 and the results compiled in Table I.

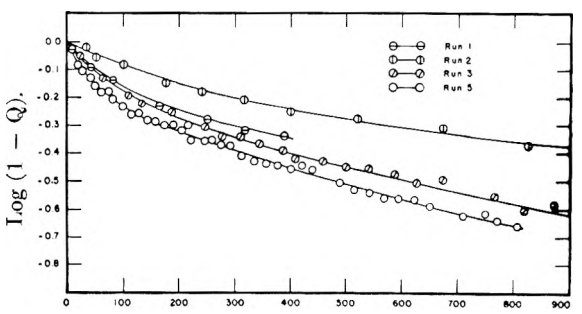

Fig. 3.—Hydrogen-cesium exchange: run 1, ⊖-⊖; run 2, -①①; run 3, ⊘-⊘; run 5, ○-○

Discussion

The film diffusion mechanism predicts that the non-zero slope $(1 - KD_B^\circ/D_A^\circ) \times 0.4343$ will differentiate this rate process from one chemically controlled. Since K, D_A° and D_B° are all positive quantities, the limits of variation for the slope m are

$$0.4343 > m > -\infty \tag{15}$$

If film diffusion were the rate-controlling process for the two exchange systems, H–CsR and Na–CsR, their slopes should be 0.274 and 0.172, respectively, as calculated from the data compiled in Table II.[11] Whereas the experimental slope, 0.263 for the Na–CsR exchange compares favorably with the calculated value, the slopes for the H–CsR exchange, ranging as high as 0.47, exceed even the maximum allowed value 0.4343.

TABLE II

DISTRIBUTION COEFFICIENTS AND DIFFUSION CONSTANTS

Reaction: HR + X = H + XR

X	K[12]	$D \times 10^{6}$
Li	0.61[a]	11.5
Na	1.20[a]	15.5
NH_4	1.20[a]	
K	1.50[a]	18.2
Cs	2.04[b]	19.1
Rb	2.22[b]	18.6
Tl	8.60[b]	
Ag	8.70[b]	
H	1.00	25.4

[a] Solution concentration 0.1 N. [b] Solution concentration 0.01 N.

It is of interest to note that particle diffusion dependent rate data tends to give a straight line when plotted according to the film diffusion equation, 4. Thus for the hydrogen ion exchange, a pure particle diffusion equation was fitted at one point, the remaining points calculated and, when graphed, a straight line with slope 0.41 was obtained, seemingly independent of the point used in fitting the equation to the experimental points. Therefore a straight line in a film diffusion plot does not serve in itself to distinguish film and particle diffusion although a non-zero slope rules out mass action immediately.

A second test for the film mechanism is that the ratio of the rate constant divided by the outer solution concentration, k/C°, should be invariant at constant flow velocity. This is found to hold true for the Na–CsR exchange. However, in the H–CsR exchange runs 1 and 5 show that k itself does not vary with concentration at constant flow velocity.

In an attempt to fit run 5 for the H–CsR exchange to a particle diffusion equation, it was found that the experimental curve could be sandwiched between two curves according to whether the constant $\pi^2 D/R^2$ is evaluated at the start or the end of the run. This effect can be interpreted in terms of a varying diffusion coefficient, D. Initially, the transport of H^+ ion into and through the resin is rate controlling while at the close of the exchange, the exceedingly low cesium concentration dominates the exchange rate. The intermediate region reflects this transition of control from hydrogen initially to cesium toward the end.

Although the H–CsR exchange is controlled mainly by particle diffusion and the Na–CsR exchange by film diffusion, each shows evidence that the other type of diffusion is present. Thus, film diffusion character is indicated for the H–CsR exchange by runs 3 and 5 since the rate constant increases with flow velocity at constant concentration. In the Na–CsR exchange, particle diffusion

(11) These values are presented as approximations since their use is open to theoretical objection.

(12) W. C. Bauman and J. Eichhorn, *J. Am. Chem. Soc.*, **69**, 2830 (1947).

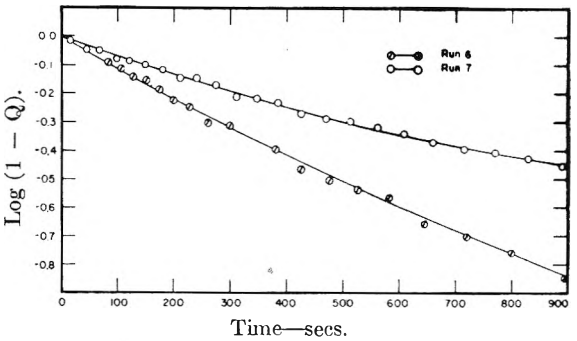

Fig. 4.—Sodium–cesium exchange: run 6, ⊘-⊘; run 7, ○-○.

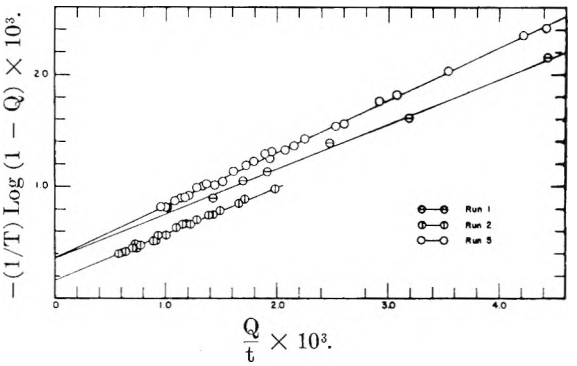

Fig. 5.—Film diffusion test, H–CsR exchange: run 1, ⊖-⊖; run 2, ⓘ-ⓘ; run 5. ○-○.

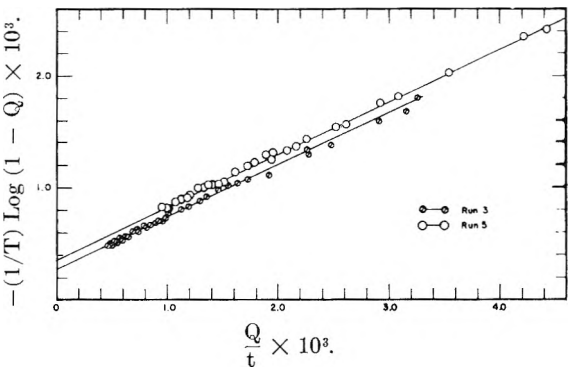

Fig. 6.—Film diffusion test, H-CsR exchange: run 3, ⊘-⊘; run 5, ○-○.

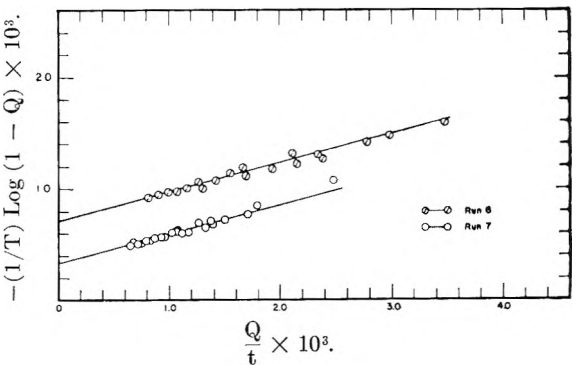

Fig. 7.—Film diffusion test, Na-CsR exchange: run 6, ⓘ-ⓘ; run 7, ○-○.

is indicated in the fact that the slope is 1.5 times greater than that calculated.

The quantity which regulates the diffusional type is, from equation 12, $RD^\circ f/DR^\circ$. It is related to the transcendental equation

$$m_a R = (1 - \theta R) \tan m_a R$$

derived from the boundary condition, equation 6, governing the eigenvalues m_a which are solutions of the simultaneous equations

$$y = \tan s \quad (16)$$
$$y = (1/b)\, s \quad (17)$$

where $s = m_a R$ and $b = 1 - \theta R = 1 - RD^\circ f/DR^0$. This ratio, expression 12, can vary between the limits 0 and ∞ for film and particle diffusion respectively. Representative intermediate diffusion is designated by setting the ratio equal to unity.

The film and particle diffusion constant ratio is approximately equal to 5 for alkali metal cations and does not vary greatly. One would predict only minor variations in the diffusional character with different members in a given series. This has been discussed by Boyd, Adamson and Myers.[4] The geometric volume and steric hindrance of large molecules can greatly increase the frictional coefficient for particle diffusion and thereby increase the diffusion coefficient well beyond 5. This effect has been reported by Kressman and Kitchener[2] for an exchange employing the large $PhNMe_2$-CH_2Ph^+ ion.

The film thickness, R°, is governed by hydrodynamical stability and it appears to be established that there is a minimum thickness attainable depending upon the agitation procedure.[2] Though it may not be possible to obtain a film sufficiently thin to allow particle diffusion to dominate the exchange rate, reducing the flow velocity will favor film diffusion. A more flexible method would be to vary the particle size, R, from colloidal particles to millimeter spheres.

Concentration effects are perhaps of greatest interest. The diffusion efficiency, $f = C_A V/\alpha Q_A E$, equation 9, is related to that fraction of the ions which are free to diffuse out of the resin phase as compared with those free to diffuse in the resin phase itself. Decreasing the outer solution concentration decreases f favoring film diffusion. On the other hand, Q is the mole fraction on the resin sites only if the resin is completely ionized. When a chemical equilibrium exists, as in the case of a weak acid resin, the fraction of ions available for diffusion in the resin phase is decreased to αQ where α is the degree of ionization.[13] Hence f becomes larger, favoring particle diffusion. The fact that the H–CsR exchange is governed by particle diffusion can be understood in this way, for even though the diffusion rate of hydrogen is larger than that for sodium, the sulfonic acid equilibrium is capable of reducing the particle hydrogen ion concentration sufficiently to permit particle diffusion to become rate controlling.

f depends also upon the ratio V/E. Comparing resins of equal porosity V, a greater exchange capacity favors film diffusion while for resins with equal exchange capacity, a greater porosity (less crosslinking for example) favors particle diffusion.

(13) Since α is dependent upon the degree of exchange, it will vary throughout the exchange and the equations are incomplete for this case. However, the degree of ionization is always less than unity and the effect on f always favors particle diffusion. The explicit expression for α for the weak acid type resin in an exchange similar to the H–CsR system can be shown to be

$$\alpha = 2\left[\left(\frac{4(K_H + 1 - Q_H)}{K_H^2} + 1\right)^{1/2} + 1\right]^{-1}$$

ELECTROCHEMICAL PROPERTIES OF A PERMIONIC ANION MEMBRANE[1]

BY J. T. CLARKE, J. A. MARINSKY, W. JUDA, N. W. ROSENBERG AND S. ALEXANDER

Ionics, Incorporated, 152 Sixth Street, Cambridge, Massachusetts

Received August 30, 1951

Correlation of diffusion, transport number and conductivity data with the chemical equilibria considered to exist in a weakly basic anion exchange medium has been reported. The data are consistent with the assumption that the resin studied (PERMIONIC ARX-44) has the properties of a simple electrolyte solution phase in which the resin salt is partially dissociated with a dissociation constant less than 1 and greater than 0.1.

In this paper, Donnan diffusion, transport number and conductivity data have been compiled in an attempt to define the chemical nature of PERMIONIC (Trade-mark) ARX-44, a weakly basic anion membrane (a continuous sheet of anion-exchange material). On the basis of these data, correlation of the electrochemical properties of the anion membrane with the chemical equilibria considered to exist in a membrane–solution system has been made and is reported.

An ion-exchange resin has been considered as an essentially homogeneous solid electrolyte solution containing randomly distributed immobile ions extended from a solid–insoluble matrix into an aqueous gel phase which contains mobile ions of opposite and equivalent charge. The electrochemical properties of such a system are expected to be determined by this physical structure, the chemical nature of the ion-exchanger, and the chemical system in which it is utilized. The presence of a high ion density in the gel phase of the ion-exchange resin should reduce diffusion into the exchanger of any ionized electrolyte in equilibrium with it. Electrochemical properties, for example conductivity and permselectivity, in a highly dissociated and concentrated ion-exchange resin gel phase are primarily a property of the mobile ions present in the gel phase. A literature survey of investigations con-

(1) Presented at the Ithaca, N. Y., Symposium on Complex Ions and Polyelectrolytes, June, 1951.

cerning Donnan diffusion, membrane potentials, and conductivities of membranes has been given elsewhere.[1a]

Preliminary Concepts

Donnan Equilibrium Involving Ion-exchange Gels.—The concepts underlying the equations which account for the chemical and electrochemical nature of ion-exchange materials considered as electrolytes have been discussed in detail in a separate paper (covering earlier work on strongly acid cation-exchange membranes) which has been submitted for publication elsewhere.[1] Considering an aqueous solution of salt M^+X^- in equilibrium with the resin gel phase, R^+X^-, a modified Donnan relation has been derived on the basis of the assumption of the equality of the activity of the component, MX, in the two phases, namely

$$K_D = [M^+]_r[X^-]_r/[M^+]_w[X^-]_w \qquad (1)$$

where M^+ and X^- are the activities of these ions and where the subscripts r and w denote the resin and water phases.

The Donnan constant K_D in equation (1) reduces to unity only when the ionization constants of the component, MX, and the standard state chemical potentials of MX are equal in both phases. Considering the resin as a partially ionized, homogeneous medium an internal ionization constant has been defined (2)

$$K_R = [R^+]_r[X^-]_r/[RX]_r \qquad (2)$$

where K_R is the ionization constant of the resin and R^+ and RX are the activities of the fixed positive ion and undissociated fixed group, respectively.

In the specific case of an anion membrane in the chloride form, RCl, in equilibrium with an aqueous NaCl solution, equation (1) takes the form of equation (3). However, the concentration of Cl^- ion in the resin gel phase is fixed by the requirement of electroneutrality and is equal to the sum of the Na^+ ion concentration and the R^+ concentration, equation (3a). Furthermore, the concentration of Cl^- ion in the solution must equal the concentration of Na^+ ion in the solution, equation (3b). Combination of these equations leads to equation (4).

$$K_D = \frac{[Na^+]_r[Cl^-]_r}{[Na^+]_w[Cl^-]_w} = \frac{(Na^+)_r(Cl^-)_r}{(Na^+)_w(Cl^-)_w} \times \frac{y^2_{\pm r}}{y^2_{\pm w}} \qquad (3)$$

$$(Cl^-)_r = (Na^+ + R^+)_r \qquad (3a)$$

$$(Na^+)_w = (Cl^-)_w \qquad (3b)$$

$$K_D' = K_D \frac{y^2_{\pm w}}{y^2_{\pm r}} = \frac{(Na^+)_r(Na^+ + R^+)_r}{(Na^+)^2_w} \qquad (4)$$

where ( ) = concentration, $y_\pm$ = mean ionic activity coefficient of NaCl, R^+ = fixed ionized resin groups.

The derivation of the above equations has considered a system at constant temperature, external pressure and charge. Even though the condition of constant charge may not be valid at the interface where a charge distribution may exist, an electrically neutral volume enclosing the interface and extending over a very short distance into each phase may be visualized and the uncertainty of electroneutrality in the system is probably not serious. The neglect of osmotic pressures exerted upon the interface, which in concentrated resin gels can be considerable,[1] is not a serious omission in the case of the anion membrane to be discussed in this paper. The internal volume of this PERMIONIC anion membrane does not vary greatly and the relations obtained by Gregor,[2] who considers the internal pressure effect, become the same as those given above for this reason.

Membrane Potentials and Transport Numbers.—An accepted technique for measuring transport numbers[3,4,5] in permselective membranes is the measurement of the electrochemical potential which arises when two solutions of different activities a_{w_1} and a_{w_2}, of the same salt are separated by a membrane. When silver–silver chloride electrodes are used as reference electrodes in equilibrium with the two solutions, then it has been shown[1] that the potential between the two electrodes is that of a concentration cell with transference (the mean ionic activity of NaCl in the resin phase at the interfaces, namely, a_{r_1} and a_{r_2}, being proportional to a_{w_1} and a_{w_2}, respectively). When calomel electrodes are used as references electrodes, then the measured potential gives the membrane potential directly subject to the presumably negligible error due to the difference in junction potentials between the saturated KCl and the NaCl solutions at activities a_{w_1} and a_{w_2}. The following derivation is similar to that given elsewhere,[1] except that the equations are derived for a system including calomel electrodes. The average transport number through the membrane can be related to the potential of this cell by considering several arbitrary cells which, when combined, are equivalent to the cell under study.

These cells include a calomel–AgCl cell, an AgCl in solution–AgCl in resin cell at equilibrium NaCl activities a_w and a_r and an AgCl in resin at activity of NaCl, a_{r_1}–AgCl in resin at activity of NaCl a_{r2}, cell with transference. The molar free energy changes, ΔF, involved in these cells are given by equations (5–9). The series summation of cells 5–9 results in cell 10, the cell under study, and the summation of the free energies involved yields the free energy change of this cell from which the potential of the cell can be expressed (equation 10).

$$Hg/Hg_2Cl_2\ (S),\ KCl\ (satd.)\ \vdots\ NaCl\ (a_{w_1}),\ AgCl/Ag \qquad (5)$$

$$\Delta F = \Delta F^\circ - RT \ln (Cl_{w_1} = a_{w_1})$$

$$Ag/AgCl,\ NaCl\ (a_{w_1})\ \vdots\ NaCl\ (a_{r_1}),\ AgCl/Ag \qquad (6)$$

$$\Delta F = 0$$

$$Ag/AgCl,\ NaCl\ (a_{r_1})\ \vdots\ NaCl\ (a_{r_2}),\ AgCl/Ag \qquad (7)$$

$$\Delta F = 2(1 - \bar{t}_-)\ RT \ln (a_{r_2}/a_{r_1} = a_{w_2}/a_{w_1})$$

$$Ag/AgCl,\ NaCl\ (a_{r_2})\ \vdots\ NaCl\ (a_{w_2}),\ AgCl/Ag \qquad (8)$$

$$\Delta F = 0$$

$$Hg/Hg_2Cl_2\ (S),\ KCl\ (satd.)\ \vdots\ NaCl\ (a_{w_1})\ \vdots\ NaCl\ (a_{r_1})\ \vdots \qquad (9)$$
$$NaCl\ (a_{r_2})\ \vdots\ NaCl\ (a_{w_2})\ \vdots\ KCl\ (satd.),\ Hg_2Cl_2/Hg\ (S)$$

$$\Delta F = RT\ (2\bar{t}_- - 1) \ln a_{w_2}/a_{w_1}$$

$$E = RT/F^*\ (2\bar{t}_- - 1) \ln a_{w_2}/a_{w_1} \qquad (10)$$

where $\bar{t}$ = transport number across the membrane,

(1a) W. Juda, N. W. Rosenberg, J. A. Marinsky and A. A. Kasper, in press.

(2) H. P. Gregor, *J. Am. Chem. Soc.*, **73**, 642 (1951).

(3) S. K. Mukherjee and C. E. Marshall, THIS JOURNAL, **55**, 61 (1951).

(4) K. Sollner, *ibid.*, **55**, 61 (1951).

(5) M. R. J. Wyllie and H. W. Patnode, *ibid.*, **54**, 204 (1950).

averaged with respect to ln a between the limits at the two membrane faces; F^* = Faraday constant.

An ideally permselective anion membrane has an activity-independent t_- equal to unity. Hence, the limiting value of equation (10) is given by equation (11). The average value of t_- with respect to a_r in the range $a_{r_1} - a_{r_2}$ is then defined by equation (12). Thus, a knowledge of the activities of the two aqueous solutions in contact with a membrane and a measurement of the potential between them when separated by a membrane will yield the value of an average transport number $\bar{t}_-$ in the membrane phase

$$E_0 = RT/F^* \ln a_{w_2}/a_{w_1} \quad (11)$$

$$\bar{t}_- = \frac{E + E_0}{2E_0} = \frac{E}{2E_0} + 0.5 \quad (12)$$

If the differences between the concentrations of aqueous solution equilibrated with the resin is small, a negligible error is introduced by assuming that t_- is linear in ln $[a]_w$. The measured t_- then becomes equal to that obtainable in the limit, in a solution of ionic activity given by the geometric mean of the two ionic activities of the solutions used in the measurements.

Membrane Conductivity.—It has been assumed that the transport number of an ideally permselective anion membrane is unity. In the present case, the physical nature of the idealized membrane is such that presumably only the mobile ion group (Cl^-) is capable of transferring current; thus, the electrical conductivity of the membrane may be written as in equation (13). Since t_- is defined by equation (14) and since the Donnan diffused electrolyte contributes to the conductance, the actual conductivity of the membrane is given by equation (15).

$$1000\,\kappa^\circ = \lambda^\circ_{Cl}(Cl^-)^\circ_r \quad (13)$$

$$t_- = \frac{\lambda^\circ_{Cl}(Cl^-)_r}{\lambda^\circ_{Cl}(Cl^-)_r + \lambda_{Na}(Na^+)_r} = \frac{1}{1 + \frac{\lambda_{Na}(Na^+)_r}{\lambda_{Cl}(Cl^-)_r}} = \frac{1}{1 + \frac{\lambda_{Na}(A)}{\lambda_{Cl}(A + R^+)}} \quad (14)$$

$$1000\kappa = \lambda_{Cl}(Cl^-)_r + \lambda_{Na}(Na^+)_r = \lambda_{Cl}(A + R^+) + \lambda_{Na}(A) \quad (15)$$

where λ = equivalent ionic conductance in the resin phase, κ = specific conductivity of resin phase.

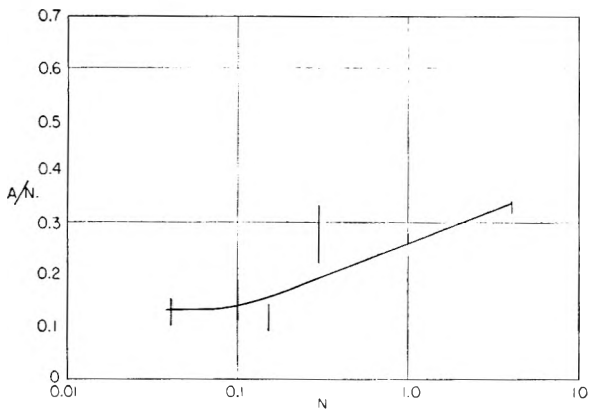

Fig. 1.—Donnan diffusion of NaCl into PERMIONIC ARX-44.

Experimental

All measurements were made exclusively with felt-backed membranes, the felt constituting about 10% of the membrane strip on the basis of its wet weight. These membrane samples were cycled between the Cl^- and NO_3^- ion forms at least once before any measurements were made. A description of the experimental technique used follows.

Capacity Determination.—Membrane samples, 7.5 cm. long, 1.9 cm. wide and 0.1 cm. thick in the Cl^- ion form and in equilibrium with 1 N HCl were leached by rapid stirring for 15–30 minute intervals with three 100-ml. portions of distilled water adjusted to a pH value of 2.1–2.5 with HCl. A fourth and final equilibration of 15 hours in the slightly acid leach water was accomplished next. The membrane samples were then contacted and agitated for 15-minute intervals with three successive 100-ml. portions of 1 N $NaNO_3$ about 0.01 N in HNO_3 to convert the resin to the NO_3^- ion form, the Cl^- ion released from the membranes being determined by the Mohr method. The samples were then reconverted to the Cl^- ion form, after leaching as before, with three 15-minute contacts with 100-ml. portions of 1 N HCl. The leaching and capacity determination steps were then repeated.

Moisture and Density Determination.—Samples of leached Cl^- ion form membrane were wiped dry and the dimensions of each sample were obtained by direct measurement, the thickness being determined with a micrometer. The samples, weighed to the nearest 0.01 g., were then dried at 110° for 1 hour to constant weight and were reweighed.

The capacity, moisture content and density of the felt-backed PERMIONIC anion membrane studied are presented below in Table I. In this table, the capacity is expressed in normality (meq./ml. of wet membrane), the moisture content is given in g./wet g. of membrane and the density is reported in g./ml. of wet membrane. All these determinations are reproducible to about 5%.

TABLE I

CHARACTERISTICS OF PERMIONIC ARX-44

Capacity (normality)	1.75 ± 0.05
Water content (g./wet g.)	0.45 ± 0.02
Density (g./ml.)	1.20 ± 0.03

Donnan Diffusion Determinations.—Weighed samples of membrane material converted as before to the leached Cl^- ion form were equilibrated by three 15–20 minute contacts with 100-ml. portions of NaCl solution of the concentration, N, under investigation. Before equilibration, all NaCl solutions employed were adjusted to a pH value of 2.1–2.5 with HCl. After equilibration, the membranes were removed, wiped dry and finally agitated for 10–15 minute periods with three successive portions of the slightly acid leach solution. The combined leachings were then evaporated to dryness to evolve HCl and were titrated for Cl^- ion after solution of the NaCl residue in a small volume of distilled water. In the dilute region, Na was detected directly by radiochemical assay of 3 y Na^{22} added to the equilibrating systems.

The Donnan diffusion data obtained from measurements made over a range of solution concentrations varying from 0.03 to 3.0 N are plotted in Fig. 1 with the ratio of adsorbed to solution chloride, A/N, as the ordinate, and the solution concentration, N, as the abscissa. The width of the lines designating these observed points indicate the probable error of the measurement.

Membrane Potential Measurements.—A Lucite cell consisting of two individual chambers, 1.3 cm. thick and 1.3 cm. in diameter (3-ml. capacity) was fitted with calomel electrodes as shown in Fig. 2. For the potential measurements at various concentration ranges, membrane samples 0.1 cm. thick and 2 cm. in diameter were inserted into this cell and the continuous flow of two NaCl solutions of concentration N_1 and N_2 with N_1/N_2 always equal to 2 was initiated. Steady potential readings on a Leeds and Northrup Type K-2 Potentiometer were always obtained in a time interval of 5–10 minutes, the final potential value being obtained at very rapid flow rates of 10–100 ml./min. where the potential was found to be independent of flow rate.

Table II presents the experimental potentials, E (precise to ±0.2 mv.), and the theoretical E° values in mv. which cor-

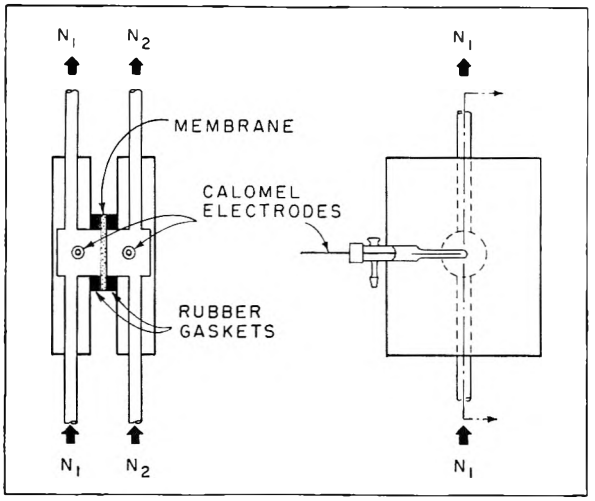

Fig. 2.—PERMIONIC membrane cell for the determination of transport numbers.

respond to each pair of concentrations for the NaCl solutions studied.

TABLE II

EXPERIMENTAL AND THEORETICAL MEMBRANE POTENTIAL VALUES

$N_1 - N_2$, N	E_0	E
3.2 -1.6	−21.9	− 9.9
1.6 -0.8	−18.3	−12.5
0.8 -0.4	−16.9	−13.3
0.4 -0.2	−16.6	−14.0
0.2 -0.1	−16.2	−14.8
0.8 -0.05	−16.5	−15.5
0.05-0.025	−16.7	−15.7

In Fig. 3, the transport number of Cl^- ion in the anion membrane equilibrated with NaCl is plotted *vs.* $\bar{N}$ where $\bar{N}$ is the geometric mean of N_1 and N_2. To obtain the Cl^- ion transport number as a function of solution concentration, the observed potential, E, was divided by $2E_0 = 108 \log a_1/a_2$ (where a_1 and a_2 were the known activities (Harned and Owen) of the various solutions of concentration N_1 and N_2) and 0.5 was added to the resultant value.

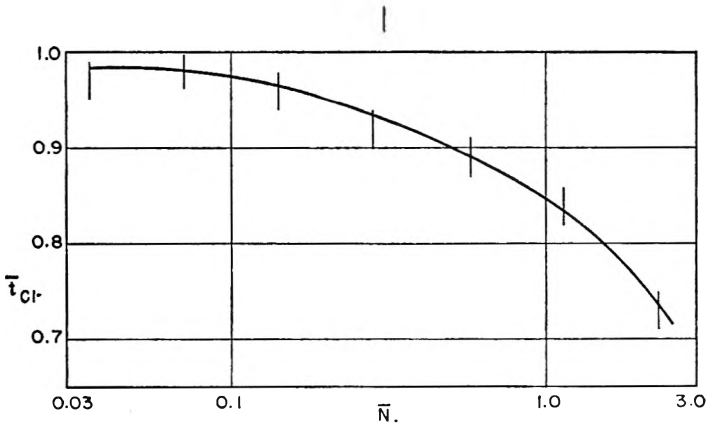

Fig. 3.—Chloride transport numbers across PERMIONIC ARX-44 in NaCl solutions.

Conductivity Determinations.—The conductance of thin membrane strips was determined using a "Solu-Bridge" (Industrial Instrument Company, New Jersey), a simple 60 cycle a.c. bridge circuit without capacitance correction. The strips were converted to the Cl^- ion form, were completely leached, and were then equilibrated with a solution of the desired concentration, the various solutions used being adjusted to a *p*H value of 2.1–2.5 as before. After wiping the strips free of adhering solution and protecting them from moisture loss by a thin latex wrapper paper, they were clamped into place by the electrode fingers of the cell as illustrated in Fig. 4 and bridge readings were made. The cell constant was obtained by a measurement of the dimensions of the membrane. The reliability of this simple method has been established previously by comparison with considerably more elaborate Jones bridge conductance measurements on cation membranes.[1]

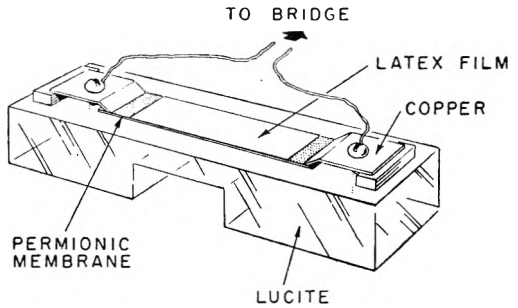

Fig. 4.—Cell used for the determination of the conductivity of PERMIONIC membranes.

A logarithmic plot of the conductivities measured is compared with the conductivity of NaCl in Fig. 5. As before,

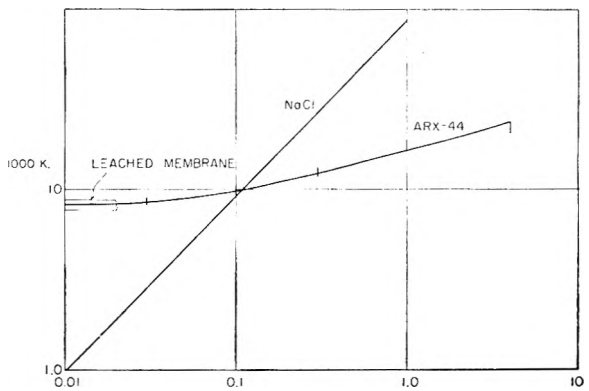

Fig. 5.—Specific conductivity of PERMIONIC ARX-44 compared with specific conductivity of NaCl.

the width of the lines designating the measured points are an indication of the probable error in these data.

The weakly basic nature of PERMIONIC ARX-44 required the careful definition of experimental procedure as described above. For example, it was found that during equilibration of the Cl^- ion form of the membranes with distilled water, hydrolysis of the resin always decreased the *p*H value of the leach water to 2.5 with a consequent decrease in Cl^- ion capacity. For this reason, the chloride form of the membrane was always kept in contact with solution at a *p*H value of 2.1–2.5.

It was also determined that the resin capacity for Cl^- ion was, as expected, a function of the *p*H of the Cl^- ion solution employed during conversion; the lower the *p*H value, the higher the Cl^- ion capacity. A standard conversion procedure was therefore selected. A solution of HCl rather than NaCl was employed to avoid variations in capacity due to hydrolysis of a membrane during numerous conversions. Once the membrane is partially converted to the basic form by hydrolysis, the Cl^- ion from NaCl cannot exchange with the weakly dissociated basic form of the resin.

Since the Cl^- ion capacity of these membranes is a function of *p*H, sufficient time was necessarily allowed during the leaching steps with dilute HCl (*p*H 2.1–2.5) to permit equilibration of the system. It was found that if the fourth leach of 15 hours were not incorporated in the procedure,

high and inconsistent values were obtained for the Cl^- ion capacity of ARX-44.

Discussion

The only evidence for non-conformity of membrane behavior with that expected on the basis of theoretical considerations has been the observation that the Donnan salt ratio, A/N, apparently is constant in the dilute region (Fig. 3). It was felt that in the dilute region A/N would continue to decrease since an increasingly stronger screening effect is expected due to an increase in the fraction of R^+ ions from a partially ionized anion membrane.

Good agreement between the observed behavior of PERMIONIC ARX-44 and that predicted from the preliminary concepts discussed earlier has been obtained in every other respect. It has been found that the resin salt, RCl, is apparently only partially ionized, the value of its ionization constant falling between 0.1 and 1.

In obtaining this result, the mathematics employed in an earlier paper[1] was applied. A series of K_R values were selected and equation (2) was solved to determine R^+ as a function of adsorbed Cl^- ion (A) for each K_R value. In Fig. 6, a family of R^+ *versus* A curves obtained in this manner are compared with "experimental" R^+ values calculated from equation (14). Each synthetic curve corresponds to an arbitrarily chosen value of K_R. The experimental R^+ curve is obtained by employing $\bar{t}_{Cl}$ values measured in the course of this study; the width of the line representing each "experimental" R^+ value is an estimate of the possible deviation of each value which arises from experimental error in the transport number measurements.

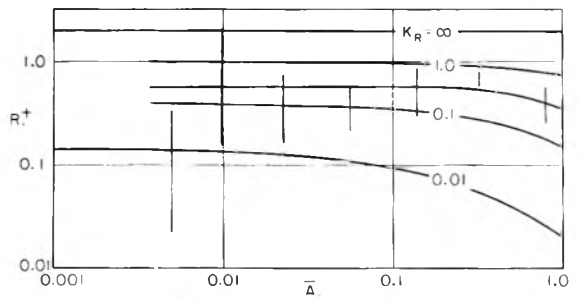

Fig. 6.—R^+ *versus* $\bar{A}$ for various K_R values compared with "experimental" R^+ *versus* $\bar{A}$ values.

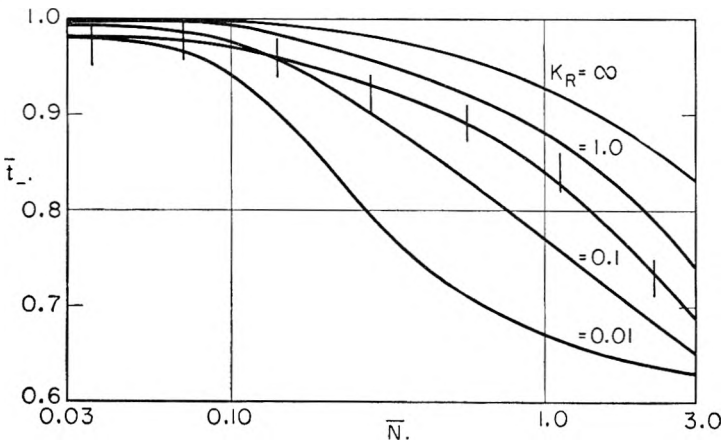

Fig. 7.—Comparison of experimental $\bar{t}_-$ values with calculated $\bar{t}_-$ values assuming various K_R values for the PERMIONIC ARX-44 membrane in NaCl solutions.

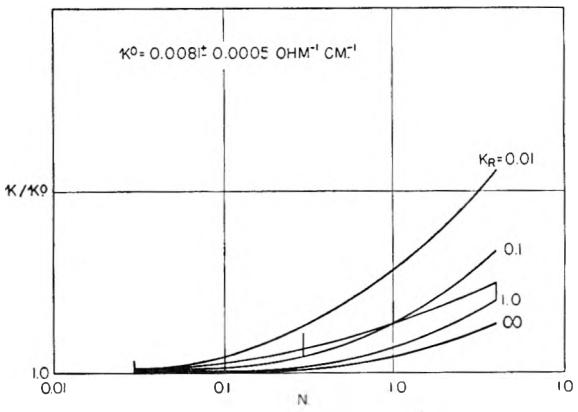

Fig. 8.—Experimentally determined $K/K°$ values compared with $K/K°$ values assuming various K_R values for the PERMIONIC ARX-44 membrane.

The values of R^+ (synthetic) were then substituted in equation (14) to obtain a family of $\bar{t}_{Cl}$ *versus* A curves corresponding to the selected K_R values. In Fig. 7 these curves are compared with $\bar{t}_{Cl}$ values experimentally determined for the membrane equilibrated with NaCl solutions (Fig. 3).

Finally a family of $\kappa/\kappa°$ curves corresponding to these K_R values were calculated by dividing equation (13) by equation (15). These are compared in Fig. 8 with the experimental data obtained for NaCl, the specific conductivity of the leached membrane being employed as the $\kappa°$ value.

$$K_R = \frac{[R^+]_r[Cl^-]_r}{[RCl]_r} = \frac{[R^+]_r[A + R^+]_r}{[C - R^+]_r} \times \frac{y_r^{\pm}}{y} \quad (2)$$

$$1000\,\kappa° = \lambda°_{Cl}(Cl^-)_r° = \lambda°_{Cl}(R^+)_r° \quad (13)$$

$$\bar{t}_{Cl} = \frac{\lambda_{Cl}(Cl^-)_r}{\lambda_{Cl}(Cl^-)_r + \lambda_{Na}(Na^+)_r} = \frac{1}{1 + \frac{\lambda_{Na}(Na^+)_r}{\lambda_{Cl}(Cl^-)_r}} = \frac{1}{1 + \frac{\lambda_{Na}(A)}{\lambda_{Cl}(A + R^+)}} \quad (14)$$

$$1000\kappa = \lambda_{Cl}(Cl^-)_r + \lambda_{Na}(Na^+)_r = \lambda_{Cl}(A + R^+) + 0.61\lambda_{Cl}(A) \quad (15)$$

For these calculations the capacity (C) reported for the felt-backed membrane in Table I could not be used. Correction for the 10% inert felt material present in the membrane samples studied was necessary. Considering the density of resin and felt to be approximately equivalent, the measured capacity, expressed in normality per ml. of membrane, was therefore multiplied by a factor of 1.1 to estimate the actual capacity of the resin samples.

Successful correlation of the electrochemical properties of the anion membrane with the chemical equilibria considered to exist in the membrane–solution system has resulted. The experimental $\bar{t}_{Cl}$, R^+ and $\kappa/\kappa°$ curves indicate quite clearly that the ionization constant K_R, of the Cl^- ion form of ARX-44, is a value less than 1 and greater than 0.1.

A more quantitative interpretation of the data should not and will not be attempted because of errors introduced by making the simplifying assumptions necessary to facilitate this correlation. For example, the ionic activity coefficients in the gel phase were considered to be equal to unity as a first approximation. With respect to application of equation (14) the value of $\lambda_{Na}/\lambda_{Cl}$, in the absence of independent measurements of the ionic mobilities in the membrane, was taken to be constant and equal to 0.61, the limiting value determined from t^+ measurements of the PERMIONIC CR-41 membrane in concentrated NaCl solutions at 25° and 1–3 *N* in concentration.

For the purpose of comparing the conductance data, the assumption of the constancy of ion mobility as well as ion mobility ratios was made when employing equations (13) and (15).

REMARKS

ARTHUR W. ADAMSON: The use of the Donnan equation raises the question of the relative relevance of the Mass Action and Donnan approaches. The two systems are summarized below for the anion exchange

$$M^+, X^- + RY = RX + M^+, Y^-$$

	Mass action	Donnan
(A)	$K_a = \frac{a_{RX}a_{Y^-}}{a_{RY}a_{X^-}}$	$1 = \frac{(a_{X^-})_R a_{Y^-}}{(a_{Y^-})_R a_{X^-}}$

since

$$(a_{M^+})_R(a_{X^-})_R = a_{M^+}a_{X^-}$$
$$(a_{M^+})_R(a_{Y^-})_R = a_{M^+}a_{Y^-}$$

Standard state definitions:

(B)
$$a_{RX} \longrightarrow N_{RX} \text{ as } N_{RX} \longrightarrow 1$$
$$(a_{Y^-})_R \longrightarrow (c_{Y^-})_R \text{ as } (c_{M^+})_R \longrightarrow 0$$
$$a_{RY} \longrightarrow N_{RY} \text{ as } N_{RY} \longrightarrow 1$$
$$(a_{X^-})_R \longrightarrow (c_{X^-})_R \text{ as } (c_{M^+})_R \longrightarrow 0$$

If resin phase is ideal:

(C) $$K_N = N_{RX}a_Y/N_{RY}a_X \qquad 1 = c_{RX}a_Y/c_{RY}a_X$$

Comparison of equations (A) and (B) demonstrates the thermodynamic identity of the two formulations, and that the equilibrium constants differ numerically only because of the difference in the formulation of the standard states. However, when ideal behavior is assumed, then the two treatments diverge considerably.

From the Mass Action viewpoint, the ideal system is one of a resin solid solution. Since the resin salt, RX, is essentially insoluble, the activity of the *exchangeable ion on the sites* is very low; there is more or less void space, and this is occupied by solution of essentially the same composition as externally. Thus, in the present case, there would be two "types" of chloride ion in the resin phase: chloride ion which is occupying a site position, and chloride ion in the interstitial solution.

From the Donnan viewpoint, the resin phase, ideally, is merely an aqueous salt solution with a special charge restriction due to the fact that one of the ions (R) cannot migrate. All the chloride ion is identical, and hence the activity of chloride ion, ideally, is the sum of the capacity of the resin, and of the "sorbed" salt. The Donnan viewpoint is certainly the proper model for the case of two solutions separated by a membrane, but can be overdone in heterogeneous equilibrium. A simple illustration will suffice. The ideal equation (4) is given for the amount of "sorbed" salt in the case of RCl immersed in NaCl, and leads to the conclusion, for example, that in 1 *M* NaCl there is about 0.2 *M* Na^+ within the resin phase. Now the system AgCl in NaCl is formally entirely analogous to the above, yet I am sure that no one would argue the even approximate validity of (4) in this case! Here, clearly the Mass Action approach is best.

I have stressed the differences between the idealized versions of the two approaches because, firstly, of the tendency to assume that neglect of activity coefficients for the resin phase will *not* introduce *major* errors. A glance at equation (C) makes it apparent that such neglect is more serious with the Donnan ideal equation than with the Mass Action one since, while equilibrium constants do remain roughly *constant* over a range of resin composition, they in general will differ considerably from the value of *unity* predicted by the Donnan equation. I would therefore question the authors' assumption that such neglect will permit even approximate validity to their treatment of the dissociation constant for RX (what is the activity coefficient value for R^+?).

The second reason for stressing this different between the two approaches is that the models upon which they are based suggest quite different interpretations of the conductance and transference results. Thus, on the basis of the Donnan approach, the authors can predict that t^- will decrease with increasing external solution concentration because of the increase in "sorbed" electrolyte given by (4); conversely, from the data, the concentration of the latter can be calculated if it is assumed that the mobilities of Na^+ and Cl^- ions bear a prescribed ratio in the resin phase. This last calculation does not involve any approximations with activity coefficients. The authors find that a somewhat better fit to their data is obtained if it is assumed that 90% to 99% of the capacity is non-ionic (corresponding to their K_R value of 0.1 to 0.01), or, essentially, that this fraction of the Cl^- on the exchange sites is *different* from that in solution.

The above finding is virtually what would be *predicted to begin with* by the Mass Action approach, namely, that the ions on the sites are different, and do not contribute to the activity of the interstitial electrolyte. It seems quite likely, moreover, that the entire set of data could very reasonably be explained from the Mass Action point of view. The conductivity of the resin in pure water would now be considered to be due to two dimensional diffusion (this effect is quite important for salts adsorbed on such surfaces as glass, and there is no *a priori* reason not to expect it with exchangers). The increase in conductivity and decrease in t^- with increasing external solution concentration would be due to an increasing contribution of the interstitial electrolyte. The two unknowns (surface diffusion constant and mobility of the ions in the interstitial solution—undoubtedly different from the bulk value because of the "random" walk effect of the internal capillaries[6]) correspond to the two, K_R and K_0, used by the authors in their treatment.

Virtue can be claimed for one or the other of these models only insofar as can be justified empirically. The present transference and conductance data seem to be rather strong evidence that the ideal Mass Action approach is more nearly valid than the ideal Donnan approach. A second justification for the former is the one mentioned above, that resin phase activity coefficients are smaller when computed on the Mass Action formulation than when computed by the Donnan equations.

(6) The random walk treatment is being developed by Mr. J. J. Grossman.

ELECTROMIGRATION IN A CATION EXCHANGE RESIN. II. DETAILED ANALYSIS OF TWO-COMPONENT SYSTEMS

BY K. S. SPIEGLER AND C. D. CORYELL

Massachusetts Institute of Technology, Cambridge, Massachusetts, and Weizmann Institute of Science, Rehovoth, Israel[1]

Received August 30, 1951

Electromigration in a cation-exchange column flushed with deionized water was observed by tagging laminas of adsorbate with radiotracers and observing their migration in an electric field. It was shown that conductance is ionic and the current is carried only by the cations. Broadening of the tagged band occurs as electrolysis proceeds. As in aqueous solutions, the character of the boundary between two layers of cations depends on the ratio of their mobilities and remains sharp only if the slower ions follow the faster. When Dowex-50 in the sodium form is electrolyzed between platinum electrodes, the faster hydrogen ions produced at the anode penetrate the sodium layer by virtue of their higher mobility, slowing down the rate of migration of a tagged sodium lamina. The observed rate of migration of the band is somewhat higher than the rate calculated from the principle of independent ionic mobilities. If, on the other hand, a zinc anode is used, the boundary between sodium and zinc ions remains sharp. Applications of these phenomena for separations of ions and resin regeneration are discussed.

In a previous publication[2] there was presented a brief summary of an investigation of electromigration in columns of the cation-exchange resin Dowex-50. An electric potential was applied to a column of resin particles flushed continuously with deionized water. The migration of a layer of cations tagged with a radioisotope was observed by means of radioactive counting equipment. These studies are now extended and evaluated quantitatively for typical systems. The results are of general electrochemical interest and provide a framework for possible future application for separating ionic constituents of different mobility in the adsorbed state as well as for regenerating ion-exchange resins without the use of solutions.

It will be shown that the electromigration phenomena observed in cation-exchange resins are analogous to those observed in solutions and investigated in connection with the moving-boundary method for the determination of transference numbers in solutions.[3,4] On the other hand, as the resins are solid in the gross physical sense, certain disturbing factors, such as thermal convection,[5] are eliminated for the resins. Owing to the stoichiometric nature of ion binding and the high capacity, the resinous ion exchangers provide a very useful system for study.

Theory

When an electric potential is applied to a resin column containing different ionic species, concentration changes occur owing to the differences in the mobilities of these ions and also as a consequence of electrode reactions. It was shown[2] that the following electrode reactions occur when sodium Dowex-50 is electrolyzed between platinum electrodes

$$\text{Anode: } 4R^- + 2H_2O = 4HR + O_2(g) + 4e^-$$

$$\text{Cathode: } 4e^- + 4NaR + 4H_2O = 4R^- + 4Na^+ + 4OH^- + 2H_2(g)$$

where R^- represents one gram-equivalent of resin anion. A zinc anode reacts in the following manner

$$2R^- + Zn = ZnR_2 + 2e^-$$

These changes may lead to the formation of limited regions of different composition separated by sharp boundaries. The theory of the concentration changes occurring in electromigration in solutions was developed by F. Kohlrausch[6] and H. Weber[7] and their main conclusions were verified by the study of moving boundaries in aqueous solutions. Briefly, it was postulated and confirmed that if an electric field is applied to a solution phase, the ionic species tend to form a series of bands in the order of their mobilities. If initially a boundary exists between two solutions of electrolytes such that the faster ionic species is behind the slower one with respect to the direction of migration, mixing occurs, the faster ions tending to overtake the slower ones. In the reverse case, the boundary remains sharp provided the ratio of the equivalent concentrations c_{AX} and c_{BX} of the two solutions satisfies the relation

$$\frac{c_{AX}}{c_{BX}} = \frac{T_A}{T_B} \qquad (1)$$

where T_A and T_B are the transference numbers of cations A and B, respectively, with X the common anion.

In a cation-exchange resin in equilibrium with pure water, the cross-linked resin matrix remains in place and the current is carried by the cations only. (A proof of this assumption is given below in Table II.) Hence the transference numbers T_A and T_B and their ratio are unity. At a boundary between two regions AR and BR on Dowex-50, the ratio of the concentrations of A and B (defined in milliequivalents (meq.) per ml. of column space) is also approximately unity as the capacity of this resin (defined in the same units) for different cations is nearly the same. Hence condition (1) is always satisfied and the boundaries between AR and BR may be expected to remain sharp during electromigration provided the slower ions follow the faster.

The theoretical treatment of the concentration changes occurring in the presence of two types of resin-adsorbed ions in an electric field is considerably simplified by these considerations. It will be convenient to present this simplified treatment and to extend the theory to the interpretation of our

(1) This work was carried out in the Department of Chemistry and Laboratory for Nuclear Science and Engineering of the Massachusetts Institute of Technology.

(2) K. S. Spiegler and C. D. Coryell, *Science*, **113**, 546 (1951).

(3) L. G. Longsworth, *J. Am. Chem. Soc.*, **67**, 1109 (1945).

(4) D. A. MacInnes and L. G. Longsworth, *Chem. Revs.*, **11**, 171 (1932).

(5) A. Tiselius, *Nova Acta Reg. Univ. Upsaliensis*, **7** (4) (1930).

(6) F. Kohlrausch, *Wied. Ann.*, **62**, 209 (1897).

(7) H. Weber, *Sitz. Preuss. Akad. Wiss.*, 1897, p. 936; also "Die partiellen Differentialgleichungen der mathematischen Physik I," 4th ed., F. Vieweg, Braunschweig, 1900, pp. 481–506.

observations. As a first approximation, the resin column is treated as a homogeneous medium and diffusion is neglected. Some useful conclusions can be drawn from this approach although the resin columns are more complicated than this simple model.

Consider an element of a column of cross-section 1 cm.^{2} and length dz cm. containing two adsorbed ionic species A and B (Fig. 1) the concentrations of which at z are c_A and c_B meq. per ml. of column space. The potential gradient at z is E volt cm.$^{-1}$.

The conservation conditions for ions A and B, respectively, are

$$m_A E \left(\frac{\partial c_A}{\partial z}\right)_t + m_A c_A \left(\frac{\partial E}{\partial z}\right)_t + \left(\frac{\partial c_A}{\partial t}\right)_z = 0$$
$$m_B E \left(\frac{\partial c_B}{\partial z}\right)_t + m_B c_B \left(\frac{\partial E}{\partial z}\right)_t + \left(\frac{\partial c_B}{\partial t}\right)_z = 0 \qquad (2a, b)$$

where m_A and m_B are the ionic mobilities in cm.^{2} volt^{-1} sec.$^{-1}$, which are assumed to be independent of c_A and c_B. The time t is measured in seconds.

If the mobilities of A and B were equal (which is approximately true if they are isotopes of the same element), the potential gradient along the whole column would be uniform. Hence equation (2a) would reduce to

$$m_A E \left(\frac{\partial c_A}{\partial z}\right)_t + \left(\frac{\partial c_A}{\partial t}\right)_z = 0$$

The general solution of this equation is

$$c_A = f_A(z - m_A E t) \qquad (3)$$

f_A being an arbitrary function.

The shape of f_A for a particular problem is determined by the distribution of ions A at $t = 0$ and the meaning of equation (3) is that the band of ions A migrates at the rate $m_A E$ without changing its shape.

If the mobilities of the two ionic species are different, the potential gradient depends on their relative concentrations. In an ion-exchange resin, c_A and c_B are related by the equation

$$c_A + c_B = c_R \qquad (4)$$

where c_R is the (volume) capacity of the resin in meq. per ml. column space, independent of z and t. By subtracting (2b) from (2a) and substituting for c_B from (4) we obtain

$$2E \left(\frac{\partial c_A}{\partial z}\right)_t + (2c_A - c_R)\left(\frac{\partial E}{\partial z}\right)_t + \left(\frac{\partial c_A}{\partial t}\right)_z \left(\frac{1}{m_A} + \frac{1}{m_B}\right) = 0 \qquad (5)$$

This equation still contains the two variables $E(z, t)$ and $c_A(z, t)$; it may be reduced to an equation containing only one variable as follows: The number n of milliequivalents discharged per cm.^{2} sec. with current density of i milliamperes (ma.) per cm.^{2} is given by

$$n = \frac{i}{F} = E(c_A m_A + c_B m_B) = E[c_A(m_A - m_B) + c_R m_B] \qquad (6)$$

where F is the faraday constant. Defining a conductivity term $C(t, z)$ by

$$C(t,z) \equiv \frac{1000k}{F} = c_A(m_A - m_B) + c_R m_B \qquad (7)$$

where $k(t,z)$ is the specific conductivity of the resin

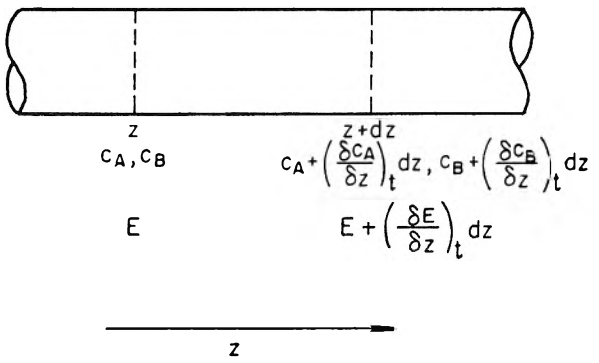

Fig. 1.—Section through an ion-exchange resin column. Current flows from left to right.

column element in mho cm.$^{-1}$, equation (6) can be written in the following manner

$$E = n/C \qquad (8)$$

As the current is constant along the column, n is independent of z. If the electrolysis is carried out at constant current, it is also independent of time. Hence

$$\left(\frac{\partial E}{\partial z}\right)_t = -\frac{n}{C^2}\left(\frac{\partial C}{\partial z}\right)_t \qquad (9)$$

Combining equations (7), (8) and (9), equation (5) can thus be written in terms of the variable C only

$$\left(\frac{\partial C}{\partial z}\right)_t + \frac{C^2}{nc_R m_A m_B}\left(\frac{\partial C}{\partial t}\right)_z = 0 \qquad (10)$$

It is convenient to transform this equation by introducing a resistance term θ defined by

$$\theta(z,t) \equiv \frac{(nc_R m_A m_B)^{1/2}}{C} = \frac{(nc_R/M)^{1/2}}{c_A(M-1) + c_R} = \frac{(nc_R/M)^{1/2}}{c_B\left(\frac{1}{M} - 1\right) + c_R} \qquad (11)$$

when M is the mobility ratio m_A/m_B.

It is seen that for a given resin and pair of ions, $\theta(z,t)$ is proportional to the specific resistance of the column element. Hence equation (10) reduces to

$$\left(\frac{\partial \theta}{\partial t}\right)_z + \theta^2\left(\frac{\partial \theta}{\partial z}\right)_t = 0 \qquad (12)$$

which describes the changes of specific resistance occurring along the column under the influence of a current of density nF. From θ the concentrations of the ionic species can be calculated using equation (11) provided the ratio of their mobilities and the capacity of the resin are known.

The general solution of equation (12) can be written only in the implicit form

$$\theta = f(z - \theta^2 t) \qquad (13)$$

where f is an arbitrary function which can be determined if, at the time $t = 0$, the values of θ are known for the length of the column.

One can represent $\theta(z,t)$ in a three-dimensional, rectangular system of coördinates. The geometrical meaning of equation (13) is the equality of all θ values corresponding to the straight lines in the z,t-plane whose equation is

$$z - \theta^2 t = \text{constant}$$

In other words, if at $t = 0$ a certain value θ_0 is

found at z_0, this same value θ_0 will be found at all points z, t defined by

$$z - \theta_0^2 t = z_0 \qquad (14)$$

Thus equation (14) represents the "equation of motion" of a certain concentration ratio c_A/c_B. The straight lines in the z,t-plane defined by equation (14) are called the characteristics of equation (12). Their slope $1/\theta_0^2$ is proportional to the square of the specific conductance of the resin element at $z = z_0$ and $t = 0$.

Figure 2 represents a plot of the characteristics for electromigration in a resin column containing an initial boundary between ZnR_2 and NaR at $z_0 = 0$.

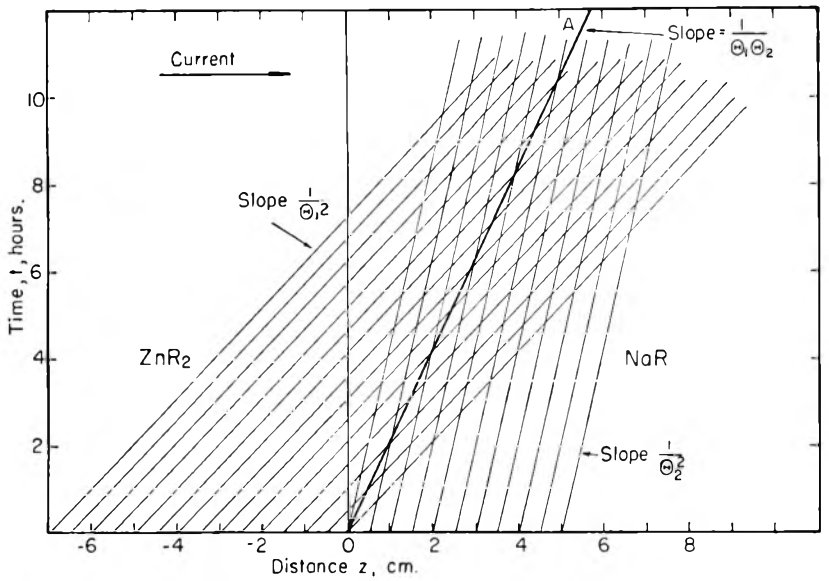

Fig. 2.—Characteristics of the system ZnR_2–NaR: R = Dowex-50 [80–100 mesh, (dry basis)]; i = 25 ma. c_R = 1.96 meq./ml.; $M = m_{Zn}/m_{Na} = 0.49$; $\theta_1 = 0.98$ cm.$^{1/2}$ hr.$^{-1/2}$ (ZnR_2 region); $\theta_2 = 0.48$ cm.$^{1/2}$ hr.$^{-1/2}$ (NaR region). Line OA describes the progress of the ZnR_2–NaR boundary.

The sodium ions migrate in front of the zinc ions. The slopes of the characteristics were obtained by substituting the experimental data for c_R (1.96 meq. per ml. column space), n (0.93 meq. cm.$^{-2}$ hr.$^{-1}$), and M (0.49) in equation (11). Left of the origin $c_A = c_{Zn} = c_R$ and right of it $c_B = c_{Na} = c_R$. Thus we obtain from equation (11) for the ZnR_2–NaR system at $t = 0$ left of the origin

$$\theta_1 = \left(\frac{n}{c_R M}\right)^{1/2} = 0.98 \text{ cm.}^{1/2} \text{ hr.}^{-1/2}$$

and right of the origin

$$\theta_2 = \left(\frac{nM}{c_R}\right)^{1/2} = 0.48 \text{ cm.}^{1/2} \text{ hr.}^{-1/2}$$

It is to be noted that the θ values are not properties of the compounds but of the system. The characteristics originating in these regions have the slopes $1/\theta_1^2$ or $1/\theta_2^2$, as shown in Fig. 2.

It is seen that in a definite region these characteristics intersect and hence θ is not unambiguously defined there. However, as at any point only one value of θ has a physical meaning, it may be concluded that in this region the value of θ can be either θ_1, as in the ZnR_2 layer, or θ_2, as in the NaR layer. Hence mixing of zinc and sodium ions does not occur and the boundary remains sharp. The rate of migration of the boundary, dz_B/dt, is given simply by the ratio between ion flux and concentration

$$\frac{dz_B}{dt} = \frac{n}{c_R} = \frac{i}{Fc_R} = \theta_1\theta_2 \qquad (15)$$

which is the reciprocal of the geometric mean of the slopes of the two sets of characteristics. The position of the boundary is given by line OA in Fig. 2. It is independent of M.

A different situation prevails if the fast ions are initially behind the slow ones. Figure 3 shows a plot of the characteristics for such a case, namely, an initial boundary between the hydrogen and sodium forms of the resin at $z = 0$, the latter being in front of the former. The values of c_R and n are the same as for Fig. 2. Using M' for the mobility ratio m_H/m_{Na}, which has the value 8.55, we have for left of the origin at time zero, $c_A = c_H = c_R$ and the θ_3 value of 0.236, and for right of the origin, $c_B = c_{Na} = c_R$ and the θ_4 value of 2.02. The two groups of parallel characteristics from the left and right branches of the z-axis do not intersect and leave the values of θ in the region between them as yet undetermined. This region, marked by lines converging on the origin, will be called the mixed region.

At the origin ($t = 0$, $z = 0$), θ changes discontinuously from θ_3 to θ_4. One might expect that the characteristics in the mixed region should pass through the origin and that their slopes will be related to their corresponding values, θ_i, by equation (14). It can indeed be shown rigorously (9) that the equations of the characteristics in this region are

$$t = z/\theta_i^2 \qquad \theta_4 > \theta_i > \theta_3 \qquad (16)$$

Hence

$$\theta_i = \sqrt{z/t}$$

which satisfies the basic equation (12) and represents a θ surface passing continuously into the planes $\theta = \theta_3$ and $\theta = \theta_4$ corresponding to the two groups of parallel characteristics based on θ_3 and on θ_4.

From equations (11) and (16) we obtain the relation

$$c_A = c_H = \frac{1}{M-1}\left[\left(\frac{nc_R M t}{z}\right)^{1/2} - c_R\right] \qquad (17)$$

which is valid only in the mixed region. Thus the concentration c_A which remains constant along each characteristic may be calculated from the slope of the latter. Using this equation, the characteristics in Fig. 3 have been labeled in terms of $c_{Na} = c_B = c_R - c_A$.

From this plot the distribution of the ions along the column at any time t_x can be easily found by drawing a parallel to the z-axis at $t = t_x$. This

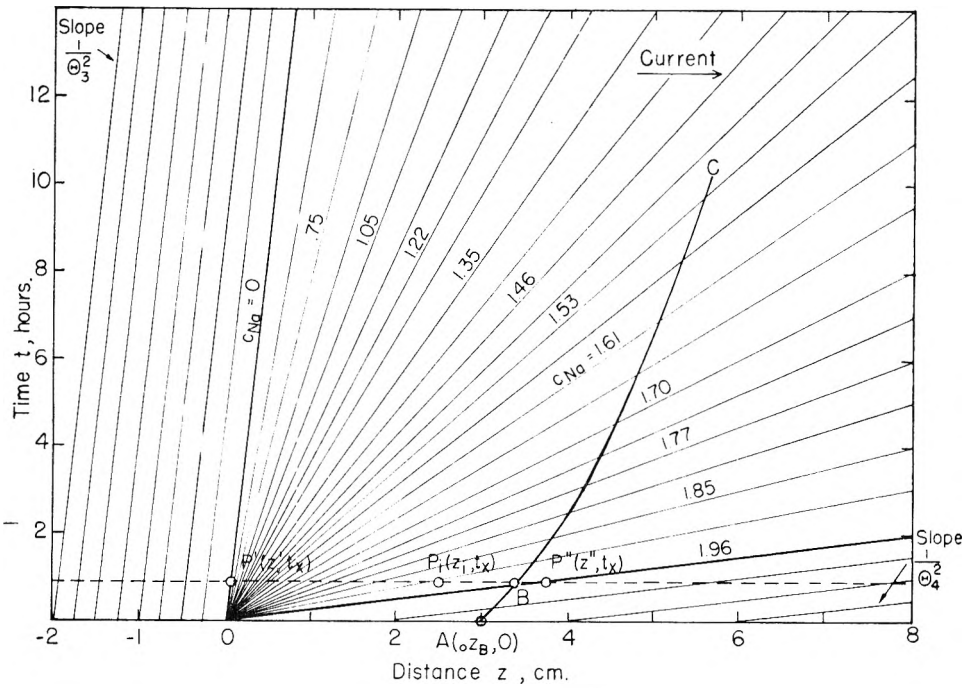

Fig. 3.—Characteristics of the system HR–NaR: R, i, c_R, as in Fig. 2; $M' = m_{HR}/m_{NaR} = 8.55$; $\theta_3 = 0.236$ (HR region); $\theta_4 = 2.02$ (NaR region). The line ABC describes the progress of a tagged element initially at $_0z_B$.

line intersects the characteristics at points $P_i(z_i, t_x)$ and by plotting the c_{Na} values of the characteristics at time t_x against z_i, the sodium ion distribution is obtained as a function of z. Such curves are shown in Fig. 4 for times t_x of 0, 2, 4, 6 and 9 hours after the start of electrolysis.

It is seen that there are three distinct regions in the z,t-plane (Fig. 3). In the first ($z < z'$) the resin is completely in the hydrogen form. In the second, the mixed region ($z' < z < z''$), both hydrogen and sodium ions are found. In the third region ($z > z''$) the resin is completely in the sodium form. The length of the mixed region is proportional to the time of electrolysis.

Consider now a traced lamina of sodium ions initially at A and assume that the mobility of the Na^{22} isotope is equal to that of Na^{23}. As long as no hydrogen ions have reached the lamina, it progresses with sharp boundaries and its position z_B is defined by equation (15) (straight line AB in Fig. 3). If it is assumed that the sodium ions do not overtake each other, the total amount of sodium between the origin and the traced lamina should remain constant, and hence its position at any time should be defined by the definite integral

$$\int_0^{z_B} c_{Na} dz = {}_0z_B c_R$$

A convenient method of obtaining z_B is planimetric evaluation by trial and error from the plots of c_{Na} *versus* z (Fig. 4). The resulting curve $z_B(t)$ representing the progress of the tagged lamina is plotted in Fig. 3 (curve BC). As a consequence of penetration by hydrogen ions, a fall in concentration in the tagged lamina, associated with a spread, is predicted to occur, as shown in the successive shaded areas of Fig. 4.

Platinum and zinc electrodes were used in our experiments. By virtue of the electrode reactions outlined above, the anodes produce the hydrogen and zinc forms of the resin. Hence from the point of view of the theory they are equivalent to initial layers to the left of the origin of hydrogen resin and zinc resin, respectively.

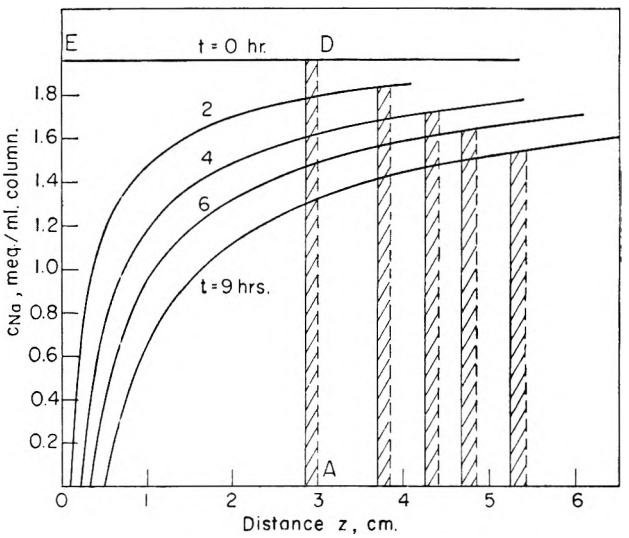

Fig. 4.—Computed variation (from Fig. 3) of the sodium concentration along a resin column with an initial HR–NaR boundary at the origin. Successive shaded areas represent a traced lamina of the sodium resin, showing penetration by hydrogen resin.

Experimental

Resin electrolysis was carried out in a thin lucite cell with plexiglass headers and perforated circular electrodes. The inner diameter of the tube was 1.6 cm. and its length 10 cm. The electrodes were lightly pressed against the resin in order to ensure good contact. In the process of filling the cell a thin layer of resin containing the tracer was embedded in the column, usually 3 cm. from the anode, or the radiotracer was adsorbed there in a thin band by the regular chromatographic technique.

The activity at the beginning of the experiment and after passage of a constant current for a given time was measured by inserting the cell in a slide propelled by a screw under a Geiger-Mueller tube. This tube was mounted on a lead brick 9 cm. high, covered with aluminum sheet to absorb most of the γ-radiation except for a narrow beam passing through a slit of width 2 mm. cut in the brick under the tube. As different parts of the cell were exposed, the radiation emanating from each was recorded. The position of the cell could be read to an accuracy of $^1/_{32}$ inch. Voltage and current were measured at regular intervals and a fast stream of deionized water (specific resistance, 10^6 ohm cm.) was passed through the resin from anode to cathode in order to keep the resin temperature constant and to remove the sodium hydroxide formed at the cathode and the gases formed at both electrodes. It has been verified that within a period equal to the length of the experiment only a slight spread of radioactive material occurs unless an electric potential is applied.

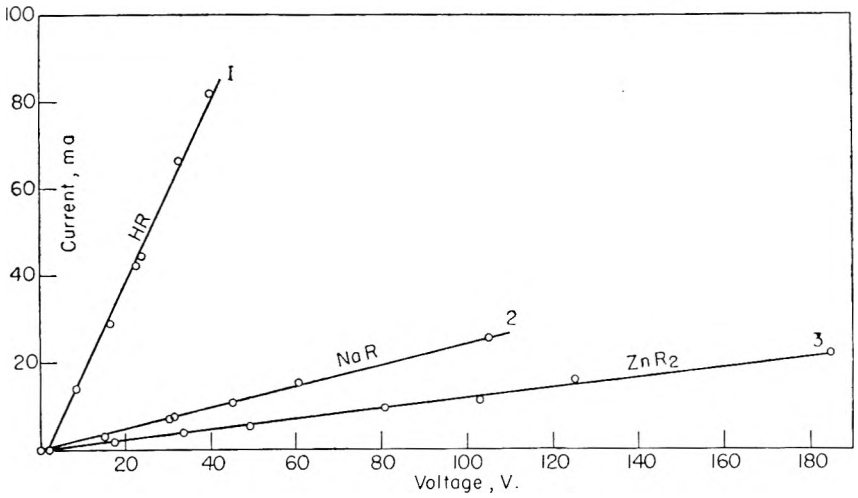

Fig. 5.—Current–voltage curves of Dowex-50 [80–100-mesh (dry basis)] in different states at 27.5°: curve 1, HR between platinum electrodes; curve 2, NaR between platinum electrodes; curve 3, ZnR_2 between zinc electrodes.

The current was taken from a high-voltage power supply with a stabilizer and was measured by calibrated voltmeter and milliammeter. The accuracy of these instruments was within 2%. Figures 2, 3, and 4 are based on a current density of 25 ma. and data taken at other current densities were corrected on a linear basis.

The resistance of the resin changed as the electrolysis proceeded, owing to temperature changes, packing effects, and the changes in the composition of the resin brought about by the electrode reactions. These changes were particularly pronounced in the electrolysis of the sodium resin. In all cases the average current density was determined by planimetric evaluation of the time integral of the current.

The a.c. conductivities at 60 and 1000 cycles were measured by means of a Serfass conductivity bridge with a magic-eye zero-point indicator, without capacitance compensation. The conductivity increased appreciably during the first 10 minutes after stopping the flow of the rinse water and changed only very slowly thereafter. The reported values represent the average after 10 minutes between the 60- and 1000-cycle values, which usually differed by a few per cent.

The resin used in these experiments was Dowex-50 furnished by courtesy of the Dow Chemical Company, Midland, Michigan. It was ground in a ball-mill, fractionated by sieving and converted to the appropriate form by column regeneration with nitrates of A.R. quality. In most experiments the fraction between 80- and 100-dry mesh (U.S. Standard) was used.

The deionized rinse water had a head of about 20 ft. and was prepared by passing distilled water through a monobed containing Dowex-50 and Dowex-2. The rinse rate varied between 10 and 20 ml. per minute and resin column cross-section of 1 cm.^{2}

The radioactive tracers, 2.6 y Na^{22} and 250 d Zn^{65}, were furnished by the M.I.T. Cyclotron Group.

Results

Current-Voltage Curves of HR, NaR and ZnR_2.—In Fig. 5 the current–voltage curves for HR, NaR and ZnR_2 are shown. An appreciable decomposition voltage (about 2 volts) was noticed only in the case of an HR column between platinum electrodes. The apparatus used was not suitable for an accurate investigation of the low-voltage region, but in previous experiments[8] with small resin particles a preliminary study of the decomposition potential, which is characteristic of the adsorbed species, had been made. Compared to the voltage applied in the electrolysis experiments the decomposition voltage is negligible.

From the slope of the current–voltage curves the specific conductivities of these three resin forms were calculated and are summarized and compared to the measured a.c. specific conductivities in Table I.

TABLE I

SPECIFIC CONDUCTIVITIES k AT 27.5° OF PLUGS OF DOWEX-50 80–100-MESH (DRY BASIS) IN DIFFERENT FORMS

	k, ohm^{-1} cm.$^{-1}$ From current–voltage curve	From a.c. bridge	Ionic mobility, cm.^{2} volt^{-1} hr.$^{-1}$
HR between platinum electrodes	10.4×10^{-3}	9.7×10^{-3}	0.1845
NaR between platinum electrodes	1.22×10^{-3}	1.22×10^{-3}	.0232
ZnR_2 between zinc electrodes	0.60×10^{-3}	0.59×10^{-3}	.0112

In the last column the ionic mobilities are given, as calculated from the a.c. bridge conductances and the value of 1.96 meq. per ml. of column space, for the resin capacity determined with respect to hydrogen ions. In computing these values the assumption was made, justified by the experiments quoted in the next section, that the transference number of the cations is unity.

Resin conductivity was found to increase considerably with temperature. Owing to the evolution of heat during electrolysis, higher temperatures (up to 37°) prevailed in the migration studies. However, it will be noticed that only ratios M of mobilities and not their individual values m_A and m_B appear in the final equations. It was assumed that these ratios vary but little with the temperature and hence it is justifiable to use the mobility data of Table I in Figs. 3 and 4.

Migration of a 250 d Zn^{65} Band in ZnR_2.—Figure 6 shows the migration of a lamina traced with 250 d Zn^{65} embedded in a column of ZnR_2 between zinc electrodes. The rate of migration of the maximum is seen to be constant (see insert in Fig. 6) and in very close agreement with the rate calculated from the time integral of the current under the as-

(8) K. S. Spiegler, unpublished results.

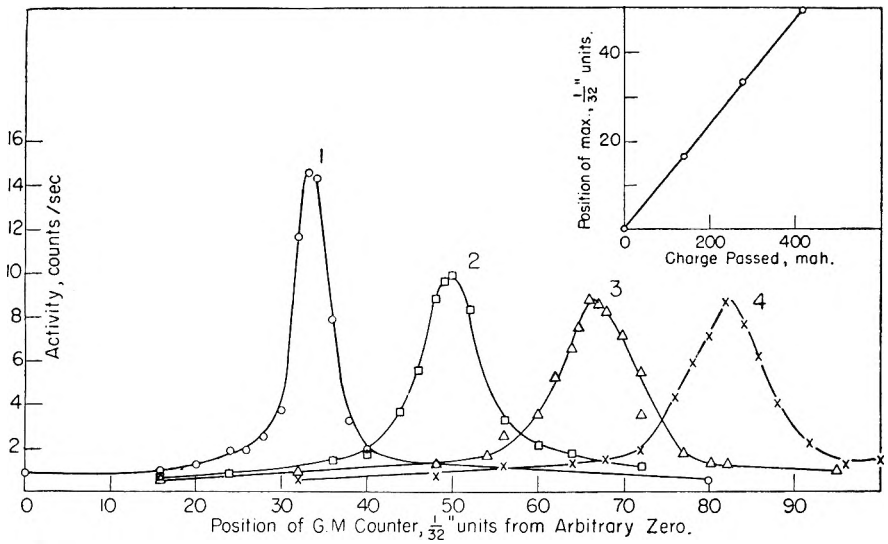

Fig. 6.—Electrolysis of ZnR_2 between zinc electrodes: progress of a lamina traced with 250 d Zn^{65} originally 3.6 cm. from the anode; resin, Dowex-50; current, 50 ma.; curve 1, original position of lamina; curves 2, 3, 4 after 2.72, 5.52 and 8.34 hr., respectively; activity corrected for room background.

sumption that the transference number of the zinc ions equals unity (first line of Table II).

TABLE II

COMPARISON OF THE OBSERVED MIGRATION OF THE ACTIVITY MAXIMUM WITH THE VALUES CALCULATED FROM EQ. (15) AND CHECK OF FARADAY'S LAW

	Total charge passed (mah)	Displacement of activity maximum (cm.) obsd.	calcd.	Loss of weight of zinc anode (mg.) obsd.	calcd.
Zn^{65} in ZnR_2	418	3.94	3.96	470	510
Zn^{65} at the ZnR_2-NaR boundary	437	4.16	4.21	488	534

As also shown in Table II, the observed loss of weight of the zinc anode is about 8% less than calculated from the anode reaction

$$Zn + 2R^- = ZnR_2 + 2e^-$$

This discrepancy is probably due to the production of some HR and to the fact that the zinc anode was found to be pitted and slightly oxidized after electrolysis and thus the real loss of zinc is higher than the observed loss of weight of the electrode. The agreement between the calculated and the observed rate of band migration proves that the transference number of the zinc ions in ZnR_2 in a medium of deionized water equals unity within the experimental error.

It is seen that the band spreads while it progresses. The spread occurred mainly during the first two stages of the electrolysis and this result was verified by a repeat experiment. When the current was reversed, the band continued to spread. The problem of the spread is discussed in greater detail in a later section.

Migration of a Zinc-Sodium Boundary Traced with 250 d Zn^{65}.—Figure 7 shows the migration of a band of Zn^{65} at the boundary between ZnR_2 and NaR, the first following the latter. A zinc anode and platinum cathode were used. The rate of migration of the activity maximum was again proportional to the time integral of the current (see insert) and agreed closely with the value calculated from equation (15) (see line OA in Fig. 2). The boundary remained sharp and the spread was comparatively small. The check of transference number and of Faraday's law for this experiment are given in the second line of Table II, with results very similar to those for the pure ZnR_2-system.

Migration of a 2.6 y Na^{22} Band in NaR with HR Formed at the Anode.—A more complicated case was studied in the migration of a band of $Na^{22}R$ in a column of NaR electrolyzed with platinum electrodes. In this case HR was produced by the anode reaction mentioned above. Thus the system is equivalent to a column containing an initial boundary between HR and NaR at the anode.[2]

Figure 8 shows the migration of a band tagged with 2.6 y Na^{22} in NaR. It is seen that the rate of migration of the activity maximum decreases with time and that the band spreads considerably. At the end of the electrolysis a 1 *M* solution of sodium nitrate was passed through the column and the nitric acid formed by elution of hydrogen ions from the resin was titrated in the eluate. The total amount of HR was thus found to be 14.3 meq.;

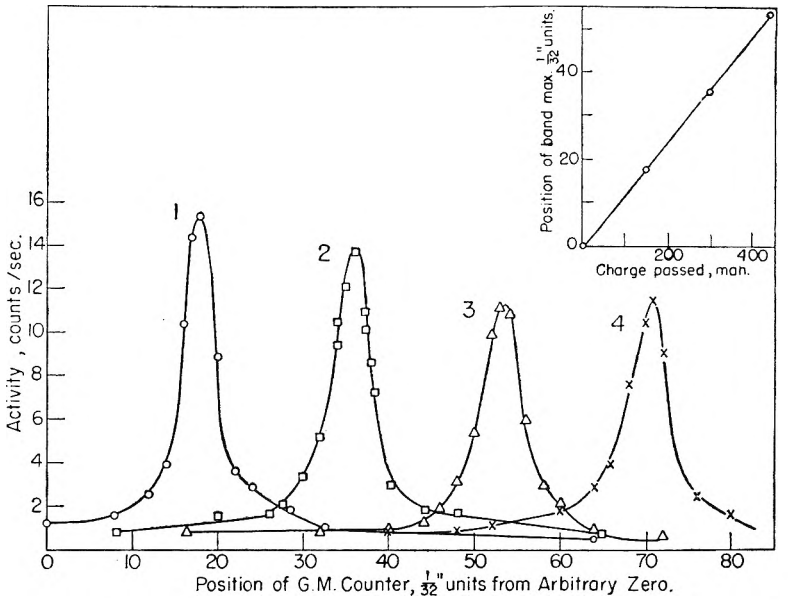

Fig. 7.—Electrolysis of the system $-Pt|NaR|ZnR_2|Zn+$: NaR-ZnR_2 boundary traced with 250d Zn^{65}; resin, Dowex-50; current, 50 ma; tagged layer initially 3.6 cm. from anode; curves 1, 2, 3, 4 correspond to electrolysis periods of 0, 2.8, 6.0 and 8.75 hours.

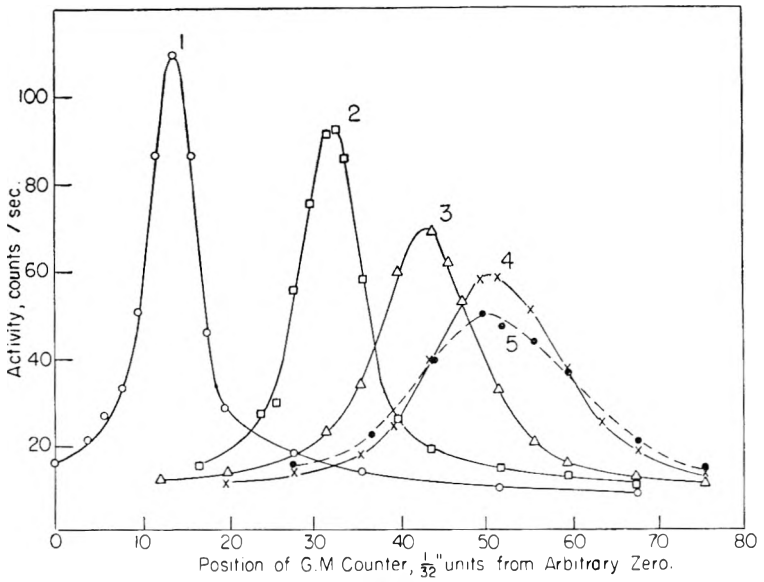

Fig. 8.—Electrolysis of Dowex-50 in the sodium form traced with 2.6 y Na^{22}, with HR formed at the anode: resin, Dowex-50; current, 140 ma.; tagged layer initially 3 cm. from anode; curves 1, 2, 3, 4 after electrolysis periods of 0, 1.0, 2.08 and 3.04 hr., respectively, covering 8 hr. between the measurement of curves 1 and 4; curve 5 after 100 hr. without further electrolysis.

the amount of charge passed was 15.9 millifaraday. The difference probably represents loss of HR[2] in the cathode reaction

$$2HR + 2e^- = H_2 + 2R^-$$

The rates of migration of the activity maximum in this experiment, as well as those in three other experiments in which smaller current densities prevailed, can be seen in Fig. 9, which shows the position of the activity maximum as a function of the total charge passed between the electrodes (in mah). It is seen that the data for the different experiments fall approximately on one curve. For comparison there is also plotted curve ABC, taken from Fig. 3 representing the position of a tagged lamina of infinitesimal thickness originally in the same position as the actual activity maximum. The correlation between these two curves is discussed in the next section.

Discussion

Comparison of the experimental results with the theory shows that the assumption of unit transference number for the cations in the resin is justified. The measured a.c. and d.c. conductivities of the sodium and zinc forms agree closely and the values for the hydrogen form differ only by several per cent. (Table I). Slight differences between the a.c. conductivities at 60 and 1000 cycles were found. The accuracy of the bridge did not permit definite conclusions to be drawn from these differences, but they are probably due to effects of dipole rotation as assumed by Albrink and Fuoss[9] for an anion-exchange membrane of low capacity whose d.c. and a.c. conductivities did not agree. Our measurements show that in the case of a Dowex-50 column, the a.c. component is small in comparison with the purely electrolytic d.c. component.

From equation (3) it is obvious that except for a small effect due to the very small difference in the mobility of the isotopes, no spread of the tagged band of Zn^{65} in ZnR_2 should occur in a continuous medium if diffusion may be neglected. As the spread of the band in the absence of an electric field was shown to be negligible in a period equal to the length of the electrolysis, it is believed that the spread is related to the inhomogeneous nature of the resin column. In the latter such properties as viscosity, ionic concentration, and diffusion rate vary in space; it can be shown that these variations may lead to a considerable spread of the band. Inhomogeneous packing of the column, producing channels of different resistance, and gradients of rinse water flow rate and of temperature in the cell are possible additional reasons for the spread. However, at the present stage, the authors cannot offer proof for any of these suggestions. In particular it is not known whether the spread is related to lack of uniformity on a macroscopic or molecular scale. It is seen that the spread is roughly symmetrical and we have therefore assumed in our conclusions that the position of the activity maximum is representative of the position of the center of the tagged lamina, *i.e.*, that if equation (3) were satisfied, the position of the lamina would be identical with the observed position of the activity maximum.

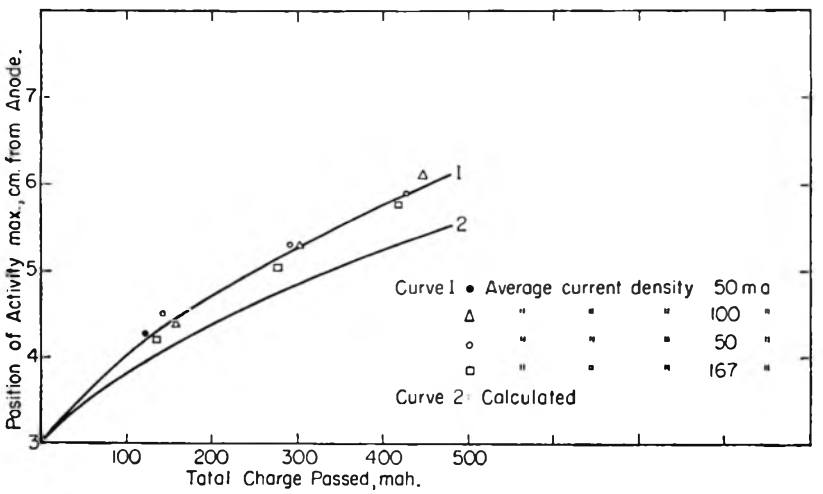

Fig. 9.—Progress of the activity maximum in the system Pt | NaR | Pt tagged with a lamina of $Na^{22}R$ initially 3 cm. from the anode.

This assumption may even be extended with reasonable approximation to the electrolysis of NaR between platinum electrodes in spite of the asymmetric nature of the spread of band caused by the penetration of the hydrogen ions. For it is seen

(9) W. S Albrink and R. M. Fuoss, *J. Gen. Physiol.*, **32**, 453 (1949).

from Fig. 4 that within the range considered here, the asymmetric spread due to this effect is small compared to the considerable observed spread.

If the activity maximum is considered representative of the tagged layer, its displacement should agree with curve ABC (Fig. 3). Comparison of this curve with the observed data (Fig. 9) shows that after the passage of 450 mah cm.$^{-2}$, the displacement was about twenty per cent. higher than predicted from the theory. The reason for this discrepancy lies probably in the interaction between the hydrogen and sodium ions causing the ratio of their mobilities in the mixed form of the resin to be different from the ratio of their mobilities in the pure forms HR and NaR, respectively, on which Figs. 3 and 4 are based. Even in dilute aqueous solutions departures from the Kohlrausch principle of independent ionic mobilities exist.[10] Thus in a mixture of aqueous hydrochloric acid and potassium chloride, the mobility of the hydrogen ion is lower and of the potassium ion higher than in solutions of the single electrolytes at the same ionic strength. Hence, one might indeed expect the observed rate of migration of the activity maximum to be faster than predicted.

If the spread of the bands could be sufficiently reduced, resin electrolysis might prove a suitable method of separation. Its aspects are different from those of regular ion-exchange chromatography, as frictional resistance to ionic movement and voltage gradient determine the migration of a band in an electric field, while in regular chromatography the mobility of a band is determined by the distribution of the adsorbate between solid and solution and by the rate of flow of the eluant. On the other hand, compared to electroseparations in solution, the solid exchanger should offer advantages such as reduced diffusion and freedom from the disturbances caused by thermal convection.

Separation of two ionic species, A and B, is possible if a layer of resin containing both of them is sandwiched between resin layers containing ions C and D, respectively, such that C has a higher mobility than A or B and migrates in front, while D has a lower mobility than A or B and migrates behind the mixed layer.

Thus preliminary results show that some separation of sodium from potassium occurs in the system

$$- \text{Pt} \mid \text{HR} \mid \begin{matrix}\text{NaR} \\ +\text{KR}\end{matrix} \mid \text{ZnR}_2 \mid \text{Zn} +$$

and further experiments on this aspect of resin electrolysis as well as extension of these observations to resin membranes are in progress.

Acknowledgments. — The authors thank Professor John W. Irvine, Jr., of M.I.T. for his many helpful suggestions throughout the course of the work, Mr. Charlie Fisher of the Commissariat à l'Energie Atomique, Paris, for his assistance at the beginning of this research, and Mrs. Elizabeth W. Backofen for purification of the tracers Na^{22} and Zn^{65} One of the authors (K.S.S.) is holder of a Weizmann Institute Postdoctoral Fellowship. The work was also assisted by the A.E.C.

(10) H. S. Harned and B. B. Owen, "The Physical Chemistry of Electrolytic Solutions," Reinhold Publishing Corp., New York, N. Y., 2nd ed., 1950, p 142.

ION EXCHANGE STUDIES OF COMPLEX IONS AS A FUNCTION OF TEMPERATURE, IONIC STRENGTH, AND PRESENCE OF FORMALDEHYDE[1]

BY JACK SCHUBERT

Division of Biological and Medical Research, Argonne National Laboratory, Chicago, Illinois

Received August 30, 1951

The use of ion exchange materials for the study of complex ions is reviewed. Experimental details are given of the ion exchange method utilizing carrier-free radiotracers for the determination of the composition and stability of complex ions. The effect of temperature and ionic strength on the stability of the strontium citrate complex ion was determined. The stability of several complex ions of Ca^{++} and Sr^{++} was determined in the presence and absence of formaldehyde at an ionic strength of 0.16, $t = 25°$, and *p*H 7.2–7.3. The ligands studied were aspartic, succinic, and malic acids, butylamine, ethanolamine, and formaldehyde.

Introduction

Consider the complex ion $(MA_n)^c$, where M is a cation, A an anion, n the number of moles of A relative to M, and c the net charge on the complex. When the solution of the complex ion is in contact with a cation exchange resin, the degree to which unbound M exchanges with the cation in the exchanger is related quantitatively to the extent to which M is bound by the ligand A. The same situation holds for the uptake of the anionic components by an anion exchange resin.

The first reports of the use of ion exchangers for the investigation of complex ions were published in 1922 by Guenther-Schulze.[2,3] As in all such work done prior to the discovery of the organic ion exchangers by Adams and Holmes[4] in 1935, Guenther-Schulze employed an inorganic zeolite. He studied the complex ions formed between Cl^- and divalent cations. He assumed that the presence of Cl^- in the cation exchanger was due to the sorption of $(MCl)^+$. Recently Samuelson carried out similar experiments with an organic cation exchanger[5] and concluded that Guenther-Schulze's experiments

(1) Presented at the Twenty-fifth National Colloid Symposium, which was held under the auspices of the Divisions of Colloid and Physical and Inorganic Chemistry of the American Chemical Society at Ithaca, New York, June 18–20, 1951.

(2) A. Guenther-Schulze, *Z. Elektrochem.*, **28**, 89 (1922).

(3) A. Guenther-Schulze, *ibid.*, **28**, 387 (1922).

(4) B. A. Adams and E. H. Holmes, *J. Soc. Chem. Ind.*, **54**, 1T (1935).

(5) O. Samuelson, *Iva*, **17**, 17 (1946).

were invalid because the chloride was adsorbed on the permutite, instead of undergoing exchange.

Guenther-Schulze's work led Gustavson[6,7] to investigate the complex ions of chromium—a problem of great interest to the leather chemist. Gustavson subsequently[8-14] applied the synthetic organic resins to the problem with greater success because of the marked chemical stability of the organic exchangers, particularly in acid solutions, as compared to the inorganic exchangers. Further studies on chromium complexes, especially ones involving organic acids, have been made.[15-17] In these investigations the general procedure involved contact of the hydrogen form of the organic cation exchanger with the solution containing chromium salts. It was assumed that the cationic complexes are removed by the exchanger, while the neutral and anionic fractions remain in the effluent. Analysis of the original salt solution, the effluent after contact with the resin, and the effluent following elution of the sorbed chromium, is used to determine the composition of the complexes present in the initial solution. Both static and dynamic techniques have been employed. Further examination of the filtrate with an anion exchanger has been suggested.[8]

Samuelson[18,19] employed synthetic anion exchangers to elucidate the structure of Graham's salt. He also employed a cation exchanger to determine the composition and stability of the ferrimetaphosphate complex.[20]

In experiments in which the concentration of M relative to A and to the capacity of the cation exchanger is negligible, as is often the case when carrier-free radiotracers are employed, the formulation of the necessary equations for the complex ion constants, and the experimental techniques are simplified considerably. Investigations along this line were begun in 1944[21] and eventually led to determinations of the composition and stability of complex ions formed between the alkaline earths, including Ra^{++}, and various organic acids.[22-28] Subsequently, the ion exchange technique utilizing radiotracers has been employed for the study or detection of complex ions formed between the rare earths and citric acid,[29-31] cerous and inorganic anions,[32-34] zirconium and niobium with fluoride and other inorganic ions[27] and between transuranic elements and the chloride ion.[35] Anion exchange resins have been used to deduce information regarding anionic complex ions resulting from the interaction of Zr, Nb, Pd, Fe and other metals with halides.[36-38]

In this paper are presented results showing the effect of temperature and ionic strength on the interaction between strontium and citrate. Such thermodynamic studies are of fundamental importance for the elucidation of the nature of the binding forces in complex ions as was emphasized recently by J. Bjerrum.[39] In addition, data on the interaction between Ca^{++} and Sr^{++} with some organic acids and nitrogenous derivatives are included. In most instances, the measurements were made (at $\mu = 0.16$ and pH 7.2) in order to approximate physiological conditions.

Experimental

In the experiments described here the procedures, unless otherwise stated, were as follows: to each of a series of ten flasks containing 100 mg. of the sodium form of the synthetic organic cation exchanger, Dowex-50,[40] a sulfonated polystyrene resin, were added 25 ml. of veronal buffer[41] at pH 7.2–7.3, and 0.16 M in Na^+. The buffer contained tracer levels of $^{45}Ca^{++}$ or $^{89,90}Sr^{++}$, and, where indicated, formaldehyde or phenol as a preservative. To each flask was added a predetermined volume of a given ligand. The ligand-containing solution was adjusted to a pH 7.2–7.3 and to 0.16 M in Na^+ with NaCl. Finally, the volume in each flask was brought to 100 ml. with 0.16 M sodium chloride solution. Generally, from four to eight different concentrations of the ligand were employed, the concentration range chosen depended on the ligand's affinity for Ca^{++} and Sr^{++}. Two of the ten flasks contained zero concentration of the given ligand, and an additional two flasks containing only buffer plus sodium chloride were run as blanks. After shaking the flasks mechanically for three hours, an aliquot of the supernatant from each was removed for radiochemical assay. To each flask was added subsequently, in some cases, 1 ml. of a 0.16 M NaCl solution containing carrier-free $^{89,90}Sr^{++}$. After an additional three hours shaking period, aliquots were removed for $^{89,90}Sr$ assay. In other runs the $^{89,90}Sr$ was already present in the buffer.

A typical system involving strontium citrate and the experimental data are given in Table I.

Materials.—All reagents were of C.P. grade. Solutions of the ligands were prepared just before use by dissolving weighed amounts of either the sodium salts, acid or base, and diluting to a known volume after adjustment to pH 7.2–7.3 with dilute NaOH. Solid sodium chloride was added, when necessary, to bring the total Na^+ to 0.16 M.

Buffer.—A universal veronal buffer, devised by Michaelis,[41] was employed. This buffer was chosen because it contains no anions which form insoluble compounds with

(6) K. H. Gustavson, *J. Am. Leather Chem. Assoc.*, **19**, 446 (1924).
(7) K. H. Gustavson, *Ind. Eng. Chem.*, **17**, 577 (1925).
(8) K. H. Gustavson, *Svensk. Kem. Tid.*, **56**, 14 (1944).
(9) K. H. Gustavson, *J. Colloid Sci.*, **1**, 397 (1946).
(10) K. H. Gustavson, *J. Intern. Soc. Leather Trades' Chemists*, **30**, 264 (1946).
(11) K. H. Gustavson, *Svensk. Kem. Tid.*, **58**, 2 (1946).
(12) K. H. Gustavson, *ibid.*, **58**, 274 (1946).
(13) K. H. Gustavson, *J. Am. Leather Chemists Assoc.*, **44**, 388 (1949).
(14) K. H. Gustavson, *J. Soc. Leather Trades' Chemists*, **34**, 259 (1950).
(15) R. S. Adams, *J. Am. Leather Chemists Assoc.*, **41**, 552 (1946).
(16) E. J. Serfass, E. R. Theis, T. C. Thorstensen and R. K. Agarwal, *ibid.*, **43**, 132 (1948).
(17) E. R. Theis and T. C. Thorstensen, *J. Intern. Soc. Leather Trades' Chemists*, **31**, 124 (1947).
(18) O. Samuelson, *Svensk. Kem. Tid.*, **56**, 343 (1944).
(19) O. Samuelson, *ibid.*, **61**, 76 (1949).
(20) O. Samuelson, *Iva*, **17**, 9 (1946).
(21) J. Schubert, Manhattan Progress Report, CN-2563, issued February, 1945.
(22) J. Schubert, THIS JOURNAL, **52**, 340 (1948).
(23) J. Schubert and J. W. Richter, *ibid.*, **52**, 350 (1948).
(24) J. Schubert and J. W. Richter, *J. Am. Chem. Soc.*, **70**, 4259 (1948).
(25) J. Schubert, E. R. Russell and L. S. Myers, Jr., *J. Biol. Chem.*, **185**, 387 (1950).
(26) J. Schubert and A. Lindenbaum, *Nature*, **166**, 913 (1950).
(27) J. Schubert, *J. Colloid Sci.*, **5**, 376 (1950).
(28) J. Schubert, *Anal. Chem.*, **22**, 1359 (1950).
(29) C. E. Crouthamel and D. S. Martin, Jr., *J. Am. Chem. Soc.*, **72**, 1382 (1950).
(30) A. D. Tevebaugh, Document AECD-2749, issued November 29, 1949, Technical Information Division, Oak Ridge, Tenn.
(31) E. R. Tompkins and S. W. Mayer, *J. Am. Chem. Soc.*, **69**, 2859 (1947).
(32) R. E. Connick and S. W. Mayer, *ibid.*, **73**, 1176 (1951).
(33) S. W. Mayer and S. D. Schwartz, *ibid.*, **72**, 5106 (1950)
(34) S. W. Mayer and S. D. Schwartz, *ibid.*, **73**, 222 (1951).
(35) K. Street, Jr., and G. T. Seaborg, *ibid.*, **72**, 2790 (1950)
(36) K. A. Kraus and G. E. Moore, *ibid.*, **72**, 4293 (1950).
(37) K. A. Kraus and G. E. Moore, *ibid.*, **73**, 9 (1951).
(38) K. A. Kraus and G. E. Moore, *ibid.*, **73**, 13 (1951)
(39) J. Bjerrum, *Chem. Revs.*, **46**, 381 (1950).
(40) W. C. Baumann and J. Eichhorn, *J. Am. Chem. Soc.*, **69**, 2830 (1947).
(41) L. Michaelis, *Biochem. Z.*, **234**, 139 (1931).

TABLE I

EXPERIMENTAL SYSTEM AND RESULTS OBTAINED FOR THE STRONTIUM CITRATE COMPLEX

Resin, sodium form of Dowex-50, 100–150 mesh; buffer, veronal buffer, 0.16 *M* in Na^+, 0.7% by weight of phenol, *p*H 7.2–7.3; sodium citrate solution 0.02 *M* in citrate, 0.16 *M* in Na^+; sodium chloride, 0.16 *M*, *t* 25°; shaking time, 3 hours.

Flask no.	Resin, mg.	Buffer, ml.	NaCl, ml.	Sodium citrate, ml.	Final citrate concn., moles/l.	$^{89,90}Sr$ activity in equil. soln. c./m./ml.	Average amount $^{89,90}Sr$ in separate phases, % Resin (calcd.)	% Soln.	K_d	k_f
1	0	10.0	90.0	0	0	189.9	...	...	.....	...
2	0	10.0	90.0	0	0	185.3				
3	100.0	10.0	90.0	0	0	50.9	27.30	72.70	2.6630	...
4	100.0	10.0	90.0	0	0	51.5			(K_d°)	
5	100.0	10.0	82.0	8.00	.0016	81.5	43.57	56.43	1.2952	658
6	100.0	10.0	82.0	8.00	.0016	81.9				
7	100.0	10.0	80.0	10	.0020	86.1	45.88	54.12	1.1796	629
8	100.0	10.0	80	10	.0020	86.0				
9	100.0	10.0	75	15	.0030	98.2	52.74	47.26	0.8961	658
10	100.0	10.0	75	15	.0030	99.5				
11	100.0	10.0	70	20	.0040	107.8	57.20	42.80	0.7483	641
12	100.0	10.0	70	20	.0040	106.8			Average k_f 647 =12	

the alkaline earth cations. Under the experimental conditions the buffer anions exert negligible complexing action (unpublished work). The buffer is essentially a 0.16 *M* solution of sodium chloride and contains a mixture of acetate and diethyl barbiturate ions, each at a concentration of 0.02856 *M*. Each liter of ^{45}Ca containing buffer had about 0.1 mc. of ^{45}Ca. The ^{45}Ca was obtained from Oak Ridge and had a specific activity of 1.54 mc./mg. The concentration of all polyvalent cations in the ^{45}Ca-containing buffer was less than 10^{-6} *M*, *i.e.*, negligible relative to the ligand concentration, and sufficiently low so that the distribution coefficient of free Ca^{++} in the resin would be unaffected by gross changes in the concentration of Ca^{++} or metallic impurities.

Resin.—The synthetic organic cation exchanger, Dowex-50, was used particularly because its capacity is independent of *p*H over a wide *p*H range,[40] thus avoiding the necessity for the type of calibration curve in earlier studies.[23] The air-dried resin was classified by means of U.S. standard sieves, to 100–150 mesh particle size. The resin was put through several alternate Na^+–H^+ cycles with 5% solutions of NaCl and HCl. After saturation with excess NaCl, the resin was equilibrated with excess 0.16 *M* NaCl solution. The supernatant solution in contact with the resin was adjusted to *p*H 7.2–7.3 with dilute NaOH solution. After the mixture was stirred an hour the *p*H of the supernatant was tested, and readjusted, until no change in *p*H took place after stirring. The resin was filtered through a buchner funnel, and rapidly washed free of adhering salt solution with distilled water. The washed resin was spread in a thin layer on a tray and air-dried. All experiments were conducted with the air-dried resin. Analysis showed that the air-dried resin contained 3.86 milliequivalents Na per gram and 12.5% moisture as determined by drying to constant weight at 110°.

Radiochemical Assays.—In order to avoid corrections for self-absorption "infinitely thick" samples (40–50 mg./cm.^{2}) of precipitated calcium oxalate were mounted and counted. Results were consistently reproducible to about 1–2%.

$^{89,90}Sr$ Assay.—Depending on the level of radioactivity a measured volume (usually 1–5 ml.) was removed from the solution in the flasks after the 3-hour equilibration period, and deposited directly into 10-ml. flat bottom porcelain dishes. Sufficient water was added to ensure a uniform deposit of salts upon drying. The aliquots were dried by overhead heating with an infrared bulb. The samples were allowed to stand at least 15 days before counting for radioactive equilibrium to be attained.

Counting Procedure.—Samples were counted by means of a thin (2–3 mg./cm.^{2}) end mica-window Geiger tube. All samples were placed in a reproducible position beneath the counter window. At least a total of 10,000 c.p. were taken on each sample. The counting rates were sufficiently low (2000 c.p.m.) so that coincidence corrections were avoided. The $^{89,90}Sr$ samples were counted through a 54 mg./cm.^{2} aluminum absorber when ^{45}Ca was present so as to screen out the weak beta particles emitted by ^{45}Ca.

General Comments

In separate experiments, the effect of shaking time on the distribution coefficient for the particular experimental conditions described in this paper was tested. It was found that a steady state was attained in less than an hour in the presence or absence of a complex forming ligand. For example, the formation constant for strontium malate was found to be identical, within experimental error, for contact times varying from one hour to two days.

In none of the cases described here was any significant adsorption of the ligand by the resin or walls of the flasks found. The reliability of the experimental procedures was also checked in the manner described elsewhere.[25]

One possible source of error is the destruction, probably by bacterial action, of some organic ligands after prolonged contact (> 2 days), particularly at elevated temperatures. For this reason all solutions were made up fresh. The buffer solution was kept refrigerated when not in use. Neutral antibacterial agents in small concentrations such as phenol, (~0.05–0.1%) and formaldehyde (~0.5%) have been found to prevent decomposition without affecting the ion exchange reaction or complex formation.

Results

The dissociation constant, k_c, for the complex ion, $(MA_n)^c$, in terms of the equilibrium ion exchange formulation is[25]

$$k_c = \frac{(A)^n}{(K_d^\circ/K_d) - 1} \qquad (1)$$

where K_d° and K_d are the distribution coefficients obtained in the absence and presence, respectively, of the ligand A. The distribution coefficient for the cation M is defined as

$$K_d = \frac{\%\ \text{M in exchanger}}{\%\ \text{M in solution}} \times \frac{\text{volume of solution}}{\text{mass of exchanger}} = \lambda \times \frac{v}{m} \qquad (2)$$

where λ represents the per cent. ratio. The term K_d° can be obtained directly or from values of K_d by graphical or analytical means. It is convenient to plot $1/K_d$ *versus* $(A)^n$ and to extrapolate the straight line for proper *n* values to zero concentrations of A, as indicated by the relation

$$\frac{1}{K_d} = \frac{1}{K_d^\circ} + \frac{(A)^n}{K_d^\circ k_c} \qquad (3)$$

The use of equation (1) assumes that the cation, M, is complexed only by A, *i.e.*, that complex formation by other anions in the solution is negligible. This is not always true. The equations necessary to describe the more complicated situations are to be reported elsewhere. Under the experimental conditions described in this paper, the factors needed to convert all values to a standard solution, say 0.16 *M* NaCl or 0.16 *M* sodium perchlorate, are relatively minor, amounting to less than 5% in most of the cases. Consequently, equation (1) will be used without modification. Equation (1) is valid for the conditions employed even when

the complex ion is itself adsorbed, *i.e.*, has a net positive charge.

In all the ligands studied here, it was found that Ca^{++} and Sr^{++} formed a 1:1 complex. The formation constant, k_f, found for several of these complex ions is summarized in Table II, the constant $k_f = 1/k_c$ is the mass action equilibrium constant for the reaction

$$M + A \rightleftarrows MA \qquad (4)$$

where the charge on the complex ion, MA, is less than +2 for M^{++}. The value of k_f at infinite dilution is given by the term k_f°.

TABLE II

EFFECT OF TEMPERATURE ON THE FORMATION CONSTANT OF STRONTIUM CITRATE

Systems and experimental conditions given in Table I. Successive runs made on same series of solutions following withdrawal of 5.0-ml. aliquot from respective flasks for analysis at given temperature.

Run order	Date of run	Temp., °C.	Soln. vol., ml.	Mass resin, mg.	K_d°	k_f	log k_f
1	4/13/51	25	100.0	100.0	2.66_3	647 ± 12	2.81
2	4/16	25	95.0	100.0	2.44_1	571 ± 16	2.76
3	4/16	3	90.0	100.0	2.00_7	697 ± 17	2.84
4	4/17	15	85.0	100.0	2.12_0	632 ± 21	2.80
5	4/18	25	80.0	100.0	2.18_6	606 ± 39	2.78
6	4/18	40	75.0	100.0	2.44_0	651 ± 28	2.81
7	4/19	25	70.0	100.0	1.90_3	639 ± 16	2.81

In all cases, the observed value of K_d° agreed with that obtained by extrapolation of $1/K_d$ to where A = 0 as shown by the examples in Figs. 1 and 2. The values of K_d° for Ca^{++} when, Na^+ 0.16 *M*, *p*H 7.2–7.3, and the solution contained 1 ml. of buffer for every 3 ml. of 0.16 *M* sodium chloride, generally fell in the range 1.31–1.46. The corresponding K_d° value for Sr^{++} fell in the range 2.38–2.47. The value of the formation constant is unaffected by relatively large differences in the absolute value of K_d° in different runs.

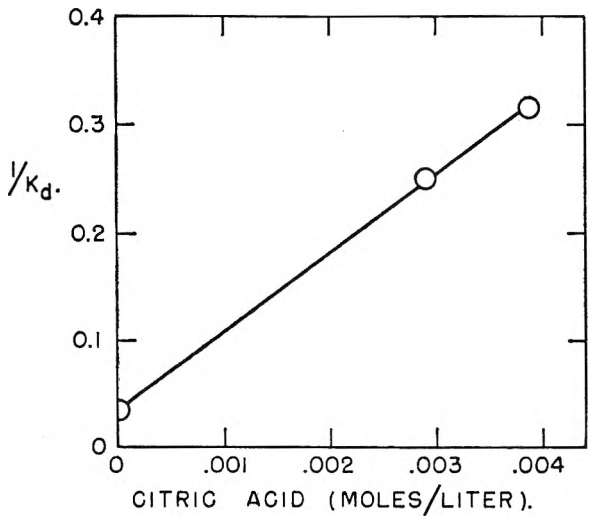

Fig. 1.—Variations of the reciprocal of the distribution coefficient for Sr^{++} *versus* the concentration of citric acid at t = 25°, *p*H 7.2–7.3, and μ = 0.048.

Temperature and Ionic Strength Effects on Complex Ion Stability.—The formation constant of strontium citrate was studied in the temperature range 3–40° at μ 0.16 and *p*H 7.2–7.3. The values of k_f at the different temperatures were obtained by utilizing the original system (Table I) and withdrawing successive 5-ml. aliquots after shaking the flasks in a thermostat controlled water-bath at a given temperature. The experimental observations for the first 25° point are recorded in Table 1 for illustrative purposes. The sequence of temperatures studied was as follows: 25, 25, 3.0, 15, 25, 40 and 25°. In this way, any decomposition of citrate or other effects which might affect the results are detected by comparison with the 25° point used as a reference.

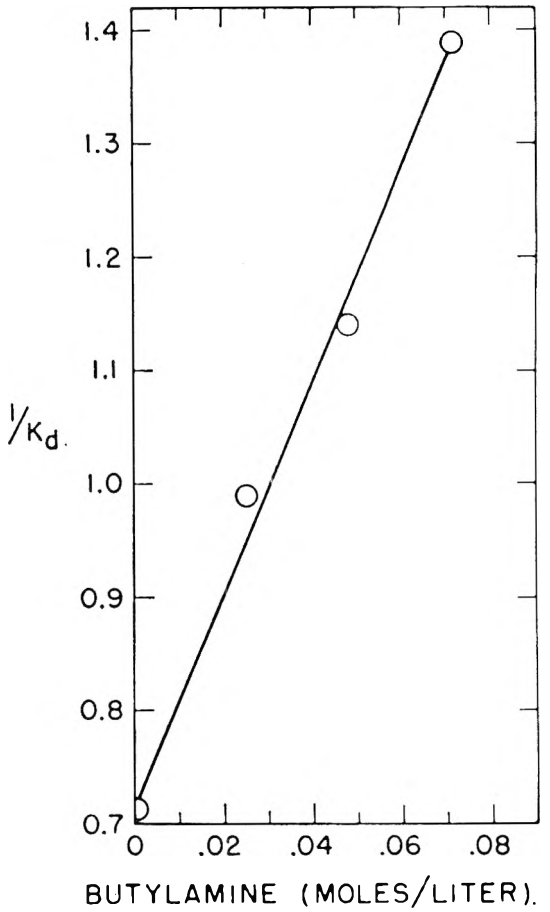

Fig. 2.—Variations of the reciprocal of the distribution coefficient for Ca^{++} *versus* the concentration of butylamine, t = 25, and μ = 0.16 and *p*H 7.2–7.3.

In the temperature range 3–40° the formation constant is, within experimental error nearly unchanged (Table II). This is probably to be expected if it is assumed that the variation of k_f for strontium citrate is very small as was observed by Bates and Pinching for the temperature coefficients of the ionization constants of citric acid over the same temperature range.[42]

In Table III are presented data relating to the effect of ionic strength on the formation constant of strontium citrate obtained by successive dilutions of the starting solutions. Two different concentrations of citrate were em-

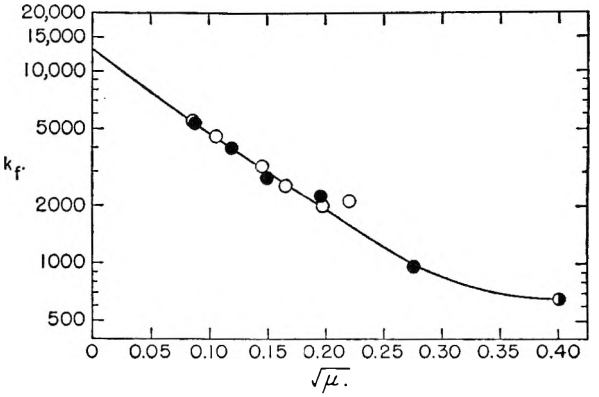

Fig. 3.—Variation of the formation constants of strontium citrate with ionic strength. The symbols ○, ◑, ● represent separate experiments. See text for a discussion of the slope of the curve in the extrapolated region.

(42) Bates and Pinching, *J. Am. Chem. Soc.*, **71**, 1274 (1949)

TABLE III

INTERACTION OF $^{89,90}Sr^{++}$ WITH CITRIC ACID AT DIFFFRENT IONIC STRENGTHS

The initial solutions were 100 ml. in volume and equilibrated with 10 mg. of the sodium form of Dowex-50 at $t = 25°$, and pH 7.2–7.3.

Expt.	μ	K_d°	$K_d^\circ \times (Na^+)^2 \times \gamma^2_{Na^+} \times 10^2$	Ratio of activity coefficient[a] $\gamma_{(SrCit)^-}/\gamma_{Sr^{++}}\gamma_{Cit^{\equiv}}$	k_f	log k_f	log k_f° (inf. dilu.)[b]
A	0.16	2.66	3.60	(62)	660	2.82	4.6
B	.076	11.7	4.32	13	982	2.99	4.1
C	.048	28.8	4.52	9.2	2,130	3.33	4.3
B	.039	42.3	4.43	7.7	2,280	3.36	4.2
C	.038	40.7	4.11	7.7	2,020	3.31	4.2
C	.027	87.7	4.67	5.9	2,550	3.41	4.2
B	.022	101	3.63	4.9	2,800	3.45	4.1
C	.021	135	4.40	4.9	3,230	3.51	4.2
B	.014	172	2.60	3.4	3,940	3.60	4.1
C	.011	296	2.90	3.4	4,620	3.67	4.2
B	.0074	413	1.88	2.9	5,560	3.74	4.2
	0	....	..	1.0	13,000‡	4.11[c]	...

[a] Activity coefficient ratio calculated from individual ion activity coefficients as tabulated by Kielland.[43] It was assumed that $\gamma_{(SrCit)^-}$ is equal to $\gamma_{(H_2Cit)^-}$. [b] Calculated by multiplication at a given ionic strength of k_f value by the activity coefficient ratio. [c] Obtained by extrapolation of a plot of log k_f vs. $\sqrt{\mu}$.

TABLE IV

INTERACTION OF $^{89,90}Sr^{++}$ AND $^{45}Ca^{++}$ WITH ORGANIC ACIDS AND NITROGENOUS DERIVATIVES IN THE PRESENCE AND ABSENCE OF FORMALDEHYDE

The solutions were equilibrated with the sodium form of Dowex-50 at $t = 25°$, $\mu = 0.16$, pH 7.2–7.3, $v = 100$ ml., $m = 100$ mg., 25 ml. of veronal buffer.

Ligand	Structural formula	Concn. range of ligand, moles/liter	k_f Ca	k_f Sr	log k_f Ca	log k_f Sr	Constants when HCHO present[a] k_f Ca	k_f Sr	log k_f Ca	log k_f Sr
Aspartic acid	HOOC—CH_2—CH(—NH_2)—COOH	0.015-0.12	2.8 ± 0.7	7 ± 2	0.44	0.8	67 ± 8	31 ± 3	1.8	1.5
Butylamine	CH_3—CH_2—CH_2—CH(NH_2)—CH_2	.02 - .07	14 ± 2	....	1.1	....	14 ± 2	....	1.1	...
Ethanolamine	HO—CH_2—CH(NH_2)—CH_2	.02 - .07	9.2 ± .8	12.8 ± 1	0.96	1.1	13 ± 1	17 ± 2	1.1	1.2
Succinic acid	HOOC—CH_2—CH_2—COOH	.005- .04	9 ± 1	8 ± 2	1	0.9	12 ± 2	....	1.1	...
Malic acid	HOOC—CH(—OH)—CH_2—COOH	.004- .04	116 ± 8	27.9 ± 1.4	2.06	1.45	....	....	...	...
Formaldehyde	HCHO	2.3 -6.9	0.02	0.02	−1.7	−1.7	....	....	...	...

[a] The formaldehyde concentration was 10% by weight.

ployed at the outset, 0.008 M and 0.006 M in one series and 0.0052 and 0.0039 M in another series. The starting systems consisted of 10 mg. of Dowex-50 and 100 ml. of solution. All samples were run in triplicate.

In separate experiments it was found that the ion exchange equilibria were reversible, that is, if to the system at $\mu = 0.01$ we add sufficient NaCl to bring the μ back to $\mu = 0.04$, the values of K_d° and k_f check the values originally obtained at $\mu = 0.04$, despite a fourfold change in the v/m ratio.

The agreement between the extrapolated value of k_f° at infinite dilution (Fig. 3) and that calculated from the individual ion activity coefficients is satisfactory considering the fact that the extrapolation was made over a fairly wide concentration range. The slope of the extrapolated region of the curve in Fig. 3 should, according to the Debye-Hückel limiting law be about −6.1 below a $\sqrt{\mu} = 0.05$. The limiting slope as drawn is about −5. The resulting $\Delta F°_{298} = -5{,}700$ cal. The corresponding value of log k_f° for calcium citrate, using Kielland's[43] values for the individual ion activity coefficients inserted into the data of Muus and Lebel,[44] is 4.64, giving a $\Delta F°_{298} = -6{,}300$ cal.

Some information on the ion exchange reaction

$$Sr^{++} + 2NaR \rightleftharpoons SrR_2 + 2Na^+ \qquad (5)$$

where R represents the immobile anionic part of the cation exchanger is also obtained from the data in Table III. The ion exchange reaction can be written[45]

$$K_d^\circ(Na^+)^2\,\gamma^2_{Na^+} = \frac{\lambda^2_{NaR}\,\lambda_{Sr^{++}}}{\gamma_{SrR_2}} = \sim \text{Constant} \qquad (6)$$

assuming the pressure–volume terms are negligible. Since NaR is kept essentially constant, and the activity coefficient ratio is kept essentially constant under the experimental conditions, we would expect that the product $K_d^\circ(Na^+)^2\gamma^2_{Na^+}$ would be approximately constant in the range (Table III). More accurate values must include analyses of the Na content of the resin phases for each of the NaCl concentrations employed and the degree of swelling of the resin.

Effect of Formaldehyde on Complex Ion Stability.—The addition of formaldehyde increased the affinity of aspartic acid for Ca^{++} and Sr^{++} markedly, but exerted little effect on the other $-NH_2$ containing compounds. The amount of formaldehyde added, as formalin, corresponded to the amounts used in the formol titration[46] of amino acids. At pH 7.2–7.3 no physiologically significant complex formation took place between Ca, Sr, and the nitrogen containing compounds, including the dicarboxylic amino acid, aspartic. Formaldehyde itself is practically devoid of complex forming properties with the alkaline earths. Malic acid is several times more powerful than succinic acid in complex formation, showing the marked effect of an –OH group. A similar enhancement of complexing properties for Ca and Sr by a single –OH group was shown for the citric–tricarballylic acid pair.[26,44] Additional –OH groups do not increase complex forming ability in the case of the alkaline earths as shown by the fact that k_f for the calcium tartrate complex at $\mu = 0.16$ is 60.5,[28] *i.e.* weaker than the malic acid complex.

(43) J. Kielland, *J. Am. Chem. Soc.*, **59**, 1675 (1937).

(44) J. Muus and H. Lebel, *Danske Vidensk. Selsk., Math.-fys. Medd.*, **13**, No. 19 (1936).

(45) H. P. Gregor, *J. Am. Chem. Soc.*, **70**, 1293 (1948).

(46) C. L. A. Schmidt, "The Chemistry of the Amino Acids and Proteins," 2nd edition, C. C Thomas, Springfield, Illinois, 1945.

Discussion

The positively charged $-NH_3^+$ group in the aspartic acid molecule can be expected to repel a positively charged ion from the adjacent carboxyl anion.[47] Under the experimental conditions aspartic acid, insofar as its complexing action is concerned, can be considered to be the equivalent of a monocarboxylic acid anion. The addition of formaldehyde in the amounts stated at constant *p*H increases the acid ionization constant of the amino group from 2.5×10^{-10} to about 1.6×10^{-7},[46] thus reducing the net positive charge. In addition, the formaldehyde reacts with the uncharged amino group.[47] The net result is to increase markedly the bound fraction of Ca^{++} or Sr^{++}. Since the resulting formation constant becomes roughly equivalent to that of the malate anion with Ca^{++} or Sr^{++} rather than succinate, it appears that the group formed on the amino acid molecule between HCHO and $-NH_2$ exerts a complex forming action similar to the –OH group in malate. A further discussion of these points will be deferred until more data are obtained.

The relatively minor effects of temperature on the complex formation constant of strontium citrate appears characteristic for the alkaline earth–organic acid complexes in the 3–55° range. A systematic and more extensive study of the effects of temperature, ionic strength, *p*H and dielectric constant on the complexes found between the alkaline earths, transition elements, and organic acids is in progress.

The technical assistance of Mr. R. C. Lesko is gratefully acknowledged. The writer is indebted to Dr. A. Lindenbaum for the development of the radiochemical assay method for ^{45}Ca, and to Mr. R. Bane and Mr. R. Telford for the chemical analysis of the resin.

(47) E. J. Cohn, and J. Edsall, "Proteins, Amino Acids and Peptides," Reinhold Publishing Corporation, New York, N. Y., 1943.

REMARKS

ISAAC FELDMAN: I should like to point out that there are certain, as yet unstated, limitations on the method of Dr. Jack Schubert. Considering the complex $aMx\ Ay \rightarrow bMm + ay$A. A straight-line log plot using Schubert's method is obtained only when $a = b$, and therefore $x = M$. This limitation becomes important for hydrolyzable ions such as beryllium, since in basic solutions beryllium may polymerize, even in tracer concentration. Even in the case where $a = b$ and $x = m$, one must still determine "m" or "x" by an independent method. That is, the original assumption that $Mx\ Ay$ is equivalent to $MA y/x$ is subject to limitations.

These facts were first pointed out to me by Dr. Loft Toribara of our laboratory.

RESPONSE ADDED IN PROOF.—Dr. Feldman's comments apply generally to practically all methods used for the measurement of formation constants of complex ions. The extent of polymerization of a complex ion if any, would have to be determined in supplementary experiments.

ION EXCHANGE SEPARATIONS BASED UPON IONIC SIZE

BY T. R. E. KRESSMAN

The Permutit Co., Ltd., London, England

Received August 30, 1951

The molecular pores of "Zeo-Karb 225," a sulfonated cross-linked polystyrene resin, are shown to be smaller than those of the phenol sulfonate resin "Zeo-Karb 215." In spite of this the rate of exchange between the NH_4-form of "Zeo-Karb 225" and various quaternary ammonium salts is greater than that with "Zeo-Karb 215." As with "Zeo-Karb 215" the kinetics of exchange are controlled by particle diffusion (P-kinetics). Whilst the smallest pores in "Zeo-Karb 215" are larger than the effective size of the phenyldimethylbenzylammonium ion, those in "Zeo-Karb 225" are smaller than the tetramethylammonium ion. Differences of rates of exchange on "Zeo-Karb 215" have already been employed to effect separations between cations of different size: when "Zeo-Karb 225" is used, the degree of separation is enhanced by virtue of the limited saturation capacity for the larger ions. The study is extended to the absorption of acids on "De-Acidite E" and on the highly porous "Decolorite." Inorganic acids, *e.g.*, H_2SO_4, HCl are taken up rapidly by both resins from 0.01 *N* solution at 22°. Some dye acids are also taken up rapidly by "Decolorite," and more slowly and to a limited extent by "De-Acidite E." In every case the rate determining step is diffusion in the solid particle as indicated by the form of the kinetics and by interruption tests. The results can be used as a basis for the separation of inorganic salts from dye solutions with "De-Acidite E," and the feasibility of separating dye acids one from another with "Decolorite" is also indicated.

Since the mechanism of ion exchange is determined among other factors by the size of the exchanging ion, it is natural to suppose that its contribution could be exploited for effecting separations. The separation of ions by exploiting differences in rates of exchange has already been demonstrated in a preliminary manner by Kressman and Kitchener[1] and the feasibility of separations based on differences in saturation capacities is suggested by the results of Richardson which showed that the saturation capacity for acids decreases with increasing ionic size in the anion exchanger "De-Acidite B".[2]

In the present paper the pore size distributions of the phenolsulfonic acid resin "Zeo-Karb 215" and the sulfonated polystyrene resin "Zeo-Karb 225" are compared and their effect on separations based upon rates and total capacity is studied. The study is extended to the absorption of acids, having large molecules, on the anion exchanger "De-Acidite E" and the highly porous anion exchanger "Decolorite." The application of the results to the separation of inorganic salts from dyes and to the separation of high molecular weight acids among themselves is indicated.

Both the anion exchange resins are of the weakly basic type and the equilibrium absorption of acids, if not the relative rate of absorption, is considerably influenced by the dissociation constant of the acid in question. In order to eliminate this as far as possible, dyestuffs containing free SO_3H groups

(1) T. R. E. Kressman and J. A. Kitchener, *Disc. Faraday Soc.*, No. 7, 90 (1949).

(2) H. W. Richardson, *Nature*, 164, 916 (1949).

were used in the study since the acid strength of these groups is not greatly influenced by their number and by their environment (at least in the absence of adjacent NH_2 groups).[3]

Experimental

Materials.—"Zeo-Karb 225" is a unifunctional cation exchanger in bead form prepared from sulfonated cross-linked polystyrene and that used was a sample of "Permutit" laboratory grade resin sieved 16/30 B.S.S. mesh. It was converted to the H-form by flowing an excess of N HCl through a column of the resin until sodium ions were only just detectable in the effluent with a flame photometer. The resin was washed with distilled water until the effluent was free of acid, then air-dried.

The NH_4-form of the resin was prepared by flowing a 0.5 N solution of ammonium chloride through the column of the H-form until no more acid appeared in the effluent and washing off the excess ammonium chloride. The resin was filtered at the pump and surface moisture removed by mopping between filter papers. The mopped resin was then kept in a tightly stoppered bottle.

The H-form of the resin was used for the experiments illustrated in Fig. 5 and the NH_4-form for those in Figs. 2 and 3.

The "De-Acidite E" and "Decolorite," both weakly basic anion exchangers in granular form, were likewise samples of laboratory grade resins and they were converted to the free base forms by flowing a 3 N solution of ammonia through a column of the resin until chloride was undetectable in the effluent. The excess ammonia was washed from the resin with distilled water until the water emerging had a pH of about 7.5. The granules were graded by elutriation. The washed resins were kept in distilled water and sufficient for immediate needs was filtered at the pump, mopped between filter papers until surface dry and then kept in stoppered bottles. No mopped resin was used which was more than 30 hours old, a fresh quantity being taken from the large batch under distilled water, rinsed by several decantations with distilled water, then filtered and mopped as before.

The resins were used in the free base form throughout.

Determination of Effective Sphere Radius of the Swollen Resin Particles.—This was determined by the method previously described.[1] Briefly the method consists in weighing a known number of water swollen particles and determining their density (ρ) with the aid of a density bottle. The effective sphere radius r is calculated from

$$4/3.\pi r^3\rho = w$$

where w is the average weight of one particle. The "Zeo-Karb 225" particles were, in fact, in the form of spheres and the method gives the average radius of the spheres. This was found to be 0.40 mm. The effective radii of the "De-Acidite E" and "Decolorite" granules were 0.39 and 0.42 mm., respectively.

Determination of Exchange Velocity.—The technique already described[1] using the limited bath method was adhered to exactly, the speed of rotation of the stirrer being kept constant at 1000 r.p.m., a speed previously shown to be the optimum.[1]

In the experiments illustrated in Figs. 4 and 5, 2.92 meq. of swollen H-resin were used together with 125 cc. of solution originally 0.01 N in both NH_4^+ and NEt_4^+. In Figs. 2 and 3, 2.50 meq. NH_4-resin were used with 125 cc. solution, 0.02 N in total cations. In the experiments with "De-Acidite E" 1 g. of swollen resin was used and, because of its lower capacity, 2-g. lots of "Decolorite" were used. 125 cc. of solution containing 1.25 meq. acid was used for each experiment.

Determination of Total Capacity.—The total number of exchangeable hydrogen ions in the "Zeo-Karb 225" was determined by stirring a known weight—1 to 2 g.—of the resin with about 50 cc. of water containing about 20 mg. of NaCl and titrating the total acid liberated with 0.1 N NaOH to methyl red end-point. The total number of exchangeable ammonium ions in the NH_4-form was determined by distilling a known weight with dilute NaOH solution into standard acid and back titrating in the usual way.

(3) Landolt-Börnstein Tabellen, *Band II*, 1137 *et. seq.* (1936).

This method was not practicable for measuring the total capacity for organic cations and the method previously described[4] was used here. The solution of the quaternary salt was flowed slowly through a column of H-resin and the acid in the effluent titrated with alkali. The column was allowed to stand for 24 hours with the resin immersed in the quaternary salt solution and the flow of solution restarted and continued until no more acid appeared in the effluent: this acid was titrated. This was repeated until on running off the salt solution after the 24 hours standing no titratable amount of acid appeared in the effluent. The total acid liberated is a measure of the quaternary ion entering the resin.

Since the two anion exchangers are weakly basic their capacities were measured as a function of pH. Two-gram samples of the water swollen resins were weighed into a series of stoppered bottles and known volumes of nitric acid solution added to each. The initial acid concentration was different in every bottle and ranged from 0.01 to 0.5 N. After allowing 36 hours for equilibrium to be attained the pH of the solution in each bottle was measured and the residual acid titrated in an aliquot with standard alkali. Figure 1 shows the curves obtained.

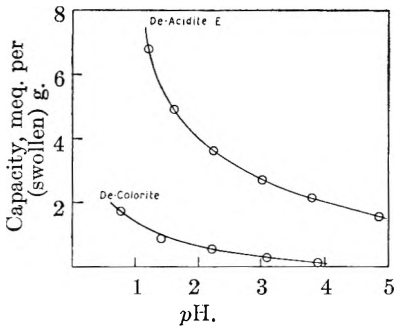

Fig. 1.—Capacity–pH curves for "Decolorite" and "De-Acidite E."

Determination of Total Water Content of the Fully Swollen Resins.—Samples of the fully swollen resins, blotted between filter papers, were weighed and dried to constant weight at 110°. The values thus obtained for the water contents, expressed as g. water per g. oven dried resin, are: "Zeo-Karb 225" H-form 0.80 g./g.; "Zeo-Karb 225" NH_4-form 0.53 g./g.; "De-Acidite E" 0.47 g./g.; "Decolorite" 2.54 g./g.

Preparation of Pure Free Dye Acids.—These were prepared from the impure sodium salts by ion exchange. A solution of the salt was prepared, containing about 30 meq. total cations in about 1 liter of water. This was passed through a column of "Zeo-Karb 225" in the H-form (25 cm. × 1.5 cm.) and then through a column of "De-Acidite E" (25 cm. × 1.0 cm.). The former converted all the salts present to the free acids and the latter absorbed the inorganic acids, while allowing the dye acid to pass through. The solution of the dye acid was then brought to 0.01 N by appropriate dilution and electrometric titration with standard alkali.

1 - Amino - 8 - naphthol - 3,6 - disulfonic acid was prepared from the monosodium salt by neutralizing a solution with sodium hydroxide and then passing this through a column of "Zeo-Karb 225" (H-form). It was then brought to 0.01 N by appropriate dilution.

Dyes Used.—In addition to 1-amino-8-naphthol-3,6-disulfonic acid, the dyes studied were Chlorazol Sky Blue, [3,3′ - dimethoxydiphenyl - 4,4′ - bis-(2 - azo - 8 - amino - 1-hydroxynaphthalene - 5,7 - disulfonic acid)]; Carmoisine [naphthalene - 1 - sulfonic acid - 4 - (2 - azo - 1 - hydroxynaphthalene - 4 - sulfonic acid)]; Orange II [2 - hydroxynaphthalene - 1 - azobenzene - p - sulfonic acid] and Orange G [2 - hydroxynaphthalene - 6,8 - disulfonic acid - 1 - azobenzene]. The major diameters of these dyes are approximately 30, 20, 15 and 15 Å., respectively; that of the aminonaphtholdisulfonic acid is about 10 Å.

Discussion

Ionic size contributes directly to the mechanism

(4) T. R. E. Kressman and J. A. Kitchener, *J. Chem. Soc.*, 1190 (1949).

of both cation and anion exchange reactions in two ways: (1) it affects the position of equilibrium, and (2) it affects the rate of attainment of equilibrium. Above a certain minimum size (depending upon the exchanger) it contributes indirectly by determining the total or saturation capacity. For the exchange of the alkali metal, ammonium and hydrogen ions the size function determining the equilibrium is the distance of closest approach a_0 in the Debye–Hückel equation,[4,5] the affinity decreasing with increasing ionic size, *i.e.*, increasing a_0. This and other evidence suggest that the cations are bound to the resin by Coulomb forces. Large organic cations show higher affinities, provided the pores of the exchangers are of sufficient size and, in contrast to the simple metal ions, the affinities *increase* with increasing ionic size. This suggests that van der Waals forces contribute largely to the affinity, the Coulomb forces being less important. Qualitative support of this is provided by the observation that the affinities of some quaternary ammonium ions increase with the number of atoms in contact with a surface.[6]

Considerably less work has been carried out with anion exchangers (see, however, refs. 7, 8, 9), and it is impossible from the data available to determine the contribution made by the size of the anion. The present work, however, indicates that in the absorption of free acids by a weakly basic, highly porous exchanger, the position of equilibrium is independent of ionic size.

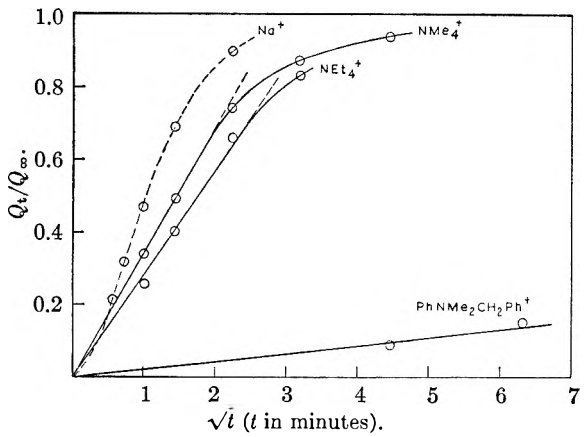

Fig. 2.—Tests of mechanism—"Zeo-Karb 225."

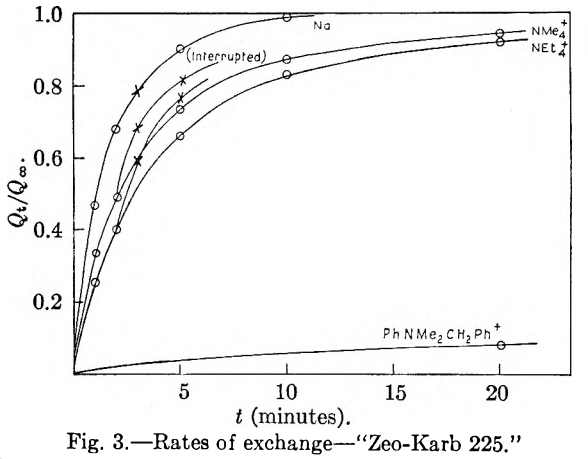

Fig. 3.—Rates of exchange—"Zeo-Karb 225."

In so far as ionic size affects the rate of attainment of cation exchange equilibrium two mechanisms can be distinguished, where the rate is controlled by diffusion in the particles of the exchanger (P-mechanism) and in the bounding Nernst film (F-mechanism), respectively. Some evidence of an intermediate (I) mechanism where the rate is influenced by diffusional resistance in *both* phases has also been obtained.[1] The form of the kinetics is often dependent upon circumstances; for example, with the sodium ion on a phenolsulfonate type resin P-kinetics at relatively high concentration can give way to F-kinetics at lower concentration[10,11]; and P-kinetics at lower temperature to F-kinetics at higher.[12] With quaternary ammonium ions on "Zeo-Karb 215" the kinetics appeared to be controlled by particle diffusion under all circumstances[1] and, as would be expected, the rate decreases as the size of the cation increases.

The saturation capacity of a sulfonic acid resin is the same for all ions when the ions are very small. With increasing size of the ion, however, a critical size is reached at which the ion is larger than some of the pores of the resin and a limited capacity only is exhibited. A resin of higher capacity will generally require a higher degree of cross-linking if similar swelling characteristics are to be maintained, because of the hydrophilic nature of the exchange active groups, and this results in smaller pores. Thus the smallest pores of "Zeo-Karb 215" (total capacity 2.8 meq./g. dry H-resin) are larger than the effective size of the phenylbenzyldimethylammonium ion (major diameter 11.2 Å.) although they are smaller than that of the tetrabenzylammonium and the quininium ions.[6] The smallest pores of "Zeo-Karb 225" (total capacity 5.2 meq./g.) on the other hand, are appreciably smaller than the tetramethylammonium ion (4.6 Å. diameter) and are probably about 2 or 3 Å. diameter only.

Now the rates of exchange of several quaternary ammonium ions with the NH_4-form of "Zeo-Karb 225" are found to be controlled by particle diffusion, as indicated by the initially straight lines obtained on plotting Q_t/Q_∞ against $\sqrt{t}$ (Fig. 2) and direct evidence of the existence of a concentration gradient within the solid is provided by a discontinuity in the velocity–time curves (Fig. 3) after a period of interruption.[12] It would be expected, therefore, that a greater diffusional resistance would be exhibited by "Zeo-Karb 225" for a given quaternary ion than by "Zeo-Karb 215." However, the times for half-change are, in fact, *less* with "Zeo-Karb 225" than with "Zeo-Karb 215," as shown in Table I, suggesting that the larger

(5) G. E. Boyd, J. Schubert and A. W. Adamson, *J. Am. Chem. Soc.*, **69**, 2818 (1947).

(6) T. R. E. Kressman and J. A. Kitchener, *J. Chem. Soc.*, 1208 (1949).

(7) W. C. Bauman, quoted by J. Schubert, *Anal. Chem.*, **22**, 1367 (1951).

(8) R. Kunin and R. J. Myers, THIS JOURNAL, **51**, 1111 (1947).

(9) R. Kunin and R. J. Myers, *J. Am. Chem. Soc.*, **69**, 28 (1947).

(10) G. E. Boyd, A. W. Adamson and L. S. Myers, *ibid.*, **69**, 2836 (1947).

(11) D. K. Hale and D. Reichenberg, *Disc. Faraday Soc.*, **No. 7** 79 (1949).

(12) T. R. E. Kressman and J. A. Kitchener, *ibid.*, **No. 7**, 101 (1949).

pores of the polystyrene resin are concentrated near the external surface of the spheres. The rates of exchange of the sodium ion are practically identical with both resins, as would be expected where the rate is controlled by diffusion in the liquid film. (In this table the times for half change on "Zeo-Karb 215" are taken from ref. 13 and are corrected for particle size ("Zeo-Karb 215" 0.45 mm. radius; "Zeo-Karb 225" 0.40 mm. radius) by multiplying the measured $t_{1/2}$ for the quaternary ions (P-diffusion) by $(0.40/0.45)^2$ and for the sodium ion (F-diffusion) by 0.40/0.45).

TABLE I

Ion	Time for half-change "Zeo-Karb 215"	"Zeo-Karb 225"
Na^+	1.25 mins.	1.25 mins.
NMe_4^+	2.7 mins.	1.75 mins.
NEt_4^+	10.0 mins.	3.0 mins.
$PhNMe_2CH_2Ph^+$	*ca.* 3 weeks	*ca.* 1 week

The equilibrium exchange values (*i.e.*, Q_∞) for these four ions on "Zeo-Karb 225" deserve brief mention. Under the experimental conditions used the equilibrium amounts of NH_4^+ liberated by the four ions are: Na^+ 1.17 meq., NMe_4^+ 0.5 meq., NEt_4^+ 0.74 meq., $PhNMe_2CH_2Ph^+$ 1.6 meq. If the saturation capacities were the same for all the ions these equilibrium values would increase in the order Na^+, NMe_4^+, NEt_4^+, $PhNMe_2CH_2Ph^+$. The observed order is explained by the limited saturation capacities of the resin for the organic ions. That for NMe_4^+ is 76% and that for NEt_4^+ 62% of the maximum; however, that for $PhNMe_2CH_2Ph^+$ is unexpectedly high (74% of the maximum) and the intrinsically high affinity of this ion for the resin enables a comparatively high Q_∞ value to be reached. The abnormally high saturation capacity for the $PhNMe_2CH_2Ph^+$ ion suggests either that some orientation of the molecule occurs in its passage along the resin pores, its effective diameter thus being something between its major (11.2 Å.) and its minor (4.6 Å.) diameters; or that considerable distortion of the resin structure can occur if the attractive force is sufficiently large. In this connection it is noteworthy that the bivalent ion $[CH_2N(C_2H_5)_3]_2^{++}$ also exhibits a higher saturation capacity (83% of the maximum) than its major diameter of 10.7 Å. would suggest.

The separation of inorganic ions from organic by exploiting their different rates of exchange on "Zeo-Karb 215" has been demonstrated.[1] The degree of separation is enhanced when "Zeo-Karb 225" is used by virtue of the limited saturation capacity for the larger ion. This is illustrated in Figs. 4 and 5, which show the concentration of H^+, NH_4^+ and NEt_4^+ in a solution (initially equimolar with respect to NH_4^+ and NEt_4^+) during the course of exchange experiments with "Zeo-Karb 215" and "Zeo-Karb 225," respectively. The solution becomes enriched in NEt_4^+ in each case, but whereas a 1.3-fold enrichment in 4 minutes occurs with "Zeo-Karb 215" the enrichment with "Zeo-Karb 225" after the same time is 1.6-fold.

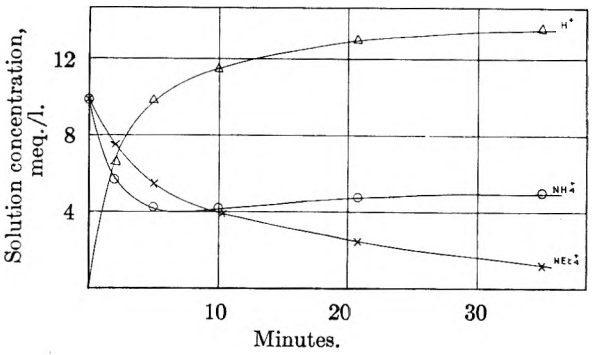

Fig. 4.—Exchange of NH_4^+ and NEt_4^+ for H^+ on "Zeo-Karb 215."

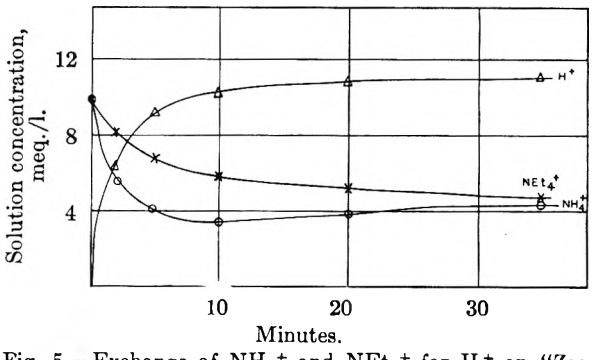

Fig. 5.—Exchange of NH_4^+ and NEt_4^+ for H^+ on "Zeo-Karb 225."

The rates of absorption of acids on "De-Acidite E" likewise decrease with increasing size of the acid molecule, and a specific effect of valency of the anion is observed, sulfuric acid exchanging at a greater rate than hydrochloric acid—Fig. 6. This is consistent with the results of Kunin and Myers[8] who supposed the effect to be due to the greater attractive force between the resin and the more highly charged ion. This is in marked contrast to cation exchange where increased valency results in a *lower* rate of exchange.[13]

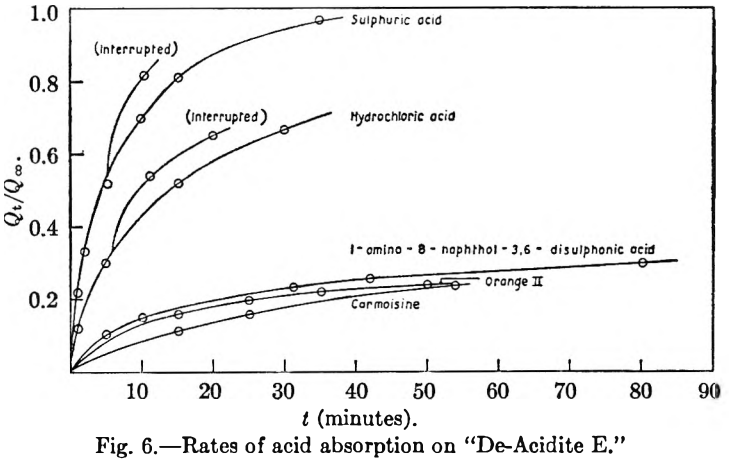

Fig. 6.—Rates of acid absorption on "De-Acidite E."

The rates of absorption of 1-amino-8-naphthol-3,6-disulfonic acid, Orange II, Carmoisine and Chlorazol Sky Blue are very low and it is evident

(13) T. R. E. Kressman and J. A. Kitchener, *Disc. Faraday Soc.*, No. 7, 95 (1949).

that a limited saturation capacity is available for these ions: with "Decolorite" the effect is observed only with the Chlorazol Sky Blue ion (*cf.* Table II).

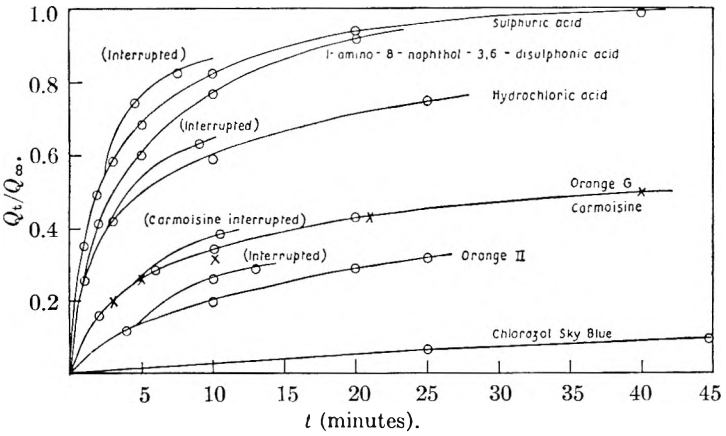

Fig. 7.—Rates of acid absorption on "Decolorite."

The specific effect of valency on the rate of acid absorption is observed also with "Decolorite" (Fig. 7) and it is seen to apply not only to inorganic acids like hydrochloric and sulfuric but also to the large organic dyes. Thus, Orange G and Orange II are of similar molecular structure differing only in the position and number of SO_3H groups. The considerably greater rate of exchange of the former with its two SO_3H groups compared with the latter with one is very marked: $t_{1/2}$ values are not available but the times for $^1/_4$-change are 4.5 and 15 min., respectively. Although Carmoisine possesses two naphthalene rings and Orange G only one, the rates of exchange are almost identical: this is remarkable since, even if the molecule enters with its major axis roughly parallel with that of the pores, the two naphthalene rings would be expected to encounter a greater diffusional resistance than the one.

The curves of Q_t/Q_∞ against $\sqrt{t}$ for both "DeAcidite E" and "Decolorite" all exhibit an initial straight portion (Figs. 8 and 9) indicating that diffusion through the solid particles is the rate determining step, and this is confirmed by the discontinuity in the rate curves exhibited after periods of interruption (Figs. 6 and 7). This is surprising in the case of the inorganic acids on "Decolorite" since the pores must be many times larger than the acid molecules and it would be expected that rapid movement through the pores would occur. It suggests that the rate step is not controlled only by simple diffusion.

The effect of valency on the equilibrium position is very marked with "Decolorite," where the acids can be divided into two groups—those with univalent anions showing an equilibrium absorption of 0.45 ± 0.01 meq. per gram, and those with bivalent showing an equilibrium absorption of 0.51 ± 0.01 meq. per gram (see Table II). The absence of any specific effect of structure is remarkable in view of the extent to which it influences the equilibrium position in cation exchange. The comparatively low degree of cross-linkage in the resin might, however, account for this.

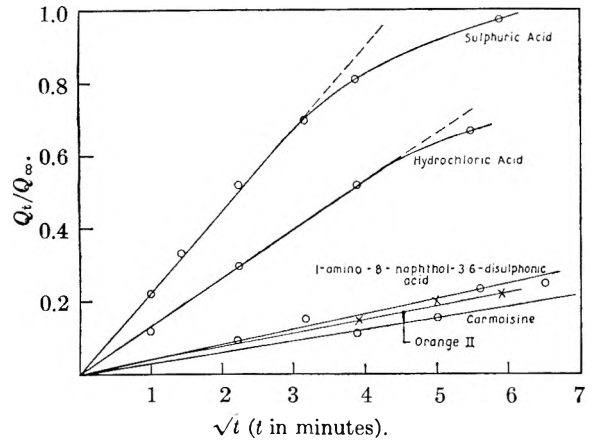

Fig. 8.—Tests of mechanism—"De-Acidite E."

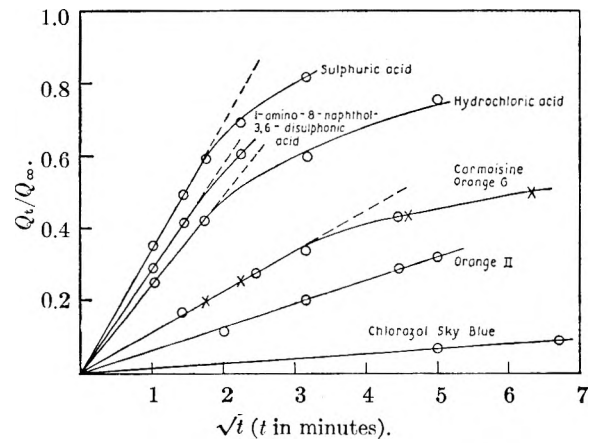

Fig. 9.—Tests of mechanism—"Decolorite."

TABLE II

EQUILIBRIUM ABSORPTION ON "DE-ACIDITE E" AND "DECOLORITE"

	"De-Acidite E" (meq./g.)	"Decolorite" (meq./g.)
Hydrochloric acid	1.00	0.44
Sulfuric acid	1.22	.50
1-Amino-8-naphthol-3,6-disulfonic acid	0.68	.45
Orange G	..	.52
Orange II	.24	.46
Carmoisine	.36	.45
Chlorazol Sky Blue FF	<.1	.32

Separations

The results discussed above indicate the feasibility of separating ions by exploiting differences in their behavior toward ion exchangers brought about by differences in ionic size. The advantage of using "Zeo-Karb 225," containing smaller pores than "Zeo-Karb 215," for this purpose is illustrated in Figs. 2 and 3.

The ability of "De-Acidite E" to absorb rapidly the simple inorganic acids while absorbing the large dye acids only very slowly, and to a limited extent, immediately suggests that the resin could be used in conjunction with a hydrogen exchanger to purify dyes from contaminating inorganic salts. Details of such a purification are given in the Experimental section. Specifically the purification of Carmoisine was carried out as described and, after bringing the solution emerging from the resin columns to *p*H 7 with sodium hydroxide, it was evaporated to dryness. The pure

dye so obtained was ashed and the ash converted to the sulfate. Ash so found 28.8%: calculated 28.3%.

The appreciable separation between the several rate curves in Fig. 7 suggests that "Decolorite" could be used to separate among themselves acids having large molecules. A preliminary qualitative experiment with a mixture of the dye acids of Orange G and Sky Blue FF confirmed this: when a solution containing a mixture of these dyes, each in 0.005 *N* concentration, was passed through a column of "Decolorite" 21 cm. × 1.2 cm. at 10 cc./min. an immediate breakthrough of the Sky Blue occurred and its concentration rapidly increased to 0.005 *N*. When the experiment was stopped after 20-bed volumes had passed Orange G had still not appeared in the effluent. When the experiment was repeated at twice the rate of flow, some Orange G also appeared in the effluent.

Acknowledgment.—Thanks are due to the Directors of The Permutit Co. Ltd., London, for permission to publish this work.

ISOBARIC AND ISOTHERMAL STUDIES IN THE SYSTEM SOAP–WATER. II[1]

BY W. O. MILLIGAN AND ARTHUR L. DRAPER[2]

Department of Chemistry, The Rice Institute, Houston, Texas

Received August 30, 1951

Sorption–desorption isotherms at 12 and 2° have been obtained for certain crystalline forms of both sodium stearate and sodium palmitate, using water vapor as the adsorbate. The soaps studied include the β-form produced by dehydration of the α-hemihydrate in a high vacuum at 35°, and the β-, δ-, and ω-forms. The adsorption isotherms for the β-form (small crystals) produced by the dehydration of the α-form and for the δ- form have two inflection points below 0.3 p/p_0, while those for the β- (larger crystals) and ω-forms are quite regular in this region. At high pressures all of the isotherms rise rapidly. A Hüttig plot yields two straight lines with similar slopes but different intercepts, suggesting that two separate adsorption processes occur consecutively. The BET function gives only one linear portion.

Heats of adsorption calculated by the Clausius–Clapeyron equation decline rapidly from extremely high values at low pressures, rise slightly at intermediate pressures, and subsequently decline to approach the heat of liquefaction of water at the saturation pressure. The shape of the adsorption isotherms may be attributed in part to the plate-like character of the soap crystals; the secondary maximum in the heat of adsorption curves may be attributed to lateral interactions of the adsorbed molecules.

The desorption isotherms exhibit low pressure hysteresis, even at very low pressures. A slight upward drift in the zero point is attributed to some chemisorption occurring in the system. Pore radii calculated from the desorption isotherms are too small to be significant. No current theory accounts for the hysteresis observed in this system.

Systematic adsorption studies have not been carried out on pure soap samples of known crystalline form. Recent investigations have been directed toward the practical determination of soap–water phase diagrams, and toward the complex problem of soap polymorphs and hydrates.[3,4]

In previous work in this Laboratory[5–8] dehydration isobars were obtained for the four clearly defined crystalline forms characterized by Ferguson, Rosevear and Stillman.[4]

The purpose of this present paper is to report the results of isothermal absorption studies carried out on a limited number of carefully chosen crystalline soap samples of known history, previously used in isobaric dehydration experiments.

Experimental

Preparation of Samples.—The soap samples employed in this investigation were especially prepared (*cf.* ref. 20) by the Procter & Gamble Company. All of the samples had been previously dehydrated at 35° in a high vacuum during the determination of dehydration isobars[7,8], and the isotherms reported here were obtained on these samples in dehydrated form. The crystalline form of these soaps before and after vacuum dehydration is given in Table I.

The identity of β-, δ- and ω-phases with the corresponding phases described by Ferguson, Rosevear and Stillman[4,9] was ascertained by comparing the powder X-ray diffraction patterns of the samples after the completion of the isotherms with the original X-ray negatives obtained by these investigators.

Adsorption Isotherms.—The adsorption isotherms were obtained at both 12 and 2° in a multiple apparatus employing 15 fused silica springs,[10] which has already been described.[11] Temperatures were measured with a thermometer calibrated by the National Bureau of Standards, and were checked by a comparison of the observed and calculated saturation vapor pressure during each isotherm. The temperature was held constant during each isotherm to approximately ± 0.001°.[11]

Samples of the crystalline soaps listed in Table I, with the exception of the δ-sodium palmitate (Sample G), were initially placed in the apparatus and dehydration isobars were obtained from −20 to 35°.[8] The dehydrated samples were left in the platinum buckets, and without opening the apparatus, the temperature was lowered to 12°. Water vapor from the adsorbate source was made available to the samples during the temperature lowering in order to prevent the samples from robbing each other of water and thus delaying the attainment of equilibrium conditions. In the determination of the isotherms at least 48 hours were required to reach equilibrium at each pressure setting, longer periods being necessary particularly in pressure regions where the amount of adsorption was changing rapidly. After completion of the isotherm at 12°, the temperature was lowered to 2°, the samples having access to water vapor during the lowering of the temperature. After the weight of the samples had become constant, the 2° isotherms were obtained.

(1) Presented before the twenty-fifth National Colloid Symposium, which was held under the joint auspices of the Division of Colloid Chemistry and the Division of Physical and Inorganic Chemistry of the American Chemical Society at Ithaca, New York, June 18–21, 1951.

(2) Procter & Gamble Fellow, 1948–1950. Humble Oil and Refining Company Fellow, 1950–1951 Present address: Carter Oil Company, Tulsa, Oklahoma.

(3) M. J. Buerger, L. B. Smith, F. V. Ryer and J. E. Spike, Jr., *Proc. Natl. Acad. Sci. U. S.*, **31**, 226 (1945).

(4) R. H. Ferguson, F. B. Rosevear and R. C. Stillman, *Ind. Eng. Chem.*, **35**, 1005 (1943).

(5) G. L. Bushey, Ph.D. Thesis, The Rice Institute, 1948

(6) A. L. Draper, M.A. Thesis, The Rice Institute, 1949.

(7) A. L. Draper and W. O. Milligan, *Texas J. Sci.*, **2**, 209 (1950).

(8) W. O. Milligan, G. L. Bushey and A. L. Draper, THIS JOURNAL, **55**, 44 (1951).

(9) R. H. Ferguson, *Oil & Soap*, **21**, 6 (1944).

(10) J. W. McBain and A. M. Bakr, *J. Am. Chem. Soc.*, **48**, 690 (1926).

(11) W. O. Milligan, W. C. Simpson, G. L. Bushey, H. H. Rachford, Jr., and A. L. Draper, *Anal. Chem.*, **23**, 789 (1951).

After the completion of the isotherms, the samples were removed and identified by means of their X-ray diffraction patterns. This was done as rapidly as possible to preserve the actual form of the crystalline soaps at the completion of the isotherms. The results of these X-ray examinations are summarized in Table I.

TABLE I

X-RAY EXAMINATION

Sample	Original form	Form after vacuum dehydration
A	α-Sodium stearate hemihydrate	β-Sodium stearate (small crystals)
B	β-Sodium stearate	β-Sodium stearate (larger crystals)
C	δ-Sodium stearate	δ-Sodium stearate
D	ω-Sodium stearate	ω-Sodium stearate
E	α-Sodium palmitate hemihydrate	β-Sodium palmitate (small crystals)
F	β-Sodium palmitate	β-Sodium palmitate (larger crystals)
G	δ-Sodium palmitate	δ-Sodium palmitate
H	ω-Sodium palmitate	ω-Sodium palmitate

A few typical isotherms are plotted in Figs. 1–4. The adsorption branch of the isotherms is indicated by open circles, the desorption branch by closed circles. The solid line represents the isotherms at 12°, the dashed line at 2°. Figure 1 gives the isotherms for the sample of the β-sodium stearate produced by the dehydration of the α-form (sample A). The small differences observed in the isotherms for different samples of β-sodium stearate and β-sodium palmitate is attributed to variation in crystal size. Since grinding may alter the structural form of soaps,[4,9] the samples were not homogenized before the isobars and isotherms were obtained. The magnitude of these differences in the beta samples is extremely small, but is considered to be significant, inasmuch as the differences are observed in both the 2° and the 12° isotherms. Figures 2–4 represent the complete isotherms for β-, δ- and ω-sodium stearate, respectively. The isotherms for the sodium palmitate samples are quite similar in appearance, and are not reproduced here.

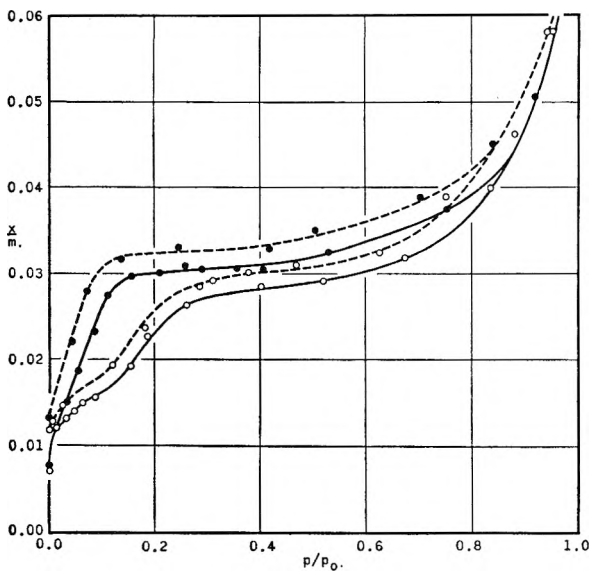

Fig. 1.—Sorption–desorption isotherms for water vapor on β-sodium stearate produced by the dehydration of α-sodium stearate at 12° (solid line) and 2° (dashed line).

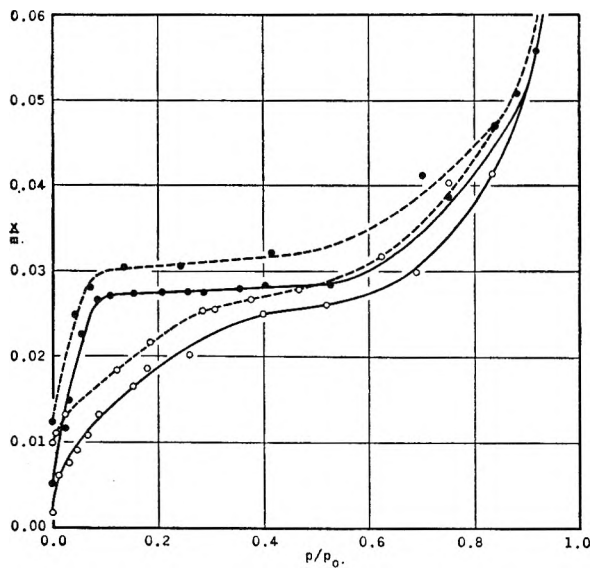

Fig. 2.—Sorption–desorption isotherms for water vapor on β-sodium stearate at 12° (solid line) and 2° (dashed line).

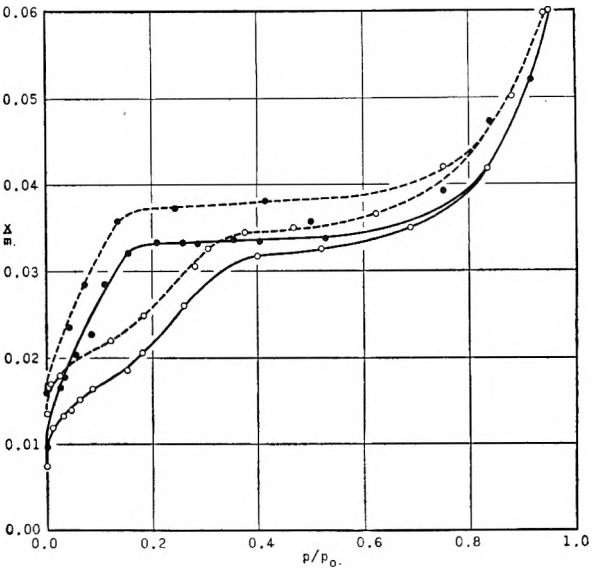

Fig. 3.—Sorption–desorption isotherms for water vapor on δ-sodium stearate at 12° (solid line) and 2° (dashed line).

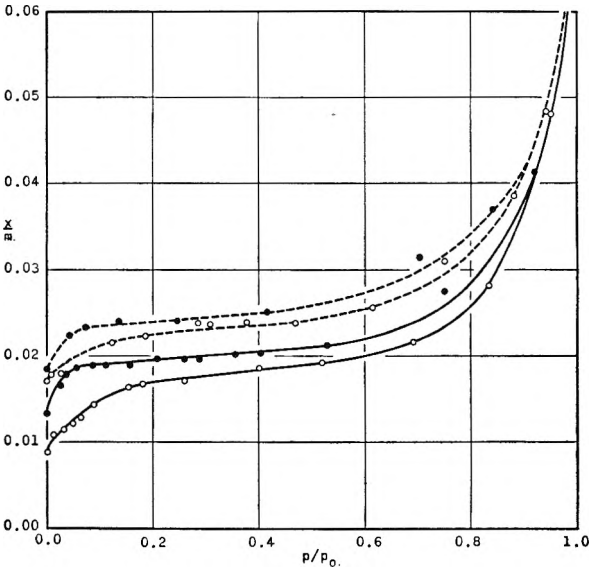

Fig. 4.—Sorption–desorption isotherms for water vapor on ω-sodium stearate at 12° (solid line) and 2° (dashed line).

Discussion

Adsorption Isotherms.—The isotherms given in Figs. 1–4 are typical of those obtained for all of the dehydrated crystalline soaps. Corresponding crystalline forms of sodium stearate and sodium palmitate give similar isotherms. At the two

temperatures, the curves tend to parallel each other. The isotherms for the β-phase produced from the dehydration of the α-sodium stearate hemihydrate and for δ-sodium stearate possess two inflection points below 0.3 p/p_0, whereas the β- and ω-forms do not show this characteristic.

Isotherms with two inflection points at low pressure have been reported infrequently in the literature. Katz[12] and McBain and Lee[13-15] observed no such isotherms in their investigations. Orr[16] obtained isotherms of this shape for the adsorption of argon, krypton and carbon monoxide on large, uniform crystals of potassium chloride. Bangham and Mosallam[17] found that isotherms of methyl alcohol on mica showed an abrupt discontinuity at 0.1 p/p_0. Cornet[18] reported curves of this type for the adsorption of ammonia on montmorillonite. Recently, Bielanski and Tompkins[19] obtained similarly shaped isotherms for the adsorption of water vapor on dehydrated single crystals of potash alum. Taylor[20] reports that oxygen, argon and krypton give such isotherms on ionic lattices.

This type of isotherm can be expressed mathematically only by an empirical equation. It is evident that first order equations cannot fit such data. The BET or Hüttig[21] adsorption equations are first order, as they may be expressed in linear form. Brunauer, Emmett and Teller[22] extended their equation to a second order approximation by including a pair of c-type constants. Ferguson and Barrer[23] have treated the Hüttig equation similarly. Such second order equations involve a ratio of two c-values, so that smooth sigmoid curves are obtained.

A plot of the soap-water adsorption data in terms of the simple Hüttig function is given in Figs. 5, 6 and 7 for the isotherms of Figs. 1, 2 and 4. It is interesting to note that two linear curves are obtained, generally of similar slopes but different intercepts. The graph for ω-sodium stearate (Fig. 7) exhibits both different slopes and intercepts. The isotherms plotted in this manner fall away from the linear portion above 0.7 p/p_0, the usual limit to which data may be expressed by the Hüttig equation. Plots of these data in terms of the BET function likewise result in a linear region at low pressures, then tend rapidly upward, a behavior which is characteristic of the usual limit to which data may be expressed by the BET equation.

The "surface area" of these soaps as calculated from the slope of the Hüttig equation is approximately 60 m.^{2}/g. This numerical value is not considered to be significant.

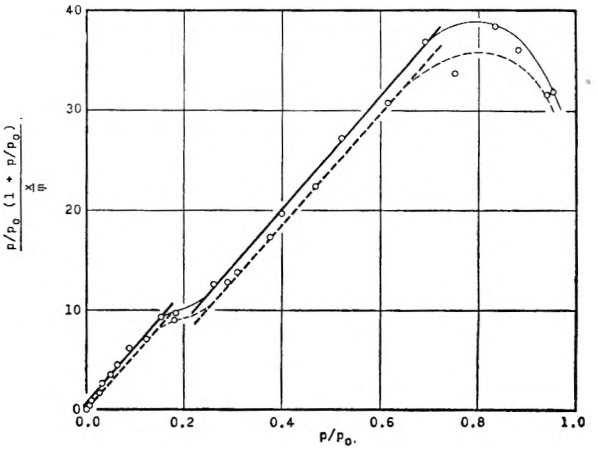

Fig. 5.—Sorption isotherms for water vapor on β-sodium stearate (sample A) produced by the dehydration of α-sodium stearate at 12° (solid line) and 2° (dashed line) according to the Hüttig equation.

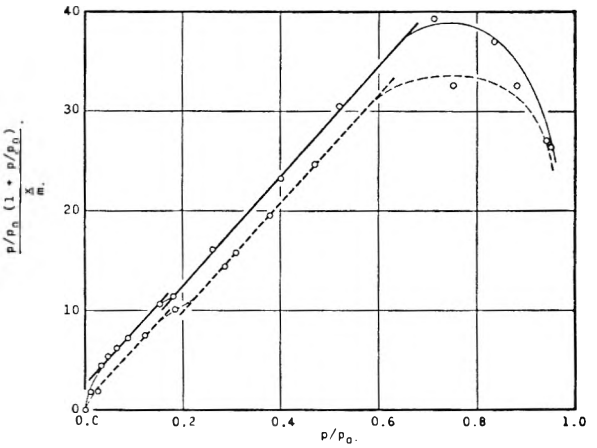

Fig. 6.—Sorption isotherms for water vapor on β-sodium stearate (sample B) at 12° (solid line) and 2° (dashed line) according to the Hüttig equation.

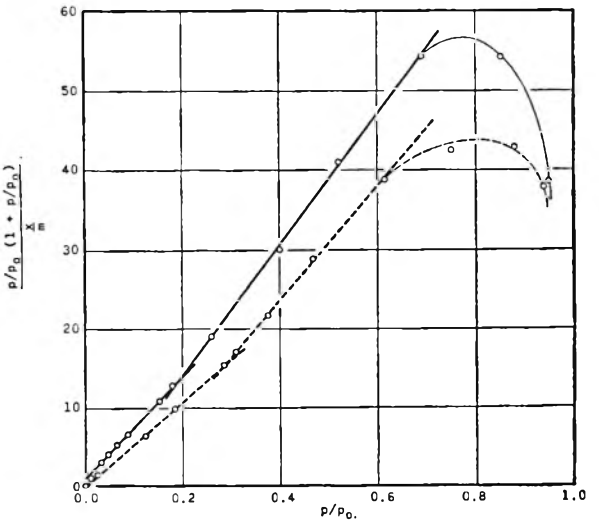

Fig. 7.—Sorption isotherms for water vapor on ω-sodium stearate at 12° (solid line) and 2° (dashed line) according to the Hüttig equation.

(12) J. R. Katz, *Kolloidchem. Beihefte*, **9**, 1 (1917).
(13) W. W. Lee, Ph.D. Thesis, Stanford University, 1941.
(14) J. W. McBain and W. W. Lee, *Ind. Eng. Chem.*, **35**, 784 (1943).
(15) J. W. McBain and W. W. Lee, *Oil & Soap*, **20**, 17 (1943).
(16) W. J. C. Orr, *Proc. Roy. Soc.* (*London*), **173A**, 349 (1939).
(17) D. H. Bangham and S. Mosallam, *ibid.*, **166A**, 558 (1938).
(18) I. Cornet, *J. Chem. Phys.*, **11**, 217 (1943).
(19) A. Bielanski and F. C. Tompkins, *Trans. Faraday Soc.*, **46**, 1072 (1950).
(20) H. S. Taylor, "Frontiers in Chemistry," Vol. VIII, "Frontiers in Colloid Chemistry," Burk and Grummitt, Editors, Interscience Publishers, Inc., New York, N. Y., 1950, p. 1.
(21) G. F. Hüttig, *Monatsh.*, **78**, 177 (1948).
(22) S. Brunauer, P. H. Emmett and E. Teller, *J. Am. Chem. Soc.*, **60**, 309 (1938).
(23) R. R. Ferguson and R. M. Barrer, *Trans. Faraday Soc.*, **46**, 400 (1950).

Halsey[24] suggests an empirical equation to describe the phenomenon of coöperative adsorption, in which an adsorbed molecule favorably influences the adsorption of its neighbors. Some of the isotherms reported here give the characteristic log p/p_0 *versus* log x/m plot predicted by this equation, but a physical interpretation of this result cannot be readily made.

The adsorption isotherms (Figs. 1–4) could possibly be interpreted on the basis of phase transitions in a two-dimensional gas in accordance with the work of Gregg.[25] A discontinuity in the compressibility or spreading pressure curve, identified with first-order transition, results from an inflection point in the isotherm. However, such considerations require a mobile layer for the adsorbed molecules in order to approximate a two-dimensional gas, but the high heats of adsorption observed in this system indicate that the molecules are held tightly.

Heats of Adsorption.—Figure 8 gives the heats of adsorption calculated by means of the classical Clausius–Clapeyron equation for the β-sodium stearate produced by the dehydration of the α-form and for the β- and δ-forms. Figure 9 details the heat of adsorption in the low pressure region for the β-phase produced by the dehydration of the α-form. These curves show a regular decline from extremely high values at low pressure, a rise to a secondary maximum at intermediate pressure, and a decline at high pressures with the heat of adsorption approaching the heat of liquefaction, indicated by a horizontal line in Figs. 8 and 9.

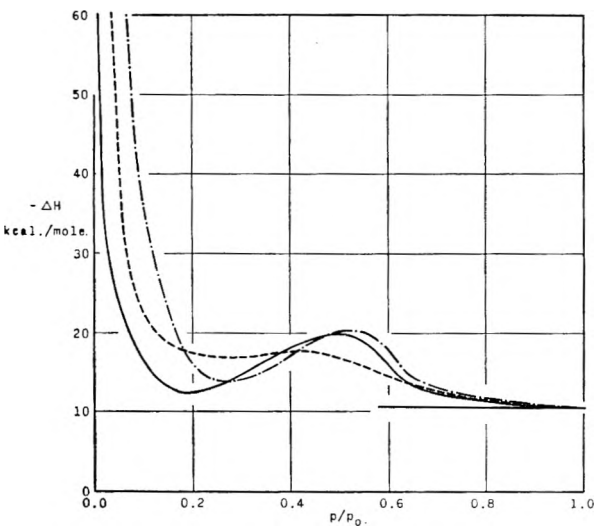

Fig. 8.—Heats of adsorption computed by means of the Clausius–Clapeyron equation at 7° for the adsorption of water on β-sodium stearate produced by the dehydration of α-sodium stearate (solid line), β-sodium stearate (dashed line) and δ-sodium stearate (dashed-dotted line).

The variation of the heat of adsorption with the amount of gas adsorbed is similar to that observed by Joyner and Emmett[26] for the adsorption of nitrogen on certain carbon blacks. The secondary maximum occurs at about the same value of p/p_0 in the two sets of data; the variation at low pressure (Fig. 9) closely resembles their results on Spheron, for with Graphon a more pronounced maximum occurs before the monolayer is complete. These results have been recently discussed in detail by Hill, Joyner and Emmett.[27] Orr[16] obtained heats of adsorption with a secondary maximum; and interpreted the position of this maximum to correspond to the monolayer. Consideration of his isotherms shows that the maxima occur at approximately the same location as those reported here and by Joyner and Emmett.[26] Halsey[24] quotes Orr's interpretation in substantiation of the coöperative theory, and Taylor[20] suggests that a secondary maximum in the heat of adsorption co-incident with the completion of the monolayer is characteristic of coöperative adsorption.

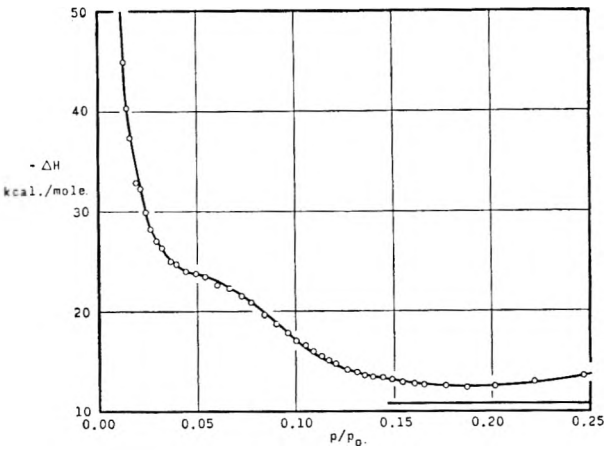

Fig. 9.—Heats of adsorption computed by means of the Clausius–Clapeyron equation at 7° for the adsorption of water of β-sodium stearate produced by the dehydration of α-sodium stearate.

Ferguson, Rosevear and Nordsieck[28] observed a continuous variation in the X-ray spacings of soaps with relative humidity. This characteristic of plate-like materials was first observed in the montmorillonite clays by Hofmann, Endell and Wilm.[29] Marshall[30] gives a complete review of such data, using it to explain the ammonia–montmorillonite isotherms obtained by Cornet.[18] Microscopic observations of the soap samples used in these studies indicate a plate-like structure.

Halsey and Taylor[31] and Sips[32] attributed smooth adsorption isotherms to a distribution of adsorption sites with respect to their energy corresponding to a regular exponential or Gaussian curve. An adsorbent with a plate-like structure would have large areas of planar surfaces; if the adsorption sites on these surfaces possessed the same energy,

(24) G. D. Halsey, Jr., *J. Chem. Phys.*, **16**, 931 (1948)

(25) S. J. Gregg "Surface Chemistry, a Special Supplement to Research," Interscience Publishers Inc., New York, N. Y., 1949, p. 205.

(26) L. G. Joyner and P. H. Emmett, *J. Am. Chem. Soc.*, **70**, 2353 (1948).

(27) T. L. Hill, L. G. Joyner and P. H. Emmett, results presented at the 119th Meeting of the American Chemical Society, which was held in Boston, Mass., April 1–7, 1951.

(28) R. H. Ferguson, F. B. Rosevear and H. Nordsieck, *J. Am. Chem. Soc.*, **69**, 141 (1947).

(29) U. Hofmann, K. Endell and K. Wilm, *Kolloid-Z.*, **86A**, 340 (1933).

(30) C. E. Marshall, "The Colloid Chemistry of the Silicate Minerals," Academic Press, New York, N. Y., 1949.

(31) G. D. Halsey, Jr., and H. S. Taylor, *J. Chem. Phys.*, **15**, 624 (1947).

(32) R. Sips, *ibid.*, **16**, 490 (1948).

the distribution curve would show a peak at this point. This condition obtains in the soaps and clays, and possibly in the ionic lattices, where extensive planar areas of similar atoms in equivalent positions result from the crystal structure.

The isotherms for an adsorbent with this type of distribution would rise rapidly at the pressure where the large number of sites was being filled. The heat of adsorption would show little change in this region. These characteristics may be seen in the isotherms and in the heat of adsorption curves for the beta-sodium stearate (sample A) given in Figs. 1 and 9. If the planar sites did not have a unique energy, a smoother isotherm would be obtained, such as for sample B (Fig. 2). The structural changes of polymorphic inversion of the other forms to the omega form produced by severe dehydration may destroy the planar surfaces, thus accounting for the absence of the inflection point in the omega phase isotherms shown in Fig. 4.

Planar domains with numerous sites of similar energy do not account for the magnitude of the heats of adsorption or the secondary maxima which are observed. The magnitude of the heats suggests that some chemisorption is occurring.

Desorption Isotherms.—The desorption isotherms indicated by the filled circles in Figs. 1–4 show hysteresis principally at low pressures. Many isotherms have been observed which exhibit hysteresis over the entire pressure range, such as those obtained by Bangham and Mosallam[17] for benzene on mica. These, however, do not possess a distinct step-like descent at the lower pressures.

Milligan, Weiser and Simpson[33] obtained isotherms on certain alumina samples (γ-AlOOH) which are of interest. The samples are known to be plate-like, but the adsorption isotherms show no inflection point at low pressures. The desorption isotherms exhibit hysteresis over the entire pressure range. In the high pressure range, a well-defined inflection point occurs, so that the hysteresis at these pressures may be readily explained by pores in accordance with the Kelvin equation. However, a definite step may be detected in the low pressure region of the desorption isotherms. Since pronounced hysteresis does not occur at high pressure in the soap–water isotherms, the enhanced low pressure hysteresis appears at a distinct phenomenon.

Since the desorption branch drops sharply after the curve has reached the low pressure region, a pore diameter calculated from the Kelvin equation corresponds to slightly more than the diameter of one molecule. The application of this equation in the low pressure region gives questionable results; Pierce and Smith[34] and others believe that pore radii corresponding to less than four molecular diameters are meaningless. Extension of the Kelvin equation to planar rather than cylindrical pores gives plate separations half the size of the corresponding radii.

It is considered that the plate-like form of the several adsorbents, such as the soaps, γ-AlOOH, mica, and certain clays, is closely related to the special adsorption–desorption characteristics of these materials. However a quantitative explanation must await the accumulation of additional information. Although the existence of extensive planar areas with large numbers of equivalent absorption sites may account for the shape of the adsorption isotherms, the low pressure hysteresis is not explained. Indeed, low pressure hysteresis has been observed in this Laboratory for the adsorption of water vapor on several samples of zirconia, which are essentially amorphous to X-rays.

The adsorption and desorption curves considered together indicate that there is occurring some phenomenon not previously observed, in which hysteresis occurs because the desorption process differs from the adsorption process. The adsorption process considered in terms of a two dimensional gas[25] might be expected to show hysteresis on desorption by considering a first order transition as a suspended change. This is considered unlikely in view of the magnitude of the heats of adsorption which are involved. The coöperative theory as presented by Halsey[24] does not imply hysteresis on desorption. Hill[35] has recently extended this idea to derive an equation for adsorption on small nuclei and planes. His equation contains many constants which cannot be evaluated. However, the equation possesses discontinuities which enable it to be used as an approximation. Considering the first inflection point to represent completion of the monolayer, the data for the beta form of sodium stearate produced by the dehydration of the alpha form are plotted in Fig. 10 together with a plot of the Hill equation. The solid line represents the equilibrium path of the isotherm, and the dashed line the theoretical curve. The similarity of this curve to that for equations of state through gas–liquid phase transitions will be noted. On this approximate basis, the coöperative theory partially explains the entire isotherms.

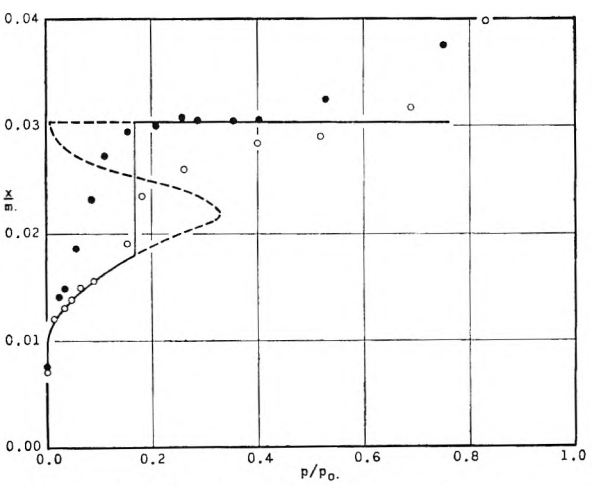

Fig. 10.—Sorption–desorption isotherms for water vapor on β-sodium stearate produced by the dehydration of α-sodium stearate at 12° according to the Hill equation.

However, the assumptions of this theory concern the influencing of the adsorption of neighboring

(33) W. O. Milligan, H. B. Weiser and W. C. Simpson. Results presented at the 105th Meeting of the American Chemical Society which was held in Detroit, Mich., April 12–16, 1943.

(34) C. Pierce and R. N. Smith, THIS JOURNAL, **54**, 784 (1950).

(35) T. L. Hill, *ibid.*, **54**, 1186 (1950).

molecules, and do not directly treat the lateral interactions of the adsorbed molecules. Ferguson and Barrer[23] point out that no successful treatment of lateral interactions has been made. Orr[16] interprets his isotherms on the basis of molecular rearrangements on the surface, but does not discuss the nature of the lateral interactions. de Boer[36] in an extensive treatment of this subject records no theory which predicts the behavior observed here. Everett, Smith and Whitton[37] in a discussion of the thermodynamics of adsorption hysteresis point out that no complete explanation of the phenomenon exists.

(36) J. H. de Boer, "Advances in Colloid Science," Vol. III, Interscience Publishers Inc., New York, N. Y., 1950, p. 1.

(37) D. H. Everett, F. W. Smith and W. I. Whitton, results presented at the 120th Meeting of the American Chemical Society which was held in New York, N. Y., Sept. 3–7, 1951.

The large domains of planar sites available in the soaps and in the other plate-like adsorbents present an opportunity for lateral interactions by the adsorbed molecules. For the adsorbates discussed here, such as water, ammonia, and methyl alcohol, interactions between molecules might consist in the information of hydrogen bonds, the energy of this stabilization process thus accounting for the secondary maximum observed in the heat of adsorption. However, lateral interactions on the uniform planar surfaces do not account for the type of hysteresis observed here in the soap–water isotherms, nor that reported by Milligan, Weiser and Simpson.[33]

The authors are grateful to the Procter & Gamble Company, which made these studies possible by the establishment of a fellowship program at the Rice Institute.

CHARACTERISTIC X-RAY SPECTROMETER PATTERNS OF THE SATURATED SODIUM SOAPS[1a,1b]

ROBERT D. VOLD, JOSEPH D. GRANDINE, 2ND,[2] AND HANS SCHOTT[3]

Department of Chemistry, University of Southern California, Los Angeles 7, California

Received August 30, 1951

It is confirmed that the sodium salts of the saturated fatty acids may exist in a large number of different states at room temperature, giving rise to X-ray diffraction patterns which differ discontinuously from modification to modification, but which are substantially the same for all samples prepared within the field of formation of a given modification, when studied at room temperature at constant relative humidity. Characteristic X-ray spectrometer patterns are presented to permit easy identification of these modifications. The formation of this multiplicity of forms apparently requires the presence of water during the processing of systems at higher temperatures before cooling to room temperature. Evidence is presented tending to show that the zeta and epsilon modifications cannot be stoichiometric hydrates but are probably solid solutions. Despite certain limitations, several of these patterns appear to be interpretable in terms of a structure consisting of a randomly stacked array of two-dimensional lattices. Striking success was also obtained in terms of this hypothesis in accounting for changes in spacing occurring on drying zeta and epsilon samples over phosphorus pentoxide, and on changing the chain length of soaps in the zeta modification.

Although much effort has been spent on study of the solid forms of the sodium soaps[4–15] the subject is still in a state of rather chaotic confusion. The present work was undertaken in the first instance to clarify the situation by providing a set of reproducible X-ray spectrometer patterns which can be used for unambiguous identification of the "modification"[16] present, and to correlate previous nomenclature with this set of standard patterns.

A further important consideration was the degree of constancy or variation of pattern of a given modification over a range of preparative conditions, such data establishing whether the large number of postulated forms actually exist as discrete modifications or are merely different members of a smaller number of continuously variable solid solution forms. The role of water was also investigated with respect to whether its presence is essential for the formation of the different modifications or whether it serves merely as a plasticizer permitting mechanical agitation of the samples, and as to its state of combination with the soap. Finally, the applicability of the hypothesis of stack-

(1) (a) Presented before the Twenty-fifth National Colloid Symposium which was held at Cornell University, Ithaca, N. Y., June, 1951. (b) For material supplementary to this article order Document 3368 from American Documentation Institute, 1719 N Street, N. W., Washington 6, D. C., remitting $1.00 for microfilm (images 1 inch high on standard 35 mm. motion picture film) or $1.20 for photocopies (6 × 8 inches) readable without optical aid.

(2) Experimental Station, E. I. du Pont de Nemours and Co., Wilmington, Del.

(3) Textile Research Institute, Princeton, N. J.

(4) M. J. Buerger, L. B. Smith, A. de Bretteville, Jr., and F. V. Ryer, *Proc. Nat. Acad. Sci., U. S.*, **28**, 526 (1942).

(5) M. J. Buerger, L. B. Smith, F. V. Ryer and J. E. Spike, *ibid.*, **31**, 226 (1945).

(6) M. J. Buerger, L. B. Smith and F. V. Ryer, *J. Am. Oil Chem. Assoc.*, **24**, 193 (1947).

(7) R. H. Ferguson, F. B. Rosevear and H. Nordsieck, *J. Am. Chem. Soc.*, **69**, 141 (1947).

(8) R. H. Ferguson, F. B. Rosevear and R. C. Stillman, *Ind. Eng. Chem.*, **35**, 1005 (1943).

(9) J. W. McBain, O. E. A. Bolduan and S. Ross, *J. Am. Chem. Soc.*, **65**, 1873 (1943).

(10) J. W. McBain, A. de Bretteville, Jr., and S. Ross, *J. Chem. Phys.*, **11**, 179 (1943).

(11) J. W. McBain and W. W. Lee, *Oil and Soap*, **20**, 17 (1943).

(12) W. O. Milligan, G. L. Bushey and A. L. Draper, THIS JOURNAL, **55**, 44 (1951).

(13) P. A. Thiessen and E. Ehrlich, *Z. physik Chem.*, **19B**, 299 (1932).

(14) P. A. Thiessen and J. Stauff, *ibid.*, **A176**, 397 (1936).

(15) R. D. Vold, THIS JOURNAL, **49**, 315 (1945).

(16) Throughout this paper the term "modification" is used in the same special sense as by McBain and Mysels, THIS JOURNAL, **52**, 1471 (1948), and Vold and Smith, *J. Am. Chem. Soc.*, **73**, 2006 (1951), to denote a material having clearly different properties but without commitment as to whether it is or is not a discrete phase.

ing disorder to interpretation of those diffraction patterns was examined.

To indicate the complexity of the field it is useful to consider briefly the existing nomenclature and hypotheses concerning the nature of these solids. Thiessen, *et al.*,[13,14] recognized two forms, alpha and beta, beta being produced by heating the alpha form, which contained an unspecified but small amount of water. McBain, *et al.*,[9,10] distinguished four forms, alpha and beta like those of Thiessen, and also gamma and hydrous gamma. Buerger, Smith, *et al.*,[4,5,17] postulate the existence of at least nine discrete phases of saturated soaps, alpha, beta, gamma, delta, sigma, epsilon, mu, kappa and zeta, regarding most or all of them as stoichiometric fractional hydrates. Ferguson, *et al.*,[7,8] maintain that there are but four distinguishable phases, alpha, beta, delta and omega, alpha being a hemihydrate and beta, and presumably the others, solid solutions of water in soap.

X-Ray Technique

Most of the present results were obtained with the Norelco X-Ray Spectrometer, Type 12021, patterns being automatically recorded by a Brown Potentiometer, No. 153 x 12V-X-30, although numerous comparisons were also made of the positions of peaks as recorded and as determined by direct counting. The general procedures followed were similar to those described in previous papers.[18] Air-dry samples were studied with bare surfaces of 15 mm. diameter, while "wet" or P_2O_5-dry samples were studied with surfaces of 12 mm. diameter covered with a 0.0015 in. thick polystyrene film (Plax Corp.).

Since the differences between the diffraction patterns of the soap modifications are sometimes rather small, involving differences in line position of less than 0.1 Å., and occasionally chiefly differences in line profiles, half-widths or relative intensities of two partially resolved peaks, it was first necessary in this investigation to establish definitively the reproducibility and accuracy of the results obtainable with sodium soaps with the X-ray spectrometer. This involved hundreds of runs with various standard materials and with soaps to investigate the effects of changing such instrumental variables as slit widths, degree of damping and amplification of the recorder, chart speed, scanning speed, magnitude of background fluctuation at various intensity levels, orientation of the sample surface by stroking, and to determine the accuracy and precision of measurement of line positions, apparent intensities, half-widths and resolving power.[19] All reported values are the average of at least two independent runs on different surfaces.

Once the instrument is properly aligned the location of peaks is unaffected by slit and recorder settings. Values of Bragg spacings (calculated using $CuK_{\alpha 12}$ = 1.5418 Å.) in duplicate runs on the same preparation showed maximum deviations of 0.1° in 2 θ, corresponding to differences of not more than 0.01 Å. at angles larger than 20°. Runs on a given soap modification prepared at different compositions or temperatures also usually showed agreement in line positions within ± 0.01 Å., although there were occasional differences of 0.02 Å. Since most of the peaks were of roughly comparable shape, "absolute" intensities were taken as the height of the peak in scale units above the continuous background rather than as the area under the peak, relative intensity being defined as the quotient of the "absolute" intensity of the peak divided by that of a given strong peak in the pattern. For completely resolved peaks the average deviation of the relative intensity of a given peak from the average relative intensity of that peak in all similar samples was ± 20%. The half-widths were similarly reproducible within about ± 20%. A small part of the evidence for these assertions concerning the precision of the experimental results will be found in the exemplary data incorporated in the body of the paper.

The resolving power of the instrument was tested by studying mixtures such as sodium sulfate and disodium hydrogen phosphate which have certain lines close together. With the slit and slide settings usually employed (5 and medium) and the usual scanning speed of 1° per min. peaks differing in position by only 0.015 Å. were clearly resolved. This is pertinent to the question as to whether the broadness of certain peaks is due merely to lack of resolution of a number of sharp lines or to an intrinsic broadness resulting from small particle size or disorder within the lattice. Even in cases where only partial resolution was obtained, the positions of the peaks were nevertheless essentially unaffected. Hence, poor or varying resolution of overlapping peaks is excluded as an explanation of the differences in diffraction pattern which are here attributed to the existence of different soap modifications.

There had been some question as to whether intensity changes or absences of lines due to possible orientation of crystallites during preparation of the sample as an extended flat surface might not result in uncontrollable variations of X-ray spectrometer patterns such as to make precise characterization of the results illusory. This matter was investigated by determination of spectrometer curves on surfaces prepared by a variety of methods from samples of different microscopic particle size, and also by comparison of these results with conventional photographs of rotating powder samples. The latter were made with the Norelco X-Ray Diffraction Unit, Type 12033, and a cylindrical powder camera with a radius of 57.3 mm.

A very much abbreviated summary of these data is presented in Table I.[20] It is evident that the value of the long spacing and the other line positions are identical within the experimental precision as determined by the two methods, although it must be added that there are some differences in the relative intensities and the number of lines detected by the two methods, indicative of orientation effects occurring in one or both. Such differences, as might be predicted, were most pronounced with the alpha, epsilon and kappa modifications, which have the greatest tendency to occur in plate-like or fibrillar habit. The effects of sample orientation might be expected to differ greatly between a stroked, flat surface studied by reflected X-rays and a tamped, cylindrical sample studied by transmitted X-rays. Since there is no significant difference between the results by the two methods except the absence of some lines in some rotation photographs it follows that it is extremely unlikely that varying sample orientation in the X-ray spectrometer can account for the differences in diffraction pattern which are here interpreted as evidence for the existence of discrete soap modifications.

Materials, Preparation of Samples and Phase Maps

The soaps used were prepared[21,22,23] from fatty acids which were purified by a variety of methods, and all had chemical constants (m.p., equivalent weight, iodine value) close to the theoretical values. Different preparations were all found to give the same experimental results.

Alpha, delta, epsilon, zeta, kappa and mu samples received from Dr. L. B. Smith were described as having been prepared by the following procedures.

Alpha, crystallized from 0.3% solution in 95% ethyl alcohol; delta, working 70% sodium stearate with 30% water at 60° for ½ hour; epsilon, working 70% sodium palmitate with 30% water at 76.7° for ½ hour; zeta, working 70% sodium palmitate with 30% water at 99° for 10 minutes;

(17) K. W. Gardiner, M. J. Buerger and L. B. Smith, THIS JOURNAL, **49**, 417 (1945).

(18) R. D. Vold and T. D. Smith, *J. Am. Chem. Soc.*, **73**, 2006 (1951).

(19) Complete details of this work can be found in the various research reports and Ph.D. dissertations of J. D. Grandine, 2nd, and Hans Schott, on file in the Library of the University of Southern California. It is currently in process of preparation for publication.

(20) To conserve space, Tables I, II, V, VI, VIII and IX, as well as a description of the details of preparation and chemical characterization of the soaps used, have been prepared on microfilm and are available from the American Documentation Institute, 1719 N. St., N. W., Washington 6, D. C.

(21) P. J. Fryer and F. E. Weston, "Technical Handbook of Oils, Fats and Waxes," Vol. II, Cambridge Univ. Press, 1939.

(22) J. M. Philipson, Research Report, University of Southern California Library, Spring, (1945).

(23) J. M. Philipson, M. J. Heldman, L. L. Lyon and R. D. Vold, *Oil and Soap*, **21**, 315 (1944).

kappa, working 70% sodium myristate with 30% water at 93.3° for 10 minutes; mu, working 70% sodium myristate with 30% water at 43.3° for 1/2 hour.

α-Sodium stearate prepared in this Laboratory was likewise made by crystallization from dilute solutions in alcohol. β-Sodium stearate was prepared by heating alpha in an open container to 54–56°, and also by desiccation at room temperature over P_2O_5. γ-Sodium stearate was prepared by heating alpha in an open container to 105–112°. σ sodium stearate was prepared by heating alpha in an open container to 118 or 135°, and also by melting sodium stearate (previously dried to constant weight at 110°) in a sealed tube, cooling to about 122°, and then quenching in Dry Ice–acetone. ρ-Sodium stearate was prepared by heating 25

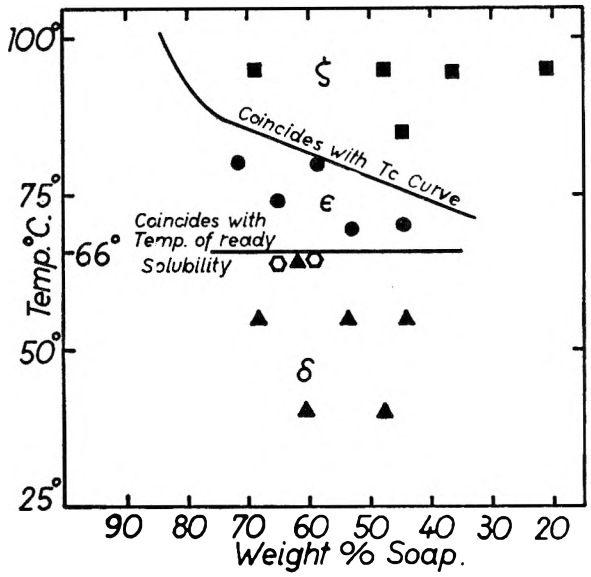

Fig. 1.—Distribution of samples on the phase map for sodium palmitate-water. The modifications resulting at room temperature in the present work are: ■, zeta (worked samples); ●, epsilon (worked samples); ▲, delta (worked samples); ⟨⟩, zeta (unworked samples).

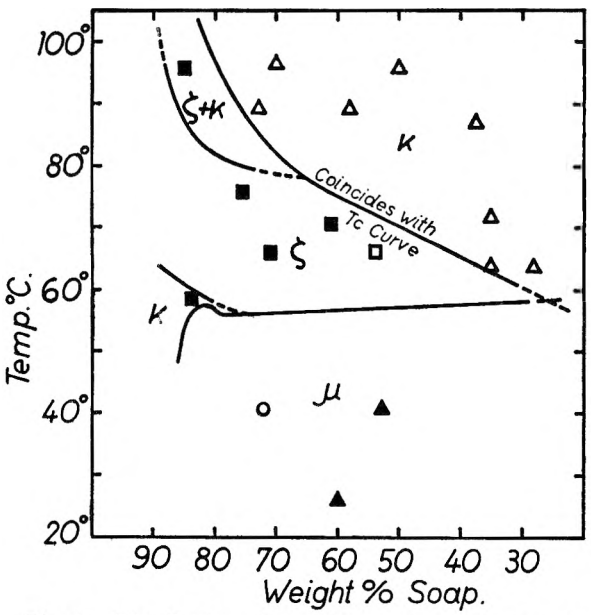

Fig. 2.—Distribution of samples on the phase map for sodium myristate–water. The modifications resulting at room temperature in the present work are: △, kappa; ■, zeta; □, mixed kappa and zeta; ▲, mu; ○, possible new pattern.

and 61% systems to 160°, tempering at 72°, followed by cooling to room temperature over a four-hour period.

The general procedure employed in preparation of the aqueous systems was to seal weighed-out soap and water (about 1.5 g.) into a heavy-walled Pyrex tube, leaving a vapor space of not more than 7 to 10 ml. The system was then heated at 170–180° for at least two hours, at which temperature all systems were either soapboiler's neat soap or a mixture of soapboiler's neat soap and middle soap,[11] mixing the contents several times by inverting the tube. Tempered samples were prepared simply by cooling in the oven (four hours to cool from 65 to 25°) to the desired temperature and letting stand.

Where mechanical working was desired the sample was transferred at room temperature after homogenization to a converter consisting of a cylindrical tube of about 9.5 mm. interior diameter, through which is moved a piston with thirty holes of 0.038-in. diameter at a rate of 13 strokes per minute over a distance of 24 mm. This is surrounded by a jacket through which water is circulated from a 2-l. beaker, serving to control the temperature during working and during cooling. Where worked and quenched samples were desired the hot mass was squeezed directly from the converter into a cap-closed vial without exposure to air, and the vial immediately immersed in Dry Ice–acetone. The moisture content of all worked mixes was determined from the loss of weight during drying to constant weight at room temperature plus the additional 2.5–3.5% from heating the air-dry samples 1.5 hours at 150° in order to establish the composition of the samples immediately after working, since occasionally, especially at the higher temperatures, jacket water leaked into the converter thus diluting the system. Representative of the treatment of all worked samples is the preparation of the epsilon samples given in Table II. The resulting solids at room temperature correspond to the descendent phases of Buerger and Smith.[5]

The distribution of the other aqueous samples with respect to composition and temperature of working is shown on the phase maps of Figs. 1 and 2, taken from previously published results.[5,6] These phase maps should not be confused with equilibrium phase diagrams; they are merely a representation of the regions of temperature and composition from which worked samples after cooling to room temperature give the same X-ray diffraction pattern. All the modifications so produced cannot be stable equilibrium forms at room temperature, since their number is greater than is compatible with the requirements of the phase rule for a two-component system. Nevertheless, since the nature of the modification at room temperature is found to change drastically depending on whether the system is worked below or above some elevated temperature, it seems likely that such diagrams can be used to deduce valid information concerning the course of phase boundaries at the higher temperatures. However, the descendent form may be structurally related to the equilibrium phase from which it was quenched, or to other forms stable at intermediate temperatures, or to mixtures of the two.

The present results with sodium palmitate agree completely with the published phase map, ζ-, ε- and δ-sodium palmitate resulting in all cases where samples were prepared from these fields. In the case of sodium myristate there is also general agreement with the published phase map although here, as is evident from study of Fig. 2, there are some discrepancies. More particularly, it seems likely that the regions at high concentrations of soap and lower temperatures described as forming the kappa modification should be curtailed or eliminated, since in the present work systems prepared in this field gave a zeta pattern. One sample prepared at 72% soap and 41° gave a pattern differing from any of the standard patterns, but which could be interpreted as resulting from a mixture of the mu and zetz modifications.

Results and Discussion

Characteristic X-Ray Spectrometer Patterns.—The Bragg spacings and relative intensities characterizing each of the modifications are assembled in Table IV, and the curves of intensity *vs.* diffraction angle which facilitate recognition of the different forms are shown in Figs. 3 and 4. Although only values on samples prepared in this

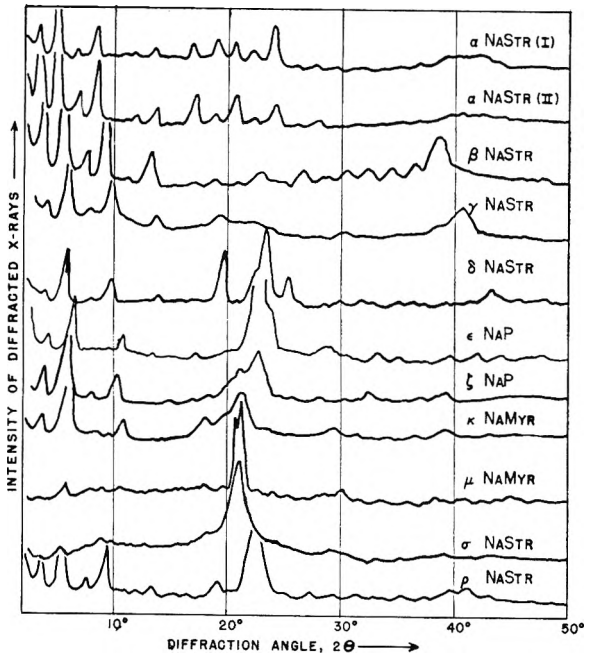

Fig. 3.—Characteristic X-ray spectrometer patterns of the saturated sodium soap modifications.

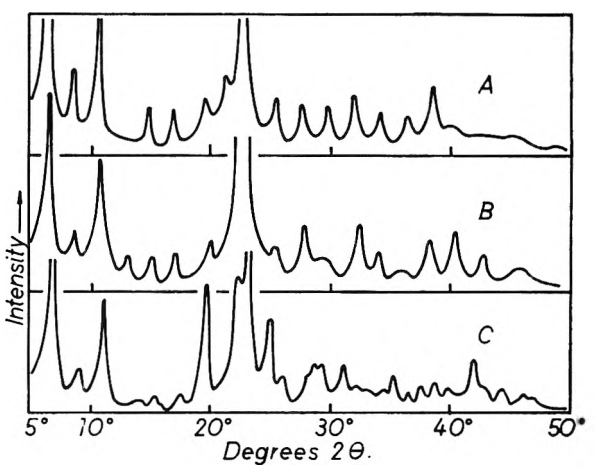

Fig. 4.—X-Ray spectrometer patterns of sodium palmitate modifications: A, zeta; B, epsilon; C, delta.

Laboratory are tabulated, results obtained earlier on samples furnished through the courtesy of Dr. L. B. Smith agreed within the stated precision with the present data in all cases. Deviations shown are maximum and not average deviations and so set an upper limit to the permissible variation in pattern for a given modification provided proper X-ray technique is employed. Even the weaker lines are quite distinctive on the original curves although not easily detectable in the pantograph reductions to $^1/_8$ scale of Fig. 3. Figure 4, which shows some of the patterns reduced fivefold in the angle scale but only 2.5 fold in the intensity scale, is more revealing.

Table III

Nomenclature of Soap Modifications in Different Laboratories

Present work	B, S, *et al.*[6]	McB, *et al.*[9]	F, R, N, *et al.*[8]	Th., *et al.*[14]
α NaStr	α	α	α	α
β NaStr	β	β	β	β
γ NaStr	γ	γ	ω	..
δ NaStr	δ	hydrous γ	δ	..
ε NaP	ε	..	..	..
ζ NaP	ζ	..	β	..
κ NaMyr	κ	..	..	..
μ NaMyr	μ	..	..	..
σ NaStr	σ	..	ω	..
ρ NaStr	..	..	..	..

The nomenclature of these patterns follows the usage of Buerger, Smith, *et al.*,[5] since the discrete existence of all the pattern types recognized by them is confirmed by the present work. Table III is an attempt to show the equivalent names of these same forms in the terminology of other investigators. The situation is somewhat complicated by the fact that some investigators have studied only a small number of forms while others use the same name for two or more of the present modifications. Thus Ferguson, *et al.*,[8] use the term beta for the patterns not only of samples prepared by thermal decomposition of the hemihydrate, alpha, but also of those resulting from cooling of samples containing 30% water. Their beta pattern may also have some characteristics of the epsilon pattern, although corresponding most closely to zeta.[5]

It is hoped that the present table of spectrometer patterns, accompanied by reproductions of the curves to aid in distinguishing patterns differing more in relative intensity and degree of resolution than in line position, will be a convenience to all workers interested in the identification of soap forms by X-ray diffraction. This is all the more true since neither of the schemes now in use is satisfactory, one[8] permitting gross variation in pattern for each form and identifying them by the presence of one or two "characteristic" short spacings, the other[5] publishing photographs for comparison and assigning a new name to any pattern showing an appreciable difference.

It is convenient in the process of identifying an unknown in terms of these standard patterns to look for the presence of components according to the following scheme. (1) Alpha is marked by the presence of five intense peaks in the range between 3.7 and 5.2 Å. in addition to other less intense spacings, and has a distinctively large long spacing. (2) Delta and rho have the three most intense peaks, exclusive of low orders of the long spacing, in the range of 3.6 to 4.6 Å. (3) Beta and gamma have the most intense peak, except for low orders of the long spacing, in the range of 2 to 2.5 Å. (4) Epsilon, zeta, kappa, mu and sigma have a principal peak near 4.0 Å. with or without resolvable shoulders, plus others of much lower intensity. The different modifications within groups (2) and (3) can be distinguished easily by the differences in their long spacing. Distinction between the different members of group (4) requires a more detailed comparison of both the Bragg spacings and the relative intensities. In identification of the modifications present in simple mixtures it is also necessary to consider the relative intensity of the different lines in order to determine whether the presence of some proportion of any given

TABLE IV

CHARACTERISTIC X-RAY SPECTROMETER PATTERNS OF THE SATURATED SODIUM SOAPS[a]

Modification	α-NaStr				β-NaStr			γ-NaStr			σ-NaStr			δ-NaP[e,f]		
No. of prepns.	8				3			2			2			7		
No. of runs	30				5			4			3			16		
Long spacing[b]	51.63 ± 0.15				47.16 ± 0.46			44.77 ± 0.20			44.49 ± 0.10			41.23 ± 0.17		
"Short spacings"[c]	d/n, Å.	Max. dev. Å.	$I/I_0^{(I)d}$	$I/I_0^{(II)d}$	d/n, Å.	Max. dev. Å.	I/I_0	d/n, Å.	Max. dev. Å.	I/I_0	d/n, Å.	Max. dev. Å.	I/I_0	d/n, Å.	Max. dev. Å.	I/I_0
	5.76	0.02	0.07	0.04	5.26	0.01	0.17	4.66	0.03	0.53	4.69	0.03	0.24	4.59	0.02	0.71
	5.18	.03	.57	1.00	4.72	.02	.29	4.54	.02	.47	4.39	.03	.23	4.18s	01	.13
	4.68	.03	.50	0.44	..	..	..	4.37	.02	.36	4.05	.01	1.00	4.01s	.02	.31
	..	..	..	..	4.03	0	.26	4.12	.03	.86	3.90	.01	.31	3.89	.01	1.00
	4.32	.02	.50	.98	3.93	.03	.53	3.99	.02	.29	3.74	0	.13	3.62	0	.46
	4.01	.02	.36	.28	3.40	.02	.39	3.91	.04	.70	3.44	.01	.07	3.49	.01	.13
	3.71	.01	1.00	.77	3.16	.01	.22	3.84	.03	.21	3.24	.02	.03	3.16	.02	.12
	3.46	.01	.08	.15	2.97	.01	.37	3.23	.02	.26	3.07	.01	.04	3.09	.01	.15
	3.24	.01	.17	.37	2.80	.01	.26	3.01	.02	.27	2.96	.01	.08	2.91	.01	.18
	3.06	.01	.09	.03	2.63	.02	.25	2.88	.02	.14	2.35	.02	.04	2.73	.01	.11
	2.88	.02	.06	.02	2.50	.02	.31	2.66	.01	.11	2.25	0	.09	2.64	.01	.09
	2.73	.01	.05	.10	2.37	.01	1.00	2.36	0	.46	2.03	.01	.08	2.57	.01	.15
	2.46	.01	.14	.12	2.26	0	.11	2.26	.02	1.00				2.49	.01	.06
	2.35	.01	.15	.08										2.41	.01	.10
	2.32	.01	.27	.30										2.34	.01	.10
	2.25	.01	.29	.23										2.29	.01	.11
	2.16	.01	.33	.10										2.24	.02	.07
	2.13	.01	.17	.10										2.16	01	.23
	2.09	.01	.17	.16										2.12	.02	.09
														2.06	.01	.08
														1.96	.02	.06
														Other Spacings		
														4.81	2.84	
														4.30	2.77	
														3.42	2.35	
														3.34	2.33	
														3.20	1.90	

Modification	ε-NaP[g]			ζ-NaP			κ-NaMyr			μ-NaMyr			ρ NaStr[h]		
No. of prepns.	8			9			9			4			3		
No. of runs	11			15			15			8			7		
Long spacing[b]	41.77 ± 0.43			41.82 ± 0.35			37.30 ± 0.13			37.40 ± 0.03			45.85 ± 0.28		
"Short spacings"[c]	d/n, Å.	Max. dev. Å.	I/I_0	d/n, Å.	Max. dev. Å.	I/I_0	d/n, Å.	Max. dev. Å.	I/I_0	d/n, Å.	Max. dev. Å.	I/I_0	d/n, Å.	Max. dev. Å.	I/I_0
	5.25	0.03	0.08	5.24	0.03	0.11	4.65	0.02	0.40	5.11	0.07	0.07	4.61	0.01	0.19
	4.49	.02	.09	4.52s	.06	.18	4.37s	.06	.12	4.62	.01	.45	4.35	.05	.11
	4.26s	..	.07	4.19s	.02	.26	4.24s	.02	.14	4.22s	.02	.11	3.92(S)	.01	1.00
	4.18s	..	.08	3.97	.03	1.00	4.02	.01	1.00	3.98	.01	1.00	3.77s	.02	.18
	3.94	.02	1.00	3.49	.02	.21	3.85s	.02	.09	3.74s	0	.18	3.60	.02	.09
	3.79s	.03	.11	3.22	.01	.18	3.72	.02	.16	3.52	.02	.28	3.30	.01	.09
	3.22	.01	.21	2.99	.02	.17	3.59s	.03	.14	3.39	0	.16	3.19	.02	.07
	3.02	.03	.12	2.79	.01	.23	3.37	.02	.16	3.24	.01	.10	3.09	.01	.07
	2.77	.02	.17	2.62	.01	.13	3.23	.02	.13	3.10s	.02	.11	2.90	.01	.07
	2.65	.01	.11	2.46	.01	.14	3.07s	.02	.11	3.00	.01	.18	2.75	.02	.09
	2.49	.02	.05	2.33	.01	.24	3.00	.10	.30	2.92	.01	.23	2.58	.01	.07
	2.35	.01	.14	2.24	0	.11	2.86	.02	.15	2.80s	.01	.12	2.44	.01	.06
	2.23	.01	.16	2.05H	..	.07	2.65	.01	.09	2.67	.02	.10	2.31	.01	.14
	2.12	.01	.11	Other Spacings			2.44	.01	.09	2.51H	..	.05	2.23	.01	.14
	1.99H	..	.05	4.73	3.63		2.31	.01	.20	2.33	0	.12	2.12	.01	.07
	Other Spacings			4.36	3.11		2.22	.03	.11	2.29	0	.11	2.00H	..	.03
	3.96	3.13		3.93	2.40		2.04H	..	.09	2.22	.01	.10	Other Spacings		
	3.55	3.07					Other Spacings			2.18	.01	.06	4.22		
	3.50	2.94					4.88	2.77		2.04H	..	.09			
	3.16	2.63					4.80	2.36		Other Spacings					
							3.48	2.28		5.29					
										3.74					

[a] In the case of alpha, beta, gamma and sigma modifications which were investigated while using a Geiger tube of lower sensitivity than that later employed, only diffraction maxima having amplitudes greater than 4% of the full-scale recorder reading (*i.e.*, 4 scale divisions out of 100) are tabulated. In the case of the other modifications all the lines found in all patterns of the given modification are tabulated in regular order, lines occurring in some but not all patterns being listed under the caption "Other Spacings." [b] The long spacing in each run was generally calculated as the average value from the Bragg spacings of the third to seventh or ninth orders inclusive. The deviation shown here is the maximum deviation of any of these averaged values from the over-all reported average. The mean deviation is usually very much smaller. [c] The variations shown here are likewise the maximum deviation found in any run from the reported average. Runs on wet samples under polystyrene covers were not used in computing these averages. Relative intensities, I/I_0, are likewise averaged overall runs, and generally reported in terms of the ratio of the intensity of the given line to that of the strongest line in the pattern exclusive of the low orders of the long spacing. [d] Alpha I is found after thorough grinding of the sample, while before grinding the pattern may be that of α-II or something intermediate between the two. The differences are in intensity only, and not in line position, and must result from orientation of the crystals in the unground samples, which often contained platelets up to 0.1 mm. or greater in size. [e] Values from runs on δ-sodium stearate are also included in this column. [f] s after a value of the spacing signifies that the given peak occurs as a shoulder on an adjacent very intense peak. Brackets to the right of the intensity column join peaks of unambiguous location but of uncertain individual intensities due to overlapping. [g] Left-hand brackets join values of d/n from peaks where the individual values are somewhat uncertain due to incomplete resolution. H signifies that the peak in question has an angular half width of ca. 3° in 2 θ or more, resembling a halo, in which case precise location of the maximum is uncertain. [h] The symbol (S) indicates the definite presence of a subsidiary shoulder on the given peak but the position of which cannot be determined with any certainty because of lack of resolution.

standard form must be postulated in order to obtain agreement with the experimental pattern.

Constancy of Pattern within a Given Modification.—In order to establish the validity of regarding each of these patterns as characteristic of discrete modifications it is necessary to demonstrate that any variations of pattern occurring within a given modification are negligibly small contrasted with the differences in pattern between modifications and that the change in type of pattern from one modification to another occurs discontinuously rather than continuously as a function of some variable such as composition or processing temperature. This matter was investigated by comparison of the patterns of a great many samples prepared under various conditions and studied in different manners (*cf.* Table II and Figs. 1 and 2). Preliminary experiments had shown that the patterns remained constant at room temperature, independent of time of standing at least for two years, once the samples were dried to equilibrium water content, so this variable was recorded but not closely controlled. Most patterns, however, were obtained within a day after the samples were air-dry.

It is clear from the limits of variation shown in Table IV that none of the rather considerable changes in composition or treatment caused any significant changes in the pattern of a given modification. Very rarely these resulted in better separation of a shoulder, resolution of a broad peak into a doublet, or appearance of some lines in more intense patterns which are not found in weaker patterns. In no case, however, was there any significant change in the number of lines or their positions. Moreover, with none of the air-dry samples were patterns obtained with spacings of intermediate value between those of any two modifications, although in exceptional cases patterns were obtained which corresponded to a mixture of two of the primary forms. Preparation of a given modification from any temperature or composition within its field of formation gave a material of essentially constant diffraction pattern, while any change of temperature or composition beyond these limits resulted discontinuously in the formation of another modification with a distinctively different diffraction pattern. Hence the individuality of these modifications is conclusively established regardless of the residual question as to the physical explanation of the observed differences.

Not only do the line positions remain unaltered in all members of a given modification but there is also no systematic change in half width as a function of composition or processing temperature. In addition to instrumental variables which were held constant, the half width depends on thermal motions in the crystal, absorption of X-rays by the sample, structural irregularities and disorder within the lattice, and the size of the crystallites.[24] Since the average value of the deviations in half width of all preparations of a given modification was no greater than the average deviation of a series of runs on different surfaces of the same sample it therefore seems likely that there were no very great differences in the degree of lattice disorder and the average size of crystallites.

The preparative conditions of the sample do affect the intensities even though line positions and half widths are unchanged. Relative intensities on different surfaces of the same sample were reproducible within 15 to 20%, whereas the average deviation of relative intensities of lines from different members of the same modification was 20 to 25%. Comparison of "absolute" intensities is even more informative, the average deviation for any strong line of a given sample being 5.6% contrasted with an average deviation of 15 to 23% between values from different members of the given modification.

Since the structure factor is determined by line intensities as well as positions this variation might be regarded as a serious objection to the concept of a modification as a form of soap giving the same diffraction pattern over its whole range of composition. However, line intensity is determined not only by the structure factor but also by such non-lattice variables as the size of particles and the size of crystallites, differences in intensity up to 70% having recently been attributed to these variables alone.[25] Similar effects may well account for the behavior observed in the present case.

Quenching or slow-cooling (*ca.* one hour) from the processing temperature caused only insignificant changes in the diffraction pattern of any of the modifications, as is evident from the exemplary data for δ-sodium palmitate given in Table V. Occasionally overlapping peaks were better resolved in the pattern of the quenched samples.

The Role of Water

Apparently the presence of water is actually required for the formation of the various soap modifications, mechanical agitation alone not being sufficient. This was shown by preparation of a system containing 65% sodium palmitate–35% solvent by homogenization at 220°, cooling to room temperature, working in the converter 35 minutes at 65°, and cooling to room temperature in the converter. When water was the solvent a typical delta pattern was obtained. With cetane as a solvent the pattern obtained was substantially that of the sigma modification, and was identical with respect to line positions, relative intensities and half-widths with the pattern of the solvent-free soap subjected to the same treatment with the omission of the mechanical working, in agreement with previous work[26] on greases where quite generally soaps dispersed in hydrocarbons were found to give the same diffraction pattern at room temperature as the solvent-free soaps.

Free Water.—Water in excess above the 2.5 to 3.5% present at equilibrium in air-dry samples at room temperature appears to act merely as an inert diluent, even though variation in its amount at the higher processing temperatures may change the modification which is produced. This con-

(24) C. W. Bunn, **Chemical Crystallography**, Oxford Univ. Press, 1946.

(25) Z. W. Wilchinsky, *Acta Cryst.*, **4**, 1 (1951).

(26) (a) M. J. Vold, G. S. Hattiangdi and R. D. Vold, *Ind. Eng. Chem.*, **41**, 2539 (1949); (b) M. J. Vold, G. S. Hattiangdi and R. D. Vold, *J. Colloid Sci.*, **4**, 93 (1949).

clusion, applicable to all modifications, is based on data such as are shown for κ-sodium myristate in Table VI, from which it is evident that no consequential change in the diffraction pattern results from increasing the amount of water beyond that present in the air-dry sample. Addition of water merely affected the intensities of the lines, the decrease being quantitatively similar to that found on addition of equivalent amounts of gum tragacanth, another inert diluent. A similar conclusion was reached by Ferguson, Rosevear and Nordsieck from studies on their beta sodium palmitate.[7]

Bound Water.—Below about 3%, changes in the amount of water do affect the diffraction pattern, the nature of the changes being such as to suggest that the water in the modifications studied is present in solid solution rather than as a stoichiometric hydrate. Data supporting this point of view are shown in Tables VII and VIII, which give the patterns of ζ- and ε-sodium palmitate dried to varying water contents over P_2O_5. Several

TABLE VII

COMPARISON OF PATTERNS OF AIR-DRY AND P_2O_5-DRY ζ-SODIUM PALMITATE[a]

Long spacing from l =	Original sample 41.86 ± 0.04		Rehydrated sample 42.10 ± 0.08		P_2O_5-dry sample 42.49 ± 0.11	
3, 4, 5, 7 water content, %	3.0		2.5		*ca.* 0.2	
Miller index, l	d/n, Å. Obsd.	Calcd.[b]	d/n, Å. Obsd.	Calcd.[b]	d/n, Å. Obsd.	Calcd.[b]
3	13.94	13.95	14.03	14.02	14.16	14.16
4	10.46	10.46	10.49	10.51	10.60	10.62
5	8.37	8.37	8.43	8.41	8.51	8.50
7	5.99	5.98	6.03	6.01	6.06	6.07
8	5.23	5.23	5.29	5.26	...	...
10	4.19	4.19	4.22	4.21	4.27	4.25
[c]	3.96	...	3.91	...	3.83	...
12	3.49	3.49	3.53	3.51	3.57	3.54
13	3.22	3.22	3.24	3.23	3.29	3.27
14	2.99	2.99	3.02	3.00	3.07	3.03
15	2.79	2.79	2.82	2.80	2.85	2.83
16	2.62	2.62	2.65	2.63	2.67	2.66
17	2.46	2.46	2.49	2.47	2.51	2.50
18	2.33	2.33	2.35	2.34	2.37	2.36

[a] All these patterns were obtained from samples covered with polystyrene, and contained several halos in addition to the tabulated spacings. In other experiments uncovered air-dry samples were compared with the covered sample after drying over P_2O_5. Here an air-dry sample of 2.9% initial water content had a long spacing of 42.19 Å. and the (01ζ) band at 3.93 Å. After drying to *ca.* 0.3% water content the long spacing was 42.88 and the (01ζ) band at 3.84 Å. [b] Calculated spacings were obtained in each case by dividing the tabulated value of the long spacing as calculated from the lower orders by the appropriate index l. [c] This peak appears to be the (01ζ) band of the two-dimensional net.

lines given in the standard patterns are not shown in these tables because diminution of intensity or interfering halos from the polystyrene cover made precise determination of positions difficult, particularly in the case of many of the true side spacings (*hk* bands). Half-widths and relative intensities underwent no change on drying over P_2O_5, although the absolute intensities decreased about 28%. With neither modification was there any indication of the appearance of a mixed pattern corresponding to the presence of an anhydrous form and a hydrate,[27] all patterns obtained being derivable by continuous variation of the pattern of the air-dry sample. Their beta phase was also classified as a solid solution by Ferguson and co-workers,[7] a similar conclusion also having been reached by Milligan, *et al.*[12]

Although drying over P_2O_5 resulted in small changes in line positions there were no changes in the number of diffraction maxima, their presumed crystallographic indices, or the relative intensity of the lines. Hence there is no need to classify the anhydrous soap as a different modification from the air-dry material. Moreover, this behavior also demonstrates that changes in water content cannot result in changes of pattern such as to constitute an alternative explanation of the patterns which are here attributed to the existence of the soap in different modifications. With respect to the distinctiveness of the epsilon and zeta forms, it is significant that the long spacing of the zeta modification increases with decreasing water content while that of the epsilon modification decreases.

Interpretation of Patterns in Terms of Stacking Disorder.—It has recently been proposed[18,28] that the solid soaps may constitute examples of crystals subject to stacking disorder. On the simplest form of this hypothesis the crystal consists of a randomly stacked array of regular two-dimensional lattices, which should give a diffraction pattern consisting of relatively sharp lines from the various orders of the long spacing and a small number of broad bands arising from the side spacings.

That this concept fits some of these patterns very well is clearly apparent from Table IX, where it is shown that the spacings calculated from the postulated indexing on this assumption for β-sodium stearate are in good agreement with the observed values. An assignment of indices is relatively simple where the theory applies, the first step involving calculation of the long spacing from the obvious lower orders (l = 3 to 9) of the (00l) set. All of the other lines which might be regarded from their positions as higher orders of this spacing are identified. The few remaining lines are treated as (*hk*ζ) bands and indexed by the graphical trial and error method of the monoclinic $\mathbf{b_1b_2}$ net as described by Bunn.[21] Similar agreement between observed values and patterns calculated on this basis was also found with a number of other modifications, most successfully with alpha, delta, zeta and epsilon.

Nevertheless, there is little question that this hypothesis in its simplest form is inadequate to explain the data fully. For example, the pattern for ρ-sodium stearate can be indexed on this basis only by assigning large values (3 to 8) to the h and k integers in the (*hk*ζ) bands while low values are absent. As a second example, a line at 2.79 Å. in ζ-sodium palmitate, which is matched numerically by regarding it as (0 0 15), was found in preliminary studies by Dr. Marjorie J. Vold with an orientation analyzer[29] to vary differently in intensity than the other orders of the long spacing as the sample is tipped from its normal position per-

(27) The conclusion here cannot be accepted without some reservation since it is known[18] that calcium stearate monohydrate can be completely dehydrated without demonstrable change of the powder X-ray diffraction pattern.

(28) A. J. Stosick, *J. Chem. Phys.*, **18**, 1035 (1950).

(29) L. G. Schulz, *J. Applied Phys.*, **20**, 1030 (1949).

pendicular to the plane of the incident and recorded, diffracted X-rays. Another difficulty, for example, is that for ϵ-sodium palmitate the long spacing calculated from the third to eighth orders is 41.83 ± 0.08 Å. while from the fourteenth to nineteenth orders it is 42.43 ± 0.07. Discrepancies in the same direction occur for some but not all of the other modifications. Finally, contrary to the present observations, the simple theory predicts that the ($hk\zeta$) bands will be markedly asymmetric, steeper on the low angle side and diffuse on the high angle side.

A possibly valid hypothesis is that the stacking of the two-dimensional slabs is not fully random and that the mean thickness of two slabs which pack closely is less than for two which fit poorly. In such a case the kind of average of "right" and "wrong" spacings for different orders of the long spacing can vary with the order considered.[30] In such a case ($hk\zeta$) diffraction would also be expected to be weak for ζ much different from zero, thus minimizing the asymmetry of the ($hk\zeta$) bands. Another possibility is that the Bragg equation may be satisfied near the edge rather than at the center of the (0 0 l) peaks in disordered crystals,[31] this effect resulting in a greater correction for the higher order peaks, which are broad, than for the narrower peaks of the lower orders.

Despite these possible objections, application of the stacking disorder hypothesis to interpretation of the present data has been quite fruitful. For instance, it is possible on this hypothesis to calculate from the known pattern of ζ-sodium palmitate what pattern should be expected for ζ-sodium myristate. Lines in the ζ-sodium palmitate pattern identified as ($hk\zeta$) bands, *i.e.*, true side spacings, were predicted to occur at substantially the same position in the myristate pattern, assuming no appreciable difference in packing but only in chain length. It was assumed that the same orders of the long spacing should appear in both patterns with similar relative intensity, the spacings in the myristate pattern being calculated from those in the palmitate pattern by multiplying by the ratio of the two long spacings, 37.74/41.69, as determined from the lower orders. This procedure was adopted to minimize any complications due to different "end effects" in the packing, although the calculation might have been made using exclusively the palmitate values, assuming constancy of the angle of tilt, and calculating the long spacing of the myristate from that of the palmitate by using the commonly accepted values of bond angles and atomic radii.

The agreement is good between calculated and observed patterns, as shown in Table X, and affords strong confirmation for the validity of the stacking disorder interpretation of the structure of this modification. However, it raises a problem as to the criteria for classifying soaps of different chain length as belonging to the same or different modifications. Previous investigators[8] have disregarded the value of the long spacing as being inconsequential, and have regarded the soaps as being in the same phase when the line positions of the "short spacings" matched. In some cases this may appear to work reasonably well, as for example with delta sodium palmitate and stearate, where the twelfth, eighteenth and nineteenth orders of the palmitate long spacing occur at 3.49, 2.28 and 2.16 Å., while the thirteenth, twentieth and twenty-first orders of the stearate spacing occur at 3.48, 2.26 and 2.15 Å., leading to an apparent direct matching of the patterns. In general, however, it would seem more reasonable to take as the criterion of similarity the occurrence in the two patterns of the same ($hk\zeta$) spacings and the same succession of higher orders of the long spacing with similar relative intensities, rather than a mere matching of some of the line positions.

On this view it may be necessary to re-examine the standard patterns of the various modifications when determined on soaps of different chain length to ascertain which, if any, of them may be attributed to a common crystal structure despite differences in the patterns. For instance, δ-sodium palmitate and μ-sodium myristate may be closely related in structure, although here the agreement is not as good as in the previous example.

The theory is equally successful in explaining the changes in pattern of ζ- and ϵ-sodium palmitate which occur on drying over phosphorus pentoxide (*cf.* Tables VII and VIII). All spacings of the zeta modification indexed as higher orders of the long spacing changed on drying by just the right amount to bring them precisely into agreement with the value as calculated by dividing the new value of the long spacing by the assigned index. This constitutes strong evidence for both the precision of the experimental data and the validity of the

TABLE X

CALCULATION OF ζ-SODIUM MYRISTATE PATTERN FROM THAT OF ζ-SODIUM PALMITATE[a]

ζ-Sodium palmitate[b] Long spacing 41.69 ± 0.20					ζ-Sodium myristate Long spacing 37.74 ± 0.07		
Indices			d/n, Å.			d/n, Å.	I/I_0
h	k	l	Obsd.	I/I_0	Calcd.	Obsd.	Obsd.
0	1	ζ	..	..	..	4.85	0.09
0	0	8	5.22	0.09	4.72	4.71	.24
1	0	ζ	4.52s	.18	4.52s	4.45s	.11
0	0	10	4.19	.52	3.77	3.79	.22
..	..	..	..	..	..	4.32s	0.12
0	0	9	..	..	4.19	4.18s	.15
1	$\bar{1}$	ζ	3.98	1.00	3.98	4.02	1.00
0	0	11	3.85s	0.39	3.43	3.43	0.13
0	0	12	3.49	.15	3.15	3.15	.20
0	0	13	3.22	.15	2.90	2.90	.14
0	0	14	2.99	.13	2.70	2.69	.14
1	1	ζ	2.78	.28	2.78	2.78	.22
0	0	15	2.78	.28	2.52	2.50	.10
0	0	16	2.62	.09	2.36	2.35	.20
0	0	17	2.46	.10	2.22	2.21	.05
0	2	ζ	2.39	.10	2.39	2.41	.09
0	0	18	2.33	.21	2.09	2.04H	0.08

[a] The ζ-sodium palmitate pattern given here was obtained by J. D. G. on a sample supplied by Dr. L. B. Smith. [b] The assignment of indices given here differs somewhat from that proposed recently by Stosick.[25] Although similar in general nature, Stosick's assignment was based on the presumed presence of lines at 4.37 and 3.85 Å., both of which occur as shoulders on stronger peaks, and the positions of which were not properly identified in the earlier unpublished work. When there are so few distinctive lines in the pattern, it is not possible to be sure that any given assignment of indices on the present basis is necessarily unique regardless of how closely the lines are matched.

(30) R. E. Franklin, *Acta Cryst.*, **4**, 253 (1951).
(31) A. J. C. Wilson, *ibid.*, **2**, 245 (1949).

assigned indexing. This is further confirmed in the instance by the fact that all spacings attributed to the b_1b_2 net decrease slightly on drying while the other values increase. Just as good agreement is also found with the epsilon modification except that here the spacings due to both (*hkl*) bands and orders of the long spacing decrease on drying over phosphorus pentoxide.

These small but real changes in spacing on drying below 3% water suggest a simple explanation for what has heretofore been a rather baffling mystery, namely, the persistent occurrence of discrepancies of 0.02 to 0.08 Å. between the reported positions of the same lines of the same modification as determined in different laboratories, such differences being well outside the attainable precision of the techniques employed. It seems quite probable that these differences may result from varying degrees of drying of the air-dry samples in different laboratories, the water content occasionally being reduced into the bound water range where the pattern is effected. In a few cases in the present work where air-dry samples gave patterns differing by more than the allowable amount from the standard values of Table IV it was found in every case that the long spacing calculated from the lower orders had changed by just the proper amount to account for the observed changes in the other spacings when calculated as higher orders of the long spacing.

THE SURFACE STRUCTURE AND PROPERTIES OF COLLOIDAL SILICA AND ALUMINA[1]

BY ERNST A. HAUSER AND D. S. LE BEAU

Massachusetts Institute of Technology, Cambridge, Massachusetts, Worcester Polytechnic Institute, Worcester, Massachusetts, and Midwest Rubber Reclaiming Company, East St. Louis, Illinois

Received August 30, 1951

Systematic studies of different synthetic silica gels, silicic acid gel, alumina–silica gel and magnesia–silica gels by differential thermal analysis and X-ray diffraction have offered definite proof that these products are amorphous in structure. With the exception of the magnesia–silica gel, they all show only an endothermic peak between 150 and 175°. This peak can be attributed to water adsorbed on the surface of the material because it is not shown in the cooling curve. Only the magnesia–silica gel shows an exothermic peak, at 810°, superseded by a second endothermic peak at 800°. These are most probably associated with a drastic change in the structure and the formation of a new compound which, however, is also amorphous in structure. The indicator method permitted the determination of the fact that the tested alumina and magnesia gels are not pure but are actually a mixture of alumina and magnesia gels with silica gels, respectively. Ultramicroscopic studies gave some indication that even the large particles are not solid but are aggregates. This becomes quite evident if they first have been dispersed in water. Electron photomicrographs have offered visual evidence that the large particles are aggregates, resulting in particles with exceptionally high porosity.

During the last years some research has been carried out and reported for the purpose of obtaining a better insight into the actual surface structure of naturally occurring clays and why most of the properties they exhibit depend primarily thereon. This research was mainly devoted, however, to naturally occurring aluminum silicates having particle sizes within the colloidal range of dimensions. In a paper presented before the 24th National Colloid Symposium[2] the results obtained by applying such techniques as infrared absorption, ion exchange capacity, differential thermal analysis, film formation, thixotropy, color reactions with amines, electron microscopy and the release of atomic oxygen and its implications for the surface structure of siliceous matter falling within the colloidal range of dimensions was reported in detail.

With the exception of applying the discovery that atomic oxygen is released from the surface of silica gels during dehydration or from the surface of freshly crushed silica and studying its implications in regard to the surface structure and composition,[2,3] very little attention has so far been paid to other methods which might aid in evaluating the surface structure and properties of synthetic silicates, aluminates, or mixtures of both.

To ascertain if and to what extent information derived from such studies might increase our knowledge of the structure and properties of colloidal silica and alumina, it was decided to carry out systematic research with synthetic silicates and aluminates or mixtures of both of known composition.

Chemical Analysis.—The chemical analysis of the most important samples is given in Table I. Three silica gels were investigated as well as an A. R. grade of silicic acid. Both the alumina and the magnesia gel contained large amounts of silica.

Particle Size Analysis.—Inasmuch as it could be expected that the silica gels would swell considerably in water, it was decided to carry out particle size analysis by screening after each of the samples had been dried at 105°, and then conditioned at 22°, 30% relative humidity. Table II shows the results obtained for silicic acid and for the alumina–silica gel. The screening analysis was not reliable for any of the other samples. During sieving it became evident that the particles of these samples were not compact but consisted mostly of aggregates. Ultramicroscopic observation confirmed this.

Differential Thermal Analysis.—Figure 1 and Curve 6 in Fig. 2 show the differential thermal analysis curves of three different types of commercially available silica gels. (The solid lines represent the analytical results with increasing the temperature and the dotted lines those obtained during the cooling period.) Curves 2, 4 and 6 are identical with Curves 1, 3 and 5 as far as the original silica gels A, B and C are con-

(1) Presented at the 25th National Colloid Symposium, which was held under the auspices of the Division of Colloid Chemistry of the American Chemical Society, at Ithaca, New York, June 18–21, 1951.

(2) E. A. Hauser, D. S. le Beau and P. P. Pevear, THIS JOURNAL, **55**, 68 (1951).

(3) E. A. Hauser, *ibid.*, **55**, 605 (1951).

TABLE I

Sample No.[b]	SiO_2	R_2O_3[a]	(Al_2O_3)	MgO	Na_2O	CaO	SO_4	Cl	HF non-vol.	Ignition loss
1	92.30	0.47	...	..	0.31	0.36	..	..	..	6.52
3	91.85	.42	...	..	.09	.02	..	..	..	7.61
5	99.60	...	...	..	..	..	..	..	..	0.40
9	79.77	.003	...	..	..	..	0.01	0.01	0.20	20.00
7	80.80	.10	12.50	..	.03	..	.40	..	..	6.00
11	64.67	.10	0.70	29.0	.10	.15	.50	..	..	4.56

[a] R_2O_3 in Samples 1 and 3 includes Al_2O_3 which was not determined specifically. [b] Corresponds to numbering of solid curves of Figs. 1, 2, 3.

TABLE II [a]

Particle size (diameter) in microns	Silicic acid, %	Alumina–silica gel, %
Larger than 177	1.8	1.1
Between 177–125	6.9	29.2
Between 125–88	18.9	21.8
Between 88–62	12.7	7.8
Between 62–44	17.4	14.6
Smaller than 44	41.7	25.1
Dust loss	0.5	0.4
	99.9	100.0

cerned, with the only exception that they were obtained after the product had been dried at 105°. All these samples show a more or less pronounced, but in no case drastic, endothermic peak between 140 and 175°, completely absent in the cooling curve. These results indicate that the initial endothermic peak must be attributed to adsorbed water on the surface of the material but that there is no loss of lattice water as is the case, for example, with the clay minerals halloysite, gibbsite and brucite.[2] Figure 2, Curve 7, is the differential thermal analysis curve of a standard alumina–silica gel, and Curve 8 the same after it had been dried at at 105°. Curves 9 and 10 are those obtained before and after drying at 105° of a commercially available pure silicic acid (A. R. grade, precipitated powder). Figure 3 was obtained from a commercially available magnesia–silica gel. The temperature rising curve shows a pronounced endothermic peak at about 140° and an equally pronounced exothermic peak at about 825°. This last reaction most probably is associated with the formation of a new compound comparable with the change the clay minerals halloysite and kaolinite undergo in forming spinel.[2] This is also indicated by the curve obtained during the cooling period.

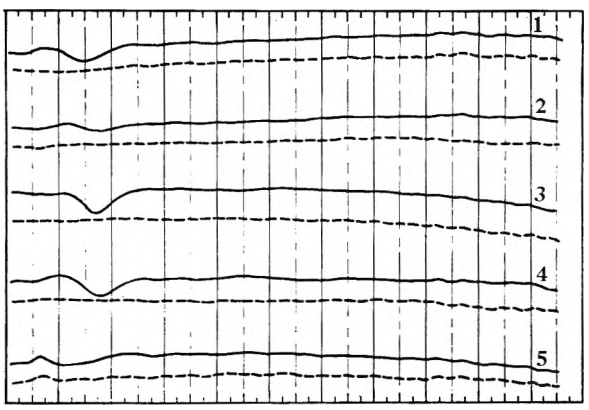

Fig. 1.—Differential thermal analysis of silica gels: 1, gel A; 2, gel A dried at 105°; 3, gel B; 4, gel B dried at 105°; 5, gel C.

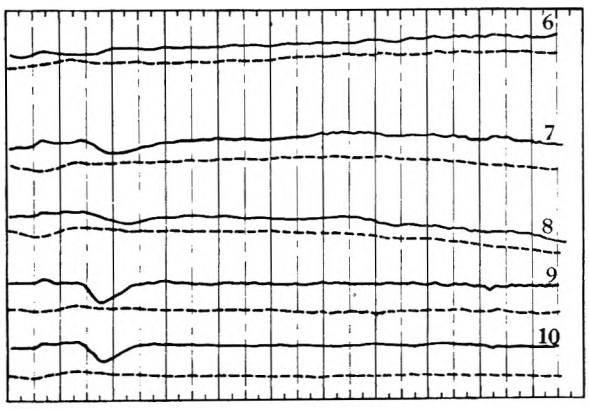

Fig. 2.—Differential thermal analysis of silica and alumina gels: 6, gel C dried at 105°; 7, alumina–silica gel; 8, alumina–silica gel dried at 105°; 9, silicic acid gel; 10, silicic acid gel dried at 105°.

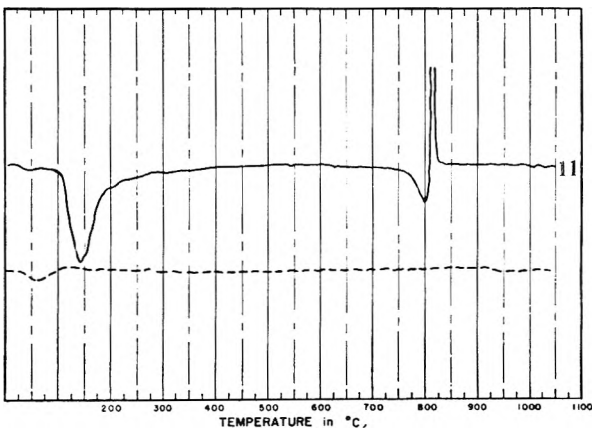

Fig. 3.—Differential thermal analysis of magnesia–silica gel.

X-Ray Diffraction.—Not one of the samples investigated gave a crystal diffraction pattern. They showed only an amorphous halo with no indication of crystallinity whatsoever (Fig. 4). This fact, which—at least to our knowledge—has so far never been stated, offers a much more plausible explanation for the reactivity of synthetic silicates than explanations depending on oriented ionic lattices, because the amorphous state is more apt to form solids with irregular

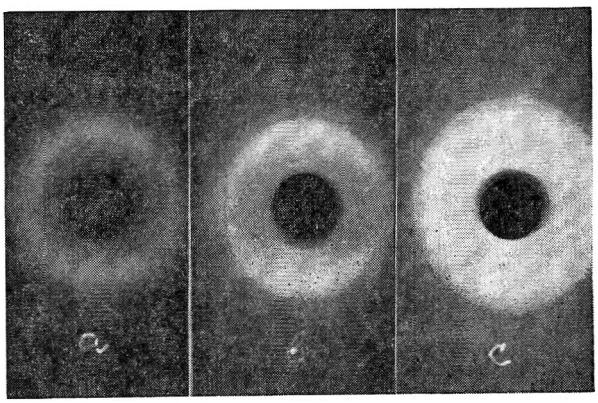

a b c

Fig. 4.—X-Ray diffraction patterns of silica gels A, B, C.

(porous) surfaces than the crystalline state. This results in a larger and more reactive interface.

Indicator Method.—All three silica gels tested by the indicator method described in detail last year[2] reacted positively. The same holds for the sample of silicic acid. The magnesia–silica gel and the alumina gel indicated very clearly that the products could not be of uniform composition because some of the particles showed a pronounced color reaction. Had they been pure magnesia or alumina gels, no color reaction would have occurred. After subjecting the products to fractionation by screening and then subjecting the individual fractions to the indicator reaction, a distinction could be made between the two components of these systems. It could be shown quite clearly that the coarser fraction is composed primarily of silica and only the finest fraction represents the magnesia or alumina and therefore did not react.

Electron Microscopy.—As previously stated, the fractionation by screening and ultramicroscopic studies indicated that most of the larger particle sizes do not consist of a compact structure but seem to be aggregates. It was felt that the only answer to this problem would be electron microscopy carried out by someone having special experience, because it is well known that silica gels have always been a difficult problem in electron microscopy.

Figures 5a, 6a, 7a and 8a[4] clearly show that what has so far always been considered to be coherent particles actually are dense aggregates of extremely small particles. Figures 5b, 6b, 7b and 8b offer visual evidence that the rise in temperature causes increased aggregation. In the case of alumina gels and magnesia–silica gels agglomeration is already quite pronounced at normal temperatures. Although the alumina gel does show a denser structure after it had been dried at 105°, neither it nor the magnesia–silica gel permits complete resolution by the electron microscope (Figs. 9 and 10).

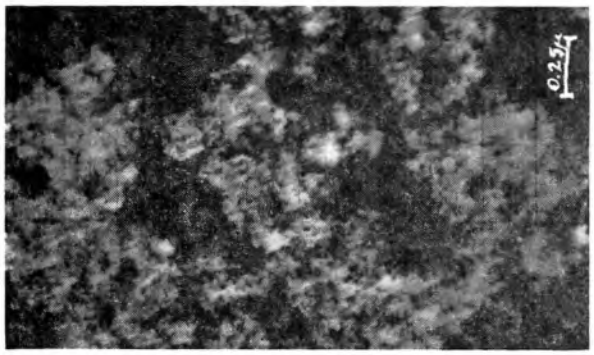

b

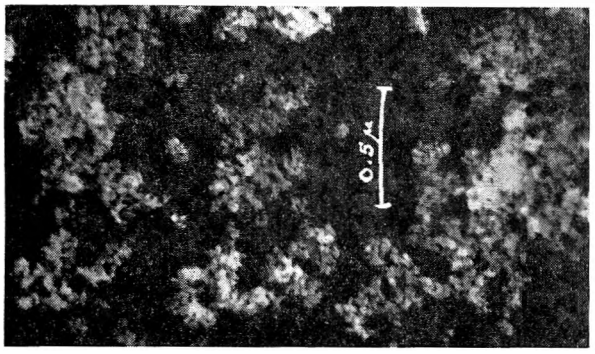

a

Fig. 5.—Electron photomicrographs of silica gel A (a) natural, (b) dried at 105°.

(4) Figures 5, 6, 7, 8, 9 and 10 as here reproduced were printed from transparent positives and therefore result in negative opacities. These have been used because they offer, in the opinion of the authors, a clearer resolution than a truly positive print of an actually white product.

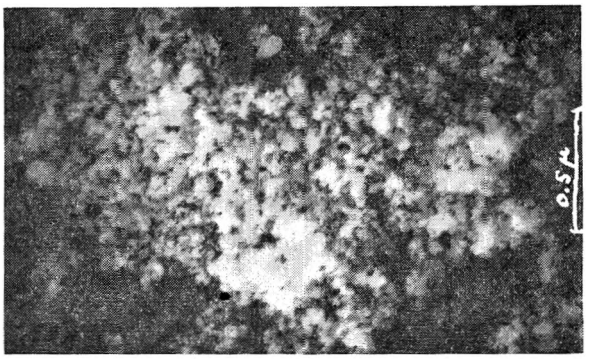

b

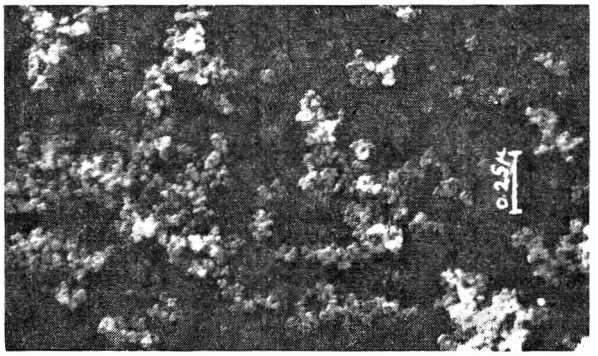

a

Fig. 6.—Electron photomicrographs of silica gel A_1: (a) natural; (b) dried at 105°.

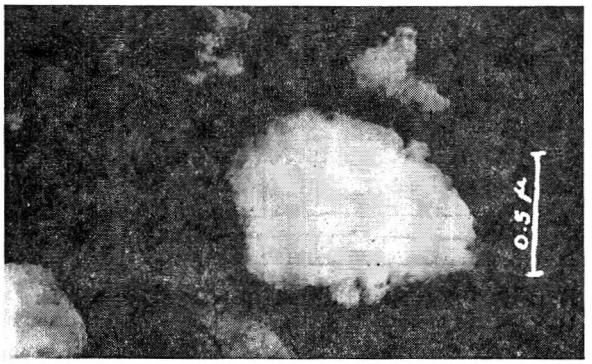

b

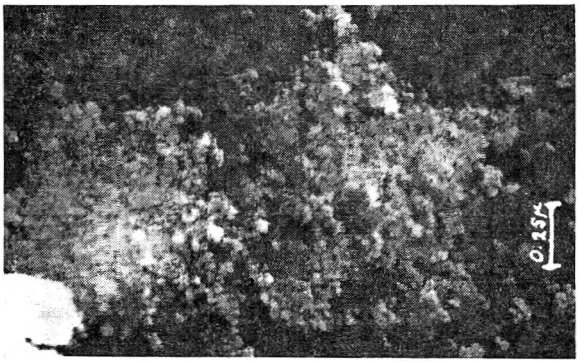

a

Fig. 7.—Electron photomicrographs of silica gel B: (a) natural; (b) dried at 105°.

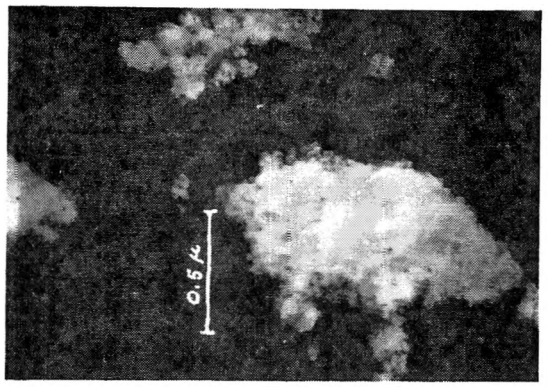

b

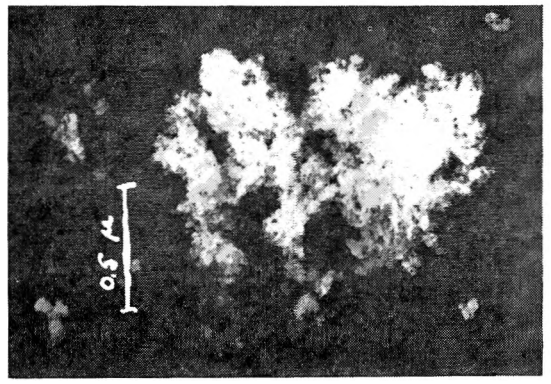

a

Fig. 8.—Electron photomicrographs of silicic acid gel C: (a) natural; (b) dried at 105°.

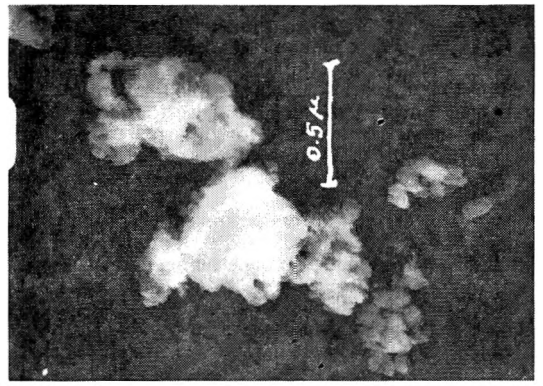

b

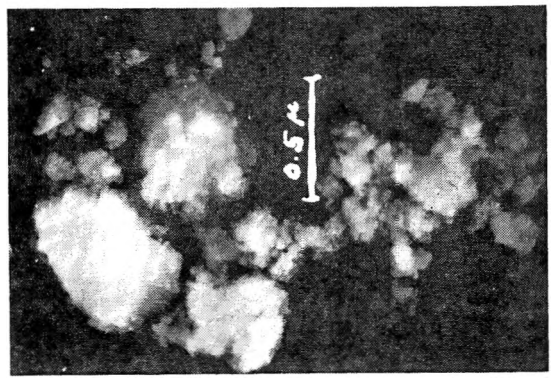

a

Fig. 9.—Electron photomicrographs of alumina gel: (a) natural; (b) dried at 105°.

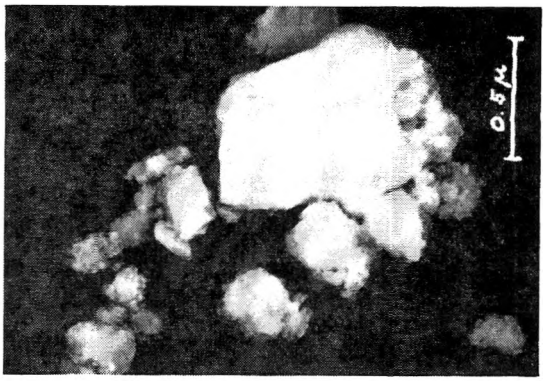

b

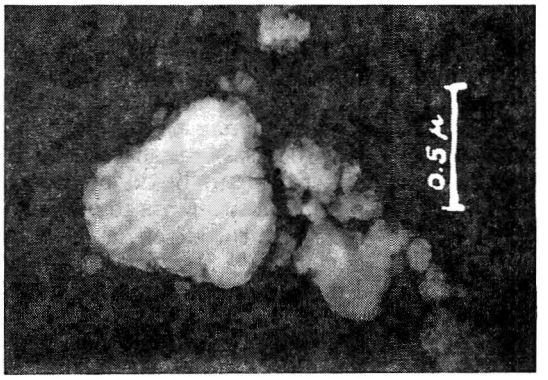

a

Fig. 10.—Electron photomicrographs of magnesia-silica gel: (a) natural; (b) dried at 105°.

Conclusions

On the basis of all these results, it is now possible to offer an explanation for the exceptionally high reactivity of these synthetic gels when used as catalysts, because even the largest particles are agglomerates of extremely small particles forming highly porous clusters. By this the over-all available surface is by far greater than if the clusters were solid particles. The fact that all these compounds are amorphous is also bound to increase their reactivity, because it assures the most reactive surface composition. It also explains why their reactivity is noticeably increased in a humid atmosphere.

These results offer further proof for the theory that the reactivity of silicates is primarily based on the ionic structure of its surfaces and that the interior crystal lattice, if existing, is of secondary importance only.

Acknowledgments.—The authors would like to express their appreciation and thanks to Dr. Theodore G. Rochow of the Analytical and Testing Division of the American Cyanamid Company, who very kindly furnished the authors with the electron photomicrographs reproduced in this paper. They are also indebted to Mr. Benjamin W. Roberts of the Physics Department of the Massachusetts Institute of Technology, and to M.I.T.'s Soil Solidification Laboratory for the differential thermal analyses.

ADSORPTION OF NITROGEN, OXYGEN, AND ARGON ON RUTILE AT LOW TEMPERATURES; APPLICABILITY OF THE CONCEPT OF SURFACE HETEROGENEITY[1]

BY J. M. HONIG AND L. H. REYERSON

School of Chemistry, University of Minnesota, Minneapolis 14, Minnesota

Received August 30, 1951

The adsorption of nitrogen, oxygen and argon on rutile has been investigated at liquid nitrogen and oxygen temperatures in the region of low relative pressure. At a given value of p/p_0 the amount of nitrogen adsorbed greatly exceeds the quantity of oxygen or argon adsorbed. The distribution of adsorption energies among surface sites has been computed and is shown to differ with each adsorbate. The reasons for these differences and the usefulness of the concept of surface heterogeneity are discussed.

During the past decade, the BET theory of physical sorption of gases on solids has considerably extended knowledge in this field. The limitations of this theory have been discussed repeatedly[2,3] and attempts to improve on the theory have been made along several lines. Various authors have obtained new isotherm equations by postulating different adsorption processes but, as was shown by Hill,[4] all such deductions are based on unsound adsorption models. Other attempts to improve on the theory have dealt with the effects of the heterogeneity of the surface,[5-7] of lateral interaction between adsorbed molecules,[8-11] and with the concept of coöperative condensation.[2,3]

A search of the literature has shown that there are only very few studies dealing with the adsorption of simple gases on well defined crystalline solids which can be used to test the above theories; in many cases investigations were not carried out at sufficiently low relative pressures to allow for a comparison of theoretical and experimental results. Among the cases suitable for theoretical study may be cited the work by Jura and Harkins[12] (nitrogen on anatase), Kington, *et al.*,[13] (nitrogen and oxygen on anatase), Arnold[14] (nitrogen, oxygen and nitrogen–oxygen mixtures on rutile), Jura and Criddle[15] (argon on graphite), Orr[16] (argon on potassium chloride), and Tompkins and Young[17] (nitrogen, oxygen, argon, carbon monoxide and mixtures on cesium iodide). In all these and other[18] cases where comparative studies on the absorption of nitrogen, oxygen, and/or argon on a given surface were available, an interesting fact was observed. At a given temperature and p/p_0 value in the low relative pressure range, the fraction of the surface covered by nitrogen greatly exceeds that covered by either oxygen or argon, while the isotherms for oxygen and argon are nearly identical.

The present experiments were designed to investigate in detail the adsorption of nitrogen, oxygen and argon on rutile in the region of low relative pressure, in order to check the findings of other investigators regarding the comparative uptake of these three gases and to test the usefulness of the concept of surface heterogeneity in explaining the results.

Apparatus, Materials and Procedure

Investigations were carried out with a standard volumetric apparatus of the type employed by Emmett and Brunauer[19] and by Jura and Harkins.[12] Pressure differences were read on a U tube manometer with a precision cathetometer to ± 0.005 cm. Repeated dead space calibrations agreed to within ± 0.1%. The sample temperature was determined by an oxygen vapor pressure thermometer. The saturation vapor pressures p_0 for nitrogen were computed from the equation of Dodge and Davis,[20] those for argon, from the equation of Born[21]; the p_0 values for oxygen were measured directly.

Nitrogen was prepared by decomposition of recrystallized and dried sodium azide. Oxygen was prepared by decomposition of purified potassium permanganate. Argon, obtained "spectroscopically pure" from commercial sources, was used without further purification.

The rutile was a synthetic material obtained through the courtesy of Dr. Walter K. Nelson of the National Lead Company, Titanium Division. A spectrochemical analysis, furnished with the sample, indicated that the major impurities consisted of alkali metal salts (1–2%) and of silica (0.3%). X-Ray diffraction patterns were stated to reveal no lines other than those of rutile.

Before each run, the sample was degassed for 18 hours at 400°; the final pressure reached in the evacuation was below 10^{-5} mm. as indicated by a McLeod gage.

Two different portions of the same sample were used in this series of runs. The results of two or more runs carried out with the same adsorbate on these two portions agreed to at least ± 0.5%, except at the very low p/p_0 values in the nitrogen runs, where large deviations occurred due to the poor precision of the pressure readings.

Results

The results are given in Table I and Figs. 1 and 2; each curve represents the average of at least two runs.

(1) This investigation was supported in part by the Grant-in-Aid for Fundamental Research contributed by E. I. du Pont de Nemours & Company.

(2) G. Halsey, *J. Chem. Phys.*, **16**, 931 (1948).

(3) G. Halsey, *J. Am. Chem. Soc.*, **73**, 2693 (1951).

(4) T. Hill, *ibid.*, **68**, 535 (1946); **72**, 5347 (1950).

(5) G. Halsey and H. Taylor, *J. Chem. Phys.*, **15**, 624 (1947)

(6) R. Sips, *ibid.*, **18**, 1024 (1950).

(7) J. Zeldowitsh, *Acta Physiochim. U. R. S. S.*, **1**, 961 (1934).

(8) R. Fowler and E. Guggenheim, "Statistical Thermodynamics," Cambridge Univ. Press, 1939, Chapter X.

(9) T. Hill, *J. Chem. Phys.*, **17**, 590, 668 (1949).

(10) A. Miller, "Adsorption of Gases on Solids," Cambridge Univ. Press, 1949.

(11) F. Volkenshtein, *Zhur. Fizicheskoi Khimii*, **21**, 163 (1947).

(12) G. Jura and W. Harkins, *J. Am. Chem. Soc.*, **66**, 1356, 1366 (1944).

(13) G. Kington, R. Beebe, H. Polley and W. Smith, *ibid.*, **72**, 1775 (1950).

(14) J. Arnold, *ibid.*, **71**, 104 (1949).

(15) G. Jura and D. Criddle, THIS JOURNAL, **55**, 163 (1951).

(16) W. Orr, *Proc. Roy. Soc. (London)*, **A173**, 349 (1939).

(17) F. Tompkins and D. Young, *Trans. Faraday Soc.*, **47**, 77, 88 (1951).

(18) A. Keenan and J. Holmes, THIS JOURNAL, **53**, 1309 (1949).

(19) P. Emmett and S. Brunauer, *J. Am. Chem. Soc.*, **59**, 1553 (1937); S. Brunauer, P. Emmett and E. Teller, *ibid.*, **60**, 309 (1938).

(20) B. Dodge and H. Davis, *ibid.*, **49**, 610 (1927).

(21) F. Born, *Ann. d. Phys.*, [4] **69**, 473 (1922).

TABLE I

ADSORPTION DATA

(p, the equilibrium pressure in cm.; $x = p/p_0$, the relative pressure; n, quantity of adsorbate held on surface in millimoles of gas per gram of solid.

Nitrogen on titanium dioxide

p	x	n
Run 1		T = 77.7°K.
0.02	0.0004	0.068
0.07	.0009	.1183
9.26	.117	.1987
Run 2		T = 77.7°K.
0.78	0.0098	0.1498
7.00	0.0881	0.1893
Run 3		T = 77.7°K.
0.01	0.0001	0.042
.02	.0003	.064
.04	.0006	.093
.60	.0076	.1457
2.21	.0278	.1648
4.12	.0519	.1765
6.16	.0776	.1860
8.64	.109	.1956
Run 4		T = 78.2°K.
0.02	0.0002	0.086
.03	.0003	.091
.03	.0003	.100
.05	.0005	.1059
.05	.0005	.1090
.06	.0007	.1137
.08	.0009	.1172
.10	.0012	.1207
.13	.0015	.1252
.16	.0019	.1290
.23	.0027	.1329
.29	.0035	.1366
.42	.0050	.1408
.55	.0066	.1445
.72	.0086	.1483
1.44	.0172	.1578
Run 11		T = 90.3 – 90.5°K.
0.005_0	0.00002_0	0.0204
$.02_0$	$.00007_0$	.0261
$.03_0$	$.00011_0$	.0316
$.04_0$	$.00014_0$	.0382
$.05_0$	$.00018_0$	.0457
$.05_5$	$.00020_0$	.0529
$.07_0$	$.00025_0$	.0692
$.16_0$	$.00058_0$	.0864
$.33_5$	$.00121_0$	.1014
$.74_0$	$.00266_0$	.1140
1.26_0	$.00457_0$	.1232
2.07_5	$.00753_0$	.1311
2.95_0	$.01079_0$	.1366
4.23_5	$.01536_0$	.1427
5.72_0	$.02075_0$	.1475
7.04_0	$.02532_0$	.1513
8.87_0	$.03246_0$	.1558
Run 12		T = 90.2°K.
0.02_0	0.00007	0.06151
0.76_0	.00278	.1154
3.57_0	.01306	.1399
11.06	.04047	.1596
14.71	.05382	.1656
20.35	.07446	.1734
27.30	.09989	.1817
34.37	.1258	.1910
42.78	.1565	.2005

Oxygen on titanium dioxide

p	x	n
Run 6	T = 77.5	–77.6°K.
0.01	0.0006	0.0128
.01	.0006	.0239
$.04_0$	.0025	.0346
$.06_0$	.0037	.0501
.11	.0068	.0601
.18	.011	.0698
.24	.015	.0827
.34	.021	.0901
.50	.031	.1048
.71	.044	.1186
.92	.057	.1319
1.13	.0711	.1418
1.37	.0854	.1516
1.65	.103	.1610
2.06	.129	.1736
2.54	.159	.1853
3.20	.200	.1990
Run 5	T = 90.3 – 90.4°K.	
0.47	0.0060	0.0429
1.11	.0142	.0616
1.66	.0211	.0726
2.14	.0273	.0809
2.87	.0367	.0915
3.46	.0444	.0986
4.93	.0632	.1141
6.12	.0788	.1247
7.96	.103	.1391
9.73	.126	.1508
Run 9-a		T = 90.0°K.
2.72	0.0366	0.0910
5.83	.0783	.1241
8.24	.111	.1429
12.69	.1702	.1691
17.47	.2347	.1912
23.88	.3214	.2184
28.96	.3898	.2388
Run 13		T = 90.2°K.
0.02_0	0.016	0.0649
.76	.050	.1025
3.57	.0793	.1247
11.06	.1287	.1517
14.71	.1769	.1716
20.35	.2537	.1975

Argon on titanium dioxide

p	x	n
Run 7		T = 77.5°K.
0.67	0.033	0.0848
0.89	.044	.0945
1.19	.0590	.1080
1.57	.0779	.1210
1.94	.0963	.1320
2.32	.115	.1423
2.72	.135	.1524
3.22	.160	.1631
3.94	.196	.1758
Run 8		T = 78.6°K.
0.03	0.001	0.0187
.08	.003	.0264
.12	.0050	.0347
.18	.0075	.0439
.27	.011	.0521
.39	.016	.0626
.52	.022	.0708
.69	.029	.0808
.88	.037	.0890
1.12	.0469	.0986
1.40	.0587	.1088
1.72	.0721	.1184
2.08	.0872	.1280
2.44	.102	.1366
2.92	.122	.1467
Run 10		T = 90.2°K.
0.06	0.0006	0.0083
.16	.0016	.0164
.38	.0038	.0251
.66	.0066	.0337
1.10	.0110	.0431
1.54	.0154	.0512
2.71	.0279	.0674
4.03	.0404	.0820
5.92	.0594	.0982
7.97	.0799	.1127
10.14	.1017	.1259
12.36	.1240	.1376
14.81	.1486	.1493

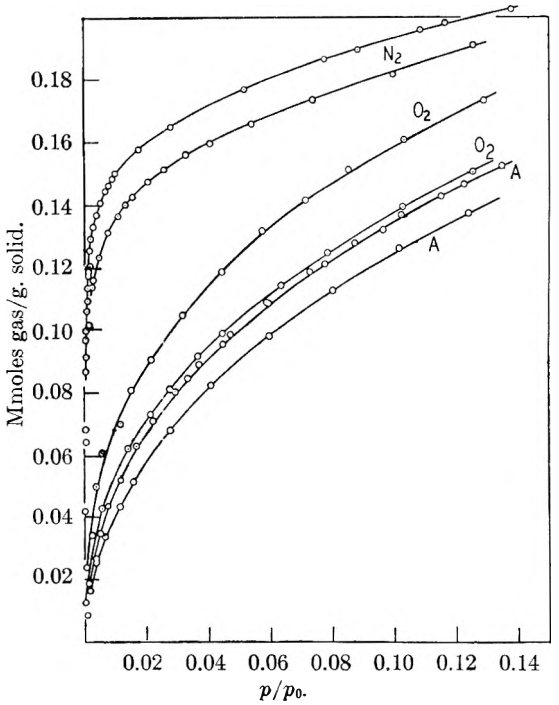

Fig. 1.—Adsorption isotherms of nitrogen, oxygen and argon on rutile.

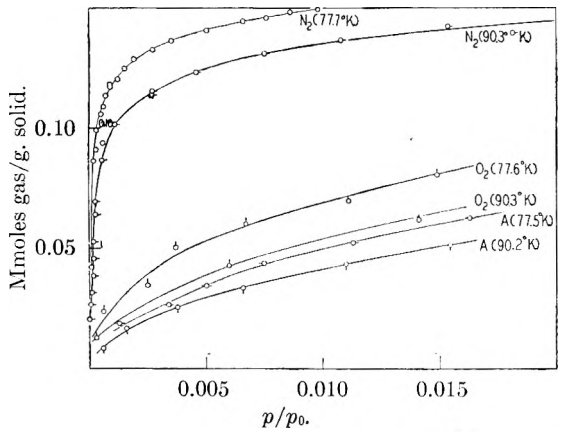

Fig. 2.—Adsorption isotherms on rutile in the region of low relative pressure.

The oxygen and argon adsorption data fit the BET equation in the range $0.05 < p/p_0 < 0.30$; in the case of nitrogen, the fit extends from the smallest p/p_0 values measured to $p/p_0 = 0.20$. A summary of the BET constants is given in Table II. The values of n_m listed in this table were used to obtain the values cited in the remaining sections of this paper.

TABLE II

BET CONSTANTS

Temp., °K.	Nitrogen n_m, millimoles/g. solid	Nitrogen c	Oxygen n_m, millimoles/g. solid	Oxygen c	Argon n_m, millimoles/g. solid	Argon c
77.4–77.7	0.179	300	0.171	48.7	0.161	28.2
90.0–90.4	0.171	300	0.165	30.3	0.157	24.5

It is seen from Table II that according to the BET theory, (a) the quantity of gas accommodated in a monolayer on the surface, n_m, decreases by roughly 5% as one passes from nitrogen to oxygen to argon; (b) that n_m decreases for all three gases with rising temperature; (c) that the constant, c, (which is a rough measure of the heat of adsorption in the first layer) for nitrogen is an order of magnitude larger than that for oxygen and argon.

From Fig. 2 and Table I, it is seen that at liquid nitrogen temperatures 66% of the surface is covered by nitrogen at $p/p_0 = 0.001$. At this same relative pressure, only 13% and 10% of the surface is covered by oxygen and argon, respectively. As another illustration of the large quantities of nitrogen taken up at very low p/p_0 values, one may note that at 90.3° K. 12% of the surface is covered in the vicinity of $p/p_0 = 0.00002$ (this value represents the lowest limit at which pressure readings could be taken). The findings of earlier studies comparing the relative uptake of nitrogen, oxygen and argon by a variety of solids thus apply also to this case.

Interpretation of Isotherms in Terms of Surface Heterogeneity.—The data of Table I can be fitted to the Sips[6] equation

$$\theta = \left(\frac{p}{p + A}\right)^c = \left(\frac{x}{x + B}\right)^c \qquad (1)$$

where

$$x = \frac{p}{p_0}; \quad A = \frac{B}{p_0}$$

which reduces to the Freundlich equation in the region of low x. A list of the constants B and c used in fitting the data to equation 1 is presented in Table III, together with the range of θ over which a good fit is obtained.

Sips[6] has shown how the adsorption isotherm may be used to determine the distribution of adsorption energies q, over a surface. If the set of sites associated with a given value of q is filled according to the Langmuir law

$$\theta_q = \frac{1}{1 + \frac{a}{p} e^{-q/RT}} = \frac{bp}{1 + bp} \qquad (2)$$

where

$$b = \frac{1}{a} e^{q/RT} \qquad (3)$$

then the distribution function corresponding to equation 1 for $q > l$ is given by

$$f(q) = \frac{1}{RT} \frac{\sin \pi c}{\pi} [e^{(q-l)/RT} - 1]^{-c} \qquad (4)$$

where

$$l = -RT \ln \frac{A}{a} \qquad (5)$$

Calculations for $f(q)$ have been carried out for each of the adsorbates at the two temperatures. Unfortunately, the adsorption isotherms do not uniquely determine the parameter l since the constant a is related by equation 3 to the Langmuir constant b, *i.e.*, to the parameters of the isotherm which would be obtained if adsorption occurred on a homogeneous surface.

However, use of a physical argument may be made to obtain approximate values of l. Mathematically, q is restricted to the range $l \leq q < \infty$; it is probable that the lower limit of q values is approached as the last bare surface sites are filled. Hence, the Clausius–Clapeyron equation was applied to compute the isosteric heats of adsorption in the region near complete surface coverage;

TABLE III

TABULATION OF CONSTANTS USED IN EQUATIONS 1 AND 2 AND RANGE OF VALIDITY OF EQUATION 1

Gas	Nitrogen		Oxygen		Argon	
Temp., °K.	77.7	90.3	77.6	90.4	77.5	90.2
c	0.097	0.126	0.366	0.412	0.417	0.486
B	0.0540	0.0676	0.140	0.147	0.151	0.163
A, cm.	4.30	18.6	2.37	11.5	3.59	16.2
Range of applicability[b] $\theta_{min.}$	0.63	0.69	0.23	0.15	0.25	0.14
Range of applicability[b] $\theta_{max.}$	0.94	1.09	1.48[a]	0.94[a]	1.40	1.42[a]
a, cm.	10×10^5	6.7×10^5	6.2×10^5	4.6×10^5	3.0×10^5	2.4×10^5
l, cal./mole	1920	1890	1940	1910	1760	1730

[a] These values do not necessarily represent upper limits since no experimental data were taken beyond this point. [b] n_m values cited in Table II were used to determine these values.

after conversion to differential heats of adsorption, these values were used in equation 4; values of a computed from equation 5 are listed in Table III.

The distribution functions are plotted against q in Fig. 3. It is to be emphasized that the shape of these curves is determined solely by the parameter c; the value of l determines only the position of these curves laterally along the q axis without affecting the actual distribution.

Inspection of Fig. 3 shows that the distribution functions for oxygen and argon are quite similar, differing only in their location along the abscissa. The number of low energy sites heavily outweighs the number of high energy sites. The larger uptake of oxygen compared to argon, as evidenced by the isotherms, is thus reflected as a shift of the distribution curve toward higher q values.

In striking contrast to these curves, the distribution function for nitrogen is very nearly uniform over a large range of q values. The enormous uptake of nitrogen compared to oxygen and argon can thus be correlated to the apparent abundance of high energy sites when nitrogen is adsorbed.

It is of interest that the nitrogen isotherms also fit the equation

$$\theta = \frac{1}{\ln k} \ln \frac{kp + C}{p + C} = \frac{1}{\ln k} \ln \frac{kx + D}{x + D} \qquad (6)$$

with $D = C/p_0$; k, C, D are constants. Equation 6 is a generalized form of the isotherm proposed by Temkin and Pyzhev.[22]

The distribution function which corresponds to this isotherm has been shown by Sips[6] to be the step function

$$f(q) \begin{cases} = \dfrac{1}{RT \ln k} \text{ for } l < q < l + RT \ln k \\ = 0 \text{ for all other } q \end{cases} \qquad (7)$$

where

$$l = -RT \ln C/a \qquad (8)$$

Again, since a is not known, we use in place of l the values of q computed from the Clausius-Clapeyron equation near $\theta = 1$, which are given in Table III. The values of $q_{max.} = l + RT \ln k$ are entered in Table IV.

The nitrogen distribution function corresponding to the Sips equation (Eq. 1) is very similar to that corresponding to Eq. 6. The value for $f(q)$ computed from 77.7° K. isotherm according to Eq. 4 at $q = 2200$ cal./mole agrees with that computed from Eq. 7. At $q = 3300$ cal./mole, the two values read 3.08×10^{-4} and 5.25×10^{-4} (cal./mole)$^{-1}$, respectively. Thus, although the nitrogen data can be made to fit two completely different types of isotherm equations, the resulting distribution functions resemble one another very closely over the range of applicability. It is of importance that we were unable to fit our oxygen or argon data to Eq. 6. This would be expected intuitively since in these cases the distributions computed from Eq. 4 are far from uniform while the applicability of Eq. 6 presupposes a uniform distribution.

(22) M. Temkin and V. Pyzhev, *Acta Physicochim. U.R.S.S.*, **12**, 327 (1940).

TABLE IV

TABULATION OF CONSTANTS USED IN EQUATIONS 6 AND 7 TO REPRODUCE THE ADSORPTION OF NITROGEN ON RUTILE; RANGE OF APPLICABILITY

Temp., °K.	k	D	$f(q)$, (cal./mole)$^{-1}$	$q_{max.}$, cal./mole	Range of validity of Eq. 6 $\theta_{min.}$	$\theta_{max.}$
77.7	2.19×10^5	0.0660	5.25×10^{-4}	3830	0.50	0.90
90.3	2.75×10^4	0.0835	5.45×10^{-4}	3740	0.43	0.93

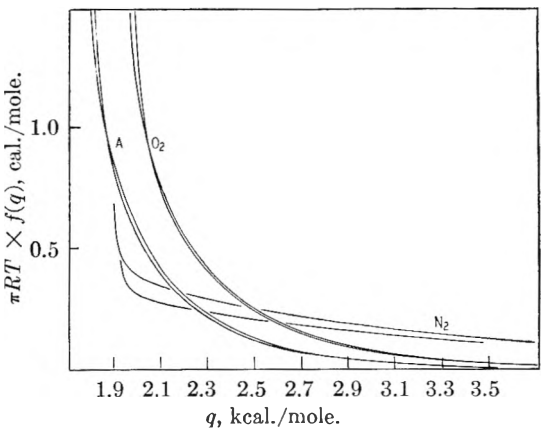

Fig. 3.—Distribution of adsorption energies among surface sites of rutile.

Discussion

The distribution functions plotted in Fig. 3 approach zero asymptotically as $q \rightarrow \infty$ and approach infinity as $q \rightarrow 0$. Since the number of sites on the surface is finite, the distribution of q values on the surface must differ from that given by equation 4 in the range of maximum and minimum q values.

Inspection of Fig. 3 shows that the function $\sin \pi c [e^{(q-l)/RT} - 1]^{-c}$ varies with different adsorbates. Since the distribution is presumably a property of the solid, these variations must be due to other factors not taken into account by the Sips

theory. One such factor is the formation of higher layers before completion of the first. This effect may be of importance for the nitrogen data which cannot be fitted to equation 1 except at $\theta > 0.63$ or to equation 6 except at $\theta > 0.49$. Another factor is the effect of lateral interaction between adsorbed particles in the first layer, which augments the quantity of adsorbate held on the surface at a given pressure when the interaction forces are attractive. A third factor not considered in the Sips analysis is the specificity of the surface toward some adsorbates. As an illustration of this effect, consider adsorption on a surface which contains a great number of constricted sites accessible to one adsorbate but not to another; the distribution functions obtained with these two gases would obviously differ considerably.

The experimental adsorption isotherm thus could be resolved into four contributions that will be broadly classified as "nonspecific solid-gas" interactions, and "lateral," "multilayer" and "specific" interactions. Obviously, the Sips analysis should be applied only to the isotherm which results upon subtracting algebraically the lateral, multilayer and specific contributions from the experimental isotherm. The resulting distribution functions obtained for the three gases after such subtraction should coincide in shape, although they might differ in location along the q axis, since the l values vary with different adsorbates. Coincidence in shape of the distribution functions obtained in this manner may, therefore, be used as a criterion to check on the correctness of the calculations dealing with lateral interactions and with multilayer formation.[23]

(23) It should be noted that when two distribution functions are identical except for their location along the q axis the corresponding isotherms will have different numerical values for some of their parameters (such as A in Eq. 1, k in Eq. 6) and will, therefore, differ in shape. Hence, examination of the isotherms does not aid in establishing the correctness of the above mentioned calculations.

In these discussions it has been tacitly assumed that the postulates, implicit in equation 2, on which the Sips theory is based are correct. For the purpose of this discussion it is useful to imagine a process whereby all sites on a given surface which are associated with the same q value are grouped in a hypothetical patch, and all the patches are arrayed on the surface in order of decreasing q. One basic assumption on which the Sips theory rests is that at any value of $0 < \theta < 1$ all patches are covered to some extent; that is, $\theta_q > 0$ for all q values. Halsey[3] has recently proposed a model involving coöperative adsorption, according to which at a given value of θ all patches down to a given $q = q_\theta$ are completely filled and the remaining patches are empty; in this model, $\theta_q = 1$ for $q \geq q_\theta$ and $\theta_q = 0$ for $q < q_\theta$. The concept of surface heterogeneity is essential to the model since a one step isotherm equation would be obtained on a homogeneous surface. It is obvious, however, that the Sips analysis cannot be applied to the Halsey model. Failure of the generalized Langmuir theory to apply may thus be the reason for the apparent variations of the distribution functions plotted in Fig. 3.

The second assumption implicit in equation 2 is that the adsorbed layer forms an immobile film on the surface of the solid. However, Hill has pointed out that one should really expect formation of a partially mobile surface film in the temperature range of 77–90° K. Surface mobility, even in the absence of strong lateral interactions, disturbs the equilibrium distribution described by equation 2. In such cases the Sips theory must be suitably modified before it can be applied.

Acknowledgments.—The authors are pleased to acknowledge their indebtedness to Mr. William Schwabacher for helpful discussions and to Mr. Robert Batdorf and Mrs. Gertrude Honig for part-time technical aid.

CRYSTAL STRUCTURE OF HEAVY METAL ORTHOVANADATES[1]

BY W. O. MILLIGAN AND L. W. VERNON

Department of Chemistry, The Rice Institute, Houston, Texas

Received October 30, 1950

The following is a brief summary of the results of this investigation: (1) The orthovanadates of cerium, praseodymium, neodymium, samarium, europium, gadolinium, terbium, dysprosium, holmium, erbium, thulium, ytterbium, lutecium, yttrium and scandium possess the zircon structure. (2) The oxygen parameters for fourteen of these orthovanadates are $x = 0.19 \pm 0.01$ and $z = 0.35 \pm 0.01$. For scandium orthovanadate the parameters are $x = 0.20 \pm 0.01$ and $z = 0.32 \pm 0.01$. (3) The oxygen tetrahedra in scandium orthovanadate are elongated in the direction of the *c*-axis. In the other orthovanadates of this series the oxygen tetrahedra are almost regular.

In a previous paper[2] from this Laboratory it was reported that the orthovanadates of praseodymium, neodymium, samarium, europium, gadolinium, terbium, dysprosium, erbium, thulium, ytterbium, lutecium and yttrium comprise a tetragonal isomorphous series. The structures of a limited number of orthovanadates have been described in the literature. Broch[3] found that yttrium ortho vanadate was tetragonal, possessing a crystal structure closely similar to that of zircon.[4,5] Brandt[6] found that chromium orthovanadate ($CrVO_4$) was orthorhombic and belonged to space group D^{17}_{2h} — Cmcm. Brandt[7] has also reported rhodium orthovanadate ($RhVO_4$) to be tetragonal and to possess the rutile structure.[8]

The results of the previous investigations in this Laboratory and the work of Brandt suggest the desirability of further quantitative studies on the heavy metal orthovanadates.

Experimental

Samples of scandium orthovanadate, holmium orthovanadate and cerium orthovanadate were prepared by the method used in the preparation of the other orthovanadates previously studied.[2] The oxide or the oxalate of the trivalent metal was mixed with ammonium metavanadate in quantities such that equimolar amounts of M_2O_3 and V_2O_5 were present. The samples were heated for periods of two hours at 750–1000°.

These powder samples were examined by standard X-ray diffraction methods, using CrK_α and CuK_α X-radiation. The diffraction patterns observed for cerium orthovanadate and holmium orthovanadate are almost identical with the X-radiograms of the other rare earth orthovanadates. The pattern obtained for scandium orthovanadate consists of relatively fewer lines and will be discussed in detail below.

The relative intensities were obtained by measuring the area under the peaks on the X-radiograms, which were produced by the Geiger-counter and Brown recorder of the Norelco X-ray spectrometer. The scanning speed of the spectrometer was one degree (2θ) per minute. The copper radiation was filtered through nickel foil to obtain the copper K_α radiation. The X-radiograms of neodymium orthovanadate, ytterbium orthovanadate and scandium orthovanadate are reproduced in Fig. 1.

Because of the limited angular range of the Norelco spectrometer, the intensities of some of the diffraction lines of scandium orthovanadate were obtained from the powder photograph using a Moll microphotometer and a "Photopen" recorder. The observed intensities which are reported in parentheses in Table IV are the ones obtained from the powder photograph by means of the microphotometer.

Crystal Structure

The approach used in determining the structure of the orthovanadates enumerated above is based on the similarity of the powder photographs and the structure of yttrium orthovanadate reported by Broch.[3]

When the X-ray diffraction lines of the orthovanadates of 14 trivalent metals (cerium, praseodymium, neodymium, samarium, europium, gadolinium, terbium, dysprosium, holmium, erbium, thulium, ytterbium, lutecium and yttrium) are indexed in a body-centered tetragonal system, the following reflections are absent: (110), (130), (002), (330), (114), (222) and (150). The absence of these reflections suggests the presence of a fourfold screw axis, an *a*-plane perpendicular to this axis, and a *d*-plane perpendicular to (110). These symmetry elements lead to the following extinctions. Reflections (*hkl*) occur only with $h + k + l = 2n$; (*hk*0) only with $h = 2n$ and $k = 2n$; (*hhl*) only with $l = 2n$ and $2h + l = 4n$. These are the characteristic extinctions of space group D^{19}_{4h} —I4/amd.

From consideration of the density of these orthovanadates it is found that the unit cell contains four molecules of MVO_4. Space group D^{19}_{4h} — I4/amd (reference 9) contains two positions with four equivalent points and three positions with sixteen equivalent points.

The special positions (*a*), (*b*), (*f*) and (*g*) (ref. 9) have additional extinctions. Because of these additional extinctions the presence of reflections (202) and (134) eliminates the possibility of the oxygen atoms being in positions (*f*) or (*g*). The oxygen atoms must be in position (*h*). The atomic positions are:

Four trivalent metal atoms in (*a*): 000; $\frac{1}{2}\ \frac{1}{2}\ \frac{1}{2}$; $0\ \frac{1}{2}\ \frac{1}{4}$; $\frac{1}{2}\ 0\ \frac{3}{4}$

Four vanadium atoms in (*b*): $0\ 0\ \frac{1}{2}$; $\frac{1}{2}\ \frac{1}{2}\ 0$; $0\ \frac{1}{2}\ \frac{3}{4}$; $\frac{1}{2}\ 0\ \frac{1}{4}$

Sixteen oxygen atoms in (*h*): $(000;\ \frac{1}{2}\ \frac{1}{2}\ \frac{1}{2}) + 0,x,z;\ 0,\ -x,z;\ x,0,\ -z;\ -x,0,\ -z;\ 0,\frac{1}{2}+x,\frac{1}{4}-z;\ 0,\frac{1}{2}-x,\frac{1}{4}-z;\ x,\frac{1}{2},\frac{1}{4}+z;\ -x,\frac{1}{2},\frac{1}{4}+z$

Calculation of Intensities.—The relative intensities were calculated by means of the equation

$$P' = k \times \frac{1 + \cos^2 2\theta}{\sin^2\theta \cos\theta} \times pF^2$$

where each term has the meaning given in ref. 9.

(1) Presented before the Division of Physical and Inorganic Chemistry at the 118th Meeting of the American Chemical Society, which was held in Chicago, Ill., September, 1950.

(2) Milligan, Watt and Rachford, THIS JOURNAL, **53**, 227 (1949).

(3) Broch, *Z. physik. Chem.*, **20B**, 345 (1932).

(4) Vegard, *Phil. Mag.*, **1**, 1151 (1926).

(5) Vegard, *ibid.*, **4**, 511 (1927).

(6) Brandt, *Arkiv Kemi Mineral. Geol.*, **17A**, No. 6 (1943).

(7) Brandt, *ibid.*, **17A**, No. 15 (1943).

(8) Wyckoff, "The Structure of Crystals," Chemical Catalog Company, (Reinhold Publ. Corp.), New York, N. Y., 1931.

(9) "Internationale Tabellen zur Bestimmung von Kristallstrukturen," Gebrüder Borntraeger, Berlin, 1935.

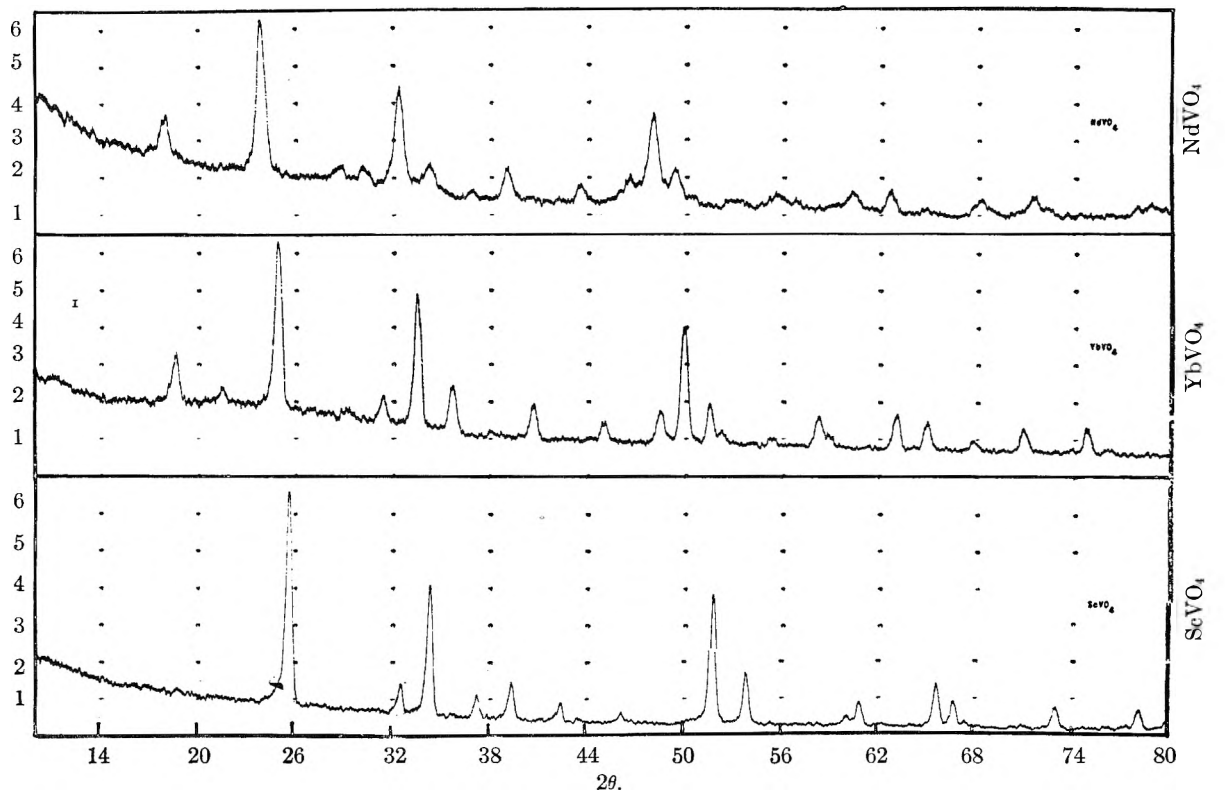

Fig. 1.—Geiger counter X-radiograms of neodymium orthovanadate, ytterbium orthovanadate and scandium orthovanadate.

After substituting the atomic positions given above and simplifying, the following structure factor is obtained for reflections with $h + k + l = 2n$:

$$F_{hkl} = 2[1 + \exp \pi i (k + l/2)][f_M + f_V \exp \pi il] + 4f_0 \{[\exp (2\pi ilz) \cos 2\pi kx + \exp (-2\pi ilz) \cos 2\pi hx] + \exp \pi i(k + l/2) [\exp (2\pi ilz) \cos 2\pi hx + \exp (-2\pi ilz) \cos 2\pi kx]\}$$

From examination of this structure factor it is seen that for reflections with $k + l/2 = 2n + 1$ the oxygen atoms alone contribute to the diffraction. It will also be noted that when l is odd the phase of the waves diffracted by the trivalent metal atoms differs by 180 degrees from the phase of the X-rays diffracted by the vanadium atoms. Reflections with $k + l/2 = 2n + 1$ should be very weak; lines with l odd should be weak and lines with l even should be strong.

Only values of x between zero and a half need be considered since for an oxygen atom at $(0xz)$ there is an equivalent atom at $(0\bar{x}z)$. Values of z between zero and a half are the only ones that need be considered since larger values would give the same results with the a and b axes interchanged.

The reflection (220) is relatively weak although l is even. From consideration of the structure factor it is seen that this means that $\cos 4\pi x$ must have a large negative value. The structure factor for the (220) plane does have a large negative value when $x = 1/4$. Although the (202) reflection is caused by the oxygen atoms only, it is relatively strong. This fact means that $\sin 4\pi z(1 - \cos 4\pi x)$ must be a large number. The function above does have large values when $x = 1/4$ and $z = 1/8$ or $3/8$. If z is equal to $1/8$, the interatomic distances in the crystal are abnormal. The values of the parameters are probably close to $1/4$ and $3/8$.

The final values of the parameters were determined by the method of trial and error. The values of the parameters were varied until a good general agreement between the calculated intensities and the experimentally determined intensities was obtained.

The X-ray diffraction lines on the powder photograph of scandium orthovanadate can be indexed in the body-centered tetragonal system. The unit cell dimensions of all of the orthovanadates studied are given in Table I in absolute ångström units. Calculation of the density using the unit cell in Table I and four molecules of $ScVO_4$ per unit cell gives

TABLE I

UNIT CELL DIMENSIONS

Compound	a, Å.	c, Å.	c/a
$ScVO_4$	6.78	6.12	0.90
$LuVO_4$	7.01	6.19	.88
$YbVO_4$	7.04	6.23	.89
$TmVO_4$	7.00	6.20	.89
$ErVO_4$[a]	7.07	6.25	.88
$HoVO_4$	7.06	6.25	.89
YVO_4	7.10	6.27	.88
$DyVO_4$	7.10	6.27	.88
$TbVO_4$	7.15	6.31	.88
$GdVO_4$	7.19	6.33	.88
$EuVO_4$	7.20	6.35	.88
$SmVO_4$	7.24	6.36	.88
$NdVO_4$	7.33	6.43	.88
$PrVO_4$	7.30	6.42	.88
$CeVO_4$	7.34	6.47	.88

[a] 25% yttrium.

a value of 3.54 g./cc. The density of scandium orthovanadate was determined experimentally by the pycnometer method and a value of 3.6 g./cc. was obtained.

TABLE II

RELATIVE INTENSITIES OF $NdVO_4$ AND $YbVO_4$

	$NdVO_4$		$YbVO_4$	
hkl	Calcd.	Obsd.	Calcd.	Obsd.
101	3.2	2.9	4.6	3.2
200	10.0	10.0	10.0	10.0
211	1.4	1.5	2.1	1.7
112	7.9	7.6	8.3	7.8
220	2.1	2.4	2.3	2.7
202	0.5	0.6	0.4	0.5
301	1.4	2.0	1.5	2.1
103	0.8	1.1	0.9	1.2
231	1.3	2.0	1.6	1.9
132	5.8	6.1	6.0	6.8
400	1.7	2.4	1.6	2.2
123	0.6	0.7	0.8	0.9
411	0.4	0.6	0.5	0.5
240	1.4	1.2	2.0	1.9
004	0.3	0.8	0.3	0.7
303	.2		.2	
402	.02	[a]	.02	[a]
332	1.5	1.7	1.6	2.0
204	1.1	1.4	1.2	1.7
233	0.1		0.2	
242	.02	[a]	.02	[a]
341	.5	0.5	.6	0.8
501	.08		.1	
224	1.2	1.4	1.2	1.5
143	0.3		0.4	
134	.01	v.w.	.01	v.w.
251	.1	v.w.	.2	v.w.
152	1.5	1.6	1.6	1.7

[a] Not observed.

TABLE III

INTERATOMIC DISTANCES IN $NdVO_4$, $YbVO_4$, YVO_4, $ScVO_4$, Å.

	$NdVO_4$	$YbVO_4$	YVO_4[a]	$ScVO_4$
V–O	1.69	1.63	1.64	1.74
$(O–O)_x$	2.78	2.68	2.70	2.70
$(O–O)_z$	2.76	2.66	2.67	2.92
M–O	2.36	2.27	2.30	2.07
M–O	2.65	2.56	2.73	2.38

[a] Reported by Broch.[6]

Indexing the reflections of scandium orthovanadate in the above manner gives a large number of extinctions (see Table IV). Examination of the absent reflections reveals that scandium orthovanadate has the same systematic extinctions as the other orthovanadates enumerated above. In addition to these systematic extinctions, scandium orthovanadate has a pseudo-extinction; many reflections with l odd are missing. If scandium orthovanadate has the same structure as the other orthovanadates enumerated above, the pseudo-extinction can be explained. When l is odd the wave diffracted by the scandium ion is 180° out of phase with the wave diffracted by the vanadium ion. Since the scattering powers of V^{+5} and Sc^{+3} are approximately the same, X-ray diffraction by planes with odd l is caused almost entirely by the oxygen atoms and in some cases the intensity will be too weak to be observed.

The intensities of the diffraction lines of scandium orthovanadate were calculated by the method outlined above. The results are given in Table IV.

TABLE IV

X-RAY DIFFRACTION DATA OF $ScVO_4$

	Interplanar spacings, Å.		Relative intensity	
hkl	Calcd.	Obsd.	Calcd.	Obsd.
101	4.50	[a]	0.00	[a]
200	3.38	3.38	10.0	10.0
211	2.71	2.71	1.4	1.4
112	2.57	2.58	6.2	6.1
220	2.39	2.39	0.7	1.1
202	2.27	2.27	1.3	1.8
301	2.12	2.12	0.5	0.9
103	1.950	1.950	.3	0.6
231	1.793	[a]	.04	[a]
132	1.755	1.760	5.9	6.2
400	1.693	1.690	2.1	2.5
123	1.695	[a]	0.2	
411	1.588	[a]	.04	[a]
004	1.525	1.530	.3	0.5
240	1.513	1.510	1.0	1.1
303	1.514	[a]	0.01	
402	1.485	[a]	0.03	[a]
332	1.415	1.420	1.9	2.1
204	1.390	1.395	1.0	1.2
233	1.382	1.380	0.3	0.3
242	1.360	[a]	.1	[a]
341	1.322	[a]	.05	[a]
501	1.322	[a]	.04	[a]
224	1.285	1.290	.9	1.0
143	1.280	[a]	.03	[a]
134	1.243	[a]	.1	[a]
251	1.231	1.230	.2	0.2
152	1.220	1.220	.9	.9
440	1.200	1.200	.4	.4
105	1.201	[a]	.07	
125	1.130	[a]	.01	[a]
404	1.133	1.135	.5	0.5
343	1.128	[a]	.01	[a]
600	1.128	1.127	.5	0.5
161	1.097	[a]	.01	[a]
352	1.086	1.086	.9	(1.0[b])
260	1.075	1.075	.4	(0.6[b])
116	0.997	0.998	.6	(.6[b])
136	.921	.921	.7	(.8[b])
712	.915	.913	1.0	(.7[b])
624	.876	.878	1.0	(.9[b])
336	.857	.854	0.3	(.5[b])

[a] Not observed. [b] From microphotometer.

Discussion

The calculated and experimental intensities of the X-ray diffraction lines of neodymium orthovanadate and ytterbium orthovanadate are given in Table II for the parameters $x = 0.19$ and $z = 0.35$. It will be noted that there is good general agreement between the calculated intensities and the intensities measured by means of the Geiger counter. Since the intensities of most of the interference maxima are not very sensitive to changes in the values of the parameters, it is difficult to estimate the accuracy of the parameters. However,

the maximum error is probably less than 0.01. A qualitative examination of the X-radiograms of all of the orthovanadates of this isomorphous series reveals no significant difference in the relative intensities of the various members of the series. Since the parameters $x = 0.19$ and $z = 0.35$ give satisfactory agreement between the calculated and experimental intensities for both neodymium orthovanadate and ytterbium orthovanadate, it is believed that the parameters ($x = 0.19 \pm 0.01$, $z = 0.35 \pm 0.01$) will give satisfactory results for each member of the isomorphous series except scandium orthovanadate.

The observed intensities of the diffraction lines of scandium orthovanadate and the calculated intensities for the parameters $x = 0.20$ and $z = 0.32$ are given in Table IV. It will be noted that the calculated intensities of the reflections that were not observed experimentally are less than one per cent. of the intensity of the strongest line. There is also good general agreement between the calculated intensities and the intensities measured by the Geiger counter of the Norelco spectrometer.

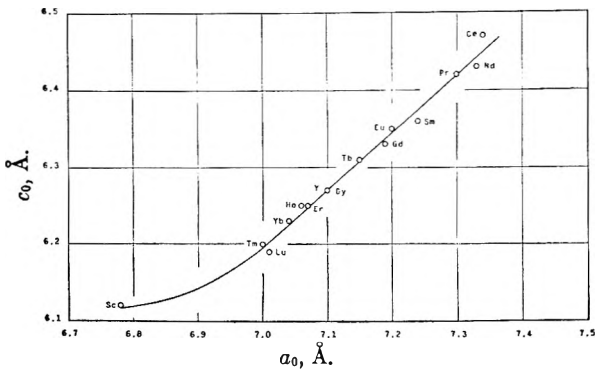

Fig. 2.—Lattice constants of the orthovanadates with the zircon structure.

The structure of the orthovanadates of this isomorphous series is the zircon type structure. The interatomic distances are given in Table III. The trivalent metal atom is surrounded by eight oxygen atoms; four of the oxygen atoms are nearer than the other four. There is a tetrahedron of oxygen atoms around each vanadium atom. In scandium orthovanadate this tetrahedron is elongated in the direction of the c-axis; in the other orthovanadates of this series the tetrahedra are almost regular.

In Fig. 2 it will be noted that a graph of the lattice constants of all of the orthovanadates of this isomorphous series is a straight line (except for scandium orthovanadate) within the probable accuracy of the available data. The unit cell of scandium orthovanadate is elongated in the direction of of the c-axis.

An explanation for the fact that the unit cell of neodymium orthovanadate was found to be larger than the unit cell of praseodymium orthovanadate[2] has been found. The previously proposed process of solid solution[2] has been confirmed in this investigation. In the X-radiogram of one of the samples of cerium orthovanadate ($CeVO_4$) some of the stronger lines of cerium dioxide were observed. When this sample was heated for a longer period of time at a higher temperature the cerium dioxide lines disappeared and the lattice constants of cerium orthovanadate became larger.

MATHEMATICS OF ADSORPTION. IV. EFFECT OF INTRAPARTICLE DIFFUSION IN AGITATED STATIC SYSTEMS

BY FRED J. EDESKUTY AND NEAL R. AMUNDSON

Department of Chemical Engineering, University of Minnesota, Minneapolis 14, Minnesota

Received November 9, 1950

The solution of the problems posed in this paper are rather special in that the types of isotherms and kinetics employed have only limited application. For the linear isotherm there are cases where this assumption is valid. The case of linear kinetics has not been investigated experimentally to any extent. For more general cases numerical methods of solutions of equations proposed here must be sought and the use of digital computers should prove to be of great help in this endeavor. This is largely because of the iterative nature of the approximate solution to the diffusion equation. This problem is being investigated at the present time and will be reported upon later.

The problem of adsorption of a solute from a solution by an adsorbent in a static non-flow system is an old one. The major emphasis in the past has been on the equilibrium attained between the adsorbate on the solid and that in the solution. There is evidence according to Amis,[1] that adsorption equilibrium obtains always in a finite time although a period of years may be required. Many equations have been proposed for adsorption kinetics, a brief review of which is given by Amis. Kinetic effects may arise in a variety of ways and it is not always clear just what effects are being measured. For example, the distribution of solute in the solution exterior to the adsorbent may not be uniform giving rise to concentration gradients. These may be minimized or eliminated completely by agitation of the whole system. Even moderately high agitation rates may still not eliminate these gradients in the neighborhood of the particles themselves and this condition manifests itself in the so-called film resistance to mass transfer at the particle surfaces. High agitation rates will reduce the film resistance to a point where there is practically no kinetic effect at the particle surface. This is tantamount to assuming that the concentration of solute at the particle surface is identical with that in the main

(1) Edward S. Amis, "Kinetics of Chemical Change in Solution," The Macmillan Co., New York, N. Y., 1949.

body of the solution. These two effects are dependent upon diffusion of the solute in the solution exterior to the adsorbent.

For particles of some size an appreciable portion of the adsorbent surface is in the interior of the particle. Adsorption can only take place on this surface after the adsorbate has diffused through the solution existing in the pore volume of the solid. This diffusion may be much slower than diffusion in a solution alone because of the increased length of the tortuous path caused by the internal structure of the solid. Eagle and Scott[2] in a recent paper made some mention of this aspect of the kinetics.

Finally, the rate of adsorption itself can be a limiting factor and this is in general the most difficult of the kinetic effects to handle analytically. Even if the rate of adsorption is so rapid that equilibrium is attained practically instantaneously, the equilibrium isotherm is generally complicated enough to preclude exact mathematical methods and some recourse to approximate numerical methods must be made. Laidler[3] has examined to some extent under what conditions adsorption kinetics will prevail.

In this paper the problem of adsorption in a static system is considered in the following way. A vessel contains W grams of porous adsorbent and V liters of adsorbate-free solvent. At time t equal to zero adsorbate is admitted to the vessel

TABLE I

NOMENCLATURE

a	$= \dfrac{p(p + K_1 + k_2\alpha)}{D(p + k_2\alpha)}$
C	= concn. in main body of solution, moles per liter
C_0	= concn. in main body of solution initially, moles per liter
c	= concn. of solution in void volume of solid, moles per liter
c_0	= init. concn. of solution in void volume of solid, moles per liter
D	= diffusivity, cm.^{2} per second
h	= LaPlace transform of c
H	= LaPlace transform of C
k	= mass transfer coefficient at particle surface
k_1, k_2	= constants in adsorption isotherm or kinetic expansion
K	$= k_1/k_2$, equilibrium constant for adsorption kinetics
n	= amount adsorbed on solid, moles per liter of apparent volume
n_0	= init. amount adsorbed on solid, moles per liter of apparent volume
N	= LaPlace transform of n
p	= LaPlace transform parameter corresponding to t
r	= radius variable in particle, cm.
R	= external radius of particle, cm.
t	= time in seconds
V	= volume of external solution, liters
W	= weight of adsorbent, grams
z	$= pR^2\gamma$
α	= fractional void volume
β	$= (k + \alpha)W/V\rho$
β'	$= D\mu/R^2$
$\Gamma(x)$	= gamma function
γ	$= \dfrac{k_1 + \alpha}{\alpha D}$
Δ	$= R\sqrt{-a}$
ϵ	$= D/Rk$
μ	$= \alpha W/\rho V$
ρ	= solid apparent density, g./cc.
ω	$= R\sqrt{-p\gamma}$

(2) S. Eagle and J. W. Scott, *Ind. Eng. Chem.*, **42**, 1287 (1950).

(3) K. J. Laidler, *Bull. soc. chim. France*, D 171 (1949).

so that the concentration in the solution is C_0. The agitation is sufficient to minimize concentration gradients in the main body of the solution but not so great as to remove the film resistance at the particle surface. The problem then is to obtain a formula which will predict the change in the solution concentration with time. It is assumed that the adsorbent is in the form of uniform porous spheres. In order that adsorbate be adsorbed on the internal surface it is first necessary that it diffuses through a resisting film at the sphere surface and then diffuses further into and through the particle.

In order to cover the case for desorption as well it will be assumed that at time t equal to zero the concentration in the main body of the solution is C_0 while the concentration of the solution in the sphere void volume is c_0 while that on the solid is n_0; c_0 and n_0 may be equilibrium values but this is not necessary. Table I gives a complete notation of symbols used in this paper.

If one considers a spherical shell of inside radius r and thickness Δr, then on equating inflow minus outflow by diffusion to the rate of accumulation in the shell there results

$$\left(4\pi r^2 D\alpha \frac{\partial c}{\partial r}\right)_{r-\Delta r} - \left(4\pi r^2 D\alpha \frac{\partial c}{\partial r}\right)_r = \left(4\pi r^2\alpha \frac{\partial c}{\partial t}\right)_{\bar{r}}\Delta r + \left(4\pi r^2 \frac{\partial n}{\partial t}\right)_{\bar{r}}\Delta r$$

where $r < \bar{r} < r + \Delta r$. This reduces, on letting $\Delta r \to 0$, to

$$D\left(\frac{\partial^2 c}{\partial r^2} + \frac{2}{r}\frac{\partial c}{\partial r}\right) = \frac{\partial c}{\partial t} + \frac{1}{\alpha}\frac{\partial n}{\partial t} \qquad (1)$$

this equation holds regardless of the adsorption mechanism obtaining inside the spheres.

The condition at the sphere surface when there is a resistance to mass transfer is given by

$$-D\frac{\partial c}{\partial r} = k(c - C), \text{ when } r = R \qquad (2)$$

This equation really defines the mass transfer coefficient k. A large value of k indicates that there is little resistance to mass transfer. In the limit as the agitation is increased k becomes infinite and Equation 2 is replaced by the equation

$$c = C, \text{ when } r = R \qquad (3)$$

In addition to these equations there is another which relates the change in concentration of the solution with the rate at which adsorbate enters the adsorbent. The rate at which adsorbate enters a single sphere is $4\pi R^2\alpha D(\partial c/\partial r)_{r=R}$. Hence the rate at which adsorbate enters W grams of spheres is $3(D\alpha W)/R\rho\,(\partial c/\partial r)_{r=R}$. The rate at which the solution is becoming depleted is $-V(\mathrm{d}C/\mathrm{d}t)$, and therefore

$$-V\frac{\mathrm{d}C}{\mathrm{d}t} = \frac{3D\alpha W}{R\rho}\left(\frac{\partial c}{\partial r}\right)_{r=R} \qquad (4)$$

This equation is merely a material balance over the adsorber made on the adsorbate.

The condition of the adsorbent and solution must be stated at time $t = 0$. In general

$$\left.\begin{aligned} c &= c_0 \\ C &= C_0 \end{aligned}\right\} \text{ when } t = 0 \qquad (5)$$

For the case of fresh adsorbent $c_0 = 0$ while for the case of desorption using fresh solvent $C_0 = 0$.

Equations 1, 2, 3, 4 and 5 are valid irrespective of the mechanism taking place inside the spheres. Two cases will be considered: in the first it is assumed that adsorption equilibrium occurs pointwise inside the spheres while in the second a kinetic relation will be assumed to hold. The former case is really a special case of the latter but it is somewhat easier mathematically to treat them as separate problems.

Case 1. Equilibrium.—If one assumes pointwise equilibrium inside the particles then the equilibrium is that of an adsorption isotherm, $n = f(c)$. In general then Equation 1 reduces to

$$D\left(\frac{\partial^2 c}{\partial r^2} + \frac{2}{r}\frac{\partial c}{\partial r}\right) = \left[1 + \frac{1}{\alpha}f'(c)\right]\frac{\partial c}{\partial t}$$

The only isotherm for which analytical solutions may be obtained is the linear one, $n = k_1 c + k_2$. It is true that this limits the applicability of the results of this paper but it has been shown in these laboratories that there are situations in which the linear isotherm can be applied. This will be done in a further paper. The diffusion equation may now be written

$$\frac{\partial^2 c}{\partial r^2} + \frac{2}{r}\frac{\partial c}{\partial r} = \gamma\frac{\partial c}{\partial t} \qquad (6)$$

Equations 2, 4, 5 and 6 make up a complete description of the system. A further condition which is obvious physically and which must be included in order to obtain a mathematical solution is that the concentration must remain finite at all times. The applicability of this condition will become clear later.

A solution will now be found which will satisfy Equations 2, 4, 5 and 6. The method is that of the LaPlace transformation, details of which can be found in Churchill.[4] Let L stand for the LaPlacian operator which is taken with respect to the variable t

$$L[c(r,t)] = \int_0^\infty e^{-pt}\, c(r,t)dt = h(r,p) = h$$

$$L[C(t)] = \int_0^\infty e^{-pt}\, C(t)dt = H(p) = H$$

On taking the transform of Equation 6 and using Equation 5 there results

$$\frac{d^2h}{dr^2} + \frac{2}{r}\frac{dh}{dr} - \gamma p h = -\gamma c_0$$

This is an ordinary differential equation whose solution can be readily shown to be

$$h = \frac{A}{r}\sin r\sqrt{-\gamma p} + \frac{B}{r}\cos r\sqrt{-\gamma p} + \frac{c_0}{p} \qquad (7)$$

Since concentrations must remain finite at all times it is clear that the constant B must be zero.

If the transforms of Equations 2 and 4 are taken, respectively

$$-D\frac{dh}{dr} = k(h - H), \text{ when } r = R$$

and

$$\frac{3D\alpha W}{R\rho}\frac{dh}{dr} = -V(pH - C_0), \text{ when } r = R$$

(4) R. V. Churchill, "Modern Operational Mathematics in Engineering," McGraw-Hill Book Co., Inc., New York, N. Y., 1944.

These two equations may be solved simultaneously to eliminate H to obtain

$$\left(\frac{3D\alpha W}{R\rho} + \frac{VDp}{k}\right)\frac{dh}{dr} = -Vph + VC_0, \text{ when } r = R \qquad (8)$$

This equation can now be used to determine the constant A in Equation 7. If the operations in Equation 8 are performed on h as given in Equation 7 then an equation in A results which may be solved for A. When this is substituted in Equation 7

$$h = \frac{R^3\gamma(C_0 - c_0)\sin r\omega/R}{r[(-3\beta + (\epsilon - 1)\omega^2)\sin\omega + (3\beta - \epsilon\omega^2)\omega\cos\omega]} + \frac{c_0}{p} \qquad (9)$$

where

$$\beta = \frac{(k_1 + \alpha)W}{V\rho};\quad \epsilon = \frac{D}{Rk};$$

$$\omega = R\sqrt{-\gamma p};\quad p = -\frac{\omega^2}{R^2\gamma}$$

Equation 9 is the transform of the concentration of the solution inside the sphere. In order to obtain the concentration itself the inverse transform must be found. This can be done by standard methods and will only be sketched here. The inverse transform is the sum of the residues of the function $e^{pt}h(r,p)$ at the poles of $h(r,p)$. The poles will occur at the zeros of the denominators of Equation 9.

If the pole at $p = b$ is a simple pole the residue is given by the formula

$$\lim_{p\to b}[(p - b)e^{pt}h(r,p)] \qquad (10)$$

If all of the poles are simple poles the Heaviside expansion theorem or its extensions may be used.

Thus since $h(r,p)$ has the fractional form $q(p)/s(p)$, the inverse transform corresponding to the zeros of $s(p)$, provided $q(p)$ is analytic, is given by

$$\sum\frac{q(p_n)}{s'(p_n)}e^{p_n t} \qquad (11)$$

where p_n is a root of $s(p) = 0$, $s'(p_n)$ is the derivative of $s(p)$ evaluated at $p = p_n$, and the summation is taken over all the roots of $s(p) = 0$ in question.

To go back to Equation 9 it is to be noted that the numerator is analytic while the zeros of the denominator are at the zeros of

$$[-3\beta + (\epsilon - 1)\omega^2]\sin\omega + (3\beta - \epsilon\omega^2)\omega\cos\omega = 0$$

Let the zeros be denoted by 0, ω_1, ω_2, ω_3, ... The residue at $p = 0$ corresponding to $\omega = 0$ can be found from Equation (10). By expanding the trigonometric terms into their respective infinite series, cancelling common terms, and passing to the limit there results

$$\frac{C_0 - c_0}{1 + \beta} + c_0 \qquad (12)$$

where the second term comes from the term c_0/p in Equation 9. The sum of the remaining residues is found using Equation 11. Here

$$q(p) = \frac{R^3}{r}\gamma(C_0 - c_0)\sin\frac{r\omega}{R}$$

$$s(p) = Q(\omega)$$

$$Q(\omega) = [-3\beta + \omega^2(\epsilon - 1)]\sin\omega + (3\beta - \epsilon\omega^2)\omega\cos\omega$$

It can be shown that

$$s'(p_n) = \frac{R^2\gamma \sin \omega_n}{2(3\beta - \epsilon\omega_n^2)} [P(\omega_n)]^{-1}$$

where

$$[P(\omega_n)]^{-1} = (3\beta - \epsilon\omega_n^2)^2 + 3(3\beta - \epsilon\omega_n^2) + (1 + 2\epsilon)\omega_n^2$$

Therefore combining Equation 12 with this result

$$c(r,t) = c_0 + \frac{C_0 - c_0}{1 + \beta} + \frac{2R}{r}(C_0 - c_0) \sum_{n=1}^{\infty} \frac{(3\beta - \epsilon\omega_n^2) \sin \frac{r\omega_n}{R}}{\sin \omega_n} P(\omega_n) e^{p_n t}$$

noting that $p_n^2 = -\frac{\omega_n^2}{R^2\gamma}$. This formula gives the concentration in the sphere as a function of time and position. In order to obtain the concentration of the external solution use will be made of Equation 4. Integration gives

$$\frac{3D\alpha W}{R\rho} \int_0^t \left(\frac{\partial c}{\partial r}\right)_{r=R} dt = -V \int_0^t \frac{dC}{dt} dt = V[C_0 - C] \tag{13}$$

Now

$$\left(\frac{\partial c}{\partial r}\right)_{r=R} = \frac{2(C_0 - c_0)}{R} \sum_{n=1}^{\infty} \frac{(3\beta - \epsilon\omega_n^2)(\omega_n \cos \omega_n - \sin \omega_n)}{\sin \omega_n} P(\omega_n) e^{p_n t}$$

$$= \frac{2(C_0 - c_0)}{R} \sum_{n=1}^{\infty} \omega_n^2 P(\omega_n) e^{p_n t}$$

On substitution into Equation 13, one obtains

$$\frac{C_0 - C}{C_0 - c_0} = 6\beta \sum_{n=1}^{\infty} P(\omega_n)(1 - e^{p_n t}) \tag{14}$$

This formula solves the problem originally posed in the paper for the case of pointwise equilibrium in the adsorbent. Note that it is valid for either adsorption or desorption. Equation 14 is in the form of an infinite series but the convergence is very rapid since for large values of ω_n the term in $P(\omega_n)$ behaves essentially as ω_n^{-4}. The roots ω_n, as n increases, behave about as n, *i.e.*, $\omega_n/n \to$ a constant for large n and $\omega_{n+1} - \omega_n \to \pi$ as n increases. Hence not more than three or four terms should be needed for calculation purposes. This equation includes the surface resistance effect of mass transfer. The magnitude of the mass transfer coefficient depends to a large extent on the degree of agitation. As the agitation level is increased k increases and should approach infinity with the result that the concentration on the sphere surface is the same as that in the main body of the solution as in Equation 3. From the definition of ϵ it is seen that as $k \to \infty$, $\epsilon \to 0$ so that Equation 14 reduces to

$$\frac{C_0 - C}{C_0 - c_0} = 6\beta \sum_{n=1}^{\infty} S(\omega_n)(1 - \epsilon^{p_n t}) \tag{15}$$

with

$$[S(\omega_n)]^{-1} = 9\beta(\beta + 1) + \omega_n^2$$

where ω_n is a root of

$$(-3\beta - \omega^2)\sin \omega + 3\beta\omega \cos \omega = 0$$

Again the summation in Equation 15 must be made to include all the roots of this transcendental equation. Equation 15 solves the problem of adsorption or desorption on porous adsorbents in a well agitated system for a linear isotherm. A problem in heat transfer similar to this problem was considered by Patterson.[5] Ebel[6] considered an analogous problem in extraction from porous spheres. Problems of a similar mathematical nature have also been considered by Kasten and Amundson[7] and Munro and Amundson.[8]

It is now necessary to examine into the character of the roots of the equation

$$s(p) = Q(\omega) = [-3\beta + (\epsilon - 1)\omega^2] \sin \omega + (3\beta - \epsilon\omega^2)\omega \cos \omega = 0$$

since this determines the nature of the poles in Equation 9. Equation 9 can be written in the form

$$h = \frac{c_0}{p} + \frac{R^2\gamma(C_0 - c_0)}{2zg(z)} \sum_{n=0}^{\infty} \left(\frac{r}{R}\right)^{2n} \frac{z^{2n}}{(2n + 1)!}$$

where

$$g(z) = \sum_{n=0}^{\infty} \frac{z^n}{n!} \phi(n)$$

and

$$\phi(n) = \frac{\Gamma(n + 2)}{\Gamma(2n + 4)} [4\epsilon n^2 + (6\epsilon + 2)n + 3(\beta + 1)]$$

with

$$pR^2\gamma = z, \quad \omega^2 = -z$$

From this definition of z it is clear that the nature of the roots in p is the same as that in z, $R^2\gamma$ being positive. Thus it is necessary to determine the roots of

$$g(z) = 0$$

By a theorem of Laguerre[9] the roots of $g(z) = 0$ are negative provided the roots of the quadratic factor considered as a function of n

$$4\epsilon n^2 + (6\epsilon + 2)n + 3(\beta + 1) = 0$$

are negative. It is obvious that there are no positive roots and the two roots will be negative if the discriminant

$$(2 + 6\epsilon)^2 - 48\epsilon(\beta + 1) = (3\epsilon - 1)^2 - 12\epsilon\beta > 0$$

If this inequality is not true the quadratic factor will have two complex roots and by an extension of the theorem of Laquerre one can show that $g(z)$ will not have more than two complex roots and possibly it may have none, all the remaining roots being negative. It is obvious of course that $g(z)$ has no positive roots since the infinite series contains terms all of which have the same sign. Consequently in terms of ω it is seen that there will be no imaginary roots, there may be two complex roots, and the real roots are symmetrical with respect to the origin since $Q(\omega)$ is an even function. It would be desirable to make a more definite statement about these roots but it is not possible at this time. Under these circumstances each case must be treated as a special one.

(5) S. Patterson, *Proc. Phys. Soc.*, **59**, 50 (1947).

(6) R. A. Ebel, Ph.D. Thesis, University of Minnesota, 1949.

(7) P. R. Kasten and N. R. Amundson, *Ind. Eng. Chem.*, **42**, 1341 (1950).

(8) W. D. Munro and N. R. Amundson, *ibid.*, **42** 1481 (1950).

(9) E. C. Titchmarsh, "Theory of Functions," Oxford University Press, London, 1939.

For the case of the infinite mass transfer coefficient the quadratic factor reduces to a linear factor, $2n + 3(\beta + 1)$, and the zero of this equation is always negative. Therefore in this case the zeroes of $g(z)$ are always negative. Consequently for the well agitated system, which the authors consider to be the most important one, the roots may be calculated with the assurance that all have been accounted for.

Case 2. Non Equilibrium.—For this case Equations 1, 2, 4 and 5 are still valid but a new assumption concerning the relation between adsorbed material and solution concentration must be made. In general the kinetic relation will replace the equilibrium isotherm and will be of the form $\partial n/\partial t = F(c,n)$, where $F(c,n)$ is a complicated function depending upon the adsorbate, solvent and adsorbent. Although a numerical method could be developed to treat a general function it is the purpose here to develop mathematical formulas and the most general relation of this type which can be used is

$$\frac{1}{\alpha}\frac{\partial n}{\partial t} = k_1 c - k_2 n \qquad (16)$$

α being introduced for convenience only.

The complete system to be solved for this case consists of Equations 1, 2, 4, 5 and 16. This problem can be handled also by means of the LaPlace transformation. Let $L[n(r,t)] = N(r,p) = N$. The transforms of Equations 1 and 16 are, respectively

$$\frac{d^2h}{dr^2} + \frac{2}{r}\frac{dh}{dr} = \frac{1}{D}(ph - c_0) + \frac{1}{\alpha D}(pN - n_0)$$

and

$$\frac{1}{\alpha}(pN - n_0) = k_1 h - k_2 N$$

If N is eliminated between these two equations the following results

$$\frac{d^2h}{dr^2} + \frac{2}{r}\frac{dh}{dr} - ah = -\frac{1}{D}\left[\frac{c_0(p + k_2\alpha) + n_0k_2}{p + k_2\alpha}\right]$$

where $a = p(p + k_1 + k_2\alpha)/D(p + k_2\alpha)$.

The solution of this equation which remains finite at $r = 0$ is

$$h = \frac{A}{r}\sin r\sqrt{-a} + \frac{c_0(p + k_2\alpha) + n_0k_2}{p(p + k_1 + k_2\alpha)}$$

The constant A may still be determined from Equation 8 with the result that the complete solution is

$$h = \frac{c_0(p + k_2\alpha) + n_0k_2}{p(p + k_1 + k_2\alpha)} + \frac{R}{r}\frac{[C_0(p + k_1 + k_2\alpha) - c_0(p + k_2\alpha) - n_0k_2]\sin\frac{r\Delta}{R}}{(p + k_1 + k_2\alpha)Z(p)} \qquad (17)$$

where $\Delta = R\sqrt{-a}$ and

$$Z(p) = \left[-\frac{3D\mu}{R^2} + p(1 - \epsilon)\right]\sin\Delta + \Delta\cos\Delta\left(\frac{3D\mu}{R^2} + p\epsilon\right) \qquad (18)$$

where $\mu = \alpha W/\rho V$. Equation 17 is the inverse transform of the concentration in the solution.

The residue at the pole $p = 0$ can be shown to be $(C_0\alpha + \mu(\alpha c_0 + n_0))/(K\mu + \alpha(1 + \mu))$, where $K = k_1/k_2$. This consists of the sum of two terms one coming from the first and the other the second term in Equation 17. There is also a pole at $p = -k_1 - k_2\alpha$. The residue at this pole can be found by evaluating the limit in the prescribed manner. Two terms are again obtained which are negatives of each other and hence their sum zero. The remaining poles occur at the zeroes of Equation 18 and the sum of the residues for these poles can be obtained from Equation 11. Direct calculation will show that

$$c(r,t) = \frac{C_0\alpha + \mu(\alpha c_0 + n_0)}{K\mu + \alpha(1 + \mu)} + \frac{R}{r}\sum_{n=1}^{\infty}\frac{[C_0(p_n + k_1 + k_2\alpha) - c_0(p_n + k_2\alpha) - n_0k_2]\sin\frac{r\Delta_n}{R}}{(p_n + k_1 + k_2\alpha)Z'(p_n)}e^{p_nt}$$

where

$$Z'(p_n) = \frac{\sin\Delta_n}{\Delta_n(3\beta + p_n\epsilon)}G(p_n)$$

$$G(p_n) = 3\beta'\Delta_n + E_n[-\Delta_n^2(3\beta' + p_n\epsilon)^2 + p_n(3\beta' + p_n\epsilon) - p_n^2]$$

$$E_n = -\frac{R^2}{2D\Delta_n}\left[1 + \frac{k_1k_2\alpha}{(p_n + k_2\alpha)^2}\right]$$

$$\beta' = D\mu/R^2$$

and p_n is a zero of Equation 18 with

$$\frac{\Delta_n^2D}{R^2} = -\frac{p_n(p_n + k_1 + k_2\alpha)}{p_n + k_2\alpha}$$

In Equation 13 it is necessary to calculate

$$\left(\frac{\partial c}{\partial r}\right)_{r=R} = \frac{1}{R}\sum_{n=1}^{\infty}\frac{[C_0(p_n + k_1 + k_2\alpha) - c_0(p_n + k_2\alpha) - n_0k_2][\Delta_n\cos\Delta_n - \sin\Delta_n]}{(p_n + k_1 + k_2\alpha)Z'(p_n)}e^{p_nt}$$

Upon using Equation 18 this can be reduced after substituting for the cosine to

$$\left(\frac{\partial c}{\partial r}\right)_{r=R} = -\frac{1}{R}\sum_{n=1}^{\infty}\frac{[C_0(p_n + k_1 + k_2\alpha) - c_0(p_n + k_2\alpha) - n_0k_2]\Delta_np_n}{(p_n + k_1 + k_2\alpha)G(p_n)}e^{p_nt}$$

Substitution into Equation X gives

$$C_0 - C = 3\beta'\sum_{n=1}^{\infty}\frac{[C_0(p_n + k_1 + k_2\alpha) - c_0(p_n + k_2\alpha) - n_0k_2]\Delta_n}{(p_n + k_1 + k_2\alpha)G(p_n)}[1 - e^{p_nt}] \qquad (19)$$

Equation 19 solves the kinetic problem for the type of kinetics assumed here completely. A mass transfer coefficient has been assumed to exist but the case for infinite mass transfer can be easily obtained by allowing $\epsilon \rightarrow 0$ with subsequent simplification of the equation defining the concentration and the roots over which the summation is to be made.

It would be highly desirable to make a statement concerning the roots of Equation 18 but it is not possible at this time. However preliminary investigation seems to indicate that for the case of no film resistance all the roots in p are negative.

THE CHEMICAL EFFECTS OF α-PARTICLES UPON SOME C_6-HYDROCARBONS IN THE VAPOR STATE

BY VICTOR P. HENRI,[1] CHARLES R. MAXWELL, WILLIAM C. WHITE AND DOROTHY C. PETERSON

National Institute of Arthritis and Metabolic Diseases of the National Institutes of Health, Public Health Service, Federal Security Agency, Bethesda, Maryland

Received November 13, 1950

Some of the chemical effects of α-particles upon *n*-hexane, cyclohexane, cyclohexene and benzene have been determined. The hydrocarbons were mixed in the vapor state with radon and allowed to stand for several weeks. The resulting gaseous mixtures were analyzed by the use of a mass spectrometer. Some of the physical properties of the liquids formed in each case were also determined.

Introduction

The effects of α-particles upon the vapors of *n*-hexane, cyclohexane, cyclohexene and benzene have been investigated by mixing these vapors with radon gas. Such mixtures were allowed to stand for several weeks until the radon had decayed to a level which was safe to handle. The gases in the bulbs were then analyzed with a mass spectrometer and, where possible, the iodine numbers and average molecular weights were determined on the non-volatile liquids formed in the flasks.

In order to obtain sufficient products for analysis and to minimize the effect of the radiation emitted in the late stages of the experiments upon the products formed in the early stages of the experiments, it was necessary to use large amounts of the radon-vapor mixture. With three-liter spherical bulbs and 250 to 500 millicuries of radon the concentration of gaseous products was such that in the least favorable case (*n*-hexane) only 7% of the total energy absorbed in the gas phase was absorbed by the products rather than by the original C_6-hydrocarbon. No attempt was made to estimate the amount of radiation absorbed by the liquid product collecting in the bottom of the flasks, but it was undoubtedly small since the solid angle presented by this material to the large spherical volume of radon was very small.

Experimental Procedure

The hydrocarbon vapor and the radon were sealed into an all-glass system in the following manner. The radon, contained in a sealed thin wall capillary, was dropped into the apparatus (Fig. 1) through the tube T. This tube was then sealed with a flame at point A.

Bulb L, which contained liquid hydrocarbon, was immersed in liquid air and the apparatus evacuated with a mercury vapor diffusion pump to a pressure less than 10^{-4} mm. Stopcock I was closed and the liquid air removed from around bulb L. When the pressure of hydrocarbon vapor reached several mm., as measured on a Hg manometer sealed onto the bulb B (in a plane not shown in Fig. 1), stopcock II was closed and the system re-evacuated. Several such flushings were made as a precaution against any dissolved gases in the liquid hydrocarbon. Finally the pressure of the hydrocarbon was allowed to reach a value a few mm. below the vapor pressure of the liquid at room temperature and the bulb was sealed from the vacuum system at the constriction C. The end of the capillary needle which contained the radon was then sheared off by a glass enclosed iron plunger actuated by a magnet.

The pressure of the system was followed for about two weeks. Within the experimental error the pressure change in the system paralleled the decay of the radon. The bulbs were allowed to stand for at least six weeks, sometimes twelve, before the contents were analyzed for reaction products.

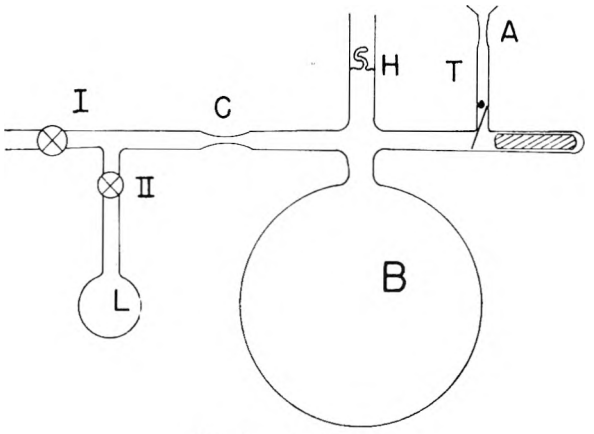

Fig. 1.—Apparatus.

The benzene was C.P. grade which had been further purified by fractional crystallization. The cyclohexene and *n*-hexane were secured from the National Bureau of Standards and were used without further purification. They were certified to be better than 99 molecular per cent. pure. The cyclohexane was obtained from Eastman Kodak Company and had a melting point of 5.70° and a boiling point range of 80.7 to 81.1°.

Analysis of the Bombarded Sample.—The composition of the gas in the flask after bombardment was determined with a Westinghouse mass spectrometer. The gas was introduced into the mass spectrometer through a capillary leak from a gas handling system designed for these particular mixtures. The bombardment flask was sealed directly to this system and the gas introduced by breaking the hook seal H (Fig. 1). The gases were moved to any desired portion of the system through mercury filled U-tube cut-offs by pressure differentials or by Toepler pumps. From the time the radon gas mixture was sealed from the original filling system until the analysis was completed the gases were in contact with nothing except glass and mercury.

The residual starting material and the saturated hydrocarbons produced by the radiation were first determined on a portion of the sample by standard mass spectrographic techniques using neon as an internal standard.

The hydrogen was determined by measuring the loss in pressure when another portion of the sample was allowed to stand in contact with a hot palladium thimble.

Since it was impossible to determine the small amounts of unsaturated gases with any degree of accuracy in the presence of the large amount of unchanged C_6-hydrocarbon, the remaining sample was divided into three fractions by the use of cold traps.

The first fraction, which was obtained by slowly pumping the gases through two liquid air traps, was found to contain H_2, CH_4 and C_2H_4. The CH_4 and C_2H_4 were determined and the H_2 was taken as the difference. Although this value for H_2 was always lower than the value obtained with the palladium thimble, the agreement was usually within 10%. The palladium figures are the ones reported.

The second fraction was obtained by pumping the remaining gas through traps immersed in Dry Ice and alcohol.

(1) National Institutes of Health Fellow (1948). Present address: Massachusetts Institute of Technology, Physics Department and Laboratory of Nuclear Science and Engineering, Cambridge, Mass.

This fraction was found to consist of C_2–C_5-hydrocarbons and a small amount of the original C_6-hydrocarbon. By this method we were able to determine very small amounts of gases which could not be detected in the unfractionated sample.

At least three analyses were made on each of the above fractions and a minimum of three samples were bombarded for each of the four compounds investigated.

In addition to the above gases there was formed in each case an oily non-volatile liquid which collected in the bottom of the spherical vessel as the bombardment proceeded. This material was clear to slightly yellow in color. The product from benzene was the most colored and the most viscous of the four. At the completion of the gas analysis the flasks were broken and as much as possible of the liquid removed for a determination of its average molecular weight and iodine number. The small amount of liquid and the large glass surface made it impractical to attempt to remove all the liquid for a direct determination of yield by weighing. The yield of liquid and the H/C ratios of the liquid reported in Table I were calculated by a simple weight balance based on the gas analysis.

TABLE I

THE CHEMICAL EFFECT OF 5–8 MEV. PARTICLES FROM RADON ON SOME C_6-HYDROCARBON VAPORS

		Compound bombarded (parent compound)			
		n-Hexane	Cyclohexane	Cyclohexene	Benzene
Molecules parent compound reacting per 100 ev. absorbed $-G_R$		8.2	9.0	16.3	4.9
$-M/N$ = Molecules removed / Ion pairs formed		2.8	3.1	5.7	1.4
Average mol. weight of liquid		330	355	360	330
Energy absorbed in parent compound, %		93	97	95	99
Parent compound reacting, %		41	40	53	24
H/C ratio parent compound		2.33	2.00	1.67	1.000
H/C ratio liquid (calcd.)		2.03	1.81	1.59	0.98
Weight % parent compound reacting found in liquid (calcd.)		73	90	86	97
Average number double bonds / Average molecule of liquid		1.25		2.00	
G_p = molecules of indicated gas formed/100 ev. absorbed	H_2	3.5	3.6	1.9	0.30
	CH_4	0.44	0.53	0.27	0.01
	C_2H_2	..	..	0.49	0.42
	C_2H_4	.08	..	1.3	0.02
	C_2H_6	.90	1.2	0.04	.006
	C_3H_4	..	..	.36	...
	C_3H_6	06	..	.19	...
	C_3H_8	1.35	0.33	.02	...
	C_4H_8	..	..	.05	...
	C_4H_{10}	1.10	.34	..	...
	C_6H_{12}	0.23	..	..	...
	C_6H_6	..	..	.07	...
	C_6H_{12}	..	..	1.07	...
Total		7.7	6.0	5.8	.76

The average molecular weights of the liquid products were determined by freezing point depression. Small amounts of the products were dissolved in benzene and in cyclohexane and the capillary melting points of the quickly frozen solutions taken. Very slow rates of heating were used and the disappearance of the last crystal was taken as the melting (freezing) point of the solution.

Where possible, iodine numbers were run on the liquids and the results calculated as the average number of double bonds found per average molecule of the liquids. The values, of course, have the errors of the molecular weight determinations and the iodine number determinations associated with them.

Calculations.—The range of the Rn α-particle was calculated for the average composition of the gases in the flask from the final analysis and the relative stopping powers for C and H as given by Livingston and Bethe.[2] The energy absorbed was then determined from a plot of the data of Maxwell and Henri[3] using the following distribution of α-emitters based on the experimental determination reported earlier.[4] Rn in gas, 100%; RaA in gas, 90%; RaC′ in gas, 40%.

The amount of energy absorbed in any gaseous constituent was calculated from the ratio of the relative stopping power of that constituent to the total relative stopping power of the gas mixture.

The yields reported in Table I were calculated on the basis of the energy absorbed in the original C_6-hydrocarbon and not the total energy absorbed in the gas phase.

Discussion

Although the number of compounds studied has been too small to warrant the formation of general rules as to the effect of structure on the reactivity of hydrocarbon molecules under the influence of ionizing radiation, the data in Table I do indicate certain trends. The reactivities of the four compounds studied are of the same order of magnitude; the larger, for cyclohexene, and the smaller, for benzene, differ only by a factor of three. These reactivities are of the same order of magnitude as those reported earlier by Lind[5] for lighter hydrocarbons.

In all cases most of the mass of the reacted hydrocarbon was found in a non-volatile liquid of higher molecular weight than the original or parent hydrocarbon. The amount of liquid varied from 73% of the reacted *n*-hexane to 97% of the reacted benzene. With all four compounds the H/C ratio was less for the liquid product than for the parent hydrocarbon. Whether the near equality of the average molecular weights of the liquids is real or an artifact the authors are not sure, although the method used for the determination gave consistent and reliable results with pure substances.

The gaseous products of the irradiation were, in general, mixtures of lower molecular weight hydrocarbons and hydrogen. For the aliphatic compounds (*n*-hexane, cyclohexane and cyclohexene) most of the lower molecular weight saturated hydrocarbons and many of the unsaturated ones were present with hydrogen being the most abundant single product. With all four compounds the relative amount of unsaturated gaseous product increased with increasing unsaturation of the parent hydrocarbon until in the case of benzene the mixture consisted almost entirely of hydrogen and acetylene.

A relatively large fraction of the reacted cyclohexene molecules (C_6H_{10}) appeared as C_6H_{12} molecules. The ratio of the 84 and 83 peaks in the mass spectrographic analysis of the gas mixture indicated that these molecules were cyclohexane. However, the complexity of the mixture made the use of lower mass peaks for the positive identification of this compound impossible and this identification can only be considered as the most probable.

(2) M. S. Livingston and H. A. Bethe, *Rev. Mod. Phys.*, **9**, 271 (1937).

(3) C. R. Maxwell and V. P. Henri, *J. Chem. Phys.*, **18**, 207 (1950).

(4) C. R. Maxwell, V. P. Henri and D. C. Peterson, *ibid.*, **18**, 179 (1950).

(5) S. C. Lind, "The Chemical Effects of Alpha Particles and Electrons," The Chemical Catalog Company (Reinhold Publ. Corp.), New York, N. Y., 1928.

Certain comparisons may be made with other studies reported in the literature. Table II compares the effect of 5–8 mev. α-particles on these

TABLE II

THE EFFECT OF STATE UPON THE CHEMICAL EFFECTS OF IONIZING RADIATION ON HYDROCARBONS

Compound	G_g = Molecules gas formed / 100 ev. absorbed		G_R = Molecules reactant reacting / 100 ev. absorbed	
	Gas[a]	Liquid[b]	Gas[c]	Liquid[b]
Benzene	0.76	0.04	4.9	0.5
n-Heptane		4.2		1.7
n-Hexane	7.7		8.2	
Cyclohexane	6.0	4.0	9.0	1.2
Cyclohexene	5.8	1.0	16.3	4.2

[a] Effect of 5.5 → 7.7 mev. α-particles. [b] Effect of 2.3 → 2.8 mev. electrons observed by Flanagan, Hochanadel and Penneman, ref. (6).

hydrocarbons in the gaseous phase with the effect of 2–3 mev. electrons on the hydrocarbons in the liquid phase.[6] In every case the chemical effect on the gas is greater than on the liquid. It is, of course, impossible to say definitely whether this difference is due to the difference in type of ionizing particle or to the difference in state of the hydrocarbon or to both. However, it is very probably due to the difference in state. Franck and Rabinowitch[7] have pointed out that in certain photochemical cases where the same decomposition reaction can be studied both as a gas and a liquid, the quantum yield of the reaction is generally lower in the liquid. This is believed to be caused by a collisional deactivation effect and/or a cage effect which is much more pronounced in the liquid. The magnitude of the deactivation effect will vary with the amount of activation energy imparted to the molecules and the "life time" of the activated molecule before decomposition. Since, as Burton[8] has pointed out, the resonating structure of benzene tends to increase this "life time," the effect of state should be most noticeable with this substance. This is what was observed.

The very high reactivity of cyclohexene is in unexplained disagreement with previous reports. Both the above work of Flanagan, Hochanadel and Penneman[6] with 2–3 mev. electrons and the work of Schoepfle and Fellows[9] with 170 kv. electrons show that the reactivity of cyclohexene (liquid) lies between the saturated hydrocarbons and the aromatics. The reported G_R for this work includes both decomposition and hydrogenation but when the total value 16.3 is reduced by 1.07 for hydrogenation, the value is still greater than those values found for the other hydrocarbons.

These observations are far too few to establish a mechanism of reaction but they are consistent with one of the simple probable mechanisms, *i.e.*, the excitation and/or ionization of the parent hydrocarbon molecule followed by the rupture of this molecule into two or more ions or free radicals. These fragments then recombine on primarily a statistical basis until all the electrical charges and free valence bonds are neutralized.

Acknowledgment.—The radon for these experiments was supplied by the U. S. Marine Hospital, Baltimore, Maryland, through the courtesy of Dr. John E. Wirth and Dr. Roger K. Taylor.

(6) J. V. Flanagan, C. J. Hochanadel and R. A. Penneman, reported by Burton in ref. 8.

(7) J. Franck and E. Rabinowitch, *Trans. Faraday Soc.*, **30**, 120 (1934).

(8) Milton Burton, THIS JOURNAL, **52**, 564 (1948).

(9) C. S. Schoepfle and C. H. Fellows, *Ind. Eng. Chem.*, **23** 1396 (1931).

THE POLYMERIZATION OF CYCLOPROPANE[1,2]

BY R. J. SCOTT AND H. E. GUNNING

Department of Chemistry, Illinois Institute of Technology, Chicago 16, Illinois

Received November 24, 1950

A study has been made of the physical and chemical properties of the polymer produced by the reaction of cyclopropane with Hg $6(^3P_1)$ atoms at 30° in a static system. The polymer is an oily liquid, normal b.p. 271°, $n^{20}D$ 1.4649. The molecular weight distribution is Gaussian, with the mean chain length at 6.1 C_3H_6 units and the most probable chain length at 5.3 units. Bromination tests indicate less than 1% unsaturation in the polymer. The results of infrared studies on the polymer and the fractions obtained therefrom by fractional distillation, coupled with the unsaturation data, suggest that the polymer is essentially a complex mixture of cycloparaffins. Previous kinetic studies on the reaction showed that the polymerization proceeds through a polymethylene biradical. The results of the present investigation indicate that the polymethylene biradicals terminate mainly by cyclization.

Introduction

In an investigation of the kinetics of the reaction of cyclopropane with Hg $6(^3P_1)$ atoms in a static system at 30°, Gunning and Steacie[3] have shown that the photoexcited mercury atoms induce a polymerization of the cyclopropane. Their results indicate that at least 98% of the cyclopropane disappearing in the reaction is used up in the formation of a liquid polymer, the mean molecular weight of which remains constant in the region of complete quenching of the Hg $6(^3P_1)$ atoms, *i.e.*, at initial pressures of cyclopropane above 40 mm. These authors postulate that the polymerization is propagated by energy-rich polymethylene biradicals in accordance with the following sequence

$$C + Hg\ 6(^3P_1) \longrightarrow R_1^* + Hg\ 6(^1S_0) \quad (1)$$
$$R_1^* + C \longrightarrow R_2^* \quad (2)$$
$$R_1^* + C \longrightarrow 2C \quad (3)$$
$$R_2^* + C \longrightarrow R_3^* \quad (4)$$
$$\vdots$$
$$R_n^* + C \longrightarrow M_n + C \quad (5)$$

where C, cyclopropane; R_1, $\cdot(CH_2)_3\cdot$; R_2, $\cdot(CH_2)_6\cdot$; etc. and M_n, polymer.

It is apparent from the foregoing that detailed information on the specific type of compound, or compounds, present in the cyclopropane polymer would be of considerable assistance in establishing the mechanism whereby polymethylene biradicals are converted into stable molecules. And the present investigation was undertaken in order to establish, as far as possible, the specific nature of the polymer formed in the reaction described above. The details of the investigation follow.

Experimental

In a static system, the cyclopropane polymer forms in tiny droplets on the window of the quartz reaction cell, through which the mercury resonance radiation is transmitted. Gunning and Steacie[3] have shown that the quantum yield of cyclopropane disappearance is 0.136 for the reaction. And if this value is combined with their light intensity of 2537 Å. radiation of 1.06×10^{-5} einstein/min., their rate of formation of polymer becomes $(1.06 \times 10^{-5})(0.136)(60)(42) = 0.0036$ g./hour. This calculation serves to show that a major problem, to be solved at the outset, was the collection of sufficient quantities of the polymer for characterization.

The design of the polymer collection unit underwent many modifications. Eventually the apparatus shown in Fig. 1 was developed. This unit operated quite satisfactorily and with little attention. It consisted essentially of a piece of quartz tubing, 30 mm. in diameter and 230 mm. in length, with walls 3 mm. thick. This reaction tube was placed inside the helical coils of a Hanovia Sc-2537 mercury resonance lamp. The quartz-to-Pyrex graded seals, X and X′, served, respectively, to connect the reaction tube to the high-vacuum system and to a calibrated 15-ml. Pyrex centrifuge tube, G, *via* a 19/38 standard taper joint.

The evacuation system was of conventional design, employing a Princeton-type, two-stage, all-glass mercury diffusion pump, backed by a two-stage Welch Duoseal mechanical pump. The pumps were isolated from the main manifold by a large high-vacuum stopcock. A McLeod gage together with a series of traps, for purifying the cyclopropane, were connected to the main manifold. The polymer collection unit made connection with the main manifold through a Stock-type mercury cut-off, indicated as S_3 in Fig. 1.

The cyclopropane used throughout the entire investigation was obtained from the Ohio Chemical and Manufacturing Company, Cleveland, Ohio. Minimum purity, guaranteed by the manufacturer, was 99.5%. The cyclopropane was further purified by several trap-to-trap distillations from Dry Ice–acetone to liquid nitrogen temperatures. Only the middle fractions from these distillations were retained for the polymer generation. In order to be certain that no appreciable quantities of olefins were present, rate data were obtained for the purified cyclopropane on an apparatus exactly similar to the one employed by Gunning and Steacie.[3] And since these authors have shown that 0.2% of propylene will cause a 5% inhibition in the initial rate of pressure decrease, this method becomes a sensitive criterion of olefin concentration. Our values for $-dP/dt$ were constant in reaction time to 1%, which was the maximum experimental error of the determinations. It was therefore concluded that olefins, if present at all, could not exceed 0.04% in concentration.

The Hanovia Sc-2537 resonance lamp was operated from the secondary of a General Electric Luminous Tube transformer. The transformer maintained a current of 120 ma. through the lamp and provided a starting potential of 5000 volts. In operation the potential drop across the lamp was 500 volts. The lamp emits a small amount of radiation at 1849 Å., which is absorbed by the oxygen in the light-path, with the formation of ozone. Since ozone absorbs the 2537 Å. radiation, an electric fan was directed on the lamp and reaction tube during operation in order to prevent the accumulation of ozone in the light-path.

Before starting a run, the reaction tube was removed from the system, cleaned with hot chromic acid solution, and "flamed out" at a red heat with a hand torch. The small tube, R, in Fig. 1 was filled with freshly-distilled mercury to a fixed mark, after which the reaction tube was sealed to the system. The calibrated receiver, G, was then attached to the system using Cenco "Sealstix" cement on the standard taper joint. The "Sealstix" cement was chosen because hydrocarbons are insoluble in it. The mercury cut-off, S_3, was then opened and the system was thoroughly evacuated. Checks on the vacuum-stability of the system showed a maximum pressure buildup of less than 10^{-5} in 24

(1) This work was supported by Contract No. AT-(11-1)-43 with the U. S. Atomic Energy Commission.

(2) Part of a dissertation submitted by R. J. S. in partial fulfillment of the requirements for the degree of Master of Science at Illinois Institute of Technology.

(3) H. E. Gunning and E. W. R. Steacie, *J. Chem. Phys.*, **17**, 351 (1947).

hours. After evacuation of the system, the cyclopropane, purified as described above, was distilled from a large trap in the purification system, which was immersed in Dry Ice–acetone, to trap T_1 which was maintained at liquid nitrogen temperature. The distillation was continued until about 25 ml. of solid cyclopropane were frozen into T_1. The polymer collection unit was then isolated from the remainder of the system by closing cut-off S_3, whereupon large dewars of Dry Ice–acetone were placed around T_1, and around the receiver, G. The pressure of cyclopropane in the system corresponded to its vapor pressure at −78.5°, *i.e.*, 55 mm. All that remained, then, was to turn on the lamp and fan and allow the polymer to collect in the receiver, G.

The distillation of the polymer was carried out in a Podbielniak Miniature "Hypercal" column assembly. The column itself was 8 mm. i.d. and 30 cm. long, with "Heligrid" packing. Both the column and the distilling flask were vacuum-jacketed.

The boiling point determinations on the polymer and the fractions were made by the method recommended by Siwoloboff.[4] The 0–360° thermometer used in the measurements was carefully calibrated against a platinum resistance thermometer in conjunction with a Mueller bridge. Check determinations made on pure liquids indicated a precision of 2° for the method.

The refractive index measurements were made with an Abbe refractometer, thermostated at 20° and illuminated by a sodium lamp.

The molecular weight determinations were first attempted using the camphor method of Rast.[5] However the results obtained seemed to be somewhat higher than might be expected on the basis of the other physical properties of the polymer fractions. This method was finally abandoned in favor of a semi-micro technique, employing carefully purified cyclohexane as solvent. The temperature changes were followed with a Beckman differential thermometer. Weighed samples of the polymer fractions of the order of 0.2 g., together with a weighed quantity of cyclohexane of the order of 25 g., were placed in an unsilvered dewar which was fitted with the thermometer and a stirrer. The dewar was, in turn, immersed in an ice-bath. Repeated checks with purified naphthalene with this method showed maximum deviations of ±2%.

The olefin content of the polymer was determined by titration of a weighed sample dissolved in chloroform, against a standardized solution of bromine in glacial acetic acid, after the method of Uhrig and Levin.[6]

Infrared absorption curves were made for some of the polymer fractions, using a Perkin-Elmer infrared recording spectrometer.

Results

Polymer Collection.—Under optimum conditions the polymer collection unit generated approximately 0.5 ml. of polymer during each 24-hour period. Since the reaction produces a small amount of hydrogen,[3] it was found advisable to freeze down the cyclopropane and its polymer in liquid nitrogen, at 12-hour intervals, and evacuate the system. By this means it was possible to prevent any inhibition in the rate of polymer formation arising from competitive quenching of the Hg $6(^3P_1)$ atoms by hydrogen molecules. This technique also reduced the possibility of hydrogenation of the polymer by H atoms.

The polymer collection was allowed to continue until 18 ml. of polymer had been accumulated. The polymer had roughly the same viscosity as a light machine oil. Furthermore, it should be noted that it had a pale yellow color when viewed in bulk.

Polymer Distillation.—For the distillation, 15 ml. of the polymer was measured into the vacuum-jacketed distilling flask of the Hypercal unit.

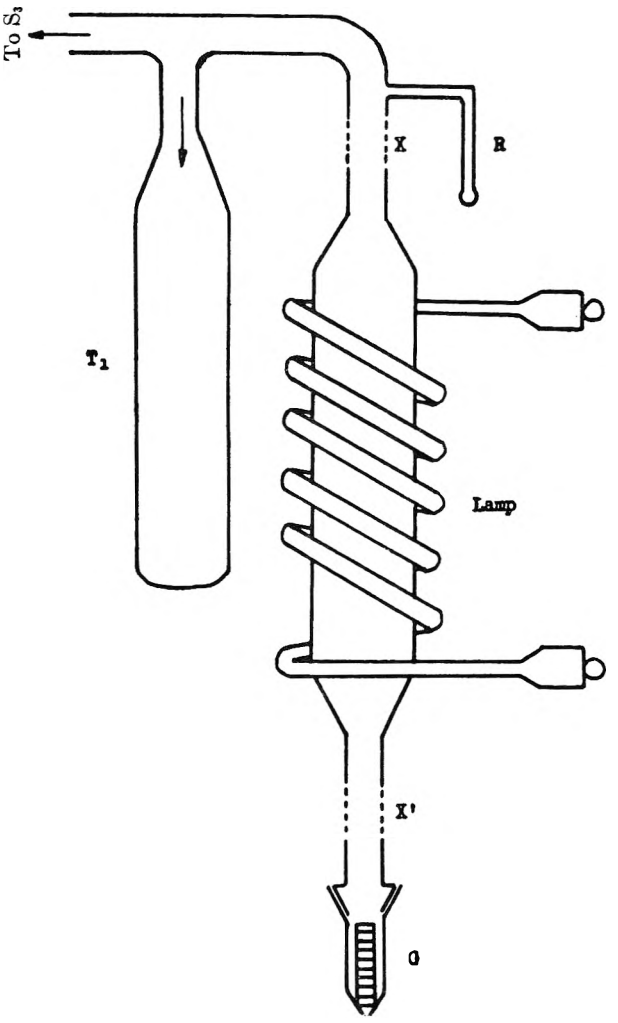

Fig. 1.—The polymer collection unit.

The distillation was carried out at atmospheric pressure for the lower fractions, and at a pressure of 100 mm. for the higher fractions. The distillation was stopped after ten fractions had been collected, owing to the high viscosity of the tenth fraction. The total volume of distillate accounted for very nearly two-thirds of the 15 ml. of polymer taken. The distillation curve revealed very strikingly that the polymer was a mixture of enormous complexity. Some twenty-two significant constant-temperature plateaus were observed in all. Since the distillation was exploratory in nature, the extensive temperature–volume data have been omitted from the present paper.

The Physical Properties of the Polymer and Its Fractions.—The boiling point, refractive index and average molecular weight were determined for the original polymer and for each of the ten fractions collected. These data, together with the volumes of each fraction, are summarized in Table I.

The Olefin Content of the Polymer.—In view of the fact that the polymethylene biradical, which propagates the polymer chain, could conceivably stabilize itself either by rearrangement to form a linear olefin, or by cyclization, the determination of the olefin content of the polymer becomes par-

(4) A. Siwoloboff, *Ber.*, **19**, 795 (1886).
(5) K. Rast, *ibid.*, **55**, 1051, 3727 (1922).
(6) K. Uhrig and H. Levin, *Ind. Eng. Chem., Anal. Ed.*, **13**, 90 (1941).

TABLE I

PHYSICAL PROPERTIES OF THE POLYMER FRACTIONS

Distillation fraction no.	Volume, ml.	B.p. at 760 mm., °C.	Refractive index $n^{20}D$	Molecular weight	No. of C_3H_6 units
Original polymer	15.00	271	1.4649	255	6.1
1	0.46	136	1.4218	130	3.1
2	.50	172	1.4371	155	3.7
3	.76	216	1.4456	192	4.6
4	1.06	240	1.4500	213	5.1
5	1.46	252	1.4545	218	5.2
6	0.46	263	1.4558	219	5.2
7	1.51	274	1.4567	243	5.8
8	2.22	280	1.4560	266	6.4
9	0.61	290	1.4618	253	6.0
10	0.51	302	1.4645	277	6.6
Undistilled residue	5.45	...	....	...	...

ticularly significant. Consequently two bromine titrations were made on the polymer by the method described above. These titrations indicated a maximum degree of unsaturation of 0.5%. This result is a vital key to the characterization of the polymer, for it can be concluded, therefore, that the polymer consists almost, if not entirely, of saturated compounds. And if the compounds are saturated, they must needs also be cyclic since they are formed by intramolecular rearrangement of the polymethylene biradical, $(C{\cdot}H_2)_{3n}{\cdot}$.

Infrared Data for the Polymer Fractions.—In order to gain further insight into the chemical nature of the polymer, infrared absorption curves were run on fractions 1, 2, 3 and 8. The data obtained are summarized very briefly in Table II.

TABLE II

PRINCIPAL INFRARED ABSORPTION PEAKS FOR THE POLYMER FRACTIONS

Wave length, microns	Fraction no. 1	2	3	8
5.79	+	+	+	+
6.04	+	+	+	+
6.83	+	+	+	+
7.25	+	+	+	+
7.78	+	−	−	−
7.94	+	+	+	−
8.20	+	−	−	−
8.58	+	+	+	−
9.23	−	+	−	−
9.76	−	+	−	−
9.85	−	−	−	+
10.36	+	+	+	+
10.97	+	−	−	−
11.23	+	+	+	+
12.25	+	+	+	−

The observed absorption frequencies for the polymer fractions have been collated with infrared data on the C_nH_{2n} hydrocarbons, both in the literature and in standard compilations.[7,8] As might be expected, the complexity of the mixtures, coupled with the paucity of infrared data on higher molecular weight hydrocarbons, renders it difficult indeed to arrive at definite conclusions concerning the presence or absence of specific configurations in the fractions. Certain tentative conclusions, however, are possible. The 12.25 frequency present in nos. 1, 2 and 3, but not in no. 8, appears to be associated uniquely with olefinic hydrocarbons. Furthermore, the frequencies associated with the cyclopropane and cyclobutane rings seem to be missing. In view of the meager data available on the macrocyclanes, it would seem unwise to carry our inferences further.

Molecular Weight Distribution in the Polymer.—Reference to various compendia[7,9,10] on the physical constants of hydrocarbons brings to light the fact that the densities of the higher cycloparaffins (*i.e.*, C^9 and higher) vary within fairly narrow limits. The total range of densities (d^{20}_4) for C_9H_{18} to $C_{20}H_{40}$ is very nearly 0.79 to 0.84. What is more, any particular group of isomers shows considerable variation within the range defined above. Consequently we may consider the densities of the polymer fractions as constant to a first approximation. With this assumption, we may derive the following relation

$$X_i = \frac{N_0}{V_0}\sum_{i=1}^{i}\frac{V_i}{N_i} \equiv \frac{N_0}{V_0}J_i = 0.40\,J_i$$

where X_i = the cumulative mole fraction up to, and including, the *ith* fraction. The summation is taken in order of increasing mean molecular weight.
N_0 = mean number of C_3H_6 units in the polymer = 6.1
V_0 = volume of polymer taken for distillation = 15.0 ml.
V_i = volume of *ith* fraction in ml.
N_i = mean number of C_3H_6 units in the *ith* fraction
J_i = value of the summation

The necessary data for the evaluation of X_i are given in Table I, and the results of the calculation are summarized in Table III. In Fig. 2, X_i is plotted against N, the number of C_3H_6 units. The slope of this sigmoidal curve is one form of the molecular weight distribution function for the polymer. The point of inflection corresponding to the maximum slope occurs at a value of N of approximately 5.3. This value will therefore be the most probable chain length for the polymer.

TABLE III

MOLECULAR WEIGHT DISTRIBUTION DATA FOR THE POLYMER

N_i No. of C_3H_6 Units	J_i	X_i
3.1	0.15	0.06
3.7	.28	.11
4.6	.45	.18
5.1	.66	.27
5.2	.94	.38
5.2	1.03	.42
5.8	1.29	.52
6.0	1.39	.56
6.4	1.73	.70
6.6	1.83	.73

(7) American Petroleum Institute, "Selected Values of Properties of Hydrocarbons," 1949.

(8) H. M. Randall, R. G. Fowler, N. Fuson and R. G. Dangl, "Infra-red Determination of Organic Structures," D. Van Nostrand Company, Inc., New York, N. Y., 1949.

(9) M. P. Doss, "Physical Constants of the Principal Hydrocarbons," The Texas Company, New York, N. Y., 1943.

(10) G. Egloff, "Physical Constants of Hydrocarbons," Reinhold Publishing Corp., New York, N. Y., Vol. I, 1939, Vol. II, 1940.

And from Table I, we see that the average chain length is slightly higher at $N = 6.1$. In short, the distribution function appears to be of a Gaussian type.

Discussion

It will be convenient for our discussion to summarize first the results of our investigation of the properties of the polymer formed in the reaction of cyclopropane with Hg $6(^3P_1)$ atoms. These are:

(1) The polymer is a pale yellowish, oily liquid with a normal boiling point of 271° and a refractive index ($n^{20}D$) of 1.4649.

(2) The polymer consists of a complex mixture of cycloparaffins together, possibly, with a small amount (less than 1%) of olefinic compounds in the lower molecular weight region.

(3) The polymer has a mean chain length of 6.1 C_3H_6 units, while the most probable chain length is 5.3 units.

(4) Infrared absorption measurements indicate that compounds involving the highly-strained cyclopropane and cyclobutane rings are absent, as might be expected.

Probably the most interesting result of this investigation is the fact that the growing polymethylene biradical, $\cdot(CH_2)_{3n}\cdot$, does not tend to stabilize itself by the shift of an H-atom to form a linear olefin. And since Gunning and Steacie[3] have shown that there are no appreciable quantities of C_6 compounds present in the complete quenching region, we can conclude that the energy-rich biradical does not have a sufficient number of degrees of freedom to allow it to stabilize itself intramolecularly until it has attained a chain length of at least three C_3H_6 units. The fact that the most probable chain length falls between five and six C_3H_6 units would suggest strongly that the C_{15} and the C_{18} biradicals represent optimum chain lengths for intramolecular stabilization by cyclization in this reaction.

The relatively low boiling point of the polymer, taken in conjunction with its mean chain length of 6.1 units, indicates that the probability of propagation falls off rather rapidly with increasing chain length beyond $N = 6$. This is to be expected since the number of degrees of freedom for the biradical is $(27N - 6)$ or, in other words, there is an increase of 27 in the number of degrees of freedom for each unit increase in N. Consequently it should become increasingly more difficult for the propagating biradical to furnish sufficient energy, upon collision with a cyclopropane molecule, to rupture the ring.

Owing to the complexity of the polymer and the paucity of physical data, it would be difficult, indeed, to establish definitely at this time the special ring or rings present. However certain reasonable conclusions can be drawn. Exclusive head-tail cyclization leading to the formation of unsubstituted macrocyclanes such as cyclononane, cyclododecane, cyclopentadecane, etc., would seem to be ruled out on the basis of the improbability of the active ends of the biradical approaching sufficiently close to each other to allow coupling of the unpaired electrons. Furthermore the unsubstituted

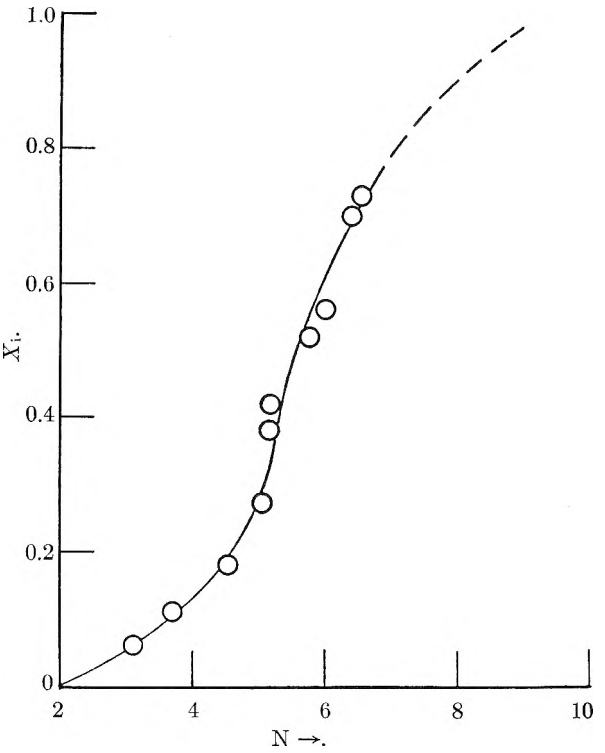

Fig. 2.—Integral molecular weight distribution curve for the cyclopropane polymer.

macrocyclanes beyond C_{11} are all solids at ordinary temperature. Cyclododecane,[10] for example, melts at 61°. And finally, exclusive head-tail cyclization would lead to the formation of a polymer containing relatively few compounds, contrary to our findings.

A study of scale models of the polymethylene biradical, $\cdot(CH_2)_{3n}\cdot$, would tend to suggest that the most probable type of compounds present would be monosubstituted alkyl cyclohexanes, and perhaps disubstituted alkyl cyclohexanes, with the substituents in adjacent positions. Of course, it is important to bear in mind that the biradical contains excess energy owing to its mode of formation, with the result that isomerization, so common to ring systems of this type, may well play a significant role in determining the nature of the stable compounds formed. In this connection we have made a fairly complete survey of all the available data on the cycloparaffins, and this survey leads us to the conclusion that the observed properties of the polymer are quite consistent with those which might be expected for a complex mixture of mono- and disubstituted cyclohexanes.

One interesting kinetic consequence of this investigation arises from the fact that Gunning and Steacie[3] have shown that the ratio of the rates of the cyclopropane-reforming reaction (k_3) to the propagation reaction (k_2), for the trimethylene biradical, can be expressed by the relation

$$k_3/k_2 = 7.3\,\bar{N} - 1$$

where $\bar{N}$ is the mean chain length of the polymer. From our data, $\bar{N} = 6.1$, leading to the result: $k_3 = 43\,k_2$. In other words, only some 2.3% of the trimethylene biradicals, generated in the primary

process, actually propagate polymer chains, the remainder reverting to cyclopropane.

Conclusions

Cyclopropane occupies a decidedly unique position among the reactions of the hydrocarbons with Hg $6(^3P_1)$ atoms,[11] in that it is the only hydrocarbon which has yet been investigated wherein the primary process definitely appears to involve the rupture of a C–C bond. Even if we restrict our comparison to the higher members of the cycloparaffin series, we find that cyclopentane,[12] methyl cyclopentane[13] and cyclohexane,[14] all decompose by the initial rupture of a C–H bond. And perhaps what is most interesting of all, recent data obtained in this Laboratory indicate that cyclobutane[13] also undergoes C–H bond rupture in its primary reaction with Hg $6(^3P_1)$ atoms.

Our present study has thrown considerable light on the specific nature of the polymerization process. And our findings complement the kinetic study of Gunning and Steacie,[3] and are in complete consonance with their basic mechanism. The cycloparaffinic nature of the polymer leads fairly unequivocally to the important generalization that polymethylene biradicals tend predominantly to stabilize themselves by cyclization rather than by olefin formation, in homogeneous gas reactions.

Acknowledgments.—The authors would like to express their appreciation to Dr. R. B. Bernstein for assistance in making the infrared measurements, to Mr. D. L. Kantro for assistance in collating the infrared data, and last, but by no means least, to Dr. Eugene Lieber for many helpful discussions.

(11) E. W. R. Steacie, "Atomic and Free Radical Reactions," Reinhold Publishing Corp., New York, N. Y., 1946.

(12) G. A. Allen, D. L. Kantro and H. E. Gunning, *J. Am. Chem. Soc.*, **72**, 3588 (1950).

(13) M. Schlochauer and H. E. Gunning, *J. Chem. Phys.*, **19**, 474 (1951).

(14) H. E. Gunning, unpublished data.

SPEED YOUR SEARCHES

of the CHEMICAL LITERATURE

with the . . .

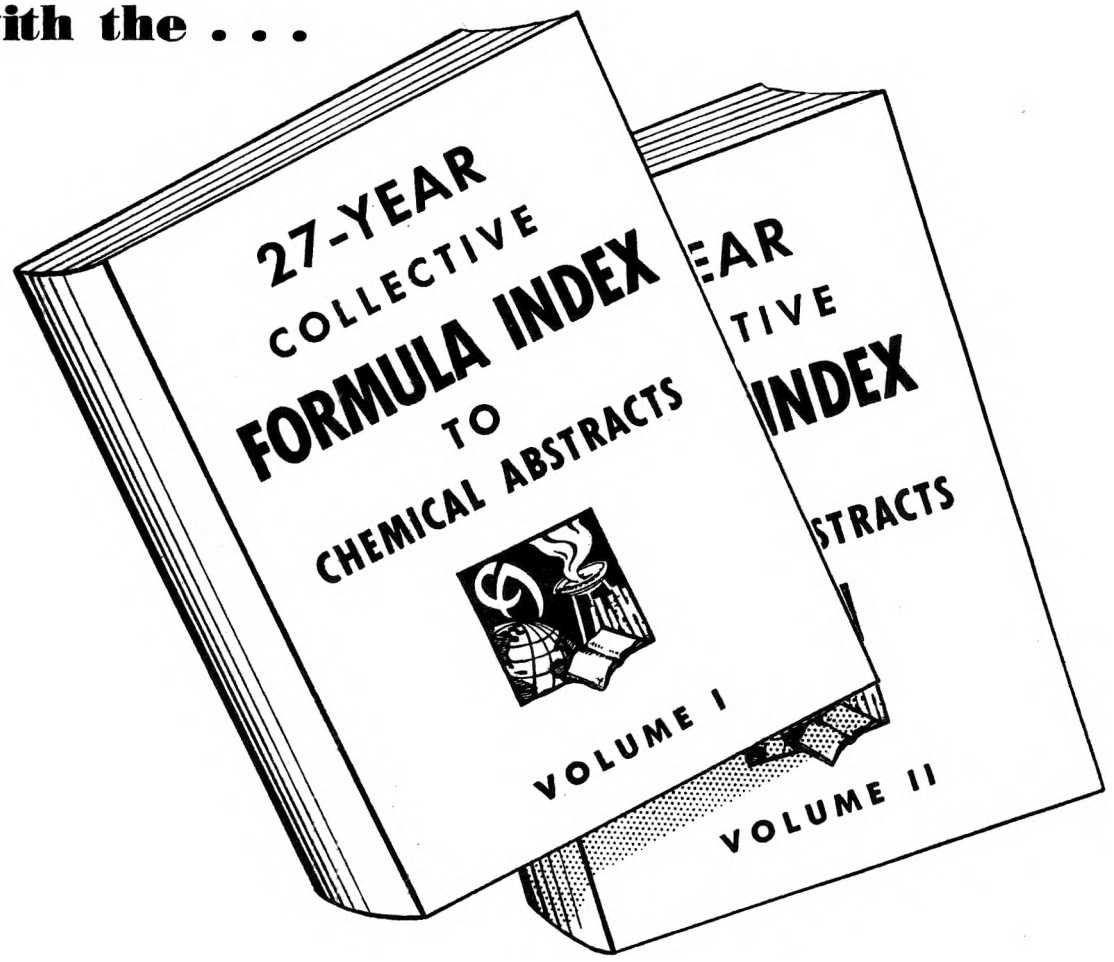

- Covering 1920–46
- Listing both organic and inorganic compounds
- Containing over half a million entries
- Giving cross references to subject indexes
- Listing compounds in simple arrangement
- With up-to-date nomenclature
- In two volumes of about 1000 pages each
  Vol. I now ready, Vol. II available in late 1951

Price: Paper bound, $80.00. Cloth bound, $85.00.
(Less $10.00 to ACS members who certify that index is for personal use. Certification form sent on request.)

Address orders and inquiries to:

SPECIAL PUBLICATIONS DEPARTMENT
AMERICAN CHEMICAL SOCIETY
1155 Sixteenth Street, N.W.
Washington 6, D.C.